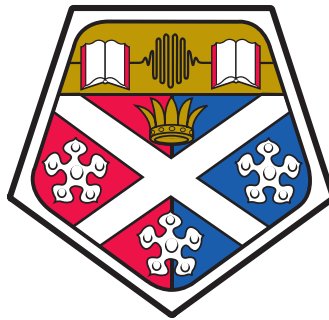


**On the impacts of climate  
change on water resources:  
Lessons from the River Nith  
Catchment and Shire River  
Basin**



**Jackson Kawala**

Department of Civil and Environmental Engineering

University of Strathclyde

A Thesis presented for the Degree of Doctor of Philosophy

September 2020

This thesis is dedicated to my beautiful wife, Susan Mwape, my children Chloe Nakawala and Jackson Kawala III, and in loving memory of my parents Jackson Kawala Snr. and Agness Kaleya.



## Declaration

This thesis is the result of the author's original research. It has been composed by the author and has not been previously submitted for examination which has led to the award of a degree.

The copyright of this thesis belongs to the author under the terms of the United Kingdom Copyright Acts as qualified by University of Strathclyde Regulation 3.50. Due acknowledgement must always be made of the use of any material contained in, or derived from, this thesis.

---

Signature

---

Date

## **Acknowledgements**

Foremost, I would like to thank God for the blessing of life, family and friends, including the opportunity to pursue this PhD.

My deepest gratitude and appreciation also goes to my Supervisor, Professor Robert M. Kalin, for all the guidance and support throughout my studies. Not only did he provide research guidance, he shared precious life experiences and mental jewels that taught me how to become a better husband, father and human being in general. I will eternally be grateful to him for the times he was patient with me on my slow progress with my dissertation and the times he would tell me “you are doing great Jackson” or “I believe in you” whenever he sensed a cloud of despair and doubt hanging over my head. Only in eternity could a true estimate of the impact of those words be measured. For that, I am truly thankful.

I would also like to thank my Second Supervisor, Dr Phillippe Sentenac for all the support, academic and otherwise, rendered to me during the course of my studies. My gratitude also goes to Dr Christopher White for his guidance and support on a lot of issues that greatly enhanced the content of this thesis.

I would also like to thank all faculty and non-faculty staff of the Civil and Environmental Engineering Department for their support, cheerfulness and hos-

pitality. You made my stay at the University of Strathclyde a memorable and wholesome experience.

To my fellow research colleagues and friends, Jonathan, Ibrahim, Charles, Jamiu, Laura, Christina, Alexandra, Jafar and many others in the CEE department, you were my beacon of light at every step of my PhD journey and for that, I remain eternally grateful.

The work that led to the writing of this thesis would not have been possible without the financial support of the Commonwealth Scholarship Commission and the University of Strathclyde. My gratitude also goes to the Copperbelt University for supporting my studies.

Last but certainly not the least, I would like to thank my lovely wife Susan and our two lovely children Chloe and Jackson, at whose expense I have had to spend long hours away from their attention in order to pursue my passion and complete this thesis. I remain highly indebted to you for your understanding, comfort and support that you offered throughout this journey. May God bless you immeasurably.

## **Abstract**

One of the most complex and challenging problems faced by the world today is that of water scarcity which has been recognized as a global risk. According to experts, freshwater scarcity affects close to two-thirds of the world's population at least one month of the year while half a billion people are estimated to be living under water scarcity throughout the year. Climate change, population growth, increased reliance on irrigated agriculture and changes in land-use threaten to exacerbate water scarcity risk. In recent decades, solutions to these challenges and threats have been proposed through various interventions such as the Millennium Development and Sustainable Development Goals (MDGs and SDGs respectively). Responsible management of water systems and resources entails having a thorough understanding of the quantity and quality of these resources. Researchers have used simplistic 1-dimensional models to complex semi-distributed models to understand how water systems such as lakes, rivers and entire basins are replenished.

However, most studies have focussed on only one aspect of the hydrologic cycle when quantifying freshwater resources. In the past decade or so, the issue of integrated hydrologic modelling (IHM) where surface- and groundwater is modelled as an integrated unit has gained traction in the research community.

More recently, it has become fashionable to couple integrated hydrologic models coupled with atmospheric models to account for climate change. Notwithstanding this development, there is still no unified and systematic methodology and/or framework that has been adopted by the water research community for integrated hydrologic modelling. This, coupled with the challenge of filtering through the many spatial climate data products offered by the climate research centres, makes the task all the more challenging. This has led to a slow adoption of these models by the water resources community.

This thesis applies integrated hydrologic models (SWAT-MODFLOW) coupled with atmospheric models to two watersheds (River Nith Catchment and Shire River Basin) from different climatic settings to determine the quantity and availability of future water resources. The River Nith Catchment (RNC) is located in South-West Scotland, UK while the Shire River Basin (SRB) is located in Southern Malawi. Downscaling of Global Circulation Models (GCMs) that were used to force the integrated hydrologic models was done using the quantile mapping method. Six GCMs and a total of thirty-six climate scenarios and hydrological models under RCP4.5 and RCP8.5 were developed for the SRB while five GCMs and a total of thirty climate and hydrological models under RCP4.5 and RCP8.5 were developed for the RNC. In total, sixty-six models were developed for the two study areas encompassing climate change and variability analyses, surface-water modelling and groundwater recharge modelling. The methodology was found to be applicable in both temperate and semi-arid climates.

This thesis documents methods that can be used to model climate change impacts on groundwater resources using a multi-GCM and integrated hydrologic modelling approach using freely available data and tools within an Integrated

Water Resources Management (IWRM) framework. It is the hope of the author that these tools and methodologies will be adopted by the wider IWRM community in an effort to meet Sustainable Development Goal number 6 (SDG 6) by 2030. The contribution to research of this thesis can be viewed from four perspectives. Firstly, a novel method for GCM subset selection incorporating Symmetrical Uncertainty (SU), Probability Density Function (PDF) ranking and the Random Forest Algorithm was developed. Secondly, this is the first time such a model has been applied for future water resources quantification in both the RNC and SRB. Thirdly, this work has demonstrated that it is possible to do high quality predictive hydrological modelling that can be incorporated into climate adaptability planning using freely available remotely-sensed climate data. Fourthly, the methodology developed in this thesis provides a basis for a unified framework (i.e. software tools adopted in this work including related software) and methodology for integrated hydrologic modelling that can be applied in different climatic settings using freely available hydro-climatic data products.

# Table of contents

List of figures	xv
List of tables	xxviii
Nomenclature	xxxi
<b>1 Introduction</b>	<b>1</b>
1.1 Background . . . . .	2
1.2 Study Sites . . . . .	3
1.2.1 River Nith Catchment (RNC) . . . . .	3
1.2.2 Shire River Basin . . . . .	5
1.2.3 Rationale for Study Site Selection . . . . .	7
1.3 Research Aims and Objectives . . . . .	9
1.4 Significance of Research . . . . .	10
1.5 Organisation of Thesis . . . . .	10
<b>2 Background</b>	<b>13</b>
2.1 Climate Change – Key Aspects . . . . .	14

---

2.1.1	Climate Change, Variability and Global Warming . . . . .	14
2.1.2	Climate and Emission Scenarios . . . . .	15
2.1.3	The Hydrologic Cycle . . . . .	18
2.2	Uncertainty in Climate Impact Studies . . . . .	21
2.2.1	Uncertainty in Climate Input Data . . . . .	21
2.2.2	Uncertainty Due to Land-use Change and Classification . .	24
2.2.3	Uncertainty in the Conceptual Understanding . . . . .	27
2.3	GCM Downscaling and Bias Correction . . . . .	29
2.3.1	Statistical Downscaling . . . . .	29
2.3.2	Statistical Downscaling Methods and Models . . . . .	30
2.4	Water-Food-Energy-Climate Nexus . . . . .	35
2.5	Methods for Quantifying Groundwater/ Surface-water Interactions	39
2.5.1	Surface-water Models . . . . .	39
2.5.2	Groundwater Flow Modelling . . . . .	39
2.5.3	Limitations of Groundwater Flow Modelling . . . . .	41
2.5.4	Integrated Hydrologic Modelling . . . . .	44
2.6	Potential Groundwater Recharge Estimation . . . . .	46
2.7	Modelling Code Selection . . . . .	48
2.7.1	MODFLOW . . . . .	48
2.7.2	Soil and Water Assessment Tool (SWAT) . . . . .	51
2.7.3	SWAT-MODFLOW . . . . .	53
2.8	Model Calibration . . . . .	53
2.8.1	Quantifying Model Performance . . . . .	53
2.8.2	Groundwater Model Calibration . . . . .	55
2.8.3	Surface-water Model Calibration . . . . .	57



---

2.9	Water Governance . . . . .	58
2.10	Research Gap . . . . .	60
2.11	Summary . . . . .	61
<b>3</b>	<b>Materials and Methods</b>	<b>62</b>
3.1	Research Design . . . . .	63
3.1.1	Research Methodology . . . . .	63
3.1.2	Comparative Analysis Approach . . . . .	63
3.2	Data collection . . . . .	65
3.2.1	Meteorological Data . . . . .	65
3.2.2	Global Circulation Models . . . . .	66
3.2.3	Topographical Maps . . . . .	66
3.2.4	Land-use and Soil Maps . . . . .	66
3.2.5	Streamflow Data . . . . .	67
3.3	GCM Selection . . . . .	68
3.3.1	Symmetrical Uncertainty . . . . .	70
3.3.2	PDF-Based Ranking . . . . .	72
3.4	Statistical Downscaling . . . . .	73
3.5	Ensemble Climate Model . . . . .	74
3.6	Handling of Missing Data . . . . .	77
3.6.1	Commonly Used Infilling or Imputation Techniques . . . . .	78
3.6.2	Adopted Infilling Method . . . . .	80
3.7	Hydrologic Models Development . . . . .	81
3.7.1	MODFLOW . . . . .	81
3.7.2	SWAT . . . . .	82
3.7.3	SWAT-MODFLOW . . . . .	84

3.8	Metrics of a “Good Model” . . . . .	87
3.8.1	SWAT . . . . .	87
3.9	SWAT and MODFLOW Calibration . . . . .	90
3.9.1	Calibaration with SWAT-CUP . . . . .	90
3.9.2	Conceptual and Theoretical Basis of SUFI-2 . . . . .	91
3.9.3	MODFLOW Calibration . . . . .	94
3.9.4	Calibration Periods . . . . .	94
3.10	Statistical Tests . . . . .	96
3.11	Additional Software and Tools . . . . .	101
3.12	Chapter Summary . . . . .	101
<b>4</b>	<b>Climate modelling</b>	<b>103</b>
4.1	Introduction . . . . .	104
4.2	Missing Data . . . . .	104
4.3	Reanalysis Products Selection . . . . .	106
4.4	GCM Selection . . . . .	107
4.5	Downscaling GCM Outputs . . . . .	109
4.6	Performance and Uncertainty Evaluation . . . . .	110
4.7	Multi-GCM Ensemble . . . . .	114
4.8	RNC Baseline and Future Climate Assessment . . . . .	115
4.8.1	RNC Baseline Climate . . . . .	115
4.8.2	RNC Baseline Downscaling . . . . .	121
4.8.3	RNC Future Climate Results and Discussion . . . . .	122
4.9	SRB Baseline and Future Climate Assessment . . . . .	130
4.9.1	SRB Baseline Climate . . . . .	130
4.9.2	Historical Precipitation Downscaling and Bias Correction .	135

4.9.3	Historical Temperature Downscaling and Bias Correction .	136
4.9.4	Historical Wet/Dry Spell Lengths . . . . .	137
4.9.5	Future Climate Results and Discussion . . . . .	143
4.10	limitations . . . . .	149
4.11	Chapter Summary . . . . .	149
<b>5</b>	<b>Hydrological Modelling</b>	<b>152</b>
5.1	Introduction . . . . .	153
5.2	Description of the Study Sites . . . . .	153
5.3	RNC Hydrologic Modelling . . . . .	155
5.3.1	Model Setup . . . . .	155
5.3.2	Model calibration and validation . . . . .	158
5.3.3	Climate change impacts on streamflow - RNC . . . . .	161
5.3.4	Blue-Green Water Nexus . . . . .	175
5.3.5	RNC Modelling Summary . . . . .	199
5.4	SRB Hydrologic Modelling . . . . .	202
5.4.1	Model Setup . . . . .	202
5.4.2	Model calibration and validation . . . . .	205
5.4.3	Climate Change Impacts on Streamflow . . . . .	207
5.4.4	Blue-Green Water Nexus . . . . .	222
5.4.5	SRB Modelling Summary . . . . .	247
5.5	Chapter Summary . . . . .	251
<b>6</b>	<b>Integrated Hydrologic Modelling</b>	<b>254</b>
6.1	Purpose and Scope . . . . .	255
6.2	Data Requirements . . . . .	255

6.3	Dumfries Basin Groundwater Modelling . . . . .	256
6.3.1	Dumfries Basin Conceptual Model . . . . .	256
6.3.2	Model Development . . . . .	262
6.3.3	Description of the Coupling Process . . . . .	268
6.3.4	Baseline and Future Recharge Estimation . . . . .	269
6.3.5	RNC Groundwater Recharge Modelling Summary . . . . .	280
6.4	SRB Groundwater Modelling . . . . .	281
6.4.1	Conceptual Model . . . . .	281
6.4.2	Model Development . . . . .	284
6.4.3	Description of the Coupling Process . . . . .	289
6.4.4	Baseline Recharge Estimation . . . . .	289
6.4.5	Future Groundwater Recharge Estimation . . . . .	293
6.4.6	Impacts of Land-use/Land-cover . . . . .	308
6.4.7	SRB Groundwater Recharge Modelling Summary . . . . .	309
6.5	Limitations . . . . .	310
6.6	Chapter Summary . . . . .	311
<b>7</b>	<b>IRWM in Developing and Transition Countries</b>	<b>315</b>
7.1	Introduction . . . . .	316
7.2	Overview of IWRM Challenges in Developing Countries . . . . .	317
7.3	Technical and Institutional IWRM challenges in Malawi . . . . .	318
7.3.1	Capacity Building Needs . . . . .	318
7.3.2	Limited Availability of Ground Truth Data . . . . .	319
7.3.3	Policy Coherence Issues . . . . .	320
7.4	Way Forward . . . . .	322
7.4.1	Data Collection and Sharing . . . . .	322

---

7.4.2	Capacity Building in IWRM Sectors . . . . .	326
7.4.3	Robust Adaptation Strategies . . . . .	333
7.4.4	Multi-objective Optimization . . . . .	334
7.4.5	Policy formulation and Implementation . . . . .	338
7.5	Summary . . . . .	339
<b>8</b>	<b>Conclusions and Recommendations</b>	<b>341</b>
8.1	Summary of Findings . . . . .	342
8.2	Recommendations . . . . .	346
8.3	Limitations . . . . .	350
8.4	Research Contribution . . . . .	352
8.5	Considerations for Future Works . . . . .	353
	<b>References</b>	<b>355</b>
	<b>Appendix A Supplementary data</b>	<b>397</b>
	<b>Appendix B Supplementary climate data</b>	<b>399</b>
B.1	Shire Basin climate modelling . . . . .	403

# List of figures

1.1	Location of the River Nith Catchment . . . . .	4
1.2	Location of Shire River Basin . . . . .	6
2.1	History of CMIPs and their contributions to IPCC Assessment Reports (ARs) . . . . .	17
2.2	A depiction of the hydrologic cycle . . . . .	20
2.3	Impact of land use and climate variability on hydrological response as a function of scale . . . . .	24
2.4	The water, energy and food security nexus . . . . .	36
2.5	Risks interconnection map . . . . .	38
2.6	Schematic representation of recharge processes from infiltration to interaquifer flow . . . . .	46
3.1	Schematic summary of the methodology used in this research . . .	64
3.2	SWAT model operation flow-chart . . . . .	85
3.3	General overview of SWAT-MODFLOW . . . . .	87

3.4	Flowchart highlighting the major steps of calibrating a predictive groundwater model . . . . .	95
4.1	Biases of raw and corrected GCM outputs in the baseline period for Chileka . . . . .	112
4.2	Biases of raw and corrected GCM outputs in the baseline period for Mangochi . . . . .	113
4.3	Biases of raw and corrected GCM outputs in the baseline period for Ngabu . . . . .	114
4.4	Exploratory data analysis plots of daily precipitation . . . . .	117
4.5	Empirical autocorrelation plots for the baseline period at Dumfries	118
4.6	RNC future precipitation under RCP4.5 as calculated by the RNC-EGCMM . . . . .	124
4.7	RNC future precipitation under RCP8.5 as calculated by the RNC-EGCMM . . . . .	125
4.8	RNC future $T_{max}$ under RCP4.5 as calculated by the RNC-EGCMM	126
4.9	RNC future $T_{max}$ under RCP8.5 as calculated by the RNC-EGCMM	127
4.10	RNC future $T_{min}$ under RCP4.5 as calculated by the RNC-EGCMM	128
4.11	RNC future $T_{min}$ under RCP8.5 as calculated by the RNC-EGCMM	129
4.12	Rainfall variability in the SRB for the baseline period (1975-2005)	133
4.13	Box plots of mean monthly precipitation in the SRB . . . . .	134
4.14	Performance of bcc-csm1-1m downscaled precipitation in the SRB	139
4.15	Performance of HadGEM2-ES downscaled maximum temperature in the SRB . . . . .	140
4.16	Performance of HadGEM2-ES in predicting wet spell lengths in the SRB . . . . .	141

4.17	Performance of HadGEM2-ES in predicting dry spell lengths in the SRB . . . . .	142
4.18	Chileka future SRB-EGCMM results for rainfall, maximum and minimum temperatures . . . . .	145
4.19	Mangochi future SRB-EGCMM results for rainfall, maximum and minimum temperatures . . . . .	146
4.20	Ngabu future SRB-EGCMM results for rainfall, maximum and minimum temperatures . . . . .	147
5.1	Watershed layouts for the RNC and SRB . . . . .	154
5.2	SWAT model inputs for the SRB . . . . .	157
5.3	Global sensitivity analysis results for the RNC . . . . .	160
5.4	Graphs of river discharge calibration and validation for selected rivers in the RNC . . . . .	163
5.5	Projected future streamflow at Scar Water at Capenoch for the RCP4.5 Scenario . . . . .	169
5.6	Projected future streamflow at Scar Water at Capenoch for the RCP8.5 Scenario . . . . .	170
5.7	Projected future streamflow at Nith at Friars Carse for the RCP4.5 Scenario . . . . .	171
5.8	Projected future streamflow at Nith at Friars Carse for the RCP8.5 Scenario . . . . .	172
5.9	Projected future streamflow ensemble (SWAT forced with the RNC-EGCMM) in the RNC under RCP4.5 and RCP8.5 scenarios . . .	173



5.10	Projected future streamflow ensemble (SWAT model averaged results, otherwise referred to as RNC-SWATEMM) in the RNC under RCP4.5 and RCP8.5 scenarios . . . . .	174
5.11	Schematic illustration of blue and green water components as defined in this study . . . . .	178
5.12	Water balance components in the RNC for the baseline period . .	180
5.13	CCSM4 RCP4.5 water balance components in the RNC for the future projected period . . . . .	183
5.14	CCSM4 RCP8.5 water balance components in the RNC for the future projected period . . . . .	184
5.15	GFDL-ESM2G RCP4.5 water balance components in the RNC for the future projected period . . . . .	185
5.16	GFDL-ESM2G RCP8.5 water balance components in the RNC for the future projected period . . . . .	186
5.17	HadGEM2-ES RCP4.5 water balance components in the RNC for the future projected period . . . . .	187
5.18	HadGEM2-ES RCP8.5 water balance components in the RNC for the future projected period . . . . .	188
5.19	INMCM4 RCP4.5 water balance components in the RNC for the future projected period . . . . .	189
5.20	INMCM4 RCP8.5 water balance components in the RNC for the future projected period . . . . .	190
5.21	MPI-ESM-LR RCP4.5 water balance components in the RNC for the future projected period . . . . .	191

5.22 MPI-ESM-LR RCP8.5 water balance components in the RNC for the future projected period . . . . .	192
5.23 Ensemble mean (RNC-SWATEMM) RCP4.5 water balance compo- nents in the RNC for the future projected period . . . . .	195
5.24 Ensemble mean (RNC-SWATEMM) RCP8.5 water balance compo- nents in the RNC for the future projected period . . . . .	196
5.25 Ensemble mean (RNC-EGCMM) RCP4.5 water balance compo- nents in the RNC for the future projected period . . . . .	197
5.26 Ensemble mean (RNC-EGCMM) RCP8.5 water balance compo- nents in the RNC for the future projected period . . . . .	198
5.27 SWAT model inputs for the SRB . . . . .	204
5.28 Global sensitivity analysis results for the SRB . . . . .	207
5.29 Graphs of river discharge calibration and validation for selected rivers in the SRB . . . . .	210
5.30 Projected future streamflow at Lichenya for the RCP4.5 Scenario	214
5.31 Projected future streamflow at Lichenya for the RCP8.5 Scenario	215
5.32 Projected future streamflow at Rivirivi for the RCP4.5 Scenario .	216
5.33 Projected future streamflow at Rivirivi for the RCP8.5 Scenario .	217
5.34 Projected future streamflow at Ruo for the RCP4.5 Scenario . . .	218
5.35 Projected future streamflow at Ruo for the RCP8.5 Scenario . . .	219
5.36 Projected future streamflow at Lichenya, Ruo and Rivirivi using the simple arithmetic mean of SWAT models for the future RCP4.5 and RCP8.5 scenarios . . . . .	220

5.37	Projected future streamflow at Lichenya, Ruo and Rivirivi using SRB-EGCMM forced SWAT model simulations under RCP4.5 and RCP8.5 scenarios . . . . .	221
5.38	Water balance components in the SRB for the baseline period . .	224
5.39	BCC-CSM1-1-M RCP4.5 water balance components in the SRB for the future projected period . . . . .	227
5.40	BCC-CSM1-1-M RCP8.5 water balance components in the SRB for the future projected period . . . . .	228
5.41	CCSM4 RCP4.5 water balance components in the SRB for the future projected period . . . . .	229
5.42	CCSM4 RCP8.5 water balance components in the SRB for the future projected period . . . . .	230
5.43	CNRM-CM5 RCP4.5 water balance components in the SRB for the future projected period . . . . .	231
5.44	CNRM-CM5 RCP8.5 water balance components in the SRB for the future projected period . . . . .	232
5.45	GFDL-ESM2G RCP4.5 water balance components in the SRB for the future projected period . . . . .	233
5.46	GFDL-ESM2G RCP8.5 water balance components in the SRB for the future projected period . . . . .	234
5.47	HadGEM2-ES RCP4.5 water balance components in the SRB for the future projected period . . . . .	235
5.48	HadGEM2-ES RCP8.5 water balance components in the SRB for the future projected period . . . . .	236

5.49	MPI-ESM-LR RCP4.5 water balance components in the SRB for the future projected period . . . . .	237
5.50	MPI-ESM-LR RCP8.5 water balance components in the SRB for the future projected period . . . . .	238
5.51	Ensemble mean (SRB-SWATEMM) RCP4.5 water balance compo- nents in the SRB for the future projected period . . . . .	241
5.52	Ensemble mean (SRB-SWATEMM) RCP8.5 water balance compo- nents in the SRB for the future projected period . . . . .	242
5.53	Ensemble mean (SRB-EGCMM) RCP4.5 water balance components in the SRB for the future projected period . . . . .	245
5.54	Ensemble mean (SRB-EGCMM) RCP8.5 water balance components in the SRB for the future projected period . . . . .	246
6.1	Permian Geology of the Dumfries Basin . . . . .	257
6.2	Quaternary geology of the Dumfries Basin . . . . .	259
6.3	Cross-section showing deposits in Dumfries . . . . .	261
6.4	Schematic conceptual flow model of the Dumfries Basin aquifer . .	263
6.5	Average baseline daily recharge (mm/day) provided by SWAT to each MODFLOW Grid Cell . . . . .	270
6.6	Percentage differences in groundwater recharge (GWRch) between the baseline period and future periods for the Dumfries Basin as simulated by CCSM4 . . . . .	271
6.7	Percentage differences in groundwater recharge (GWRch) between the baseline period and future periods for the Dumfries Basin as simulated by GFDL-ESM2G . . . . .	272

6.8	Percentage differences in groundwater recharge (GWRch) between the baseline period and future periods for the Dumfries Basin as simulated by HadGEM2-ES . . . . .	273
6.9	Percentage differences in groundwater recharge (GWRch) between the baseline period and future periods for the Dumfries Basin as simulated by INMCM4 . . . . .	274
6.10	Percentage differences in groundwater recharge (GWRch) between the baseline period and future periods for the Dumfries Basin as simulated by MPI-ESM-LR . . . . .	275
6.11	Percentage differences in groundwater recharge (GWRch) as simulated by SWAT-MODFLOW between the baseline period and future periods for the Dumfries Basin . . . . .	278
6.12	Percentage differences in groundwater recharge (GWRch) as simulated by SWAT-MODFLOW between the baseline period and future periods in the SRB . . . . .	279
6.13	Geology of the SRB . . . . .	283
6.14	Long term daily average recharge for the rainy season in the SRB for the baseline period . . . . .	291
6.15	Average Cell-by-Cell Groundwater Hydraulic Head in the SRB for the baseline period . . . . .	292
6.16	Percentage differences in groundwater recharge (GWRch) as simulated by SWAT-MODFLOW between the baseline period and future periods in the SRB – BCC-CSM1-1-M . . . . .	296

6.17	Percentage differences in groundwater recharge (GWRch) as simulated by SWAT-MODFLOW between the baseline period and future periods in the SRB – CCSM4 . . . . .	297
6.18	Percentage differences in groundwater recharge (GWRch) as simulated by SWAT-MODFLOW between the baseline period and future periods in the SRB – CNRM-CM5 . . . . .	298
6.19	Percentage differences in groundwater recharge (GWRch) as simulated by SWAT-MODFLOW between the baseline period and future periods in the SRB – GFDL-ESM2G . . . . .	299
6.20	Percentage differences in groundwater recharge (GWRch) as simulated by SWAT-MODFLOW between the baseline period and future periods in the SRB – HadGEM2-ES . . . . .	300
6.21	Percentage differences in groundwater recharge (GWRch) as simulated by SWAT-MODFLOW between the baseline period and future periods in the SRB – MPI-ESM-LR . . . . .	301
6.22	Percentage differences in groundwater recharge (GWRch) as simulated by SWAT-MODFLOW between the baseline period and future periods in the SRB – SRB-SWATMFEMM . . . . .	305
6.23	Percentage differences in groundwater recharge (GWRch) as simulated by SWAT-MODFLOW between the baseline period and future periods in the SRB – SRB-EGCMM . . . . .	306
6.24	Managed Aquifer Recharge options that can be adopted by water management agencies . . . . .	307
7.1	Water points in Southern Malawi mapped by the CJF between 2011 – 2018 . . . . .	324

7.2	Figure depicting uncertainty levels and how they evolve . . . . .	335
7.3	Components of a proposed Decision Support System for IWRM in Malawi . . . . .	336
B.1	GCMs' ability to simulate precipitation for the baseline period (1981–2005) in the River Nith Catchment after bias correction. . .	400
B.2	GCMs' ability to simulate summer maximum temperature for the baseline period (1981–2005) in the River Nith Catchment after bias correction. . . . .	401
B.3	GCMs' ability to simulate summer minimum temperature for the baseline period (1981–2005) in the River Nith Catchment after bias correction. . . . .	402
B.4	Performance of CCSM4 downscaled precipitation in the SRB . . .	403
B.5	Performance of CNRM-CM5 downscaled precipitation in the SRB	404
B.6	Performance of GFDL-ESM2G downscaled precipitation in the SRB	405
B.7	Performance of HadGEM2-ES downscaled precipitation in the SRB	406
B.8	Performance of MPI-ESM-LR downscaled precipitation in the SRB	407
B.9	Performance of bcc-csm1-1m downscaled maximum temperature in the SRB . . . . .	408
B.10	Performance of CCSM4 downscaled precipitation in the SRB . . .	409
B.11	Performance of CNRM-CM5 downscaled maximum temperature in the SRB . . . . .	410
B.12	Performance of GFDL-ESM2G downscaled maximum temperature in the SRB . . . . .	411
B.13	Performance of MPI-ESM-LR downscaled maximum temperature in the SRB . . . . .	412

B.14 Performance of bcc-csm1-1m downscaled minimum temperature in the SRB . . . . .	413
B.15 Performance of CCSM4 downscaled minimum temperature in the SRB . . . . .	414
B.16 Performance of CNRM-CM5 downscaled minimum temperature in the SRB . . . . .	415
B.17 Performance of GFDL-ESM2G downscaled minimum temperature in the SRB . . . . .	416
B.18 Performance of HadGEM2-ES downscaled minimum temperature in the SRB . . . . .	417
B.19 Performance of MPI-ESM-LR downscaled minimum temperature in the SRB . . . . .	418
B.20 Performance of bcc-csm1-1-1m in predicting wet spell lengths in the SRB . . . . .	419
B.21 Performance of CCSM4 in predicting wet spell lengths in the SRB	420
B.22 Performance of CNRM-CM5 in predicting wet spell lengths in the SRB . . . . .	421
B.23 Performance of GFDL-ESM2G in predicting wet spell lengths in the SRB . . . . .	422
B.24 Performance of MPI-ESM-LR in predicting wet spell lengths in the SRB . . . . .	423
B.25 Performance of bcc-csm1-1-1m in predicting dry spell lengths in the SRB . . . . .	424
B.26 Performance of CCSM4 in predicting dry spell lengths in the SRB	425



B.27 Performance of CNRM-CM5 in predicting dry spell lengths in the SRB . . . . .	426
B.28 Performance of GFDL-ESM2G in predicting dry spell lengths in the SRB . . . . .	427
B.29 Performance of MPI-ESM-LR in predicting dry spell lengths in the SRB . . . . .	428
B.30 bcc-csm1-1-1-m seasonal and annual future projections for rainfall in the SRB. . . . .	429
B.31 CCSM4 seasonal and annual future projections for rainfall in the SRB. . . . .	430
B.32 CNRM-CM5 seasonal and annual future projections for rainfall in the SRB. . . . .	431
B.33 GFDL-ESM2G seasonal and annual future projections for rainfall in the SRB. . . . .	432
B.34 HadGEM2-ES seasonal and annual future projections for rainfall in the SRB. . . . .	433
B.35 MPI-ESM-LR seasonal and annual future projections for rainfall in the SRB. . . . .	434
B.36 bcc-csm1-1-1-m future projections for maximum temperature in degree Celsius. Shaded region represents baseline period (1975–2005)	435
B.37 CCSM4 future projections for maximum temperature in degree Celsius. Shaded region represents baseline period (1975–2005) . .	436
B.38 CNRM-CM5 future projections for maximum temperature in degree Celsius. Shaded region represents baseline period (1975–2005) . .	437

- B.39 GFDL-ESM2G future projections for maximum temperature in degree Celsius. Shaded region represents baseline period (1975–2005) 438
- B.40 hadGEM2-ES future projections for maximum temperature in degree Celsius. Shaded region represents baseline period (1975–2005) 439
- B.41 MPI-ESM-LR future projections for maximum temperature in degree Celsius. Shaded region represents baseline period (1975–2005) 440
- B.42 bcc-csm1-1-m future projections for minimum temperature in degree Celsius. Shaded region represents baseline period (1975–2005) . . 441
- B.43 CCSM4 future projections for minimum temperature in degree Celsius. Shaded region represents baseline period (1975–2005) . . 442
- B.44 CNRM-CM5 future projections for minimum temperature in degree Celsius. Shaded region represents baseline period (1975–2005) . . 443
- B.45 GFDL-ESM2G future projections for minimum temperature in degree Celsius. Shaded region represents baseline period (1975–2005) 444
- B.46 hadGEM2-ES future projections for minimum temperature in degree Celsius. Shaded region represents baseline period (1975–2005) 445
- B.47 MPI-ESM-LR future projections for minimum temperature in degree Celsius. Shaded region represents baseline period (1975–2005) 446

## List of tables

1.1	Summary description of study sites . . . . .	8
2.1	History of prominent sets of emissions scenarios . . . . .	16
2.2	Overview of representative concentration pathways (RCPs) . . . .	18
2.3	Summary of conceptual model errors encountered in groundwater and environmental modelling . . . . .	27
3.1	UKBN2 rivers in the RNC suitable for hydrological trend analyses	67
3.2	Performance of the infilling technique adopted in this study . . . .	81
3.3	SWAT and MODFLOW calibration periods for the RNC and SRB	96
4.1	Percentage of missing data for the baseline period in the SRB . .	105
4.2	Selected GCMs for the SRB and RNC climate downscaling . . . .	108
4.3	Selected stations for bias correction method verification . . . . .	111
4.4	Results of Mann–Kendall, Pre-Whitened Mann-Kendall and Sen’s slope estimator statistical tests for Dumfries station conducted on monthly and seasonal time scales . . . . .	120
4.5	Selected meteorological stations in the SRB . . . . .	130

5.1	Distribution of LU/LC classes in the River Nith Catchment . . .	156
5.2	Distribution of Soil classes in the River Nith Catchment . . . . .	158
5.3	Description of SWAT parameters used in the RNC calibration process	162
5.4	Calibrated parameter values with their range for the RNC arranged according to their sensitivity in decreasing order . . . . .	164
5.5	Summary of RNC future streamflow changes with respect to the baseline period . . . . .	200
5.6	Summary areal mean change of projected future water balance components in the RNC with respect to the baseline period . . .	201
5.7	Distribution of LU/LC classes in the Shire River Basin . . . . .	205
5.8	Distribution of Soil classes in the Shire River Basin . . . . .	206
5.9	Description of SWAT parameters used in the SRB calibration process	208
5.10	Calibrated parameter values with their range for the SRB arranged according to their sensitivity in decreasing order . . . . .	209
5.11	Summary of SRB projected future streamflow changes with respect to the baseline period . . . . .	248
5.12	Summary areal mean change of projected future water balance components in the SRB with respect to the baseline period . . .	250
6.1	Goodness-of-fit statistics used to compare the performance of SWAT and SWAT-MODFLOW (SWAT-MF) in simulating monthly stream- flow in the RNC . . . . .	267
6.2	Summary areal mean percentage change in projected groundwater recharge (GWRch) in the RNC with respect to the baseline period	281

---

6.3	Goodness-of-fit statistics used to compare the performance of SWAT and SWAT-MODFLOW (SWAT-MF) in simulating monthly stream-flow in the SRB. . . . .	288
6.4	Summary areal mean percentage change in projected groundwater recharge (GWRch) in the SRB with respect to the baseline period	309
7.1	Applications of multi-objective optimization techniques in water resources management . . . . .	337
A.1	Main characteristics of each RCP after van Vuuren et al. (2011) .	398

# Nomenclature

## Greek Symbols

$\Sigma$	Summation
$\sigma$	Standard Deviation

## Acronyms / Abbreviations

95PPU	95 Percent Prediction Uncertainty
AMALGAM	A Multi-algorithm Genetically Adaptive Multi-Objective Method
ANN	Artificial Neural Network
AOGCM	Atmospheric and Oceanic General Circulation Model
ARIMA	AutoRegressive Integrated Moving Average
BCM	Bias Correction Method
BCSD	Bias Correction and Spatial Downscaling
BFI	Baseflow Index

---

BMLFP	Bi-Level Multi-Objective Linear Fractional Programming
BP	Bi-level Programming
BW	Blue Water
BWF	Blue Water Flow
CCP	Chance-Constrained Programming
CDF	Cumulative Distribution Function
CEDA	Centre for Environmental Data Analysis
CFSR	Climate Forecast System Reanalysis
CJF	Climate Justice Fund
CMIP5	Coupled Model Intercomparison Project Phase 5
CRS	Coordinate Reference System
CRU	Climatic Research Unit
CV	Coefficient of Variation
DB	Dumfries Basin
DDM	Data-Driven Model
DEM	Digital Elevation Model
DEM	Digital Elevation Model
DHRU	Disaggregated Hydrologic Response Unit

---

DJF	December, January, February
DSS	Decision Support System
DTR	Diurnal Temperature Range
ECDF	Empirical Cumulative Distribution Function
ESD	Empirical Statistical Downscaling
ET	Evapotranspiration
FAO	Food and Agriculture Organization
FB	Fractured Basement
FOSS	Free and open-source software
GBSO	Gini-coefficient Based Stochastic Optimization
GCM	General Circulation Model
GDP	Gross Domestic Product
GHG	Greenhouse gas
GHGES	Greenhouse Gases Emissions Scenarios
GIS	Geographic Information System
GLCC	Global Land Cover Characterization
GoM	Government of Malawi
GoM	Government of Malawi



---

GRDC	Global Runoff Data Centre
GRT	Groundwater Response Time
GSFLOW	Groundwater and Surface-water FLOW
GUI	Graphical User Interface
GW	Green Water
GWF	Green Water Flow
GWP	Global Water Partnership
GWRch	Groundwater Recharge
GWS	Green Water Storage
GW/SW	Groundwater/Surface-water
HK	Horizontal Hydraulic Conductivity
HPC	High-Performance Computing
HRU	Hydrologic Response Unit
HSPF	Hydrological Simulation Program Fortran
IAM	Integrated Assessment Model
IFMONLP	Intuitionistic Fuzzy Multi-Objective Non-Linear Programming
IHM	Integrated Hydrologic Model
IPCC	Intergovernmental Panel on Climate Change

---

ITCZ	Inter Tropical Convergence Zone
JICA	Japan International Cooperation Agency
JJA	June, July, August
LAI	Leaf Area Index
LFP	Linear Fractional Programming
LSV	Lower Shire Valley
LU/LC	Landuse/Landcover
M95PPU	Average or 50% Percent Prediction Uncertainty
MAM	March, April, May
MAR	Managed Aquifer Recharge
MIS	Management Information System
MLBMA	Maximum Likelihood Bayesian Model Averaging
MME	Multi-model Ensemble
MMS	Malawi Meteorological Services
MoAIWD	Ministry of Agriculture, Irrigation and Water Development
MOO	Multi-Objective Optimization
MOOC	Massive Open Online Course
MOP	Multi-Objective Programming

---

MORDM	Many Objective Robust Decision Making
NFC	Nith at Friars Carse
NGO	Non-Governmental Organisation
NLPCA	Non-linear Principal Component Analysis
NRFA	National River Flow Archive
NSE	Nash-Sutcliffe Efficiency
NSGA	Non-dominated Sorting Genetic Algorithm
NWRA	National Water Resources Authority
PDF	Probability Density Function
PEST	Parameter Estimation Tool
PRMS	Precipitation Runoff Modeling System
QA	Quaternary Alluvial
QM	Quantile Mapping
RAM	Random-Access Memory
RCP	Representative Concentration Pathway
RF	Random Forest
RNC	River Nith Catchment
RNC-EGCMM	River Nith Catchment Ensemble GCM Mean

RNC-SWATEMM River Nith Catchment SWAT Ensemble Model Mean

RNC-SWATMFEMM River Nith Catchment SWAT-MODFLOW Ensemble Model  
Mean

SC Storage Coefficient

SDGs Sustainable Development Goals

SDSM Statistical DownScaling Model

SOM Self-Organizing Map

SON September, October, November

SPEA2 Strength Pareto Evolutionary Algorithm 2

SRB Shire River Basin

SRB-EGCMM Shire River Basin Ensemble GCM Mean

SRB-SWATEMM Shire River Basin SWAT Ensemble Model Mean

SRB-SWATMFEMM Shire River Basin SWAT-MODFLOW Ensemble Model  
Mean

SRES Special Report on Emission Scenarios

SRTM Shuttle Radar Topography Mission

SSP Shared Socio-economic Pathways

SU Symmetrical Uncertainty

SUFI Sequential Uncertainty Fitting

---

SVM	Support Vector Machine
SWAT	Soil & Water Assessment Tool
SWAT-CUP	SWAT Calibration Uncertainties Program
SWC	Scar Water at Capenoch
SY	Specific Yield
UK	United Kingdom
UKBN2	United Kingdom Benchmark Network 2
UNESCO	United Nations Educational, Scientific and Cultural Organization
UNFCCC	United Nations Framework Convention on Climate Change
USGS	United States Geological Survey
VK	Vertical Hydraulic Conductivity
WASH	Water, Sanitation and Hygiene
WB	Weathered Basement
WEAP	Water Evaluation And Planning system
WEF	Water-Energy-Food
WFP	Water Futures Programme
WMA	Water Monitoring Assistant

—The greatest challenge to any  
thinker is stating the problem in  
a way that will allow a solution.

Bertrand Russell

# 1

## Introduction

*This chapter provides a brief discussion on the background, context and motivation of the work presented in this thesis. Section 1.1 provides a short background to the study in terms of the challenges associated with anthropogenic climate change and its impact on water resources. Section 1.2 introduces the study sites that were selected in this thesis and also discusses the rationale behind the choice of the same. Section 1.3 provides the aims and objectives of this study. Section 1.4 is a statement on the significance of this research and lastly, Section 1.5 provides a brief description of the structure of this thesis.*

## 1.1 Background

Changes in the hydro-climatic and socio-economic landscapes has led many researchers and policy makers worldwide to conclude that there is a sustained and increasing pressure on freshwater resources (Veldkamp et al., 2016). In particular, an ever increasing global population, adoption and expansion of irrigated agriculture, higher demands for freshwater due to changing lifestyles and a changing climate has aggravated water scarcity both at regional and global levels (Mekonnen and Hoekstra, 2016; Veldkamp et al., 2016). It is estimated that approximately 4 billion people globally experience severe water scarcity at least 1 month of the year (Mekonnen and Hoekstra, 2016) and that generally, about half of the world's population will be living in water-stressed areas by 2025 (WHO, 2017).

Climate change impacts on the hydrologic cycle is an interesting and active area of research riddled with a lot of uncertainty. However, there has been significant efforts made by different organisations and research groups to understand and reduce the uncertainty associated with climate change impacts on future hydrological cycles. For instance, many research groups have successfully employed the multimodel ensemble approaches as a way of reducing uncertainty when investigating climate change impacts on water resources (e.g. Allen and Ingram, 2002; Christensen and Lettenmaier, 2007; Tebaldi et al., 2004; Tebaldi and Sanso, 2009; Tebaldi et al., 2005). Thus, more skilful and reliable climate predictions are increasingly being generated and incorporated into future hydrological impact studies worldwide.

While a lot of climate change impacts research has been done with respect to discrete aspects of the hydrological cycle (i.e., atmospheric processes, surface water,

groundwater etc.), most of the research has focussed on impacts and management of surface-water systems. Few studies have investigated the potential effects of climate change on subsurface resources and fewer still have studied in detail all aspects of the hydrological cycle as a single system composed of multiple processes and subsystems that interact with each other. Groundwater is an important fresh water resource globally estimated to be the main source of potable water for more than 1.5 billion of the Earth's population (Healy, 2010). Approximately 98% of the world's fresh water reserves are stored underground and thus groundwater is an important buffer against surface-water shortfalls in drought years (Margat and VanDerGun, 2013). Although, it is true that there has been an accelerated interest in understanding groundwater response to climate change in the last decade, there is need for multi-disciplinary efforts aimed at improving our understanding of climate change on surface- and groundwater as an integrated unit and the resulting feedback on other processes of the hydrological cycle. Moreover, from an adaptation to global change perspective, it is only prudent that potential future climate impacts on water resources be studied from a holistic perspective that aims to understand all aspects of the hydrological cycle (Green et al., 2011a).

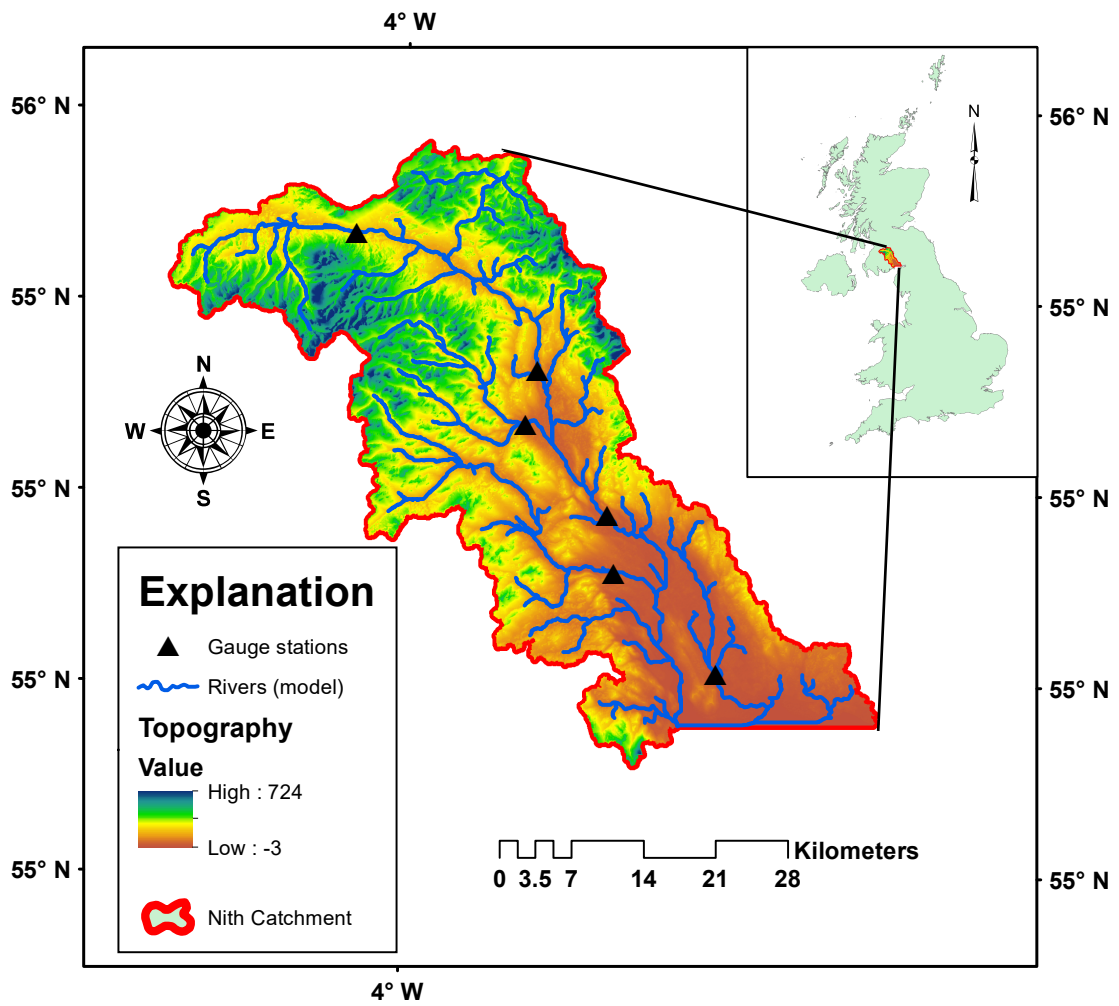
## 1.2 Study Sites

### 1.2.1 River Nith Catchment (RNC)

The River Nith Catchment (RNC) derives its name from the River Nith which is the largest river in south-west Scotland, United Kingdom (UK) (see Figure 1.1). The catchment covers an area of approximately 1450 km<sup>2</sup>.

The River Nith begins lies in the hills of East Ayrshire and discharges into





**Figure 1.1** Location of the River Nith Catchment

the Solway Firth at Airs point. The RNC extends east to the Lowther Hills and south to the Solway Firth (CBEC, Mott MacDonald, Walking-the-Talk, 2013). The RNC is drained by the River Nith and its tributaries. Historical Baseflow indices (BFIs) of the Nith and its tributaries ranges from 0.38 to 0.53. Mean annual rainfall in the RNC is approximately 1429 mm but varies spatially within the catchment – the north receiving more rainfall than the south.

Because of the integrated modelling approach adopted in this thesis, climate and surface-water modelling was done for the entire RNC while groundwater

modelling focussed only on the Dumfries Basin (DB) aquifer, a subarea of the RNC. The DB is located in the lower portion of the RNC and is one of the most productive aquifers in Scotland (MacDonald et al., 2005).

### 1.2.2 Shire River Basin

The Shire River Basin is located south of Malawi and is drained by the Shire River, Malawi's largest river. The Shire River is the only outlet of Lake Malawi and flows for about 520 km south of Malawi before it merges with the Zambezi River in Mozambique. The SRB is part of the larger Zambezi River Basin. Strictly speaking, the "Shire River Basin" refers to the hydrological basin that is south of Lake Malawi and also *within* Malawi (more of a planning unit than a hydrological basin). In this thesis however, SRB is used in the context of a hydrological trans-boundary basin as shown in Figure 1.2. The SRB covers approximately 16% of Malawi in area.

Malawi's water resource includes natural lakes, perennial and seasonal rivers, groundwater aquifers, several small- to medium-size reservoirs and a few large multi-purpose reservoirs (Chidammodzi and Muhandiki, 2017). In the SRB, the Shire River is the largest River which is a source of domestic and industrial water. It is divided into three stages namely; the Upper, Middle and Lower Shire. The Upper Shire sits at about 470 metres above sea level (masl) where it flows through Lake Malombe and through the Kamuzu Barrage at Liwonde. The Middle Shire begins from Liwonde where it drops seven metres in 50 km as it flows across a broad plain before steeply dropping 360 m over a distance of 70 km (MoAIWD, 2017). Thus this portion of the river is ideal for hydropower generation due to availability of head.

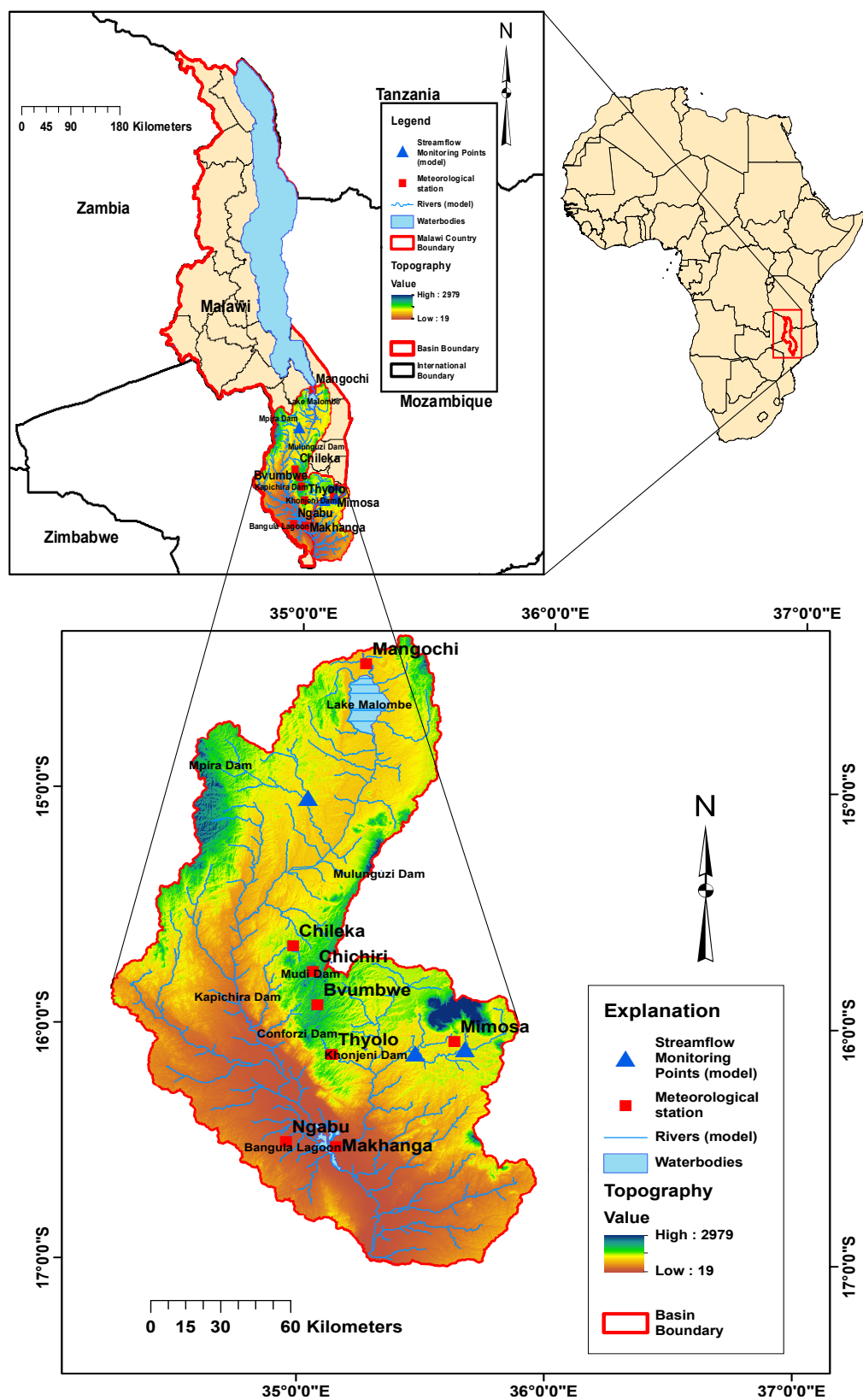


Figure 1.2 Location of Shire River Basin

The Lower Shire emanates from Kapichira falls where it flows through a floodplain and a wetland called the Elephant Marsh. It is in this region where a lot of settlements can be found which rely on the river for traditional and commercial agriculture among other needs (MoAIWD, 2017). Baseflow indices at selected gauges in the SRB range from 0.90 to 0.97 (Shire River gauges) and 0.19 to 0.64 (tributaries of the Shire River) according to Kelly et al. (2019).

### 1.2.3 Rationale for Study Site Selection

Two sites from two continents were selected as study sites in this thesis (see Table 1.1). The main reason for this is so that a comparative study can be undertaken between a data-rich region (River Nith Catchment) and a data-scarce region (Shire River Basin). In particular, we endeavoured to establish the efficacy of methods developed and tested in data-rich regions when applied to data-scarce regions. Additionally, the two study sites have completely different climate types so it would be interesting to test whether the methodology developed here is suitable for different climatic settings. Thus, in as far as analyses and application of developed methodologies in this thesis are concerned, except in limited cases, it was determined to maintain uniformity between the two regions.

The DB aquifer is one of the most productive aquifers in Scotland which provides domestic and industrial water needs of Dumfries town. The aquifer has been studied extensively in the last few decades but, to the best of our knowledge, few studies have been done to investigate surface-water and groundwater recharge and availability under climate change in this region.

Due to an increasing population in the SRB (estimated at 22% of Malawi's population), pressure on freshwater resources is increasing. Climate change coupled

**Table 1.1** Summary description of study sites

Description	Catchment	
	SRB (Malawi)	RNC (UK)
Area (km <sup>2</sup> )	28076.18	1450.49
Type of Climate	Warm Subtropical	Temperate Maritime
Annual Rainfall (mm)	1133	1429
Average Temperature	24 °C	9 °C
Dorminant Landcover	Savanna (47.2% of basin)	Dryland cropland and pasture (91.6% of catchment)
Population	4,500,000	64,000

with competing demands for water for domestic, agricultural, industrial and power generation threatens the security of water resources in the SRB. These threats are recognized by the Government of Malawi (GoM) as highlighted in “The Malawi Growth and Development Strategy (MGDS III)” which is the fourth medium-term national development strategy formulated to contribute to the attainment of Malawi’s long-term development aspirations as enshrined in the Vision 2020 and will be implemented from 2017 to 2022 (Government of Malawi, 2017). Thus there is a call for the promotion of research, technology development and transfer in climate change and meteorology in order to improve climate change management in the country.

Lessons drawn from research efforts in the RNC, which is a First World and data-rich region, can be used to inform similar research efforts in the SRB. This, in addition to insights gained from testing the applicability of these methods in different climate settings, is the motivation for this work.

## 1.3 Research Aims and Objectives

The main aim of this thesis is to investigate future availability of freshwater resources in the RNC and SRB using a holistic approach. This entails thorough analyses of different components of the hydrologic cycle. Another important aspect, which can be considered to be a sub-aim, is the use of free and/or open source software (FOSS) in this research as a way of promoting openness, shareability and reproducibility of results. Additionally, researchers from developing countries find it uneconomical to obtain licenses for commercial and proprietary software thus limiting the types of research they can do. FOSS curtails some of the limitations associated with acquiring expensive proprietary licenses for research purposes. The main aim will be accomplished through the following specific objectives:

- (1) Downscaling of twenty-nine Couple Model Intercomparison Project Phase 5 (CMIP5) Global Circulation Models (GCMs) to local watershed scales for the RNC and SRB.
- (2) Selection of a subset of GCMs to be used for forcing hydrologic models in the RNC and SRB. A methodology of combining the GCM subset to form ensemble climate models will also be explored.
- (3) Development of SWAT hydrologic models for the study areas to investigate future streamflow, blue and green water availability up to the end of the 21<sup>st</sup> century.
- (4) Development of MODFLOW models to simulate groundwater recharge including surface-water/groundwater interactions. In order to simulate the hydrologic cycle as an integrated system with respect to climate change, the SWAT model which simulates land-atmosphere interactions will be

coupled to MODFLOW-NWT, a model capable of simulating subsurface processes such as groundwater recharge, vadose zone percolation via the UZF1 package, river-aquifer interactions and evapotranspiration among many other uses (Bailey et al., 2016).

- (5) Assessment of whether the methodology developed in this research is applicable in different climate and development settings i.e. temperate versus semi-arid climate and data-rich RNC versus data sparse SRB.

## 1.4 Significance of Research

Understanding the impacts of climate change on water resources requires a holistic assessment of surface- and groundwater resources and their interactions. In this thesis, a methodology that quantifies future surface- and groundwater availability has been presented. A method aimed at downscaling GCMs from regional to local watershed scales is discussed along with a comprehensive methodology for the selection of a subset of GCMs from the many models provided by different research institutions. Furthermore, for the first time in the study areas, integrated hydrologic models aimed at understanding land-atmosphere interactions have been developed. Results arising from this research will inform parallel and future research efforts and also feed into climate change adaptation planning especially in the SRB.

## 1.5 Organisation of Thesis

This thesis is composed of eight chapters. A short description of the chapters is given in this section.

**Chapter 1:** Chapter one is a short introduction of the study areas and also provides a brief description of the problem and motivation of the thesis.

**Chapter 2:** Chapter 2 is a detailed background and literature review of climate change and its impact on water resources. Furthermore, a detailed analysis of the tools and methods that have previously been employed to simulate climate change, surface hydrology and groundwater hydrology are discussed.

**Chapter 3:** In chapter 3, a detailed discussion of the methods employed in this thesis is presented. The methods and tools discussed in this chapter are related to climate change assessments, surface water hydrology, groundwater hydrology and integrated hydrologic modelling. Details of the General Circulation Models selected and for modelling climate change in the two study areas are also presented.

**Chapter 4:** Chapter 4 presents climate change modelling efforts and results for the River Nith Catchment and Shire River Basin using a multi-GCM approach.

**Chapter 5:** Chapter 5 discusses the development and application of hydrological models for the RNC and SRB. Impacts of future climate change on streamflow of selected rivers are presented and discussed. Furthermore, future climate change impacts in the context of the Blue-Green Water Nexus are presented and discussed as well.

**Chapter 6:** Chapter 6 discusses the development of groundwater models aimed at understanding the impact of climate on groundwater resources. Additionally, development and application of integrated hydrologic models in the context of future climate change impacts is presented.



**Chapter 7:** Chapter 7 discusses challenges in the implementation of IWRM solutions and principles in Malawi in light of the findings and recommendations of Chapters 4 to 6.

**Chapter 8:** Chapter 8 is a summary and synthesis of the research findings in this thesis.

—We live on an island surrounded  
by a sea of ignorance. As our is-  
land of knowledge grows, so does  
the shore of our ignorance.

John Archibald Wheeler

# 2

## Background

*This chapter provides a detailed review of the state of the art in anthropogenic climate change and associated impact on water resources availability. A review of the analytical tools used in climate, surface- and groundwater modelling is also presented.*

## 2.1 Climate Change – Key Aspects

### 2.1.1 Climate Change, Variability and Global Warming

Climate change encompasses natural processes and anthropogenic changes in the composition of the atmosphere or on land. These changes or variations have to be statistically significant with respect to the mean state of the climate or “*average weather*” over an extended period of time, ideally decades or longer (IPCC, 2001). In 1992, the United Nations Framework Convention on Climate Change (UNFCCC) made a distinction between climate change and climate variability by attributing the former to human or anthropogenic activities and the latter to natural causes (UNFCCC, 1992).

Global warming, on the other hand, is the increase in the average terrestrial temperature as a result of the build-up of greenhouse gases (GHGs). Greenhouse gases’ (carbon dioxide, methane, nitrous oxide, ozone and water vapour) concentrations have been measured for decades and historical concentrations reconstructed for the last hundreds of thousands of years (Keeling et al., 1976; Thoning et al., 1989). These are responsible for the dramatic changes in the climate and the hydrologic cycle. Of all the greenhouse gases, atmospheric  $CO_2$  concentration is the primary indicator of climate change. According to Petit et al. (1999), current levels of  $CO_2$  and  $CH_4$  are unprecedented during the past 420,000 years. In essence, going by the aforementioned definition of climate change, global warming is just one aspect of climate change (USGS, 2018).

### 2.1.2 Climate and Emission Scenarios

Socio-economic and emission scenarios are tools used to understand the complex interactions of the global climate system, ecosystems and how much humans could contribute to future climate change. More precisely, emission scenarios provide descriptions of potential future discharges of substances that can alter the Earth's radiation balance such as GHGs and aerosols; including information on related biophysical processes such as land-use and land-cover. Climate scenarios, on the other hand, are representations of plausible future climate conditions (i.e., rainfall, temperature, etc.) (Moss et al., 2010). Other types of scenarios include *environmental* and *vulnerability* scenarios. In this research, the term “scenarios” is used as a generic term encompassing all forms of scenarios as applied in climate science.

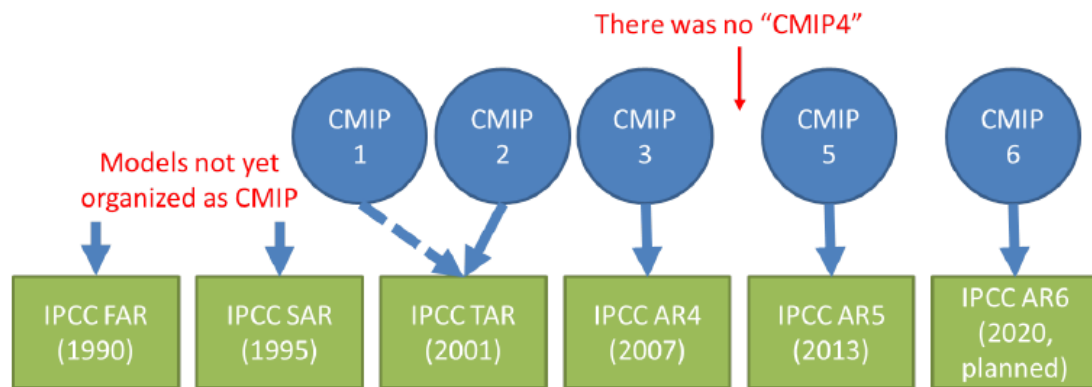
In the context of climate change research, scenarios are not necessarily used to predict the future but to explore and evaluate the uncertainty about human contributions to climate change and the implications of different plausible futures (Bjørnæs, 2013; Moss et al., 2010). Scenarios are used as input for climate models runs and provide a basis on which possible climate impacts, mitigation strategies and costs can be assessed (van Vuuren et al., 2011). Climate models or General Circulation Models (GCMs) can be defined as computer methods and tools that describe the physical processes of the climate system. Using mathematical equations, these models are capable of simulating the transfer of energy and materials in the atmosphere and thus describe atmospheric processes such as the frequency of monsoons and El Niño events. Table 2.1 provides an overview of the history of emission scenarios.

**Table 2.1** History of prominent sets of emissions scenarios after Bjørnæs (2013)

Year	Name	Used in
1990	SA90	First Assessment Report
1992	IS92	Second Assessment Report
2000	SRES - Special Report on Emissions and Scenarios	Third and Fourth Assessment Reports
2009	RCP - Representative Concentration Pathways	Fifth Assessment Report

Historically, a variety of scenarios have been used by climate and water researchers to understand and model climate change impacts on water resources. The climate scenarios are varied with respect to their philosophical underpinnings and assumptions ranging from stylized emission trajectories (i.e., annual percentage increases in global average GHGs) to advanced representations of emissions and socio-economic factors that influence greenhouse gas emissions (Bjørnæs, 2013; Van Vuuren and O'Neill, 2006). Scenarios are derived from information produced by integrated assessment models (IAMs). By combining key elements of biophysical and economic systems, IAMs can depict how increased discharges of GHGs in the atmosphere can affect temperature and thus economic dynamics.

Figure 2.1 depicts the history of Coupled Model Intercomparison Project (CMIP) models that have contributed to the IPCC assessment reports. In preparation for the Fifth Assessment Report (AR5), a new approach for developing and selecting scenarios in climate change research was developed (Bjørnæs, 2013). This change stemmed from the need to have a new set scenarios from the research community and policy makers. It was argued, for example, that in addition to the



**Figure 2.1** History of CMIPs and their contributions to IPCC Assessment Reports (ARs); adapted from Fig.1 of Emori et al. (2016)

no-climate-policy scenarios explored previously (e.g. Special Report on Emission Scenarios, SRES and prior to that IS92), there was need to explore the impact of different climate policies (Moss et al., 2010; van Vuuren et al., 2011). Based on recommendations from an IPCC expert meeting held in September, 2007 in Noordwijkerhout, The Netherlands (Moss et al., 2008), four representative concentration pathways (RCPs) radiative forcing levels (see Table 2.2) were chosen (van Vuuren et al., 2011). The current RCPs are set to be replaced by the Shared Socio-economic Pathways (SSPs) (Kriegler et al., 2012) from CMIP6 (Bjørnæs, 2013).

In this research, climate change impacts were tested at RCP4.5 (comparable to SRES scenario B1) and RCP8.5 (comparable to SRES scenario A1 F1) radiative forcing levels. RCP4.5, developed by the Pacific Northwest National Laboratory, United States, represents a future with ambitious emissions reductions and can be considered as an intermediate mitigation scenario (Bjørnæs, 2013; van Vuuren et al., 2011). RCP8.5 was developed by the International Institute for Applied System Analysis in Austria and is a high emission scenario consistent with a future with no deliberate policy changes to ensure that emissions are reduced (Bjørnæs, 2013;

**Table 2.2** Overview of representative concentration pathways (RCPs); adapted from van Vuuren et al. (2011)

RCP	Description	Reference – IAM
RCP8.5	Rising radiative forcing pathway leading to 8.5 W/m <sup>2</sup> (~1370 ppm CO <sub>2</sub> eq) by 2100.	(Riahi et al., 2007) – MES-SAGE
RCP6	Stabilization without overshoot pathway to 6 W/m <sup>2</sup> (~850 ppm CO <sub>2</sub> eq) at stabilization after 2100	((Fujino et al., 2006; HI-JIOKA et al., 2008) – AIM
RCP4.5	Stabilization without overshoot pathway to 4.5 W/m <sup>2</sup> (~650 ppm CO <sub>2</sub> eq) at stabilization after 2100	(Clarke et al., 2007; Smith and Wigley, 2006; Wise et al., 2009) – GCAM
RCP2.6	Peak in radiative forcing at ~3 W/m <sup>2</sup> (~490 ppm CO <sub>2</sub> eq) before 2100 and then declines to 2.6 W/m <sup>2</sup> by 2100).	(van Vuuren et al., 2007, 2006) – IMAGE

van Vuuren et al., 2011). The main characteristics of each RCP are summarised in Table A.1.

### 2.1.3 The Hydrologic Cycle

The hydrologic cycle is simply a description of the continuous movement of water within the Earth and atmosphere and usually described in terms of three main processes, namely evaporation, condensation, and precipitation (see Figure 2.2). Climate change and variability affects the hydrologic cycle in subtle ways that can be observed over short or longer time frames. For example, Smith (1978) reports that the terrestrial environment which includes runoff, surface-water and

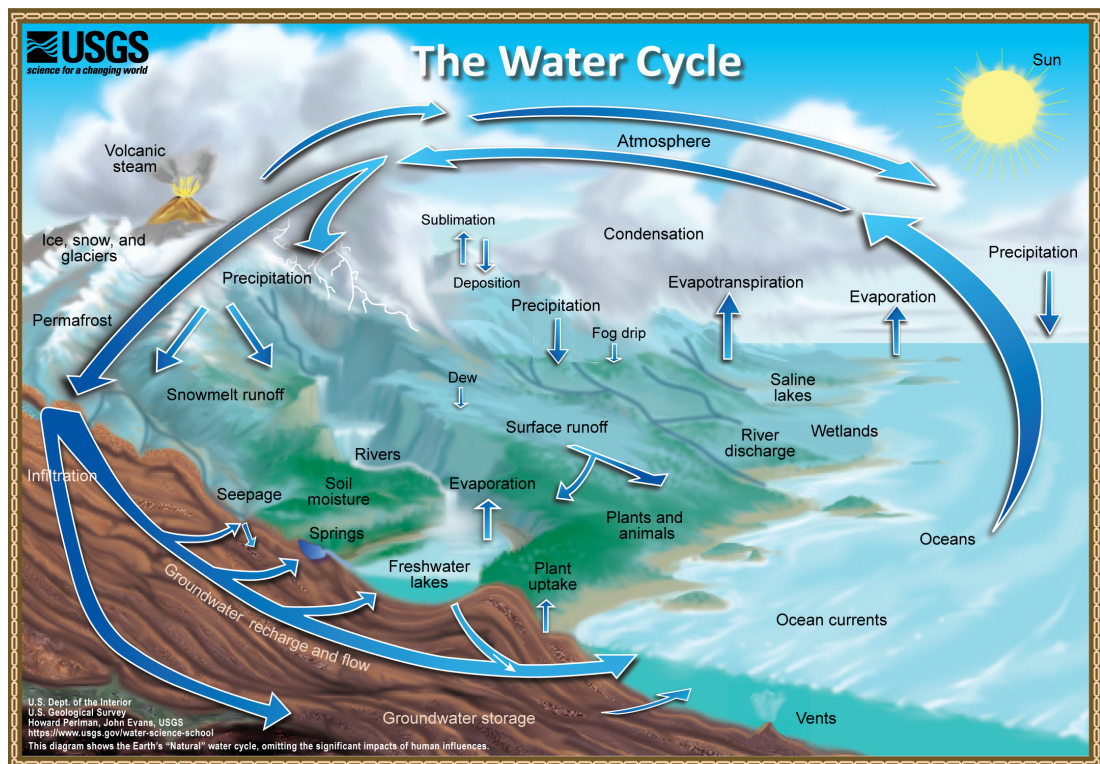
biological processes responds rapidly to climate change; usually within a year. On the other hand, continental ice sheets and oceans take a considerably longer time, on the order of decades or even centuries, before significant changes are measurable (Smith, 1978).

#### **2.1.3.1 Impact on Surface- and Groundwater Resources**

Climate change and its impact on surface water bodies has been studied extensively in the literature. Abbaspour et al. (2009) investigated the impact of climate change on precipitation and water resources (blue and green water) in Iran using the SWAT model where it was projected that wet regions would get wetter while dry regions would get drier. Globally, temperate regions are rarely expected to experience drought while arid to semi-arid regions are expected to experience droughts and extreme events such as heatwaves and floods. Kishiwa et al. (2018) used a coupled SWAT and WEAP model to assess current and future surface-water availability under a changing climate in the Pangani River Basin in Tanzania. Their study projected future increase in rainfall and consequently long-term streamflow in the Pangani River Basin. A common theme in most of the studies that have used transient GCMs coupled with rainfall-runoff models is the variability in the results from one GCM to another. This deficiency in GCMs is expected to diminish with improved GCM skill and the use of multi-model GCM ensembles (Greve et al., 2018; Zhao et al., 2018).

While many studies exist that have investigated the availability and security of surface-water resources, the same cannot be said about groundwater. However, in the last decade or so, there has been increasing interest in groundwater and climate change. More recently, studies in integrated hydrologic modelling have also





**Figure 2.2** A depiction of the hydrologic cycle (Source: USGS Water Science School).

emerged to more accurately represent the different components of the hydrologic cycle. One of the possible reasons why groundwater (flow with respect to climate change) is less studied may be attributed to lack of ground truth data (Taylor et al., 2013). Worldwide and especially in developing countries, there is a shortage of groundwater level monitoring data without which verification and validation of groundwater models would be difficult.

Generally, groundwater is affected by climate change directly and indirectly. Groundwater is affected directly by changes in focussed (e.g. from ephemeral streams and lakes e.t.c.) or diffuse rain-fed recharge and indirectly via changes in groundwater abstraction for industrial and agricultural purposes (Taylor et al., 2013). Havril et al. (2018) studied the impacts of climate change on groundwater flow systems in the Tihany Peninsula in Hungary. Their study revealed that

decreasing recharge significantly affects the groundwater flow system hierarchy. In another study, McCallum et al. (2010) investigated impacts of climate change on groundwater in Australia with a particular emphasis on groundwater recharge. Their study concluded that groundwater recharge (diffuse) is mostly affected by changes in rainfall intensity.

In this thesis, using methods described in Chapter 3, the impact of potential climate change on precipitation and consequently diffuse and focussed groundwater recharge is investigated by quantifying changes in rainfall intensity and groundwater/surface-water interactions.

## **2.2 Uncertainty in Climate Impact Studies**

### **2.2.1 Uncertainty in Climate Input Data**

There are many sources of uncertainty in climate change impact studies. One of these sources, and evidently the largest contributor to uncertainty in hydrological impact assessments, is climate change projections from Global Circulation Models (GCMs) and Greenhouse Gases Emissions Scenarios (GHGES) (Chen et al., 2011). Mahlman (1997) posited that “significant reduction of key uncertainties” in projections of anthropogenic climate warming “will require a decade or more”. More than two decades later, uncertainty in hydrological impact studies is still mostly attributed to output from GCMs (see for example, Brisson et al., 2015; Chen et al., 2012, 2013, 2016; Fang et al., 2015; Ficklin et al., 2016; Shen et al., 2018). It is therefore important to recognise, explore, quantify and reduce the inevitable uncertainty associated with societal impact studies, especially in cases where results of such studies can influence policy formulation by water resources

managers and political leaders.

Many studies have been done to assess, quantify and reduce uncertainty in climate change impact studies. For example, Wilby and Harris (2006) presented a probabilistic framework for evaluating different components of uncertainty in climate change impact studies using changing low flows in the River Thames. An ensemble of four GCMs, two statistical methods, two emission pathways, two hydrological model (CATCHMOD) structures and parameters, were used to explore the uncertainty in low flows for the River Thames by the 2080s. Wilby and Harris (2006) concluded that low flows were most sensitive to inherent uncertainty in climate change scenarios and choice of GCM while the hydrological model parameters and the increase in the emission pathway with time was comparatively insignificant. Chen et al. (2011) investigated how the choice of a downscaling method (see Section 2.3) can be a source of uncertainty in hydrological impacts of climate change studies. Using an ensemble of seven GCMs, three GHGES, six downscaling methods and a rainfall-runoff model (HSAMI), they discovered that a large uncertainty envelope was linked to the choice of a downscaling method. Overall, the study concluded that regression-based statistical downscaling methods contribute the most to the uncertainty envelope than other statistical downscaling techniques. Shen et al. (2018) estimated the uncertainty and its temporal variation in relation with GCMs in quantifying climate change impacts on hydrology. A total of twenty CMIP5 GCMs under RCP4.5 and RCP8.5 emission pathways were used in the study to determine the uncertainty envelope for future climate and streamflow using the HMETTS hydrological model. The study developed a methodology, using a set of statistical metrics (i.e. mean, median, extremes etc.), that combine statistical techniques such as wavelet analysis, Mann-Kendall

trend test and polynomial regression to evaluate the temporal variation. In other studies, the uncertainty stemming from GHGES has been investigated. For example, Maurer (2007) used eleven GCMs and two emission pathways to investigate hydrologic impact uncertainty due to choice of a GCM and GHGES. The study concluded that emission pathways play an important role in determining the extent and degree of impacts to water resources. In a similar investigation for the same region, Ficklin et al. (2016) used Coupled Model Intercomparison Project Phase 5 (CMIP5) projections to evaluate the hydrologic impact on snowmelt-dominated mountain runoff-generating regions of the western United States. The study found that, while projections made using the older generation CMIP3 GCMs were still valid, there was need to “re-evaluate” the projected climatic impacts on the water resources; indicating that there are differences in potential impacts modelled using equivalent emission pathways of the CMIP3 and CMIP5 projections (see also Ayers et al., 2016).

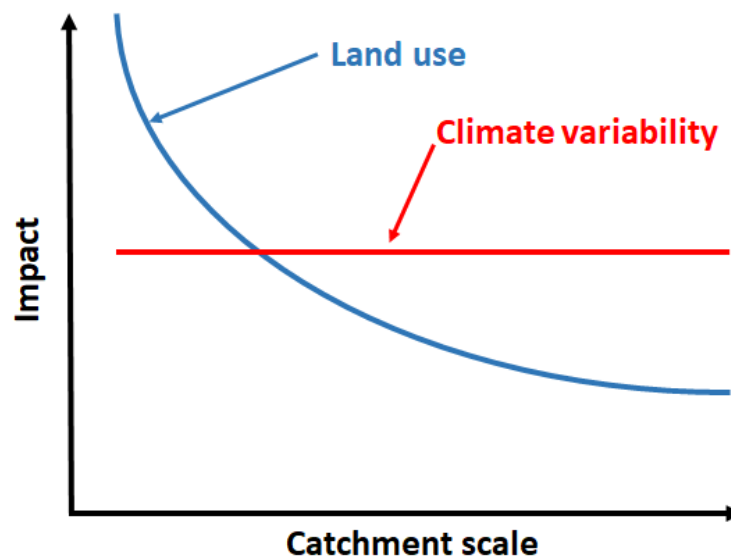
These and many more studies in the literature signify the paramount need to pay particular attention to hydrological model climate inputs uncertainty before carrying out any hydrological modelling and interpretation.

One of the ways in which uncertainty in climate impact assessments can be reduced is through the use of multi-model projections (e.g. Christensen and Lettenmaier, 2006; Fischer et al., 2012). Tebaldi and Knutti (2007) reports of cases where the El Niño Southern Oscillation (ENSO) forecasts have been found to be better than single-model forecasts. The premise on which this idea is anchored derives from the assumption that combining different models, each with their own inherent structural and parametrization weaknesses, results in a partial cancellation of these errors leading to better prediction skill than their constitutive

models (Tebaldi and Knutti, 2007). In this research, a multi-model climate ensemble approach using CMIP5 projections was employed. In a study conducted by Knutti and Sedlacek (2013) to test the robustness of CMIP5 projections, the authors conclude that some uncertainties are persistent ‘and may even grow temporarily’ but that this should not stop professionals working on climate impacts from making decisions and directing policy (Knutti and Sedlacek, 2013).

### 2.2.2 Uncertainty Due to Land-use Change and Classification

Anderson (1976) defines land use simply as “man’s activities on land which are directly related to the land”. Land cover, on the other hand, “is the result of land use at a certain moment in time” (Mucher et al., 1993).



**Figure 2.3** Impact of land use and climate variability on hydrological response as a function of scale (Adapted from Fig.1 of Bloeschl et al. (2007).)

Anthropogenic influences on the hydrology of watersheds such as land use

change have been investigated extensively in the literature. In particular, the issue of tropical deforestation and its effect on climate and biodiversity has received a lot of attention since the 1980s (Bonell, 1999). However, investigating the impacts of land cover/use change on the hydrologic components of a catchment is problematic because of several reasons. Firstly, hydrologic components (e.g. streamflow) can be influenced by atmospheric processes such as local climate, and thus influence the amount and timing of streamflow (Bruijnzeel, 2006). Secondly, the classic methodology of studying such problems (i.e. “paired catchment experiment”), in which streamflow from preferably two adjacent catchments of comparable characteristics (e.g. topography, geography, vegetation) are expressed in terms of each other and subsequently compared under a changing land cover, is time-consuming (typically > 5 years) and expensive. Thus, there is a decline in the number of such experiments in the last few decades with an inclination towards a *computer simulations* approach (Bruijnzeel, 2006).

Generally, approaches to understanding the impacts of land-use change on the hydrologic components of a catchment need to consider the effects of scale (Bloeschl et al., 2007; Costa and Foley, 1997). According to Kiersch et al. (2002), “impacts of land use activities on hydrological and sediment-related processes can only be verified at smaller scales (upto some tens of square kilometres) where they can be distinguished from natural processes and other sources of degradation”. Figure 2.3 is a hypothesized understanding of the impact of land use and climate variability on hydrological response as a function of scale after Bloeschl et al. (2007).

However, despite this understanding, there is need to investigate the interplay of many other factors between catchment-scale land-use change and hydrological processes. Many studies have attempted to address some of these issues such

as the effect of land-use change on flood frequency, runoff-generation processes and the relationship between land-use and internal dynamics of the hydrological cycle (Bronstert, 2004). Costa et al. (2003) documents, for example, that the annual mean discharge for the Tocantins River in the Tocantins basin in central Brazil, increased by 24% due to a deforestation of about 30% in the basin. Due to the structural differences and varying dynamics between watersheds, it is difficult to infer that watersheds (even at the same spatial scale) would respond in the same way when subjected to similar external stresses. Furthermore, there is a high degree of uncertainty associated with the parameterisation of land cover properties because of the difficulty involved in obtaining or measuring reliable observations (Eckhardt et al., 2003). Also, upscaling of point measurements to basin scale can lead to loss of information and thus induce some uncertainty.

To this extent, there is some degree of uncertainty from the land-use inputs introduced into watershed models when assessing the impact of climate change and variability on a hydrological system. The land-use used in this study, for example, was considered to be stationary for the baseline period and further assumed to be stationary during the projected future period. Historical and emerging studies have recognised the need for distributed watershed models to dynamically simulate land-use changes in the reference or baseline (observed) period. Recently, a new model (Moriassi et al., 2019) developed in the Python programming language is able to dynamically update land-use in the SWAT model while running multi-year simulations (see also Section 8.5).

### 2.2.3 Uncertainty in the Conceptual Understanding

Uncertainty in groundwater and environmental modelling in general can arise due to errors in the conceptual model (structural uncertainty). While most research is focussed on the determination of optimal parameter values using parameter estimation methods, the uncertainty in the conceptualization process itself is typically ignored by these methods (Rojas et al., 2008). Typically, groundwater modellers rely on a single hydrogeological conceptual model (which is translated to a mathematical model) of the site being modelled. This, according to Neuman (2003b), leads to the errors summarised in Table 2.3.

**Table 2.3** Summary of conceptual model errors encountered in groundwater and environmental modelling

Model Error	Case
Type I	Arises when one rejects or omits valid alternative models
Type II	Arises when one adopts or fails to reject an invalid conceptual model

Generally, Type II errors lead to statistical bias in the analyses of model uncertainty due to reliance on an invalid model while Type I errors lead to underestimation of uncertainty through under sampling of the relevant model space. Most studies focus on the bias and uncertainty introduced through model parameterization yet reliance on an inadequate conceptual-mathematical model is a source of relatively much larger biases and uncertainty, leading to unjustified overconfidence in the model results (Neuman, 2003b).

Having recognized the seriousness of this type of uncertainty, especially when modelling complex environmental problems, many strategies have been proposed to reduce such uncertainty. Refsgaard et al. (2006) proposed a six step frame-



work for assessing the predictive uncertainties of environmental models used for extrapolation (i.e. where field data is unavailable for calibration). The methodology involves the use of multiple conceptual models which are assessed with respect to their predictive bias and uncertainty. This approach is desirable in situations where field data or observations are lacking. Traditionally, when field data is available, the model is calibrated against a sample of the available data and model predictions compared with an independent set of field data. The differences between the simulated and observed values are then used to make inferences about the model's conceptual error leading to its acceptance, rejection or refinement. Where data are unavailable, a more robust methodology is required to quantify and reduce the conceptual error. Neuman (2003b) proposed a Maximum Likelihood Bayesian Model Averaging (MLBMA) method of assessing the joint predictive uncertainty of many competing deterministic or stochastic models. Similarly, Rojas et al. (2008) suggested a method (see also Rojas et al., 2010a,b) that combines generalized likelihood uncertainty estimation (GLUE) and Bayesian model averaging (BMA) to assess model structural uncertainty. The authors applied the methodology to a three-dimensional hypothetical case and determined that conceptual model uncertainty alone contributed up to 30% of the total uncertainty.

In this study, watershed models were calibrated using field data and thus the uncertainty associated with the parameterization and conceptual understanding was quantified. Similarly, for the groundwater models, model calibration and uncertainty quantification was performed based on ground truth data. Improvements and recommendations of how to refine the conceptual understanding were advanced.

## 2.3 GCM Downscaling and Bias Correction

### 2.3.1 Statistical Downscaling

Statistical downscaling (SD) is a process where quantitative statistical relationships are established between large-scale atmospheric variables (predictors) and local-scale variables (predictands) (Wilby et al., 2004). Implicit in this definition is the assumption that the relationship between predictor variables and local climate variables (e.g. precipitation at weather station) will always be the same. SD methods can be used in climate impact studies and especially hydrological assessments provided sufficient point meteorological observations are available to derive the statistical relationships (Green et al., 2011b). Wilby and Wigley (1997) classified SD models into four categories:

**Regression methods:** In these methods, linear or non-linear relationships between predictors and predictands are established. Generally, a regression equation relating the predictors and the predictands is derived before being ‘forced’ using data from a GCM (Wilby and Wigley, 1997). Future precipitation and temperature values are then predicted by the model.

**Synoptic weather typing:** where observed station or area-average meteorological data are statistically related to a weather classification scheme. Local-scale meteorological variables are then ‘conditioned’ on the corresponding (daily) weather patterns by deriving conditional probability distributions for the observed data (Wilby and Wigley, 1997). Future climate scenarios are then constructed by resampling from the observed data distributions or by the use of combined Monte Carlo and Markov chain techniques to generate

synthetic data and then resampling from this data (Green et al., 2011b).

**Stochastic weather generators:** In these methods, local climate data is generated by modifying parameters of first- or multiple-order Markov chain weather generators scaled in direct proportion to corresponding parameters in GCMs (Green et al., 2011b).

**Limited-area climate models:** This is where a higher resolution limited-area climate model (LAM) is embedded within a GCM using transient boundary conditions defined by the GCM. One of the limitations of these methods is that they demand considerable computing resources and are just as expensive to run as a traditional GCM (Wilby and Wigley, 1997).

### 2.3.2 Statistical Downscaling Methods and Models

There are many methods and software currently in use for statistical downscaling of GCMs. Statistical DownScaling Model (SDSM) (Wilby et al., 2002b) and the Long Ashton Research Station Weather Generator (LARS-WG) (Racsko et al., 1991; Semenov and Barrow, 1997; Semenov et al., 2002, 1998), are probably the two most widely used canned statistical downscaling software. Many researchers worldwide have conducted climate impact assessments using the help of these decision support tools. Some studies (e.g. Dibike and Coulibaly, 2005; Hashmi et al., 2011; Hassan et al., 2014) have compared the performance of the two models in quantifying the effects of climate change at local scales. Generally, the two models are capable of simulating extreme events with a high level of confidence (Hashmi et al., 2011). Hassan et al. (2014) applied SDSM and LARS-WG to simulate and downscale meteorological variables such as precipitation and temperature in the Peninsular of Malaysia and concluded that SDSM performed better LARS-WG

despite slightly underestimating wet and dry spells. In almost all cases, the two models do not provide identical results. This is attributed to the differences in the underlying approaches and philosophy of the two models. However, the statistical trends that are inferred from time-series generated by the two models are usually in agreement (Hassan et al., 2014). The next sections describe the main differences in simulation approach of the two models.

### 2.3.2.1 LARS-WG

LARS-WG is a stochastic weather generator developed at the UK Long Ashton Research Station (Semenov and Barrow, 1997) capable of simulating weather data for a single station under both current and future climate scenarios (Racsko et al., 1991; Semenov et al., 2002). Fundamentally, the weather generator uses observed point station data such as maximum and minimum temperature, precipitation and solar radiation, to determine a set of parameters for probability distributions of weather variables. The correlations between the weather variables are then estimated and the resulting set of parameters used to generate synthetic weather time series of arbitrary length by randomly selecting values from the appropriate distributions (Semenov, 2007).

Dry and wet days are distinguished depending on whether precipitation is greater than zero. Probability distributions of dry and wet series, daily precipitation, minimum and maximum temperatures and solar radiation, are approximated in LARS-WG by a semi-empirical distribution (SED), defined as the cumulative probability distribution function (PDF) (Semenov and Stratonovitch, 2010). Previously, LARS-WG used ten intervals ( $n$ ) in the SED but in the current version, LARS-WG5, 23 intervals are used offering a more accurate representation of the

observed distribution. For each climatic variable  $v$ , a value of a climatic variable  $v_i$  corresponding to the probability  $p_i$  is calculated as;

$$v_i = \min\{v : P(v_{obs} \leq v) \geq p_i\} i = 0, \dots, n \quad (2.1)$$

Where,  $P$  is the probability based on the observed data,  $\{v_{obs}\}$ .  $P_o$  and  $P_n$ , for each climatic variable, are fixed with the value of 0 and 1, respectively, with corresponding values of  $v_o = \min\{v_{obs}\}$  and  $v_n = \max\{v_{obs}\}$ . Furthermore, to allow for accurate approximation of the extreme values of a climatic variable, some  $p_i$  are assigned close to 0 or 1, dependent on whether the values of the variables are extremely low or high respectively, while the remaining values of  $p_i$  are distributed evenly on the probability scale (Semenov and Stratonovitch, 2010).

In order to simulate events with extremely high daily precipitation that occur with very low probability such as hurricanes and typhoons, 3 values close to 1, allowing for better approximation, are used in LARS-WG (i.e.,  $p_{n-1} = 0.999$ ,  $p_{n-2} = 0.995$  and  $p_{n-3} = 0.985$ ). Also, owing to the fact that very low daily precipitation (i.e.,  $< 1mm$ ) which has a high probability of occurrence and has little effect on the output of a process-based model,  $v_1$  and  $v_2$  equal to  $0.5mm$  and  $1mm$  respectively, were proposed by Semenov and Stratonovitch (2010) to simulate rainfall within the interval  $[0,1]$  and the corresponding  $p_i$  defined as;

$$p_i = P(v_{obs} \leq v_i), i = 1, 2 \quad (2.2)$$

Similarly, for maximum and minimum temperature, 2 values close to 0 and 2 values close to 1 (i.e.,  $p_2 = 0.01$ ,  $p_3 = 0.02$  and  $p_{n-1} = 0.99$  and  $p_{n-2} = 0.98$ ) are

used in SEDs to account for extremely low and high temperatures respectively. For extremely long wet and dry series,  $p_{n-1} = 0.99$  and  $p_{n-2} = 0.98$  (both close to 1) are used in the SEDs. In the case of radiation, all  $p_i$  values for  $0 < i < n$  are distributed evenly between the extreme values (Semenov and Stratonovitch, 2010).

### 2.3.2.2 SDSM

SDSM is a robust statistical downscaling and decision support tool for assessing local climate change impacts. It is described as a hybrid of a stochastic weather generator and regression based methods (Wilby et al., 2002a, 2003). Generally, SDSM uses local-scale weather generator parameters, such as precipitation occurrence and intensity, to linearly condition large-scale coarse GCM and National Center of Environmental Prediction (NCEP) output, usually referred to as *predictors* ( $j = 1, 2 \dots, n$ ) as follows:

$$\omega_i = \alpha_0 + \sum_{j=1}^n \alpha_j \hat{u}_i^{(j)} \quad (2.3)$$

where  $\omega_i$  is the conditional probability of precipitation occurrence on day  $i$ ,  $\alpha_j$  are regression coefficients approximated via ordinary least squares method for each month, and  $\hat{u}_i^{(j)}$  are normalized predictors. By stochastically comparing  $\omega_i$  with the output of a linear random-number generator,  $r_i$ , wet- and dry-spell sequences can be determined.

In the second step, a conditional distribution is constructed if precipitation occurrence is established (i.e.  $\omega_i \leq r_i$ ) by regressing precipitation (can be *fourth root*, *Natural log* or *inverse-normal* transformed) amounts at the station on large-

scale predictors using:

$$Z_i = \beta_0 + \sum_{j=1}^n \beta_j \hat{u}_i^{(j)} + \epsilon \quad (2.4)$$

where  $Z_i$  is the  $z$ -score,  $\beta_j$  are regression coefficients approximated via ordinary least squares method for each month, and  $\epsilon$  is an error term modelled stochastically by a series of serially independent Gaussian numbers (Semenov and Stratonovitch, 2010). In other words, the rainfall  $y_i$  on day  $i$  can be approximated by:

$$y_i = F^{-1} [\phi(Z_i)] \quad (2.5)$$

where  $\phi$  is the normal cumulative distribution function and  $F$  is the empirical function of  $y_i$  (Hassan et al., 2014).

### 2.3.2.3 Quantile Mapping

A survey of published literature reveals two different reasons for applying quantile mapping (QM): 1) it is commonly used as a bias correction method applied to observed and simulated climate model data at similar scales and 2) as a way of downscaling coarse climate data to finer local scales (either observed or gridded reanalysis data) (Cannon et al., 2015). Furthermore, the software tools discussed above, despite being popular, are not easily amenable to automation. In fact, even if LARS-WG is free for research purposes, one is required to register with the author to obtain a license. The QM method has been implemented in free software languages such as Python and R and can thus be easily automated for reproducibility and scalability.

In this study, QM was applied for both bias correction and downscaling, and as such, hereinafter, the method is referred to as Bias Correction and Spatial

Downscaling (BCSD) (e.g. Ahmed et al., 2013; Maurer and Hidalgo, 2008; Sanglantoni et al., 2018). The details of the implementation used in this thesis is given in Chapter 3.

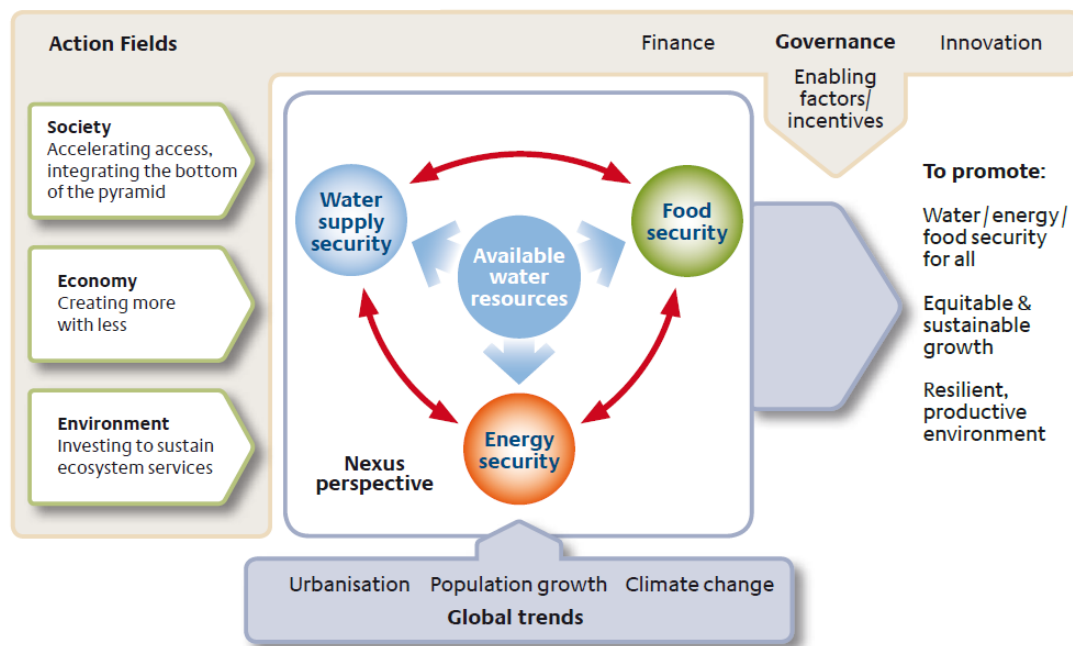
## 2.4 Water-Food-Energy-Climate Nexus

The global population is faced with a myriad of interrelated wicked and complex problems that threaten national and international security (Bazilian et al., 2011). At the heart of this so-called *nexus* of looming threats, three main areas, namely, water, energy and food security, are identified. These threats, on their own, are major threats to economic and security stability especially in developing countries, but become increasingly important when examined from a climate change perspective. Consequently, water security has been identified as the proverbial *gossamer* linking together this web of food, energy and climate (World Economic Forum Water Initiative and others, 2012). Addressing these challenges demands fresh perspectives and flexible forms of governance (Leck et al., 2015).

Water, energy and food (WEF) sectors are at the heart of the nexus approach because of the way they are inextricably linked to each other. The nexus approach aims at overall resource use efficiency and benefits in production and consumption by addressing externalities across these sectors. Furthermore, the interrelations across and between sectors, and how the actions of one system impacts the others, are described in the nexus approach (Hoff, 2011).

As can be seen from Figure 2.4, water supply security, food security and energy security are all dependent on the availability of water resources. Water supply is dependent on the availability of energy, hydropower energy production is dependent on the availability of water resources and food production is dependent on the



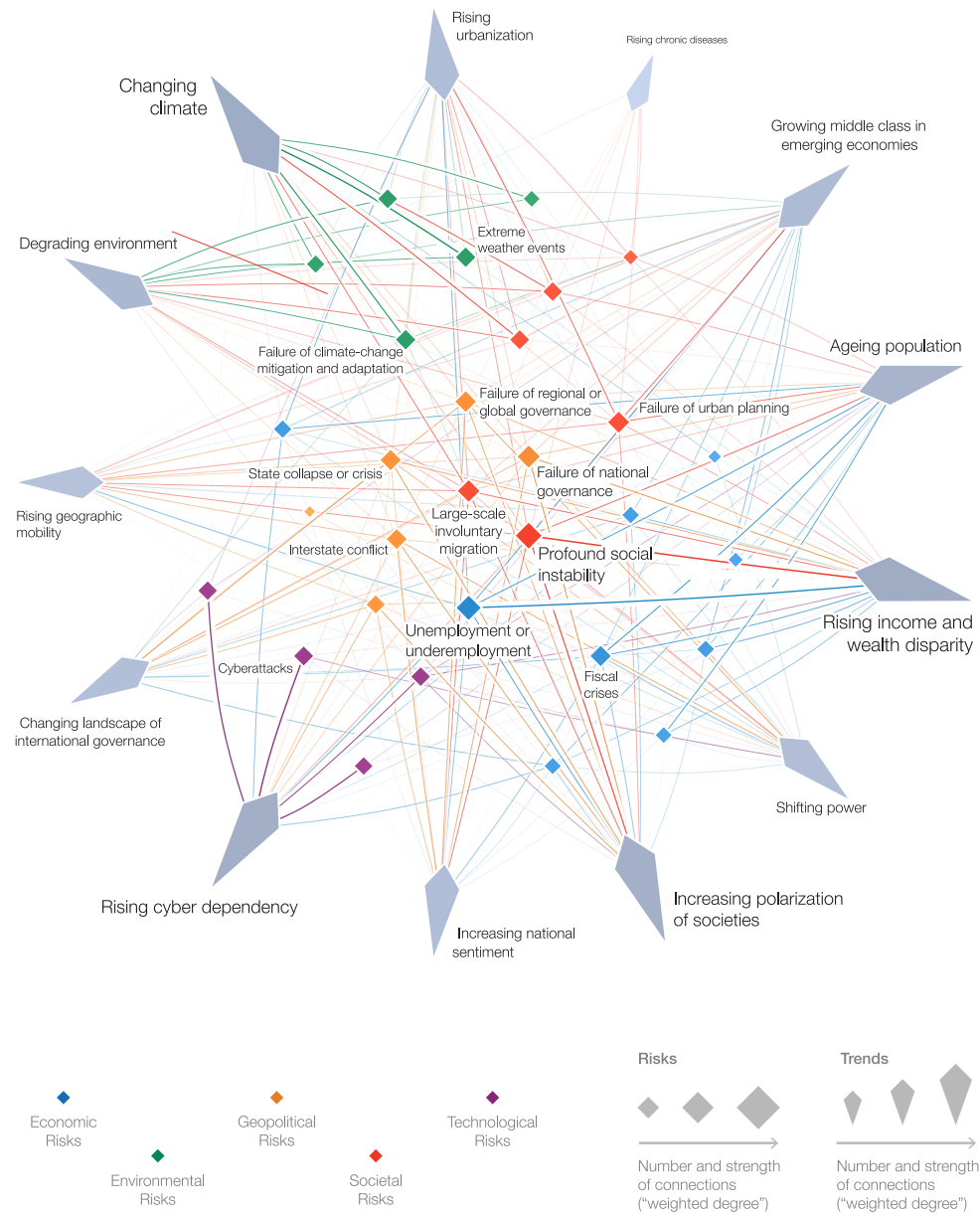


**Figure 2.4** The water, energy and food security nexus (Hoff, 2011)

availability of water resources. This interdependency is one of the foundations of the nexus paradigm and needs to be taken into account by policy makers and other stake holders. A threat to the security of any of the WEF and associated components results in a threat to many other system components due to their interconnectedness as depicted in Figure 2.5. In most cases, the perspective of the policy-maker determines the approach taken towards the WEF nexus (Bazilian et al., 2011; Harris, 2002). For example, from an energy perspective, water and biomass in form of energy crops are generally an input or resource requirement and food is considered to be the output; from a water perspective, food and energy systems are consumers of the resource; from a food perspective, energy and water are inputs. The approach or perspective adopted will largely influence the policy design (Bazilian et al., 2011).

The WEF nexus differs from the IWRM approach and similar holistic ap-

proaches to environmental decision-making in that the latter “takes water as its point of departure” while the former approaches WEF from a systems dynamics point of view (Leck et al., 2015). The point remains, however, that path dependency in modelling and data availability, together with other complexities, often results in policy makers operating along nexus lines, adopting one perspective and later incorporating others (Bazilian et al., 2011; Leck et al., 2015; Rees, 2013).



**Figure 2.5** Risks interconnection map (WEF, 2017)

## 2.5 Methods for Quantifying Groundwater/ Surface-water Interactions

### 2.5.1 Surface-water Models

River basin models such as SWAT and PRMS have modules that calculate groundwater/surface-water (GW/SW) interactions (see Section 3.7.3). PRMS and SWAT can both calculate groundwater storage, inflows and outflows to and from each HRU. Baseflow and groundwater flow out of the model domain that is not due to streamflow constitute *outflows* while recharge constitutes *inflow* (Markstrom et al., 2015). However, the simulation of groundwater processes is not adequate in these models when compared to MODFLOW. Thus PRMS has in the last decade been coupled with MODFLOW-NWT to form GSFLOW; and more recently, SWAT has been coupled with MODFLOW-NWT to form SWAT-MODFLOW. This allows for a comprehensive assessment of GW/SW interactions.

### 2.5.2 Groundwater Flow Modelling

The use of groundwater flow models in understanding important aquifers has been in existence for decades. For example, in 1978, the Regional Aquifer System Analysis (RASA) program of the U.S. Geological Survey was for the first time employed to simulate large scale aquifer systems (Zhou and Li, 2011). This culminated into production of hundreds of reports which continue to inform the insights of modern day groundwater modellers. More importantly, groundwater flow models are still being employed, more so than ever before, in understanding subsurface water flow and aquifer systems, especially as technology has progressed

and more computational power is available to groundwater professionals. A *model* is simply an approximation or representation of a real system (Fetter, 2000). Groundwater flow models can either be *physical* or *numerical*. An example of a physical model is a laboratory-scale tank with columns filled with sand and saturated with water so that groundwater heads and flows can be observed and measured directly (Anderson et al., 2015; Kresic, 2006).

Groundwater modelling is particularly useful for predicting or forecasting future conditions and also for understanding how current conditions came to be (Kresic and Mikszewski, 2012; Rushton, 2003). In the context of *Integrated Water Resources Management (IWRM)*, groundwater management decisions can benefit from insights generated by groundwater models. Anderson et al. (2015) state that since “...*the subsurface is hidden from view and analysis is hampered by lack of field observations, a model is the most defensible description of a groundwater system for informed and quantitative analyses as well as forecasts about the consequences of proposed actions*”. This reason and perhaps many more, strengthen the need and importance of performing groundwater flow modelling at the beginning of every hydrogeological investigation.

Using specialized packages such as the UZF (Unsaturated-Zone Flow package) (Niswonger et al., 2006), SFR (Streamflow-Routing package) (Niswonger and Prudic, 2005) and RIV (river package) (Harbaugh et al., 2000), one is able to simulate GW/SW exchanges between streams and aquifers. In this thesis, the RIV package was used to simulate and account for GW/SW fluxes.

### 2.5.3 Limitations of Groundwater Flow Modelling

Although groundwater flow models can aid our understanding of subsurface flow and related phenomena, it is important not to lose sight of the many assumptions made in trying to simulate the environment. Thus, it is necessary for groundwater modelling results to be presented in a context where uncertainty and the nature thereof is explicitly stated (Anderson et al., 2015). The importance of such information to end users such as policy makers or environmental managers cannot be overstated. The major weaknesses associated with groundwater modelling are discussed below.

#### 2.5.3.1 Uncertainty

In the context of hydrological modelling, uncertainty can be further classified into *aleatory/intrinsic* and *epistemic* uncertainties. Aleatory uncertainties relate to apparent random variability and can be quantified by probabilistic terms whereas epistemic uncertainties arise from a limitation or lack in knowledge and understanding. The latter, it is suggested, can be reduced by taking more precise measurements or by using new techniques altogether (Beven and Young, 2013) while the former cannot be reduced either by the availability of more information or by new science (Anderson et al., 2015). Thus aleatoric uncertainties are more amenable to probabilistic description methods. Currently, Bayesian multimodel averaging (BMA) (Neuman, 2003a,b) is the most popular of such probabilistic methods where the uncertainty in the knowledge of the physics underlying hydrological processes is characterized using multiple structures (Gong et al., 2013).

Uncertainty in groundwater models can arise from many sources. Limited

understanding of the geology, code selection (Anderson et al., 2015), conceptualization of the groundwater model and input parameters used to calibrate and constrain the model are possible sources of uncertainty. With regard to the conceptual model, geological uncertainty mainly arises from two sources: the medium in which flow is occurring and the hydraulic parameters of the medium (Refsgaard et al., 2012). Accounting for this type of uncertainty is still an active area of research. One of the ways in which this uncertainty can be reduced is by the use of a *multimodel* approach (Refsgaard et al., 2012). For example, Poeter and Anderson (2005) demonstrated the usefulness of multimodel inference based on Kullback-Leibler (K-L) information in selecting the best model. This approach lends itself well to the *equifinality* concept, advocated for by Beven (2006a), where multiple models are accepted as possible representations of the hydrological system. However, challenges related to model evaluation and model error representation still remain. For example, in order to simulate different scenarios or hypotheses about the environment, one needs to have observations or parameterisations of those processes to be simulated (in most cases this is actually a *hindcasting* problem) (Beven, 2006a). One way of achieving this is by stochastic generation of hydrological models. However, this leads to the problem of *overparameterization* and thus no matter how perfect a model is defined from a mathematical perspective, it will still be subject to equifinality even if non-error-free parameters are used to define the boundary conditions and to drive the model (Beven, 2006a).

Although the equifinality thesis may seem as an attractive method of specifying and quantifying uncertainty related to hydrological modelling, it is often shunned in policy and decision making situations where one best model or solution is desired (Anderson et al., 2015). Thus, it behoves climate and water experts to

develop systematic and pragmatic guidelines for environmental managers and policy makers tasked with the heavy responsible of translating probabilities into adaptation responses (Wilby and Harris, 2006). In this research, calibration constrained approaches such as those available in the PEST (Doherty et al., 1994) and SWATCUP (for the surface-water models) software suites were used to estimate the uncertainty in the hydrological models.

### 2.5.3.2 Nonuniqueness

In surface- and groundwater model calibration the inverse problem is almost always expected to be *underdetermined* and thus mathematically *ill-posed* (Anderson et al., 2015). In other words, there are more unknown parameters than there are observations or field measurements. Thus it is not reasonable to constrain the model calibration to one solution since many different combinations of parameters are able to reproduce the observed values. Herein lies the problem or shortcoming with history matching. The modeller is thus faced with the task of picking one solution from many to present to decision-makers who, in many instances, demand for a single unique solution (Anderson et al., 2015).

While it is true that there are multiple solutions to the inverse problem in hydrologic model calibration, it is usually the case that some of the solutions are geologically or hydrologically infeasible. Thus the modeller is expected to either select the best and realistic solution or regulate the calibration using advanced calibration tools such as Tikhonov regularization (Tikhonov and Arsenin, 1977) and singular value decomposition (SVD). Hunt et al. (2019) revisited Freyberg's (1988) classroom problem which revealed problems associated with 'point calibration' aimed at getting a good historical fit "even at the expense of geological realism"



(Hunt et al., 2019), including the shortcomings of simplistic trial-and-error methods where no rigorous quantitative evaluation of the results can be made (Hunt et al., 2019). Their findings established the following; a) that even after thirty-one years since Freyberg's classroom experiment and in spite of the great strides that have been made in automated parameter estimation tools, the nonuniqueness problem still exists but can now be better handled via soft-knowledge Tikhonov regularization and SVD, b) that introducing pilot points (highly parameterized inversion) yields better performance in the calibration process and that, c) to achieve better results from the calibration campaign, suggestions offered by Anderson et al. (2015) to the effect that, both head and flux targets should be used since the correlation between hydraulic conductivity and recharge cannot be overcome using only head data for calibration, are valid.

In this thesis, it has been proposed that (see Chapter 7) that alongside recommendations proposed by Hunt et al. (2019) and Anderson et al. (2015), particularly in groundwater model calibration, a secondary step in the form of multi-objective optimization (MOO) should be performed to help the decision-maker select not only the best model but the most probable given a set of constraints.

#### **2.5.4 Integrated Hydrologic Modelling**

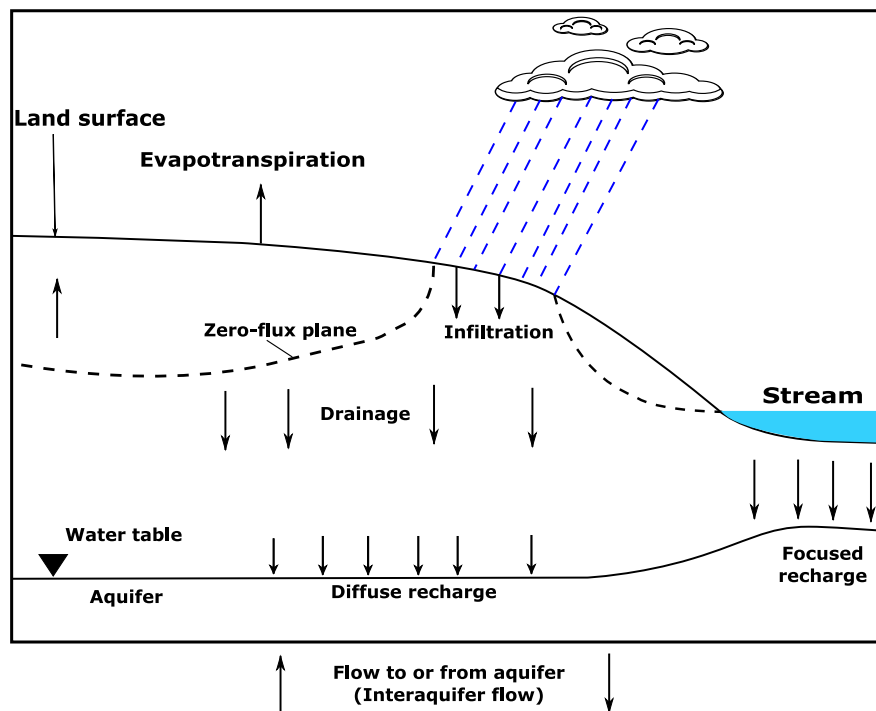
Integrated hydrologic models (IHMs) present exciting opportunities to understand groundwater/surface-water interactions which could lead to a holistic approach to managing both surface and subsurface water resources. Recently, a lot of research has been devoted to the study and application of IHMs to the solution of complex hydrologic and environmental problems. For example, Dehghanipour

et al. (2019) explored sustainable management options for agricultural production and downstream flow to the shrinking Urmia Lake using a coupled dynamically coupled MODFLOW and WEAP model. Somers et al. (2019) used the GSFLOW model to test the extent to which, in the future, groundwater will buffer the loss of glacial meltwater in the typically proglacial Shullcas Watershed in central Peru. Their study concluded that the groundwater component improves our current understanding of the interplay between glaciers, surface- and groundwater under a changing climate. Chunn et al. (2019) applied the SWAT-MODFLOW model to the Little Smoky River watershed in western Alberta, Canada in a bid to evaluate potential impacts of climate change and water withdrawals on groundwater–surface water interactions. Their study revealed that uncontrolled groundwater abstractions could have more immediate effects on streamflow than climate change.

Despite the many advantages of IHMs, they require specialised knowledge and a lot of temporal-spatial data input to set-up, calibrate, validate and apply (Tian et al., 2018). More specifically, model preparation requires one to have highly specialised GIS and computer programming skills (Gardner et al., 2018). In recent years, however, tools aimed specifically at easing the laborious exercise of input data preparation for free and open-source IHMs have been developed. Gardner et al. (2018) for example developed a python toolset that builds input for GSFLOW while Park et al. (2019) developed a QGIS plugin (QSWATMOD) that is used to prepare and run SWAT-MODFLOW models. In this thesis, QSWATMOD was used to prepare, run and post-process SWAT-MODFLOW results.

## 2.6 Potential Groundwater Recharge Estimation

Groundwater recharge is defined as the vertical flow of water reaching the phreatic surface or water table and adding to the groundwater storage (Healy, 2010). Water flowing from other aquifers through a semi-permeable layer such as an aquiclude, for example, is included by some authors in their definition of recharge. Others refer to such flow as *interaquifer flow*. Herein, the definition of groundwater recharge is limited to two forms i.e. *diffuse* and *focussed* recharge as illustrated in Fig. 2.6.



**Figure 2.6** Schematic representation of recharge processes from infiltration to interaquifer flow (adapted from Healy (2010)).

Diffuse recharge, sometimes referred to as *local* or *direct* recharge, is defined as

recharge that reaches the water table by infiltrating the soil surface and percolating the unsaturated zone in response to a precipitation event and is usually distributed over large areas (Allison, 1988; Healy, 2010; Simmers, 2017). Focussed recharge is defined as “the movement of water from surface-water bodies, such as streams, canals, or lakes, to an underlying aquifer” and usually varies spatially than diffuse recharge (Healy, 2010). Infiltration refers to the entry of water from the ground surface into the subsurface. It is more aptly referred to as *potential* recharge since it may become recharge when it reaches the water table or return to the atmosphere via evapotranspiration or simply remain in the vadose zone for some time (Healy, 2010; Rushton, 2017). Aquicludes or low permeability materials may prevent the downward movement of water in the vadose zone and thus create perched aquifers and induce other types of groundwater flow such as forcing water from lakes or springs (Mansour et al., 2018). In this thesis, because these processes are neither examined in detail nor accounted for, the terms “groundwater recharge” and “infiltration” are used interchangeably to mean *potential recharge*.

Many techniques including water-budget, modelling, physical, chemical and heat tracer methods have been used to estimate recharge. Stable environmental isotopes such as deuterium ( $^2H$ ) and oxygen-18 ( $^{18}O$ ) and radioactive isotopes such as tritium ( $^3H$ ) and carbon-14 ( $^{14}C$ ) have been used extensively since the early 1950s to estimate average recharge to groundwater (e.g. Gaye and Edmunds, 1996; Kalin, 2000; Sharma and Hughes, 1985).

Some groundwater recharge estimation methods such as numerical modelling, chemical and tracer methods etc., are data-intensive while others such as hydrograph separation methods require less data. Arnold et al. (2000) used two methods, i.e., SWAT’s water balance method and a modified hydrograph recession

curve displacement technique, to estimate groundwater recharge in the Upper Mississippi river basin, Cairo, Illinois, United States. The authors point out that the hydrograph recession displacement method simulated recharge just as well as the SWAT model with the only data input requirement being daily streamflow records.

## 2.7 Modelling Code Selection

### 2.7.1 MODFLOW

MODFLOW is a modular three-dimensional finite difference groundwater flow modelling code developed by the United States Geological Survey (USGS)<sup>1</sup> (McDonald and Harbaugh, 1988) and is widely considered to be the de-facto groundwater modelling code. Many iterations (referred to as “core versions”) of the code have been released as open source code to the public since its early development in the 80s (i.e. MODFLOW-88, MODFLOW-96, MODFLOW-2005 and MODFLOW-6).

MODFLOW solves the following governing partial differential equation for three-dimensional groundwater flow:

$$\frac{\partial}{\partial x} \left( K_{xx} \frac{\partial h}{\partial x} \right) + \frac{\partial}{\partial y} \left( K_{yy} \frac{\partial h}{\partial y} \right) + \frac{\partial}{\partial z} \left( K_{zz} \frac{\partial h}{\partial z} \right) + W = S_s \frac{\partial h}{\partial t} \quad (2.6)$$

where  $K_{xx}$ ,  $K_{yy}$  and  $K_{zz}$  are values of hydraulic conductivity along the  $x$ ,  $y$  and  $z$  coordinate axes, which are assumed to be parallel to the major axes of hydraulic conductivity ( $L/T$ ),  $h$  is the potentiometric head (L),  $W$  is a volumetric flux per unit volume representing sources and/or sinks of water, with  $W < 0$  for

---

<sup>1</sup><http://water.usgs.gov/ogw/modflow>

flow out of the groundwater system and  $W > 0$  for flow into the system ( $T^{-1}$ ),  $S_s$  is the specific storage of the porous material ( $L^{-1}$ ) and  $t$  is time ( $T$ ).

Numerous MODFLOW versions, other than the core versions, have been developed, mainly to address specific problems. Issues of saltwater intrusion, solute transport, surface and groundwater interactions, karst groundwater flow modelling, local refinement with nested and unstructured grids, and problems associated with unconfined groundwater flow problems have led to the development of many MODFLOW variants such as MODFLOW-NWT, MODFLOW-USG, GSFLOW, MODFLOW-OWHM, MODFLOW-LGR and SEAWAT.

Of particular note is the problem of the occurrence of “dry cells” which has been documented extensively in the literature (e.g. Bedekar et al., 2012; Hunt and Feinstein, 2012; Painter et al., 2008). Generally, when the calculated head in a cell falls below the base of the cell, the cell becomes “dry” and is excluded from future calculations as it is considered to be *inactive* by MODFLOW. Doherty (2001) has summarised the problems associated with the occurrence of dry cells as follows:

- Recharge assigned to a cell by MODFLOW may never enter the groundwater model domain if the respective cell is declared inactive. Although this can be circumvented by assigning recharge to the top *active* cell of the grid as opposed to specific cells, recharge can still be lost if the bottom layer dries out and thus lead to a propagation of dry cells within the model domain.
- The drying/rewetting capability of some MODFLOW solvers (e.g. BCF2 (McDonald et al., 1991)) causes numerical instability and non-convergence issues. To alleviate this problem, the convergence criterion can be set to an unusually higher value and the iteration interval between rewetting of dry cells also set high; although this could lead to unacceptable budget errors and

questionable groundwater flow solutions.

- Calibrating MODFLOW models using nonlinear parameter estimation codes such as PEST or UCODE, rewetting of cells can introduce a degree of granularity to model outputs. Furthermore, the inversion process can be severely hampered when observation wells are situated in dry cells.

To solve the drying/rewetting issue in MODFLOW, Waterloo Hydrogeologic<sup>1</sup> developed MODFLOW-SURFACT (Panday and Huyakorn, 2008) and more recently, the USGS released MODFLOW-NWT (Hunt and Feinstein, 2012; Niswonger et al., 2011). MODFLOW-NWT is a Newton-Raphson formulation for MODFLOW-2005 that is designed to improve the solution of unconfined groundwater flow problems (Niswonger et al., 2011). Recently, it has become fashionable to couple watershed models with MODFLOW-NWT such as GSFLOW (Markstrom et al., 2008) and SWAT-MODFLOW (Bailey et al., 2016). The Newton-Raphson solver (NWT) in MODFLOW-NWT has also been implemented in MODFLOW-OWHM (Hanson et al., 2014), MODFLOW-USG (Panday et al., 2013) and in MODFLOW 6 (Hughes et al., 2017; Langevin et al., 2017), the current core version release of MODFLOW.

In this research, MODFLOW-NWT was used to solve the groundwater flow problem. MODFLOW-NWT was fully coupled with the SWAT model for form SWAT-MODFLOW. All MODFLOW models were developed using free and open-source software.

---

<sup>1</sup><https://www.waterloohydrogeologic.com/>

### 2.7.2 Soil and Water Assessment Tool (SWAT)

The Soil and Water Assessment Tool (SWAT) is a comprehensive, semi-distributed river basin or watershed scale model developed by Dr. Jeff Arnold for the United States Department of Agriculture (USDA) Agricultural Research Service (ARS) (Arnold et al., 2012, 1998; Neitsch et al., 2011). Swat has been designed and used to model the impact of management on water, evaluation of streamflow (e.g., Githui et al., 2009; Govender and Everson, 2005; Patil and Ramsankaran, 2017; Rahman et al., 2013; Strauch et al., 2012; Thampi et al., 2010; Vazquez-Amabile and Engel, 2005; Wang et al., 2008), simulation of sediment, nutrient and pollutant transport (e.g., Ayele et al., 2017; Betrie et al., 2011a,b; Jha et al., 2004a; Lemann et al., 2016) in gauged and ungauged watersheds (Douglas-Mankin et al., 2010; Gassman et al., 2007). The SWAT model has proved to be a robust tool for these types of problems and many researchers worldwide have adopted it as a tool of choice among many competing alternatives (e.g., PRMS (Leavesley et al., 1983), Hydrologic Engineering Center - River Analysis System (HEC-RAS) (Brunner, 2010), etc.). A detailed description of how the SWAT model simulates hydrological processes is given in Section 3.7.2.

Many researchers have used SWAT to assess the impacts of climate change on surface water resources. For example, Ficklin et al. (2009) used the SWAT model to simulate the hydrological response to climate change of the San Joaquin River watershed, California, in the United States. Specifically, the study investigated how varying atmospheric CO<sub>2</sub>, temperature and precipitation can affect the hydrological regime of a watershed. Using a SWAT model conditioned on monthly streamflows, the study concluded that a changing climate has significant effects on water yield, streamflow, evapotranspiration and irrigation water use. Eckhardt and



Ulbrich (2003) investigated the potential impact of anthropogenic climate change on groundwater recharge and streamflow in a central European low mountain range. The study used a modified version of SWAT to simulate projected recharge and streamflow under two climate change scenarios. The results of the study indicated that there were changes in the projected mean annual cycle of groundwater recharge and streamflow.

From an ecohydrological and climate change perspective, impacts of land-use/landcover and climate changes on future streamflows and other watershed hydrological components have been modelled globally using the SWAT model (see for example Leemhuis et al., 2017; Pandey et al., 2017; Rodrigues da Silva et al., 2018; Setyorini et al., 2017; Yin et al., 2017b). Determination of the hydrological response of highly pressured ecosystems or watersheds to various external stresses is important for water managers and policy makers from a sustainability viewpoint.

In the context of Malawi, very few studies have been conducted to assess the impact of climate and landuse/landcover (LU/LC) changes on the hydrological regime of different watersheds in the country. One study by Palamuleni et al. (2011) applied the SWAT model to assess the impact of LU/LC changes in the Upper Shire River Basin. To date, this is the only study that has addressed this issue using a combination of GIS techniques and a hydrological model. In this study, future hydrologic forecasts were conducted using the SWAT model but the LU/LC was considered to be stationary – that is, conditions existing during the baseline period were considered to persist into the future.

### 2.7.3 SWAT-MODFLOW

SWAT-MODFLOW (Bailey et al., 2016), an amalgamation of SWAT and MODFLOW, was selected for integrated hydrologic modelling because of its wide application in different settings across the world (e.g., Aliyari et al., 2019; Bailey et al., 2016; Chung et al., 2015; Gao et al., 2019a; Kim et al., 2017; Molina-Navarro et al., 2019a; Semiromi and Koch, 2019; Wei and Bailey, 2019). Details of the software and its application in this thesis can be found in Section 3.7.3.

GSFLOW was also considered as a possible tool for integrated hydrologic modelling. However, due to the fact that PRMS (surface-water modelling engine in GSFLOW) has not been applied extensively, especially in semi-arid or arid regions, SWAT-MODFLOW was adopted instead. It should be noted that GSFLOW uses MODFLOW-NWT (also used in SWAT-MODFLOW) as the groundwater modelling engine. Future work considerations may look at the applicability of GSFLOW to Malawi and subsequently assessment of uncertainty associated with different IHMs.

## 2.8 Model Calibration

### 2.8.1 Quantifying Model Performance

One of the main limitations of hydrologic and hydroclimatic models is uncertainty and nonuniqueness (Anderson et al., 2015). This is because the parameter space (i.e. the set of all possible combinations of values of parameters that are used to simulate the environment by a model) can contain many different combinations of spatial parameters that can lead to mathematically equivalent predictions (BEVEN

and BINLEY, 1992). Modern practice requires the environmental modeller to report multiple calibrated models or error bounds constructed around a preferred calibrated model forecast but, as has been discussed earlier, this is not desirable in IWRM where decisions with societal impacts often have to be made based on one “correct” model (Anderson et al., 2015; Beven, 2006b).

During calibration of atmospheric or hydrological models, it is necessary to quantify the performance of the model (also referred to as *Model Evaluation*). Here, the “goodness-of-fit”, or in other words, how closely the simulated results fit the observed data, is determined by pairwise comparisons of simulated results and observed data. Sometimes, a visual inspection of the goodness-of-fit is carried out by plotting simulated and observed values on a graph and judging whether the model is simulating the system correctly based on the “match” between the two plots. The state-of-the-art, however, is to use statistical techniques to quantify the performance. The most widely used statistical metrics to assess how well a model can simulate reality include the *Pearson’s product-moment correlation coefficient* ( $r$ ) and the *coefficient of determination* ( $R^2$ ) (Legates and McCabe, 1999). However, according to Legates and McCabe (1999), these metrics can indicate that a model is a good simulator when in fact it is not. This is because correlation-based measures are oversensitive to outliers and are insensitive to additive and proportional differences between model predictions and observation (Legates and McCabe, 1999). Other measures of goodness-of-fit that have been considered in this research include *Nash-Sutcliffe Efficiency* (NSE) (Nash and Sutcliffe, 1970b), *Modified Nash-Sutcliffe Efficiency* (mNSE), *Relative Nash-Sutcliffe efficiency* (rNSE), *Mean Error* (me), *Mean Absolute Error* (mae), *Root Mean Square Error* (RMSE), *Normalized Root Mean Square Error* (nrms), *Ratio of Standard Deviations* (rSD),

*Index of Agreement* (d) (Willmott, 1981), *Modified Index of Agreement* (md), *Relative Index of Agreement* (rd), *Coefficient of Persistence* (cp), *Percent Bias* (pbias), *Kling-Gupta efficiency* (KGE), *the coefficient of determination multiplied by the slope of the linear regression between simulated results and observed data* (bR2), and *volumetric efficiency* (VE). A discussion of how some of these metrics were applied to assess model performance is given in Chapter 3.

## 2.8.2 Groundwater Model Calibration

Groundwater models are a highly simplified representation (conceptual understanding) of the subsurface system. This is because subsurface systems and aquifers are never known exactly and as such they must be mapped to a model space that adequately represents field conditions i.e. translating the conceptual model into a numerical model. This translation is necessary but further simplifies the conceptual model so that the numerical model is computationally tractable (Anderson et al., 2015, p. 376).

Model input parameters are measured in the field but often represent a small portion of the subsurface system (Carrera et al., 2005). In spite of this shortcoming, the values of heads and fluxes measured in the field usually have a higher degree of confidence associated with them than parameter values. Thus, model calibration, as is applied in groundwater modelling, belongs to a class of numerical methods known as “inversion” because the groundwater model in this case is posed as an inverse problem (Anderson et al., 2015, p. 376). In other words, the known (heads) must be *inverted* to find the unknown (aquifer properties) (Anderson et al., 2015, p. 397).

Practically, field observations are usually limited in number and thus relatively

few parameters can be estimated. Moreover, because of the spatial-temporal distribution of model inputs, the pool of parameter values could easily be infinite. Through a process referred to as *parameterization*, model inputs can be defined using a limited number of parameter values (Hill and Tiedeman, 2006, p. 5).

In this research, the popular groundwater calibration software, Parameter ESTimation Tool (PEST), was used to calibrate the groundwater flow models. PEST is a model-independent, non-linear parameter estimation software and currently one of the most advanced software for environmental model calibration and uncertainty analysis (Doherty, 2003; Doherty et al., 1994). PEST is an open-source (but also supported in commercial graphical user interfaces [GUIs]) software that can be downloaded from <http://www.pesthomepage.org/PEST.php>. Detailed theory on which PEST is based can be found in (Doherty, 2015).

Many examples of the application of PEST for the calibration of hydrological models can be found in the extant literature. Al-Abed and Whiteley (2002) used PEST to calibrate water-quantity parameters of the Hydrological Simulation Program Fortran (HSPF) model for the Grand River watershed located in southern Ontario, Canada. The study concluded that automatic calibration using the PEST model produced reliable results for the watershed and recommended that GIS data is used in the model development process. Baginska et al. (2003) performed a sensitivity analysis of the key parameters of the Annualized Agricultural Non-point Source (AnnAGNPS) model in a study aimed at predicting the export of nitrogen and Phosphorous from Currency Creek, a small catchment in the Sydney region, South Australia. In their study, PEST was recommended as a tool that can considerably reduce the time needed for identification of key parameters and consequently selection of input values.

### 2.8.3 Surface-water Model Calibration

For the calibration of surface water models (i.e SWAT models), the popular calibration tool, SWAT Calibration Uncertainties Program (SWAT-CUP) (Abbaspour et al., 2007) was used. The following algorithms are implemented in SWAT-CUP:

- Sequential Uncertainty Fitting version 2, SUFI-2 (Abbaspour et al., 2004, 2007)
- Particle Swarm Optimization, PSO (Eberhart and Kennedy, 1995; Kennedy and Eberhart, 1995)
- Generalised Likelihood Uncertainty Estimation, GLUE (BEVEN and BINLEY, 1992)
- Parameter Solution, ParaSol (van Griensven and Bauwens, 2003)
- Markov Chain Monte Carlo, MCMC (Kuczera and Parent, 1998)

It is important to note that SWAT calibration is not limited to the aforementioned algorithms. For example, Bekele and Nicklow (2007) successfully used a multi-objective automatic calibration routine employing the Non-dominated Sorting Genetic Algorithm II (NSGA-II) to calibrate a SWAT model for daily stream-flow and sediment concentration. Zhang et al. (2010) compared the performance of a multi-algorithm, genetically adaptive multi-objective method (AMALGAM) with two evolutionary multi-objective optimization methods (i.e. Strength Pareto Evolutionary Algorithm 2 (SPEA2) and Non-dominated Sorted Genetic Algorithm II (NSGA-II)) for multi-site calibration of SWAT. The authors concluded that AMALGAM performed better or as good as the single-algorithm methods for multi-site calibration of the SWAT model.

Recently, SUFI-2 has been used extensively for calibrating SWAT models. It's sudden popularity can be attributed to the fact that it is easily accessible via

SWAT-CUP and also because of the readily available documentation for application of the algorithm to SWAT calibration. Furthermore, some studies have compared the performance of SWAT-CUP based algorithms and recommended SUFI-2 as the best performing algorithm. Wu and Chen (2015), for example, used GLUE, SUFI-2 and ParaSol to evaluate uncertainty estimates in hydrological modelling for the Wenjing River watershed, China. The study concluded that, while ParaSol produced slightly higher NSE values than SUFI-2 (0.77 vs 0.75 respectively), SUFI-2 generated more balanced prediction uncertainty ranges than the other methods. Additionally, SUFI-2 and ParaSol required fewer simulations to achieve good results in comparison to GLUE, highlighting their computational efficiency. Schuol et al. (2008a) applied SUFI-2 algorithm to the calibration of a SWAT model aimed at estimating freshwater availability for a large area (4 million km<sup>2</sup>) covering eighteen countries in West Africa. The authors concluded that SUFI-2 was very efficient in localizing an optimum parameter range with a relatively small number of iterations considering the vastness of the area being modelled and the associated computational demand.

In this study, SUFI-2 algorithm was used for calibration of the SWAT models. Details of the SWAT-CUP calibration routine applied in this study are given in Chapter 3.

## 2.9 Water Governance

According to the Global Water Partnership (GWP) water governance (Rogers and Hall, 2003) is defined as follows; ‘Water governance refers to the range of political, social, economic and administrative systems that are in place to develop and manage water resources, and the delivery of water services, at different levels

of society.’ The term “governance” itself denotes some form of administrative authority through an agreed upon set of laws so as to prevent anarchy within a society. Such authority, usually exercised by governments, should be extended to the management of water resources to ensure equitable and sustainable use of the water resources. However, it has been argued by some analysts that governance should not be assumed to be synonymous with *government*; that it is instead a convergence point of different actors and stake-holders from public and private institutions including civil society and the general population (Tortajada, 2010). Thus, by it’s very nature, IWRM cannot thrive without effective water governance especially in the face of climate change and shortage of freshwater resources.

Many studies have emerged that have concentrated on forecasting future availability of water resources in the face of climate change and extreme weather (e.g., de Moraes Takafuji et al., 2019; Donevska and Panov, 2019; Erler et al., 2019; Mirmasoudi et al., 2019; Qian et al., 2018). However, without effective water governance and attendant policies, inequitable allocation and delivery of water supplies including many other challenges associated with water security could soon become irremediable especially in developing countries. Thus, *good governance* and consequently effective water governance, is central to the success of IWRM in developing countries such as Malawi.

Some researchers (e.g, Castro, 2007; Pahl-Wostl et al., 2008) have posited that to enhance water governance (including the *global water governance (GWP) paradigm*), there should be a healthy interplay between ‘techno-scientific, socio-economic, political, and cultural aspects of water management activities’ (Castro, 2007). In this thesis, techno-scientific aspects of the research and their potential application to the solution of IWRM challenges especially in the developing world,



are presented and discussed in Chapter 8.

## 2.10 Research Gap

Groundwater and surface water are often studied in isolation with respect to climate change and variability even though the two systems are related and considered as one resource from a hydrological perspective. Many studies have been published that have investigated the effects of climate change and variability on surface water resources globally (for example, Chiew and McMahon, 2002; Ficklin et al., 2009; Jha et al., 2004b; Jones et al., 2006; Luo et al., 2013; Miller et al., 2003; Stonefelt et al., 2000; Yilmaz and Imteaz, 2011). Meanwhile, few studies have investigated the effects of climate change on groundwater resources and fewer still have simulated both surface water and groundwater and the interactions thereof with respect to climate change and variability. As Hunt et al. (2013) note, using a simplistic method such as applying a percentage reduction (or increase) in the steady-state groundwater recharge rate, one can thus simulate a climate change scenario. However, such a simplistic methodology can come at a cost of missing important “inter-annual temporal characteristics of climate change” or interactions between the groundwater system and other hydrologic systems (Hunt et al., 2013). In the past decade, many IHMs have been developed and applied to the study of hydrologic systems under climate stress conditions. However, there are still relatively few studies that have applied these models to help solve IWRM problems around the world. By harnessing the power of integrated hydrologic modelling, it is hoped that the contribution made through this thesis will help to inform IWRM policy decisions in Malawi and in the UK in the quest to meet the expectations of SDG6.

## 2.11 Summary

In this chapter a review of the state-of-the-art in climate change impacts on hydrology/hydrogeology has been presented. Uncertainty in these types of studies is a critical issue that needs to be taken into consideration. Such uncertainties can propagate from GCMs to hydrologic models – a situation which can be further exacerbated by structural uncertainties in the hydrologic models themselves. Thus, it is a requirement that uncertainties arising from such processes, that is climate and hydrologic modelling, are mitigated at each step of the process. With respect to integrated hydrologic modelling, it is evident that free and open-source software tools for this task are still in their infancy. GSFLOW and SWAT-MODFLOW (extensively applied) are the main players in this category with the latter being selected for integrated hydrologic modelling in this thesis.

While a lot of studies have been done to assess impacts of climate on surface-water and groundwater as separate units, few studies have been dedicated to the study of surface- and groundwater bodies as an integrated unit. In Malawi, specifically, where the impacts of climate change are hypothesized to be more severe, there is an urgent need to quantify availability of freshwater resources and formulate climate adaptation plans to be incorporated into policy documents for a sustainable future. There is enough evidence of successful application of integrated hydrologic models especially in temperate regions and a few isolated studies in semi-arid to arid regions such as Malawi. The recently developed SWAT-MODFLOW model, forced with CMIP5 projections, will be tested in a temperate and semi-arid climate to assess its suitability as a decision support tool in hydro-climatic adaptation studies.

—*The important work of moving  
the world forward does not wait  
to be done by perfect men.*

George Eliot

# 3

## Materials and Methods

*In this chapter, methods and tools that were used in this thesis are introduced. Firstly, the research design is introduced. Thereafter, data collection and data preparation methods are discussed. Software tools and methods related to climate, hydrology and hydrogeology are discussed thereafter. Finally, a series of statistical tests that are used to assess model performance are presented.*

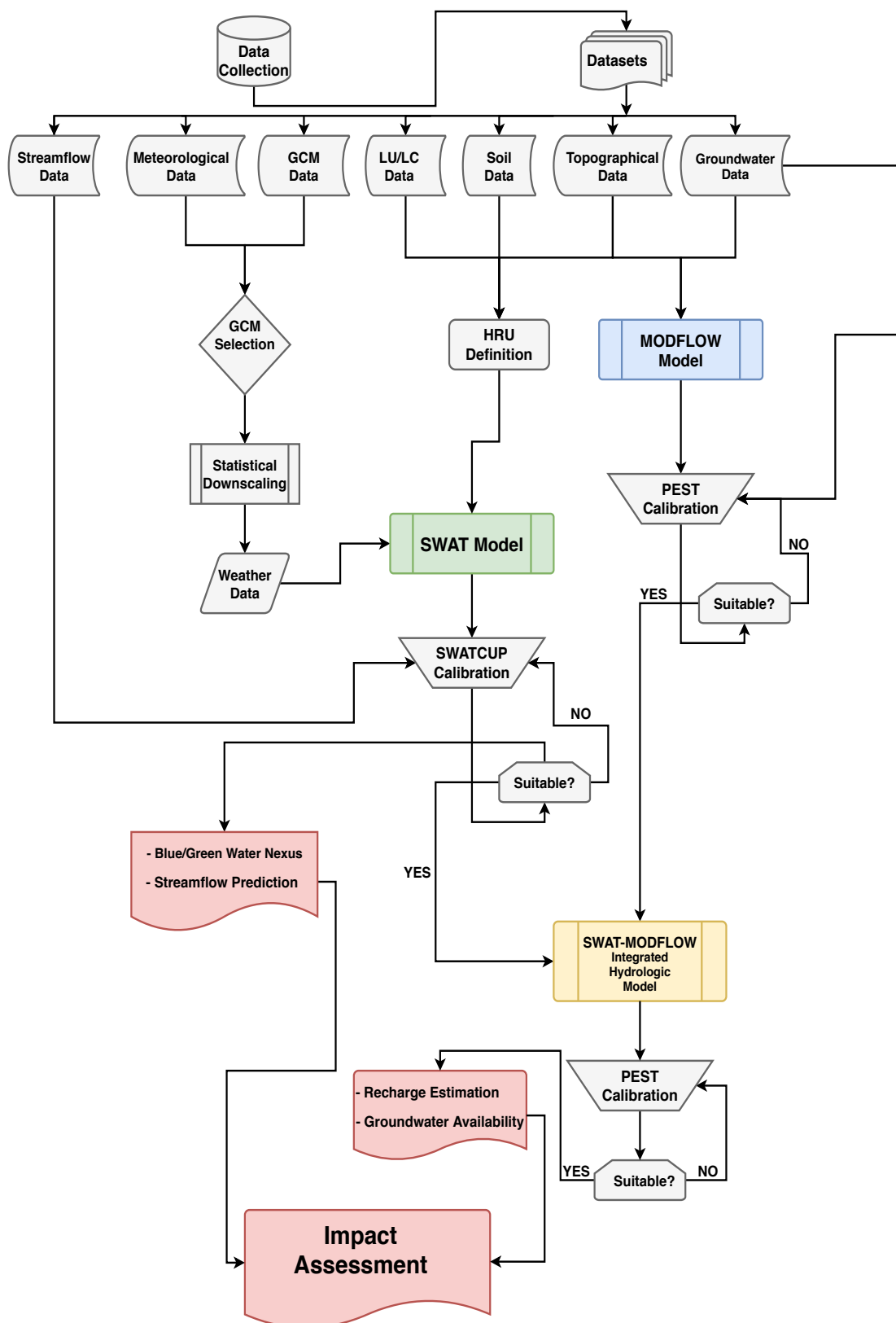
## 3.1 Research Design

### 3.1.1 Research Methodology

Quantitative research, the methodology adopted in this thesis, is a form of scholarly inquiry where data, generated in “quantitative form”, is analysed using rigorous quantitative methods (Kothari, 2004). In this paradigm, a researcher begins by formulating a theory, collecting data to support or refute the theory and finally arrives at conclusions and recommendations (Creswell and Creswell, 2017). In addition, the researcher may decide to carry out additional inquiry using a more refined approach or recommend as *possible avenues of further inquiry to other researchers*. In the context of this thesis, “quantitative research” involved firstly, analysing quantitative observations of natural and physical phenomena (e.g. climate, hydrological cycle etc.) and secondly, building models that can simulate and explain these phenomena. Specifically, Chapters 4 to 6, for example, include detailed analyses of climate, surface water hydrology and groundwater models respectively. A schematic summary of the quantitative methods used in this thesis is presented in Figure 3.1.

### 3.1.2 Comparative Analysis Approach

Application of the methods in this research begins by applying the methodology to a data-rich region before applying the same methodology to a data-scarce region (see Section 1.2.3). Thereafter, conclusions were made with respect to a) impact of climate change in the two regions and b) generalizability of the methodology (i.e can be applied in different settings).



**Figure 3.1** Schematic summary of the methodology used in this research

## **3.2 Data collection**

### **3.2.1 Meteorological Data**

#### **3.2.1.1 Shire River Basin**

The Malawi Meteorological Services (MMS) Department is responsible for meteorological data collection dating all the way back to the 1890s when the country was still a British protectorate. Until the mid 1940s, climate data was collected mostly by untrained personnel working in climate stations that also did not operate consistently. In the mid 1940s, however, a systematic network of stations under a meteorological authority began finally culminating in what is now the MMSD (MMSD, 2018). Meteorological data (rainfall, minimum and maximum temperature) were collected from the MMS.

#### **3.2.1.2 River Nith Catchment**

For the RNC, it was difficult to obtain reliable long term station data. Most stations within the catchment have records which are either outside the baseline period or within the baseline period but are too short to be used for statistical downscaling. Because of this reason, reanalysis data were used as observations to develop the statistical downscaling models. Reanalysis data are attractive in that they contain minimal or no missing data and are a consistent spatial and dynamic representation of the climate system (Deng et al., 2017). For both the RNC and SRB, the ability of two reanalysis data, namely Climatic Research Unit (CRU) (Mitchell and Jones, 2005) and Climate Forecast System Reanalysis (CFSR) (Saha et al., 2010), to reproduce the baseline hydrological regime was

compared. Pre-calibration results revealed that the CRU products were suitable for the RNC while the CFSR data produced better results in the SRB.

### 3.2.2 Global Circulation Models

Global circulation models used in this study were downloaded from the Centre for Environmental Data Analysis (CEDA) <sup>1</sup>. CMIP5 regional and global climate models were downloaded and saved on disk. To reduce computation time, the downloaded GCMs were clipped to country level scale i.e. United Kingdom in the case of River Nith Catchment and Malawi in the case of the Shire River Basin. The clipping was done using Climate Data Operators (CDO) (Schulzweida et al., 2006) software toolkit.

### 3.2.3 Topographical Maps

Topographical maps for Dumfries and the Shire River Basins were downloaded from the Shuttle Radar Topography Mission (SRTM) (van Zyl, 2001) USGS website, EarthExplorer <sup>2</sup>. For both basins, 90m digital elevation models (DEMs) were ultimately used for delineating the watersheds.

### 3.2.4 Land-use and Soil Maps

Land-use maps used in this study are derived from the USGS Global Land Cover Characterization database (EarthExplorer) with 24 classifications of land-use. Soil maps were downloaded from the TEXAS A&M UNIVERSITY SWAT website <sup>3</sup>. This product is based on the FAO-UNESCO Soil Map of the World.

---

<sup>1</sup><http://www.ceda.ac.uk/>

<sup>2</sup><https://earthexplorer.usgs.gov/>

<sup>3</sup><https://swat.tamu.edu/data/>

### 3.2.5 Streamflow Data

#### 3.2.5.1 Streamflow Data for the RNC

Streamflow data for the RNC was downloaded from the National River Flow Archive (NRFA) website<sup>1</sup>. The gauging stations from the NRFA are part of the United Kingdom Benchmark Network 2 (UKBN2) which is a subset of gauging stations from the national hydrometric network that are suitable for identification and interpretation of climate-driven hydrological trends (Harrigan et al., 2018). Table 3.1 is a summary of the gauges using for streamflow analyses for the RNC.

**Table 3.1** UKBN2 rivers in the RNC suitable for hydrological trend analyses

Station	Region	River	Location	Easting	Northing	Area (km2)	ME	BFI
79002	SEPA-SW	Nith	Friars Carse	292300	585100	799	288	0.39
79004	SEPA-SW	Scar Water	Capenoch	284500	594100	142	318.7	0.31

<sup>BFI</sup> Baseflow Index

<sup>ME</sup> Median Elevation (m AOD)

<sup>SEPA</sup> Scottish Environment Protection Agency

#### 3.2.5.2 Streamflow Data for the SRB

Streamflow data for the SRB was obtained from the Ministry of Irrigation and Water Development. Data from three gauging stations i.e. Lichenya, Rivirivi and Ruo were ultimately used for SWAT calibration and streamflow assessments under a changing climate. This is due to the large portions of missing data in the other stations rendering them unsuitable for infilling and subsequent hydrological assessments.

---

<sup>1</sup><https://nrfa.ceh.ac.uk>



### 3.3 GCM Selection

Selection of the appropriate set of GCMs to be used in climate change studies is a challenge that is yet to be unanimously resolved. Many approaches have been used in the past to tackle this problem ranging from simplistic multi-model means to complex statistical and data-driven methods (Biemans et al., 2013; Immerzeel et al., 2013; Lutz et al., 2016; Warszawski et al., 2014). In this study, a subsection from 29 GCMs for the SRB and RNC were assessed numerically and found to be capable of closely reproducing the historical record.

Several methods have been employed to assess the performance of climate models. In the literature, GCM selection methods have been classified into two broad categories namely, the past-performance approach and the envelope approach. In the former, GCMs are ranked and selected based on their ability to simulate the historical climate (Raju and Kumar, 2014) while in the latter, a subset of GCMs covering a wide range of projections is selected from the available climate models (Warszawski et al., 2014). It has become fashionable to combine both methods in order to overcome the disadvantages of the methods when used singularly. For example, the past-performance approach does not consider the agreement between GCMs in simulating the possible future climate whereas the envelope approach does not address the issue of the GCMs' ability to simulate historical climate (Pour et al., 2018; Salman et al., 2018). According to Lutz et al. (2016), a combination of the two methods can overcome these drawbacks by first screening out the models based on their past-performance and then further selecting an ensemble of GCMs based on their projections near to the higher or lower sides of the projection range (Salman et al., 2018). However, it is argued

here that because such a methodology is done sequentially, it relies heavily on the past-performance approach, which has been used extensively in the literature alongside other metrics such as the ability to reproduce extremes. Thus in this research, a combination of two methods that are past-performance based are used to rank and then select a subset of GCMs to be used for climate change impact assessment.

A survey of the literature suggests that filter and wrapper feature selection methods such as correlation coefficients, information entropy, clustering, weighted skill score, Bayesian weighting and multiple-criteria decision-making have been employed widely in the climate sciences (Pour et al., 2018). In order to select a suitable subset of GCM models for the study regions, GCMs were ranked using two methods. Firstly, a feature selection algorithm to rank the GCMs was employed. Thereafter, the GCMs were ranked using a probability density function (PDF) based skill score methodology after Perkins et al. (2007). In the first instance the information entropy based method, Symmetrical Uncertainty (Flannery et al., 1992), was used to rank the GCMs. The methodology for GCM selection and downscaling can be summarised as follows;

1. Downloading GCM ensembles with daily data
2. Development of PDFs
3. Ranking of GCMs using PDF based skill scores (Top 15 GCMs selected)
4. Development of SU models
5. Ranking of GCMs based on SU metrics (Top 10 GCMs selected)
6. Selection of final subset of GCMs (7 GCMs of which 6 were selected for the SRB and 5 for the RNC)
7. Selection of statistical downscaling method

8. Statistical downscaling of future climate
9. Development of ensemble model using the selected GCMs.

In this thesis, the GCM selection method also relied on the research by McSweeney et al. (2015) who used a multi-criteria rating system approach on a range of metrics to select a subset of GCMs that were suitable for climate change studies across multiple regions (i.e. Europe and Africa). For full details of the methodology that was used in their study, refer to McSweeney et al. (2015). Based on the evidence presented in their research where they compare their methodology to previous regional studies, the methodology used in this thesis can be considered to be robust and applicable for GCM selection in multiple regions since the results in this thesis correlate with theirs. The key difference between the methodology used in this research and theirs lies in the fact that simple numerical and statistical analyses were employed here offering many advantages such as robustness and interpretability. The methodology is described in detail in the following sections.

### 3.3.1 Symmetrical Uncertainty

*SU* is a simple goodness of feature measure that has been used in many hydro-meteorological studies. Pour et al. (2018), for example, used *SU* to select a GCM ensemble for assessment of spatial and temporal changes in rainfall of Bangladesh. Salman et al. (2018) used *SU* as part of a hybrid methodology to rank and select the GCMs for projection of spatio-temporal changes in temperature of Iraq with uncertainties.

*SU* is based on the information-theoretical concept of entropy which measures

the uncertainty of a random variable. The entropy of a variable  $X$  is defined as

$$H(X) = - \sum_i P(x_i) \log_2(P(x_i)) \quad (3.1)$$

and the entropy of  $X$  after observing values of another variable  $Y$  is defined like so:

$$H(X|Y) = - \sum_j P(y_j) \sum_i P(x_i|y_j) \log_2(P(x_i|y_j)), \quad (3.2)$$

where  $P(x_i)$  is the prior probability for all of the values of  $X$ , and  $P(x_i|y_j)$  is the posterior probabilities of  $X$  given the values of  $Y$ . The amount by which the entropy of  $X$  decreases reflects additional information about  $X$  that is provided by  $Y$ , and is called the information gain ( $IG$ ) which can be mathematically represented as:

$$IG(X|Y) = H(X) - H(X|Y). \quad (3.3)$$

Feature  $Y$ , according to this measure, is regarded to be more correlated with feature  $X$  than to feature  $Z$  if  $IG(X|Y) > IG(Z|Y)$ .

For two random variables  $X$  and  $Y$ , information gain is symmetrical. Symmetry is a desired property for a measure of correlations between features. However, information gain is biased in favour of features with more values. Moreover, the values have to be normalized to ensure they are comparable and have the same effect (Kannan and Ramaraj, 2010). Thus, we choose Symmetrical Uncertainty defined as follows:

$$SU = 2 \left[ \frac{IG(X|Y)}{H(X) + H(Y)} \right] \quad (3.4)$$

$SU$  compensates for the  $IG$ 's bias towards features with more values. These values are normalised within the range  $[0, 1]$ . The value 1 denotes that knowledge

of either one of the values completely predicts the value of the other, whereas the value 0 indicates that  $X$  and  $Y$  are independent.  $SU$  treats a pair of features symmetrically (Shreem et al., 2016).

### 3.3.2 PDF-Based Ranking

In this method, according to Perkins et al. (2007), a simple ‘skill score’ based on the comparison between simulated GCM hind-cast and observed historical data is developed. In the other words, the similarity between two PDFs is estimated by calculating the cumulative minimum value of two distributions of each binned value, whereby the common area between the two PDFs is measured (Perkins et al., 2007). Where a model replicates the historical period perfectly, a value of one is assigned. This value represents the ‘skill score’ ( $S_{score}$ ) of the GCM at that particular station or grid point in the case of gridded data. It is the total sum of the probability at each bin centre in a given PDF. Conversely, if a model simulates the historical PDF poorly, its  $S_{score}$  will be close to zero meaning there is little to no overlap between the observed and simulated PDFs (Perkins et al., 2007). Mathematically,  $S_{score}$  is represented as follows;

$$S_{score} = \sum_1^n \text{minimum}(Z_m, Z_o), \quad (3.5)$$

where  $Z_m$  and  $Z_o$  are the frequency of values in a given bin from the model and observed data respectively and  $n$  is the number of bins used to calculate the PDF for a given region.

Perkins et al. (2007) demonstrated the robustness of this method against uncertainty in the spatial-temporal coverage of the observations (Perkins and Pitman, 2009). Furthermore, this method has been found to be robust against

data limitations such as the presence of gaps and outliers as is the case in the SRB (Perkins et al., 2013). In this thesis, this method was applied to rank and filter the GCMs before applying the SU technique described in the preceding section.

### 3.4 Statistical Downscaling

The method employed for statistical downscaling of GCM models in this study is the non-parametric quantile mapping method. Non-parametric quantile mapping methods have been shown to be more reliable in reducing systematic biases in GCM outputs (e.g. Cho et al., 2016; Gudmundsson et al., 2012; Ngai et al., 2017; Themessl et al., 2011) perhaps due to the fact that they do not fit a parametric distribution to the data thus making them more flexible than other methods. However, one needs to be concerned about the possibility and dangers of using such a highly adaptable method i.e. ability to fit any quantile-quantile relation. If observed data are few (short time period of observations), potential over-fitting issues could arise and thus lead to unrealistic realisations of projected climate (Gudmundsson et al., 2012).

Generally, in quantile mapping, an attempt is made to find a function  $h$  that maps a modelled variable  $P_{sim}$  such that its new distribution equals the distribution of the observed variable  $P_{obs}$  (Gudmundsson et al., 2012). This transformation can be mathematically depicted as follows;

$$P_{obs} = h(P_{sim}) \quad (3.6)$$

and, according to Gudmundsson et al. (2012), where the distribution of the

variable of interest is known, the transformation can be formulated as,

$$P_{obs} = F_{obs}^{-1}(F_{sim}(P_{sim})), \quad (3.7)$$

where  $F_{sim}$  is the CDF of  $P_{sim}$  and  $F_{obs}^{-1}$  is the inverse CDF (i.e. quantile function) corresponding to  $P_{obs}$ .

In the case of non-parametric quantile mapping, Eq. (3.7) can be solved using the ECDFs of observed and simulated values instead of assuming parametric distributions. Tables of empirical percentiles are used to approximate ECDFs and the values in between the percentiles approximated using linear interpolation (Gudmundsson et al., 2012).

In this study, the `qmap` package by Gudmundsson et al. (2012) in the free and open source R programming environment was used to bias correct and downscale GCM model outputs for the RNC and SRB.

### 3.5 Ensemble Climate Model

In both the SRB and RNC, at least five global circulation models were adopted for climate change impact assessments. It is a well known and documented phenomenon that GCM climate projections vary from one model to the other due to the inherent structural differences in the models (Pour et al., 2018). Because each model is considered to be a possible future outcome, the experiments in this study were designed in such a way that each GCM would drive a hydrological model and only average the outputs at the end of hydrological modelling to assess climate impact. However, the case where a GCM ensemble model constructed by averaging the GCM downscaled outputs is used to drive the hydrological models

(i.e. surface- and groundwater models) was also considered. A comparison between results of such models with those of post-hydrologic simulation ensemble results was made and observations that could open up new opportunities for further inquiry in the future noted. Results are presented and discussed in Chapters 5 to 7.

A machine learning based model was developed for averaging individual GCM outputs. Machine learning, also known as statistical learning refers to a vast set of tools that are used for understanding *data* (James et al., 2013). These algorithms are sometimes referred to as ‘black boxes’ because they have little connection to the underlying physical processes related to the data they are modelling. In hydrology specifically, See et al. (2007) document that one of the criticism of these methods or *hydroinformatics* as more general term, is that they don’t add any scientific knowledge or improved understanding to the field of hydrology in general (Worland et al., 2018). However, data-driven models have the unique advantage of generating predictions or forecasts high in accuracy and in a parsimonious manner. The equations describing the multiple variables used in building the machine learning models may take a different form than the actual equations describing the physics of the hydrologic system being modelled (Cherkassky et al., 2006). Be that as it may, the power of machine learning can be harnessed in situations where accurate predictions are required over physical interpretability (Worland et al., 2018).

Data-driven models have been used extensively in the literature to simulate environmental processes such as rainfall-runoff modelling (e.g. Dibike et al., 2001; Taormina and Chau, 2015), streamflow prediction (Li et al., 2019a; Liu et al., 2019; Niu et al., 2019; Ren et al., 2018; Yan et al., 2019; Yaseen et al., 2018; Zhu



et al., 2019) and climate downscaling (Alizamir et al., 2018; Knighton et al., 2019; Ren et al., 2019; Rhee and Im, 2017; Sachindra et al., 2018; Yin et al., 2017a).

The random forest (RF) machine learning algorithm was used to build an ensemble GCM model for rainfall and temperature in the SRB and RNC using downscaled GCM variables as predictors. For completeness, a comparison between the RF model and the multi-model ensemble mean was made for purposes of determining a suitable ensemble model that can reproduce the historic or baseline climate realistically. Details of the models are given in the following sections.

#### 3.5.0.1 Random Forest

The random forest (Breiman, 2001) model, a non-parametric statistical regression algorithm, was used to generate an ensemble mean from the selected subset of GCMs.

#### 3.5.0.2 Multi-model Ensembles Mean

The multi-model ensembles mean is a simple arithmetic mean of the models which can be expressed as follows;

$$S(t) = \frac{1}{N} \sum_{i=n}^N P_n(t), \quad (3.8)$$

where  $S(t)$  is the ensemble mean at time  $t$ ,  $N$  is the total number of GCMs and  $P_n(t)$  is the projection of the  $n$ th GCM at time  $t$  (Wang et al., 2018).

## 3.6 Handling of Missing Data

Incomplete time-series data can present serious challenges in the application of climate and hydrological modelling. One of the common, scientific and principled ways that hydrologists, water managers and policy makers undertake to understand the hydrologic system is by observing changes in hydrological processes over time (Viglione et al., 2010). It follows, therefore, that inadequate, incomplete and incorrect observed data, when used to model the environment, may yield misleading results and conclusions. Hydro-meteorological data, globally, is riddled with these deficiencies but more so for developing countries such as Malawi (GYAUBOAKYE and SCHULTZ, 1994; Mwale et al., 2012). Generally, missing and dubious hydro-meteorological data occurrence can be attributed to several reasons among which are; lack of adequate resources and/or funding to support the data collection programme, lack of personnel to record readings and maintain malfunctioning instruments, lack of qualified personnel to carry out the required data quality control before presenting the data to end users, other systematic and random errors (e.g. loss of water from rain gauge during measurement, adhesion loss on the surface of the rain gauge, possible tree growth near instrument, etc.)(Teegavarapu and Chandramouli, 2005).

In Malawi, a combination of all or some of the aforementioned reasons is responsible for the lack of continuous and reliable hydro-meteorological data (Kumambala, 2010; Mwale et al., 2012). It, therefore, becomes imperative to carry out diligent quality control and estimation/imputation of gaps in observed hydro-meteorological time series data before attempting to use these data in environmental models; not only to improve the performance and confidence in the models'

ability to simulate the environment, but also to reduce the uncertainty associated with the input data (Adeloye and Rustum, 2012).

### 3.6.1 Commonly Used Infilling or Imputation Techniques

Numerous techniques have been employed for estimation of missing gaps in the physical and social sciences. Infilling or imputation in this study is defined as the process of repairing time series data where observations are missing due to disruption of data collection, systematic and random errors (Bardossy and Pegram, 2014). Generally, these methods range from simple deterministic interpolation models to complex machine learning, stochastic and data-driven methods.

While most infilling methods trace their development from the applied mathematics sciences, most applications have been in the social and bioinformatic sciences. However, the past few decades have seen a rise in application of these techniques in hydrology. A range of methods have been applied to reconstruct missing gaps in hydrology such as; univariate regressive methods (e.g. Bennis et al., 1997; Lo Presti et al., 2010), artificial neural networks (e.g. Coulibaly and Evora, 2007; Khalil et al., 2001; Kim and Pachepsky, 2010; Singh and Datta, 2007), self organizing maps (e.g. Adeloye and Rustum, 2012; Kalteh and Berndtsson, 2007; Kalteh and Hjorth, 2009; Mwale et al., 2012, 2014; Nanda et al., 2017), data-driven methods (e.g. Ahani et al., 2018; Deng and Wang, 2017; Oriani et al., 2017).

In this research, infilling was applied to streamflow and meteorological time-series data. Although gaps were present in meteorological data, application of these data in the SWAT model in particular may not be problematic. This is because the SWAT model has the ability to use a user defined weather database

to generate climatic data or to fill in gaps in observed records (Fuka et al., 2014a; Neitsch et al., 2011). The Climate Forecast System Reanalysis (CFSR) global meteorological dataset was used for this purpose in the SWAT model. However, despite this important capability of the SWAT model, reconstruction of missing gaps in the meteorological data was a necessary step before statistically downscaling GCM outputs to point or station scale. Thus meteorological data for the observed (baseline) period did not include missing gaps at the time of application in the SWAT model.

In a recent study (Javier Miro et al., 2017), ten methods for massive imputation of missing rainfall data series were tested and validated for both monthly and daily data. The results indicated that the *Non-linear Principal Component Analysis (NLPCA)* method and its variants was among the three best performing methods from a pool which featured the popular and successful *Self-Organizing Map*, (SOM) (Kohonen, 1998) method. According to Javier Miro et al. (2017), this was unexpected as the SOM method has successfully been applied in the past to reconstruct missing gaps in both rainfall and streamflow time series (e.g. Adeloye and Rustum, 2012; Kalteh and Berndtsson, 2007; Kalteh and Hjorth, 2009; Mwale et al., 2012, 2014; Nanda et al., 2017, to select a few from plenty in the literature). However, the success of the SOM in different climatic settings and watersheds cannot be overlooked. For example, in the SRB, Mwale et al. (2012, 2014) successfully used the SOM to augment observed rainfall and streamflow time series data with reported  $R^2$  values greater than 0.9 (streamflow) and 0.7 (rainfall).

### 3.6.2 Adopted Infilling Method

While the NLPCA and SOM methods have been applied successfully for infilling missing gaps in datasets worldwide, we decided not to adopt these methods. This is because these methods are essentially forms of neural networks that require additional data or ‘features’ to be used in predictive modelling. In most cases, such data is not available. For example, Mwale et al. (2012) got better results when the SOM algorithm was trained on a combination of water levels and streamflow. Where many gauges are present, a multivariate relationship is created where information in terms of *weights* from one station is used to predict or infer values in other gauges. Thus correlation (e.g., correlation between water levels and streamflow) plays a significant role in the results of the SOM and NLPCA methods.

In this thesis, a univariate method was employed for streamflow missing data imputation. Climate data was augmented and gap-filled using reanalysis products as discussed in Section 3.2.1.2. The freely available *imputeTS* (Moritz and Bartz-Beielstein, 2017) package written in the R programming language was adopted for carrying out this task.

To test the imputation methodology, streamflow records from 5 gauging stations in the RNC were relied upon. This is because of the high integrity of this data which has little to no missing gaps. Thereafter, 20% of the observations were then sampled at random without replacement and omitted using custom scripts written in the R programming language. The time period considered for all the gauging stations is from 1<sup>st</sup> January, 1970 to 31<sup>st</sup> December, 2014 for uniformity. The *imputeTS* package implements a lot of methods for imputation but in this case it was found that the `na_kalman` algorithm performed better than

the others. The `na_kalman` function implements “Imputation by ARIMA State Space Representation and Kalman Smoothing” methodology whose details can be found in Moritz and Bartz-Beielstein (2017).

Results of the imputation process are summarised in Table 3.2. With the exception of Nith at Drumlanrig, the imputation performed very well with Nash-Sutcliffe Efficiency (NSE) and  $R^2$  values  $\geq 90$ . ME and MAE values were small in all cases except for the gauging station at Drumlanrig. It should be noted that an entire year (2002) was missing from this gauging station which could potentially explain the lower NSE and  $R^2$  values. Notwithstanding this, the NSE and  $R^2$  values are satisfactory and acceptable, proving the versatility of the `na_kalman` function implemented in the `imputeTS` package.

**Table 3.2** Performance of the infilling technique adopted in this study

Station	Metric					
	ME	MAE	RMSE	PBIAS %	NSE	$R^2$
Nith at Friars Carse	-0.04	2.24	10.20	-0.10	0.91	0.91
Nith at Hall Bridge	-0.01	0.55	2.43	-0.20	0.92	0.92
Scar Water at Capenoch	-0.03	0.58	2.57	-0.50	0.90	0.90
Cluden Water at Fiddlers Ford	-0.04	2.24	10.20	-0.10	0.91	0.91
Nith at Drumlanrig	-11.30	11.82	20.08	-39.30	0.67	0.87

## 3.7 Hydrologic Models Development

### 3.7.1 MODFLOW

All MODFLOW models were designed and implemented in ModelMuse (Winston, 2009), a free graphical user interface (GUI) for MODFLOW developed by the

USGS. The GUI enables a modeller to import model input files such as topographic data is ASCII or raster data, GIS shapefiles containing model parameters and many other text files. The conceptual models were developed by pre-processing model inputs mostly in a GIS (QGIS) environment before importing them into ModelMuse.

In the future, it is intended to automate the design and implementation of these models using FloPy written in the Python programming language. This will enable independent reviewers and/or end users of the models to easily reproduce the results. The main attraction of using ModelMuse in this case is that MODFLOW outputs can readily be coupled with SWAT using tools such as QSWATMOD or SWATMOD-Prep developed by Park et al. (2019) and Bailey et al. (2017) respectively.

### 3.7.2 SWAT

For assessment of surface-water and related hydrologic components, the SWAT model was used. The model is freely available and can be downloaded from <https://swat.tamu.edu/>. In this research, SWAT 2012 version was used for simulating hydrologic processes. If model files are already prepared elsewhere, one can simply run the model using the downloaded executable files from the website. If the model files are to be prepared from scratch, two options are available via ArcSWAT and QSWAT. ArcSWAT is a public domain plugin for the commercial GIS platform ArcGIS while QSWAT, also in the public domain, is a plugin for the free GIS platform QGIS.

Depending on the purpose of the project, multiple model inputs are required for SWAT. Firstly topographic data was downloaded and fed into the model.

Initially, the watersheds were delineated using a 1 arc-second resolution DEM but achieved poor results during watershed delineation, calibration and heavy use of computer resources. When the same process was attempted using a 3 arc-second resolution DEM, results were greatly improved. Other SWAT inputs include LU/LC data which should be supplied in raster format, soil types of the study area also supplied in raster format and finally weather data supplied as text files.

In this study, the ArcSWAT interface was used to develop the SWAT models to overcome the prohibitively long processing times of QSWAT. The QSWAT interface takes a considerably longer time to process large DEMs. For example, processing the DEM for the SRB took approximately 17 hours and 22 minutes compared to 20 minutes on an HP desktop computer with an Intel Core i7-6500U processor and 16GB RAM. Because of the need to frequently revise the experiments and model structure, a decision was made to go for the advantageous speeds offered by the ArcSWAT interface. Conveniently, to enable knowledge exchange and sharing between modellers and other stakeholders, the ArcSWAT models were converted to QSWAT using a freely available tool made available by the QSWAT developers. Although there are a few visual changes such as the subbasin numbers, the structure of the model remains essentially the same.

In general, the SWAT model can and has been used to predict the impact of climate change, management on water, sediment and agricultural sediment yields in both gauged and ungauged basins (Arnold et al., 1998). The model divides a watershed or basin into smaller units referred to as subbasins. The hydrological processes in the subbasins are controlled by smaller units called "hydrologic response units" or HRUs. Model input data such as DEMs, LU/LC, climate



and soil data are then used to compute hydrological processes, sedimentation, soil temperature, crop growth, nutrients and agricultural management using subroutines coded in the FORTRAN programming language (Arnold et al., 1998). A generic SWAT model operation flow-chart is present in Figure 3.2. After developing the SWAT models, the free software tool, SWAT-CHECK, which is used to summarise and visualize SWAT results was run. The tool also provides a feature which allows to check for errors in the SWAT model.

### 3.7.3 SWAT-MODFLOW

In order to address the issue of integrated hydrologic modelling, two popular hydrological modelling tools namely, SWAT and MODFLOW, were used. The models have individual weaknesses and limitations that can be overcome by harnessing the strengths of the discrete models in a synergistic manner. For example, while SWAT has a dedicated module for simulating groundwater components (ARNOLD et al., 1993), it is not possible to calculate distributed parameters such as hydraulic conductivity because the model is lumped (Kim et al., 2008). Additionally, the SWAT model presents some difficulties when it comes to adequately expressing the spatial distribution of groundwater recharge rates and levels (Kim et al., 2008). Conversely, the strength of MODFLOW lies in its ability to adequately and accurately simulate subsurface flow. However, one disadvantage of MODFLOW is the difficulty associated with determining the groundwater recharge quantities when used as the main input to the groundwater model (Kim et al., 2017). Additionally, the issue of high correlation between hydraulic conductivity and recharge rates makes groundwater flow modelling results amenable to uncertainty. Thus, it is important to know or at least obtain the closest estimates to reality of groundwater

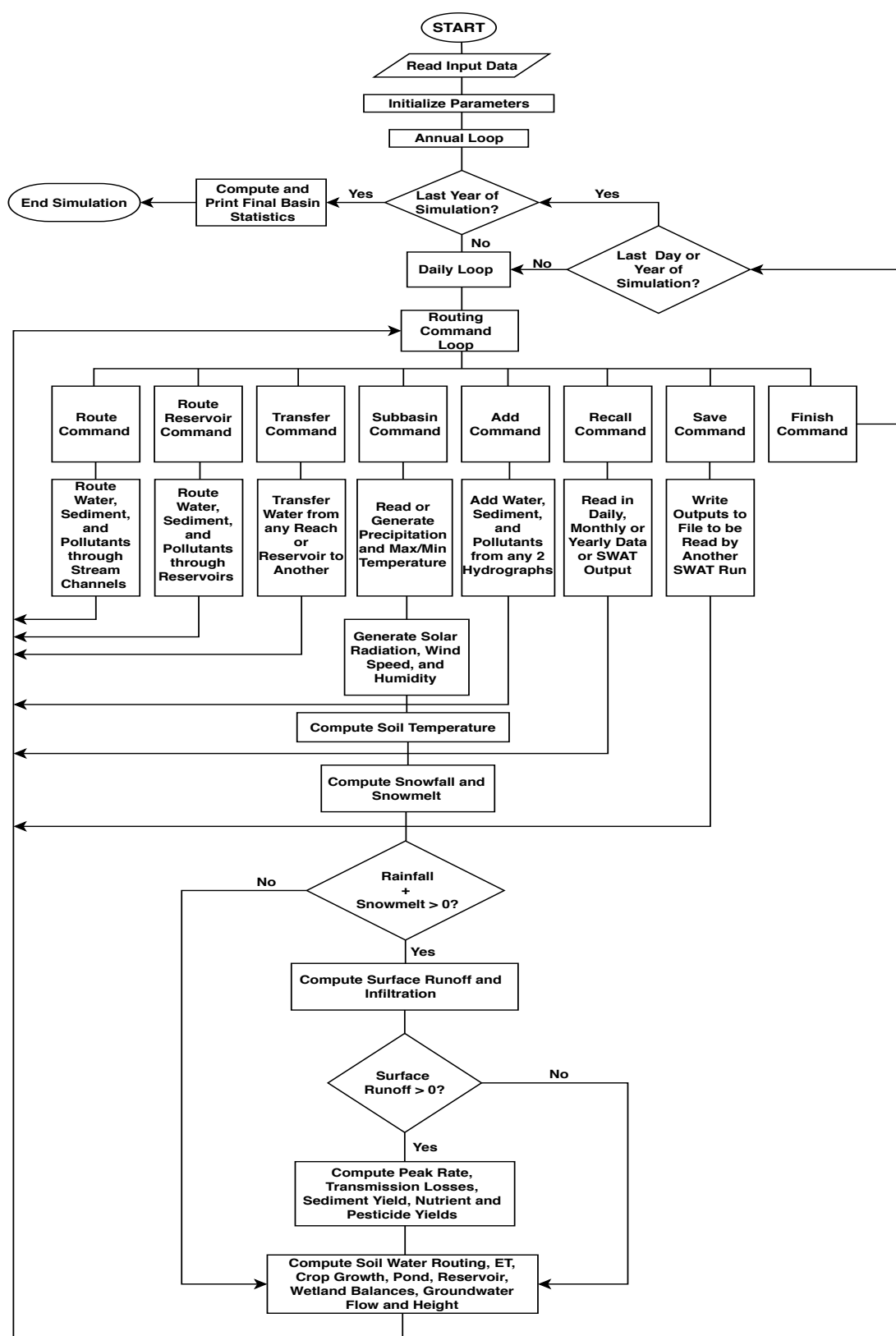
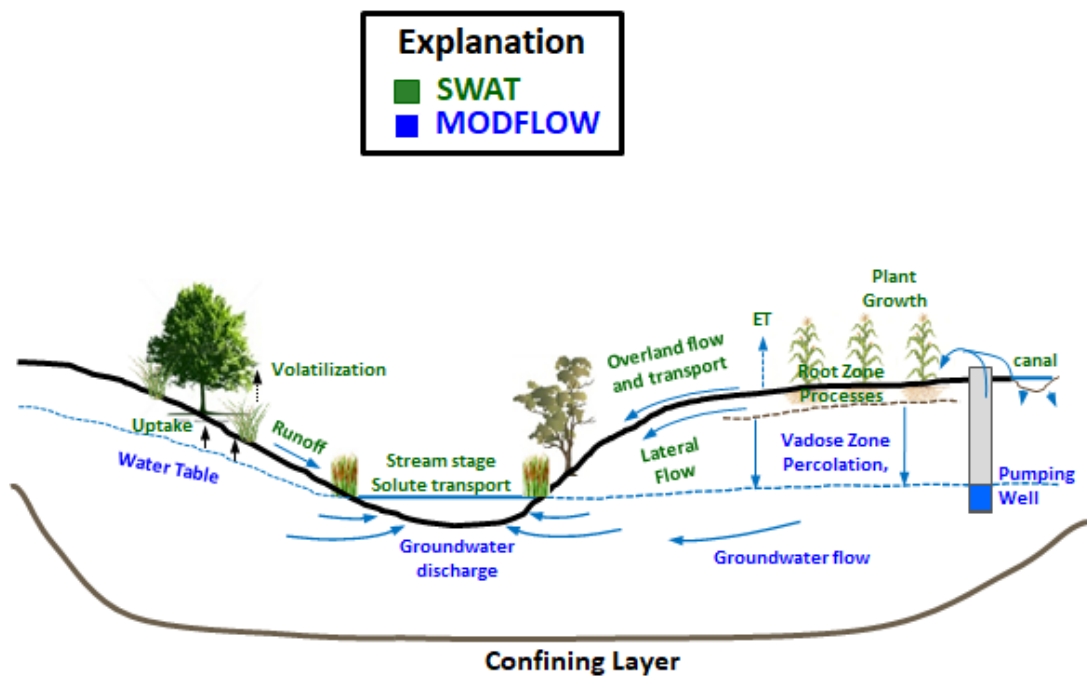


Figure 3.2 SWAT model operation flow-chart (modified from Arnold et al. (1998))

recharge rates to adequately constrain model solutions for accurate predictions. SWAT-MODFLOW provides a robust platform for integrated hydrologic modelling (IHM) where different aspects of the hydrologic cycle can be modelled.

This study employs a coupled SWAT-MODFLOW model recently developed by Bailey et al. (2016). It should be noted that there have been many other successful attempts at coupling SWAT and MODFLOW (e.g. Chung et al., 2010; Galbiati et al., 2006; Luo and Sophocleous, 2011; Sophocleous and Perkins, 2000) for application to a variety of watersheds around the world. However, the integrated model used in this study has many advantages over the previous models such as the ability to couple SWAT and MODFLOW models of varying spatial extent; an efficient Hydrologic Response Unit (HRU) grid cell mapping scheme, geographically located HRUs and the integration of MODFLOW-NWT for robust handling of dry cells in the unconfined aquifers (Bailey et al., 2016). A general overview of the capabilities of the SWAT-MODFLOW model used in this study is shown in Fig. 3.3.



**Figure 3.3** General overview of SWAT-MODFLOW (modified from Park et al. (2019))

## 3.8 Metrics of a “Good Model”

### 3.8.1 SWAT

In order to assess SWAT and MODFLOW models’ performance during calibration and validation, statistical and graphical model evaluation techniques were employed. The model evaluation statistics used in this thesis are presented here.

1. **Nash-Sutcliffe Efficiency (NSE):** The Nash-Sutcliffe efficiency (NSE), proposed by Nash and Sutcliffe (1970a) is defined as the ratio of the sum of absolute squared differences between the observed and simulated values to the variance of the observed values (Krause et al., 2005). The metric is an indication of “how well the plot of observed versus simulated data fits the

1:1 line” (Moriasi et al., 2007). It is calculated as follows:

$$NSE = 1 - \left[ \frac{\sum_{i=1}^n (Y_i^{obs} - Y_i^{sim})^2}{\sum_{i=1}^n (Y_i^{obs} - Y^{mean})^2} \right] \quad (3.9)$$

where  $Y_i^{obs}$  is the  $i$ th observed value,  $Y_i^{sim}$  is the  $i$ th simulated value,  $Y^{mean}$  is the mean of observed values and  $n$  is the total number of observations. NSE ranges between  $-\infty$  and 1 with NSE value of 1 being the optimal value.

2. **Percent Bias (PBIAS):** Percent bias is a measure of the average tendency of the predicted values to be larger or smaller than the observed values (Gupta et al., 1999; Moriasi et al., 2007). It is calculated as follows:

$$PBIAS = \left[ \frac{\sum_{i=1}^n (Y_i^{obs} - Y_i^{sim}) * (100)}{\sum_{i=1}^n (Y_i^{obs})} \right] \quad (3.10)$$

where PBIAS is the deviation of the variable being evaluated, expressed as a percentage.

3. **Coefficient of determination ( $r^2$ ):** The coefficient of determination  $r^2$  describe the degree of collinearity between simulated and observed data and the proportion of the variance in measured data explained by the model (Moriasi et al., 2007). It ranges from 0 to 1 with a value of zero denoting no correlation and a value of 1 denoting less error variance. It is calculated as:

$$r^2 = \left( \frac{\sum_{i=1}^n (O_i - \bar{O})(P_i - \bar{P})}{\sqrt{\sum_{i=1}^n (O_i - \bar{O})^2} \sqrt{\sum_{i=1}^n (P_i - \bar{P})^2}} \right)^2 \quad (3.11)$$

where  $O$  and  $P$  are observed and predicted values respectively.

4. **Mean Error (ME):** The mean error is the mean difference of the residual errors between two continuous variables defined as follows;

$$ME = \frac{1}{n} \sum_{i=1}^n (h_m - h_s)_i \quad (3.12)$$

where  $h_m$  and  $h_s$  are the measured and simulated heads respectively, and  $n$  is the number of targets. A small ME is an indication that the overall model fit is unbiased or in other words, the simulated values are generally neither too high nor too low (Anderson et al., 2015). Generally, ME is only capable of describing the model bias and is hence considered to be a poor or weak indicator of goodness of model fit.

5. **Mean Absolute Error (MAE):** The mean absolute error is defined as the mean of the absolute value of the residual (Anderson et al., 2015). It is defined as follows;

$$MAE = \frac{1}{n} \sum_{i=1}^n |(h_m - h_s)_i| \quad (3.13)$$

MAE is considered to be a better indicator of model fit because the positive and negative residuals do not cancel as is the case with ME. Thus, MAE values are usually larger than ME (Anderson et al., 2015).

6. **Root Mean Squared Error (RMSE):** is defined as the average of the squared residuals between two continuous variables. It is given by;

$$RMSE = \left[ \frac{1}{n} \sum_{i=1}^n (h_m - h_s)_i^2 \right]^{0.5} \quad (3.14)$$

One of the disadvantages of RMSE is that it is sensitive to the effects of outlier residuals and thus typically larger than the MAE.

7. **Nash–Sutcliffe Efficiency (NSE)**: This metric is particularly useful when comparing observed and simulated hydrographs for transient models (Anderson et al., 2015). Again, NSE ranges from  $-\infty$  to 1, with values close to 1 indicating good model fit.

$$NSE = 1 - \frac{\sum_{i=1}^n |(h_m - h_s)|_i^2}{\sum_{i=1}^n |(h_m - \bar{h}_m)|_i^2} \quad (3.15)$$

where  $\bar{h}_m$  is the mean of observed head.

## 3.9 SWAT and MODFLOW Calibration

### 3.9.1 Calibration with SWAT-CUP

The SWAT calibration strategy employed in this research involves the application of SUFI-2 algorithm implemented in SWAT-CUP. SUFI-2 was selected for multi-gauge streamflow calibration and prediction uncertainty due to its popularity and ease of implementation. The performance and choice of an algorithm to use for calibration is dependent on, inter alia, factors such as modeller's familiarity with the algorithm, size of watershed, strength of computational resources and time constraints. Because of the different philosophical underpinnings of the algorithms implemented in SWAT-CUP, the user is left with some freedom of how they can formulate the objective function, generalized likelihood measure or likelihood function; thus, an unbiased comparison between these algorithms is not possible and would be subjective at best (Yang et al., 2008).

### 3.9.2 Conceptual and Theoretical Basis of SUFI-2

Uncertainty in the SWAT driving variables such as rainfall and temperature including uncertainty in the conceptual model, observed data (e.g. streamflow, evapotranspiration), is accounted for in SUFI-2 by the  $P$ -factor, which is the percentage of observed data bracketed by the 95% prediction uncertainty (95PPU). The 95PPU is calculated at the 2.5% ( $X_L$ ) and 97.5% ( $X_U$ ) percentiles of the cumulative distribution of output variables obtained via Latin Hypercube (LH) sampling. 95PPUs represent an envelope of possible and good solutions generated by certain parameter ranges in a stochastic calibration approach (Abbaspour et al., 2007; Setegn et al., 2010). In a SUFI-2 calibration campaign, to quantify the fit between observed and simulated results (95PPU), two statistics are used:  $P$ -factor and  $R$ -factor. The  $P$ -factor ranges from 0 to 1, where 1 indicates perfect model simulation considering uncertainty (Abbaspour et al., 2004, 2015). For streamflow calibration, Abbaspour et al. (2015) recommend a value  $> 0.7$  or  $0.75$  to be adequate. For the  $R$ -factor, which is the ratio of the average thickness of the 95PPU band and the standard deviation of the measured variable, a value of  $< 1.5$  would be desirable (Abbaspour et al., 2015). According to (Abbaspour et al., 2007) the SUFI-2 procedure can be summarised as follows:

1. In the first instance, the objective function is formulated.
2. In the second step, meaningful parameter ranges (i.e. absolute minimum and maximum) for the parameters being optimized are defined. It is assumed that all parameters are uniformly distributed within the region bounded by the range of parameter values defined as follows:

$$b_j : b_{j,\text{abs\_min}} \leq b_j \leq b_{j,\text{abs\_max}}, \quad j = 1, \dots, m, \quad (3.16)$$



where  $b_j$  is the  $j$ -th parameter and  $m$  is the number of parameters to be estimated.

3. The third step involves an “absolute sensitivity analysis” in the initial stages of calibration for all parameters.
4. Next, initial uncertainty ranges are assigned to parameters for the first round of LH sampling as follows;

$$b_j : [b_{j,\min} \leq b_j \leq b_{j,\max}], \quad j = 1, \dots, m. \quad (3.17)$$

The ranges defined by Eq. (3.17) are generally smaller than the absolute ranges. The sensitivity analysis carried out in step 3 can be used as a guide in selecting appropriate ranges.

5. In this step, a LH sampling is carried out to produce  $n$  parameter combinations, where  $n$  is the desired number of simulations (should be between 500 – 1000). After the simulated program is run for  $n$  times, the simulated output variable(s) of interest are saved.
6. In this step the objective function,  $g(\mathbf{b})$ , is calculated and the sensitivity matrix,  $\mathbf{J}$ , of  $g(\mathbf{b})$  is computed using:

$$J_{i,j} = \frac{\Delta g_i}{\Delta b_j}, \quad i = 1, \dots, C_2^m, \quad j = 1, \dots, m, \quad (3.18)$$

where  $C_2^m$  and  $j$  are the number of rows and columns in  $\mathbf{J}$  respectively. Thereafter, the equivalent of a Hessian matrix,  $\mathbf{H}$ , and the covariance matrix,  $\mathbf{C}$ , are calculated as;

$$\mathbf{H} = \mathbf{J}^T \mathbf{J}, \quad (3.19)$$

$$\mathbf{C} = s_g^2(\mathbf{J}^T \mathbf{J})^{-1}, \quad (3.20)$$

where  $s_g^2$  is the variance of  $g(\mathbf{b})$  values resulting from the  $n$  runs.

7. In this step the 95% confidence interval and estimated standard deviation of a parameter  $b_j$  is calculated from the diagonal elements of the covariance matrix like so;

$$s_j = \sqrt{\mathbf{C}_{jj}} \quad (3.21)$$

$$b_{j,\text{lower}} = b_j^* - t_{v,0.025} s_j \quad (3.22)$$

$$b_{j,\text{upper}} = b_j^* + t_{v,0.025} s_j, \quad (3.23)$$

where  $b_j^*$  is the parameter  $b$  for one of the best solutions (i.e. parameters which produce the smallest value of the objective function) and  $v$  is the degrees of freedom ( $n - m$ ).

8. Here, parameter correlations and sensitivities are calculated using Eqs. (3.24) and (3.25) as follows;

$$r_{ij} = \frac{C_{ij}}{\sqrt{C_{ii}}\sqrt{C_{jj}}} \quad (3.24)$$

$$g = \alpha + \sum_{i=1}^m \beta_i b_i. \quad (3.25)$$

Parameter correlations are evaluated using diagonal and off-diagonal terms of the covariance matrix while parameter sensitivities are calculated by multiple regression of the LH generated parameters against the objective function values.

9. In this step, the goodness of fit is assessed by the uncertainty measures calculated from the percentage of measured data bracketed by the 95PPU

band, and the average distance  $\bar{d}$  between  $(X_L)$  and  $(X_U)$  from:

$$\bar{d}_X = \frac{1}{k} \sum_{l=1}^k (X_U - X_L)_l, \quad (3.26)$$

where  $k$  is the number of observed data points. Thereafter, the  $R$ -factor mentioned earlier is calculated using Equation (3.27);

$$\text{R-factor} = \frac{\bar{d}_X}{\sigma_X}, \quad (3.27)$$

where  $\sigma_X$  is the standard deviation of the measured variable  $X$ .

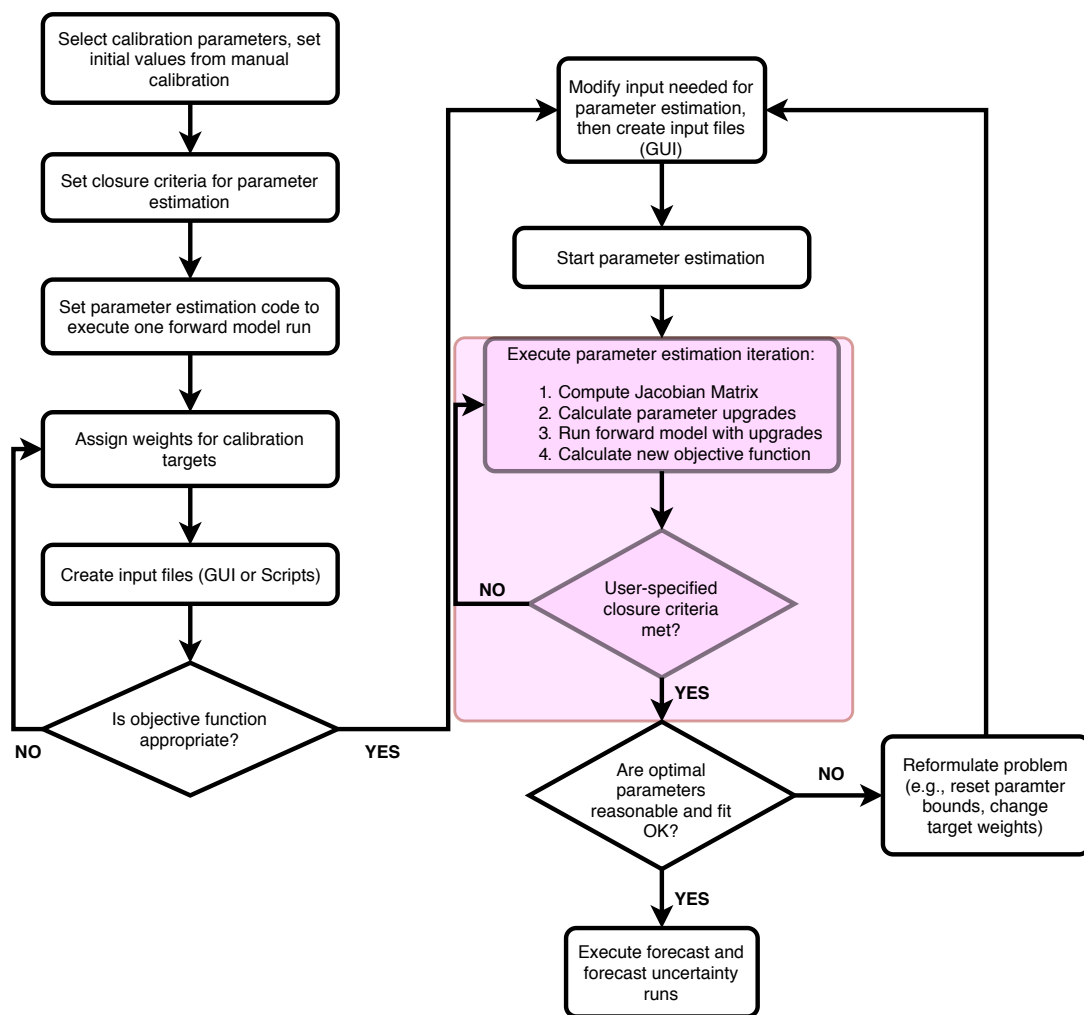
10. Finally, parameters are ranked according to their sensitivities and highly correlated parameters identified.

### 3.9.3 MODFLOW Calibration

A typical MODFLOW calibration flowchart is given in Figure 3.4. Data preparation of input files was done using a combination of GUIs (Excel) and programming scripts (Python and R programming languages). Most of the steps highlighted in Figure 3.4 are performed automatically by PEST which relies on instructions supplied by the ‘pest control file’. The pest control file contains information about the optimization algorithms and other boundary conditions specified by the modeller. During MODFLOW calibration, boundary conditions and model conceptualizations were changed before fresh calibration campaigns were performed.

### 3.9.4 Calibration Periods

For the SWAT model, calibration was done using streamflow gauge data whereas for MODFLOW, the steady-state model was calibrated using historical groundwater



**Figure 3.4** Flowchart highlighting the major steps of calibrating a predictive groundwater model (Adapted from (Anderson et al., 2015, p. 399))

heads. Calibration periods for the SWAT model were thus dependent on the streamflow time-series data for each station. For the RNC, SWAT simulation was set to run from January 1979 to December 2005 but the calibration parameters were applied according to their time definition in SWAT-CUP as shown in Table 3.3. However, the model was assigned a “warm-up” period of 6 years so results were only printed from January 1985 to December 2005. Similarly, the SRB model was assigned to run from January 1975 to December 2005 with a warm-up period of 6

years so results were only printed from January 1981 to December 2005.

**Table 3.3** SWAT and MODFLOW calibration periods for the RNC and SRB

SWAT					MODFLOW	
Station	Calibration		Validation		Calibration	
	From	To	From	To	From	To
	RNC					
Scar Water at Capenoch	Jan-85	Dec-00	Jan-01	Dec-05	Jan-79	Dec-05
Cluden Water at Fiddlers Ford	Jan-85	Dec-00	Jan-01	Dec-05		
Nith at Friars Carse	Jan-85	Dec-00	Jan-01	Dec-05		
Lochar Water at Kirkblain Bridge	Jan-85	Dec-00	Jan-01	Dec-05		
	SRB					
Rivi-Rivi River at Balaka	Jan-86	Dec-89	Jan-90	Sep-91	Jan-75	Jan-05
Ruo River at M1 Roadbridge	Jan-85	Dec-89	Jan-90	Oct-91		
Lichenya River at Mini Mini Estate	Jan-81	Dec-88	Jan-89	Oct-91		

MODFLOW for the two regions was calibrated for same period as the SWAT models with the same “spin-up” or warm-up times. However, in the case of MODFLOW, there was no need for a validation period since no observed data was withheld for validation. This follows observations and recommendations made by Anderson et al. (2015) and Doherty and Hunt (2010) against ‘withholding’ data during calibration as a groundwater model cannot be *validated*. Rather, it can only be invalidated but at a certain level of confidence (Doherty and Hunt, 2010).

### 3.10 Statistical Tests

Various statistical tests were used to assess linear relationships, variability of variables and also to detect trends in hydro-meteorological data. Beyond simple descriptive statistics, non-parametric tests were employed for trend detection since they do not assume that the data follows a particular distribution. Furthermore, non-parametric tests are more capable of handling outliers in the data including

many forms of non-normality (Kadioglu, 1997; Lanzante, 1996). The following is a brief description of the statistical methods that were employed in this research:

1. **Mann-Kendall trend test (MK test):** Introduced by Mann (1945) and modified by Kendall (1975), the Mann-Kendall trend test is one of the most popular non-parametric techniques for detecting changes in time-series data. In hydrological and climate change studies, many researchers have used this test to detect statistically significant trends in hydro-meteorological data (e.g. Ahmad et al., 2015; Gocic and Trajkovic, 2013; Tabari and Talaee, 2011; Yue et al., 2002a; Yue and Wang, 2002). The Mann-Kendall test statistic is calculated as:

$$S = \sum_{k=1}^{n-1} \sum_{j=k+1}^n \text{sgn}(x_j - x_k) \quad (3.28)$$

where  $n$  is the number of data points,  $x_k$  and  $x_j$  are data points in time-series  $k$  and  $j$  ( $j > k$ ) respectively. The term  $\text{sgn}(x_j - x_k)$  is the sign function defined as:

$$\text{sgn}(x_j - x_k) = \begin{cases} +1 & \text{if } (x_j - x_k) > 0 \\ 0 & \text{if } (x_j - x_k) = 0 \\ -1 & \text{if } (x_j - x_k) < 0 \end{cases} \quad (3.29)$$

The variance of the test statistic,  $S$ , is given by

$$\text{Var}(S) = \frac{1}{18} \left[ n(n-1)(2n+5) - \sum_{i=1}^m t_i(t_i-1)(2t_i+5) \right] \quad (3.30)$$

where  $n$  is the number of the data values,  $m$  is the number of tied groups and  $t_i$  is the number of data points in the  $i$ th group. A tied group is defined as a set of sample data having the same value. According to Kendall (1975);

Mann (1945), where the sample size  $n > 10$ , the standard normal variable  $Z$  is computed as follows:

$$Z = \begin{cases} \frac{S-1}{\sqrt{Var(S)}} & \text{if } S > 0 \\ 0 & \text{if } S = 0 \\ \frac{S+1}{\sqrt{Var(S)}} & \text{if } S < 0 \end{cases} \quad (3.31)$$

where positive values of  $Z$  indicate increasing trends while negative values of  $Z$  depict decreasing trends. Trends are tested at a specified  $\alpha$  significance level where the null hypothesis is rejected for absolute values of  $Z$  greater than  $Z_{1-\alpha/2}$  obtained from standard normal distribution tables. For example, using a significance level  $\alpha = 0.05$  (i.e 5% significance level) as was used in this research, the null hypothesis of no trend is rejected if  $|Z| > 1.96$ . At 1% significance level, the null hypothesis of no trend would be rejected if  $|Z| > 2.576$ .

2. **Effects of serial correlation:** Studies by vonStorch (1995) have shown that it is necessary to remove serial correlation from time-series data by a procedure known as “pre-whitening” (i.e. make the series free of autocorrelation). This is a necessary step in time-series data where a lag-one autoregressive AR(1) and linear trend are present. The former alters the variance of the estimate of  $S$  while the latter “alters the estimate of the magnitude of serial correlation” (Yue et al., 2002b). However, research by Yue et al. (2002b); Yue and Wang (2002) have argued that while pre-whitening can effectively remove the AR(1) component, it has the unwanted side-effect of removing a portion of the trend, if at all a trend exists; thus the slope

of the trend is smaller after pre-whitening than it is prior to pre-whitening. The net effect is that significant trends may be underestimated. The authors advocated for a trend-free pre-whitening (TFPW) approach that detrends the series before pre-whitening leading to a more accurate estimate of the true AR(1). In addition to the traditional MK test, this approach was also adopted in this research. The TFPW procedure can be summarized as follows (refer to Yue et al. (2002b) for a comprehensive mathematical treatment of the TFPW):

- Firstly, the slope of a trend in the sample is computed by the Theil–Sen approach (TSA) (Sen, 1968; Thiel, 1950a,b,c).
- Secondly, the identified trend is assumed to be linear and removed from the sample data if the slope differs from zero, resulting in a detrended time-series.
- In the third step, the lag-1 serial correlation coefficient of the detrended series from step 2 is calculated and the AR(1) component removed.
- Lastly, the modified residual series and the identified trend are combined and the tradition MK test applied to assess the significance of the trend in the combined series.

3. **Theil-Sen estimator (TSE):** Developed by Sen (1968), Theil-Sen estimator method (also referred to as the Sen’s slope estimator method) is a non-parametric technique for estimating the magnitude of trends in time-series data. In the TSE method, a linear model is used to estimate the slope of the trend and the variance of the residuals should be constant in



time (da Silva et al., 2015) as follows:

$$Q_i = \frac{X_j - X_k}{j - K} \quad \text{for } i = 1, \dots, n \quad (3.32)$$

where  $X_j$  and  $X_k$  are the data points at times  $j$  and  $k$  ( $j > k$ ), respectively. Where only one datum exists in each time period,  $N = n(n - 1)/2$ , where  $n$  is the number of time periods. Conversely,  $N < n(n - 1)/2$  if there are multiple observations in one or more time periods. Ranking the  $n$  values of  $Q_i$  in ascending order, the median of the slope or TSE is calculated as:

$$Q_{\text{med}} = \begin{cases} Q_{[(n+1)/2]}, & \text{if } n \text{ is odd} \\ \frac{Q_{[n/2]} + Q_{[(n+2)/2]}}{2}, & \text{if } n \text{ is even} \end{cases} \quad (3.33)$$

Positive and negative  $Q_{\text{med}}$  values (sign of  $Q_{\text{med}}$ ) indicate increasing and decreasing trends respectively while the magnitude of  $Q_{\text{med}}$  indicates the steepness of the trend. The confidence interval of  $Q_{\text{med}}$  at a specified probability is calculated to determine whether the median slope is statistically different from zero as follows:

$$C_\alpha = Z_{1-\alpha/2} \sqrt{\text{Var}(s)} \quad (3.34)$$

where  $\text{Var}(S)$  is as defined in Eq. (3.30) and  $Z_{1-\alpha/2}$  is obtained from the standard normal distribution. Thereafter,  $M_1 = (n - C_\alpha)/2$  and  $M_2 = (n + C_\alpha)/2$  are computed such that the upper and lower limits of the confidence interval,  $Q_{\text{max}}$  and  $Q_{\text{min}}$  are the  $(M_2 + 1)$ th largest and the  $(M_1)$ th largest of the  $n$ -ordered slope estimates (Gilbert, 1987). The slope  $Q_{\text{med}}$  is

statistically different than zero if the two limits ( $Q_{\min}$  and  $Q_{\max}$ ) have similar sign (Gocic and Trajkovic, 2013). TSE has been used recently by many researchers to estimate the magnitude of trends in hydro-meteorological time series (e.g. Kingra et al., 2018; Le Brocque et al., 2018; Sanikhani et al., 2018; Sharannya et al., 2018; Zelenakova et al., 2018).

### 3.11 Additional Software and Tools

For reproducibility, tasks that are laborious and repetitive were implemented using custom scripts written in the R and Python programming languages. For example, most of the plotting was conducted in these two languages. R is a free programming language that is used for statistical analyses and graphics and is used widely by researchers around the world. Python is a general purpose programming language that is also heavily used for machine and deep learning in industry and academia. Owing to the ubiquity of hydro-climatic packages and libraries for R and Python written by experts in these fields, it is easy to automate some analyses and results plotting. Using the powerful of such powerful scripting languages, climate and water scientists can easily handle large volumes of data and quickly get insights from the data than the traditional point-and-click method required by most canned software solutions. For some static plots and diagrams, the free professional quality vector graphics software, *Inkscape* was employed.

### 3.12 Chapter Summary

In this chapter, the methodology used in this research has been developed and discussed. For rainfall-runoff modelling, the SWAT model was proposed while

MODFLOW was proposed as a subsurface hydrological modelling tool. While most methods required the use of canned software, it was necessary at certain points to design and implement custom solutions using custom scripts developed in the R and Python programming languages. A novel technique which employs two proven and tested techniques was developed for the selection of a suitable GCM subset to be used for climate analyses. Furthermore, a methodology that can be used for studying and quantifying availability of surface- and groundwater resources in both temperate and semi-arid climates was developed. Specifically for the SRB, this is a novel approach, which at the time of writing this thesis, has never been applied before in Malawi. Previous studies have focussed on surface-water and groundwater availability and security as separate units in isolation while this study proposed to study aspects of the hydrologic cycle holistically. Additionally, the direction of this research at all times was to ensure that the methodology could be applied in different settings and reproduced using free and open source software as is recommended and preferred in modern science.

—*The trouble with weather forecasting is that it's right too often for us to ignore it and wrong too often for us to rely on it.*

Patrick Young

# 4

## Climate modelling

*In this chapter, climate analyses for the RNC and SRB are presented. Firstly, a brief description of how observed climate data was treated is presented. Secondly, proposed GCM selection and downscaling methods are applied and verified. Finally, future climate projections for the RNC and SRB are presented.*

## 4.1 Introduction

Changes in large-scale hydrological variables have been linked to an observed warming climate over several decades. Increasing atmospheric water vapour content and changes in the intensity and pattern of precipitation have been observed over the recent decades; insignia of the degree to which global warming and climate change has impacted the hydrological cycle (Bates et al., 2008). In this chapter, a multiple GCM approach has been used to investigate early, mid and late century climate change in the River Nith Catchment and Shire River basins. Outputs of GCM models have been used by many researchers as inputs to hydrological models in an effort to determine the potential impacts of climate change on water resources (surface-water and groundwater). The results from this chapter underpin the main drivers of the hydrological models (Chapter 5) developed for the RNC and SRB prior to subsequent coupling with groundwater flow models (Chapter 6) for the respective basins.

## 4.2 Missing Data

Missing data can present challenges in climate analyses such as estimation of long and short term trends, modelling extreme weather events and in the assessment of future climate projections. The methodology adopted in this thesis involves statistically downscaling coarse GCM projections to a local scale based on point meteorological data. Thus, long term complete historical records were required for the statistical downscaling exercise to be viable. For brevity, a brief description of the methodology that was used to deal with the missing data problem is presented; technical and mathematical details behind the techniques employed for infilling

are presented in Section 3.6.

In the RNC, Dumfries station data was complete and as such there was no need for further treatment beyond data quality checks. However, it was necessary to augment the RNC baseline weather data with reanalysis data due to the fact that only one station had a reliable long-term record. In the SRB, there was no single station with complete data hence an assessment of the missingness was conducted in the first instance as shown in Table 4.1.

**Table 4.1** Percentage of missing data for the baseline period in the SRB. Bold values indicate variables with more than 10% of missing data

Station	Variable		
	prcp (%)	Tmax(%)	Tmin(%)
Bvumbwe	0	3.51	4.05
Chichiri	0	4.66	4.26
Chileka	0	<0.1	0.57
Makhanga	<0.1	<b>18.86</b>	<b>20.48</b>
Mangochi	<0.1	2.53	2.56
Mimosa	<0.1	6.22	6.23
Ngabu	0	7.02	6.75
Thyolo	0	9.70	<b>11.04</b>

All stations in the SRB had complete or small gaps in the rainfall data that could easily be filled using simple techniques such as replacing missing values with the annual mean or replacing them with that of the last non-missing day. The former has the disadvantage of ignoring the seasonality of rainfall while the latter depends on the persistence of the weather; thus both methods can introduce considerable bias in the rainfall data. For this particular scenario, the number of consecutive days with no rainfall values was small enough (i.e. between one to seven consecutive days) to warrant the use of the second method. In the case of temperature, except for Chileka, all stations had significant gaps in the data

series requiring a more robust method of treatment.

### 4.3 Reanalysis Products Selection

As discussed in Section 4.2, station data was augmented with gridded reanalysis data in the RNC. For the SRB, a choice had to be made whether to use reanalysis data which had complete records or use station or point data with a lot of missing records. Before settling on the weather products to use for GCM downscaling, a thorough but simple methodology was adopted whereby the hydrologic (rainfall-runoff) model would be employed to assess the suitability of the weather products. The methodology involved constructing a hydrologic model (SWAT) and forcing it with gridded reanalysis products (Section 3.2.1.2). A selection was made between CFSR and CRU products by comparing uncalibrated streamflow hydrographs produced by each of the reanalysis products with the baseline hydrographs. The gridded products that produced the best performing hydrographs measured by the NSE and RMSE was selected for GCM downscaling and other hydrological analyses. In the case of the SRB, the model was also forced with observed station data and the resulting uncalibrated hydrographs compared with reanalysis products.

For the RNC, it was discovered that CRU products were superior in reproducing the baseline hydrology while in the SRB, station data performed better than CRU and CFSR products. In fact, CRU data was the worst performing in the SRB, highlighting the need for a careful selection of reanalysis products representative of the local climate before hydrological analyses can commence. This is especially true for regions with sparse data or for regions where station data is not readily accessible.

## 4.4 GCM Selection

In order to select a subset of GCMs to be used for climate change impact analyses in the RNC and SRB, a multi-criteria decision approach as outlined in Section 3.3 was employed. For consistency, the idea was to select a subset of GCM models that are useful for climate change impact studies in both the RNC and SRB. In other words, a subset of GCMs is selected for one region using a multi-criteria decision approach and the same subset applied elsewhere. Here, the global CFSR meteorological dataset is employed as observed variables for climate change analyses in the RNC. CFSR data was used to augment the one reliable long-term station time-series data at Dumfries. Gridded products are post-processed climate data that are derived from observed or station surface climate variables (Hewitson et al., 2014). Thus, the decision to select GCMs based on RNC climate is premised on the suspicion that the CFSR products for the RNC are more reliable than those of the SRB due to the quality, or lack thereof, of the station data that informed the latter. Detailed descriptions of the methods and algorithms used in the GCM selection procedure are provided in Chapter 3. For ease of reference, a short summary is provided here.

Firstly, a total of 29 GCMs were resampled to a spatial resolution of 38 km using bilinear interpolation to conform to the CFSR resolution since the GCMs have varying spatial resolutions. Thereafter, GCMs were ranked based on 1) the ability of the GCMs to reproduce the PDF of the observed series at each grid point in the RNC and, 2) based on the SU algorithm. Initially, 15 GCMs were selected from the 29 GCMs using the PDF system performed on rainfall data. Thereafter, based on the SU algorithm applied to both minimum and maximum



temperature, the top 10 GCMs were selected. Finally, only those GCMs (i.e. 7 GCMs listed in Table 4.2) appearing in McSweeney et al. (2015) were selected for climate change impact assessment.

A total of six GCMs were used for climate impact assessment and modelling in the SRB while five were selected for the RNC. Even though BCC-CSM1-1-M is suitable for the RNC according to McSweeney et al. (2015), it was omitted due to its poor performance in the RNC based on the methodology above. The GCMs that were selected for each region are presented in Table 4.2. For each future projection, the following three standard forecast horizons were considered: 2020s (2010-2039), 2050s (2040-2069) and late century 2080s (2070 -2099).

**Table 4.2** Selected GCMs for the SRB and RNC climate downscaling

GCM	Resolution (Lat × Lon)	Scenario	Centre
BCC-CSM1-1-M <sup>a</sup>	2.8° × 2.8°	RCP4.5 RCP8.5	Beijing Climate Center, China Meteorological Administration
CCSM4 <sup>a,b</sup>	0.94° × 1.25°	RCP4.5 RCP8.5	National Center of Atmospheric Research, USA
CNRM-CM5 <sup>a</sup>	1.4° × 1.4°	RCP4.5 RCP8.5	Centre National de Recherches Meteorologiques, France
GFDL-ESM2G <sup>a,b</sup>	2.0° × 2.0°	RCP4.5 RCP8.5	NOAA Geophysical Fluid Dynamics Laboratory, USA
HadGEM2-ES <sup>a,b</sup>	1.25° × 1.9°	RCP4.5 RCP8.5	Met Office Hadley Center, UK
INMCM4 <sup>b</sup>	1.5° × 2°	RCP4.5 RCP8.5	Institute of Numerical Mathematics of the Russian Academy of Sciences
MPI-ESM-LR <sup>a,b</sup>	1.9° × 1.9°	RCP4.5 RCP8.5	Max Planck Institute for Meteorology

<sup>a</sup> Denotes model was used in the Shire River Basin

<sup>b</sup> Denotes model was used in the River Nith Catchment

While results from McSweeney et al. (2015) indicate that more GCMs could have been included in this study (about 8 or 10), it was decided to use fewer GCMs than recommended. The decision to use fewer GCMs than were available was based on time constraints and availability of computing resources. This is because the methodology adopted required the hydrologic (SWAT) and groundwater (MODFLOW) models to be forced with one GCM at a time before calculation of the

ensemble mean using the machine learning methods described later in this chapter. This was necessary in order to determine whether using a GCM multi-model ensemble (MME) developed using robust statistical learning methods is better than the MME of the hydrologic models driven by single GCMs. Furthermore, the performance of each GCM was assessed to pick out the differences in projections in hydrologic models driven by respective GCMs. To the best of the author's knowledge, this question has not been explored fully and hence an attempt is made to address it, as part of this research's sub-aims. Moreover, the use of multiple GCMs and climate change scenarios helps water resources managers and policy makers to make decisions forearmed with the knowledge and understanding of the uncertainties captured by such studies. More importantly, McSweeney et al. (2015) note that we cannot with certainty link a model's incapability to simulate baseline climate to the plausibility of the model's future projections; thus a precautionary "one-model-one-vote" approach has in the past been adopted as a way of interpreting ensemble projections. The choice, therefore, to leave out a GCM in favour of another, is sometimes quite subjective and left to the modeller. Evidently, it would be an advantage to the climate science community to have robust methods of quantifying and reducing uncertainties in climate data ensembles in addition to decisions that are robust "against alternative future climate outcomes" and amenable to change once new evidence is made available (Dessai et al., 2009; Knutti, 2010; Lempert and Schlesinger, 2000).

## 4.5 Downscaling GCM Outputs

As discussed in Section 3.4 the nonparametric quantile mapping method (Gudmundsson et al., 2012) was used to downscale GCM data to a station-scale

resolution. Again, the reason this method was adopted is twofold; ease of implementation and success of the method in the climate, hydrology and related sciences. Further, according to Gudmundsson et al. (2012), nonparametric transformations have the “advantage that they can be applied without the specific assumptions about the distribution” of the climate data to be statistically bias corrected. Section 2.2 of this thesis discussed the many sources of uncertainty in climate change studies, not least of which is uncertainty due to the statistical downscaling method. Custom scripts written in the R programming language and the qmap (Gudmundsson et al., 2012) package were used to prepare observed data, pre-process and downscale GCM data.

Before bias-correcting GCM results for each grid point of the CFSR climate predictands in the RNC, the GCMs were downscaled to the same horizontal resolution (i.e.,  $\sim 38\text{km}$  horizontal resolution) as that of the CSFR climate data. For the SRB, the GCM outputs were downscaled to point station scale and thereafter biases statistically adjusted.

## 4.6 Performance and Uncertainty Evaluation

For the SRB, statistical downscaling and bias correction was done for twenty-nine CMIP5 GCMs and RCMs. Due to time constraints, only one downscaling and bias correction method was employed in this research and thus, it was necessary to validate it against predefined performance metrics. Raw and bias corrected GCM outputs were used to assess the ability of the bias correction method to reproduce nine metrics i.e mean, standard deviation, 25th, 50th, 75th, 90th, 95th and 99th percentiles, and maximum value as prescribed in Shen et al. (2018). Three representative stations from three clusters of meteorological stations identified in

Ngongondo et al. (2011) were used in the verification exercise (see Table 4.3).

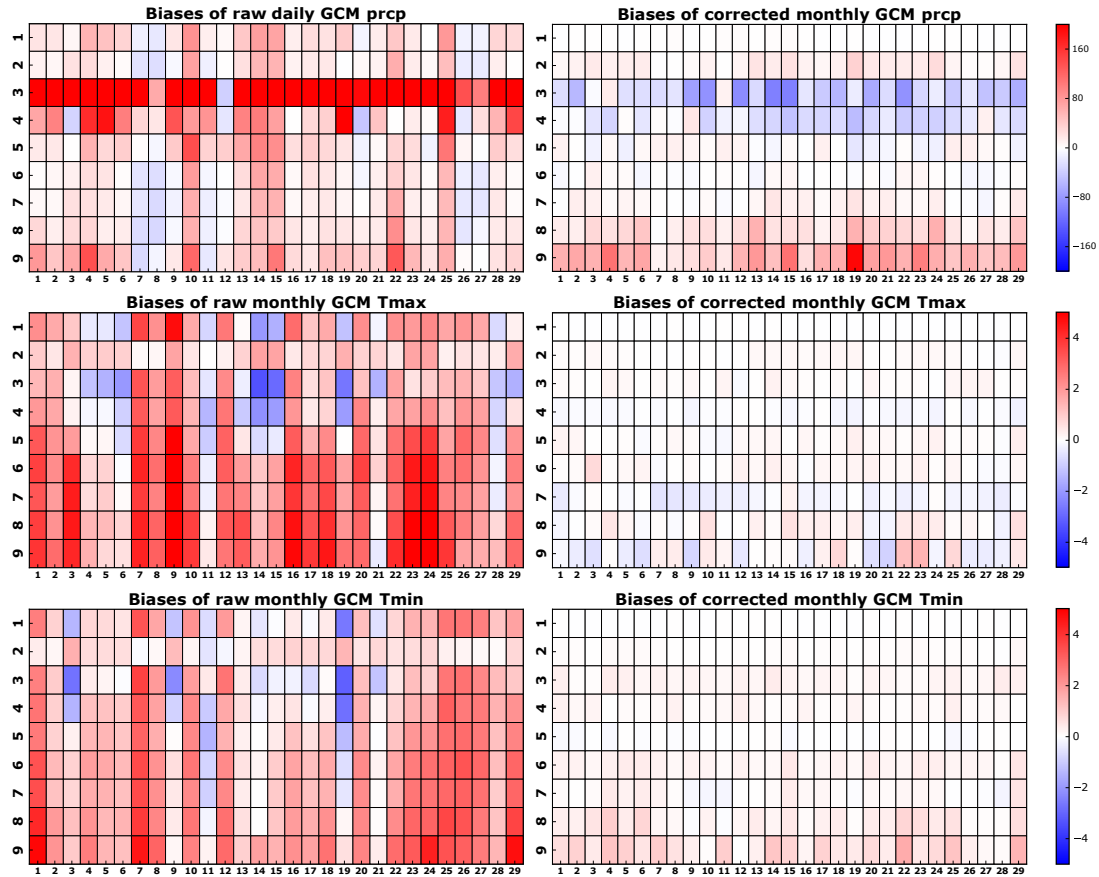
**Table 4.3** Selected stations for bias correction method verification. Stations were selected from regions identified in Ngongondo et al. (2011). Stations that have been used in this research are highlighted in bold.

Region	Stations	Representative Station
G1	Chikwawa, <b>Makhanga</b> , Nchalo, <b>Ngabu</b>	Ngabu
G2	Balaka, Chikweo, Chingale, Liwonde, <b>Mangochi</b> , Monkeybay	Mangochi
G3	<b>Bvumbwe</b> , Chanco, <b>Chichiri</b> , <b>Chileka</b> , Makoka, <b>Mimosa</b> , Mwanza, Naminjiwa, Neno, Satemwa, <b>Thyolo</b> , ZombaRTC	Chileka

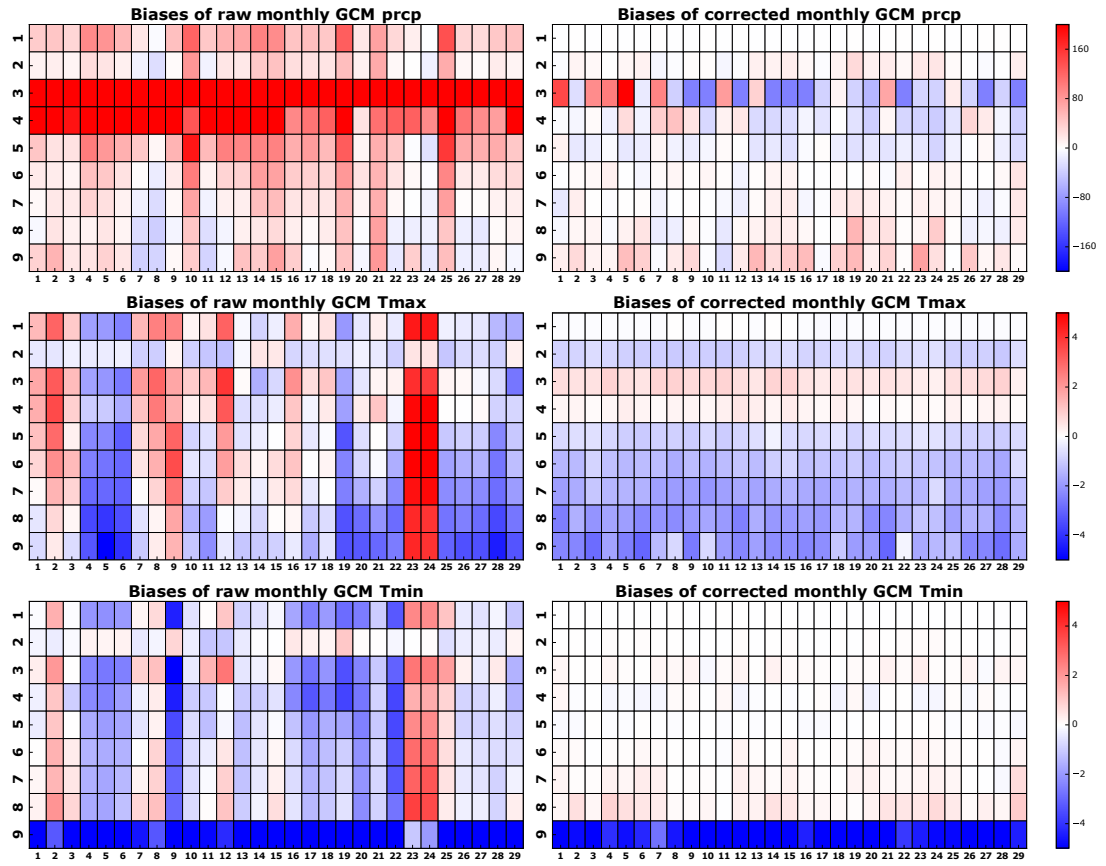
Figures 4.1 to 4.3 show the performance of the bias correction (BC) method (hereinafter referred to as *BCM*) with respect to reproducing the aforementioned performance metrics. Raw and corrected GCM statistics are presented in the left and right columns of the figures respectively. The X-axes represent the 29 GCMs that were used to verify the bias correction method while the Y-axes are the observed statistics from the mean to the maximum value numbered from 1 (mean) to 9 (maximum). The lighter the colour shading in the graphs the lesser the bias and vice versa.

All figures show a significant amount of bias in the raw GCMs. Furthermore, for all stations, the bias with respect to the observed statistics appear to be similar. For example, considerable bias in representing the 25th and 50th percentiles in precipitation can be seen in all the three representative stations. The bias correction method managed to reduce this bias significantly for all stations except Mangochi where some residual bias can be observed. The BC method was particularly efficient at reducing biases in the historical temperature simulations

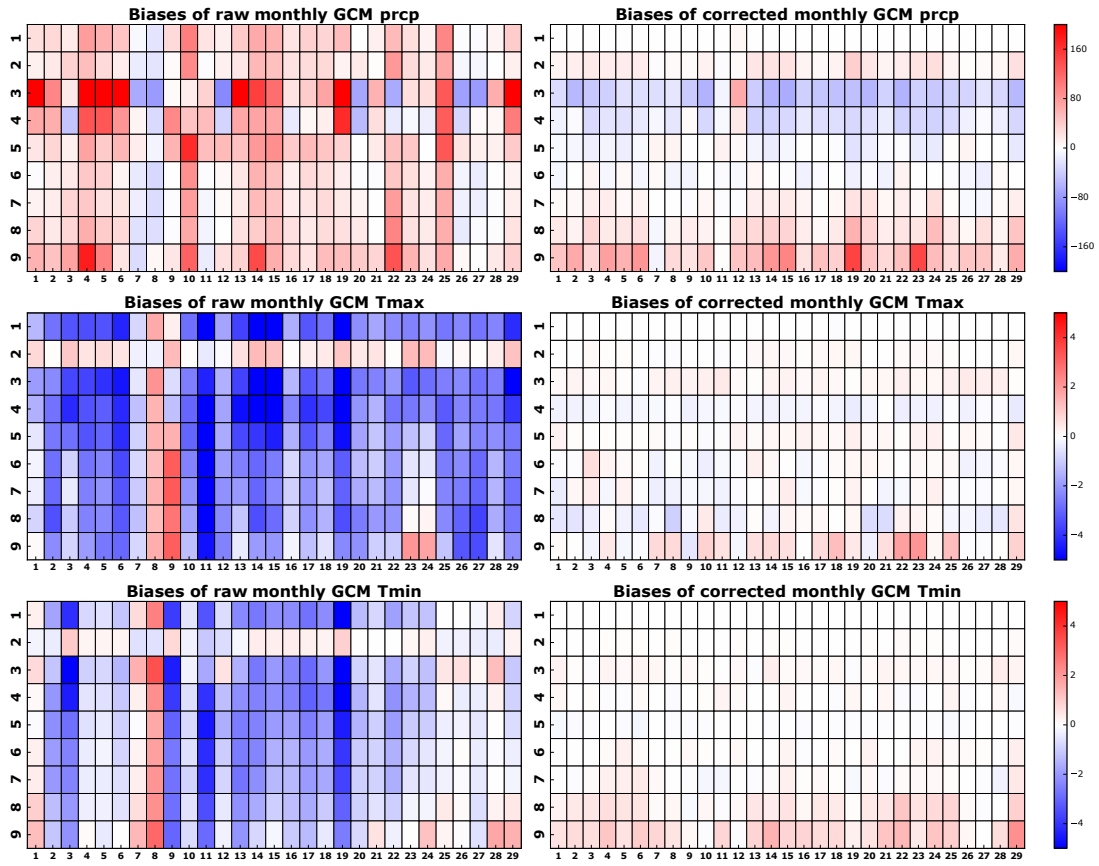
than in precipitation. Many studies in the literature have reported about the superiority of temperature simulations over precipitation (see for example, Behnke et al., 2016; Byun and Hamlet, 2018; Fowler et al., 2007; Joshi et al., 2015; Schoof and Pryor, 2001). This phenomenon can be attributed to atmospheric variability as opposed to problems in the GCM or downscaling method (Eden et al., 2012).



**Figure 4.1** Biases of raw and corrected GCM outputs in the baseline period for Chileka. The Y-axis represents nine statistics namely, mean, standard deviation, 25th, 50th, 75th, 90th, 95th and 99th percentiles, and maximum value from 1 to 9 respectively. The X-axis represents 29 GCMs that were considered for this study. Biases for precipitation are presented as the relative difference of the aforementioned statistics between the GCM and observed data while those of maximum and minimum temperatures are represented by the absolute difference



**Figure 4.2** Biases of raw and corrected GCM outputs in the baseline period for Mangochi. The Y-axis represents nine statistics namely, mean, standard deviation, 25th, 50th, 75th, 90th, 95th and 99th percentiles, and maximum value from 1 to 9 respectively. The X-axis represents 29 GCMs that were considered for this study. Biases for precipitation are presented as the relative difference of the aforementioned statistics between the GCM and observed data while those of maximum and minimum temperatures are represented by the absolute difference



**Figure 4.3** Biases of raw and corrected GCM outputs in the baseline period for Ngabu. The Y-axis represents nine statistics namely, mean, standard deviation, 25th, 50th, 75th, 90th, 95th and 99th percentiles, and maximum value from 1 to 9 respectively. The X-axis represents 29 GCMs that were considered for this study. Biases for precipitation are presented as the relative difference of the aforementioned statistics between the GCM and observed data while those of maximum and minimum temperatures are represented by the absolute difference

## 4.7 Multi-GCM Ensemble

For the RNC, the multi-GCM ensemble or River Nith Catchment Ensemble GCM Mean (RNC-EGCMM) was calculated at each grid point using the machine learning based Random Forest algorithm described in Section 3.5. The RF model has been used in many other studies to obtain a multi-model ensemble mean of

projections (see for example, Bunn et al., 2015; Keenan et al., 2011; Salman et al., 2018). The RF model was constructed using the *Scikit-learn* package in the python programming language. For the RNC, the averaging was done at each grid point whereas in the SRB it was done for each station. For brevity, performance assessments of the multi-GCM ensemble is only shown for Dumfries station in the RNC and Chileka station in the SRB.

## 4.8 RNC Baseline and Future Climate Assessment

### 4.8.1 RNC Baseline Climate

#### 4.8.1.1 Exploratory Data Analysis

In order to understand the nature of the Dumfries station climate data, initial statistical techniques aimed at discovering patterns, evaluating summary statistics and testing hypotheses were employed. These techniques are generally referred to as exploratory data analysis (EDA) and are usually graphical in nature. Fortunately, Dumfries climate data had complete records and thus no infilling and data cleaning was required.

Exploratory data analysis plots of winter precipitation for the baseline period (top three graphs of Figure 4.5) reveal unique patterns in the data. The histogram and density plot is heavily skewed to the right indicating that the data is not normally distributed. The Q-Q plot, which is a visual way of testing data for normality, shows a curved graph further confirming that the sample data are not normally distributed. Furthermore, the box plot shows that the data are positively



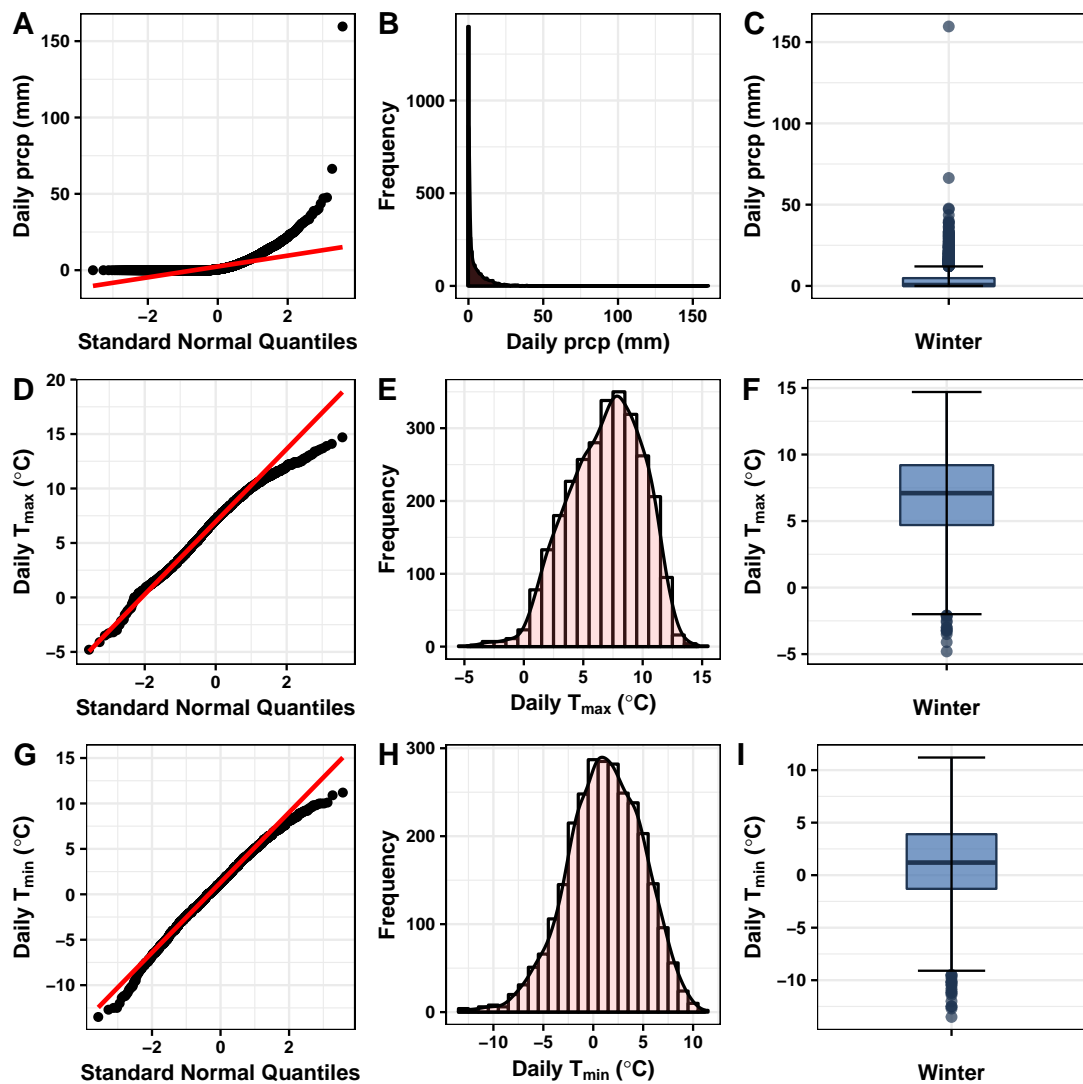
skewed and that there is a significant presence of outliers. That precipitation data are usually skewed is to expected as many researchers have investigated this phenomenon (see for example, Marchenko and Genton, 2010; Wilson and Toumi, 2005).

In the case of  $T_{max}$  and  $T_{min}$ , their Q-Q plots are nearly linear and thus an indication that the data could be normally distributed. However, for both  $T_{max}$  and  $T_{min}$ , there is clear evidence of outliers in the upper right corners of the Q-Q plots indicating that there there could be some slight skewness in the data. Further investigation using histogram, density and box plots revealed that the data are nearly normally distributed with evidence of some slight negative skewness. The box plots have a distinct shape with a few outliers towards the lower end of the temperature scale.

Figure 4.5 shows correlograms of precipitation,  $T_{max}$  and  $T_{min}$ . Correlograms or Autocorrelation Functions (ACF) are used to investigate autocorrelation or serial dependency in time series data (Khan et al., 2006). All three plots show that there is evidence of statistically significant correlation at lag 1. For precipitation, the ACF values exponentially decay before increasing again at higher lags. As the ACF values decay, they are mostly within the 95% confidence bands and are therefore insignificant. In the case of  $T_{max}$  and  $T_{min}$ , all the ACF values are significant, i.e. outside the horizontal dashed blue line, indicating that there is serial correlation in the temperature data.

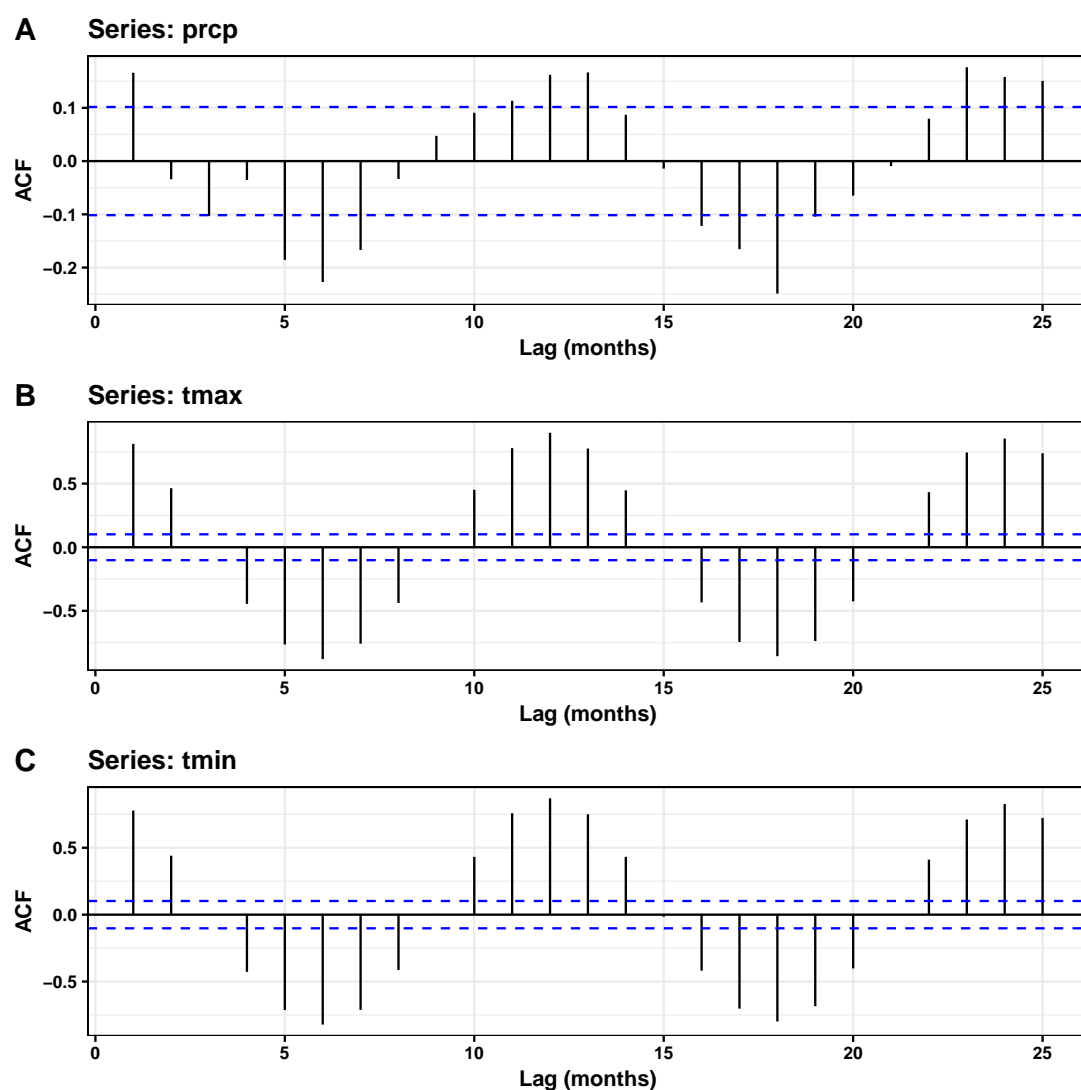
#### 4.8.1.2 Trend Analyses

As a result of the exploratory data analyses, it was concluded that non-parametric statistical tests be used to identify trends in the climate data. Non-parametric



**Figure 4.4** Exploratory data analysis plots of daily precipitation (Figs. A, B, C); daily maximum temperature (Figs. D, E, F), and daily minimum temperature (Figs. G, H, I) for winter season at Dumfries

tests are robust and less affected by the presence of outliers in the data and many forms of non-normality (Lanzante, 1996). One of the most commonly used non-parametric tools for detecting changes in climatic data is the Mann-Kendall trend test (Kendall, 1975; Mann, 1945), whose null hypothesis is that the data are independent and randomly ordered (Hamed and Rao, 1998). However, when the



**Figure 4.5** Empirical autocorrelation (Correlogram) plots of (a) monthly precipitation, (b) monthly mean maximum temperature and (c) monthly mean minimum temperature for the baseline period at Dumfries

data is characterised by the presence of positive autocorrelation, as can be seen in Figure 4.5, the probability of detecting artificial trends in the data increases. Hence, the Trend Free Pre-whitening (TFPW) (Yue et al., 2002b) procedure was employed before assessing the significance of the trend using the Mann-Kendall test.

TFPW Mann-Kendall (MK-TFPW) and Sen's slope estimator tests results are presented in Table 4.4. Results were calculated on monthly, seasonal and annual timescales where DJF, MAM, JJA and SON are winter, spring, summer and autumn respectively. Bold values indicate statistical significance at 95% confidence level. Positive values indicate an upward trend while negative values indicate a downward trend. Precipitation trends at the annual timescale are positive although not statistically significant. Similarly, increasing but insignificant trends were detected at the seasonal timescale except for autumn where insignificant decreasing trends were detected. With the exception of March, September and December, increasing trends were detected at the monthly timescale. A significant decreasing trend was detected for March (only detected via MK-TFPW) while a significant increasing trend was detected for April (detected via both MK and MK-TFPW). While the trends are statistically significant, the magnitude of change is around  $1.5 \text{ mm month}^{-1}$  and overall is insignificant at the annual and seasonal scales.

**Table 4.4** Results of Mann–Kendall, Pre-Whitened Mann-Kendall and Sen’s slope estimator statistical tests for Dumfries station conducted on monthly and seasonal time scales. Bold values indicate statistical significance at 95% confidence level.  $Z$ ,  $Z_c$ ,  $Q$ ,  $Q_c$ , pval and pvalc are the MK Z-statistic (traditional MK), TFPW-MK Z-statistic (i.e after Trend-Free Pre-whitening (TFPW)), TSE for original data series, TSE after TFPW, P-value for original data series and P-value after TFPW respectively.

Variable	Statistic	Month												Season				
		Jan	Feb	Mar	Apr	May	Jun	Jul	Aug	Sep	Oct	Nov	Dec	DJF	MAM	JJA	SON	Annual
Prcp	Z	0.00	0.90	-1.60	<b>2.75</b>	0.85	1.24	0.15	-0.20	-1.22	0.82	0.17	-0.14	0.48	0.54	0.31	-0.03	1.16
	Zc	0.54	0.61	<b>-2.64</b>	<b>2.71</b>	0.46	0.93	0.57	-0.21	-0.89	0.43	-0.04	-0.75	0.86	0.39	0.57	-0.07	0.75
	Q	0.02	1.20	-1.18	1.57	0.77	0.77	0.08	-0.17	-1.24	1.20	0.20	-0.15	0.77	1.04	0.55	-0.13	3.21
	Qc	0.54	0.96	-1.56	1.55	0.46	0.67	0.41	-0.20	-0.93	0.57	-0.03	-0.90	1.25	0.43	1.02	-0.29	1.91
	pval	1.00	0.37	0.11	<b>0.01</b>	0.40	0.21	0.88	0.84	0.22	0.41	0.87	0.89	0.63	0.59	0.76	0.97	0.25
	pvalc	0.59	0.54	<b>0.01</b>	<b>0.01</b>	0.64	0.35	0.57	0.83	0.37	0.67	0.97	0.45	0.39	0.69	0.57	0.94	0.45
Tmax	Z	1.70	<b>2.72</b>	<b>2.96</b>	1.51	1.43	-0.22	0.32	1.38	<b>3.28</b>	1.16	1.44	0.88	<b>2.67</b>	<b>3.35</b>	1.00	<b>3.14</b>	<b>3.37</b>
	Zc	<b>2.39</b>	<b>2.96</b>	<b>3.14</b>	1.75	1.03	0.43	0.71	<b>1.96</b>	<b>3.14</b>	0.82	1.46	1.61	<b>3.68</b>	<b>3.07</b>	1.64	<b>2.96</b>	<b>3.82</b>
	Q	0.06	0.08	0.09	0.04	0.04	0.00	0.01	0.05	0.07	0.02	0.03	0.03	0.07	0.06	0.03	0.04	0.04
	Qc	0.09	0.09	0.09	0.05	0.04	0.01	0.02	0.07	0.07	0.02	0.03	0.05	0.08	0.06	0.04	0.04	0.05
	pval	0.09	<b>0.01</b>	<b>0.00</b>	0.13	0.15	0.83	0.75	0.17	<b>0.00</b>	0.25	0.15	0.38	<b>0.01</b>	<b>0.00</b>	0.32	<b>0.00</b>	<b>0.00</b>
	pvalc	<b>0.02</b>	<b>0.00</b>	<b>0.00</b>	0.08	0.30	0.67	0.48	<b>0.05</b>	<b>0.00</b>	0.41	0.14	0.11	<b>0.00</b>	<b>0.00</b>	0.10	<b>0.00</b>	<b>0.00</b>
Tmin	Z	<b>2.06</b>	<b>2.07</b>	1.89	<b>2.24</b>	<b>2.75</b>	1.89	0.46	1.16	0.83	-1.00	1.70	0.24	<b>2.24</b>	<b>3.23</b>	1.63	1.34	<b>2.79</b>
	Zc	<b>2.32</b>	<b>2.14</b>	1.64	<b>2.46</b>	<b>2.28</b>	1.53	0.89	1.89	1.36	-1.21	1.28	0.71	<b>2.78</b>	<b>3.07</b>	<b>2.57</b>	1.00	<b>3.93</b>
	Q	0.08	0.06	0.06	0.04	0.06	0.03	0.01	0.02	0.03	-0.03	0.05	0.01	0.05	0.05	0.02	0.02	0.04
	Qc	0.10	0.07	0.05	0.05	0.06	0.03	0.02	0.04	0.03	-0.04	0.05	0.01	0.06	0.05	0.03	0.02	0.04
	pval	<b>0.04</b>	<b>0.04</b>	0.06	<b>0.02</b>	<b>0.01</b>	0.06	0.65	0.25	0.40	0.32	0.09	0.81	<b>0.02</b>	<b>0.00</b>	0.10	0.18	<b>0.01</b>
	pvalc	<b>0.02</b>	<b>0.03</b>	0.10	<b>0.01</b>	<b>0.02</b>	0.12	0.37	0.06	0.18	0.23	0.20	0.48	<b>0.01</b>	<b>0.00</b>	<b>0.01</b>	0.32	<b>0.00</b>

Both minimum and maximum temperatures exhibit significant upward trends at annual and seasonal scales except for summer which shows an upward but insignificant trend. The change is about  $0.4^{\circ}\text{C decade}^{-1}$  for both  $T_{max}$  and  $T_{min}$  and about  $1.24^{\circ}\text{C}$  for the entire baseline period (i.e. 1975 – 2005).

### 4.8.2 RNC Baseline Downscaling

Bias correction and statistical downscaling results of the historical GCM data for the RNC are presented in Figures B.1 to B.3. Biases in the downscaled variables were adjusted in order to have statistically similar data series for the historical period. From statistical and visual inspections, there was a good match between the observed and simulated data in the RNC.

Ensemble climate model results showed similar and in many grids superior results than individual GCMs when compared to the reanalysis data. An interesting outcome of using data-based methods to combine the GCM results is that the ensemble model was more reliable in reproducing the wet and dry spell lengths than the individual GCMs. Thus, while these methods may be considered to be “black boxes”, they hold a lot of promise for more reliability and ability to accurately simulate hydro-climatic phenomena.

One consideration to take when developing machine learning based models is to find a good balance between accuracy and generalization. Models that are overfitted during the training phase tend not to generalize well when introduced to new or unseen data and thus a trade-off needs to be made in the training and testing phases to ensure that models that generalize well (i.e., perform well during the testing phase) are favoured ahead of models that have high accuracy in the training phase but not so accurate in the testing phase. Similarly, care has to be

taken that “underfitting” is avoided.

### 4.8.3 RNC Future Climate Results and Discussion

Here, future climate is assessed using the River Nith Catchment Ensemble GCM Mean (RNC-EGCMM). Again, only seasonal differences in precipitation and temperature for the RNC are presented in Figures 4.6 to 4.11. With respect to precipitation, the highest differences between baseline and future values are observed in winter (RCP4.5 and 8.5) and least in spring (RCP8.5) and summer (RCP4.5). Mean seasonal precipitation under RCP4.5 is expected to increase by +10% to +24% in the winter season with the highest increase observed towards the end of the century. In the 2020s, spring precipitation change under RCP4.5 ranges between +3% and +5% while the 2050s experience a drop in precipitation of about -3% compared to baseline conditions. The late century sees slightly elevated precipitation changes of about +4% to +7% under RCP4.5. As alluded to earlier, summer precipitation decreases across the century with percentage changes ranging between -6% and -4%. In the autumn season, a similar trend as that observed in spring is exhibited where the 2050s experience slightly reduced precipitation by up to -2% while the 2020s and 2080s see no significant change from baseline conditions. Under RCP8.5, summer precipitation decreases significantly by up to -11% of baseline values while winter precipitation increases by up to 27%.

Maximum and minimum temperatures in the RNC are presented as absolute changes from the baseline. In the case of maximum temperature, a steady increase in the mean seasonal temperatures is immediately clear across the time horizons from Figs. 4.8 and 4.9 under both RCP4.5 and 8.5. In the winter season, maximum

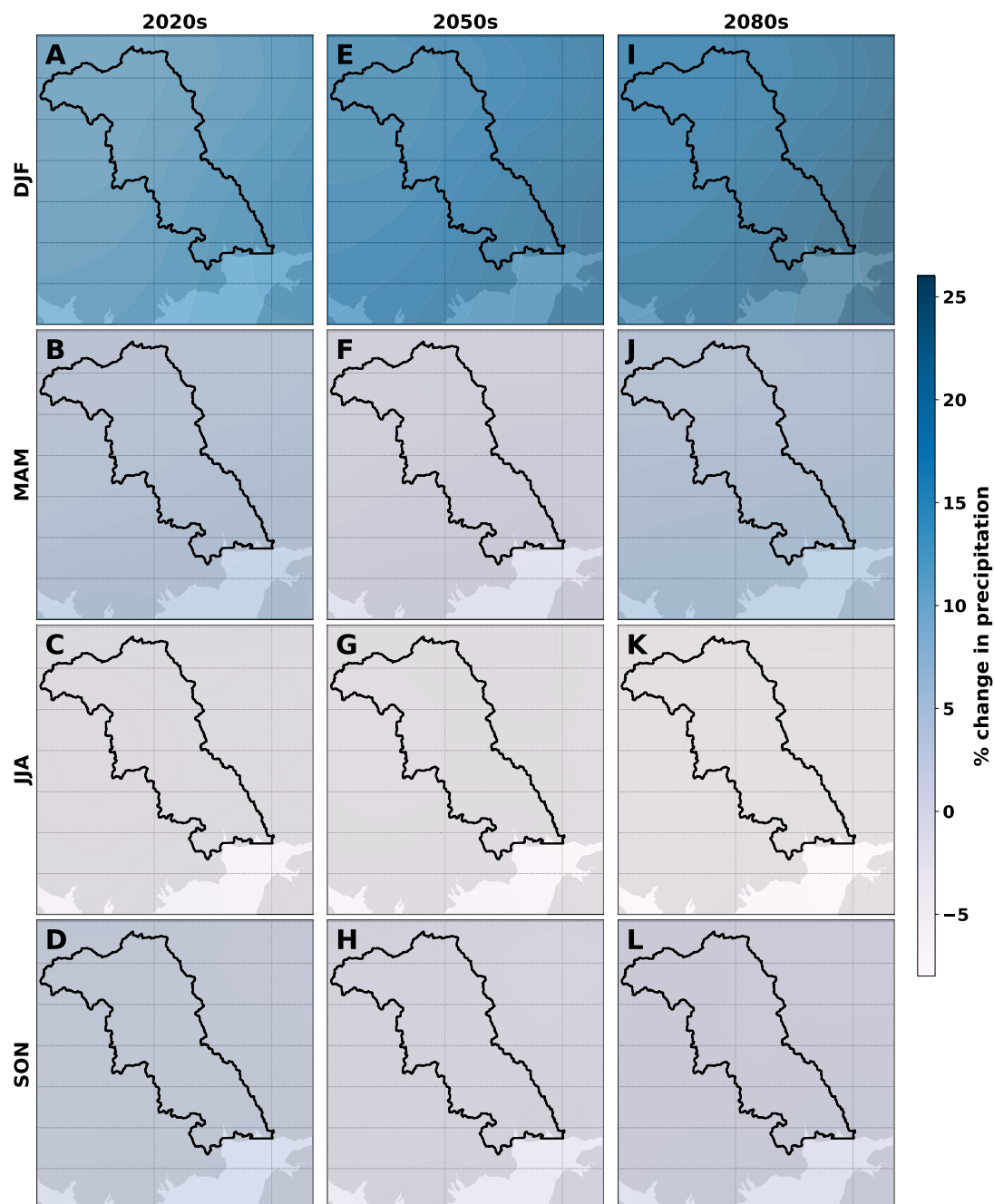
temperatures maintain baseline conditions in the 2020s with increases in the mid- to late-century of up to  $1.5^{\circ}\text{C}$  under RCP4.5 and up to  $3.8^{\circ}\text{C}$  under RCP8.5. There is a slight change of about  $+1^{\circ}\text{C}$  in spring mean  $T_{\text{max}}$  in the 2020s but minor increases of  $+1.2^{\circ}\text{C}$  to  $+1.4^{\circ}\text{C}$  observed in the mid- to late-century. The highest  $T_{\text{max}}$  changes under RCP4.5 were observed in summer where an increase of between  $+1.7^{\circ}\text{C}$  to  $+1.8^{\circ}\text{C}$  in the 2050s and up to  $+1.9^{\circ}\text{C}$  in the 2080s was observed. Similarly, under RCP8.5,  $T_{\text{max}}$  in the summer rises up to  $+3.8^{\circ}\text{C}$  by the late century.

Minimum temperatures, on the other hand, only increase by about  $+0.5^{\circ}\text{C}$  in the 2020s for all seasons except winter where an increase of up to  $+1^{\circ}\text{C}$  is observed under RCP4.5 and up to  $+2.5^{\circ}\text{C}$  under RCP8.5. In spring and autumn,  $T_{\text{min}}$  rises by  $+1^{\circ}\text{C}$  and  $+1.4^{\circ}\text{C}$  in the 2050s and 2080s respectively. Summer  $T_{\text{min}}$  rises by  $+1.4^{\circ}\text{C}$  in the 2050s and  $+1.6^{\circ}\text{C}$  in the 2080s. In winter, where the highest changes are observed,  $T_{\text{min}}$  rises by  $+1.6^{\circ}\text{C}$  and  $+1.7^{\circ}\text{C}$  in the mid- and late-century respectively under RCP4.5.

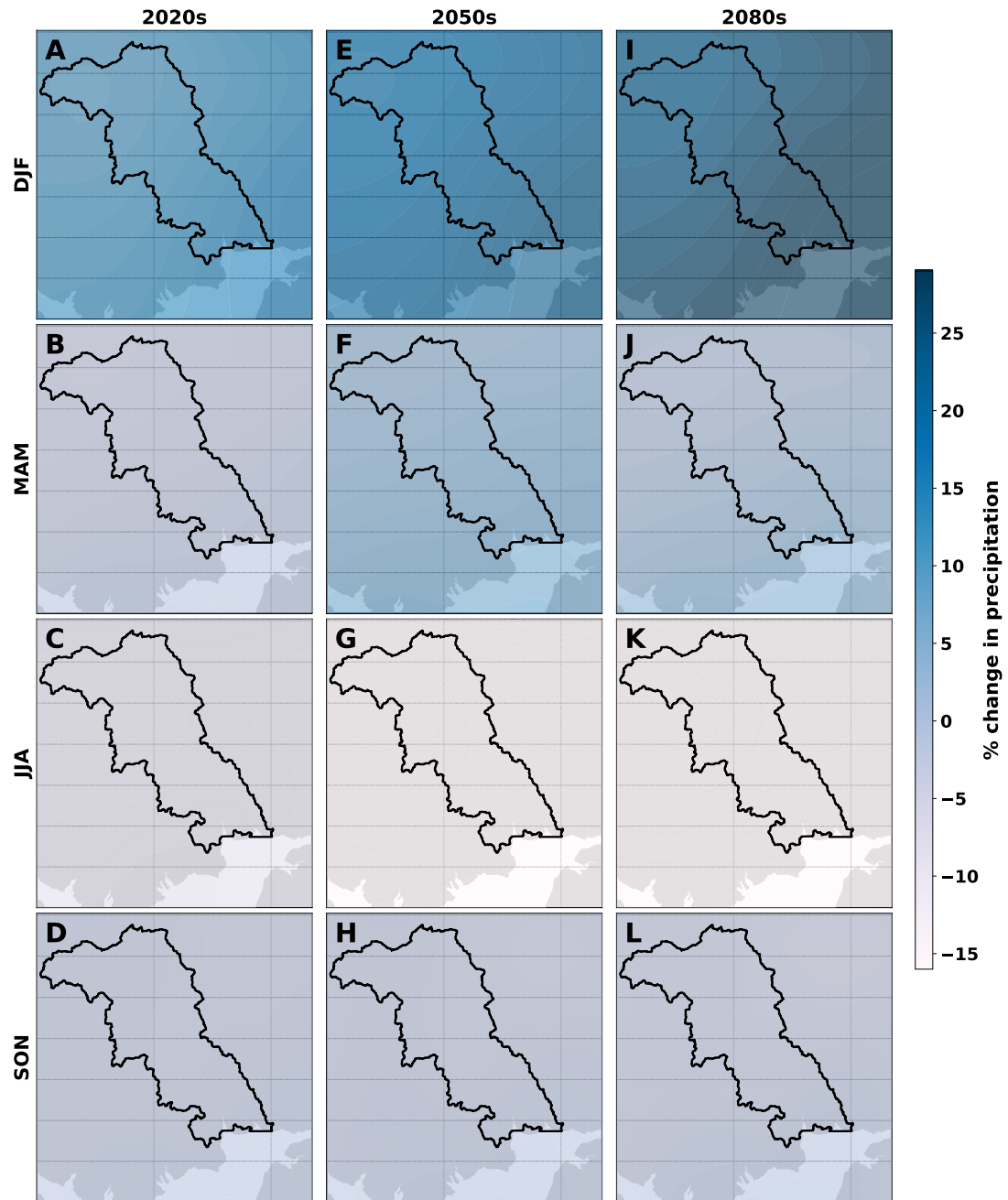
A peculiar pattern is observed for maximum and minimum temperature changes where the winters and summers get warmer by the end of the century. The rest of the seasons get warmer too but only slightly. Furthermore, the diurnal temperature range (DTR) appears to decrease, especially in winter, possibly due to the daily minimum temperatures increasing faster than the maximum daily temperatures (e.g., Braganza et al., 2004).

Increases in winter rainfall is consistent with results obtained by Watts et al. (2015) who reported similar results as well as recent findings by Murphy et al. (2018) who report “warmer, wetter winters and hotter, drier summers” over land.

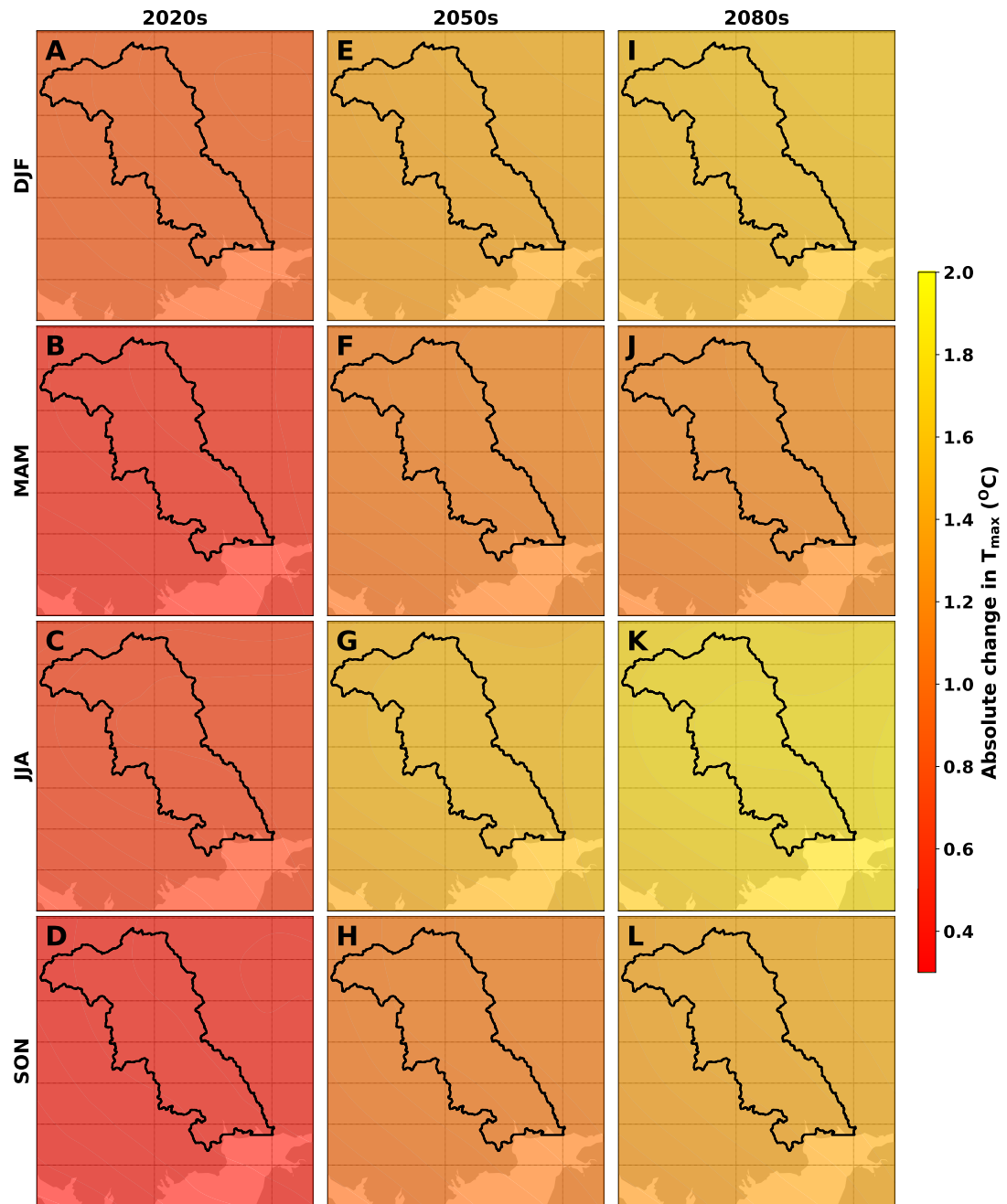




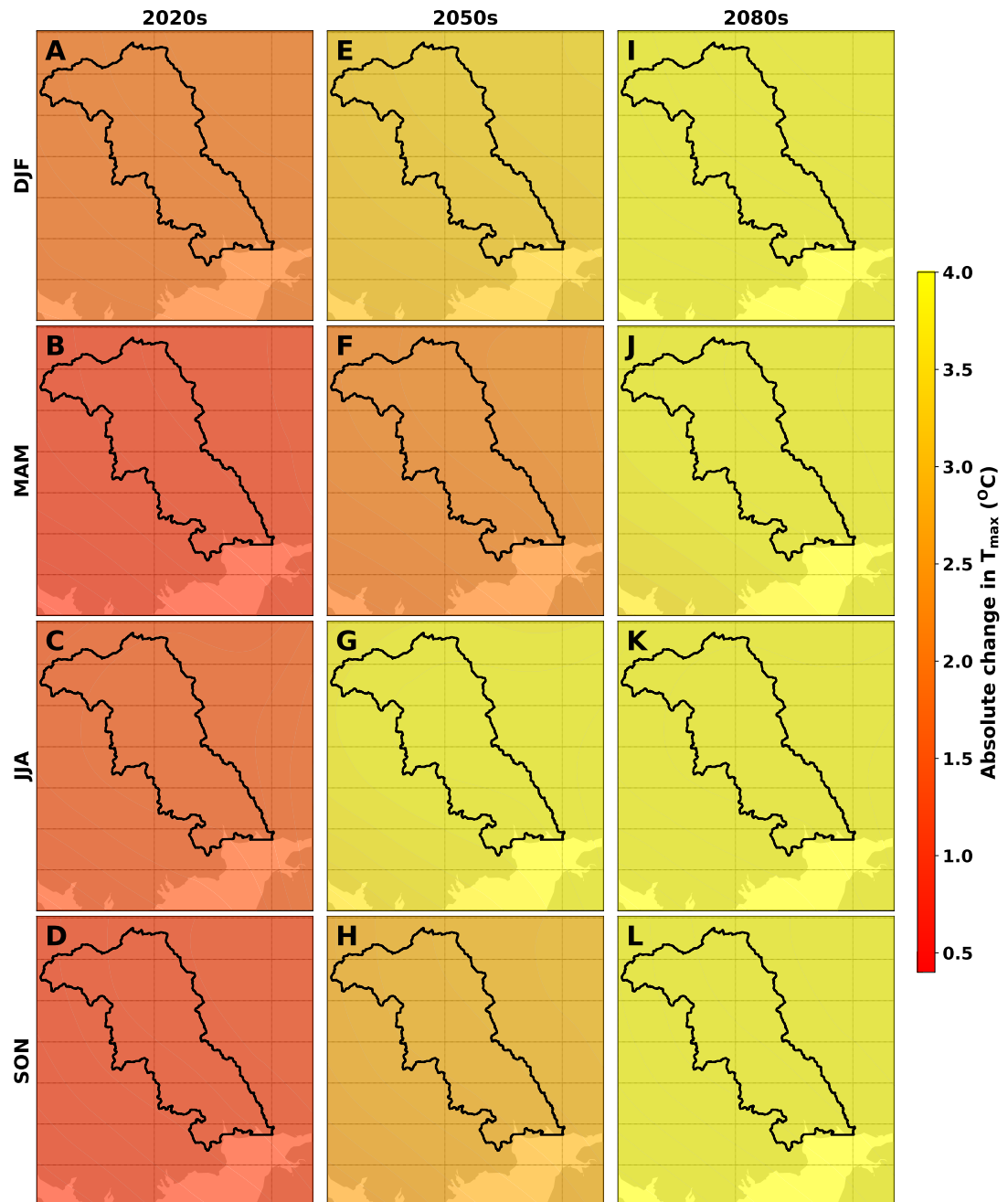
**Figure 4.6** RNC future precipitation under RCP4.5 as calculated by the RNC-EGCMM. Seasonal percentage changes in precipitation are presented row-wise while time is presented column-wise.



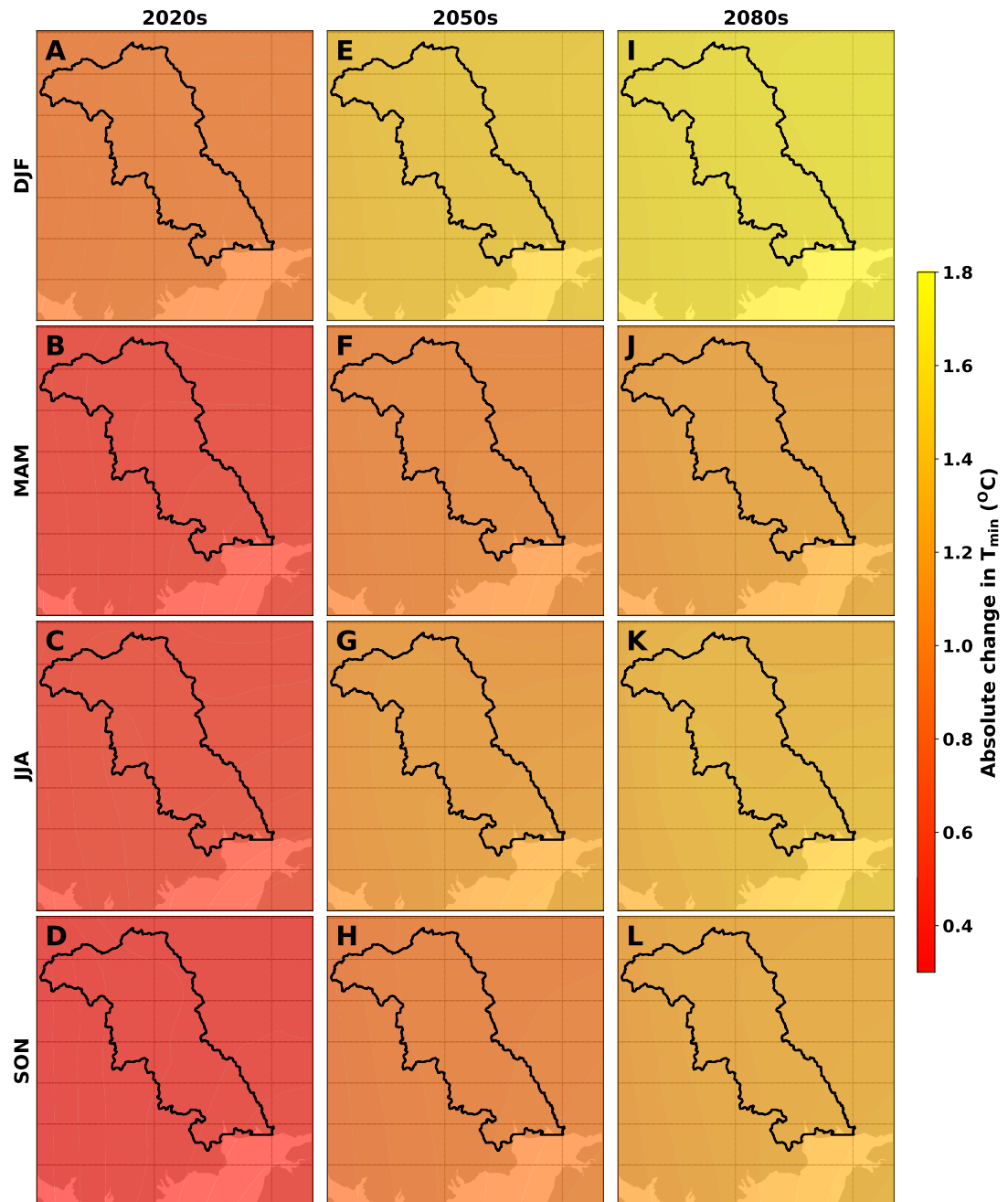
**Figure 4.7** RNC future precipitation under RCP8.5 as calculated by the RNC-EGCMM. Seasonal percentage changes in precipitation are presented row-wise while time is presented column-wise



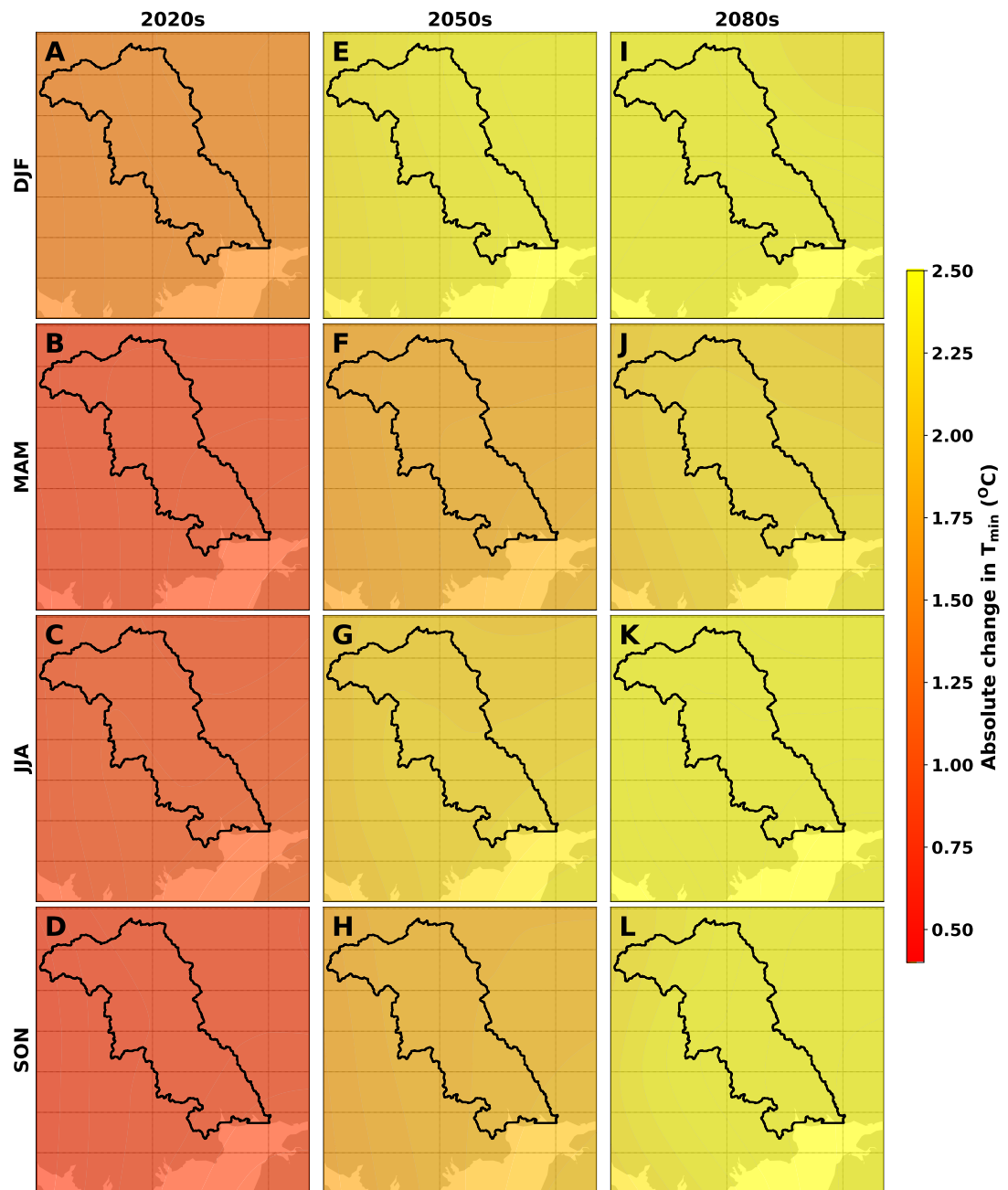
**Figure 4.8** RNC future  $T_{max}$  under RCP4.5 as calculated by the RNC-EGCMM. Seasonal absolute changes in temperature are presented row-wise while time is presented column-wise



**Figure 4.9** RNC future  $T_{max}$  under RCP8.5 as calculated by the RNC-EGCMM. Seasonal absolute changes in temperature are presented row-wise while time is presented column-wise



**Figure 4.10** RNC future  $T_{min}$  under RCP4.5 as calculated by the RNC-EGCMM. Seasonal absolute changes in temperature are presented row-wise while time is presented column-wise



**Figure 4.11** RNC future  $T_{min}$  under RCP8.5 as calculated by the RNC-EGCMM. Seasonal absolute changes in temperature are presented row-wise while time is presented column-wise

## 4.9 SRB Baseline and Future Climate Assessment

### 4.9.1 SRB Baseline Climate

For purposes of investigating the long term statistical trends for the baseline climate (i.e. 1975 – 2005) in the SRB, eight meteorological stations with less than 10% missing daily data and overlapping the baseline period were selected for analysis. Treatment of missing data is discussed in Section 4.2. Attributes of the stations and meteorological data are given in Table 4.5.

**Table 4.5** Selected meteorological stations in the SRB

No.	Station	Latitude	Longitude	Elevation (m)	Period
1	Bvumbwe	-15.92	35.07	1146	1960 – 2016
2	Chichiri	-15.8	35.05	1132	1965 – 2015
3	Chileka	-15.68	34.97	767	1949 – 2016
4	Makhanga	-16.52	35.15	76	1960 – 2015
5	Mangochi	-14.43	35.25	482	1961 – 2016
6	Mimosa	-16.08	35.58	652	1958 – 2016
7	Ngabu	-16.5	34.95	102	1960 – 2016
8	Thyolo	-16.15	35.22	820	1961 – 2015

Regional climate in the SRB is influenced by the topography and surface fluxes and the transport mechanisms of prevailing moisture organized by weather systems (Jury and Gwazantini, 2002; Torrance, 1972). Generally, Malawi's climate is sub-tropical and mostly dry except for the warm and wet season which stretches

from November to April. During this period, approximately 95% of the annual precipitation takes place (MMSD, 2017). The position of the Inter-tropical Convergence Zone (ITCZ) mainly dictates the intensity and onset of the rainy season. The oscillation of the ITCZ, which varies from year to year, and the influence of the Indian Ocean Sea Surface Temperatures are responsible for the inter-annual variability in the rainy season (McSweeney et al., 2014). In addition, the El Nino Southern Oscillation (ENSO) cycles have been reported to be a significant factor contributing to the inter-annual rainfall variability (e.g. Jury and Mwafulirwa, 2002; McSweeney et al., 2014; Ngongondo, 2006; Pilskaln, 2004). Within the SRB, analysis of the baseline climate reveals the prevalence of rainfall variability south of Malawi as can be seen from Figure 4.12.

Station Ngabu, for example, receives the least amount of rain in December but receives significantly higher rainfall than Mangochi in January. The other stations, while showing some variability, are consistent in their ranking for all the months except Mimosa which shows a significant departure from all the stations. Interestingly, analysis of the available Mimosa station rainfall data suggests that the station consistently recorded higher rainfall in March than February, a trend which was not captured by the other stations. However, from Figure 4.13, it can be seen that this trend is particularly true for the upper ranges of mean monthly rainfall in February for this station than for the lower ranges. The mean February rainfall, however, is close to the median, suggesting in general that the station consistently recorded higher rainfall amounts for this month. Furthermore, the station receives a considerable amount of rainfall during the relatively dry winter months (JJA) as can be seen from Fig. 4.12. This unusual trend was captured by another study (Nicholson et al., 2014) where a detailed analysis of rainfall



climatology for Malawi was undertaken. In their study, the authors documented that there is “a brief period of reduced rainfall in mid-February that appears to signal a shift in the prevailing rainfall and circulation regime” (Nicholson et al., 2014). Furthermore, their study concluded that the early rainy season (DJF) is dominated by tropical influences while the late rainy season (MA) is dominated by extra-tropical influences and that the interannual variability in these two periods is uncorrelated (Nicholson et al., 2014). These aspects of the SRB climate arising from Nicholson et al. (2014) study have not been further investigated in this thesis. However, it is the author’s view and recommendation that these aspects be explored in future studies from a hydrologic perspective.

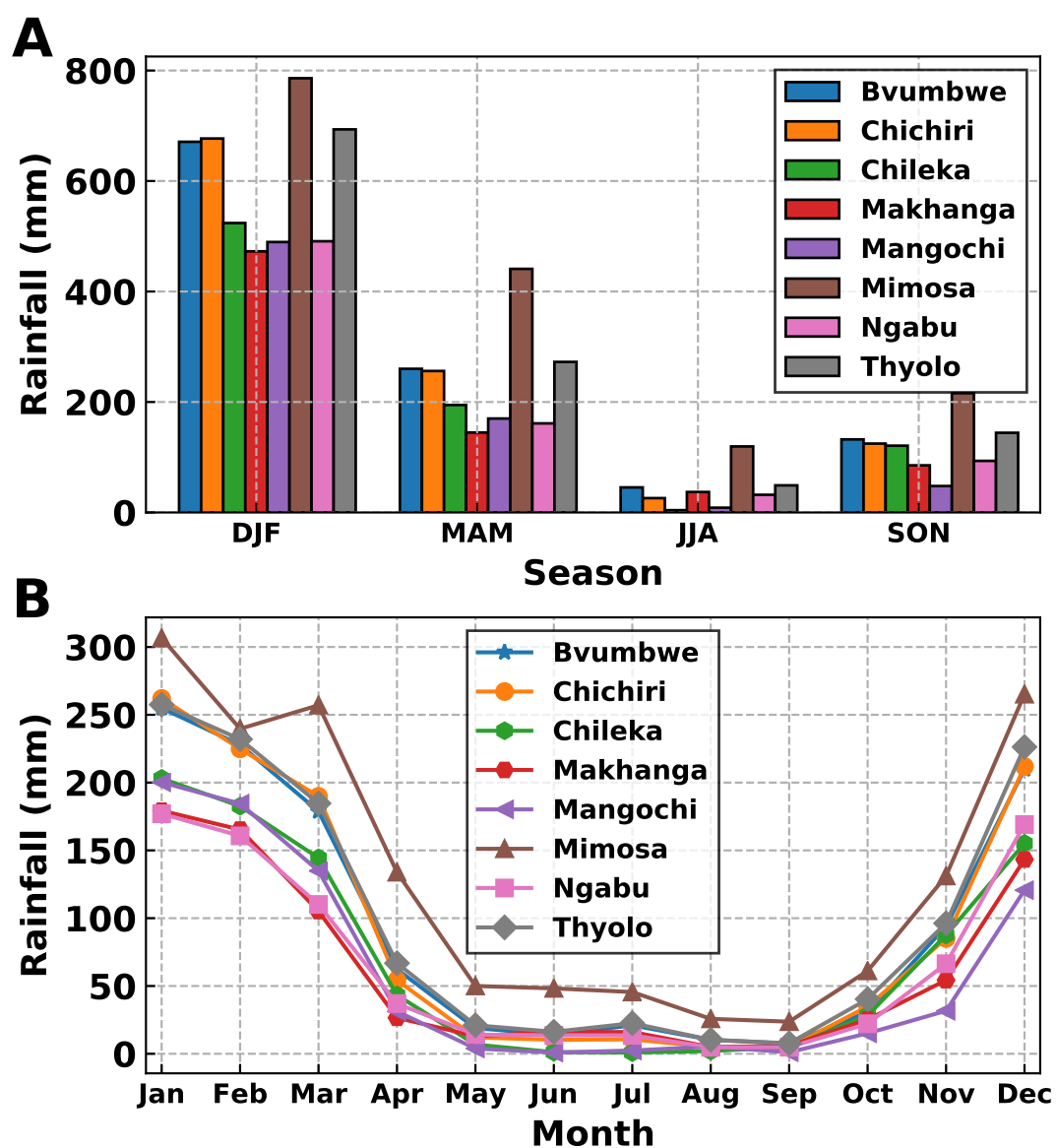
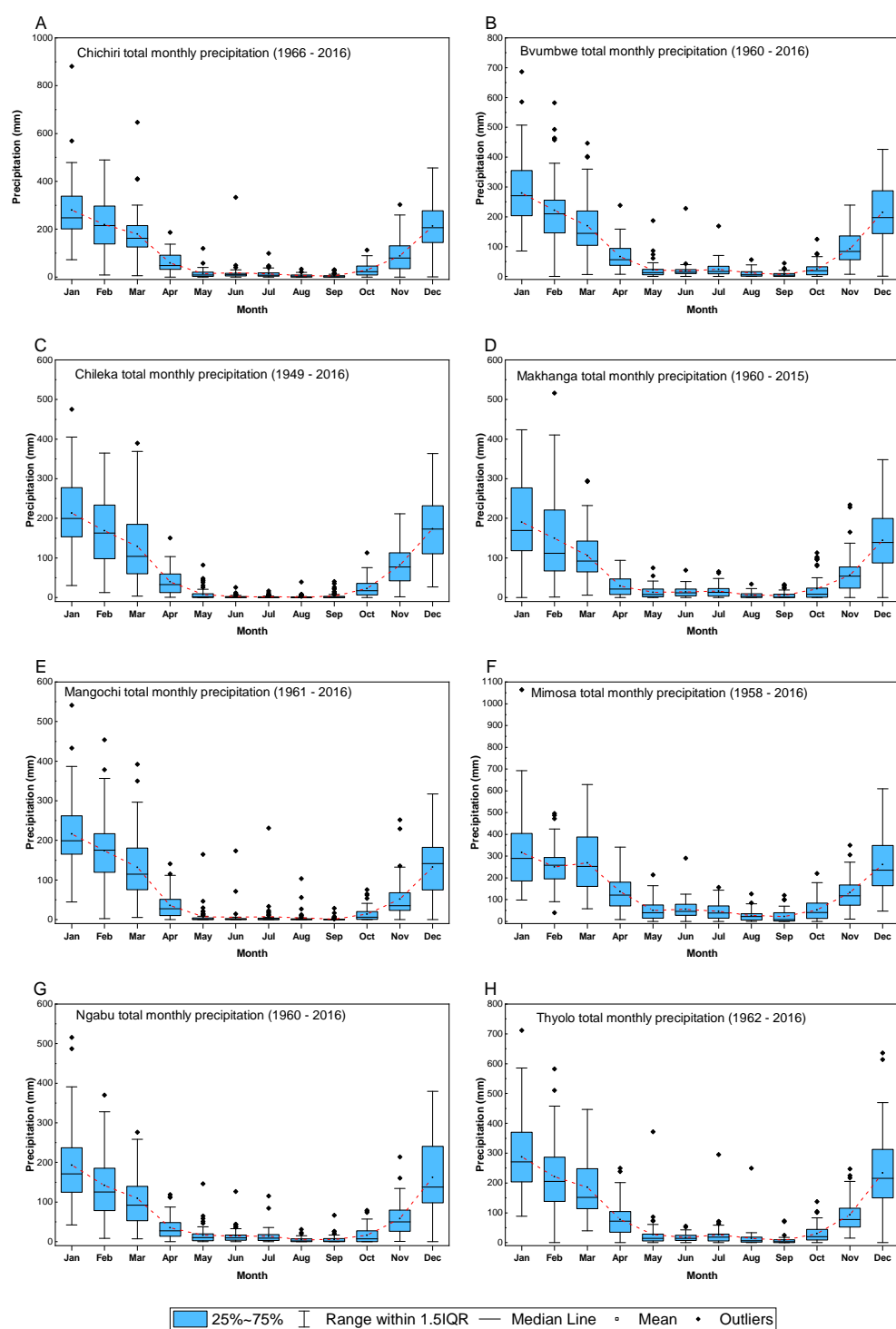


Figure 4.12 Rainfall variability in the SRB for the baseline period (1975-2005): (a) Rainfall climatologies (b) Seasonal rainfall



**Figure 4.13** Box plots of mean monthly precipitation in the SRB

### 4.9.2 Historical Precipitation Downscaling and Bias Correction

Figures 4.1 to 4.3 have shown the effectiveness of the quantile mapping bias correction method in downscaling GCM outputs to the SRB local scale. From a monthly perspective, climatologies indicate that the historical GCMs have considerable inherent bias. Taking bcc-csm1-1m GCM as an example, it can be seen from Figure 4.14 that the historical portion of the GCM before quantile mapping is biased for each of the eight climate stations in the SRB. The GCM overestimates rainfall in some months and underestimates in others. At Chileka, Makhanga, Mangochi and Ngabu, the raw GCM overestimates rainfall for almost all the months except January; whereas for Bvumbwe, Chichiri, Mimosa and Thyolo, rainfall was underestimated for all the months except April, May and June.

This trend, as expected, was not uniform for all the GCMs (see Figures B.4 to B.8). CCSM4 GCM consistently overestimated rainfall for almost all the months at all the stations except Mimosa and Thyolo where the model was able to reproduce nearly accurate estimations of the historical period before empirical adjustment. A similar trend was observed for HadGEM2-ES where a good agreement between the observed and raw GCM data can be seen at Bvumbwe, Mimosa and Thyolo. The rest of the GCMs were able to simulate the historical period fairly well except GFDL-ESM2G which had some considerable departure from historical means. This demonstrates the implicit uncertainty in the CMIP5 models and the need for using a multi-model ensemble (MME) in climate change studies.

In all cases, as discussed earlier in Section 4.6, the BCM was able to accurately downscale GCM precipitation output with respect to the control or baseline period. Many studies have reported lower skill in downscaling precipitation via the use of stochastic and multiple linear regression methods, such as those implemented in LARS-WG and SDSM respectively, than for temperature. In this study the BCM reliably downscaled and reduced the biases in the coarse GCM precipitation output.

### 4.9.3 Historical Temperature Downscaling and Bias Correction

After downscaling and correcting for biases for the historical period, the following observations were made;

- Correlation between observed and raw GCM values was significantly better for temperature than precipitation. In the case of maximum and minimum temperatures ( $T_{max}$  and  $T_{min}$  respectively), the raw GCM values were reasonably representative of the baseline period. Stations Chileka, Makhanga, Mangochi and Ngabu were accurately modelled by the GCMs. At stations Bvumbwe, Chichiri, Mimosa and Thyolo,  $T_{max}$  was overestimated by an average of 5 °C. GFDL-ESM2G (see Figure B.12) overestimated  $T_{max}$  for the wet period at Chichiri and Bvumbwe while at Makhanga and Ngabu, the GCM underestimated  $T_{max}$  by an average of 7 °C. A similar observation was made at the same stations with HadGEM2-ES (Fig. 4.15) where the overestimation was higher and the underestimation lower than GFDL-ESM2G.
- All the GCMs heavily overestimated  $T_{max}$  and  $T_{min}$  at Bvumbwe and Chichiri with the majority also overestimating Thyolo. In this regard, the

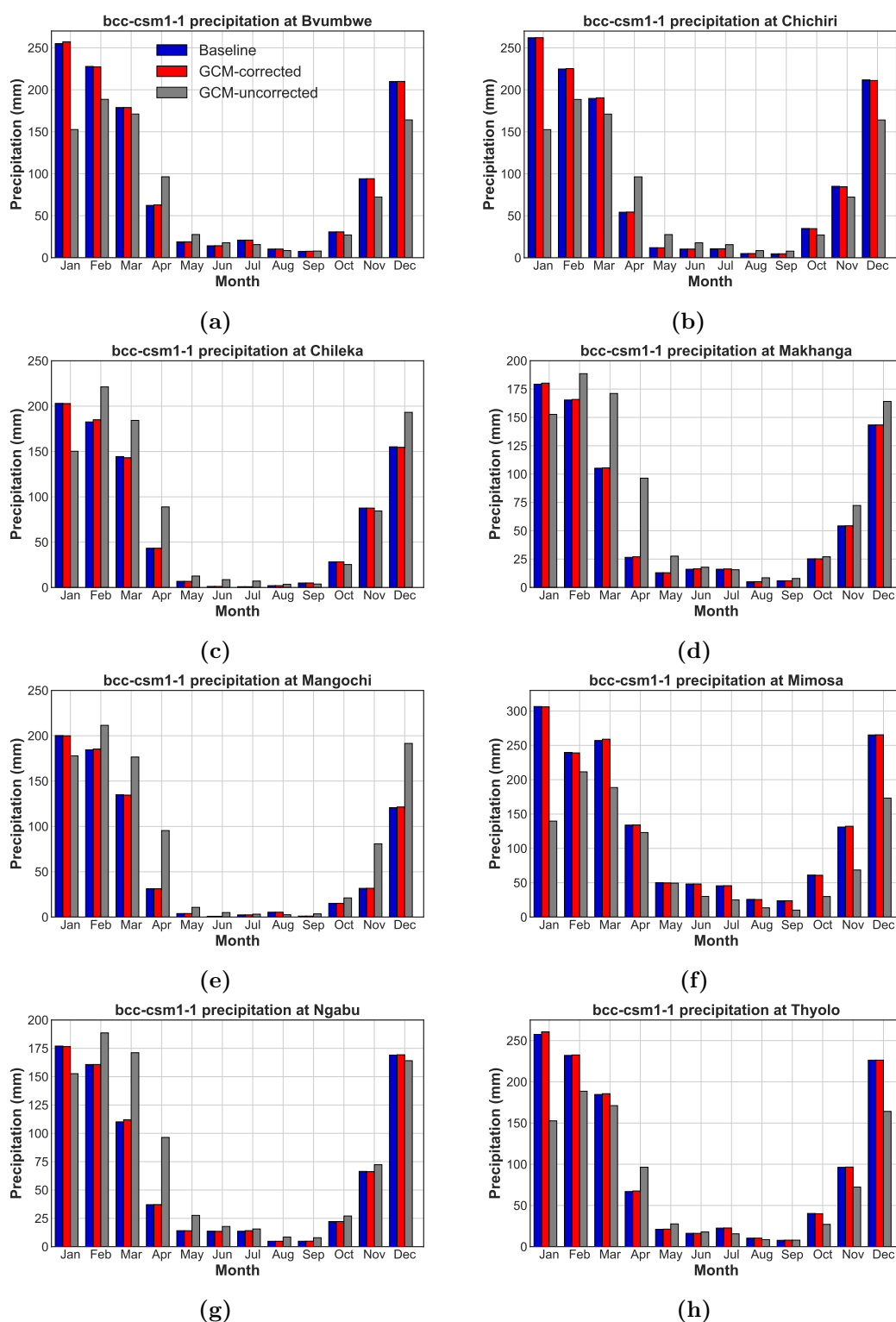
GCMs can be regarded as having moderate to good skill in reproducing the historical temperature records in the SRB. Furthermore, the BCM reliably reduced biases in the monthly mean temperatures as can be observed in Figures B.10 to B.19.

#### 4.9.4 Historical Wet/Dry Spell Lengths

The downscaled and bias corrected GCMs were also tested in terms of how well they reproduced the wet- and dry-spell lengths for the historical period. A wet (dry) spell is defined as the number of consecutive rainy (non-rainy) days (Ratan and Venugopal, 2013) and is calculated here on a monthly basis. The following observations were made;

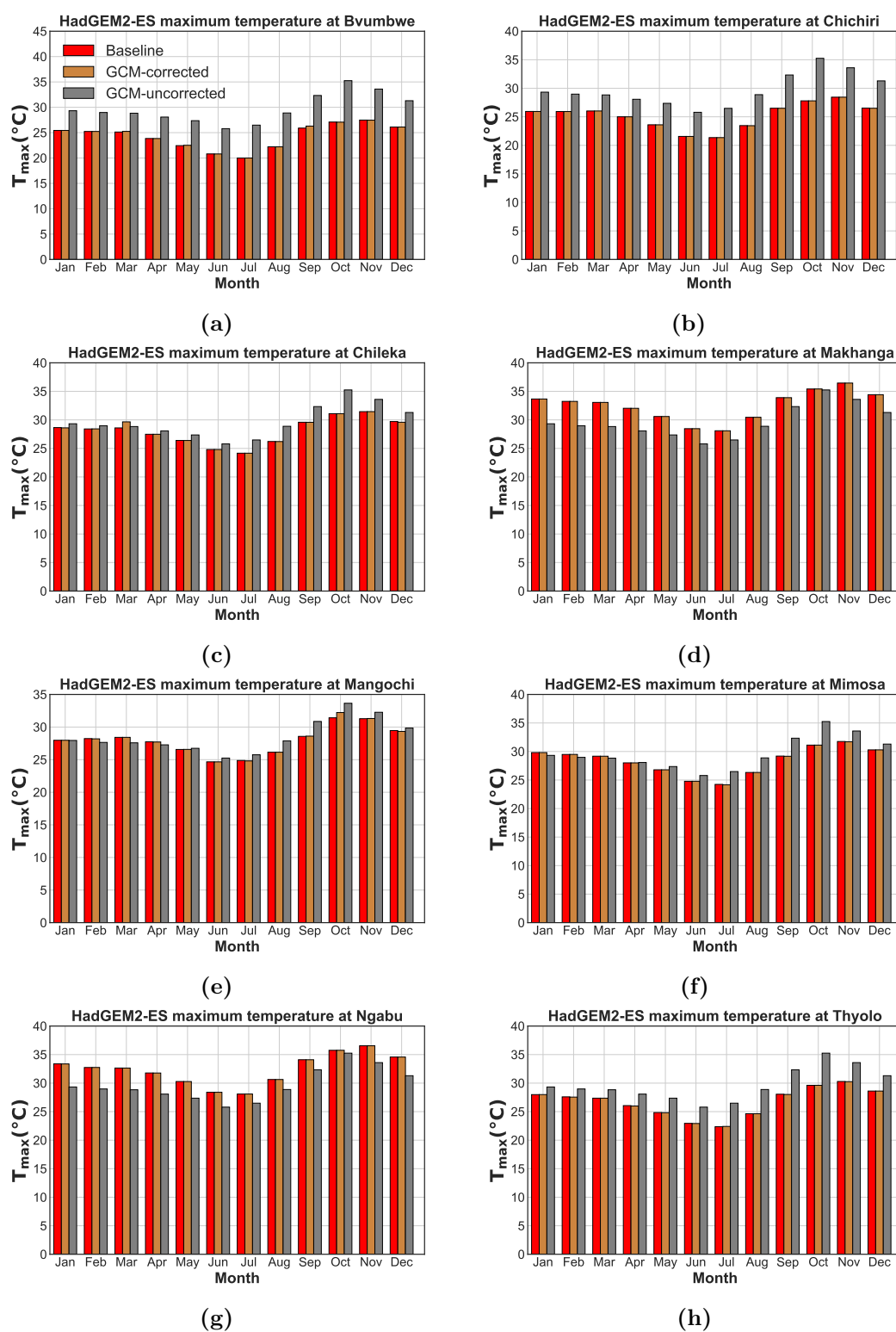
- Of all the GCMs, HadGEM2-ES and MPI-ESM-LR were more skilful in reproducing the wet-spell lengths before and after bias correction (see Figures B.24 and 4.16). Generally, the GCMs showed poor skill in reproducing the mean wet-spell lengths especially for the wet months of December, January, February, March and April. Even after bias correction, we observed poor wet-spell prediction skill among all GCMs. Corrected historical simulations for all GCMs were at least two wet-spell days longer than the observed baseline period.
- Wet-spell length prediction skill for the dry months was much higher for all GCMs and for all stations in the SRB when compared with the wet months. CCSM4 and GFDL-ESM2G showed relatively poor skill in the dry months for all stations except Chileka and Bvumbwe. In all cases, i.e. before and after bias correction, the GCMs over-predicted the wet-spell duration for the dry months by at least one day.

- In the case of dry-spell lengths, the reverse of the wet-spell prediction was observed (e.g. Figure 4.17). This means that all the GCMs showed a tendency to underestimate the wet spell lengths for the dry period while the dry-spell prediction score was higher for the wet months. Almost all the GCMs underestimated the dry-spell lengths with a few exceptions in some months in GCM MPI-ESM-LR (see Figure B.29).

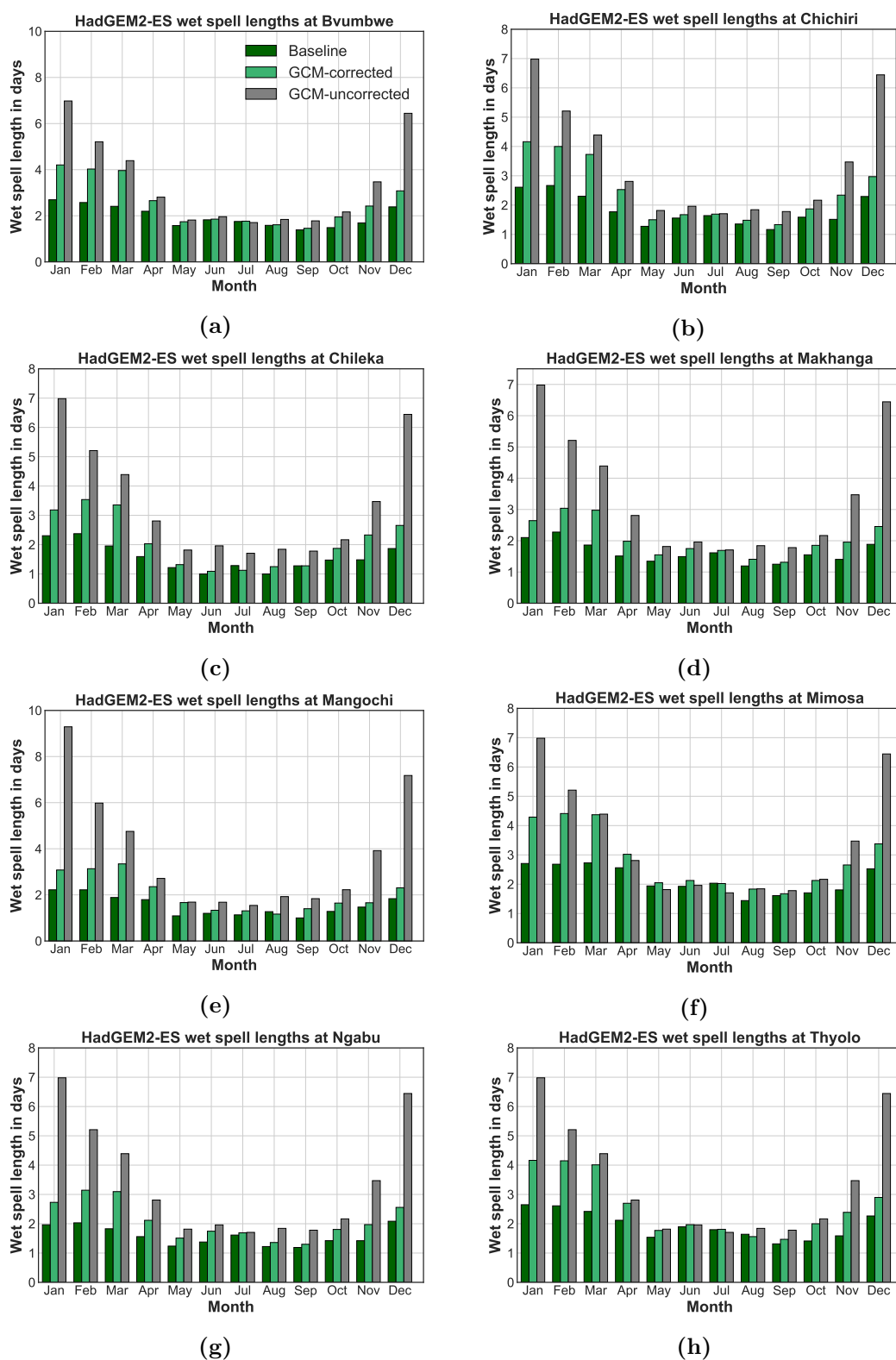


**Figure 4.14** Performance of bcc-csm1-1m downscaled precipitation in the SRB

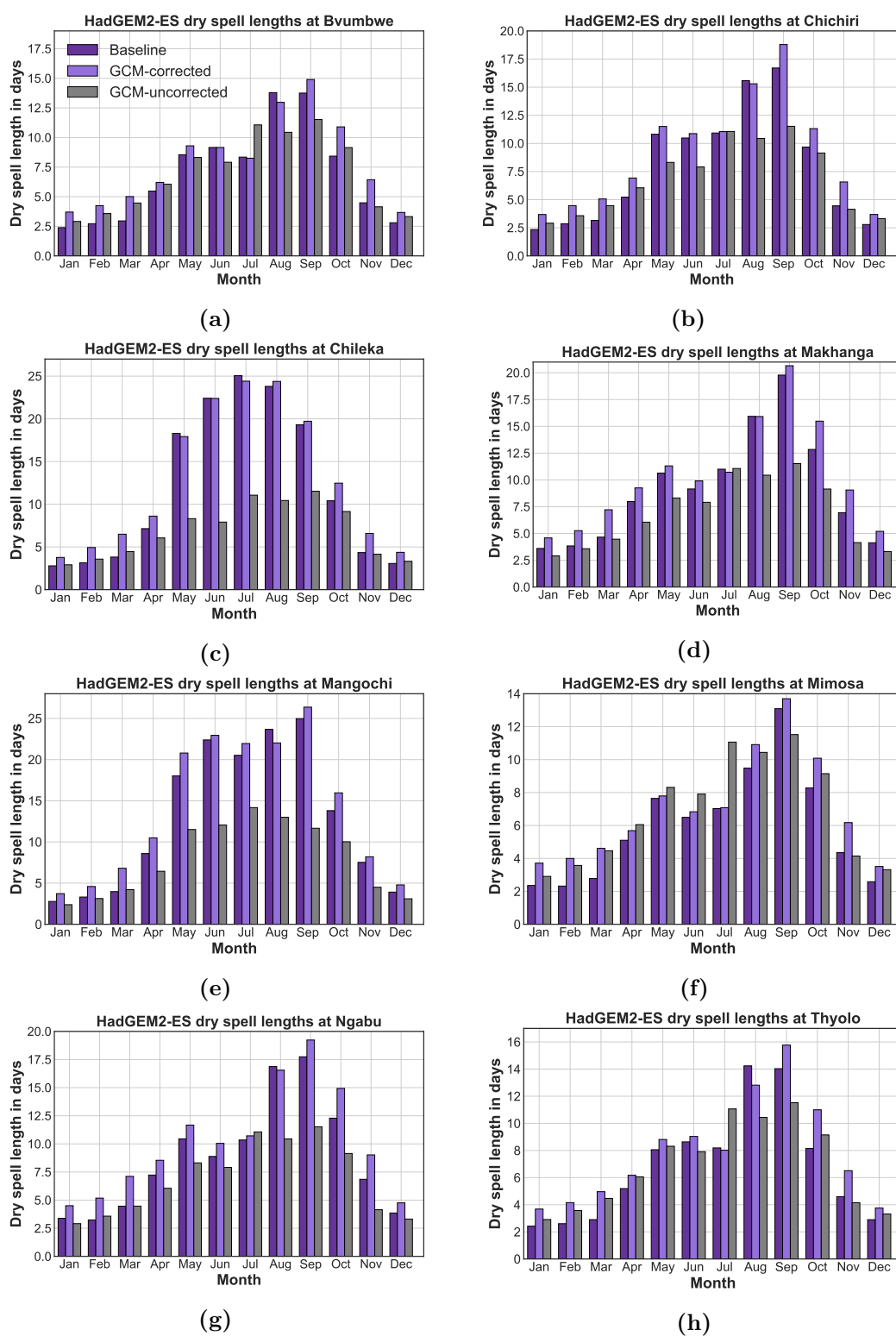




**Figure 4.15** Performance of HadGEM2-ES downscaled maximum temperature in the SRB



**Figure 4.16** Performance of HadGEM2-ES in predicting wet spell lengths in the SRB



**Figure 4.17** Performance of HadGEM2-ES in predicting dry spell lengths in the SRB

### 4.9.5 Future Climate Results and Discussion

For the future period, climate change assessment results of the ensemble model are presented for the three representative stations. Rainfall results are presented as relative changes (percentage) whereas temperature results are presented as absolute changes (see Figures 4.18 to 4.20).

#### 4.9.5.1 Rainfall

At Chileka and Ngabu, the model predicts a +5% to +8% increase in rainfall in the 2020s for the DJF months. A similar pattern was observed at Mangochi but at relatively higher percentages (increase and decrease). This could be attributed to lake effects on the precipitation regime of regions in close proximity to Lake Malawi according to a recent study by Diallo et al. (2018). Although a significant increase in precipitation was observed in regions close to the northern part of the lake, their study concluded that the lake-atmosphere interactions have significant impact on the surrounding regions. By the 2050s, RCP4.5 predicts reduced rainfall at all the representative stations for all months except DJF which depicts a slight increase ranging from +8% to +10% when compared to baseline. Under the RCP8.5 scenario, all stations show increased rainfall of up to +10% in the 2050s in the DJF period while the rest of the months depict reduced rainfall ranging between -10% to -38%. At Chileka and Mangochi, 2080s rainfall under RCP4.5 increases significantly in the DJF and JJA months by up to +25% whereas at Ngabu, rainfall is expected to increase by +15%. Under RCP8.5 the wet months of DJF see increased rainfall of up to +15% in the 2080s at all stations with the rest of the months showing significant decreases in rainfall. From an annual perspective and under all scenarios, rainfall is expected to increase slightly in the

future with the 2050s seeing less rainfall relative to the 2020s and 2080s.

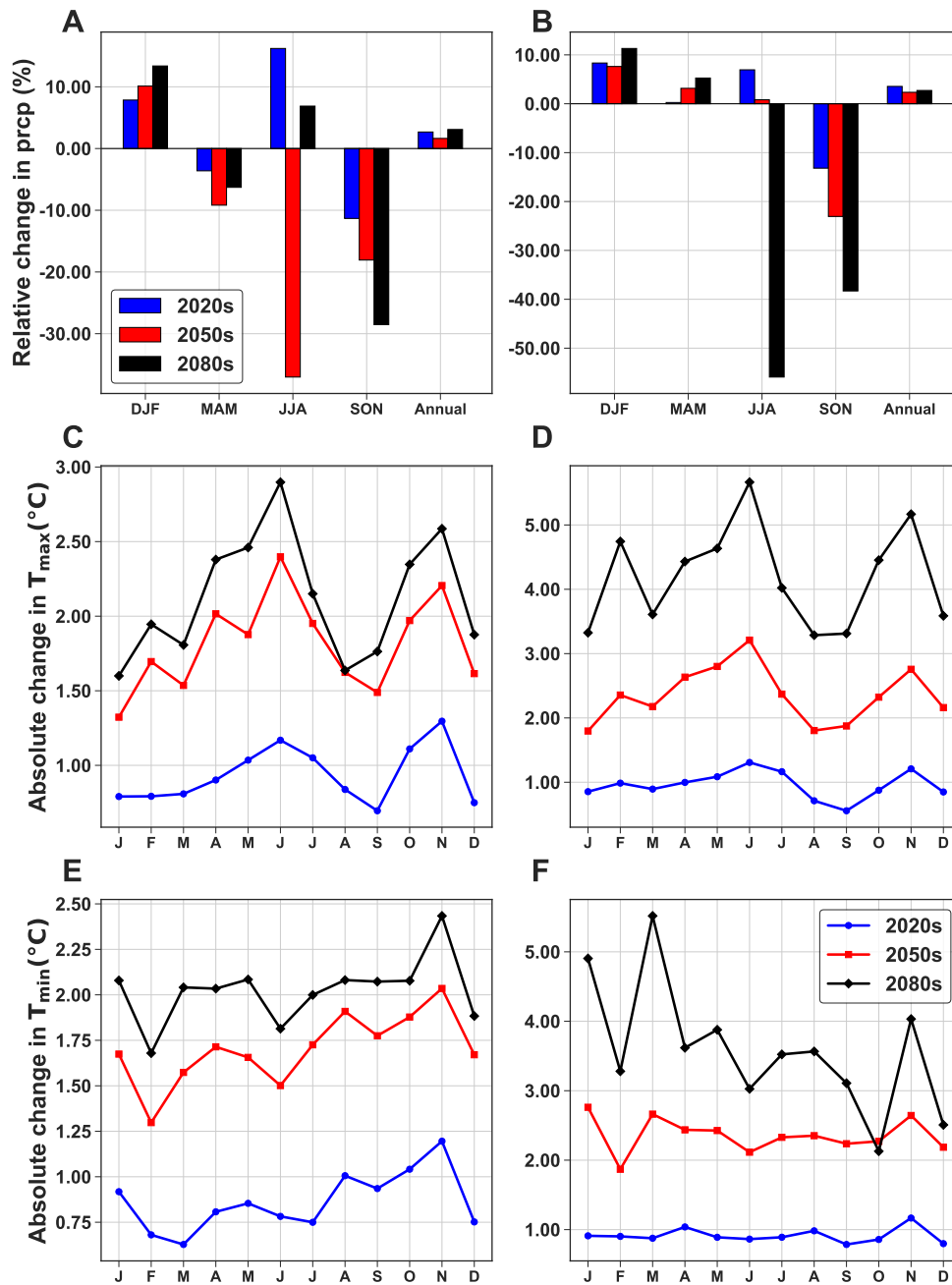
By and large, the future is expected to be wetter in the middle portion (DJF) of the rainy season and drier through the cool and dry seasons. The early and late stages of the rainy season is expected to experience decreased rainfall of up to -40% and -18% respectively. The consequence is that the rainy season may become shorter due to late onset and early cessation of rainfall. Additionally, timing of the planting season of cash crops that sustain most (60%) of the subsistence farmers in the SRB could also be affected leading to poor crop yields. Extreme precipitation events are likely to increase leading to floods in various parts of the basin. The northern part of the basin is expected to experience more rains than the south. The Shire River Basin Ensemble GCM Mean (SRB-EGCMM) results are consistent with results published in a recent study by Zuzani et al. (2019a) which showed decreasing trends in March to December rainfall in the SRB. This trend is expected to persist into the future as demonstrated by this study.

#### 4.9.5.2 Temperature

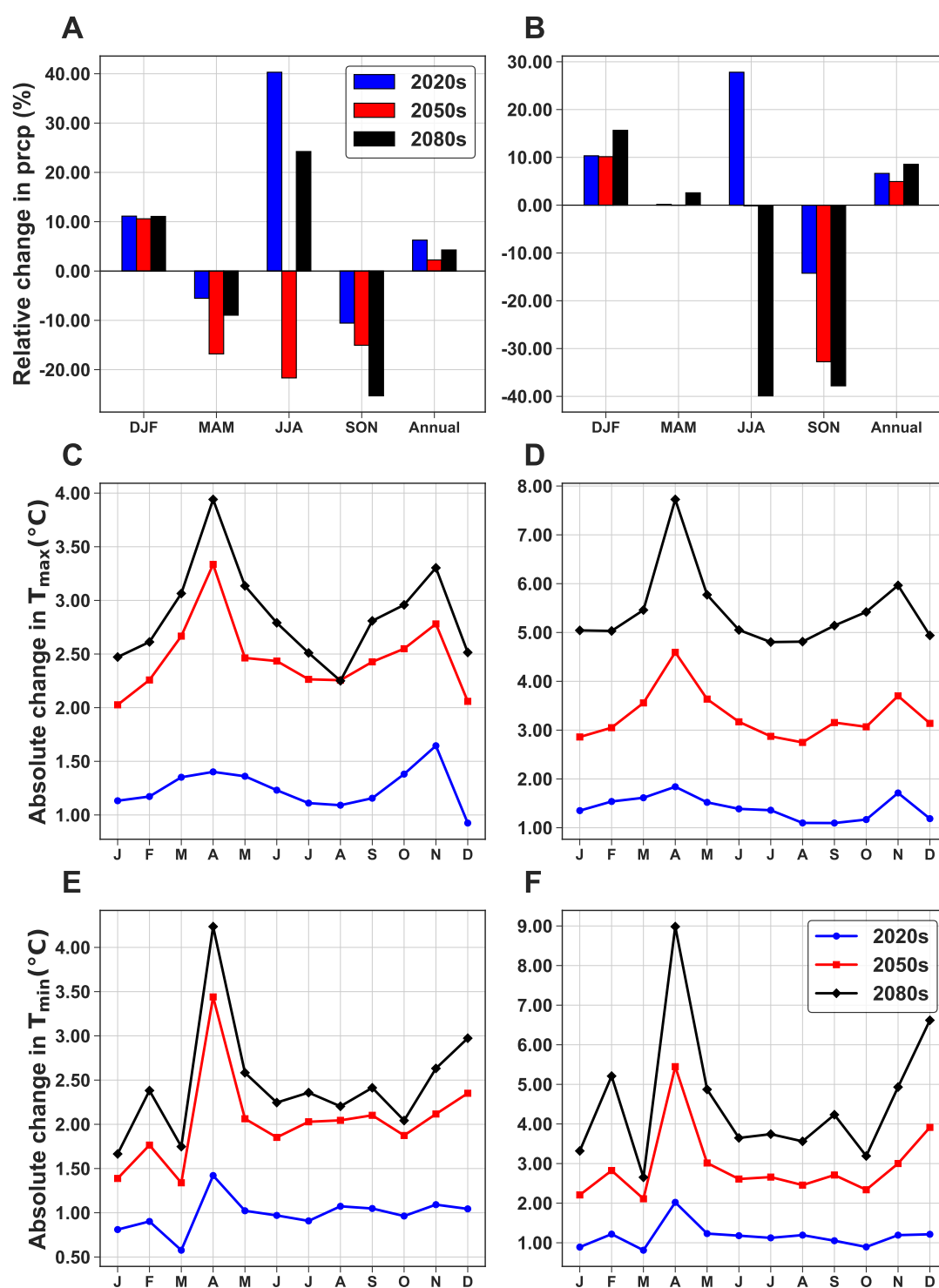
Although here, future  $T_{max}$  and  $T_{min}$  results of the ensemble model are presented, individual GCMs were in agreement with respect to the sign of the change unlike the case for rainfall. As discussed already in Chapter 2, this is to be expected since GCMs have better skill at modelling temperature than precipitation.

$T_{max}$  at all stations under RCP4.5 increases by about +0.8 °C to +1.2 °C. In the 2050s  $T_{max}$  rises by about +1.8 °C to +2.5 °C representing the largest increase between successive forecast time horizons in the century. By the 2080s,  $T_{max}$  ranges between +2 °C to +3 °C.  $T_{min}$  at all stations under RCP4.5 increases by an average of +1 °C, +1.7 °C and +2.4 °C in the 2020s, 2050s and 2080s respectively.

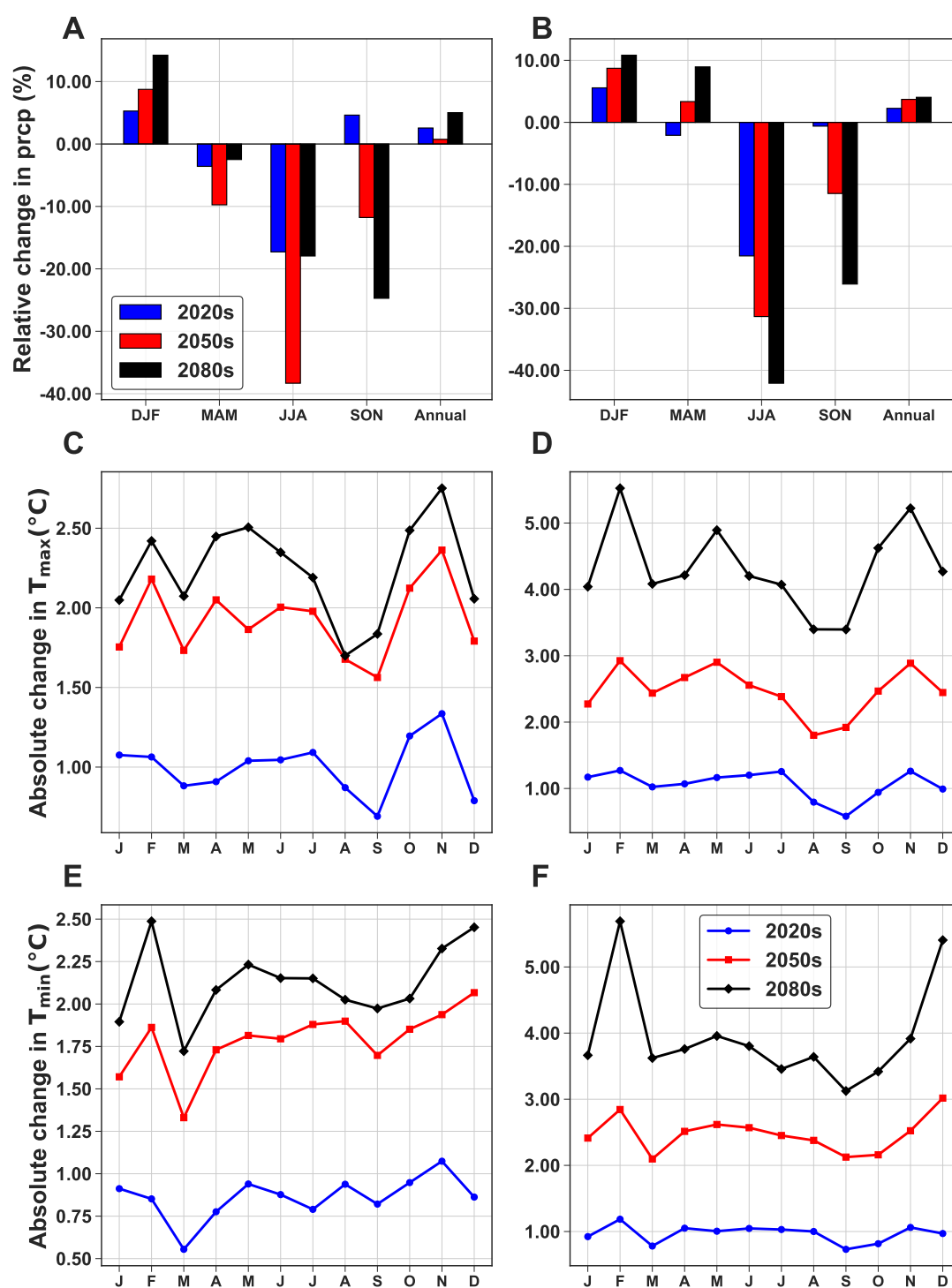
DTR reduces significantly at all stations when compared to baseline due to daily minimum temperatures increasing faster than the maximum daily temperatures.



**Figure 4.18** Chileka future SRB-EGCMM results for rainfall, maximum and minimum temperatures. Figures A,C and E are projected results under RCP4.5 while figures B,D and F represent RCP8.5 results



**Figure 4.19** Mangochi future SRB-EGCMM results for rainfall, maximum and minimum temperatures. Figures A,C and E are projected results under RCP4.5 while figures B,D and F represent RCP8.5 results



**Figure 4.20** Ngabu future SRB-EGCMM results for rainfall, maximum and minimum temperatures. Figures A,C and E are projected results under RCP4.5 while figures B,D and F represent RCP8.5 results



It was observed that all GCMs predict rising minimum and maximum temperatures for both the SRB and RNC. Generally, It has been documented by the IPCC and many other researchers in the literature that confidence in temperature estimates is higher than for other climate variables such as precipitation (Randall and Wood, 2007). While there certainly is some variations from one model to another, climate projections are all unidirectional in terms of the sign of the change. This wasn't the case with rainfall which exhibited considerable variance in projections.

In the case of the Africa, Mechoso et al. (1995) for example, talk about the 'double Inter Tropical Convergence Zone (ITCZ)' problem which remains a major source of error and uncertainty when simulating the annual cycle in the tropics in most AOGCMs (Randall and Wood, 2007). Elsewhere, climate modelling has discernibly improved but is still a challenge over Africa (James et al., 2018). Moreover, none of the current generation of GCMs were built in Africa although there are plans to start developing the first global models in African research institutions (Engelbrecht et al., 2009) that will improve models from international modelling centres over Africa (James et al., 2018). It is expected that these modelling centres will contribute to a more reliable understanding of the many factors such as the sharp gradients in temperature, strong land-atmosphere interactions, prominent modes of interannual and interdecadal rainfall variability (James et al., 2018), and the influences of the ITCZ and ENSO on the rainfall patterns and variability.

## 4.10 limitations

One of the limitations of this study, particularly for the RNC where only one station (Dumfries) was considered, was the use of CRU reanalysis data. As has been mentioned earlier, CRU and CFSR data sets were used to augment Dumfries and SRB stations' data respectively in order to have representative spatial distributions of local climate over the basins. However, reanalyses data often inherit biases from their driving models and can thus lead to optimistic verification when forecasts made with these data sets are verified against their own analysis (Monhart et al., 2018; Park et al., 2008). Due to the many climate and hydrological studies that incorporated gridded data sets and reported favourable results, the methodology that is employed in this thesis can confidently be applied in the RNC and SRB. However, it is highly recommend that future studies investigate this concern further.

Another limitation of this study is that climate impact assessments were conducted using only one downscaling method. In subsequent studies, it would be prudent to consider uncertainty with respect to the choice of the downscaling method for the SRB and RNC.

## 4.11 Chapter Summary

A total of twenty-nine GCMs were downscaled of which a subset of seven (six used in the SRB and five in the RNC) was selected for purposes of assessing future climate change under two RCPs in the SRB and RNC. In the case of the RNC, significant changes in precipitation under RCP4.5 and 8.5 are observed in winter of up to +24% and +28% respectively by the late century. The summers are

expected to be in a slight deficit of up to -4% and -16% under RCP4.5 and 8.5 respectively by the late century.  $T_{\max}$  and  $T_{\min}$ , especially in the winters and summers, are expected to increase by up to 1.9 °C and 1.8 °C respectively under RCP4.5. Significant changes are observed under RCP8.5 where  $T_{\max}$  and  $T_{\min}$  is projected to rise by up to 3.8 °C and 2.5 °C respectively by the late century. Also, the DTR decreases possibly due to the daily minimum temperatures increasing faster than the maximum daily temperatures.

In the case of the SRB,  $T_{\max}$  and  $T_{\min}$  projections by all GCMs indicate a mean rise in temperature of 1 °C, 1.5 °C and 2 °C in the short term, mid- and late century respectively under RCP4.5. Under RCP8.5, the mean rise in temperature was found to be 1 °C, 2.5 °C and 5 °C in the short, mid- and late century respectively. In the case of rainfall, there was a lot of variation in projections from one GCM to another. This is to be expected as there are a lot of factors that affect rainfall projections such as the structure of the GCMs, internal and interannual variability. In summary, by the late century, there could be increased rainfall of up to +15% in the middle stages of the rainy season while the early and late stages of the rainy season could experience decreased rainfall by up to -40% and -18% respectively. Thus, agriculture and in particular timing of the planting of cash crops such as maize is expected to be affected due to the late onset and early cessation of rains. Hence, robust climate adaptation planning and the migration to climate resilient sustainable agriculture is recommended especially in the rural parts of the SRB.

Generally, the effects of climate change are more severe in the SRB than RNC with respect to  $T_{\max}$ ,  $T_{\min}$  and rainfall. Although possible rainfall quantities have been projected, this study did not aim to assess the nature of occurrence of precipitation. It is possible that the rise in precipitation in both the RNC

---

and SRB could manifest as storms or extreme precipitation events mixed with intra-monthly droughts.

*—If you would be a real seeker after truth, it is necessary that at least once in your life you doubt, as far as possible, all things.*

Rene Descartes

# 5

## Hydrological Modelling

*Detailed hydrological analyses for the RNC and SRB are provided in this chapter. A brief discussion on the objectives of this chapter is provided first. Thereafter the rest of the chapter is split into discussions of hydrological analyses for the RNC and later the SRB. A summary of the pertinent insights gained from application of the methodology developed in this research to a data-rich versus data-scarce region is then presented. Finally, effects of climate change on water surface water resources in the two catchments are discussed.*

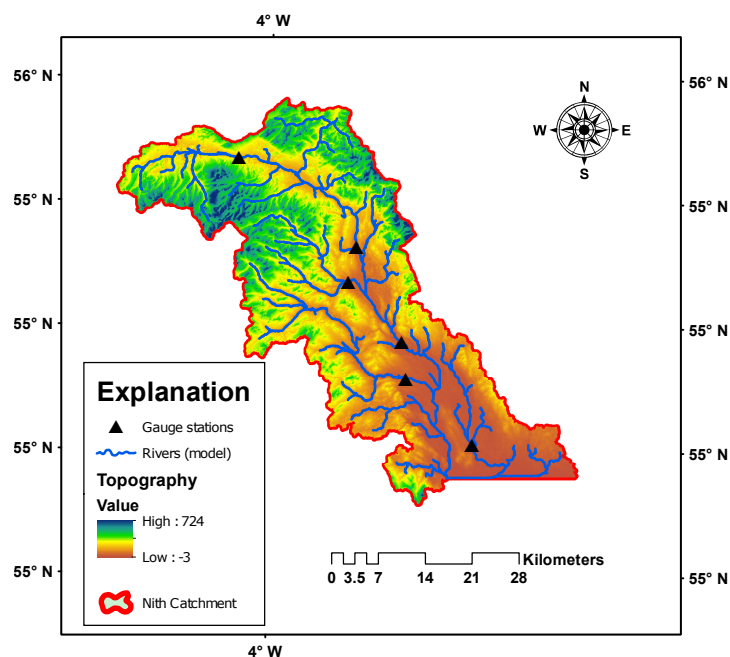
## 5.1 Introduction

To fully understand the impacts of climate change and other environmental stresses on water resources, a holistic investigation involving all the components of climate, hydrological cycle and the environment should be carried out. This chapter describes the development of semi-distributed models for the RNC and SRB based on the SWAT hydrological model. Water balance components for the two study areas were calculated for the baseline and future periods. Furthermore, using SWAT models forced with future climate predictions, quantifications of future streamflow availability was made along with the associated uncertainties.

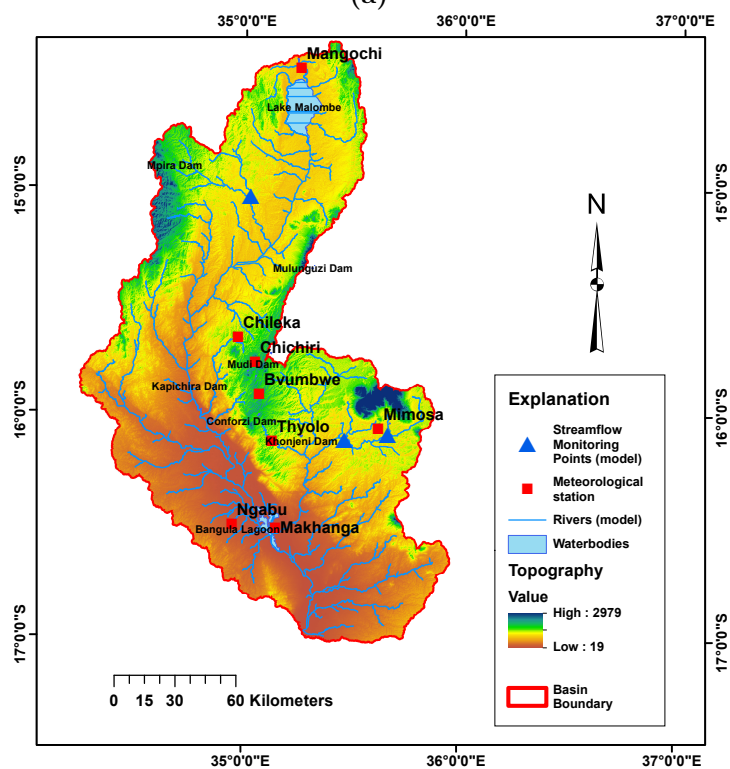
As a secondary objective and as earlier stated, hydrological models were developed for a data-rich region (i.e. RNC) first before applying the same methodology to a region with sparse data (SRB in this case). Observations were then made on whether the methodology is transferable from one region (i.e. data-rich) to the other (i.e. data-scarce). Thus, the structure of this chapter is such that the methodology and data needs for the RNC, together with the simulated results and analyses, are first presented before presenting that of the SRB. Where there was a notable deviation in methodology from that of the RNC, comments have been made accordingly.

## 5.2 Description of the Study Sites

The basic layouts of the two study basins i.e. RNC and SRB are presented in Figures 5.1a and 5.1b respectively. The RNC is mainly drained by the River Nith and its tributaries while the SRB is drained by the Shire River and its tributaries.



(a)



(b)

**Figure 5.1** Watershed layouts: (a) River Nith Catchment (UK) and (b) Shire River Basin (Malawi)

## 5.3 RNC Hydrologic Modelling

### 5.3.1 Model Setup

Model delineation, parametrization and pre-processing of input data was done using a combination of tools. Model delineation relied on tools provided in QSWAT, a QGIS based SWAT model interface used for pre- and post-processing of SWAT inputs and outputs. The QSWAT interface successfully delineated and parametrized the RNC SWAT model but was converted to the ArcGIS interface due to the latter being an order of magnitude faster. This was necessitated by the fact that conceptual modelling and parametrization was varied numerous times before a hydrologically correct model was configured. In the following sections, steps involved in the model setup are discussed in detail.

#### 5.3.1.1 Watershed Delineation

Model delineation in the SWAT model requires a spatially georeferenced DEM. The elevation of the RNC ranges between 0 and 724m amsl (Figure 5.2a). The RNC was delineated by selecting an outlet point (outlet of a watershed above the respective point) near the coastal edge of the catchment as the River Nith drains into the Solway Firth. Initial attempts to delineate the model did not result in satisfactory results. Subsequently, an attempt to improve catchment delineation by using the “Burn-in” feature of ArcSWAT (QSWAT also) was made. This method improves the hydrographic segmentation and sub-watershed boundary delineation (Luo et al., 2011) by slightly reducing the elevation of parts of the DEM intersected by the ‘real’ streams (in this case obtained via Google Earth software). Using this method, stream and watershed delineation was greatly improved. When the



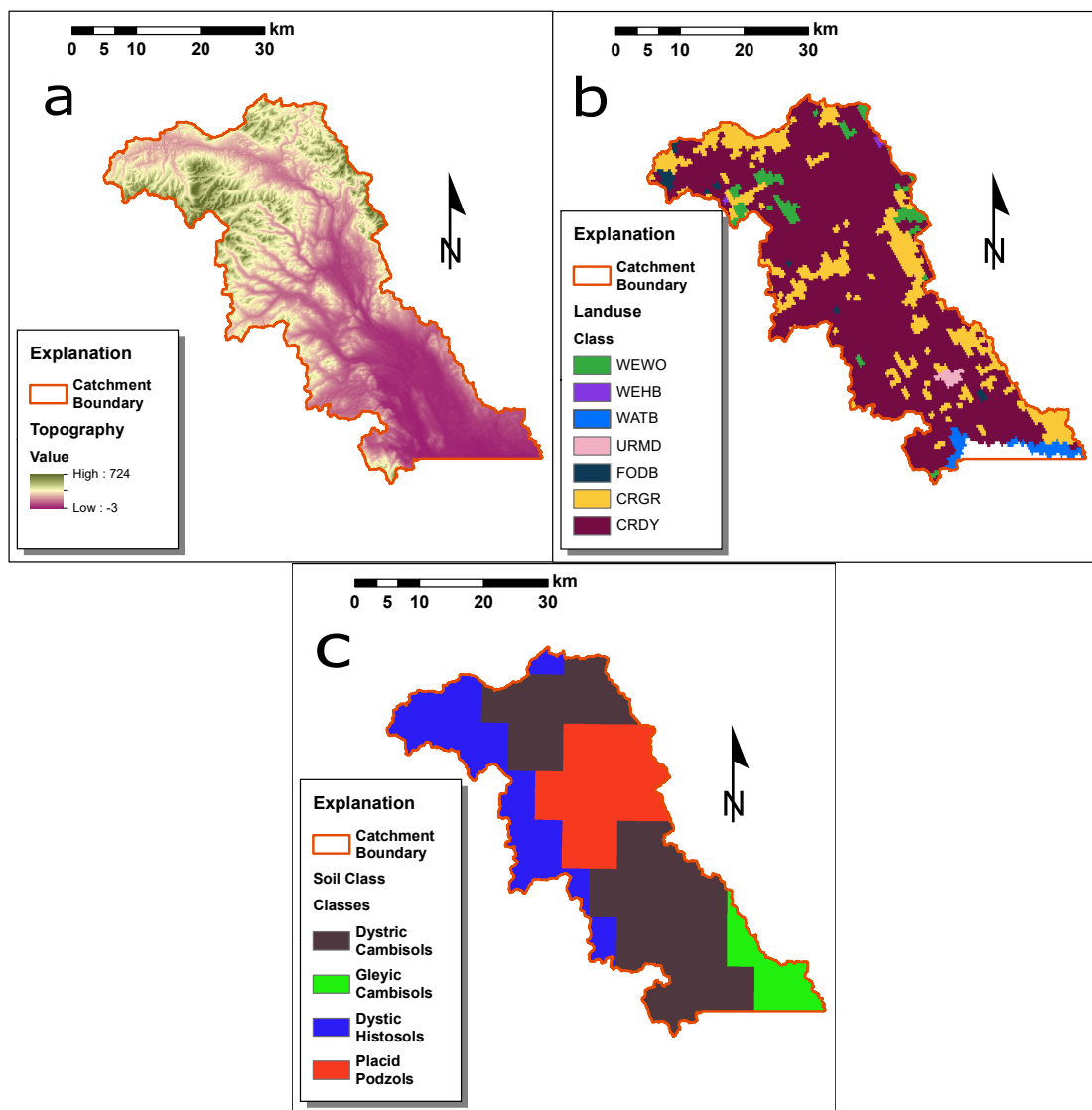
same method was applied to a 3 arc-second resolution Shuttle Radar Topography Mission (STRM) DEM (i.e. STRM 90m), even better results were achieved than earlier attempts using a 1 arc-second resolution DEM. Consequently, this method was adopted as the optimum resolution for the SWAT model. A threshold drainage area of 1000 ha was chosen as a suitable compromise between accuracy of stream delineation and number of subbasins produced since the lower the subbasins the lower the computational demand and time. This resulted in a watershed with 83 subbasins, 516 HRUs and a total area of 145049.31 ha.

#### 5.3.1.2 Land-use/Landcover

After delineation of the watershed, SWAT requires land-use data before constructing the HRUs. The land-use raster was converted to the same coordinate reference system (CRS) as the DEM and clipped to the extent of the watershed in QGIS. Within the RNC, a total of seven land-use classes were defined. From Table 5.1, it can be seen that dryland cropland and pasture (CRDY) constitutes the majority of the RNC.

**Table 5.1** Distribution of LU/LC classes in the River Nith Catchment

Land-use	Description	Area (ha)	% Watershed
CRDY	Dryland Cropland and Pasture	107129.25	76.32
CRGR	Cropland/Grassland mosaic	24726.786	17.62
WEWO	Wooded Wetland	5054.0681	3.6
WEHB	Herbaceous Wetland	244.4172	0.17
FODB	Deciduous Broadleaf Forest	1267.9468	0.9
URMD	Residential-medium density	802.0428	0.57
WATB	Water Bodies	1143.9142	0.81



**Figure 5.2** SWAT model inputs for the RNC; (A) DEM map (B) LU/LC map and (C) Soil map.

### 5.3.1.3 Soil data

Similar to the process followed in the preceding section, soil maps (see Figure 5.2c) were converted to rasters and reprojected to the same CRS as that of the DEM used to delineate the watershed. After clipping the soil layer to the watershed

extent in the QGIS environment, four soil classes were identified. The majority of the catchment is dominated by soils of type ‘Dystic Cambisols’ (Table 5.2).

**Table 5.2** Distribution of Soil classes in the River Nith Catchment

Soil Class	Description	Area (ha)	% Watershed
Bd42-1-2b-6406	Dystic Cambisols	71205.51	49.09
Bg12-2ab-6463	Gleyic Cambisols	6080.54	4.19
Od26-a-6587	Dystic Histosols	35113.09	24.21
Pp3-1b-6619	Placid Podzols	32650.17	22.51

#### 5.3.1.4 Weather data

Weather data was prepared and selected using the methodology presented in Section 4.3. Uncalibrated hydrographs in the RNC produced with CRU datasets were all above  $NSE = 0.5$  and thus the model could have been accepted as suitable for hydrological analyses without calibration (e.g. Arnold et al., 2012).

#### 5.3.1.5 Simulation period

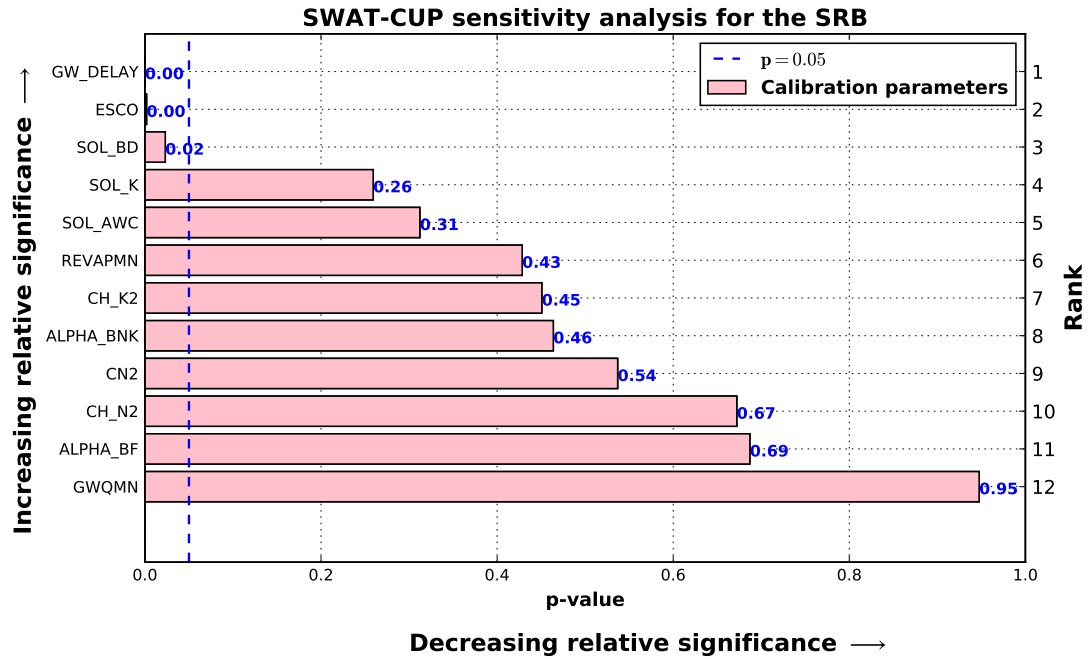
The baseline RNC SWAT model was run from 1979 to 2005. Six years were assigned to the model as a “warm-up” period. This means that SWAT ran the simulation from 1979, but only printed results for the last 21 years (i.e., 1985 to 2005).

### 5.3.2 Model calibration and validation

To calibrate the RNC model, the SUFI-2 algorithm was applied using the SWAT-CUP interface. In the first stage, a local sensitivity analysis for the four streamflow variables was performed by setting the lower and upper bounds of the calibration parameters. A total of thirteen parameters related to surface run-off and baseflow

were selected for sensitivity analysis before one iteration of 1000 simulations was run in SWAT-CUP. With respect to computation time, the RNC model took a total time of 5.78 hours to complete one iteration of 1000 simulations. It should also be noted that during model construction, the ‘Multiple HRUs’ option was selected when subdividing the watershed into HRUs. If the option ‘Dominant Land Use, Soils, Slope’, one HRU for each subbasin would be created and consequently, the dominant land use, soil, and slope class in the subbasin simulated in the resulting HRU. Similarly, if the ‘Dominant HRU’ option is selected, one HRU for each subbasin is created and the dominant unique combination of land use, soil, and slope class in the subbasin used to simulate the HRU. The Multiple and Dominant HRU options were not explored in this research but it would be interesting to see how these options affect streamflow and nutrient transport modelling in the SRB in a future study. Moreover, these options have been shown by Schuol et al. (2008b) to reduce significantly the computation time of the SWAT model calibration.

After the initial iteration was done, a global sensitivity analysis was performed by regressing the Latin hypercube generated parameter against the objective function values as discussed in Chapter 3. The objective function used in this study is the NSE. The results of the sensitivity analysis are presented in Figure 5.3 and Table 5.10. Using the p-value derived from a t-test as a measure of the relative significance, it can be seen from Figure 5.3 that parameters GW\_DELAY, ESCO and SOL\_BD were the most significant parameters. A short description of the parameters is given in Table 5.3. Parameters below the  $p = 0.05$  line are significant at the 95% confidence level and thus are a meaningful addition to the model as the changes in these parameters are related to changes in the



**Figure 5.3** Global sensitivity analysis results for the RNC. Dashed blue line is the  $p = 0.05$  line.

response variable. In the same vein, values which had very high p-values such as CH\_N2, ALPHA\_BF and GWQMN and were subsequently removed from further calibration iterations leaving a total of ten parameters in the final calibration setup. These parameters were continuously changed throughout the SUFI-2 calibration process in a campaign to maximise the objective function. Three more calibration iterations were performed for the period between 1985 to 2000 on a monthly time-step before an optimal solution was reached. When the optimal solution was reached, i.e. when a point was reached when further iterations did not lead to any improvement in the p-factor and R-factor, the calibration process was stopped and the calibrated parameters accepted as the final solution. The final corrected parameters and their calibrated ranges for the RNC model are presented in Table 5.4.

While it is possible to select any of the ten available objective functions available in the SUFI-2 algorithm, the NSE was selected due to its popularity in hydrology as a performance metric. However, it would be good science to test the effect of each of the different objective functions implemented in SWAT-CUP on the calibration process in future studies.

Because SUFI-2 is a semi-automated calibration technique, the algorithm needs to be guided between successive iterations to avoid suggesting physically impossible and meaningless parameter values. It is incumbent upon the modeller to have a fairly good understanding of the physical processes in the basin or watershed being modelled. Further, the modeller should have an appreciation of the desirable SWAT parameter ranges that are recommended for successful calibration. Here, the calibration protocol in Abbaspour et al. (2015) was followed to guide the direction of the calibration process in addition to the desirable parameter range knowledge which was known a priori.

Having examined and accepted the optimal solution, one iteration of 500 simulations was run to validate the model using observations between the years of 2000 and 2005. The optimal parameters solved during the calibration stage were used without any changes during the validation period.

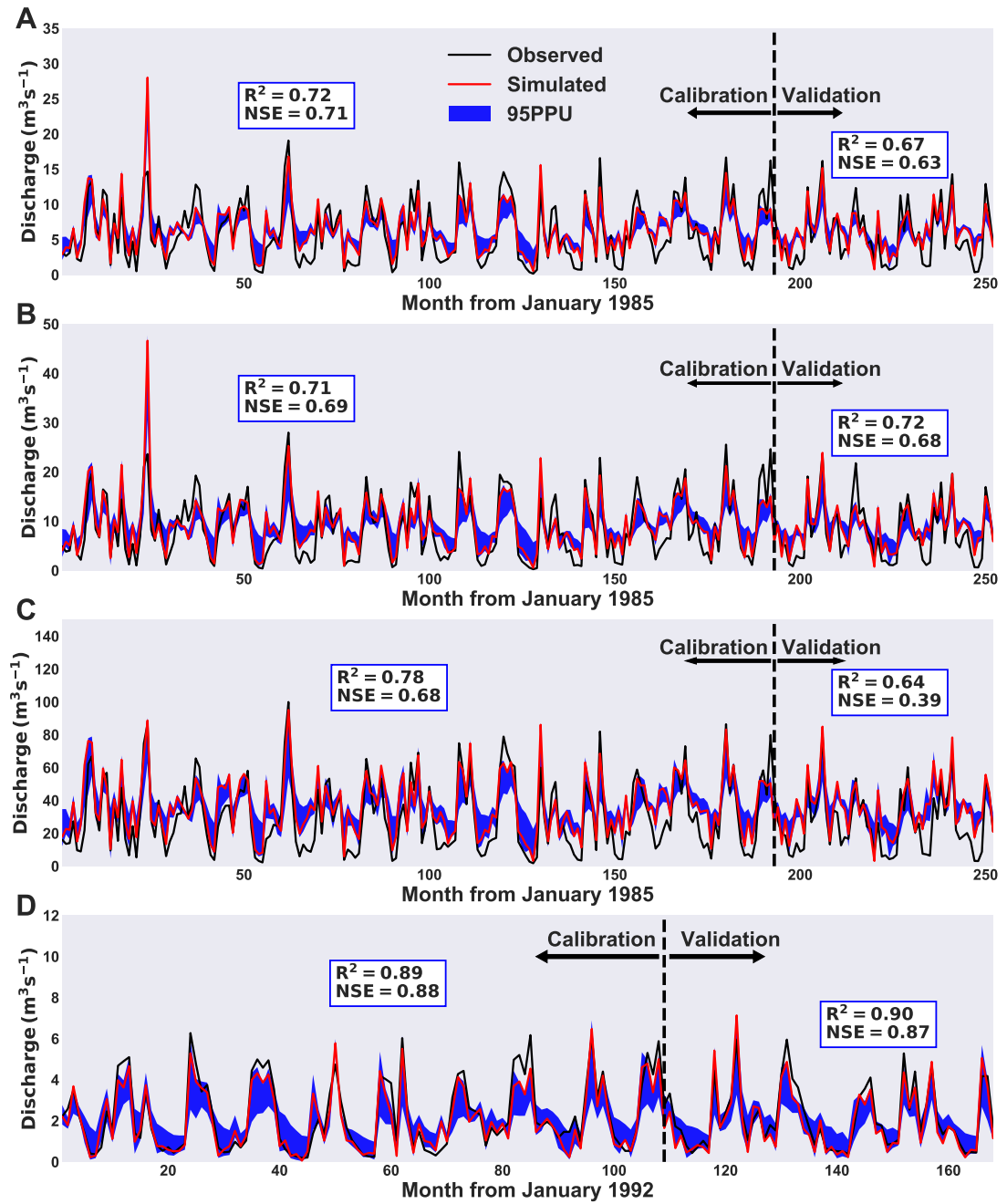
### **5.3.3 Climate change impacts on streamflow - RNC**

Changes in streamflow has been a topic of interest to water resources specialist for many decades now. These changes are usually classified into two categories i.e. climatic and non-climatic. The former can manifest as either climate change or natural variability while the latter can be due to a lot of factors such changes in LU/LC, water control and diversions, dams, bridges, tunnels and irrigation.

**Table 5.3** Description of SWAT parameters used in the RNC calibration process

No.	Parameter	Description
1	REVAPMN	Threshold water depth in the shallow aquifer for “revap” [mm]
2	GW_REVAP	Groundwater “revap” coefficient
3	CN2	Initial SCS runoff curve number for moisture condition II
4	ALPHA_BF	Baseflow alpha factor (1/days)
5	GWQMN	Threshold depth of water in the shallow aquifer required for return flow to occur (mm H <sub>2</sub> O)
6	CH_N2	Manning’s “n” value for the main channel
7	GW_DELAY	Groundwater delay time (days)
8	ESCO	Soil evaporation compensation factor
9	SOL_AWC	Available water capacity of the soil layer (mm H <sub>2</sub> O/mm soil)
10	SOL_BD	Moist bulk density (Mg/m <sup>3</sup> or g/cm <sup>3</sup> )
11	ALPHA_BNK	Baseflow alpha factor for bank storage (days)
12	SOL_K	Saturated hydraulic conductivity (mm/hr)
13	CH_K2	Effective hydraulic conductivity in main channel alluvium (mm/hr)

Analysing streamflow records for temporal trends that can be attributed to climate change, however, is a very difficult task and one fraught with many traps such as the occurrence of “change points” which can mask or amplify temporal trends (Dierauer et al., 2017). Fortunately, all the gauge records in the RNC were subjected to a hydrometric data screening process that categorized each station according to a suitability benchmark which is explained in Harrigan et al. (2018). According to the NRFA, out of all the gauging stations in the catchment, only Scar Water at Capenoch (79004) and Nith at Friars Carse (79002) were found to be most suited for identification and interpretation of long-term hydrological variability and change. Therefore, in this study, climatic change in streamflow was assessed with reference to these two stations.



**Figure 5.4** Graphs of river discharge calibration and validation for selected rivers in the RNC: a) Scar Water at Capenoch, b) Cluden Water at Fiddlers Ford, c) Nith at Friars Carse and d) Lochar Water at Kirkblain Bridge

### 5.3.3.1 Baseline Trends

Mann-Kendall trend test results at 5% significant level indicate that at SWC, there is a significant upward trend for high flows (Q5) and medium flows (Q50) while



**Table 5.4** Calibrated parameter values with their range for the RNC arranged according to their sensitivity in decreasing order

Rank	Parameter name	Op.*	File type	Fitted Value	Min. Value	Max. Value
1	GW_DELAY	v	.gw	6.0452	-1.0911	11.2340
2	ESCO	a	.hru	0.5009	0.4872	0.5713
3	SOL_BD	r	.sol	0.4026	0.2497	0.5572
4	SOL_K	r	.sol	0.4763	0.1511	0.5531
5	SOL_AWC	r	.sol	0.3647	0.2511	0.4610
6	REVAPMN	v	.gw	-0.7476	-1.7157	-0.4666
7	CH_K2	v	.rte	-23.7681	-29.4653	-21.0993
8	ALPHA_BNK	v	.rte	0.7241	0.6714	0.8465
9	CN2	v	.mgt	0.0551	0.0517	0.1033
10	CH_N2	v	.rte	0.2489	0.2145	0.2527

\* Denotes the *mathematical operation* being applied on the parameter where *v* means the existing parameter is to be replaced by a given value, *a* means a given value is added to the existing parameter value and *r* means an existing parameter value is increased by the given value as a percentage.

for low flows (Q95) there is an insignificant upward trend. At NFC, both high flows and medium flows show a significant increasing trends at the 5% significant level. Again, low flows trends are positive (increasing) but insignificant. Generally, Harrigan et al. (2018) report that analyses show there is an increase in annual mean flows (AMF) across the UK but especially in Scotland. Additionally, the trends reveal a tendency for an increase in high flows over the past 50 years. Detailed UK-wide streamflow trend analyses can be found in Harrigan et al. (2018).

### 5.3.3.2 Future Streamflow Impacts

Climate results downscaled from 5 GCMs were used to force SWAT models under RCP4.5 and RCP8.5 scenarios. The relative percentage change between future periods and the observed period for stations 79002 and 79004 was then calculated.

Percentage changes were calculated for the winter period (DJF) because of two reasons. Firstly, this is the wettest period in the RNC and secondly, all the GCMs predicted an increase in precipitation in the winter period.

Figures 5.5 to 5.10 show results from streamflow analyses for the future period. The “No\_Observation” module of SWAT-CUP was used to calculate the uncertainty (95PPU) associated with the future simulations using the calibrated parameters shown in Table 5.4. Ideally, the future simulations should be compared with observed baseline values but as was demonstrated in Section 5.3.2, the model cannot simulate the baseline period with absolute accuracy. By comparing future simulated values with the actual observed values, biases from the model simulated results can lead to spurious effects and thus lead to erroneous interpretations of impact (Shen et al., 2018). To negate the effect of such biases, simulated future streamflow was compared with model simulated baseline streamflow; a method which has been successfully employed in many other studies (e.g., Chen et al., 2011; Jung et al., 2012; Minville et al., 2008; Shen et al., 2018).

**Scar Water at Capenoch (SWC):** As expected, the changes in streamflow are not in agreement from one GCM to another. The sign of the change, however, is more consistent than the magnitude of the change. For example, at least three of the five GCMs are in agreement with the sign of the change (i.e. decrease in monthly streamflow) at Scar Water at Capenoch in the 2020s for all RCPs. However, due to structural differences in the GCMs, uncertainties exist in the climate inputs which further propagate through the SWAT models; thus the magnitude of change is significantly different from one GCM to the next. A similar downward trend is projected in the 2050s by almost all GCMs under RCP4.5 while almost all GCMs indicate

an upward shift in monthly streamflow. In the late century, at least three of the GCMs show an upward trend under all scenarios. Generally, the relative changes are insignificant when compared to the baseline when analysed at the *M95PPU*. However, it should be noted that there is significant uncertainty associated with these projections as is depicted by the shaded bands.

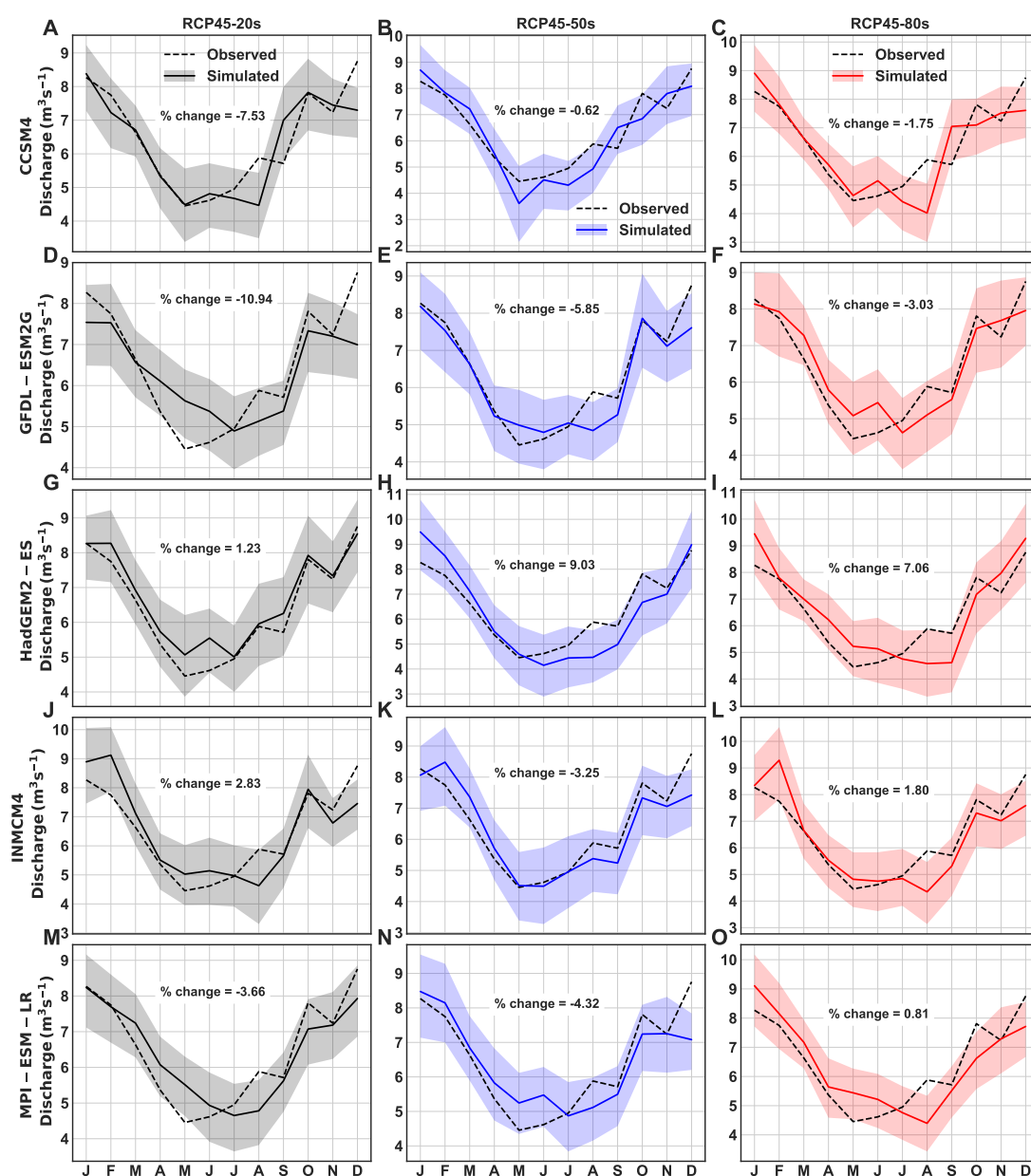
**Nith at Friar's Carse (NFC):** Similar to the case of SWC, noticeable differences in both the sign and magnitude of the change in streamflow was observed. Under RCP4.5 the general consensus is that there will be a slight decrease in monthly streamflow in the 2020s except for HadGEM2-ES and INMCM4 which project positive changes in the streamflow. Under RCP8.5, the projection is negative for all GCMs except for INMCM4 which shows a significant change in the opposite direction. There is a further decrease (about 3%) in streamflow in the mid-century from 3 GCMs under RCP4.5 while the late-century sees an increase in streamflow from most of the GCMs. Under RCP8.5, most of the models project an increase in streamflow in the mid- to late-century.

**Ensemble Models:** One of the problems that has been considered in this thesis is the issue of ensemble modelling. It is widely accepted in the literature that ensemble models offer better predictions or projections by overcoming biases inherent in individual models and also uncertainties arising due to the structural composition of the models. In fairness, hydrological models are fraught with many uncertainties that have been discussed in detail in Section 2.2. In climate studies, however, the issue of how to average model results has been heavily studied and is still an active area of research. The

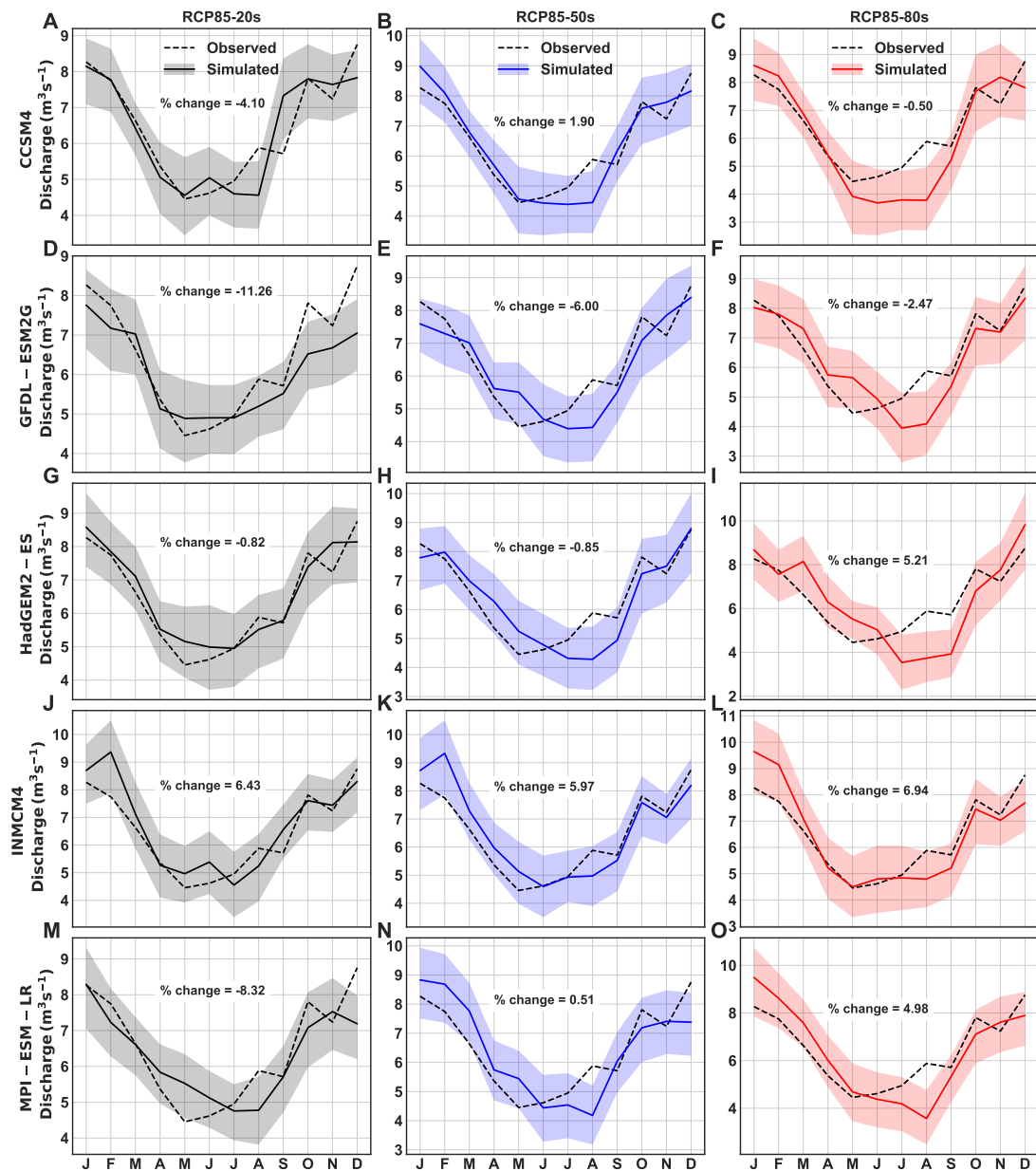
goal in this thesis was to understand how climate change affects aspects of the hydrologic cycle in the RNC and SRB. As such, it is important to consider issues of how to combine different projections and incorporate them into impact studies. After GCM selection, one issue considered in this research is the fact that each GCM realisation is a possible future which has to be taken into consideration; which begs the question – how are the model results to be combined and/or averaged? Is it at the GCM selection stage or at the hydrological modelling stage? With respect to streamflow, the findings for the RNC are summarised as follows;

- ☞ Hydrologic projections were found to be different from one model to another. In the RNC for example, for each time-scale, it was rare that 4 out of 5 GCMs would depict the same sign or direction in streamflow change. While it is numerically implausible to expect the same magnitude of change, where the sign of change is in agreement, most of the models show similar magnitudes of change.
- ☞ Figures 5.9 and 5.10 show results of a hydrologic model forced with the River Nith Catchment Ensemble GCM Mean (RNC-EGCMM) and the River Nith Catchment SWAT Ensemble Model Mean (RNC-SWATEMM) – a simple arithmetic average of the SWAT models, respectively. From these two figures, it is unclear which approach should be recommended. For example, both results agree on the direction of change, and to some extent on the magnitude of change, under all scenarios. The two figures are in agreement that the 2020s will experience a slight decrease in streamflow while the 2050s and 2080s see an increase when compared to the baseline values.

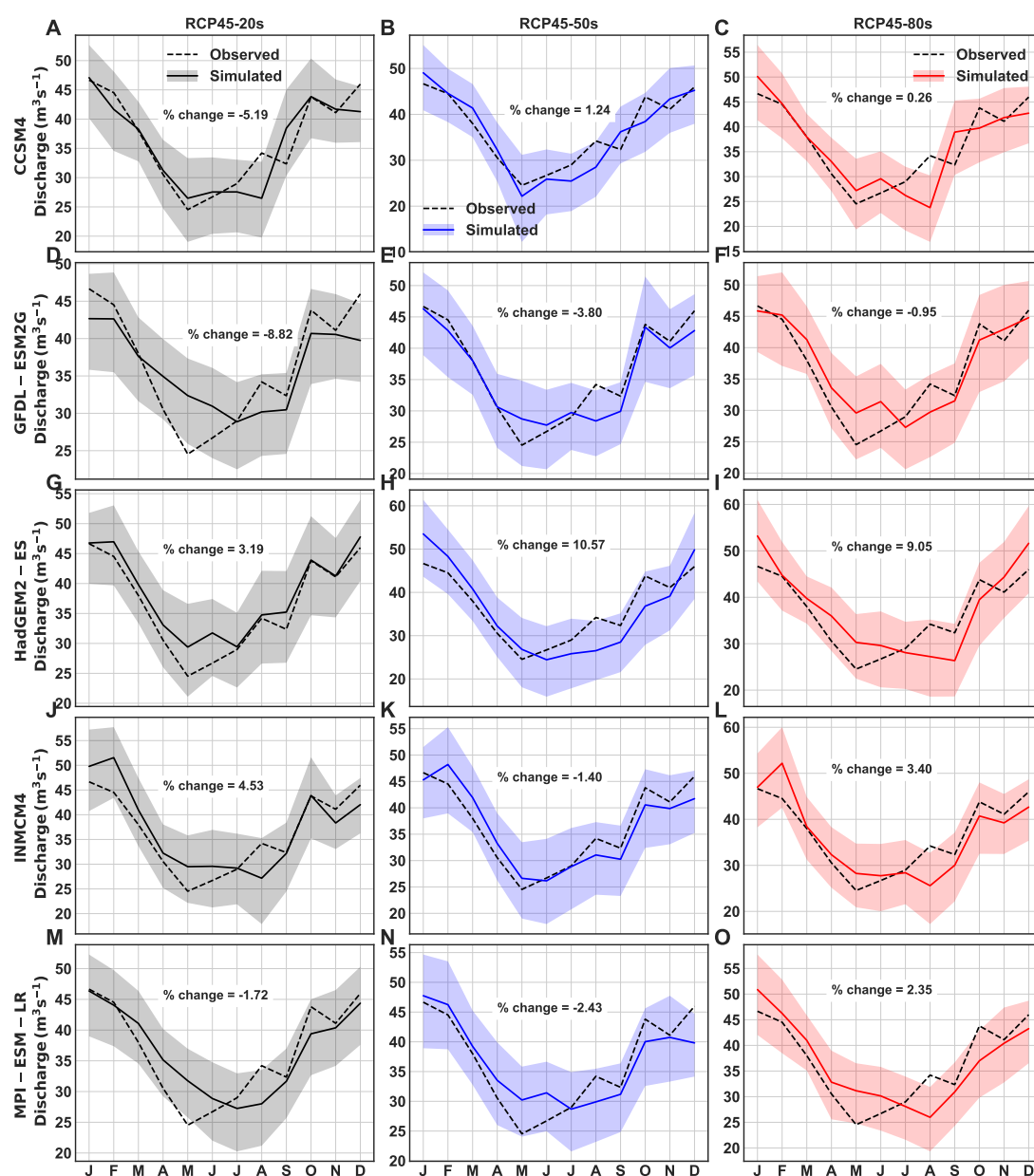
From a modelling perspective, and based on experience, constructing hydrologic models based on an ensemble GCM climate model is the more parsimonious approach especially in developing countries with limited computing and manpower resources. Whether this approach is transferable to other regions is investigated further by using the SRB case study (see Section 5.4.3).



**Figure 5.5** Projected future streamflow at Scar Water at Capenoch for the RCP4.5 Scenario. Each GCM is represented row-wise and time-scales column-wise. Shaded bands are the 95 percent prediction uncertainty (95PPU) bands for the simulated future period. The solid simulated lines are the average of the 95PPU (M95PPU)

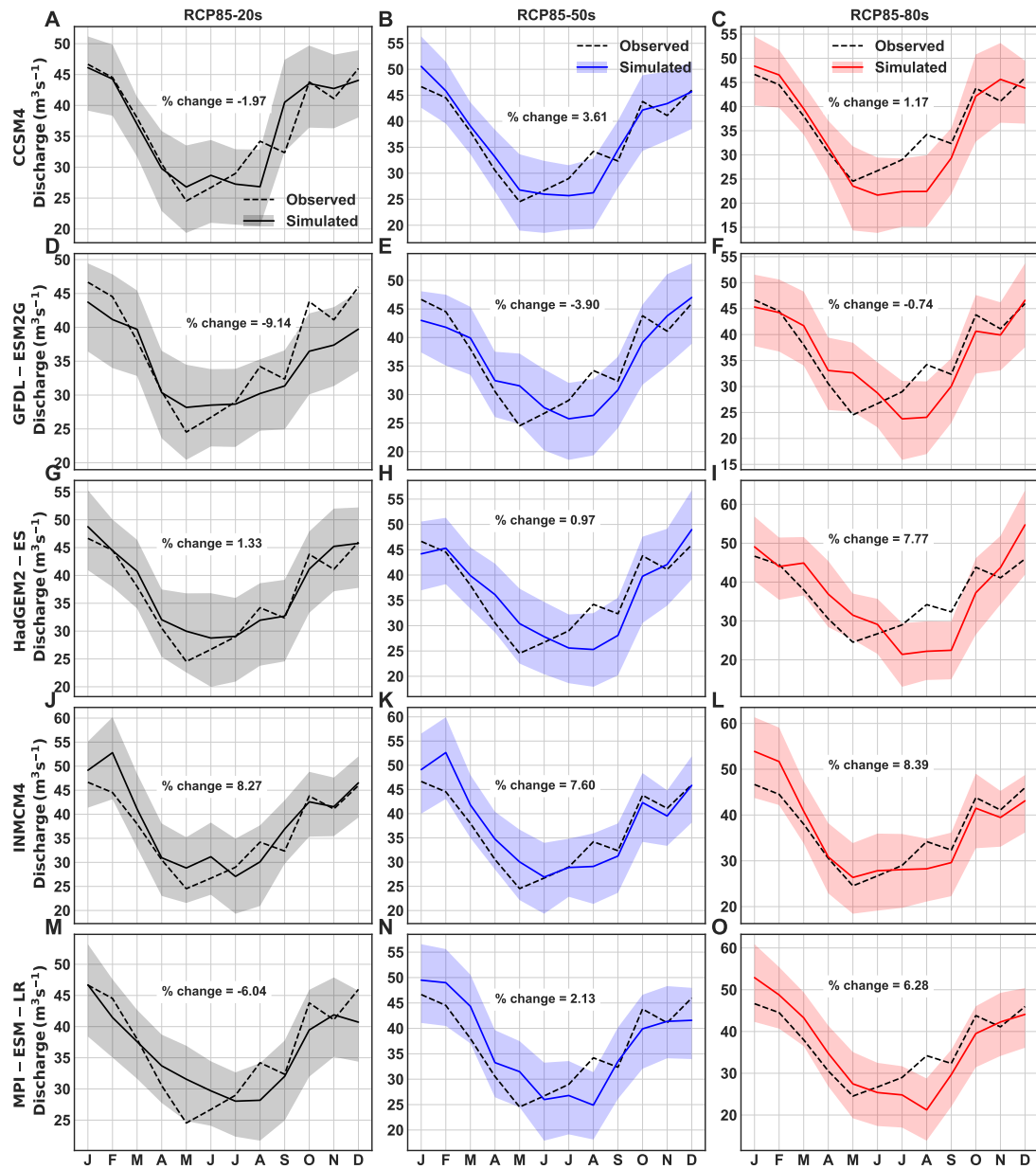


**Figure 5.6** Projected future streamflow at Scar Water at Capenoch for the RCP8.5 Scenario. Each GCM is represented row-wise and time-scales column-wise. Shaded bands are the 95PPU bands for the simulated future period. The solid simulated lines are the average of the 95PPU (M95PPU)

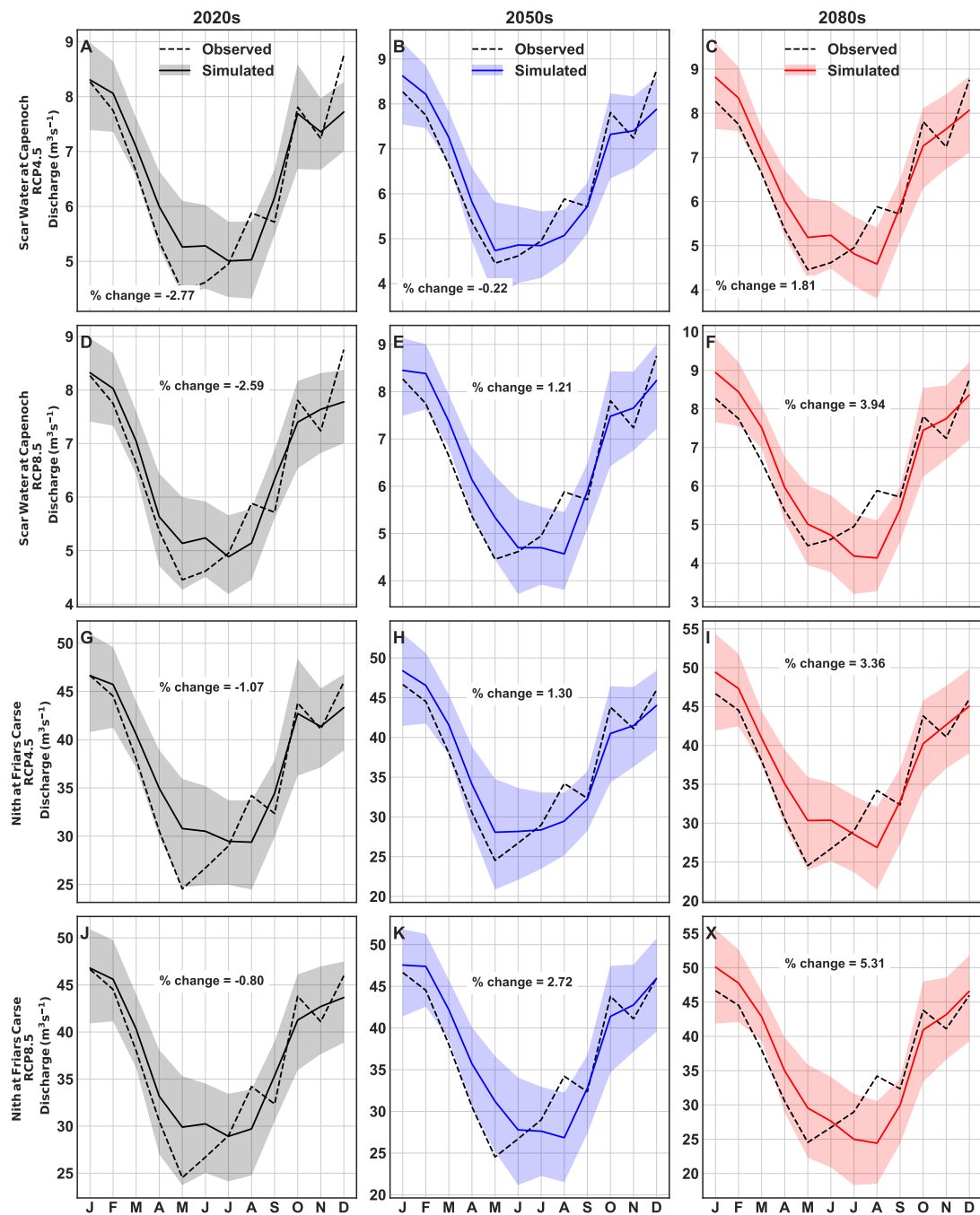


**Figure 5.7** Projected future streamflow at Nith at Friars Carse for the RCP4.5 Scenario. Each GCM is represented row-wise and time-scales column-wise. Shaded bands are the 95PPU bands for the simulated future period. The solid simulated lines are the average of the 95PPU (M95PPU)

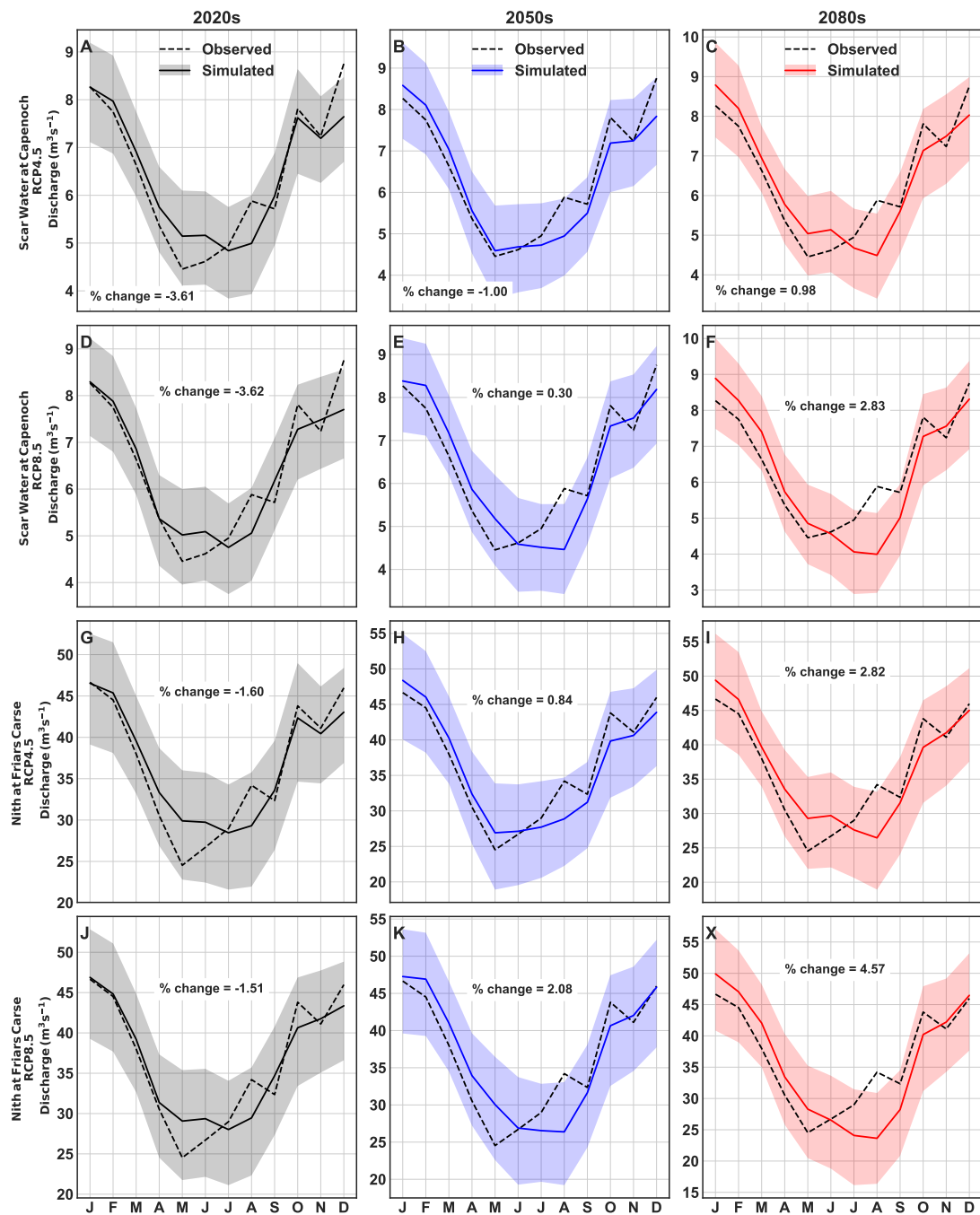




**Figure 5.8** Projected future streamflow at Nith at Friars Carse for the RCP8.5 Scenario. Each GCM is represented row-wise and time-scales column-wise. Shaded bands are the 95PPU bands for the simulated future period. The solid simulated lines are the average of the 95PPU (M95PPU)



**Figure 5.9** Projected future streamflow ensemble (SWAT forced with the RNC-EGCMM) in the RNC under RCP4.5 and RCP8.5 scenarios. Each GCM is represented row-wise and time-scales column-wise. Shaded bands are the 95PPU bands for the simulated future period. The solid simulated lines are the average of the 95PPU (M95PPU)



**Figure 5.10** Projected future streamflow ensemble (SWAT model averaged results, otherwise referred to as RNC-SWATEMM) in the RNC under RCP4.5 and RCP8.5 scenarios. Each GCM is represented row-wise and time-scales column-wise. Shaded bands are the 95PPU bands for the simulated future period. The solid simulated lines are the average of the 95PPU (M95PPU)

### 5.3.4 Blue-Green Water Nexus

Following the analyses of the response of river discharges to climate change in the early, mid and late 21<sup>st</sup> century, freshwater availability was analysed for the RNC. For consistency, the time discretization for the model was the same as for river discharge. Again, the semi-distributed hydrological model SWAT was used to quantify the water balance components in the RNC and therefore compute freshwater availability.

Freshwater, as defined in the context of this research, is composed of *blue water flow (BWF)*, *green water flow (GWF)* and *green water storage (GWS)*. Generally, blue water refers to water found in aquifers, lakes and dams while green water is the water found as moisture in soil (commonly referred to as blue and green water resources). It follows, therefore, that water flow in these media can be defined as blue water flow (water flowing through rivers and aquifers) and green water flow (water vapour flowing back to the atmosphere) (Falkenmark and Rockstrom, 2006). Freshwater availability underpins food security, public health, ecosystem protection and many other facets critical to SDG 6 attainment. According to Schuol et al. (2008b), green water has largely been ignored as part of the water resource despite its great importance for rain-fed agriculture which stands at more than 95% in sub-Saharan Africa. Furthermore, in terms of both BW and GW, It is estimated that agriculture is globally responsible for 70% of fresh groundwater that is abstracted from aquifers, lakes and rivers (Chang et al., 2016; FAO, 2016). Till about a decade ago, the vast majority of water resources research by the academic community and water-resource planners focussed on BWF since it mostly “served the needs of engineers who were involved in water supply and infrastructure projects quite well” (Falkenmark and Rockstrom, 2006).

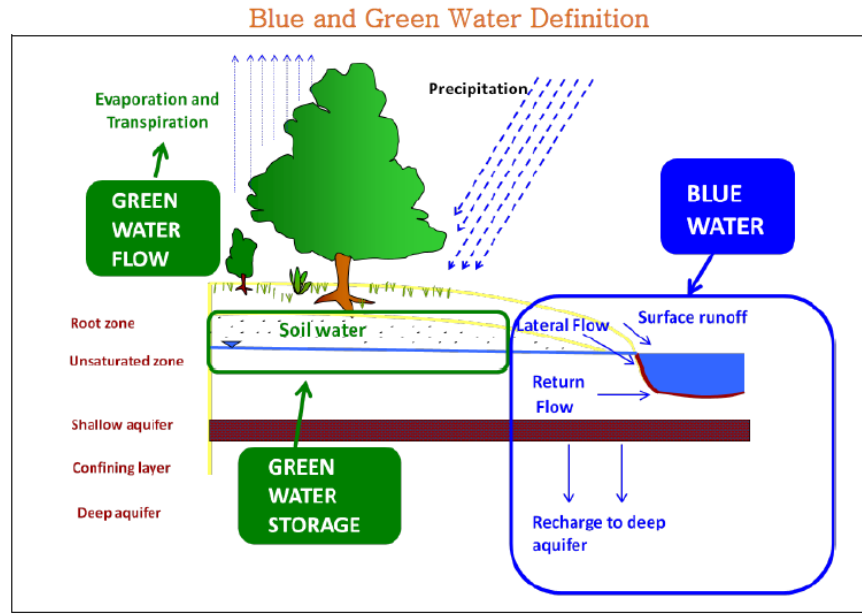
Since the realization of the importance of a holistic approach to freshwater assessments, many studies have contributed to this body of knowledge by publishing various methodologies and applications of freshwater modelling efforts and tools. Schuol et al. (2008b) modelled blue and green water availability for the whole of Africa using the SWAT hydrological model. Using the SUFI-2 algorithm, they were able to calibrate and quantify the uncertainty of the model results. They concluded that the model and its results could be used to inform policy and other studies on climate change, virtual water trade and water and food security among others. Results from this study were compared with those of Schuol et al. (2008b) even though their results were presented at continent-scale. Another study by Afshar et al. (2018) used the MIROC-ESM GCM to model long-term spatial variability of blue and green water footprints in the Kashafrud River Basin in Iran. They considered two RCP scenarios to force their SWAT model under future conditions. The study concluded that their methodology can be effectively applied in other arid or semi-arid regions. Zhao et al. (2016) studied the impacts of land-use change and climate variability on blue and green water resources in the Weihe River Basin, north-west China. In their study the authors concluded that the variability of water resources in the basin was mainly attributed to climate variability. Abbaspour et al. (2015) developed a continental-scale water quality model for Europe using the SWAT model. Their model results provided information support to the European Water Framework Directive on water availability and quality. These and many other studies have highlighted the significance of considering a blue-green water nexus approach when discussing climate adaptation strategies with respect to IWRM.

In this study, 5 GCMs described in Chapter 4 were used to assess the impacts

of climate change on freshwater resources in the RNC. Using the same time discretization as for streamflow analyses, i.e 3 time horizons dividing the 21<sup>st</sup> century, 30 models were constructed and used to compute the water balances in the RNC. Practically, one model was constructed and calibrated as discussed in the previous sections. Thereafter, the 30 scenarios were simulated in SWAT-CUP where uncertainty analyses were carried out and defined using the 95PPU. For reporting purposes, the average of the 95PPU (M95PPU) was used. Details of the 95PPU were discussed in Chapter 3. This is an essential step in environmental modelling where uncertainty of the input parameters, knowledge of the watershed and the model construction process, inter alia, have to be taken into consideration. Moreover, there exists no unique set of parameters that can be used to define and parameterize a model, a phenomenon referred to as *non-uniqueness* and discussed in detail in Chapter 2.

#### 5.3.4.1 Baseline Blue Water/Green Water availability

The main water balance components calculated for the baseline RNC model are summarised in Figure 5.11. As discussed earlier, blue water in this thesis is discussed in terms of *flow* and thus is defined as the sum of the water yield and deep groundwater recharge. Green water, according to Falkenmark and Rockstrom (2006), is separated into green water resources or storage, the renewable part that is important for rain-fed agriculture and can thus potentially generate economic returns (Cuceloglu et al., 2017). The other component is green water flow which is composed of actual evaporation (considered to be the *non-productive* part) and actual transpiration (the *productive* part); together usually referred to as actual evapotranspiration (Cuceloglu et al., 2017).



**Figure 5.11** Schematic illustration of blue and green water components as defined in this study

BWF, GWF and GWS for the baseline period were calculated and presented at the 50% probability level of the 95PPU. The average annual values of the water balance components were calculated and are presented in Figure 5.12.

Further, in order to illustrate the reliability of blue and green water resources, the coefficient of variation (CV) was calculated for the entire baseline period in each subbasin. According to Schuol et al. (2008b), the CV “is an indicator for the reliability of a freshwater resource”. The CV was calculated as follows;

$$CV = \frac{\sigma}{\mu} \times 100 \quad (5.1)$$

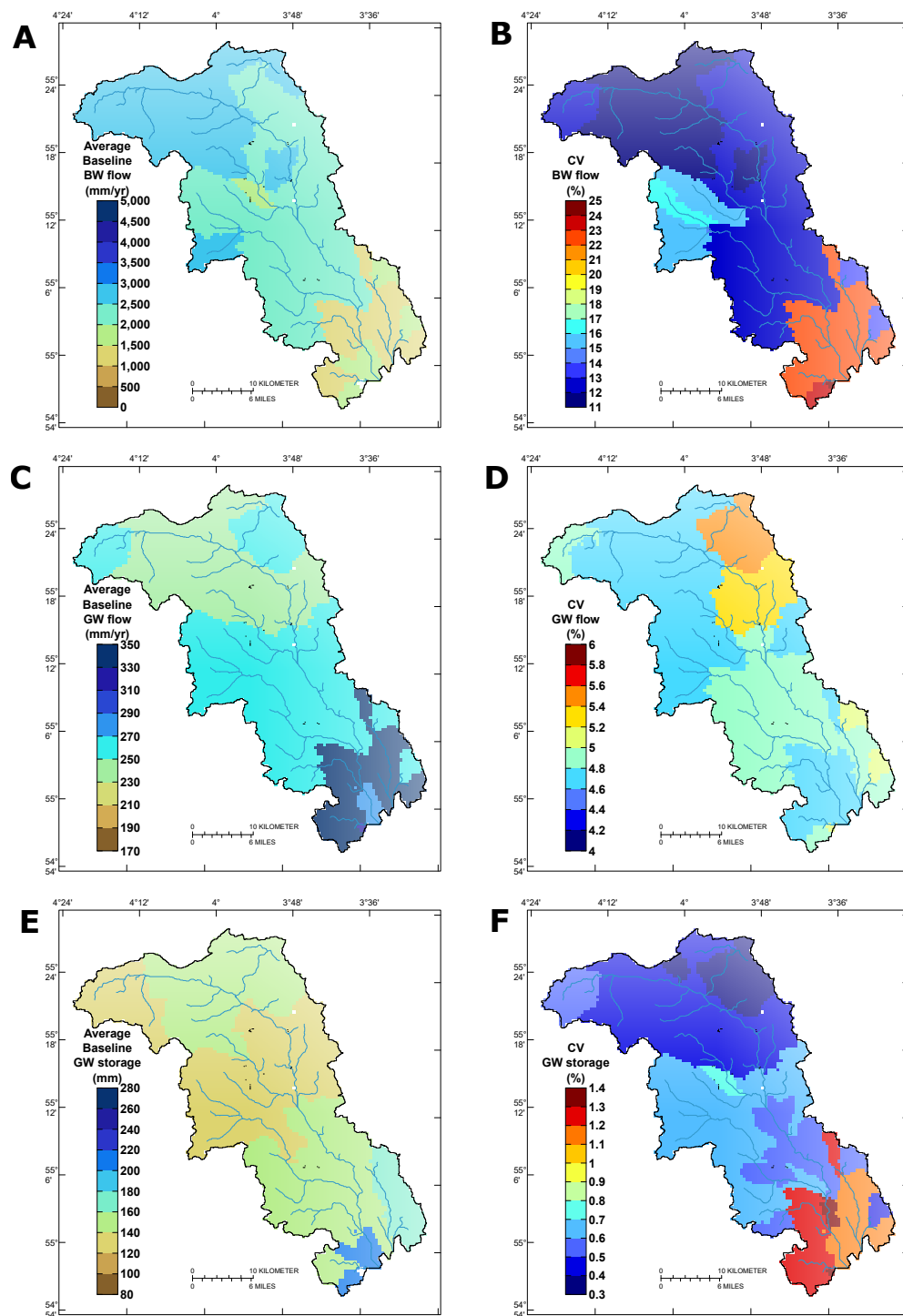
where  $\sigma$  is the standard deviation and  $\mu$  is the mean of the annual variables for each season for each subbasin. A lower value of the CV indicates lower interannual variability and hence higher reliability while larger values of CV indicate higher interannual variability and consequently less reliability of water resources.

The average BWF for the entire watershed is 2500 mm y<sup>-1</sup>. Some subcatchments have BWF potential of up to 3000 mm y<sup>-1</sup>. For the most part, the model shows BW CV values ranging from 11% to 25%. The average baseline BW CV for the RNC is around 12% and lower (indicating lower interannual variability) especially in the northern part towards New Cumnock, East Ayrshire. Towards the south, the model shows increasing BW CV values and is therefore an indication of higher interannual variability of BWF when compared to the rest of the catchment.

GWF values are approximately 250 mm y<sup>-1</sup> for most of the basin except towards the south of the catchment where GWF is consistently over 300 mm y<sup>-1</sup>. This could be as a result of increasing industrial farming activities in the Dumfries area. CV values for GWF are low throughout the RNC indicating low prevalence of interannual GWF variability.

With regard to GWS, there is an increase of GWS towards the south. The reason for this trend is likely a combination of land-use and soil cover in the RNC. On a catchment scale, the average GWS is about 150 mm. CV values for GWS are generally low, although Figure 5.12F shows increasing interannual variability southwards. For practical purposes, there is little to no indication of interannual variability in the GWS values for the baseline period.





**Figure 5.12** Water balance components in the RNC for the baseline period; (a) Blue Water Flow (BWF), (b) Green Water Flow (GWF), (c) Green Water Storage (GWS), (d), (e) and (f) are coefficients of variation expressed as a percentage for BWF, GWF and GWS respectively.

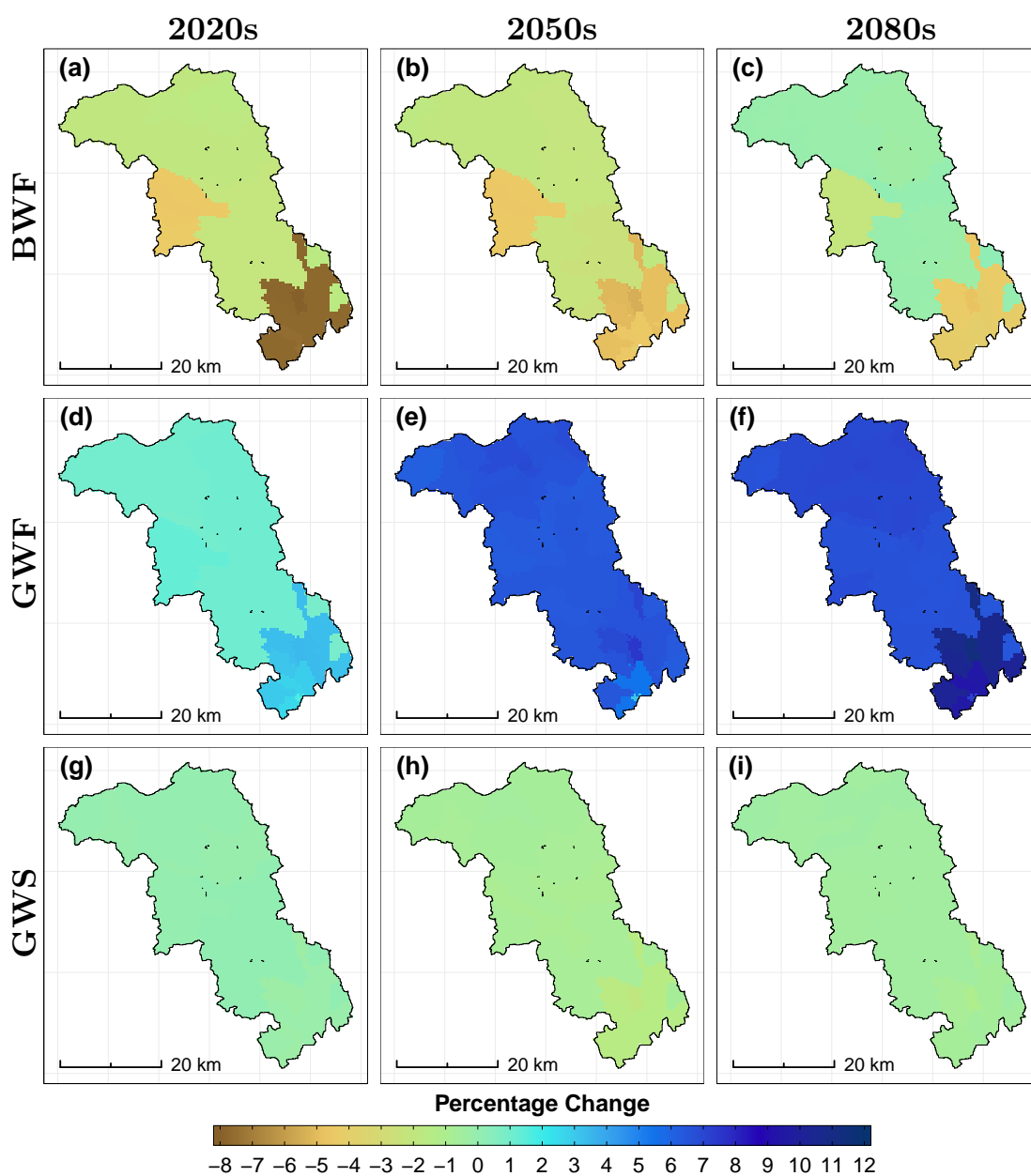
#### 5.3.4.2 Future BW/GW availability

Future BW/GW availability was assessed by constructing SWAT models forced with a) single GCMs and b) an ensemble GCM climate model (MMEGCM-SWAT described earlier). Thereafter, results were compared to the baseline values to determine projected changes in BW/GW availability.

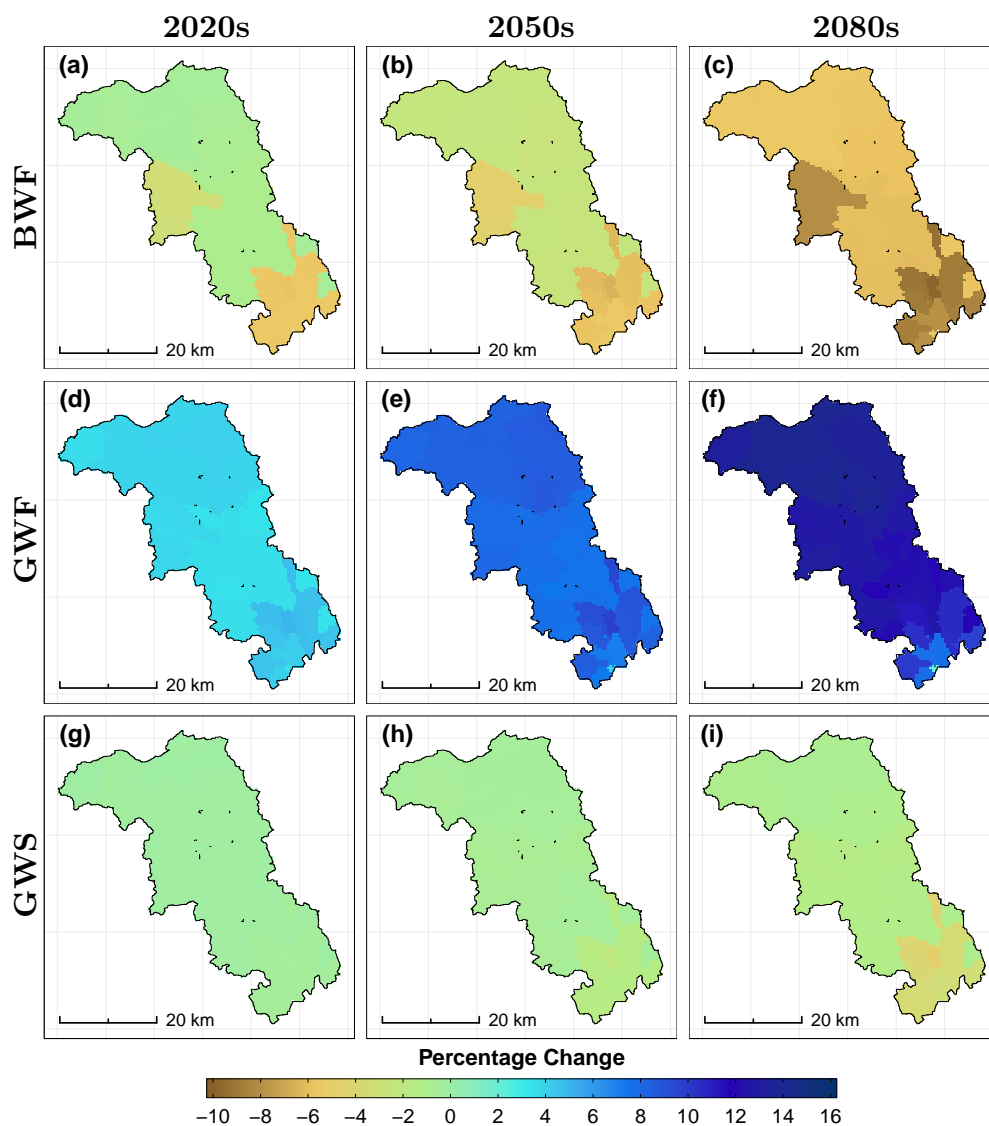
Figures 5.13 to 5.26 show percentage differences in BW/GW availability for the future period in the SRB. Positive values indicate an increase in the component being simulated compared to the baseline whereas negative values indicate a decrease in BW/GW. In the 2020s, BWF ranges between -8% and -1%, GWF between +0.8% and +3.5% according to CCSM4 under RCP4.5. Similarly under RCP8.5 the trend is downwards for BWF according to CCSM4, especially south of the RNC. GWS availability continues to decline throughout the century but only marginally while GWF increases by up to +12% in the late century. GFDL-ESM2G shows a slightly positive picture under RCP4.5 than CCSM4. For example, in the late-century, BWF (Figure 5.15C) is predicted to be slightly above baseline values for most of the catchment whereas GWF decreases slightly throughout the century when compared to CCSM4. GWS predictions by GFDL-ESM2G are similar to those made by CCSM4 under RCP4.5 and RCP8.5. HadGEM2-ES is consistent with the other GCMs in the prediction of BWF and GWS but predicts higher GWF values of up to +15% and +17% under RCP4.5 and RCP8.5 respectively. INMCM4 predicts little to no change from baseline values under both RCPs for most of the catchment except in the Dumfries region where slightly lower values in BWF are expected as the century progresses. Similar results were obtained by models forced with MPI-ESM-LR under all RCPs except for GWF where values of up to +11% and +20% are expected under RCP4.5 and RCP8.5

respectively.

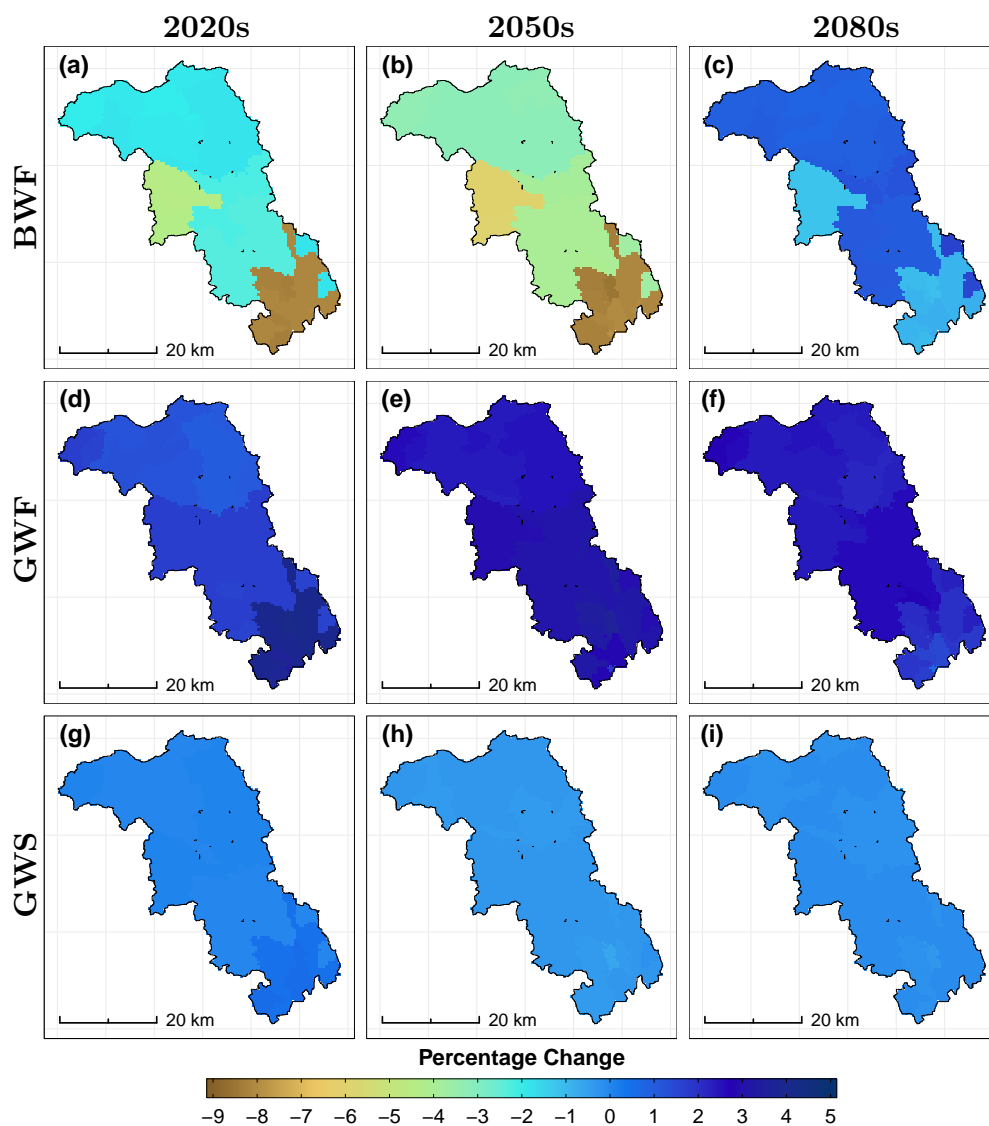
For the most part, all the 5 GCMs are in many instances agreeable on the magnitude and direction of the change. Generally, all GCMs predicted little to no change (on average a range of 1% to 3% in either direction) in GWS. Most of the variation in predictions are related to BWF followed by GWF. Accordingly, uncertainties calculated using the 95PPU were higher for BWF than GWF and GWS. A possible explanation for this phenomenon could be related to the selection of parameters used in the calibration process and omission of important processes such as springs and irrigation. Following the guidelines provided by Abbaspour et al. (2018), parameters related to snow-melt (e.g. SFTMP, SMTMP etc. ) are not to be calibrated simultaneously with other parameters to avoid introducing identifiability problems. Thus these parameters (not shown in Figure 5.3 and Table 5.3) were fitted first, set to their best values and subsequently removed from further calibration as per Abbaspour et al. (2018). It is against this background that it was suspected snow-melt parameters could have played a role in the large uncertainty observed in BWF simulations. Furthermore, it is possible that important hydrological processes such as reservoirs and springs could have been missed leading to miscalculations in the water balances.



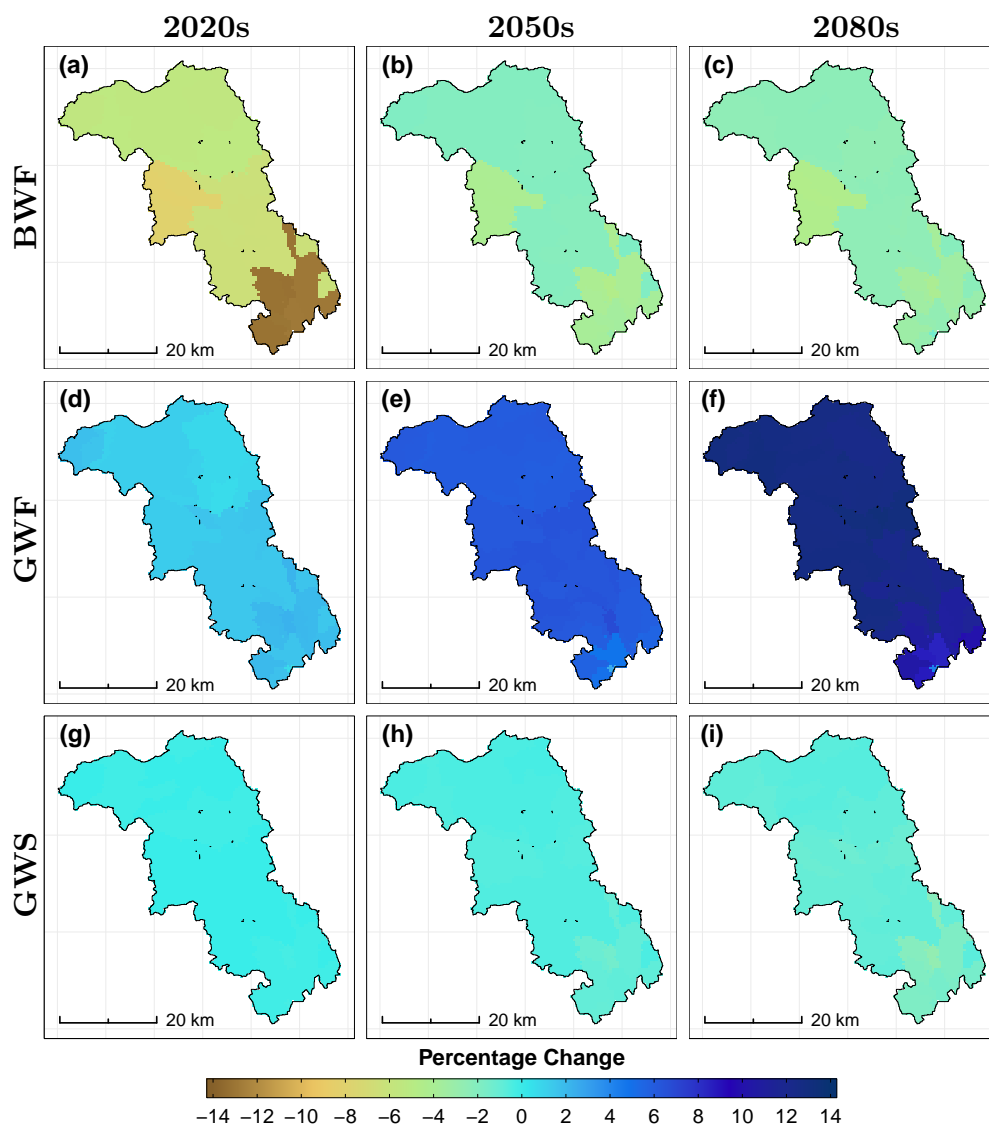
**Figure 5.13** CCSM4 RCP4.5 water balance components in the RNC for the future projected period. BW is blue water and GW is green water. Results are percentage differences from baseline period using the M95PPU



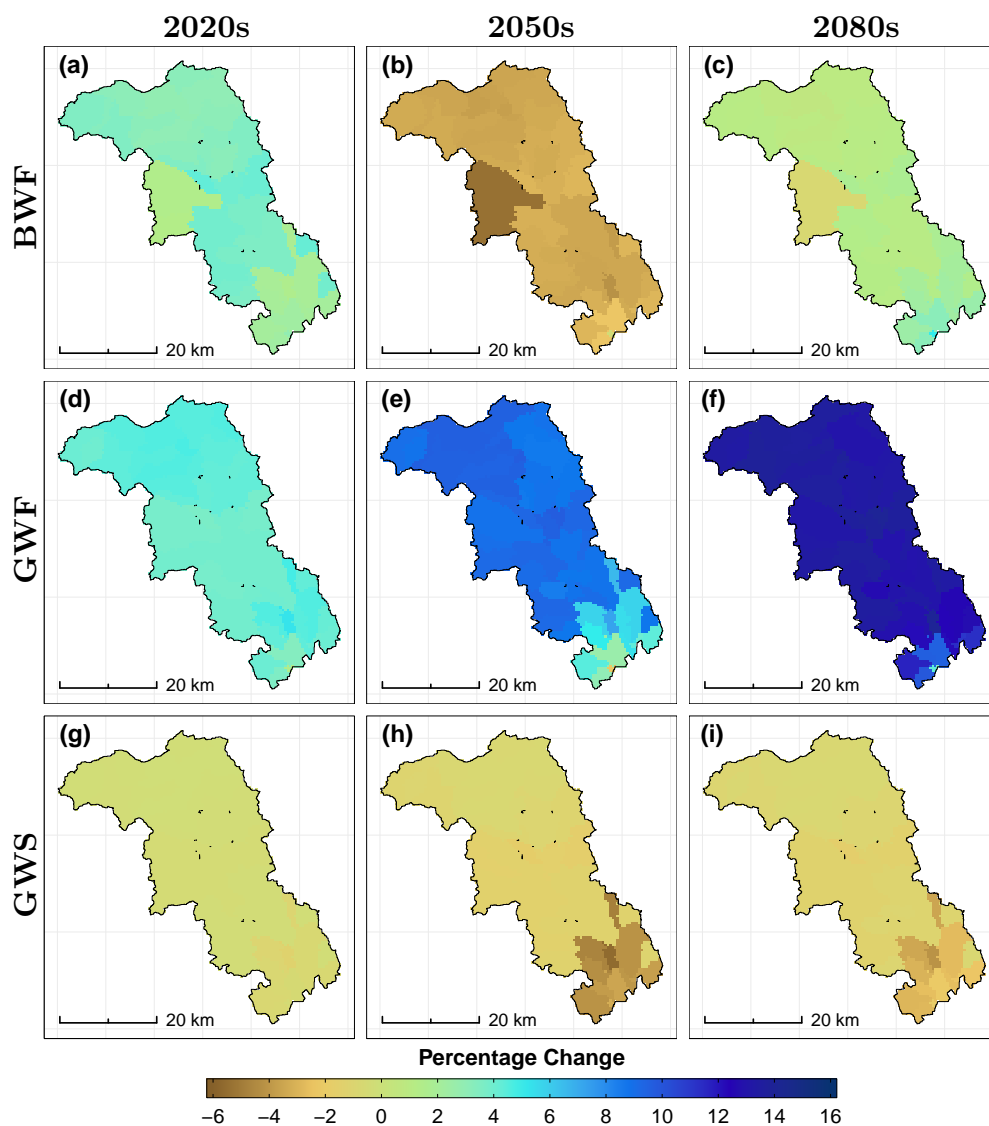
**Figure 5.14** CCSM4 RCP8.5 water balance components in the RNC for the future projected period. BW is blue water and GW is green water. Results are percentage differences from baseline period using the M95PPU



**Figure 5.15** GFDL-ESM2G RCP4.5 water balance components in the RNC for the future projected period. BW is blue water and GW is green water. Results are percentage differences from baseline period using the M95PPU

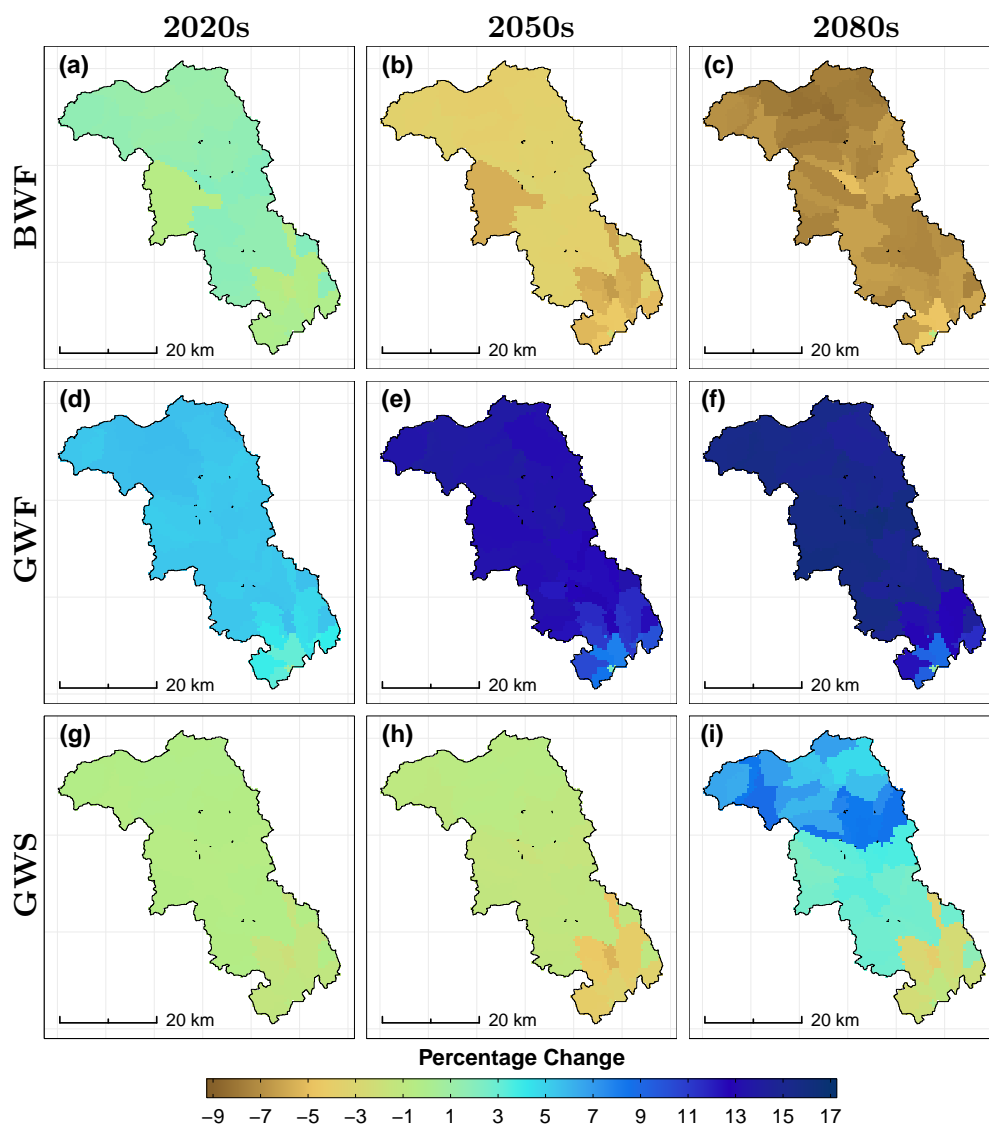


**Figure 5.16** GFDL-ESM2G RCP8.5 water balance components in the RNC for the future projected period. BW is blue water and GW is green water. Results are percentage differences from baseline period using the M95PPU

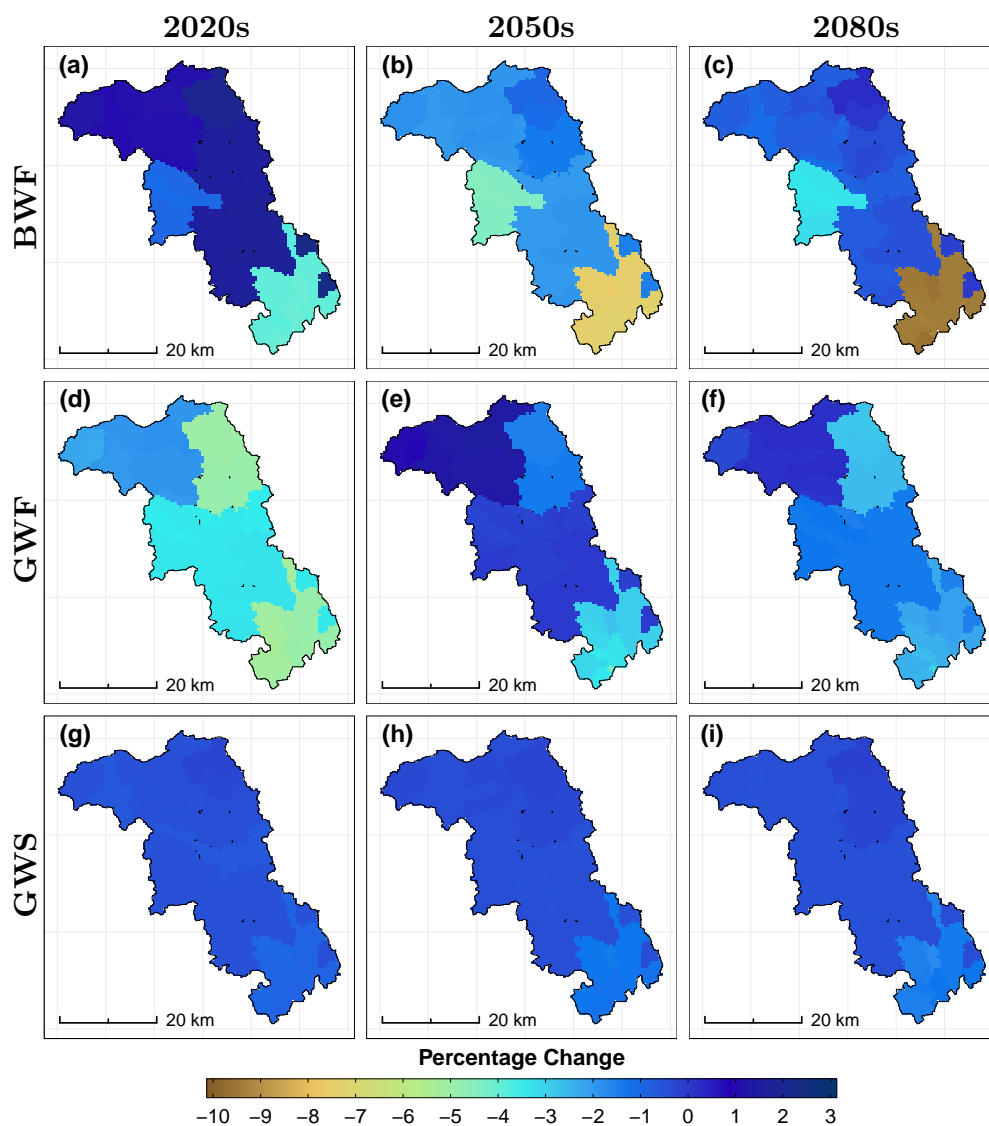


**Figure 5.17** HadGEM2-ES RCP4.5 water balance components in the RNC for the future projected period. BW is blue water and GW is green water. Results are percentage differences from baseline period using the M95PPU

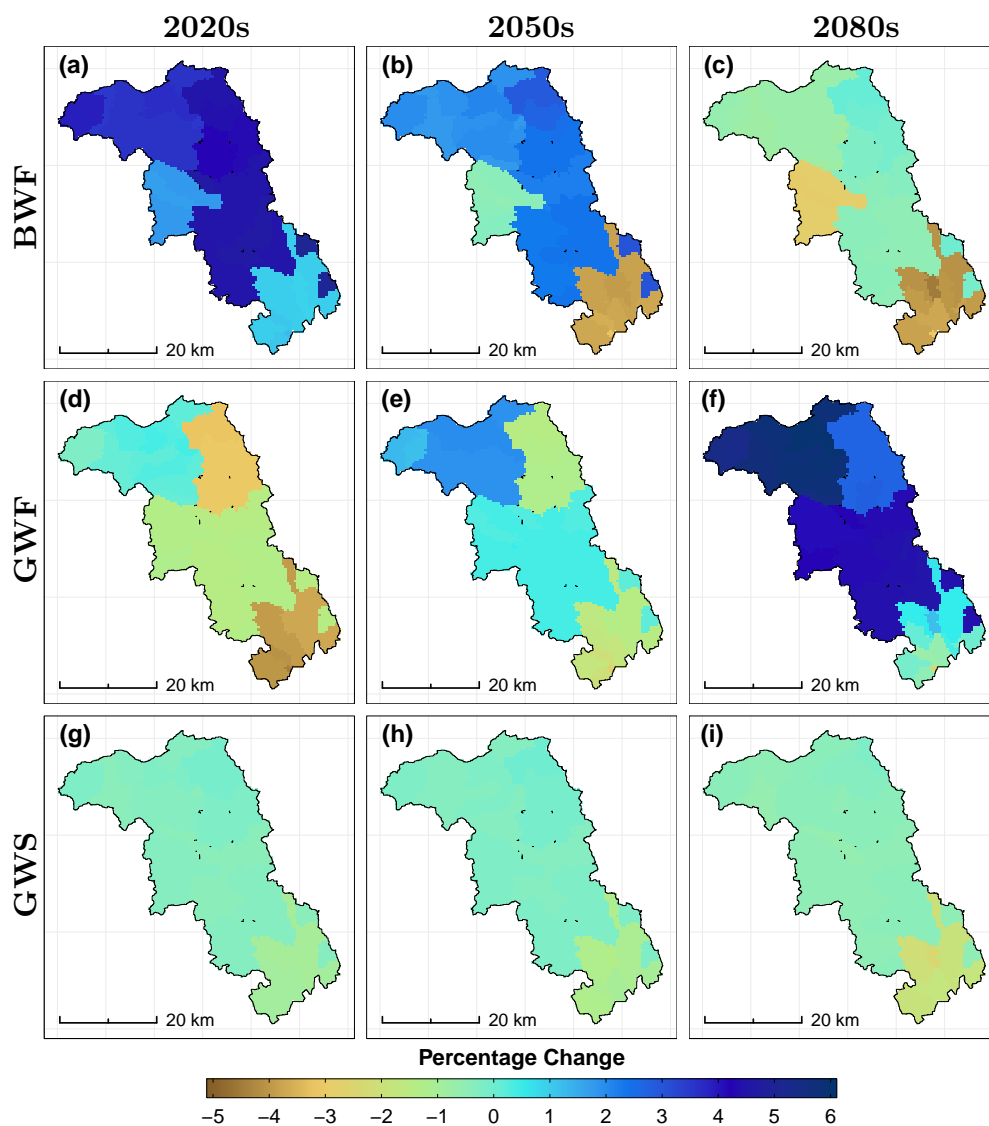




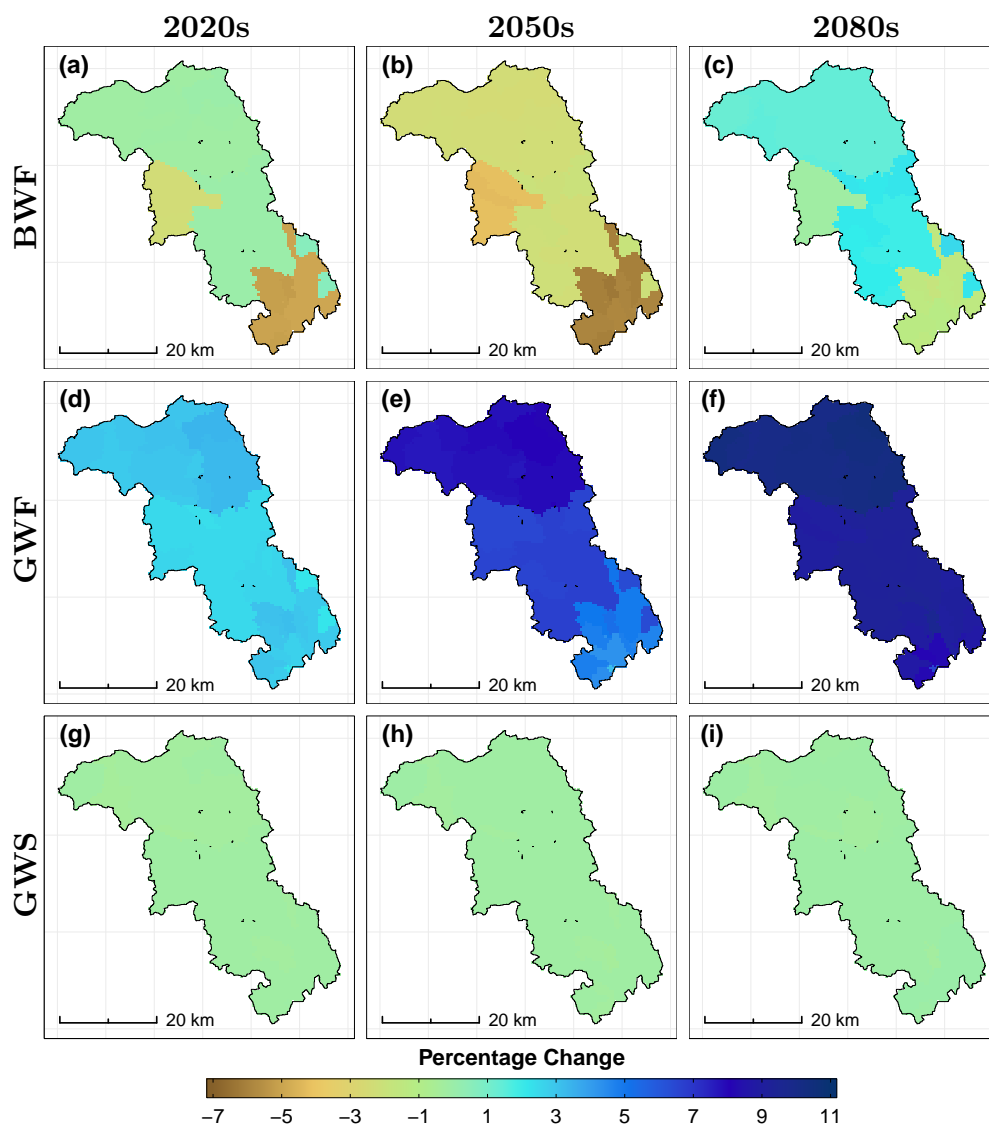
**Figure 5.18** HadGEM2-ES RCP8.5 water balance components in the RNC for the future projected period. BW is blue water and GW is green water. Results are percentage differences from baseline period using the M95PPU



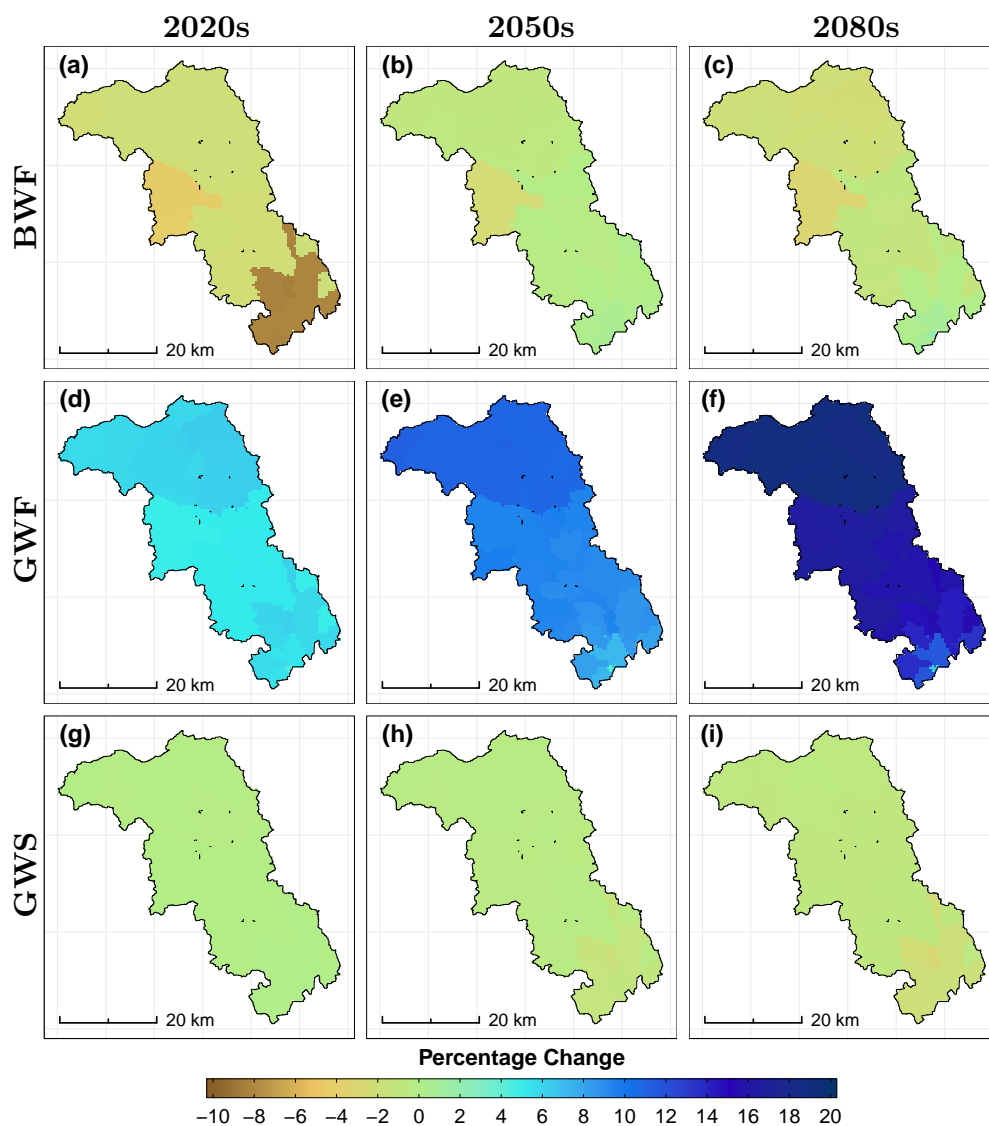
**Figure 5.19** INMCM4 RCP4.5 water balance components in the RNC for the future projected period. BW is blue water and GW is green water. Results are percentage differences from baseline period using the M95PPU



**Figure 5.20** INMCM4 RCP8.5 water balance components in the RNC for the future projected period. BW is blue water and GW is green water. Results are percentage differences from baseline period using the M95PPU



**Figure 5.21** MPI-ESM-LR RCP4.5 water balance components in the RNC for the future projected period. BW is blue water and GW is green water. Results are percentage differences from baseline period using the M95PPU.



**Figure 5.22** MPI-ESM-LR RCP8.5 water balance components in the RNC for the future projected period. BW is blue water and GW is green water. Results are percentage differences from baseline period using the M95PPU.

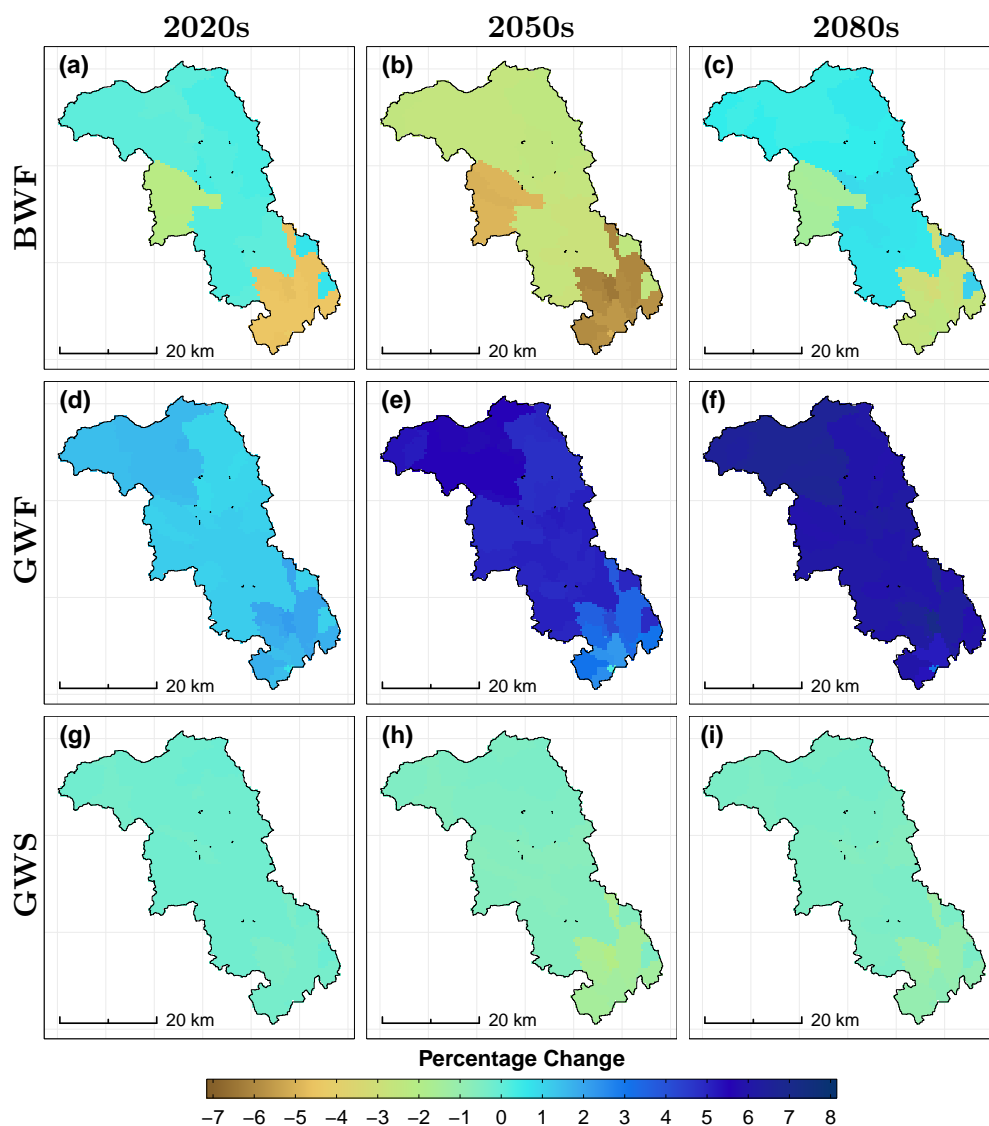
Figures 5.23 and 5.24 are averaged results of the five models presented earlier. Because of the little variation in the single models, the ensemble means are close to the results discussed earlier. Under RCP 4.5, the models show little to no increase (-6.5% to +1.5%) in BWF and GWS (-2% to 0%). GWF is expected to slowly and gradually increase up to +7.5% in the late-century. Similar values are predicted under RCP8.5 for BWF (-5.5% to 0%) and GWS (-3.5% to +1.5%). GWF ranges between +0.5% and +14%, a steadily increasing trend towards the late-century.

Results of BW/GW simulations using a SWAT model forced with the RNC-EGCMM are shown in Figures 5.25 and 5.26. Here, it is noticeable that there is a significant difference from the single models presented earlier. For example, under RCP4.5, the model predicts generally a rise in BWF availability of about +8% for the northern portion of the catchment and up to +24% south of the catchment, a trend that is consistent throughout the century according to this model. This is in contrast to the single and River Nith Catchment SWAT Ensemble Model Mean (RNC-SWATEMM) (Figures 5.23 and 5.24) models that consistently predict a decrease in BWF south of the catchment. In the case of GWF, there is a considerable decrease in GWF south of the catchment of up to -12% whereas the rest of the catchment shows a mean decrease of -4% in the 2020s. In the 2050s the values are somewhat similar but in the late-century, the model generally predicts a return to baseline levels for most of the catchment while the south remains in a deficit of up to -19%. In the case of GWS, there appears to be little to no change in the 2020s for most of the catchment except the south where a mean increase of about 3% is predicted. The results are in the same range for the rest of the century.

Under RCP8.5, the RNC-EGCMM forced model predicts marginally (roughly 2 percentage point increase across the century) higher BWF availability. The range however is similar to the one observed under RCP4.5. Thus BWF simulations according to this model represent the largest variability when compared to the models driven by a single GCM. In the case of GWF, the model predicts a steady increase up to +5% by the end of the century. In the 2020s there is a slight deficit in GWF of about -3% for the northern portion of the catchment while the south is predicted to decrease by up to -20%. In the mid-century, GWF in the northern portion of the catchment returns to baseline levels and marginally (+5% for some parts of the catchment) increases by the late-century. Notwithstanding this, the southern portion of the basin continues to be in deficit throughout the century. For GWS, the model predicts similar values as those of RCP4.5 throughout the century.

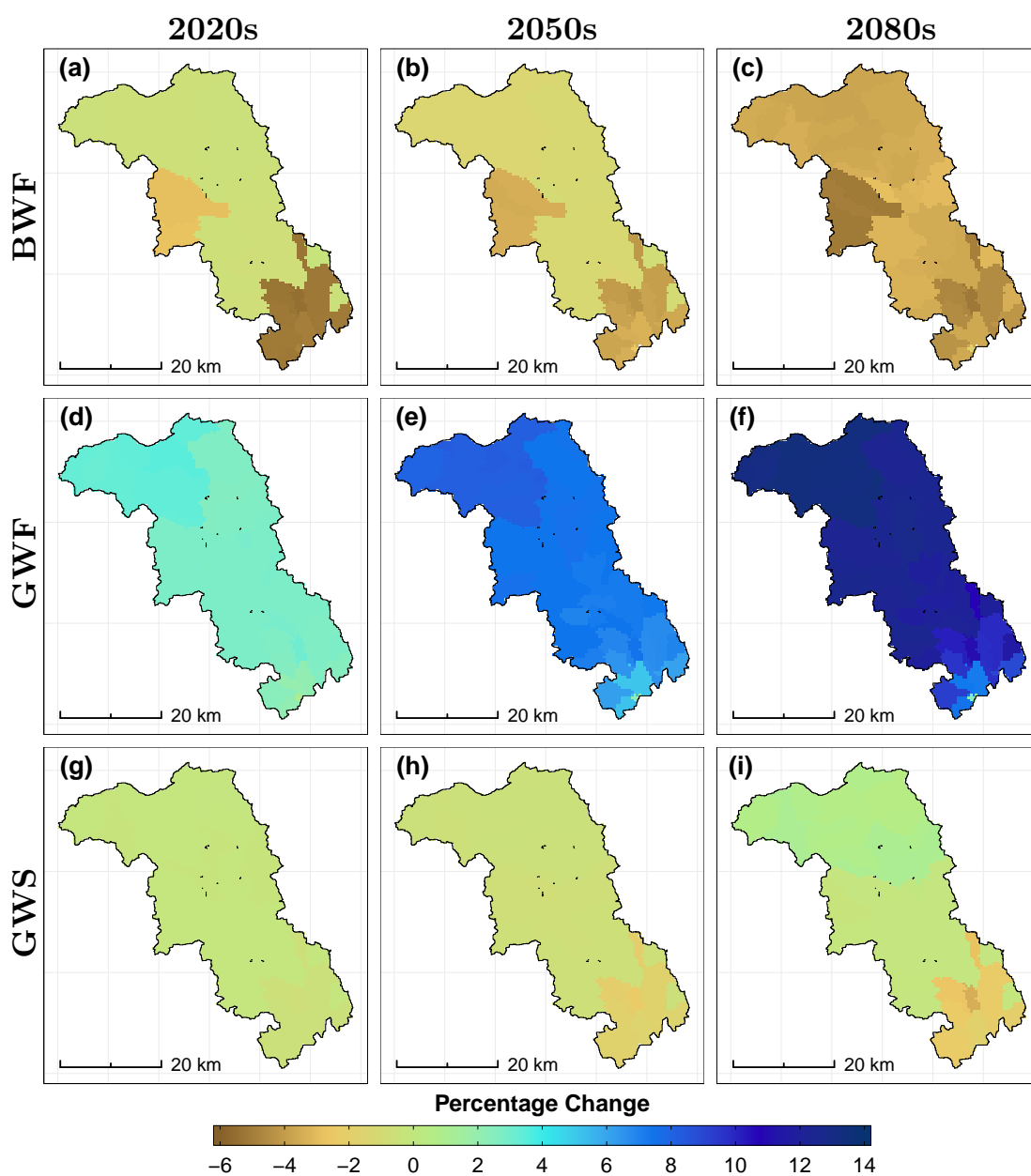
One thing that is certain is that the model forced with the RNC-EGCMM shows markedly different results than the models forced with single GCMs especially for BWF and GWF. Whether this is an artefact of the random forest model used to average the downscaled GCM outputs or simply a better representation of the future hydrological events in the catchment remains to be determined. The ensemble models are expected to cancel the biases introduced by the single models but as has been shown in this research, it remains unclear which approach should be adopted. Perhaps, a more pertinent question should be whether it is justifiable to only select a subset of GCMs to be used in impact assessment studies? The investigation of this question is explored in the literature, at least from a climate perspective, with mixed opinions and is definitely outside the scope of this research. From a hydrological point of view, the recommendation provided in Section 5.3.3.2

is reiterated to the effect that hydrologists consider constructing hydrologic models based on ensemble GCM climate outputs since a) this is the most parsimonious approach from a modelling perspective and b) ensemble climate model results are generally believed and recommended by many researchers to be more reliable than their constituent climate models.

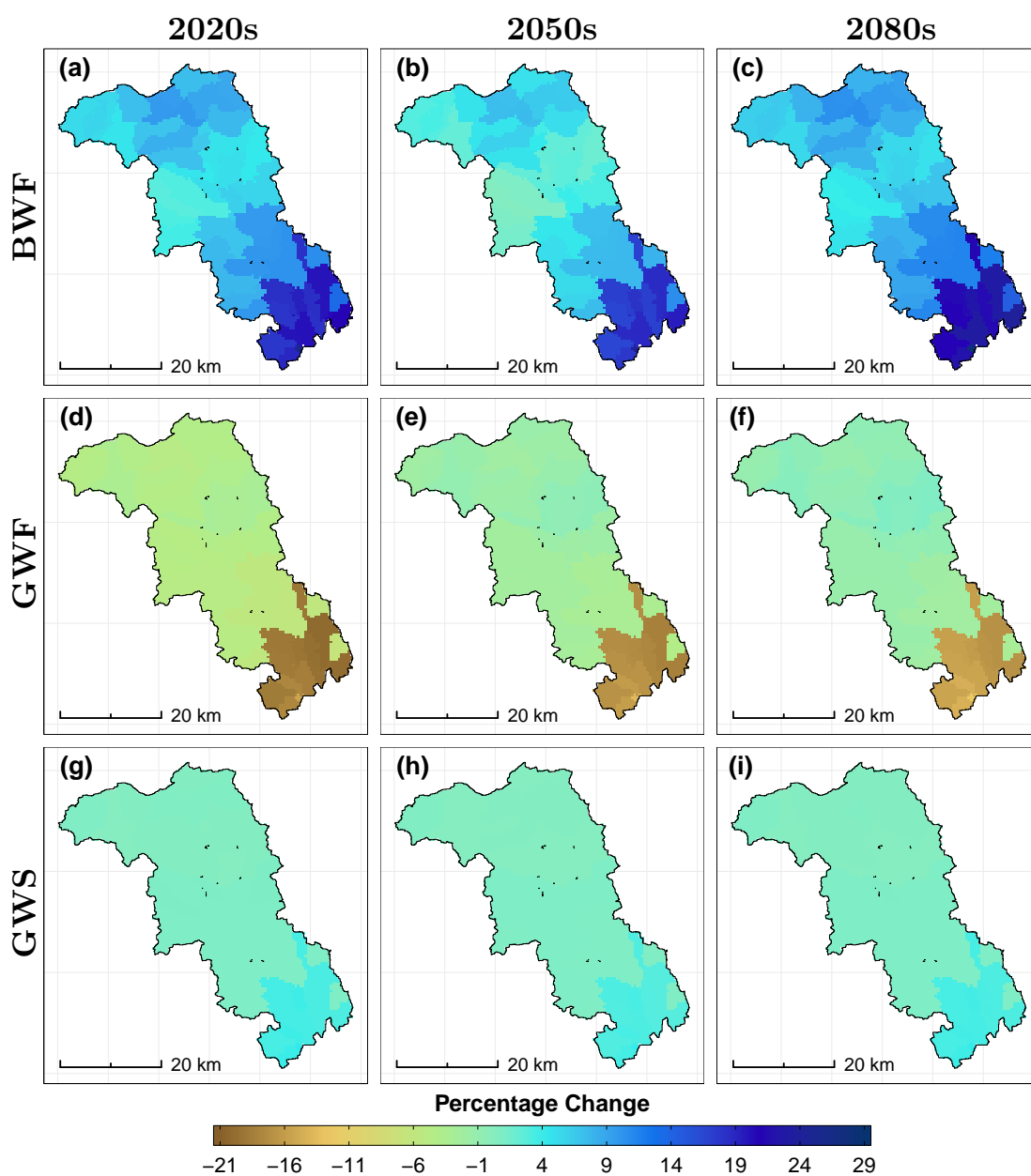


**Figure 5.23** Ensemble mean (RNC-SWATEMM) RCP4.5 water balance components in the RNC for the future projected period. BW is blue water and GW is green water. Results are percentage differences from baseline period using the M95PPU

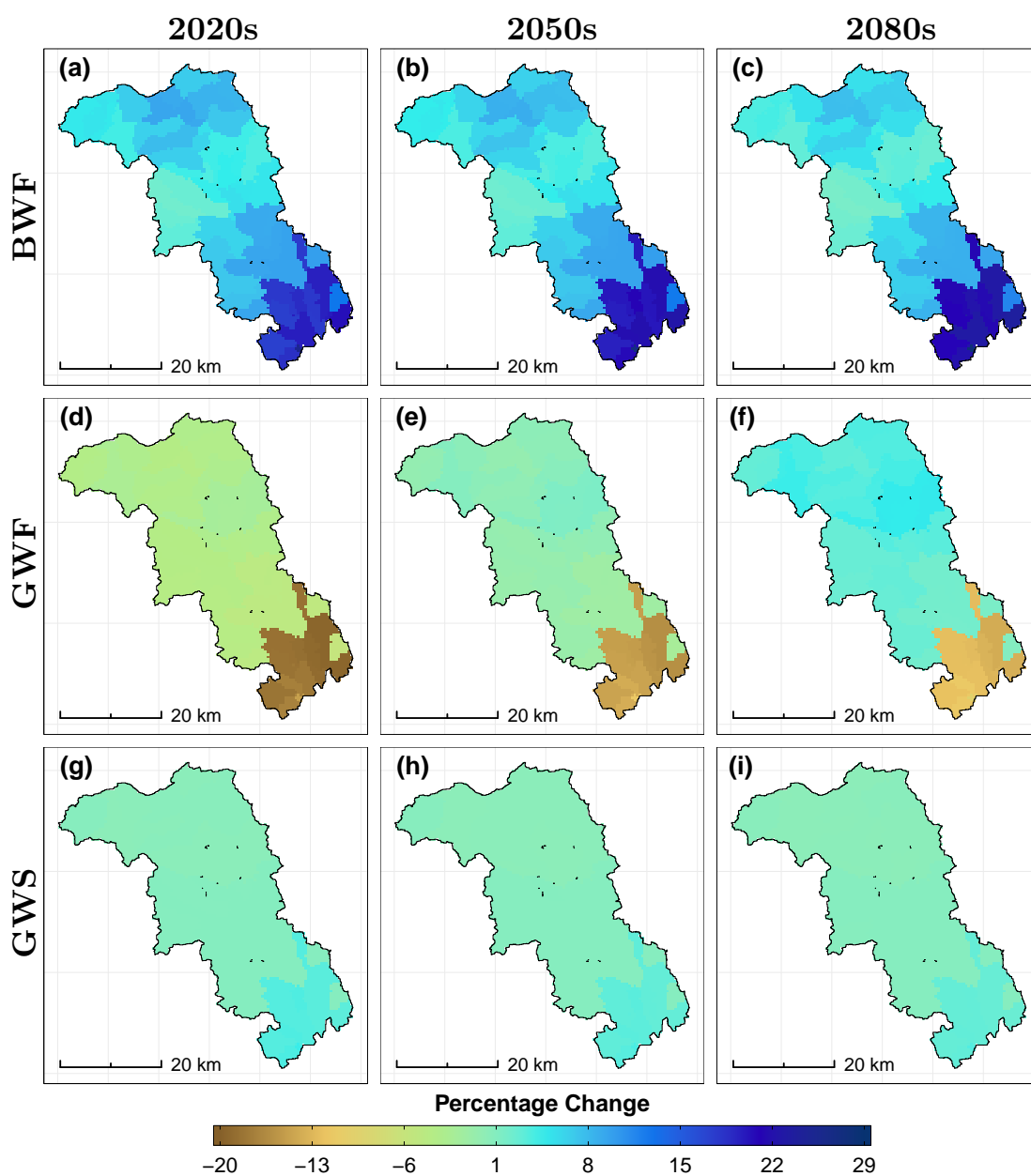




**Figure 5.24** Ensemble mean (RNC-SWATEMM) RCP8.5 water balance components in the RNC for the future projected period. BW is blue water and GW is green water. Results are percentage differences from baseline period using the M95PPU



**Figure 5.25** Ensemble mean (RNC-EGCMM) RCP4.5 water balance components in the RNC for the future projected period. BW is blue water and GW is green water. Results are percentage differences from baseline period using the M95PPU



**Figure 5.26** Ensemble mean (RNC-EGCMM) RCP8.5 water balance components in the RNC for the future projected period. BW is blue water and GW is green water. Results are percentage differences from baseline period using the M95PPU.

### 5.3.5 RNC Modelling Summary


From Table 5.5, streamflow projections from all 5 GCMs indicate that there is little to no threat on streamflow availability as a result of anthropogenic climate change in the RNC. While there could be intra-annual changes where, because of projected increases in winter rainfall resulting in winter streamflow being higher than baseline or historical values, overall streamflow availability in the future resembles baseline values throughout the century. All GCMs, except GFDL-ESM2G at SWC and HadGEM2-ES at NFC (significant downward and upward change respectively), are in agreement that there is no significant departure from baseline values.


The direction and magnitude of change is not always in agreement but varies from one GCM to another. The general consensus, however, is that the change is insignificant across all time horizons. While GFDL-ESM2G consistently predicts some decrease in streamflow availability in the 2020s under RCP4.5 and 8.5 at SWC (significant) and NFC (insignificant), the projections for other time horizons are in agreement with the other GCMs. It should be noted and emphasized here that these results assume that the LU/LC is stationary in the future. Any changes in the LU/LC and water abstractions may lead to adverse outcomes than those reported here.


Table 5.6 shows a summary of the areal mean change of projected water balance components in the RNC with respect to the baseline period. All GCMs indicate no significant change in availability of future water balance components in the RNC.

**Table 5.5** Summary of RNC future streamflow changes with respect to the baseline period. Changes within  $\pm 10\%$  of baseline values are considered to be insignificant (green boxes) whereas changes above  $+10\%$  (red boxes) and below  $-10\%$  (blue boxes) are considered to be significant.

GCM	Scenario					
	RCP4.5			RCP8.5		
	2020s	2050s	2080s	2020s	2050s	2080s
<b>Scar Water at Capenoch</b>						
CCSM4	-7.5	-0.6	-1.8	-4.1	1.9	-0.5
GFDL-ESM2G	-10.9	-5.9	-3.0	-11.3	-6.0	-2.5
HadGEM2-ES	1.2	9.0	7.1	-0.8	-0.9	5.2
INMCM4	2.8	-3.3	1.8	6.4	6.0	6.9
MPI-ESM-LR	-3.7	-4.3	0.8	-8.3	0.5	5.0
Ensemble (RNC-EGCMM)	-2.8	-0.2	1.8	-2.6	1.2	3.9
Ensemble (RNC-SWATEMM)	-3.6	-1.0	1.0	-3.6	0.3	2.8
<b>Nith at Friars Carse</b>						
CCSM4	-5.2	1.2	0.3	-2.0	3.6	1.2
GFDL-ESM2G	-8.8	-3.8	-1.0	-9.1	-3.9	-0.7
HadGEM2-ES	3.2	10.6	9.1	1.3	1.0	7.8
INMCM4	4.5	-1.4	3.4	8.3	7.6	8.4
MPI-ESM-LR	-1.7	-2.4	2.4	-6.0	2.1	6.3
Ensemble (RNC-EGCMM)	-1.1	1.3	3.4	-0.8	2.7	5.3
Ensemble (RNC-SWATEMM)	-1.6	0.8	2.8	-1.5	2.1	4.6

**Increase**  


**Insignificant Change**  


**Decrease**  


Although the results presented in Table 5.6 do not reflect spatial heterogeneity, it is evident that all the models are in agreement with each other from a general perspective. For example, even though the SWAT model forced with the RNC-EGCMM shows significant differences in water balance components between the northern and southern regions of the catchment (see Figures 5.25 and 5.26), the areal mean values do not differ significantly from the rest of the models. In the case of GWF, at least 70% of the models are in agreement that there is significant increase in this component towards the end of the century.

**Table 5.6** Summary areal mean change of projected future water balance components in the RNC with respect to the baseline period. Changes within  $\pm 10\%$  of baseline values are considered to be insignificant (green boxes) whereas changes above  $+10\%$  (red boxes) and below  $-10\%$  (blue boxes) are considered to be significant

GCM	Scenario					
	RCP4.5			RCP8.5		
	2020s	2050s	2080s	2020s	2050s	2080s
	<b>BWF</b>					
CCSM4	-3.2	-2.8	-1.0	-1.8	-3.2	-6.4
GFDL-ESM2G	-3.2	-4.5	0.5	-7.2	-2.6	-2.8
HadGEM2-ES	3.0	-3.5	1.1	1.0	-4.1	-6.9
INMCM4	0.4	-2.9	-2.2	3.4	1.1	-1.2
MPI-ESM-LR	-1.1	-3.1	1.0	-3.2	-0.6	-1.5
Ensemble (RNC-EGCMM)	8.8	6.6	10.1	8.2	8.4	7.9
Ensemble (RNC-SWATEMM)	-0.8	-3.4	-0.1	-1.6	-1.9	-3.8
	<b>GWF</b>					
CCSM4	1.4	6.5	7.3	3.8	8.1	12.6
GFDL-ESM2G	1.8	2.8	2.4	1.4	6.1	12.3
HadGEM2-ES	4.2	8.5	13.1	5.3	12.9	14.8
INMCM4	-3.5	-0.4	-1.3	-1.6	0.2	3.8
MPI-ESM-LR	2.8	6.9	9.5	5.6	9.9	17.0
Ensemble (RNC-EGCMM)	-6.8	-4.3	-3.3	-5.9	-2.5	0.7
Ensemble (RNC-SWATEMM)	1.3	4.9	6.2	2.9	7.4	12.1
	<b>GWS</b>					
CCSM4	0.0	-0.9	-0.5	-0.2	-0.8	-1.5
GFDL-ESM2G	0.1	-0.3	-0.1	-0.1	-0.5	-1.0
HadGEM2-ES	-0.4	-1.6	-1.3	-0.5	-1.5	3.8
INMCM4	-0.6	-0.5	-0.6	-0.4	-0.4	-0.7
MPI-ESM-LR	-0.3	-0.2	-0.1	0.0	-0.6	-1.0
Ensemble (RNC-EGCMM)	1.1	1.0	1.1	1.1	1.0	1.0
Ensemble (RNC-SWATEMM)	-0.2	-0.7	-0.5	-0.2	-0.8	-0.1

Increase



Insignificant Change



Decrease



## 5.4 SRB Hydrologic Modelling

### 5.4.1 Model Setup

Data required to successfully run SWAT for the Shire River Basin was obtained from sources mentioned in Chapter 3. The SWAT model requires at the minimum, four spatial input data – namely topographic, land-use/land-cover, soil and weather data. Topographic, soil and land-use inputs for the SRB are shown in Fig. 5.27. The preparation and post-processing of the data inputs was achieved using a combination of tools such as ESRI ArcGIS® (for cleaning and preparing spatial input data), ArcSWAT (Olivera et al., 2006a,b), R programming language (R Core Team, 2017) for preparation of input text files and extraction of output data and Python-Matplotlib (Hunter, 2007) for visualizing of model output results. A minimum drainage area of 10 km<sup>2</sup> was selected resulting in a discretization of 340 subbasins and 1820 HRUs.

#### 5.4.1.1 Weather data

Daily rainfall, maximum and minimum temperature data from eight climate stations were used to run the SWAT model for the baseline period. The data processing and quality assessment is described in Chapter 3 and Section 4.3. Apart from the aforementioned parameters, SWAT requires daily values of solar radiation, relative humidity and wind speed. For the SRB, observed solar radiation, relative humidity and wind speed data were not only unreliable but had large gaps such that imputation was not justified.

In SWAT, the user can create a custom weather generator in cases where observed station data are missing. This feature is also useful for estimation of

missing values in observed records (Neitsch et al., 2011). For the contiguous United States, SWAT natively includes the WXGEN weather generator model (Sharpley and Williams, 1990) to generate synthetic climate data or for imputation of missing values in observed records. For the SRB, the National Centres for Environmental Prediction (NCEP) Climate Forecast System Reanalysis (CFSR) global weather database (Dile and Srinivasan, 2014; Fuka et al., 2014b) was used for the aforementioned purposes.

In order to model the distribution of rainfall in the SRB, the skewed distribution function was used. Alternatively, one can use the modified exponential distribution which requires fewer inputs and is mostly useful in watersheds where data on precipitation events is limited (Neitsch et al., 2011). In this research, the skewed distribution was selected due to the availability of sufficient precipitation data.

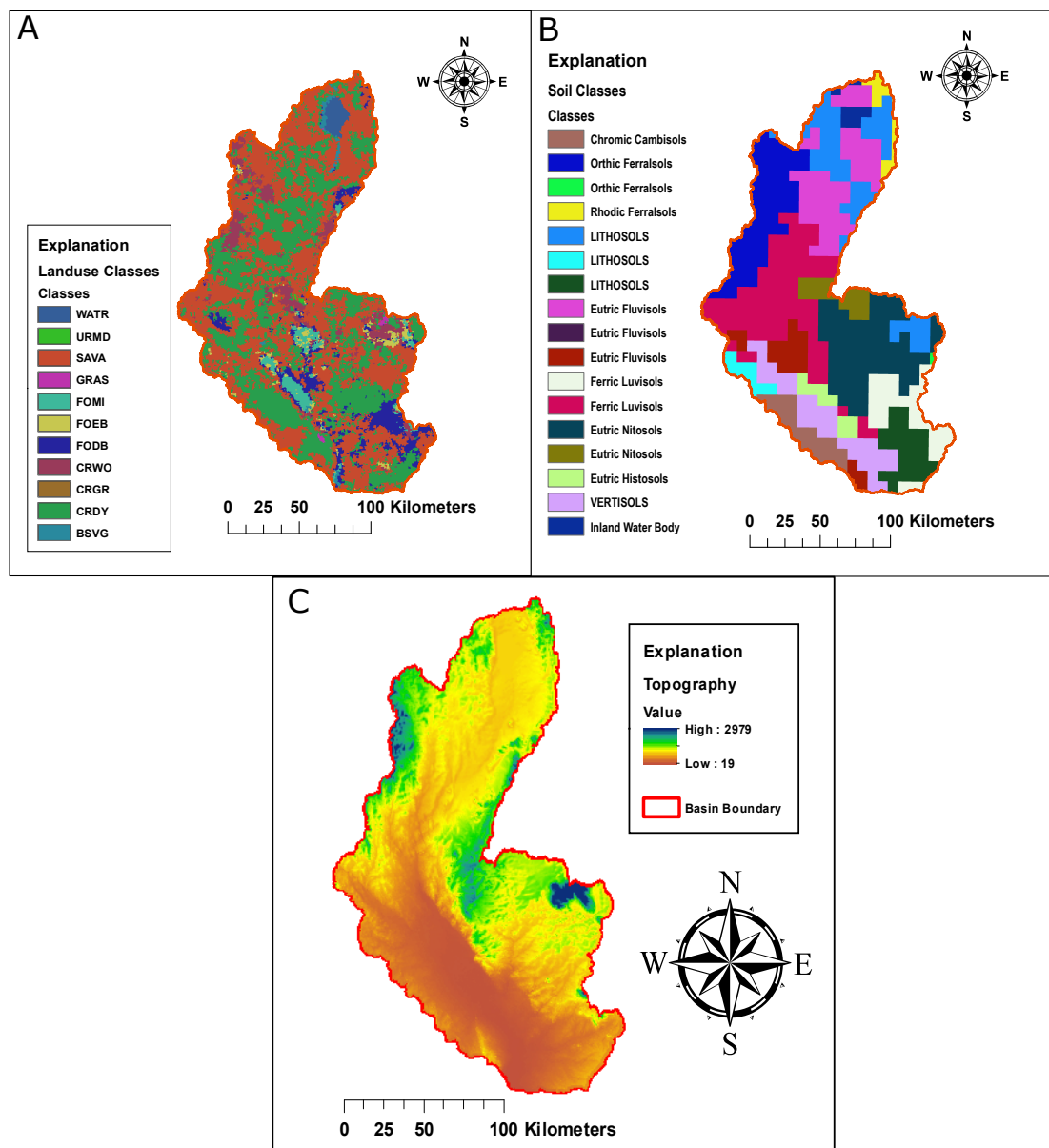
#### **5.4.1.2 Land-use/Landcover**

A total of 13 land-use classes were identified from the land-use raster and clipped to the extent of the SRB basin. The original land-use classification codes of the input raster were changed to match those used in the SWAT model. From Table 5.7, Savanna landcover dominates almost half of the basin followed by land-use of the type CRDY that covers about 35% of the watershed.

#### **5.4.1.3 Soil data**

A raster soil map classified using the FAO classification system was clipped to the watershed extent and a total of 17 soil classes identified. Soils of the type Ferric, Humic and Eutric Luvisols (Table 5.8) dominate most of the basin





**Figure 5.27** SWAT model inputs for the SRB; (A) LU/LC map map (B) Soil map and (C) Topography map.

#### 5.4.1.4 Simulation period

The baseline SWAT model was run from 1975 to 2005. Six years were assigned to the model as a “warm-up” period. This means that SWAT ran the simulation from 1975, but only printed results for the last 25 years (i.e., 1981 to 2005).

**Table 5.7** Distribution of LU/LC classes in the Shire River Basin

Land-use	Description	Area (ha)	% Watershed
CRDY	Dryland Cropland and Pasture	978264.99	34.84
SAVA	Savanna	1326194.91	47.24
WATB	Water Bodies	31656.87	1.13
BSVG	Baren or Sparsely Vegetated	19485.09	0.69
FODB	Deciduous Broadleaf Forest	173054.52	6.16
FOEB	Evergreen Broadleaf Forest	44109	1.57
GRAS	Grassland	5442.57	0.19
CRWO	Cropland/Woodland Mosaic	160662.96	5.72
FOMI	Mixed Forest	64418.67	2.29
CRGR	Cropland/Grassland Mosaic	2730.33	0.1
URMD	Residential-Medium Density	1598.13	0.06
FOMI	Mixed Forest	64418.67	2.29
CRGR	Cropland/Grassland Mosaic	2730.33	0.1

#### 5.4.2 Model calibration and validation

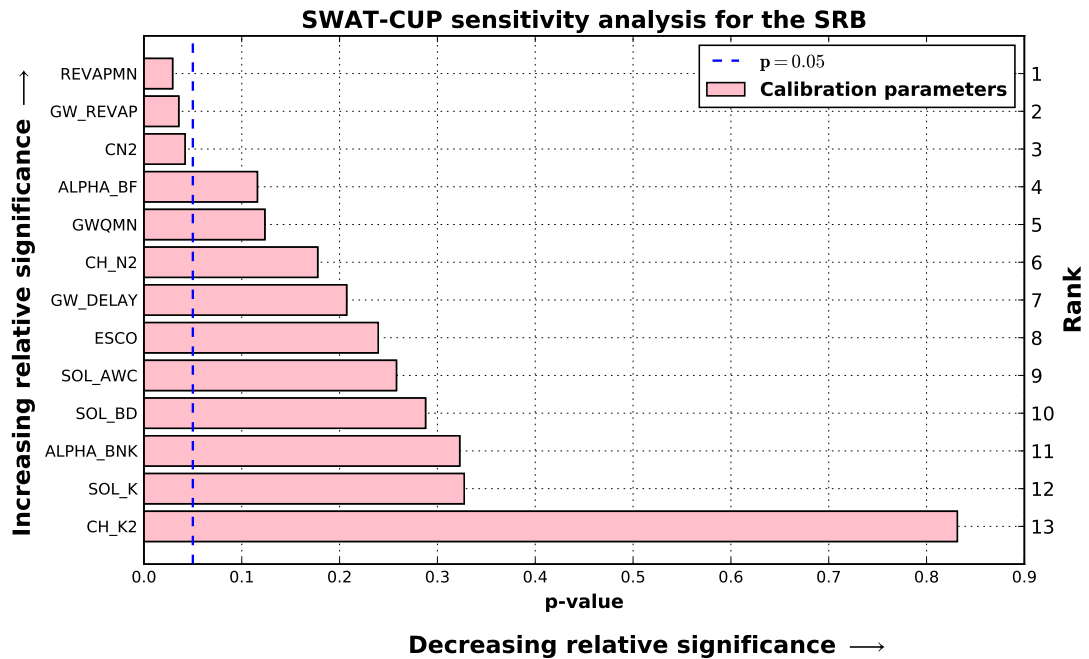
The SRB model was calibrated by applying the SUFI-2 algorithm in SWAT-CUP. A local sensitivity analysis was applied for the three streamflow variables by setting the lower and upper bounds of the calibration parameters. A total of thirteen parameters related to surface run-off and baseflow were selected for sensitivity analysis before one iteration of 1000 simulations was run in SWAT-CUP. Due to the number of HRUs in the model, computation time was significantly increased. For example, the SRB model took a total time of 26.56 hours compared to 5.78 hours for the RNC model.

Results of the global sensitivity analysis are presented in Figure 5.28. Using the p-value derived from a t-test as a measure of the relative significance, it can be seen that parameters REVAPMN, GW\_REVAP and CN2 were the most significant parameters. A short description of the parameters is given in Table 5.9. Parameters below the  $p = 0.05$  line are significant at the 95% confidence level and

**Table 5.8** Distribution of Soil classes in the Shire River Basin

Soil Class	Description	Area (ha)	% Watershed
Fr18-2-3b-572	Humic Ferralsols	46228.14	1.65
Je51-2-3a-688	Eutric Fluvisols	316793.97	11.28
WATER-1972	Water Body	34115.04	1.22
I-Bc-c-644	Lithosols	279041.40	9.94
Fo75-2-3a-534	Humic Ferralsols	311282.64	11.09
Lf88-1-2b-777	Ferric Luvisols	493557.66	17.58
Ne54-2-3b-844	Eutric Nitosols	76495.86	2.72
Ne1-3b-819	Eutric Nitosols	405959.04	14.46
Je58-2-3a-693	Eutric Fluvisols	346.68	0.01
Je7-3a-697	Eutric Fluvisols	112859.28	4.02
V1-3a-950	Vertisols	210063.33	7.48
Fo92-2-3b-554	Humic Ferralsols	2617.92	0.09
I-Bc-V-642	Lithosols	46385.64	1.65
Lf87-2-3b-776	Ferric Luvisols	164370.42	5.85
Oe4-a-857	Eutric Histosols	53885.97	1.92
Bc7-2-3b-450	Chromic Cambisols	106337.79	3.79
I-L-1b-647	Lithosols	147277.26	5.25

thus are a meaningful addition to the model as the changes in these parameters are related to changes in the response variable. In the same vein, values which had very high p-values such as CH\_K2, SOL\_K and ALPHA\_BNK and were subsequently removed from further calibration iterations leaving a total of ten parameters in the final calibration setup. These parameters were continuously changed throughout the SUFI-2 calibration process in a campaign to maximise the objective function. Four more calibration iterations were performed for the period between 1981 to 1990 on a monthly time-step before an optimal solution was reached. When the optimal solution was reached, the calibration process was stopped and the calibrated parameters accepted as the final solution. The final corrected parameters and their calibrated ranges for the SRB model are presented in Table 5.10.



**Figure 5.28** Global sensitivity analysis results for the SRB. Dashed blue line is the  $p = 0.05$  line.

Having examined and accepted the optimal solution, one iteration of 500 simulations was run to validate the model using observations between the period of 1991 and 1992. The optimal parameters solved during the calibration stage were used without any changes during the validation period. As can be seen from Figure 5.29

### 5.4.3 Climate Change Impacts on Streamflow

Assessment of historical streamflow records in the SRB and identification of change points and trends proved to be difficult for the SRB due to the many gaps in the records. Although complete records were obtained by the use of an infilling technique described in Chapter 3, it was decided against performing trend tests on such data as it may result in spurious results due to the possibility

**Table 5.9** Description of SWAT parameters used in the SRB calibration process

No.	Parameter	Description
1	REVAPMN	Threshold water depth in the shallow aquifer for "revap" [mm]
2	GW_REVAP	Groundwater "revap" coefficient
3	CN2	Initial SCS runoff curve number for moisture condition II
4	ALPHA_BF	Baseflow alpha factor (1/days)
5	GWQMN	Threshold depth of water in the shallow aquifer required for return flow to occur (mm H <sub>2</sub> O)
6	CH_N2	Manning's "n" value for the main channel
7	GW_DELAY	Groundwater delay time (days)
8	ESCO	Soil evaporation compensation factor
9	SOL_AWC	Available water capacity of the soil layer (mm H <sub>2</sub> O/mm soil)
10	SOL_BD	Moist bulk density (Mg/m <sup>3</sup> or g/cm <sup>3</sup> )
11	ALPHA_BNK	Baseflow alpha factor for bank storage (days)
12	SOL_K	Saturated hydraulic conductivity (mm/hr)
13	CH_K2	Effective hydraulic conductivity in main channel alluvium (mm/hr)

of the introduction of unnatural signals in the data. Even though infilling is a last resort measure which is desirable for water resources management and modelling, especially in watersheds where incomplete data is ubiquitous, it is contended here that analysing for trends in the synthetic data could lead to misinterpretation of trends and thus affect the implementation of adaptation plans. Projected streamflow is represented by a solid line, upper and lower bands (shaded) representing the M95PPU, U95PPU and L95PPU respectively. The percentage change in streamflow between the baseline and future periods for the wet months (DJFMA) are indicated on the graphs.

**Lichenya River:** At Lichenya, most of the GCMs predict a mean increase of streamflow of about 12% and 16% under RCP4.5 and 8.5 respectively (see

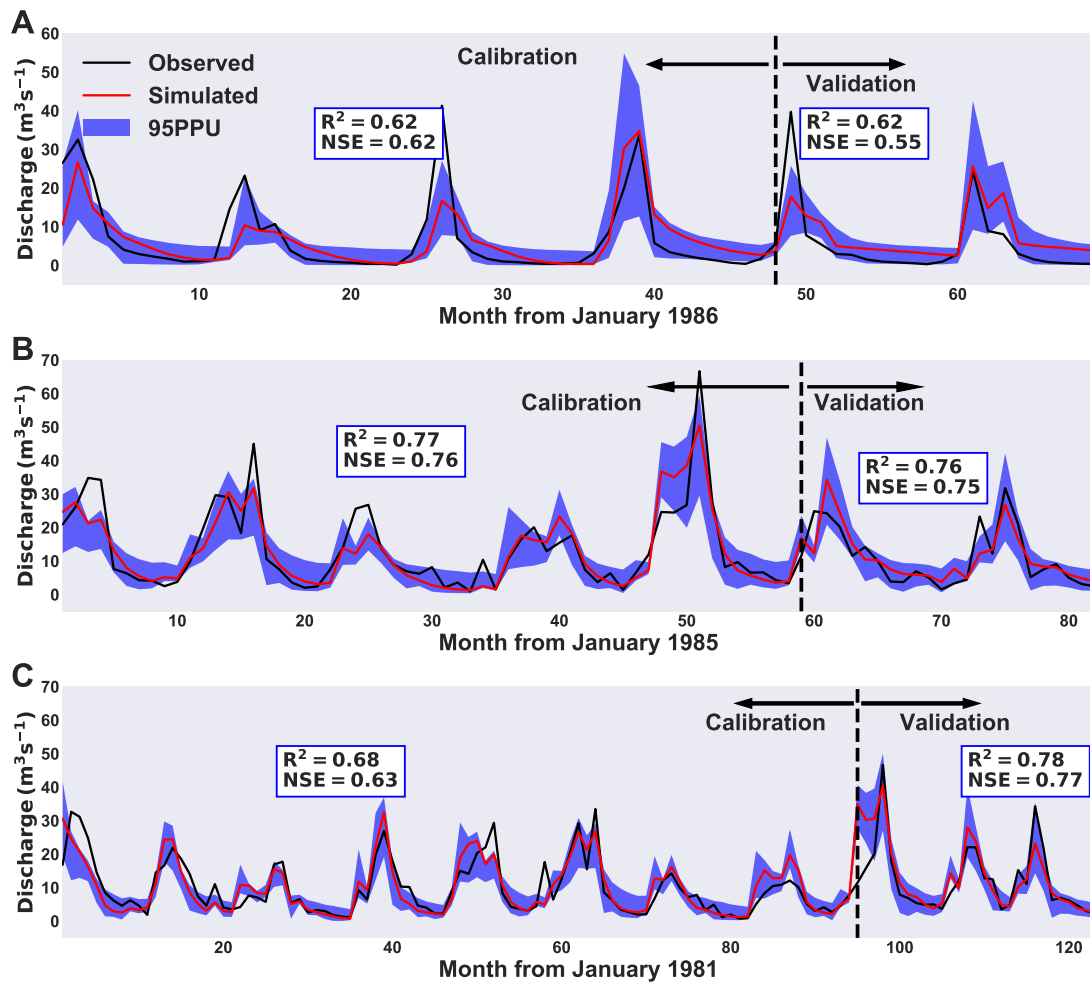
**Table 5.10** Calibrated parameter values with their range for the SRB arranged according to their sensitivity in decreasing order

Rank	Parameter name	Op.*	File type	Fitted Value	Min. Value	Max. Value
1	REVAPMN	v	.gw	85.0243	73.4199	91.5801
2	GW_REVAP	a	.gw	0.0931	0.0931	0.1225
3	CN2	r	.mgt	0.0695	0.0640	0.1336
4	ALPHA_BF	v	.gw	0.9261	0.9033	1.0335
5	GWQMN	a	.gw	0.8824	0.7865	1.3606
6	CH_N2	v	.rte	0.0762	0.0680	0.1623
7	GW_DELAY	v	.gw	348.6659	281.4008	358.2752
8	ESCO	a	.bsn	0.9209	0.9111	0.9458
9	SOL_AWC	r	.sol	-0.3538	-0.3971	-0.2678
10	SOL_BD	r	.sol	-0.4550	-0.5594	-0.3339

\* Denotes the *mathematical operation* being applied on the parameter where *v* means the existing parameter is to be replaced by a given value, *a* means a given value is added to the existing parameter value and *r* means an existing parameter value is increased by the given value as a percentage.

Figures 5.30 and 5.31). In both cases, BCC-CSM1-1-M and HadGEM2-ES project a slight decrease in streamflow signifying little or no change when compared with the baseline period. MPI-ESM-LR projects higher positive changes when compared with the other models under all scenarios and for all time periods. In the mid-century under RCP4.5, 3 GCMs project an increase in streamflow while the rest project a decline. Generally the indication is that there will be little to no change in streamflow when compared to the baseline. The same conclusion can be made for RCP8.5 where the models are split half-way between an increase or decrease in streamflow. In the late-century, at least five GCMs depict an increase in streamflow of about 12% and 14% under RCP4.5 and 8.5 respectively.

**Rivi-rivi River:** During the wet period (typically November to April), the uncertainty associated with the streamflow simulation is high as can be seen



**Figure 5.29** Graphs of river discharge calibration and validation for selected rivers in the SRB: a) Rivi-Rivi River at Balaka, b) Ruo River at M1 Roadbridge (Nsuwadzi) (Ruo) and c) Lichenya River at Mini Mini Estate

from Figures 5.32 and 5.33. When compared to the baseline, the models predict a mean rise in streamflow of about +46% in the 2020s under RCP4.5. The variation between models is much bigger under RCP8.5 with GFDL-ESM2G predicting as high +93.28% increase when compared with the baseline streamflow while the rest of the GCMs all predict approximately +30% increase in streamflow. The same trend is observed in the mid-century where all models predict an increase of approximately +40% and +60%

under RCP4.5 and 8.5 respectively. The only exception is BCC-CSM1-1-M which drastically differs from the other GCMs in terms of magnitude and direction for mid-century streamflow under RCP8.5. In the late-century, five of the six GCMs predict a mean increase in streamflow of about +37% and +48% under RCP4.5 and 8.5 respectively. Again, MPI-ESM-LR gives significantly large percentage changes of 102 and 169 under RCP4.5 and 8.5 respectively. In general the GCMs are in agreement concerning the magnitude and direction of change.

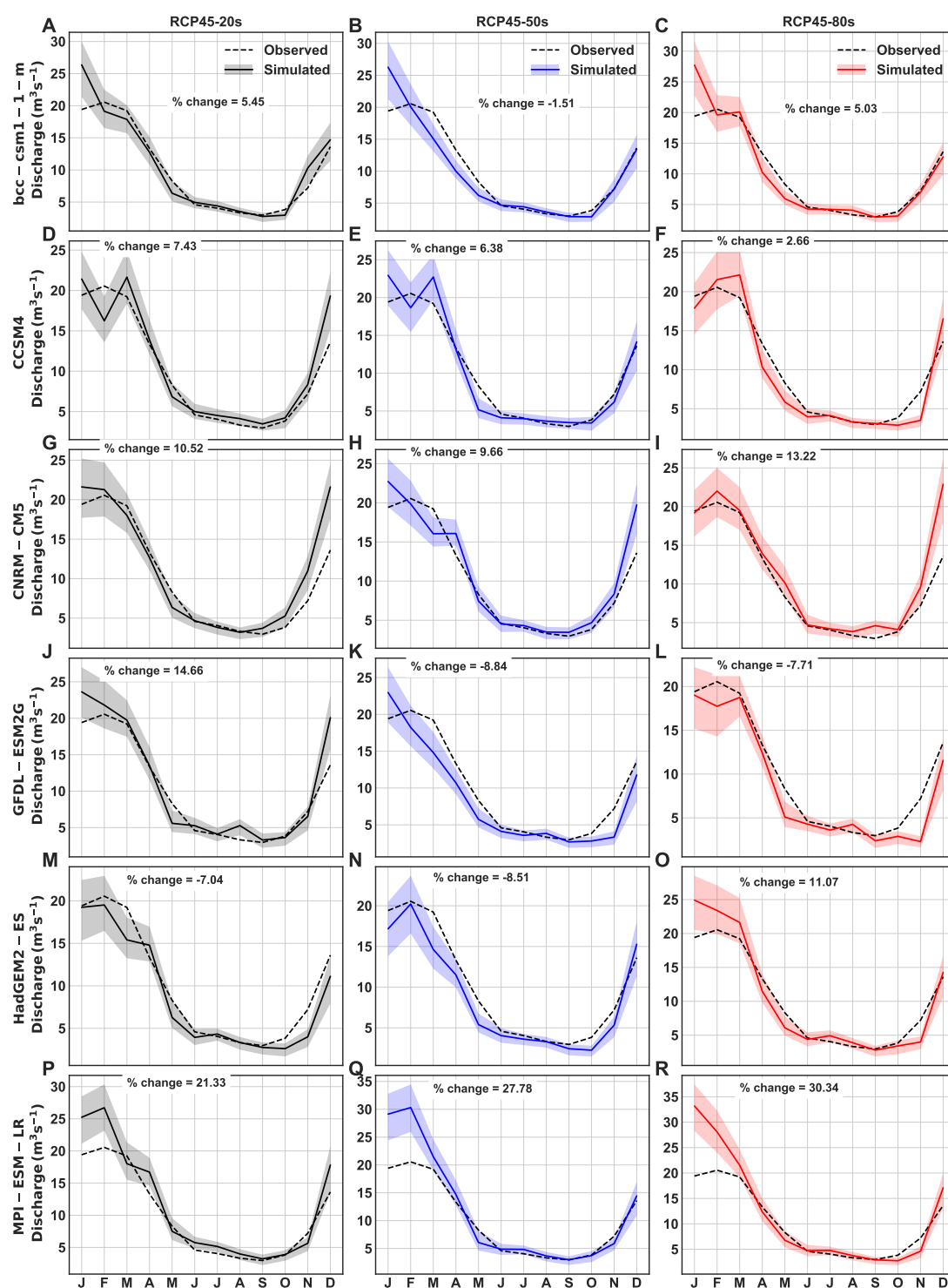
**Ruo River:** At Ruo, two GCMs (BCC-CSM1-1-M and HadGEM2-ES) under RCP4.5 in the 2020s projected a decrease in streamflow as in Lichenya above (Figures 5.34 and 5.35). On the other hand, three GCMs showed decreases in streamflow for the same time-scale under RCP8.5. In the 2050s, a similar scenario is observed where half of the GCMs are diametrically opposed in terms of the sign of change under both RCPs. Inevitably, it is difficult to interpret such conflicting results arising from the modelling exercise and thus beckoning the use of the methodology discussed in Section 5.3.3.2. Unlike the projections at Lichenya and Rivirivi, all GCMs there is a split decision regarding the direction of change for all time scales and under all RCPs. Again, the uncertainty represented by the 95PPU is wider over the wet months than the dry period.

**Ensemble models:** Figures 5.36 and 5.37 are the Shire River Basin SWAT Ensemble Model Mean (hereinafter SRB-SWATEMM) results and the results of SWAT forced with the Shire River Basin Ensemble GCM Mean (SRB-EGCMM) respectively. The SRB-SWATEMM results are a simple arithmetic mean of the SWAT models driven by individual GCMs and thus the results

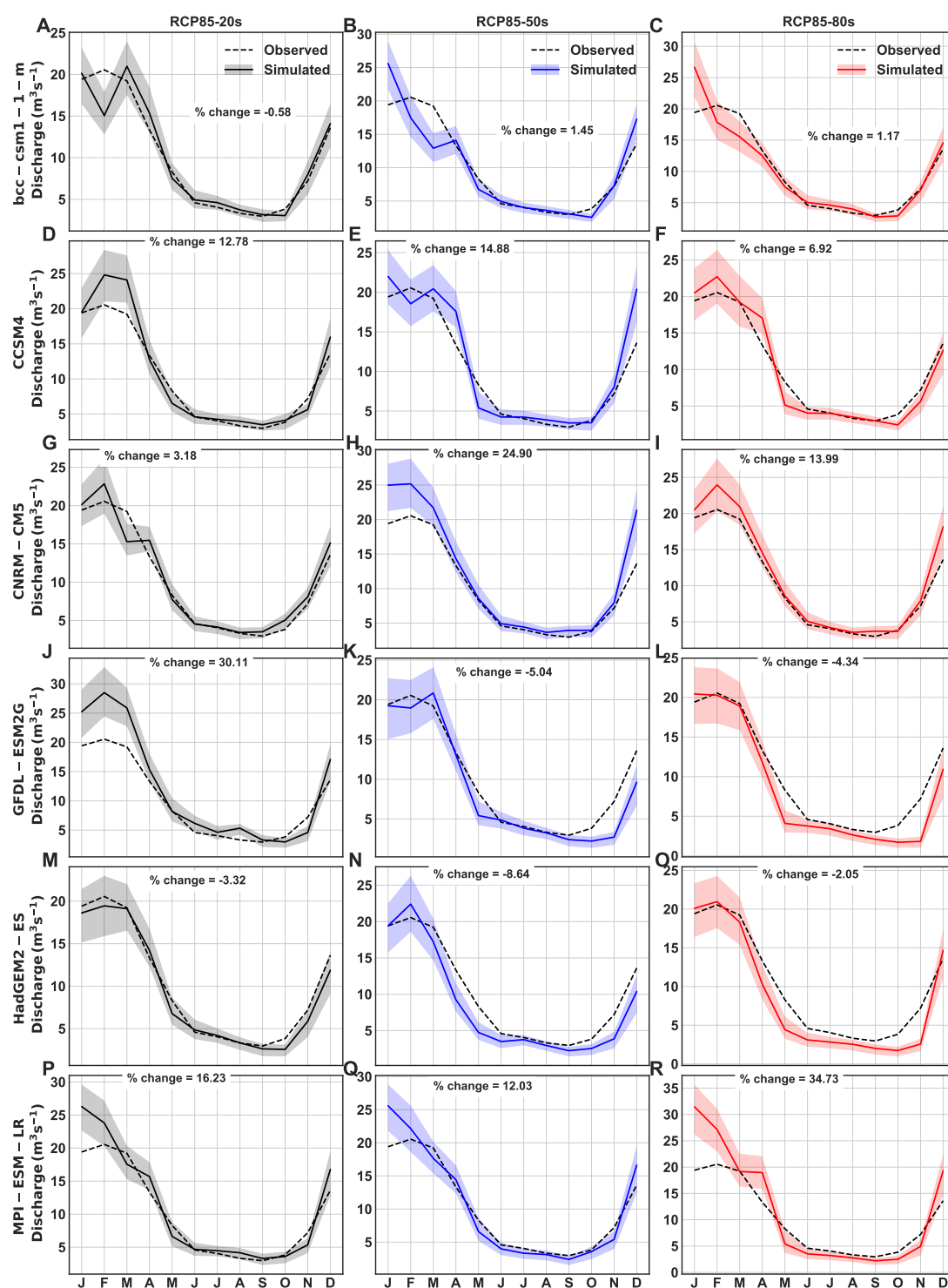


do not depart too far from the individual models. For example, from Figure 5.36, it is observed that at Rivi-rivi, the mean results predict a 46% rise in streamflow under RCP4.5 and 8.5 in the 2020s as calculated above. The median increase in the 2020s is +37% but because of two GCMs which predict as high as +50% and +90% increase, the mean as expected is slightly shifted towards the outliers. Conversely, the SRB-EGCMM forced model predicts decreased streamflow in all the rivers in the 2020s under the two RCPs. This is not surprising especially for models that had a split-choice with respect to the direction of change. However, at gauging stations where the majority of the models predicted positive changes, this was an interesting outcome strengthening the debate as to whether hydrologic models constructed with a single GCM could actually be trusted? In the 2050s, the SRB-EGCMM forced model projects on average a -10% decrease in streamflow in all the rivers. It should be noted, however, that the uncertainty range is wider at Rivi-rivi than other rivers during the wet months signifying increased uncertainty in the SUFI-2 predictions. In the 2080s, the SRB-EGCMM forced model predicts a slightly further decrease in streamflow compared to the 2050s except at Rivi-rivi where the model predicts a 10% increase under RCP8.5. Based on the ability of the ensemble GCM model to reproduce the historical streamflow period and based on recommendations from the IPCC about the use of multi-model ensembles (Stocker et al., 2010), the use of the SRB-EGCMM to force hydrologic models in impact studies is highly recommended. This can help in overcoming uncertainties associated with individual GCMs such as internal variability.

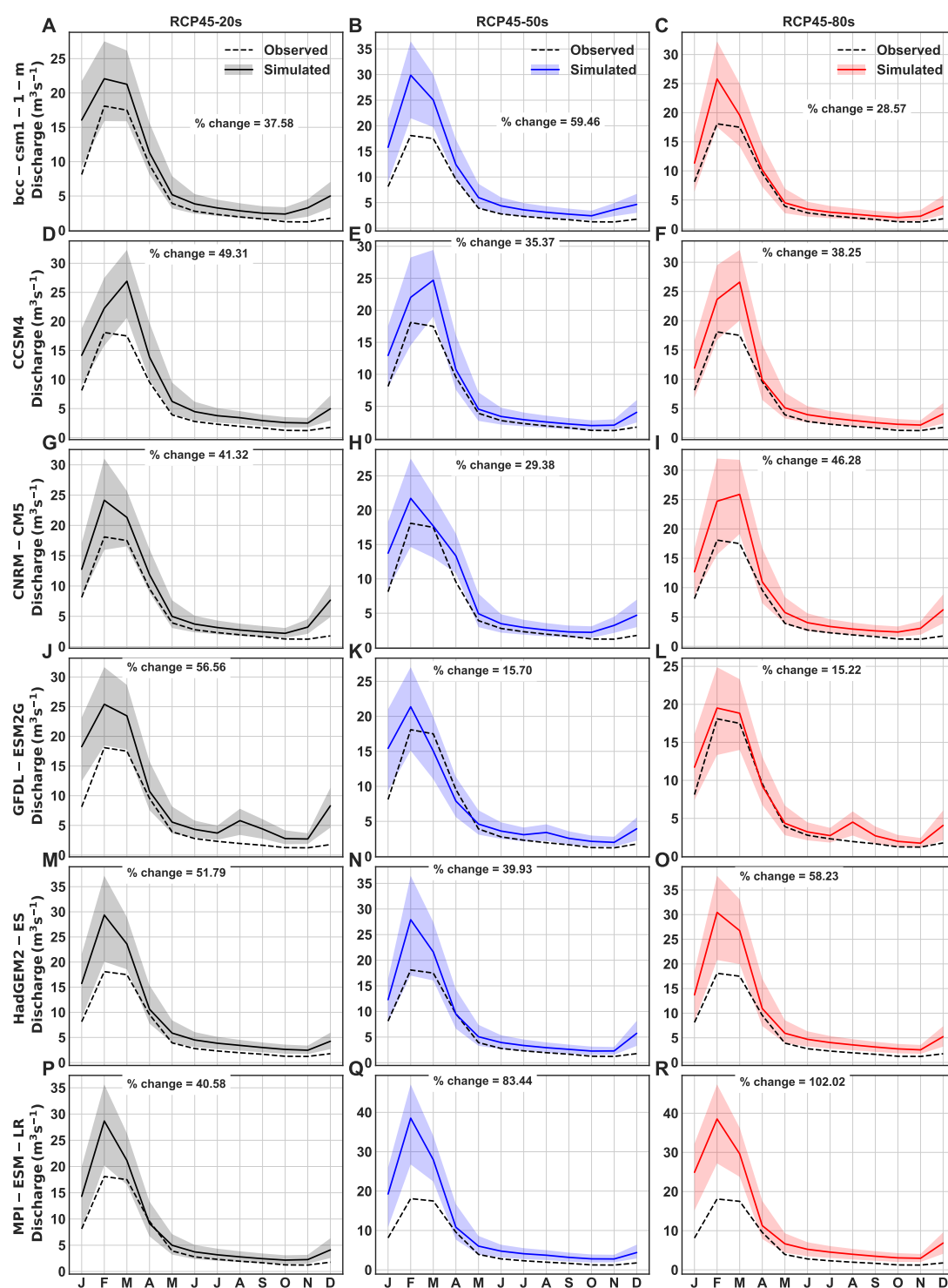
Results of the SRB-EGCMM forced model are in agreement with the future temperature and rainfall projections since on an annual basis, the SRB-EGCMM predicts for almost all stations a net rise of less than +10% in rainfall under RCP4.5 and 8.5 while temperatures rise by at least 2 °C. On a seasonal basis, almost all the stations indicate a drop in MAM precipitation in the SRB especially in the 2050s under RCP4.5. In the drier months of JJA and SON a reduction in precipitation of up to 40% especially in the mid- and late-century can be observed. In general, the change effects on streamflow are largely controlled by precipitation, although baseflow could be an important factor too. Conversely, temperature changes may also affect the streamflow regimes due to the fact that when air temperatures increase, streamflow reduces and vice versa (DeWalle et al., 2000). Other factors that could affect the future streamflow regime in the SRB include LU/LC changes, urbanisation and groundwater discharge or baseflow. In addition to the analyses here, these factors need to be incorporated into watershed management plans to mitigate against the impacts of climate change.



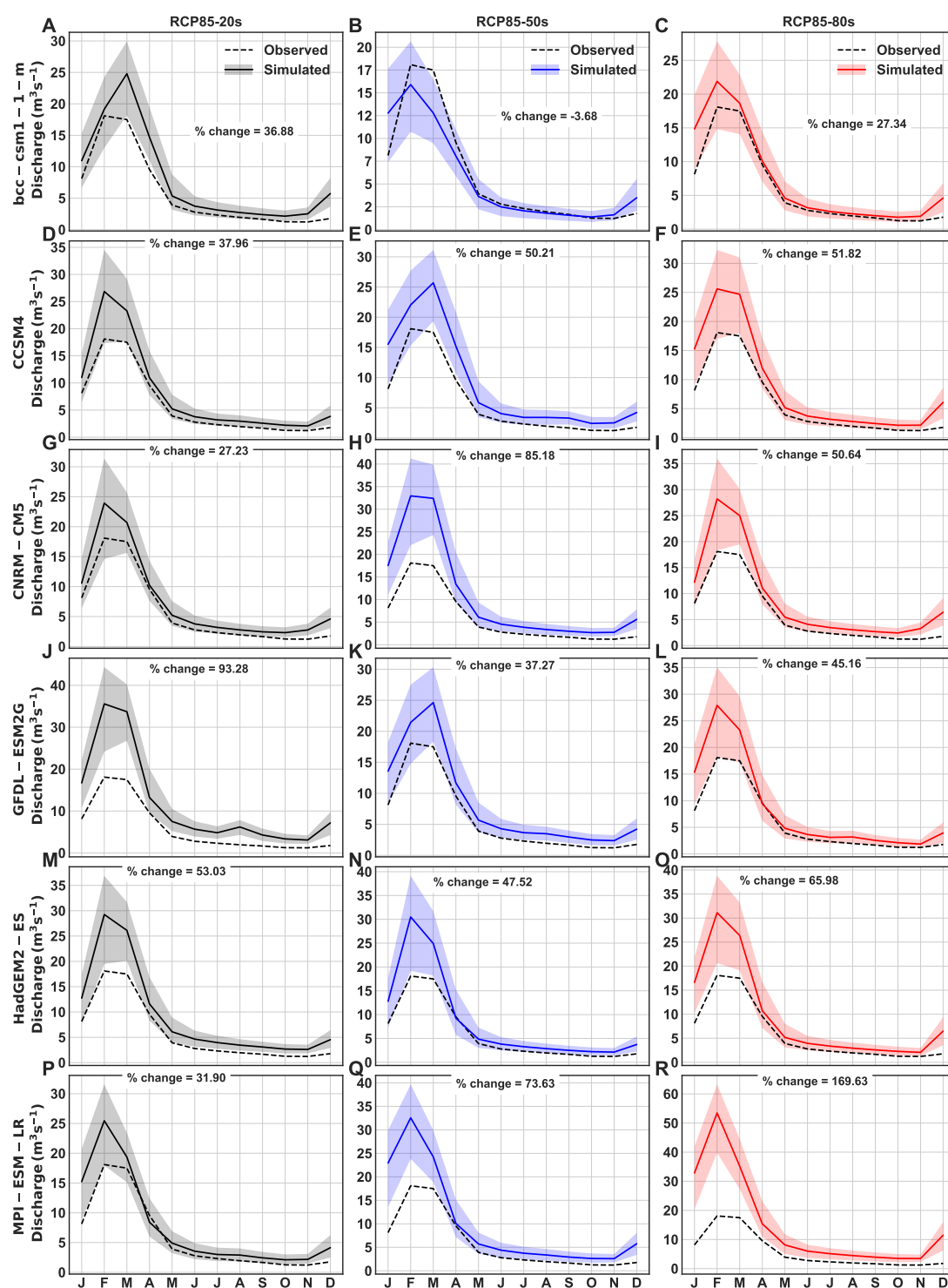
**Figure 5.30** Projected future streamflow at Lichenya for the RCP4.5 Scenario. GCMs are represented row-wise and time-scales column-wise



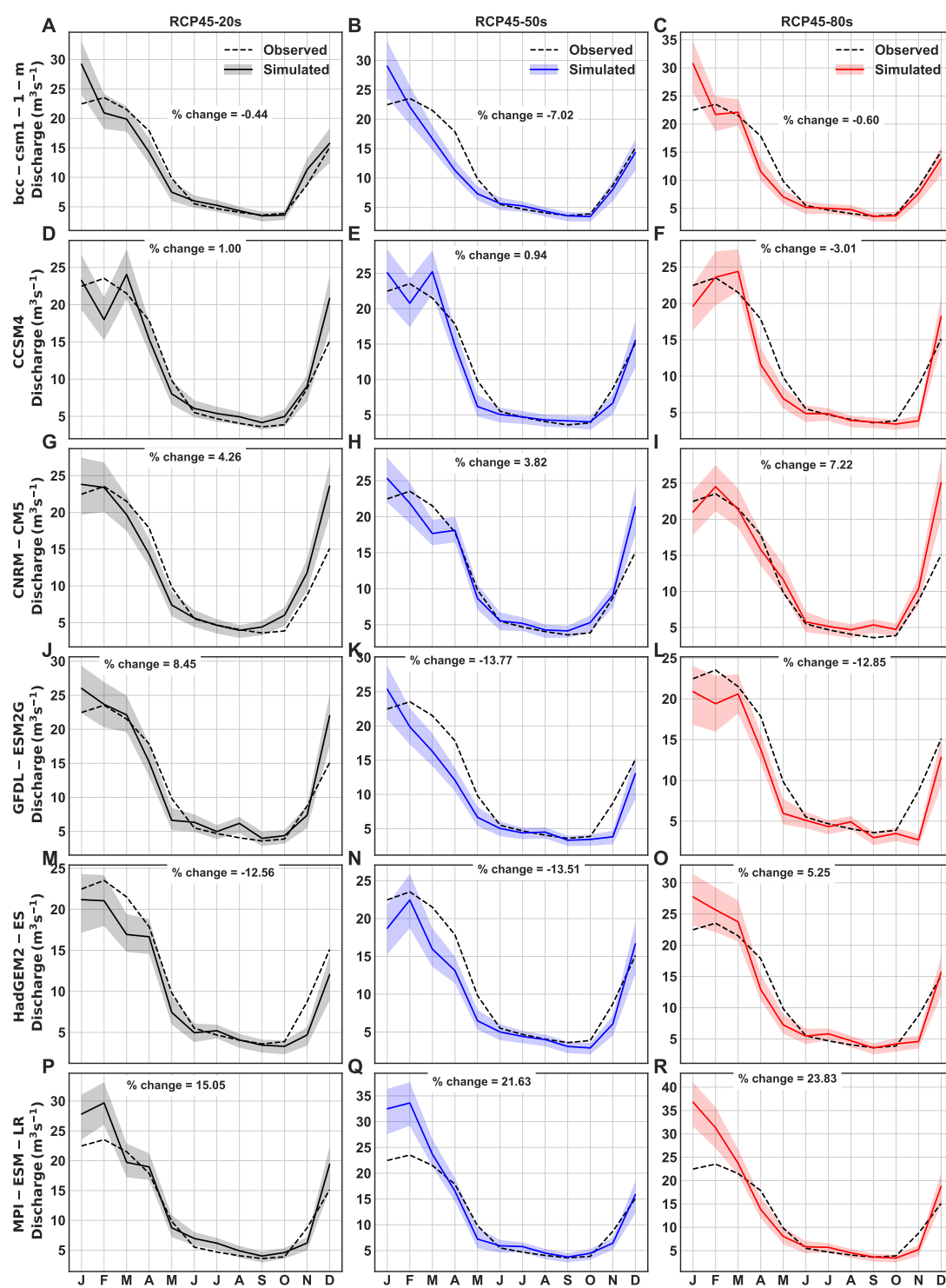
**Figure 5.31** Projected future streamflow at Lichenya for the RCP8.5 Scenario. GCMs are represented row-wise and time-scales column-wise



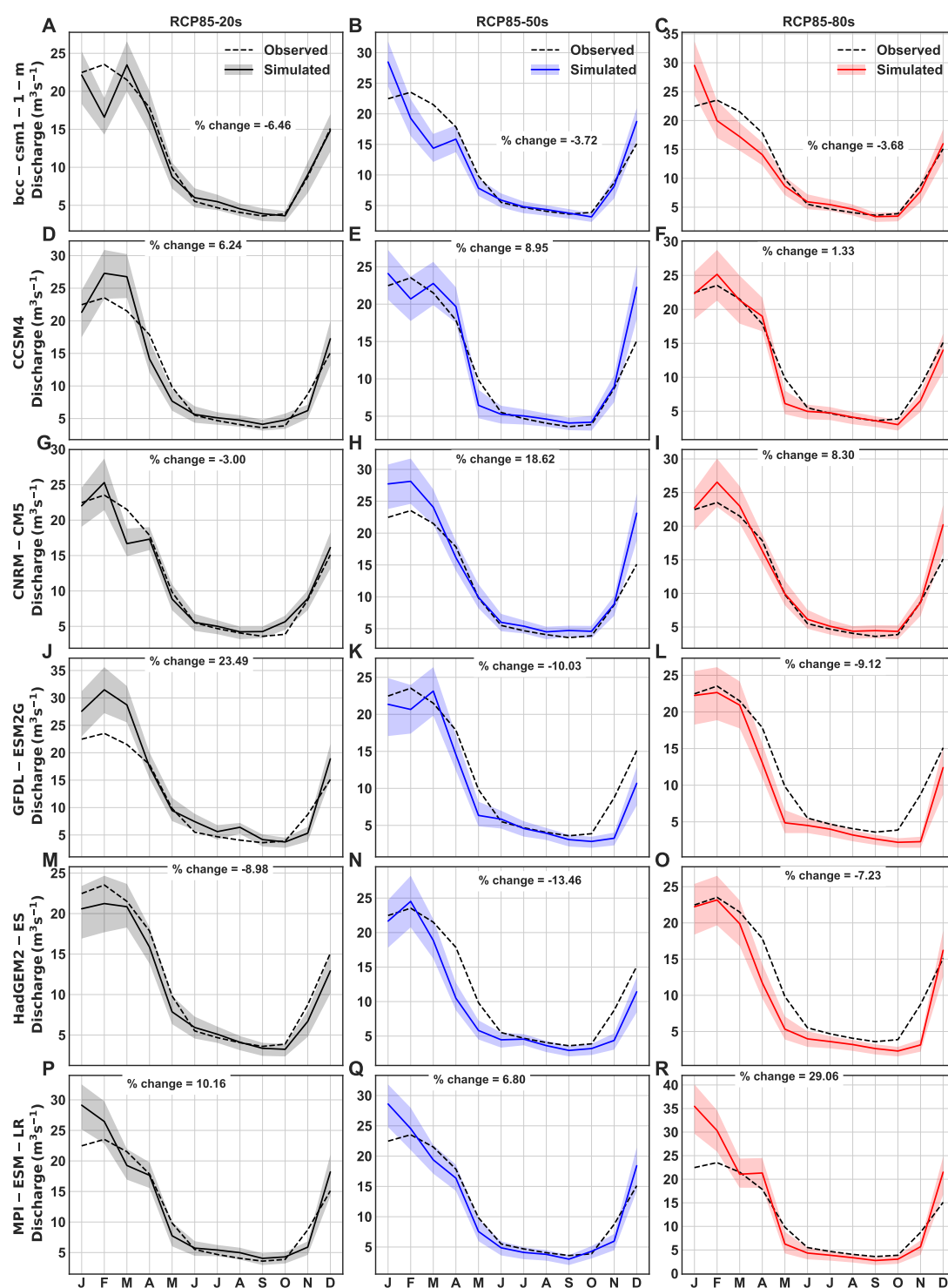
**Figure 5.32** Projected future streamflow at Rivirivi for the RCP4.5 Scenario. GCMs are represented row-wise and time-scales column-wise



**Figure 5.33** Projected future streamflow at Rivirivi for the RCP8.5 Scenario. GCMs are represented row-wise and time-scales column-wise

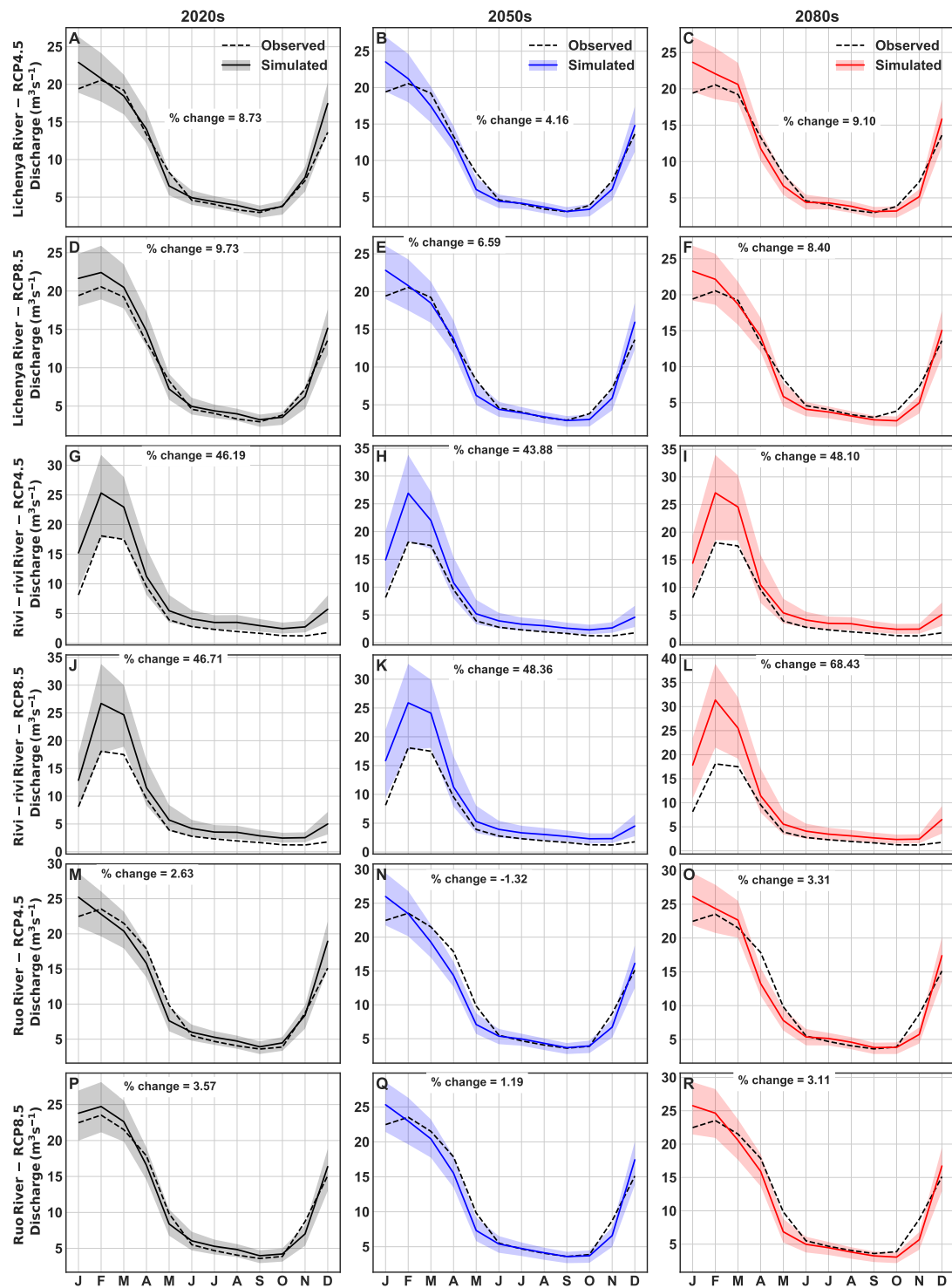


**Figure 5.34** Projected future streamflow at Ruoh for the RCP4.5 Scenario. GCMs are represented row-wise and time-scales column-wise

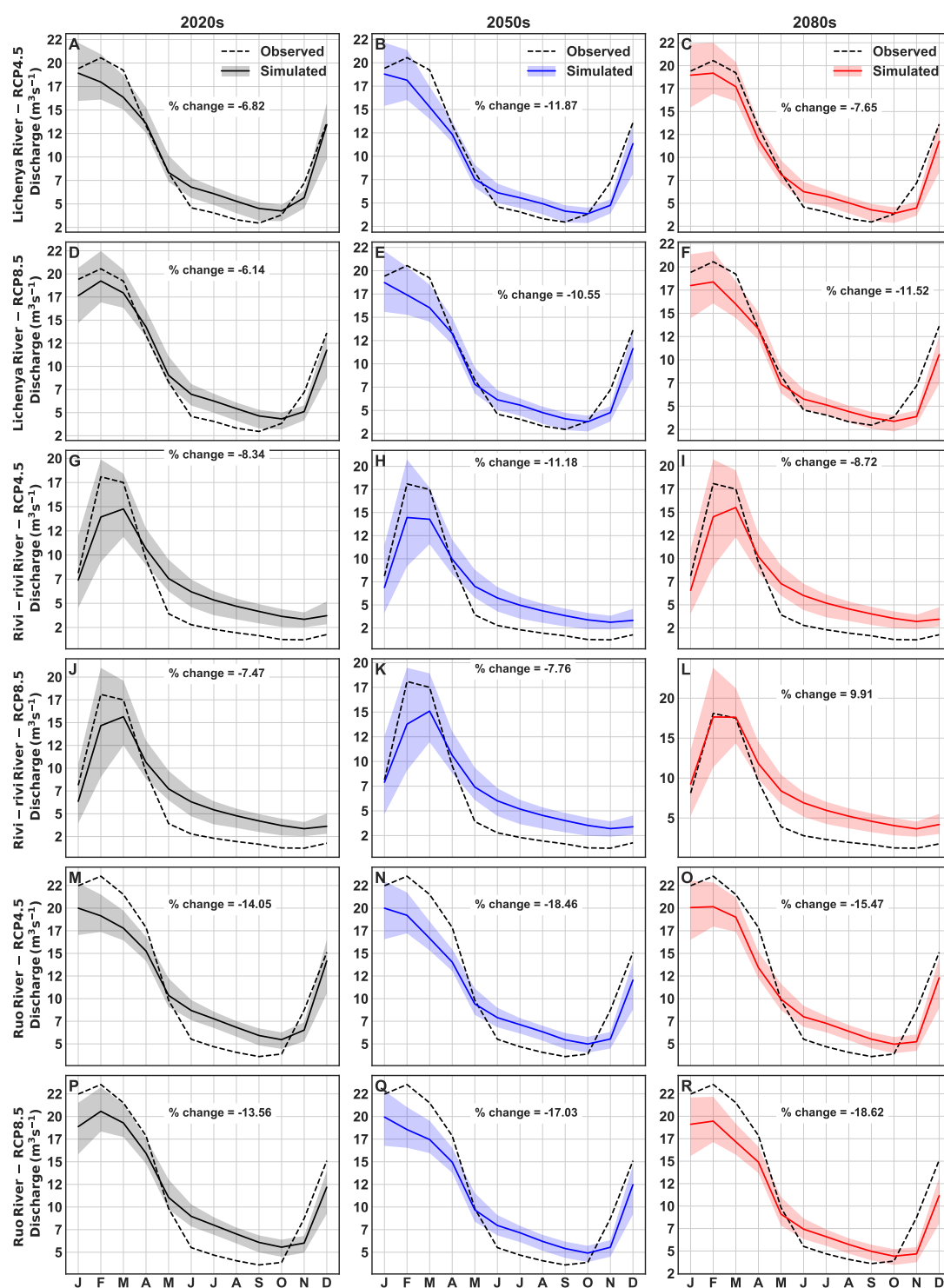


**Figure 5.35** Projected future streamflow at Ruoh for the RCP8.5 Scenario. GCMs are represented row-wise and time-scales column-wise





**Figure 5.36** Projected future streamflow at Lichenya, Ruo and Rivirivi using the simple arithmetic mean of SWAT models for the future RCP4.5 and RCP8.5 scenarios



**Figure 5.37** Projected future streamflow at Lichenya, Ruo and Rivirivi using SRB-EGCMM forced SWAT model simulations under RCP4.5 and RCP8.5 scenarios

#### 5.4.4 Blue-Green Water Nexus

At national level, Adhikari and Nejadhashemi (2016) investigated the impacts of climate change on water resources in Malawi using the SWAT model forced by six GCMs under emission scenario RCP8.5. Although the study did not distinguish categorically between green and blue water resources, some components of these water resources were modelled such as PET, ET, surface runoff, water yield and soil moisture. Their study captured spatio-temporal variations of the water balance components across Malawi projected into the future period.

In this study, a total of 6 GCMs described in Chapter 4 were used to assess the impacts of climate change on freshwater resources in the upper and lower shire basin (collectively referred to as Shire River Basin, SRB, in this thesis). Using the same time discretization as for streamflow analyses, i.e 3 time horizons dividing the 21<sup>st</sup> century, 36 models were constructed and used to compute the water balances in the SRB.

##### 5.4.4.1 Baseline Blue Water/Green Water Availability

BWF, GWF and GWS for the baseline period were calculated and presented at the 50% probability level of the 95PPU. The average annual values of the water balance components were calculated and are presented in Figure 5.38. The average BWF for the entire basin is 742 mm y<sup>-1</sup> (ranging from 240 to 1750 mm y<sup>-1</sup>). Only a few catchments have BWF potential of up to 1750 mm y<sup>-1</sup>. The western part of the basin covering Thyolo, Mulanje, parts of Blantyre and Chikwawa districts have the highest potential for bluewater ( $CV \geq 1000\text{mm y}^{-1}$ ) while the northern and southern parts of the basin (Mwanza, Balaka, Machinga, Mangochi, parts of Ntcheu, part of Chikwawa and Nsanje districts) has the lowest potential ( $CV$

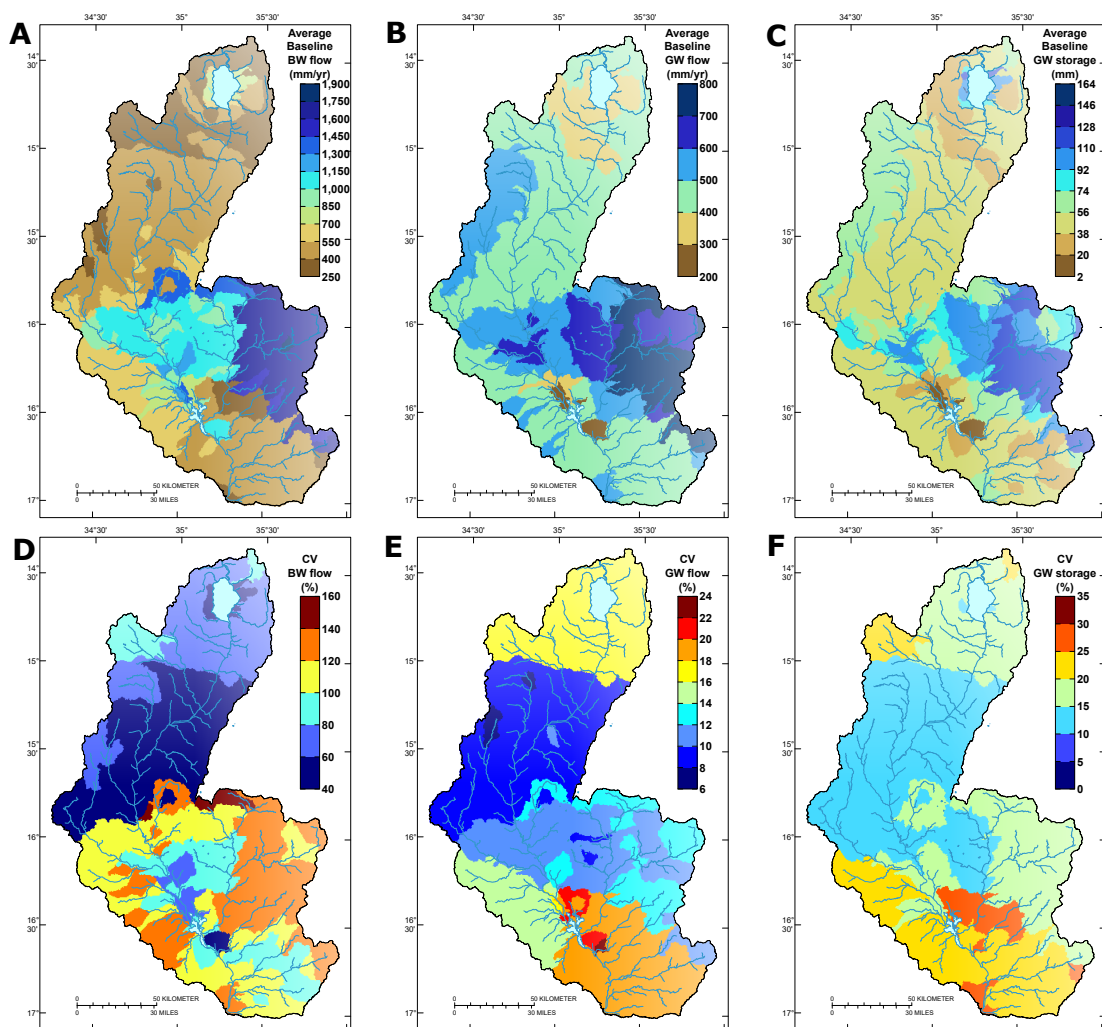
$\leq 700\text{mm y}^{-1}$ ). Mean GWF for the entire basin is  $510\text{ mm y}^{-1}$  with Mwanza, Chikwawa, Thyolo, Mulanje, Luchenza and the Mozambican town of Milange showing the highest potential for green water flow. Average GWS in the basin is  $60\text{ mm}$  with GWS potential following similar trends as for GWF.

From Figure 5.38, it can be seen that the model shows increased reliability of BW resources in parts of Blantyre, Mwanza, Neno, Balaka, parts of Ntcheu and Mangochi. In the South of the Basin, with the exception of some parts of Chiradzulu, Thyolo and Nsanje, there is evidence of higher interannual variability of BWF.

In the case of GWF, areas surrounding Blantyre, Neno, Mwanza, parts of Balaka and Ntcheu districts show increasing reliability ( $\text{CV} \leq 10\%$ ) of GW resources than the rest of the basin. Here too the model shows lower reliability ( $\text{CV} \geq 18\%$ ) in GWF south of the basin and especially the southern part of Nsanje district. Spatially, the range of CV values for GWF was much smaller than that for BWF. One explanation could be that, judging from the spatial distribution of rainfall in the basin, it appears that BWF is hugely influenced by this pattern and thus inherits and exhibits similar variability as that of rainfall. GWF appears not to be more robust to the effect of the spatial rainfall pattern. This can be explained by examining Table 5.7 and noticing that land-use classes CRDY (Dryland cropland and pasture) and SAVA (Savanna) collectively constitute approximately 82% of the entire watershed. Also, it is known that evapotranspiration is affected by vegetative cover, leaf area index (LAI), leaf shape and many other factors including soil characteristics. From the foregoing, it can be inferred that LU/LC plays a major role in controlling GWF and thus less variability in GWF, controlled mostly by LU/LC, can be seen than processes

dominantly controlled by rainfall which is less predictable.

A similar trend as that of GWF was observed in GWS. Generally, there is evidence of higher reliability ( $CV \leq 10\%$ ) of GWS in Thyolo, Blantyre, Neno, Mwanza, Balaka and Machinga districts than in the rest of the watershed. Also, it should be noted that the range in the CV is still smaller here than that observed for BWF.



**Figure 5.38** Water balance components in the SRB for the baseline period; (a) Blue Water Flow (BWF), (b) Green Water Flow (GWF), (c) Green Water Storage (GWS), (d), (e) and (f) are coefficients of variation expressed as a percentage for BWF, GWF and GWS respectively

#### 5.4.4.2 Future BW/GW Availability

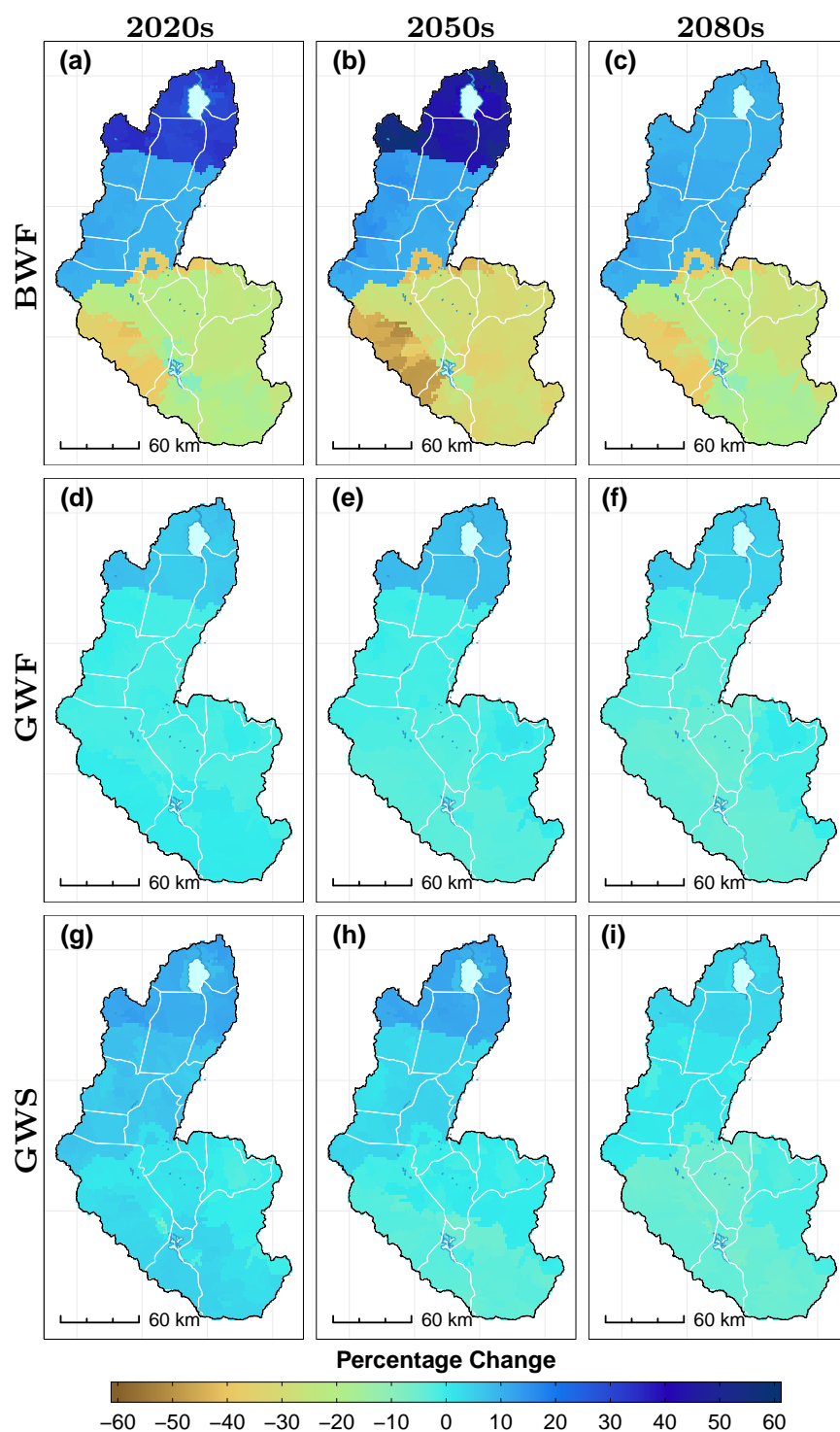
Similar to the approach in Section 5.4.3, SWAT models forced with single GCMs were constructed, the results of which were compared with MMEGCM-SWAT and the simple arithmetic mean of the singular GCM SWAT models. Figures 5.39 to 5.50 show percentage differences in BW/GW availability for the future period in the SRB. Positive values indicate an increase in the component being simulated compared to the baseline whereas negative values indicate a decrease in BW/GW. In the 2020s, BWF ranges between -45% and +40%, GWF between -13% and +14% according to BCC-CSM1-1-M, for example, under RCP4.5. The deficit in BWF is predicted in the southern part of the basin covering Chikwawa, Nsanje, Thyolo, Chiradzulu and Mulanje with the greatest deficit observed in Chikwawa and Nsanje. This trend is captured by almost all the GCMs with respect to BWF, that is, an increase in BWF in the northern parts of the SRB and a deficit in BWF in the southern parts when compared to baseline values.

In the mid-century, most GCMs predict a slight decrease in BWF when compared with 2020s values, except CCSM4 (Figure 5.42B) and CNRM-CM5 (Figure 5.44B) under RCP8.5 which predict an increase of about +25% and +55% respectively in the extreme cases when compared to the same time period. MPI-ESM-LR is a unique case where BWF is predicted to increase under all scenarios throughout the century with values as high as +105% and +165% in the late-century under RCP4.5 and 8.5 respectively. BCC-CSM1-1-M (Figure 5.40B) under RCP8.5 is also unique in that BWF decreases by up to -25% and -60% in the southern and northern parts of the basin respectively in the extreme case, when compared to baseline values. Generally, not all the GCMs agree on the magnitude and direction of change with respect to BWF. However, all the GCMs

predict an increase in BWF north of the basin and a decrease in the south. The increase in BWF in the north could be a symptom of the close proximity of Lakes Malawi and Malombe. Higher temperatures, decreased rainfall especially in the 2050s and land-use patterns could be responsible for the increasing decrease in BWF in the southern-most reaches of the basin.

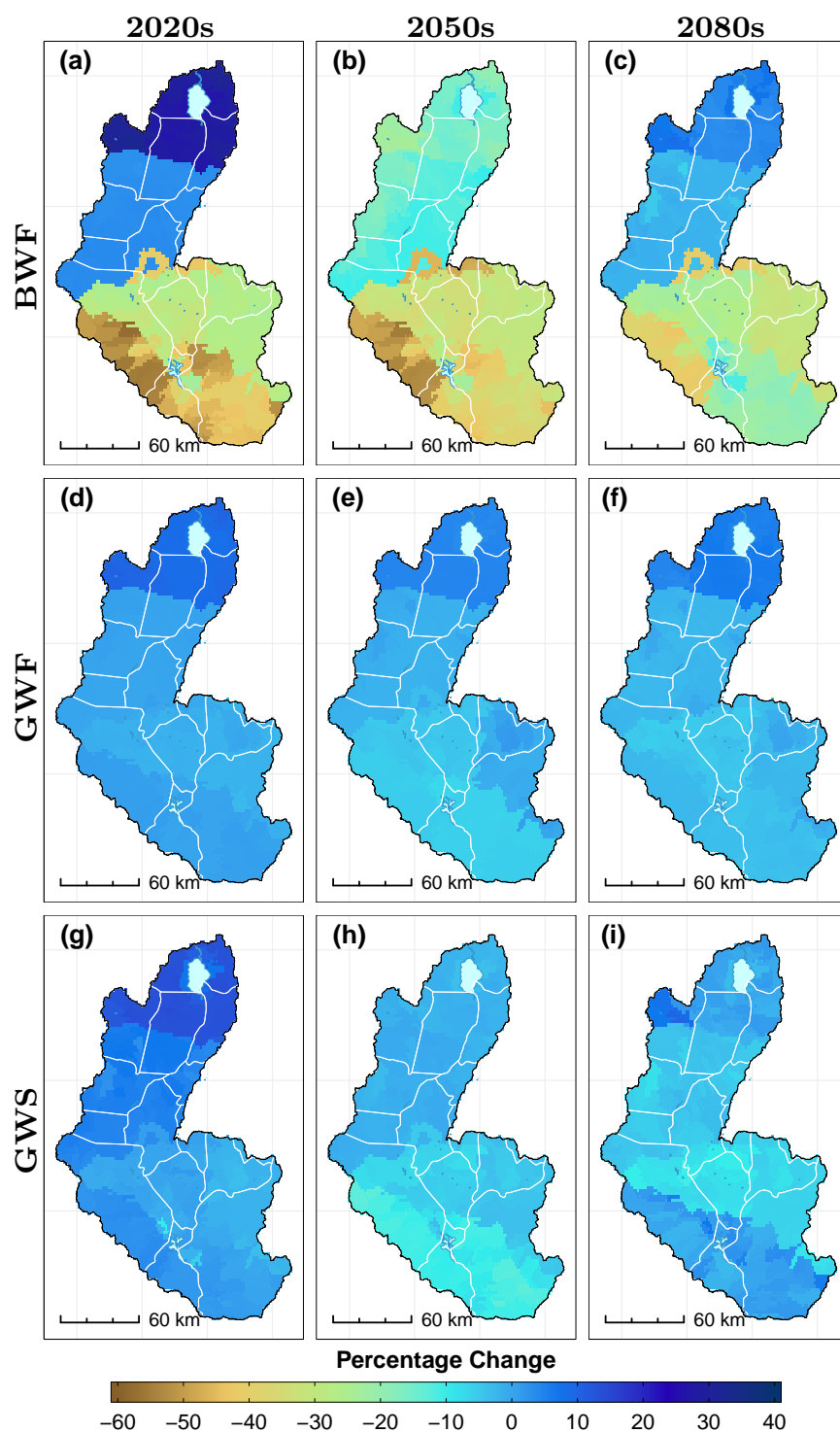
With respect to GWF, the projected changes range generally between  $\pm 12\%$  of baseline values for almost all the GCMs. In terms of the direction of change, not all the GCMs are in agreement. For example, BCC-CSM1-1-M (except under RCP8.5, Figure 5.40), CCSM4, CNRM-CM5 and MPI-ESM-LR all predict a slight increase in GWF in the 2020s, an increase of about 3 percentage points in the mid-century when compared to 2020s values and slightly lower values in the late-century, comparable to 2020s values. The rest of the GCMs predict lower-than-baseline values in the mid- and late-century.

GWS follows a similar trend as that of GWF where some GCMs predict a steady increase in GWS throughout the century and others predict a slight decline by the late-century. However, almost all the GCMs are in agreement that some parts of Blantyre, Chiradzulu, Thyolo, Mulanje and Phalombe show a decline (below baseline values by the 2050s) in GWS as the century progresses.

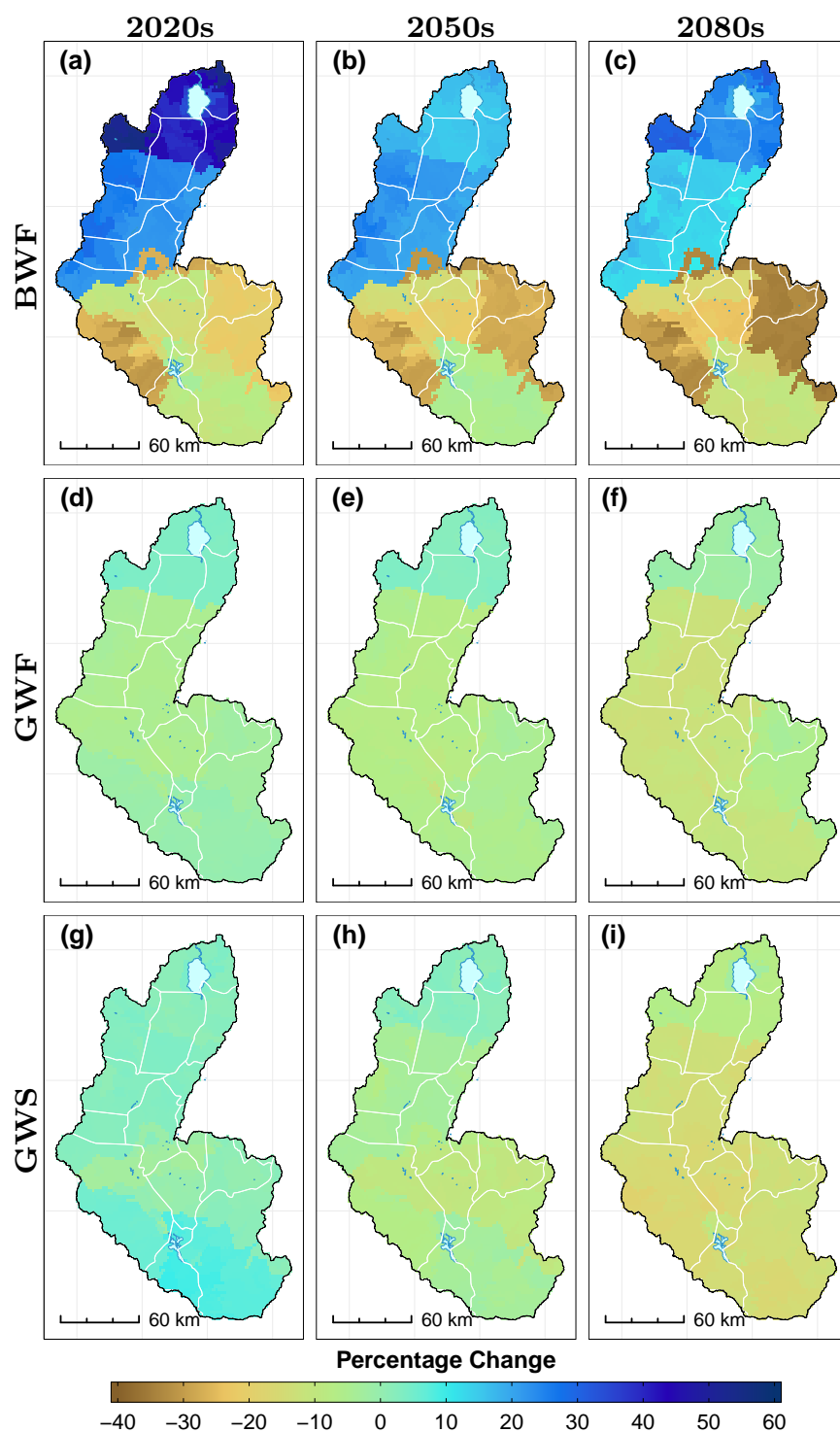


**Figure 5.39** BCC-CSM1-1-M RCP4.5 water balance components in the SRB for the future projected period. BW is blue water and GW is green water. Results are percentage differences from baseline period using the M95PPU

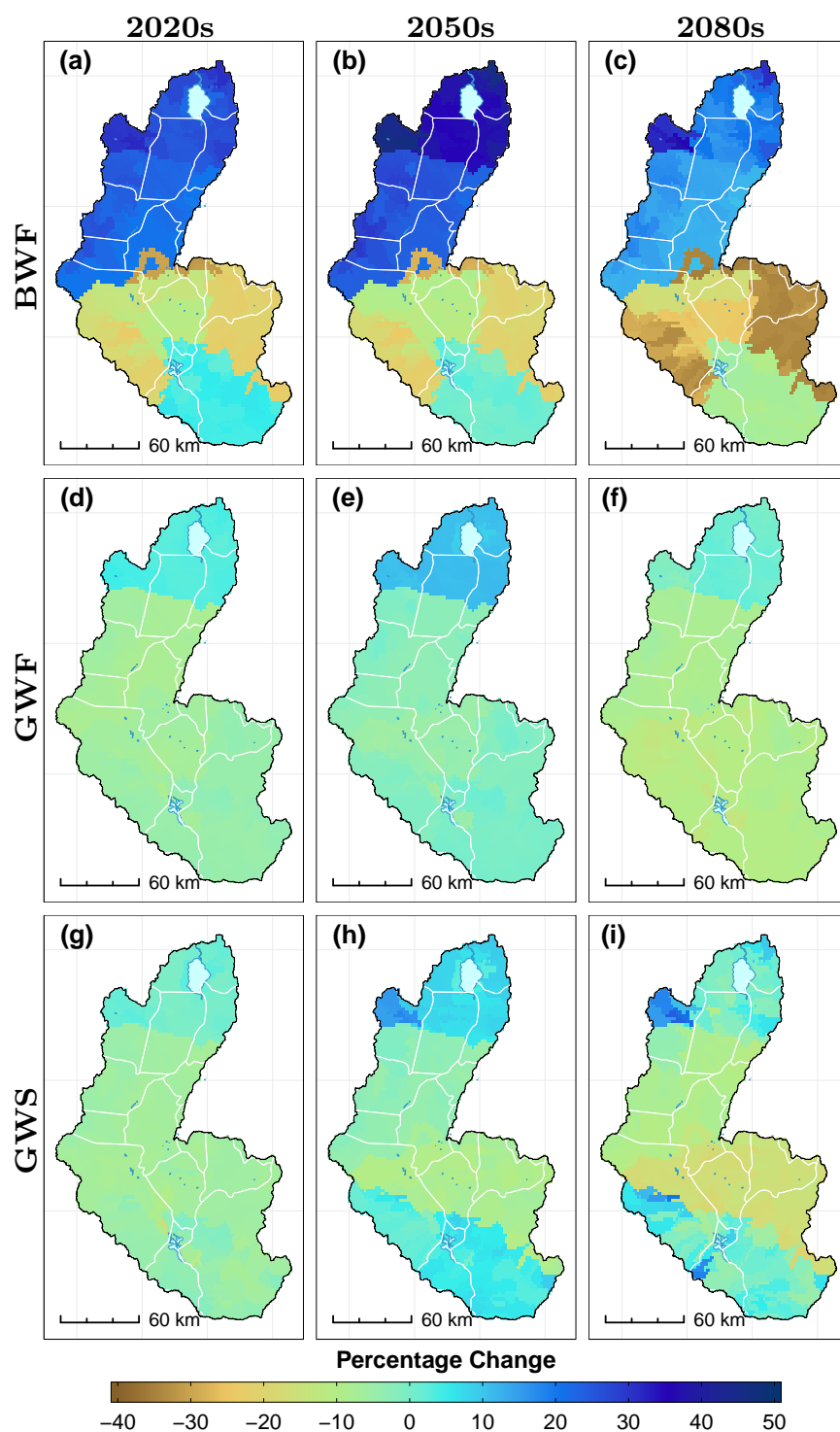




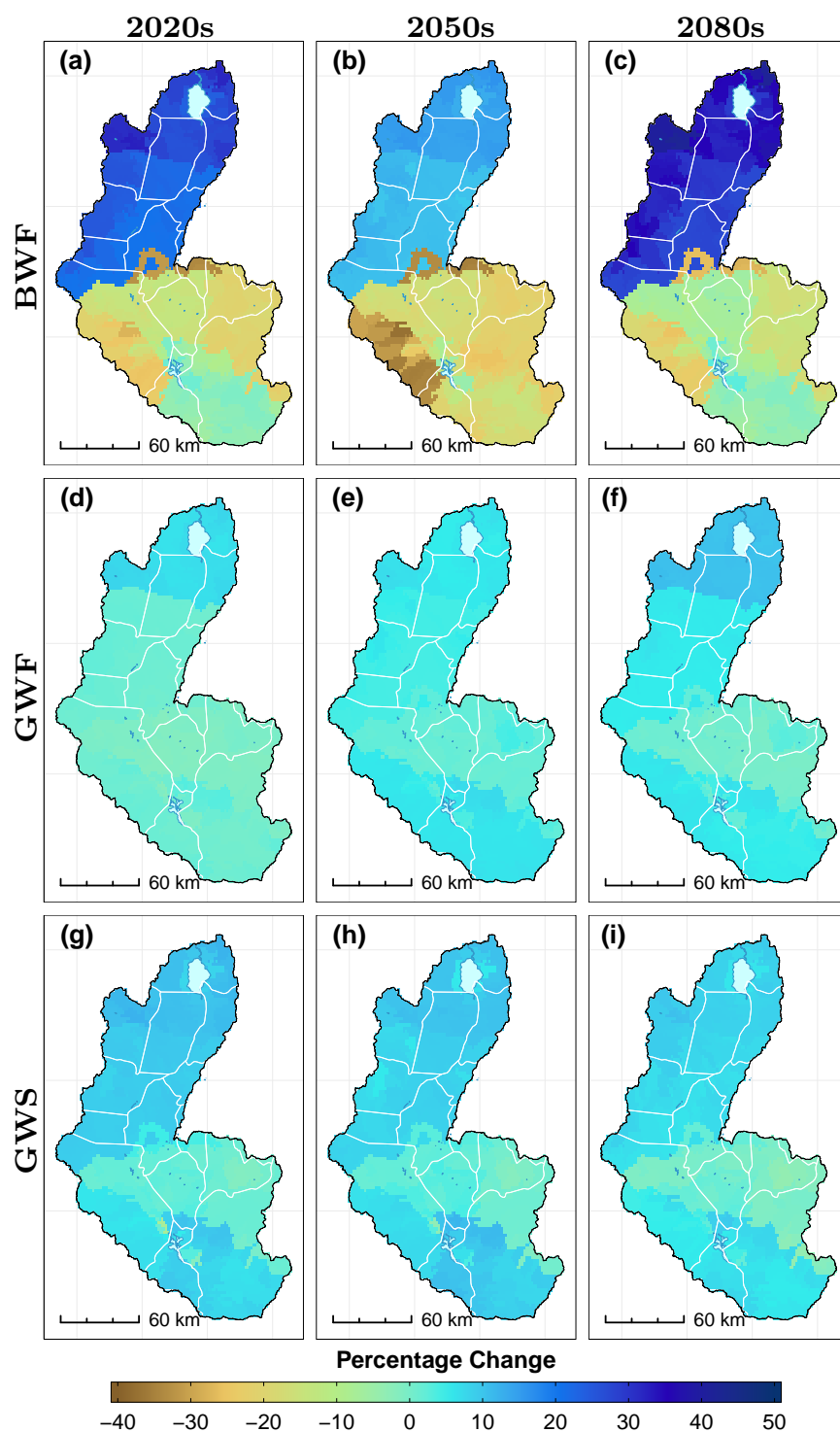
**Figure 5.40** BCC-CSM1-1-M RCP8.5 water balance components in the SRB for the future projected period. BW is blue water and GW is green water. Results are percentage differences from baseline period using the M95PPU



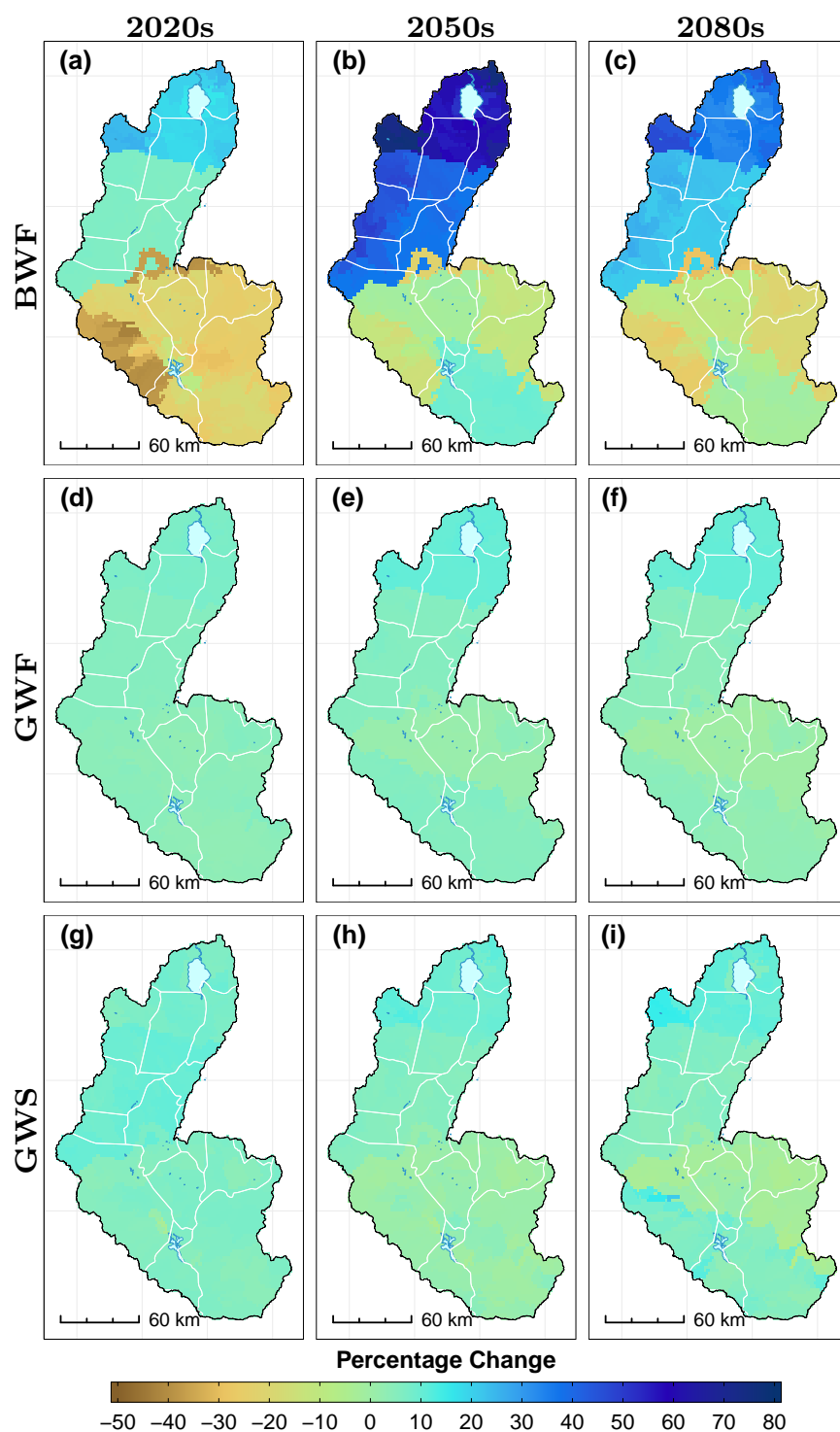
**Figure 5.41** CCSM4 RCP4.5 water balance components in the SRB for the future projected period. BW is blue water and GW is green water. Results are percentage differences from baseline period using the M95PPU



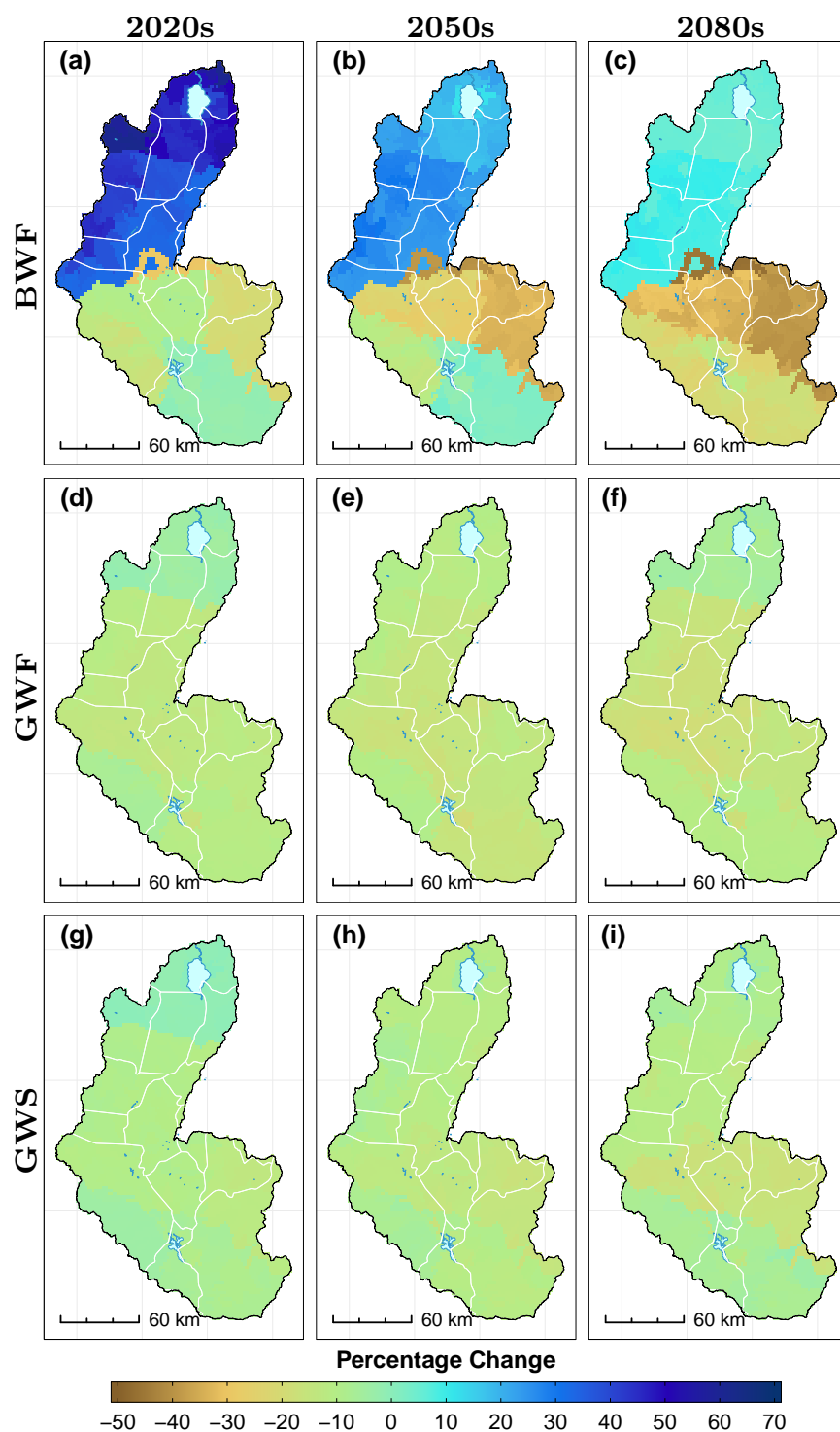
**Figure 5.42** CCSM4 RCP8.5 water balance components in the SRB for the future projected period. BW is blue water and GW is green water. Results are percentage differences from baseline period using the M95PPU



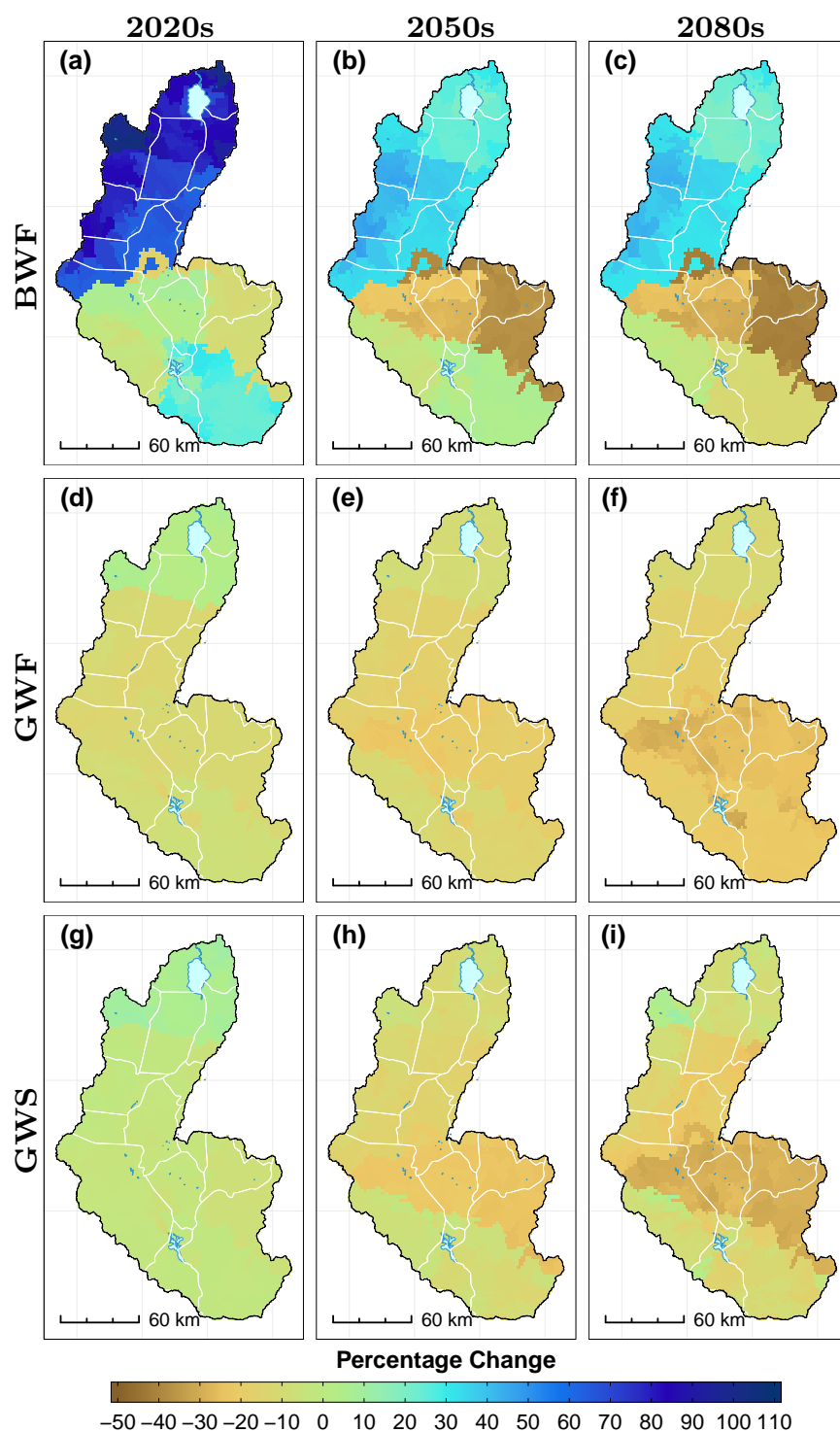
**Figure 5.43** CNRM-CM5 RCP4.5 water balance components in the SRB for the future projected period. BW is blue water and GW is green water. Results are percentage differences from baseline period using the M95PPU.



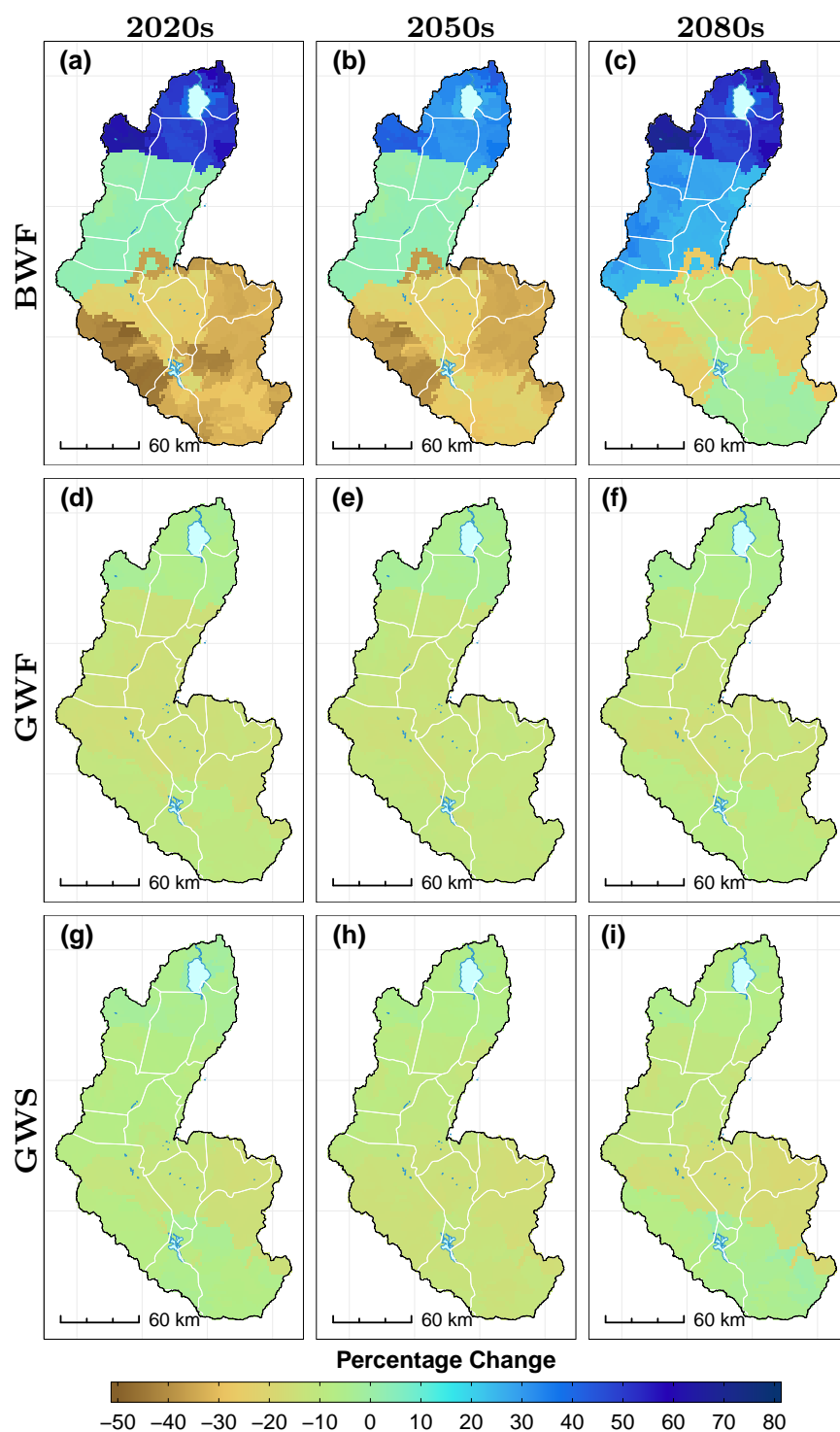
**Figure 5.44** CNRM-CM5 RCP8.5 water balance components in the SRB for the future projected period. BW is blue water and GW is green water. Results are percentage differences from baseline period using the M95PPU



**Figure 5.45** GFDL-ESM2G RCP4.5 water balance components in the SRB for the future projected period. BW is blue water and GW is green water. Results are percentage differences from baseline period using the M95PPU

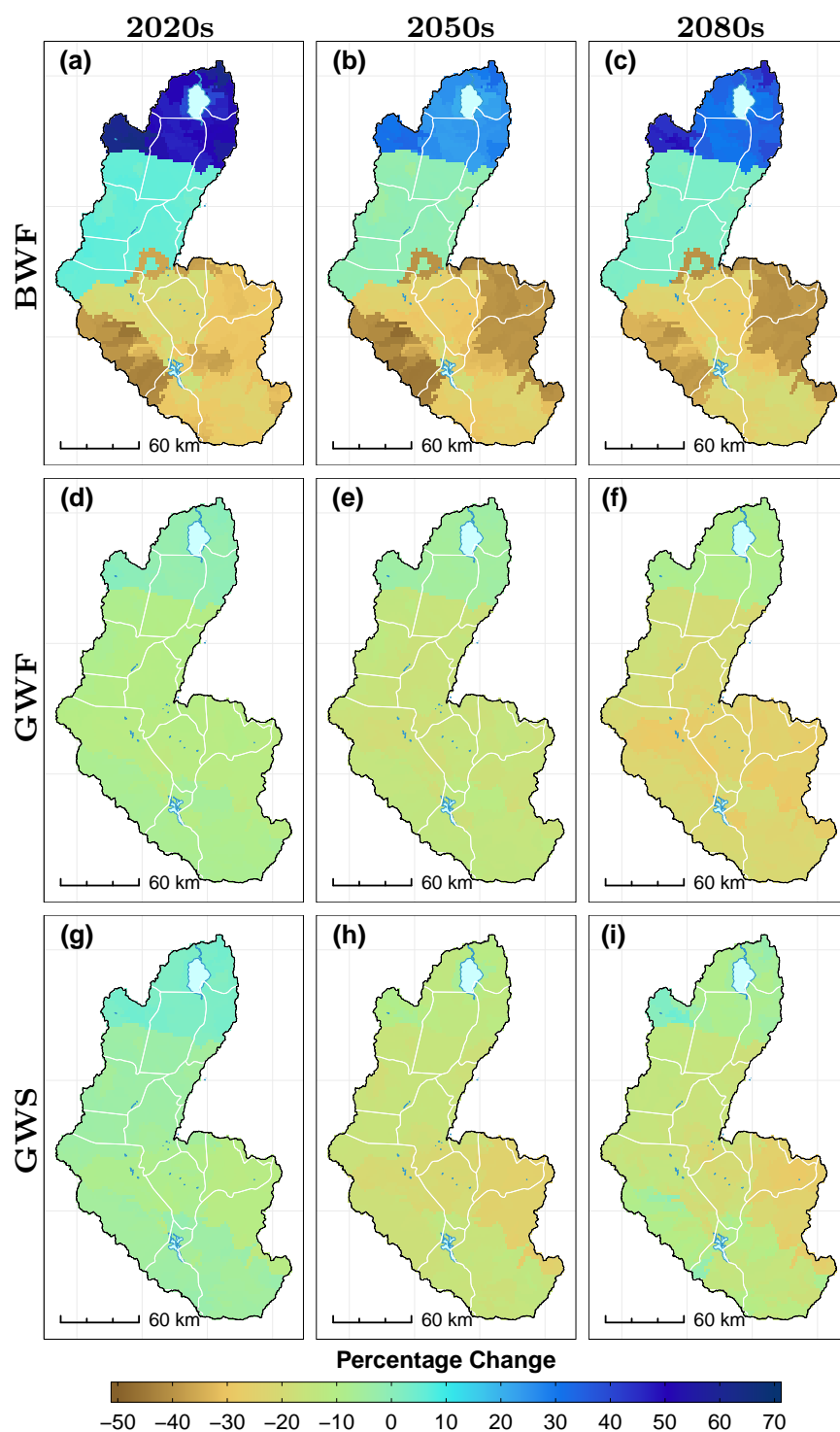


**Figure 5.46** GFDL-ESM2G RCP8.5 water balance components in the SRB for the future projected period. BW is blue water and GW is green water. Results are percentage differences from baseline period using the M95PPU

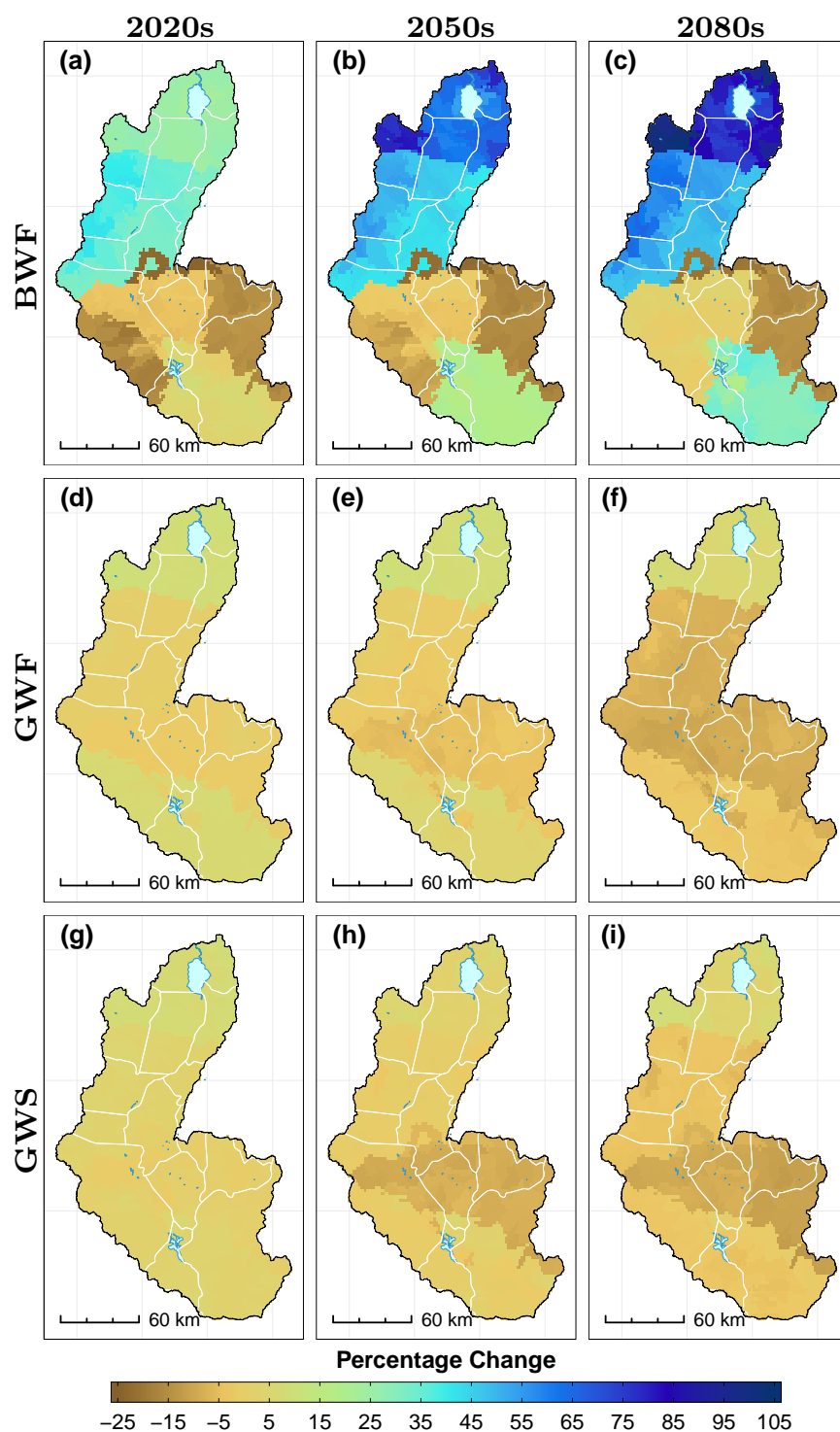


**Figure 5.47** HadGEM2-ES RCP4.5 water balance components in the SRB for the future projected period. BW is blue water and GW is green water. Results are percentage differences from baseline period using the M95PPU

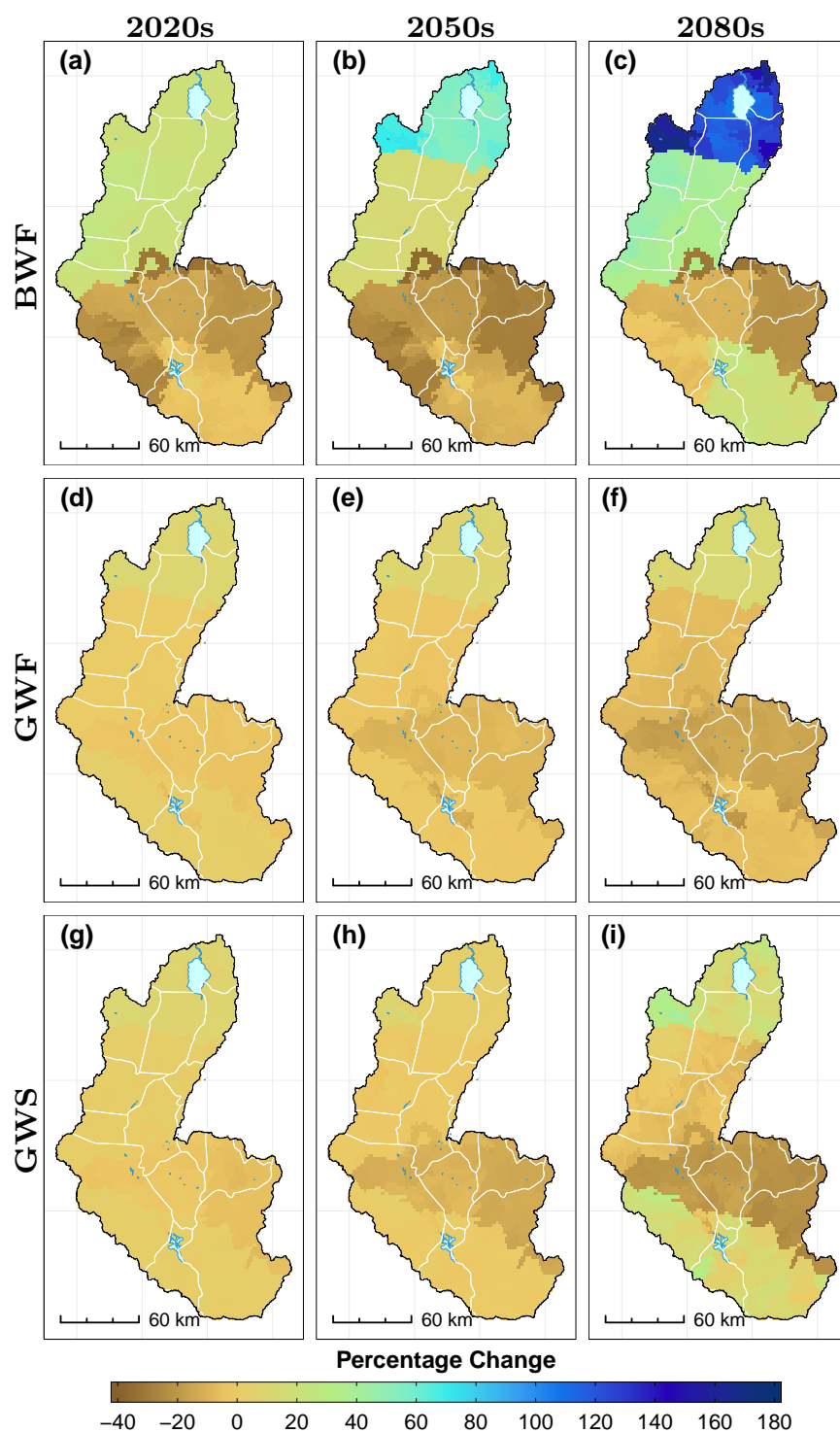




**Figure 5.48** HadGEM2-ES RCP8.5 water balance components in the SRB for the future projected period. BW is blue water and GW is green water. Results are percentage differences from baseline period using the M95PPU



**Figure 5.49** MPI-ESM-LR RCP4.5 water balance components in the SRB for the future projected period. BW is blue water and GW is green water. Results are percentage differences from baseline period using the M95PPU



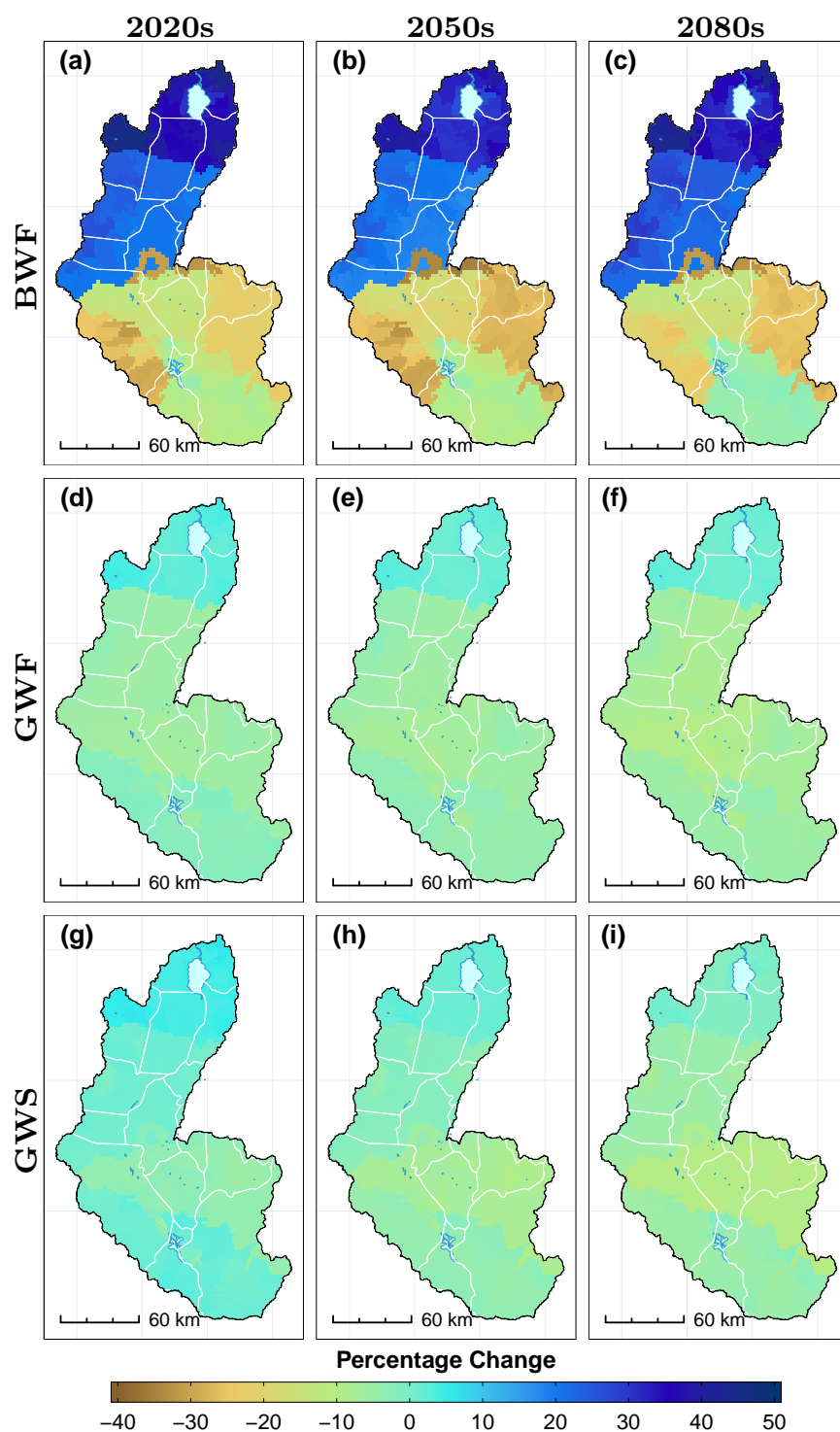
**Figure 5.50** MPI-ESM-LR RCP8.5 water balance components in the SRB for the future projected period. BW is blue water and GW is green water. Results are percentage differences from baseline period using the M95PPU

Figures 5.51 and 5.52 are averaged results of the six models presented earlier. In the case of the SRB as opposed to the RNC, BWF has been characterized by a lot of variability from one GCM to the next. Apart from the uncertainty emanating from the choice of GCM, inherent GCM variability and choice of downscaling method, it is surmised that the major source of uncertainty in BWF in the SRB is related to the model construction and parameterization. Firstly, the lack of high integrity climate data (in spite of the availability of gridded data sets such as those of the CFSR and CRU) in the region could be a potential source of error that could propagate through the climate downscaling process all the way to the hydrological assessments. As pointed out in Chapters 3 and 4, point meteorological station data performed better than CFSR and CRU in terms of reproducing uncalibrated streamflow hydrographs for selected gauging stations in the basin. However, these data had a lot of gaps which were eventually filled and augmented using the methods described in Section 3.6. The uncertainty introduced using this necessary process could easily propagate through to the hydrologic modelling and thus have an effect on the outcomes. Secondly, the region has sparse streamflow datasets that are also characterized by gaps and hence necessitating the need for infilling. Here too some uncertainty, perhaps even more insidious than the one introduced by climate processes, could have been introduced. This is in contrast to the results obtained for the RNC, where input data (climate and streamflow) are of high integrity.

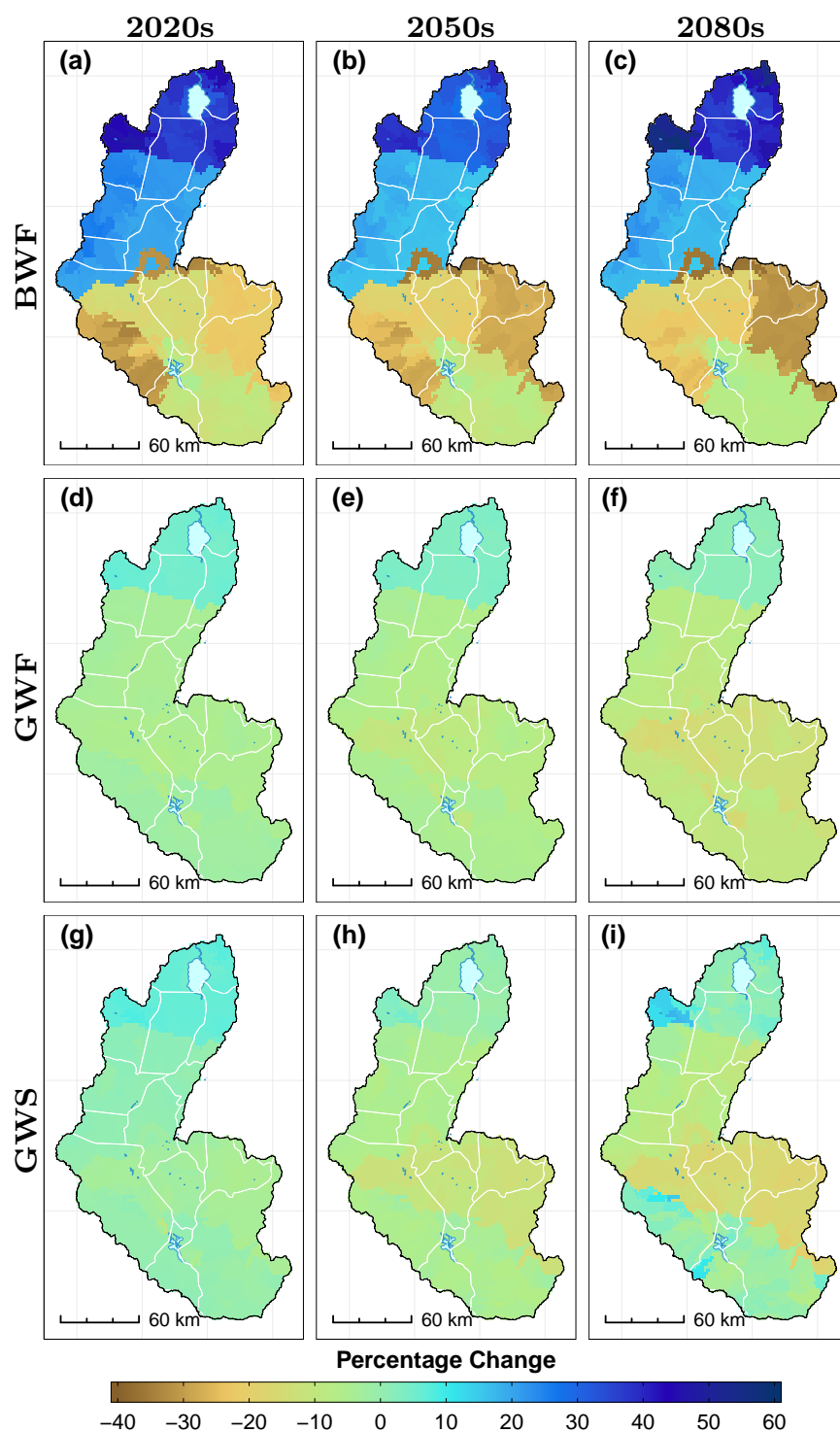
Generally under RCP4.5, BWF ranges between -36% and +45% throughout the century. In the 2050s, the deficit in the southern half of the basin is higher than the 2020s and late-century by at least 6 percentage points. On average, BWF increases by about 20% north of the basin and decreases by about 9% in

the southern portion. GWF ranges between -12% and +5% and slowly declines by at least 2 percentage points by the end of the century. Similarly, GWS ranges between -14% and +6% and slowly declines by 4 percentage points by the end of the century.

Under RCP8.5, BWF ranges between -38% and +58%. In the 2020s, BWF in the southern portion of the basin is about 16% lower than baseline values and about 23% higher in the north. A similar trend is seen in the 2050s, with the 2080s seeing BWF values increase in the south by at least 7 percentage points on average and about 10 percentage points in the north. GWF in the 2020s decreases by about 3% of baseline values for most parts of the basin except for some parts of Blantyre, Chiradzulu, Thyolo, Mulanje and Phalombe where the deficit could go up to -8%. Further north, GWF increases by up to 7%. In the 2050s, GWF values essentially remain the same as that of the 2020s while in the late-century, GWF decreases by up to -9% of baselines values for most of the basin except the northern parts of Chikwawa where the deficit goes up to -19%. GWS in the early- and mid-century ranges between -15% and +8% and essentially remains unchanged from baseline values except, again, some parts of Chikwawa, Blantyre, Chiradzulu, Thyolo, Mulanje and Phalombe where the deficit is on average about -12%. In the late-century, GWS remains unchanged from baseline values in Mangochi and Nsanje whereas in some parts of Chikwawa, Blantyre, Chiradzulu, Thyolo, Mulanje and Phalombe, GWS decreases by up to -20%.



**Figure 5.51** Ensemble mean (SRB-SWATEMM) RCP4.5 water balance components in the SRB for the future projected period. BW is blue water and GW is green water. Results are percentage differences from baseline period using the M95PPU



**Figure 5.52** Ensemble mean (SRB-SWATEMM) RCP8.5 water balance components in the SRB for the future projected period. BW is blue water and GW is green water. Results are percentage differences from baseline period using the M95PPU.

Results of BW/GW simulations using a SWAT model forced with the SRB-EGCMM are shown in Figures 5.53 and 5.54. The range in BWF values is similar to those of the multi-model means shown in Figures 5.51 and 5.52. The range in GWS and GWF is markedly wider than observed in other models.

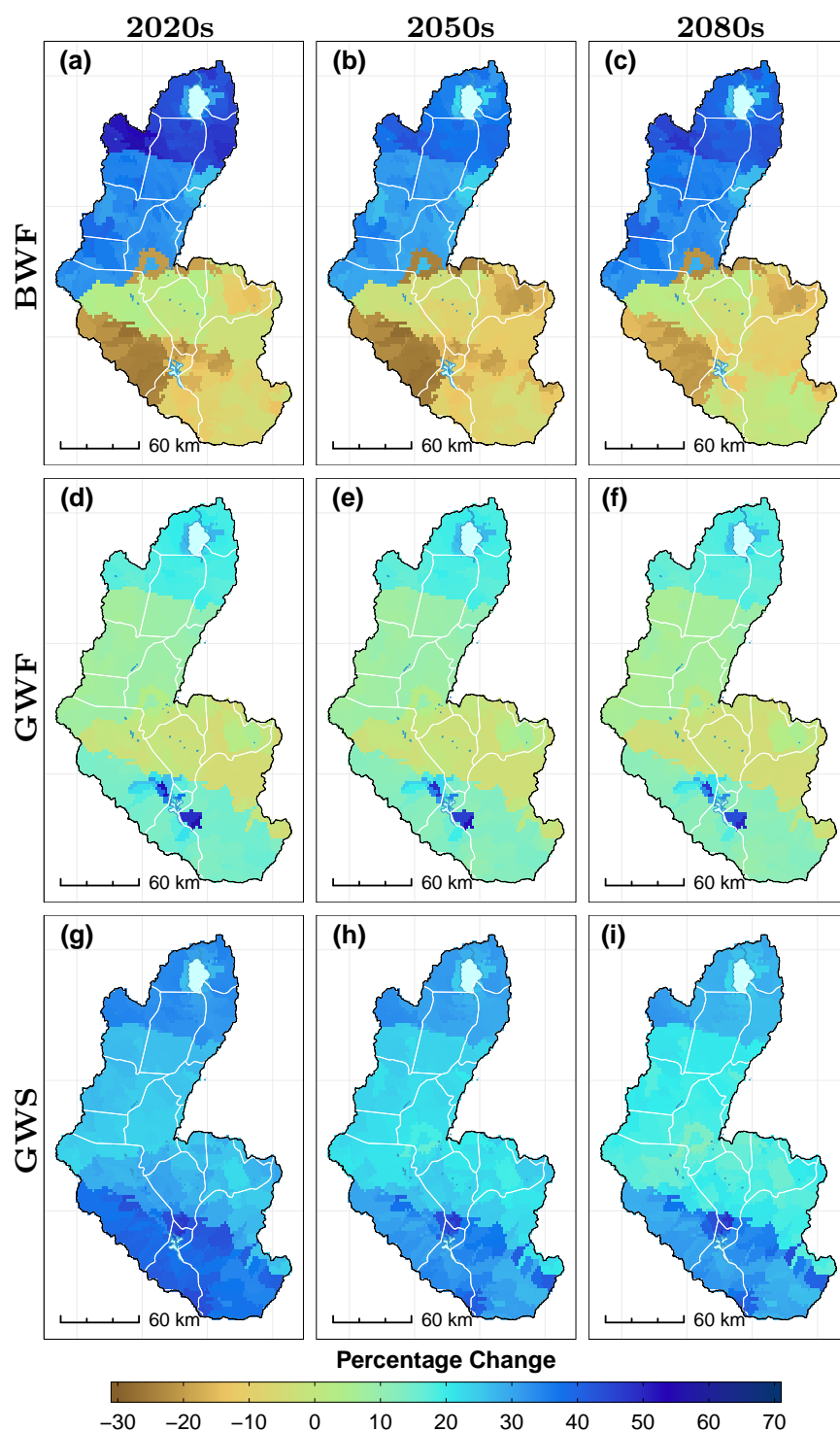
Under RCP4.5, the southern part of the basin experiences a slight decrease in BWF of about 3% from historical values except for the western part of Chikwawa where a deficit of up to -27% is expected. In this region, the values remain the same in the 2050s but the rest of the lower of the basin remains more or less the same as baseline values. The northern half of the basin is generally 25% higher than baseline values up to a maximum of 50% in the northern-most reaches of the basin by the late-century. GWF in the 2020s is generally the same as baseline values in parts of Chikwawa, Blantyre, Chiradzulu, Thyolo, Mulanje and Phalombe whereas the rest of the basin sees an increase in GWF by at least 18%. Notable exceptions are in isolated areas within the southern-most tip of Chikwawa where values are as high as +60%. These values remain, in general, the same in the mid-century with a marginal decrease towards the 2080s. GWS in the basin, with the exception of Nsanje, Mangochi and southern Chikwawa, is on average about 28% higher than baseline values and slowly decreases to about 24% by the late-century. GWS in southern Chikwawa and Nsanje is 40%, 35% and 32% higher than baseline values in the 2020s, 2050s and 2080s respectively.

BWF under RCP8.5 follows a similar trend as that of RCP4.5 but remains unchanged in the 2020s from baseline conditions for most parts in the southern half of the basin. Again, the extremes are in Chikwawa where deficits up to -31% are predicted. This trend is persistent throughout the 2050s. North of the basin, BWF availability is generally about 35% above baseline values in

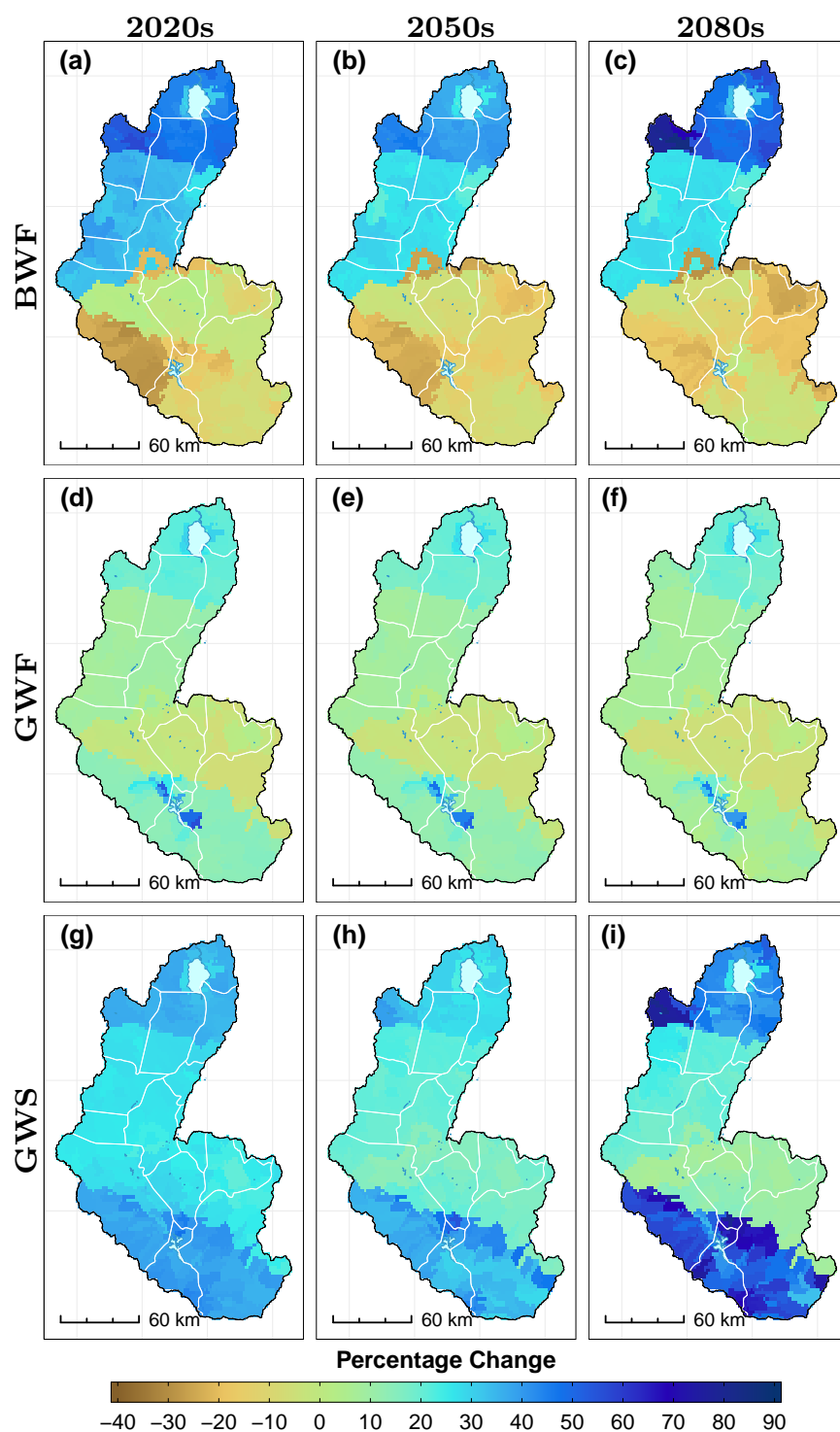


the 2020s and 2050s, eventually increasing up to 60% by the late-century in the northern-most reaches of the basin. BWF in the rest of the basin varies slightly (about +4 percentage points) from the 2050s scenario. Generally, BWF values under RCP8.5 do not change much from the RCP4.5 scenario according to this model. The same applies for GWF and GWS where the variation is within 2 percentage points, except in the late-century where GWS is expected to go as high as +80% for some parts in the north and south of the basin.

In the case of the SRB, the ensemble models are comparable with respect to BWF. As earlier stated, BWF determination is fraught with uncertainty in the SRB than in the RNC; thus, to obtain comparable figures between the two ensemble models speaks to the efficacy of averaging model results when multiple GCMs and scenarios are involved. Due to the wider ranges in GWF and GWS, values of which were in agreement in almost all the GCMs, it is surmised that the SRB-EGCMM forced model did not perform well for these variables, except for BWF which is in agreement with streamflow results from the same model. However, it is possible that this could be an artefact of the model conceptualization, calibration and other uncertainties highlighted earlier rather than an inadequacy of the methodology. Again, without considering this particular case in isolation, it is concluded that the most parsimonious ensemble method which produces results consistent with the historical period should be employed by the environmental modeller.



**Figure 5.53** Ensemble mean (SRB-EGCMM) RCP4.5 water balance components in the SRB for the future projected period. BW is blue water and GW is green water. Results are percentage differences from baseline period using the M95PPU



**Figure 5.54** Ensemble mean (SRB-EGCMM) RCP8.5 water balance components in the SRB for the future projected period. BW is blue water and GW is green water. Results are percentage differences from baseline period using the M95PPU

### 5.4.5 SRB Modelling Summary

Table 5.11 provides a summary of streamflow modelling in the SRB. Results from the modelling campaign at all stations except Rivirivi are mixed with some GCMs indicating significant increase or decrease in streamflow availability while others indicate no significant departure from baseline values.

At Rivirivi, all GCMs except SRB-EGCMM indicate significant increase in projected future streamflow. At Lichenya and Ruo, SRB-EGCMM and MPI-ESM-LR show significant departures from baseline values and sometimes from one time horizon to another. This could be attributed to the inability of the climate model (MPI-ESM-LR) to capture local climate dynamics in the region since the other GCMs do not exhibit this feature at all stations. On the other hand, going by the “one model one vote” approach, the results indicated by MPI-ESM-LR GCM could be a plausible future – further justifying the need for averaging the representations from different GCMs in an attempt to reduce the overall uncertainty. In the case of SRB-EGCMM, it is surmised that the RF algorithm could be responsible for the sharp departure from baseline values. The SRB-EGCMM tends to under-predict future streamflow availability at all stations and in almost all future time horizons. Conversely, the SWAT model ensemble (SRB-SWATEMM) reflects the mean change predicted by the six GCMs and is for the most part in contrast with results predicted by its counterpart ensemble model (SRB-EGCMM). According to SRB-SWATEMM, future streamflow availability at Lichenya and Ruo does not significantly depart from baseline values while at Rivirivi, streamflow is expected to significantly increase in the future.

**Table 5.11** Summary of SRB projected future streamflow changes with respect to the baseline period. Changes within  $\pm 10\%$  of baseline values are considered to be insignificant (green boxes) whereas changes above  $+10\%$  (red boxes) and below  $-10\%$  (blue boxes) are considered to be significant

GCM	Scenario					
	RCP4.5			RCP8.5		
	2020s	2050s	2080s	2020s	2050s	2080s
	<b>Lichenya</b>					
BCC-CSM1-1-M	5.5	-1.5	5.0	-0.6	1.5	1.2
CCSM4	7.4	6.4	2.7	12.8	14.9	6.9
CNRM-CM5	10.5	9.7	13.2	3.2	24.9	14.0
GFDL-ESM2G	14.7	-8.8	-7.7	30.1	-5.0	-4.3
HadGEM2-ES	-7.0	-8.5	11.1	-3.3	-8.6	-2.1
MPI-ESM-LR	21.3	27.8	30.3	16.2	12.0	34.7
Ensemble (SRB-EGCMM)	-6.8	-11.9	-7.7	-6.1	-10.6	-11.5
Ensemble (SRB-SWATEMM)	8.7	4.2	9.1	9.7	6.6	8.4
	<b>Rivirivi</b>					
BCC-CSM1-1-M	37.6	59.5	28.6	36.9	-3.7	27.3
CCSM4	49.3	35.4	38.3	38.0	50.2	51.8
CNRM-CM5	41.3	29.4	46.3	27.2	85.2	50.6
GFDL-ESM2G	56.6	15.7	15.2	93.3	37.3	45.2
HadGEM2-ES	51.8	39.9	58.2	53.0	47.5	66.0
MPI-ESM-LR	40.6	83.4	102.0	31.9	73.6	169.6
Ensemble (SRB-EGCMM)	-8.3	-11.2	-8.7	-7.5	-7.8	9.9
Ensemble (SRB-SWATEMM)	46.2	43.9	48.1	46.7	48.4	68.4
	<b>Ruo</b>					
BCC-CSM1-1-M	-0.4	-7.0	-0.6	-6.5	-3.7	-3.7
CCSM4	1.0	0.9	-3.0	6.2	9.0	1.3
CNRM-CM5	4.3	3.8	7.2	-3.0	18.6	8.3
GFDL-ESM2G	8.5	-13.8	-12.9	23.5	-10.0	-9.1
HadGEM2-ES	-12.6	-13.5	5.3	-9.0	-13.5	-7.2
MPI-ESM-LR	15.1	21.6	23.8	10.2	6.8	29.1
Ensemble (SRB-EGCMM)	-14.1	-18.5	-15.5	-13.6	-17.0	-18.6
Ensemble (SRB-SWATEMM)	2.6	-1.3	3.3	3.6	1.2	3.1

**Increase**

**Insignificant Change**

**Decrease**

Areal mean change in water balance components in the SRB are presented in Table 5.12. As expected, results from one GCM to another are not always in

agreement. While these results do not show the spatial-temporal changes (e.g. as presented in Figures 5.39 to 5.50) in the basin, they provide a summary picture of the realisations from each model and the variation thereof. The variability in the models are more visible for BWF than GWF and GWS since all three possible outcomes (denoted by the coloured cells in Table 5.12) are predicted.

In the case of SRB, the performance of the model forced with the SRB-EGCMM is not so different than the rest of the models. This is in contrast with the scenario observed in the RNC. However, the model tends to overestimate the availability of water balance components in the SRB when compared with the rest of the models. In the case of GWS for example, the results of SRB-EGCMM deviate significantly from the rest of the models. Thus, the results from this model should be interpreted with caution.


GFDL-ESM2G and HadGEM2-ES consistently project decreased future GWF and GWS availability in almost all time horizons. Not only are the two models in agreement with respect to the direction of change, they both predict similar magnitudes of change. This is in sharp contrast with the other models which indicate that there is minor change in GWF and GWS future availability when compared with baseline values. This highlights the importance of considering results from a committee of models as opposed to relying on a single GCM prediction.

Generally, water balance components in the SRB when investigated from a regional spatio-temporal perspective, indicate that there are regional variations in future BWF, GWF and GWS availability. The greatest variability is observed for BWF which is expected to increase in the north while the south is expected to be in deficit.


**Table 5.12** Summary areal mean change of projected future water balance components in the SRB with respect to the baseline period. Changes within  $\pm 10\%$  of baseline values are considered to be insignificant (green boxes) whereas changes above  $+10\%$  (red boxes) and below  $-10\%$  (blue boxes) are considered to be significant

GCM	Scenario					
	RCP4.5			RCP8.5		
	2020s	2050s	2080s	2020s	2050s	2080s
	<b>BWF</b>					
BCC-CSM1-1-M	-5.1	-6.1	-9.0	-14.3	-26.8	-14.9
CCSM4	5.1	-1.4	-4.5	4.5	7.3	-4.3
CNRM-CM5	3.0	-6.2	8.1	-8.6	20.1	5.7
GFDL-ESM2G	12.4	0.8	-12.5	37.1	6.1	1.5
HadGEM2-ES	-7.8	-9.6	9.4	-5.3	-13.8	-9.9
MPI-ESM-LR	10.3	23.7	32.2	1.1	3.0	31.9
Ensemble (SRB-EGCMM)	12.0	7.7	11.9	12.0	7.1	9.7
Ensemble (SRB-SWATEMM)	3.0	0.2	4.0	2.4	-0.7	1.7
	<b>GWF</b>					
BCC-CSM1-1-M	0.6	0.1	-1.6	1.4	-1.9	-1.4
CCSM4	-2.0	-4.7	-8.9	-4.2	0.2	-7.8
CNRM-CM5	1.8	4.4	5.0	5.0	5.4	4.0
GFDL-ESM2G	-10.4	-13.5	-13.0	-8.4	-15.5	-19.9
HadGEM2-ES	-11.7	-10.9	-10.5	-8.3	-13.7	-20.0
MPI-ESM-LR	3.1	1.0	-4.3	1.3	-2.3	-5.8
Ensemble (SRB-EGCMM)	9.6	9.1	7.8	9.9	8.9	6.4
Ensemble (SRB-SWATEMM)	-3.1	-3.9	-5.6	-2.2	-4.6	-8.5
	<b>GWS</b>					
BCC-CSM1-1-M	4.8	2.0	-1.3	3.7	-5.0	-3.1
CCSM4	2.9	-4.5	-13.1	-4.6	-0.8	-6.2
CNRM-CM5	6.8	6.6	5.0	7.3	3.7	4.6
GFDL-ESM2G	-7.5	-11.1	-10.9	-1.7	-14.5	-17.2
HadGEM2-ES	-8.4	-11.7	-10.3	-4.7	-17.2	-14.5
MPI-ESM-LR	3.2	-1.8	-3.7	1.7	-3.3	-0.9
Ensemble (SRB-EGCMM)	31.0	26.9	24.1	31.4	25.4	31.5
Ensemble (SRB-SWATEMM)	0.3	-3.4	-5.7	0.3	-6.2	-6.2


**Increase**



**Insignificant Change**



**Decrease**



The implication of these results, especially in the central and southern part of the SRB, is that firstly, there will be decreased availability of “liquid” or “blue” water availability for domestic and industrial usage. Since this type of water is abstracted from rivers, lakes and from groundwater aquifers, there is need for optimised use of these water resources amidst many competing needs. Secondly, decreased BWF and GWF (possibly due to increasing temperatures) availability in the central and southern portions of the basin indicate decreased capacity for irrigated and rainfed agriculture. This could threaten food security for thousands of people in rural Malawi who are dependent on these two traditional forms of crop production. Robust agricultural and water policies aimed at sustainable management and equitable distribution of limited water resources should be formulated and implemented by the GoM and other stakeholders. For example, irrigation methods that are inefficient and unsustainable could be replaced with efficient irrigation methods such as drip irrigation.

## 5.5 Chapter Summary

In this chapter, comprehensive hydrological analyses were carried out to determine the impacts of climate change on water resources in the RNC (data-rich region) and SRB (data-sparse region). The main objective of this chapter was to assess future availability of freshwater resources in the RNC and SRB using open-source software tools. Future projected streamflow and water balance components were simulated in both regions using a similar methodology. This was done so as to determine whether the methodology developed here is applicable globally i.e. first world regions with high integrity ground truth data vs developing regions with sparse or non-existent ground truth data. The results indicate that the



methodology developed here can be used in multi-regional studies effectively. Also, forcing discrete hydrological models with discrete GCMs and only averaging their results afterwards is a promising methodology albeit expensive. Most literature use an ensemble GCM mean to force hydrological models as recommended by the IPCC but the consequences of this approach on hydrological results and uncertainty has not been thoroughly investigated. Here, it is proposed that going by the ‘one vote per model’ approach, also advocated for by the IPCC, each GCM from a subset of GCMs selected for the particular region should be allowed to manifest itself singularly in the hydrological model before a committee of such models is averaged. In countries fraught with power shortages and lack of or limited access to computing infrastructure, this could be a challenge. Possible solutions to this dilemma are discussed in Chapter 7.

In general, there is little impact on future streamflow and water balance components in the RNC. The southern part of the RNC is expected to be in slight deficit with respect to BWF (approximately 7 to 9% lower than baseline values) in the short- to medium term (i.e. 2020s and 2050s). Similarly, future streamflow in the RNC varies by about  $\pm 9\%$  from baseline values indicating no significant change. These results indicate that the RNC, and in general temperate regions, are more robust to climate change and variability.

In the SRB, results indicate that some regions (especially northern portions of the SRB) will experience an increase in streamflow while others are expected to experience a decrease in streamflow. This trend is consistent with findings from Zuzani et al. (2019b) that show that historical streamflow records in the SRB exhibit both increasing and decreasing trends. Regions with increased streamflow will basically be more vulnerable to floods while regions with decreased streamflow

may experience challenges in the agricultural, energy and domestic water supply sectors. In the same vein, central and southern portions of the SRB are expected to receive reduced BWF or “liquid” water which can also affect agricultural, energy and water supply sectors. The need for robust climate change adaptation and preparedness plans in the SRB, especially in the rural setups where the most vulnerable groups are women and children, cannot be overemphasized. In terms of irrigated agriculture, commitment should be made to ensure that inefficient and unsustainable irrigation methods are replaced by more efficient systems such as *drip irrigation*.

Following streamflow and water balance simulation campaigns in the RNC and SRB, one thing is certain – effects of climate change are more severe in the SRB than the RNC. Regional impacts of climate change have been studied extensively and well documented in the literature. Unsurprisingly, these results are in agreement with previous studies that have asserted that climate change impacts are more severe in the tropics than in temperate regions. The most important outcome of the findings in this chapter, however, is to mobilise interest and effort in ensuring that adaptive capability in vulnerable regions such as the SRB is enhanced.

—We are at the very beginning of time for the human race. It is not unreasonable that we grapple with problems. But there are tens of thousands of years in the future. Our responsibility is to do what we can, learn what we can, improve the solutions, and pass them on.

Richard Feynman

# 6

## Integrated Hydrologic Modelling

*This chapter discusses the development and application of integrated hydrologic models in the RNC (particularly Dumfries Basin) and later in the SRB. SWAT models developed in the previous chapter were coupled with regional groundwater flow models developed with MODFLOW-NWT. The focus of the discussion is on the impacts of climate change on groundwater recharge in the early, mid- and late-century. A total of thirty-six scenarios were developed for the SRB using integrated hydrologic models while for the Dumfries Basin thirty scenarios were considered under RCP4.5 and RCP8.5.*

## 6.1 Purpose and Scope

As mentioned in the preamble to this chapter, the impact of climate change on groundwater processes, and in particular groundwater recharge, is assessed for the Dumfries and Shire Rivers Basins. The SRB groundwater model is a regional scale model and is thus intended to simulate basin-wide effects rather than localized effects while the Dumfries Basin is intended to simulate spatio-temporal processes at the aquifer scale. The groundwater flow models were specifically intended to simulate spatio-temporal patterns of groundwater recharge through the vadose zone to the aquifers. Again, the analyses begin with the Dumfries Basin, a region with relatively abundant ground truth data of high integrity, then on to the SRB where data is sparse and in some cases non-existent. Furthermore, the efficacy of ensemble models is investigated as has been pointed out in the previous chapters.

## 6.2 Data Requirements

Distributed recharge models require a lot of input data and tremendous effort by the modeller to prepare the data in a format acceptable by the model. In the case of SWAT-MODFLOW, data inputs used to construct the separate SWAT and MODFLOW models are shared between the two linked models in the recharge calculation process (described in Section 6.3.4). Climate data for each day is required to run the model on a daily basis. For the SRB, station meteorological data obtained from the MMS was used in the construction of the SWAT model and downscaled future climate projections, described in Chapter 4, were used to simulate future hydrological trends in the basin. For the RNC, Dumfries station data augmented with CRU climate data was used in the baseline SWAT

model construction while projected future climate was used for future hydrological analyses. 90m horizontal resolution SRTM DEMs were used to construct the SWAT and MODFLOW models for both the SRB and RNC as discussed in Chapter 5.

## **6.3 Dumfries Basin Groundwater Modelling**

### **6.3.1 Dumfries Basin Conceptual Model**

#### **6.3.1.1 Aquifer definition**

The Dumfries aquifer is a 25 km long and 10 km wide semi-elliptical basin containing the Quaternary sediments of the River Nith and Lochar Water including their tributaries. It is divided into two layers consisting of the upper Quaternary deposits and the underlying Permian sediments which are in hydraulic contact. Groundwater is inferred to flow from the north to the south-east in the northern part of the basin while in the central portion of the basin, groundwater flow is towards the rivers.

#### **6.3.1.2 Bedrock Geology**

The DB is characterized by two types of sediments from distinct geological periods (i.e. Quaternary and Permian periods) infilled to depths greater than 1000m (MacDonald et al., 2000). The Permian sediments of the Dumfries basin, as can be seen from Figure 6.1, is divided into two formations: the Locharbriggs Sandstone formation in the east and the Doweel Breccia Formation in the west (Brookfield, 1978; MacDonald et al., 2000).

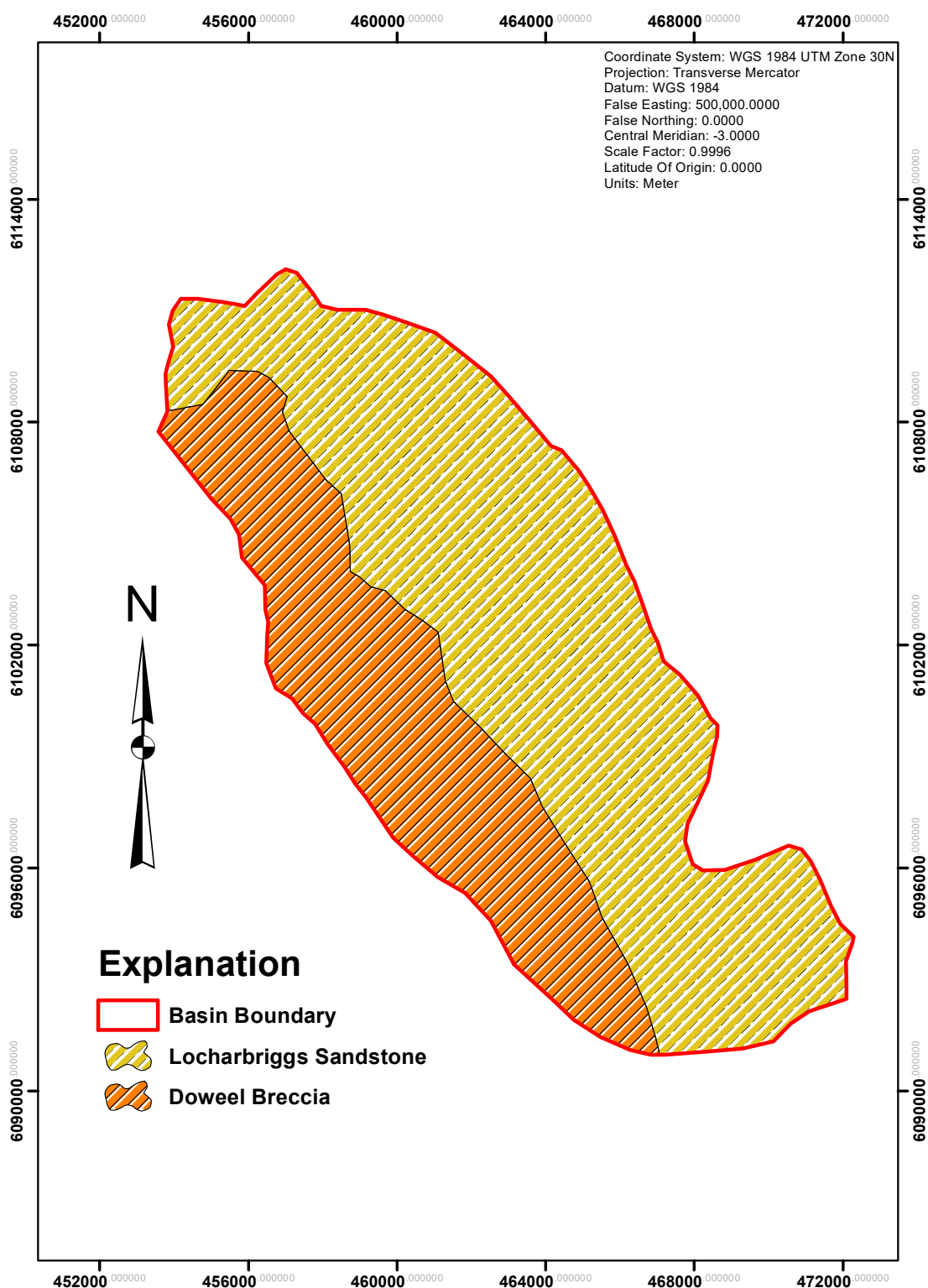
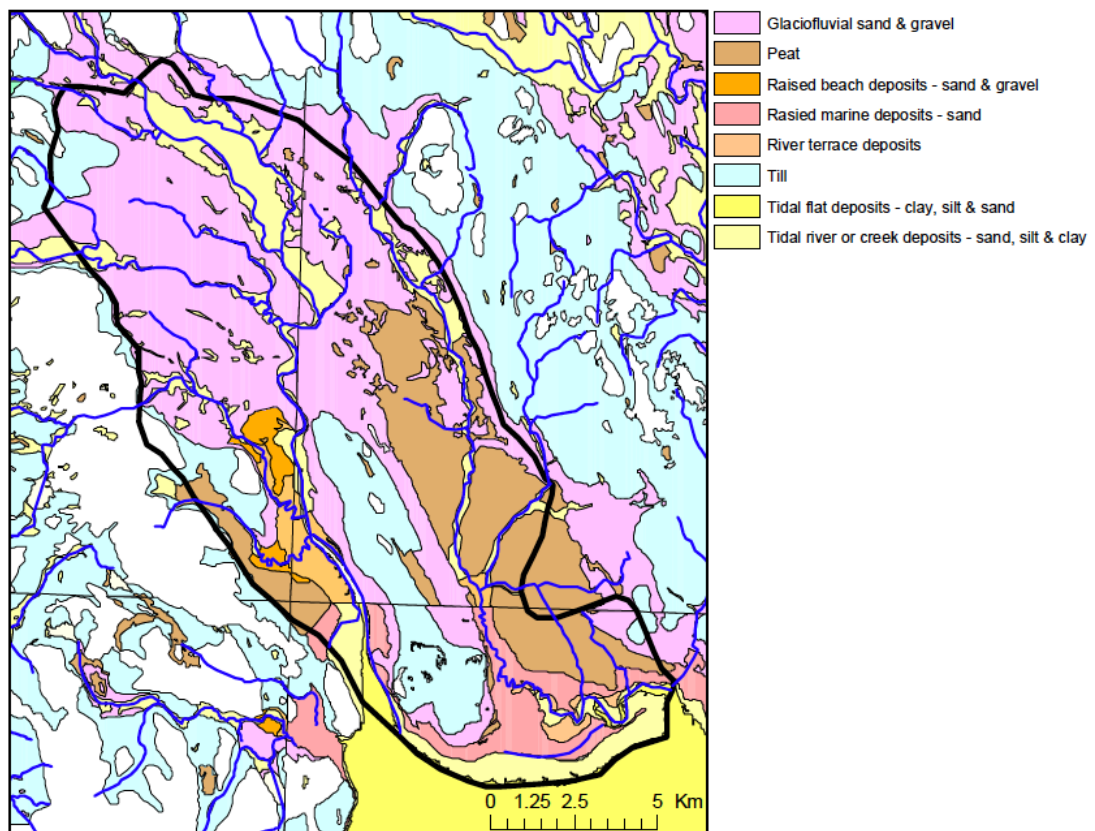


Figure 6.1 Permian geology of the Dumfries Basin (after Jackson et al., 2004)

The Doweel Breccia is predominantly composed of sedimentary breccia interbedded with sandstone, extending eastward toward the centre of the basin where it interfingers with the Locharbriggs Sandstone (Jackson et al., 2004). The Locharbriggs Formation is a conglomerate of medium to fine-grained aeolian sandstone with large scale cross bedding. The sandstone is predominantly constituted of sub rounded to very well rounded quartz with less than five percent basalt and feldspar, weakly cemented by silica (MacDonald et al., 2000). A steeply dipping succession of grey, fine-grained, wacke sandstone and mudstone of Silurian age that is intruded by the Criffel-Dalbeattie granodiorite to the south-west of the basin is overlain by unconformably by the Permian basin-fill sequence (Jackson et al., 2004). The Permian basin-fill sequence is estimated to be between 1.1 and 1.4 km thick by air-born gravity modelling data. Bouger gravity anomaly data suggests the basin to be fault-bounded by a series of en echelon faults along its western margin and fault bounded also to the north-east (Jackson et al., 2004; Robins and Ball, 2006).

#### **6.3.1.3 Quaternary Geology**

The superficial deposits of the Dumfries Basin consist mostly of glacial deposits formed during the main late Devensian (MLD) glaciation (Jackson et al., 2004; McMillan et al., 2011). Figures 6.2 and 6.3 show a summary of the depositional units or Quaternary domains in the basin. To the north-west of Dumfries, an overconsolidated sandy diamicton with wacke and sandstone clasts deposit sits atop the Permian deposits. It is considered to be the lodgement till of the Dimlington Stadial ice sheet (Robins and Ball, 2006). Ice, originating in the Southern Uplands, formed a streamlined topography of rock ridges aligned towards the south-east



**Figure 6.2** Quaternary geology of the Dumfries Basin (Jackson et al., 2004)

of the basin. Active retreat of the Nith glacier during deglaciation took place in a north-westerly direction to pinning points (bedrock highs) at Cargenbridge, Maxwelltown and Locharbriggs (Jackson et al., 2004).

To the south-east of Locharbriggs, deposits of fine sand, silt and clay, with dropstones, ended up in ephemeral glacial lakes. Tabular spreads of cross-bedded sand and pebbly gravel overlay these glaciolacustrine deposits (Robins and Ball, 2006). Further deglaciation advanced the Nith glacier resulting in the formation of a moraine, characterised by moundy topography that extends in an arc between Locharbriggs and Cargenbridge (Jackson et al., 2004). The gravel and till deposits of the moraine, which are estimated at over 30m in thickness, comprise most



of the moraine but beds of sheared glaciolacustrine sand and silt can also be found (Robins and Ball, 2006). Post-deglaciation relative sea level rise resulted in the deposition of extensive deposits of bedded sand, clay and silt to the south of Dumfries.

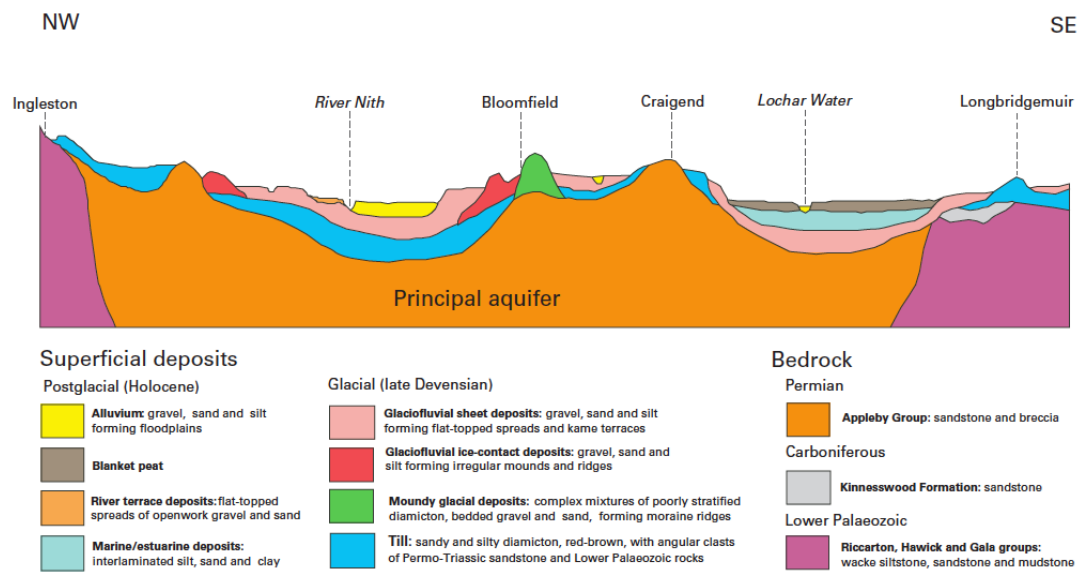
These deposits now form dissected terraces which generally lie at an elevation of 10 to 15m *aOD* as a result of isostatic rebound (Jackson et al., 2004).

#### 6.3.1.4 Surface Water

The DB is drained mainly by the River Nith which flows onto the basin from its northern edge and discharges south into the Solway Firth. The Nith has many tributaries but from the DB perspective, Cluden Water is its major tributary. The second catchment in the Dumfries Basin is that of the Lochar Water which is a smaller river that runs approximately parallel to the Nith from north to south along the eastern edge of the aquifer (Jackson et al., 2004). Flows in these rivers are measured using permanent gauging stations, each located on one of the three major rivers in the basin as discussed in Chapter 4. Using a combination of results from the three permanent and temporary spot gauging stations, Jackson et al. (2004) made the following observations;

1. River Nith, Cluden Water and Cargen Water are responsible for most of the water flowing onto the basin during the summer period
2. There is increased flow in the southern portion of the Lochar Water that is suspected to be a combination of water yield from the peat deposits, drainage and spring flow from the high ground to the west and from the Wath Burn.

Robins and Ball (2006) alludes to the fact that lack of comprehensive surface



**Figure 6.3** Cross-section north-west to south-east showing the superficial deposits in the Dumfries Basin (Robins and Ball, 2006)

water flow data can cause uncertainties in the conceptual and groundwater modelling processes, citing in particular the lack of flow records as close as possible to the tidal limit of the River Nith. This is crucial for an accurate assessment of the water balance in the Nith catchment.

### 6.3.1.5 Groundwater

Generalisations have been made about groundwater flow in the DB as groundwater monitoring points are mostly located in the central part of the basin. Generally, groundwater flow direction in the northern part of the basin is towards the south-east while flow in the central part of the basin is predominantly towards the rivers; finally, in the southern part of the basin, flow is inferred to be occurring away from the Larchfield-Caerlaverock Ridge (Jackson et al., 2004).

### 6.3.1.6 Summary of Conceptual Model

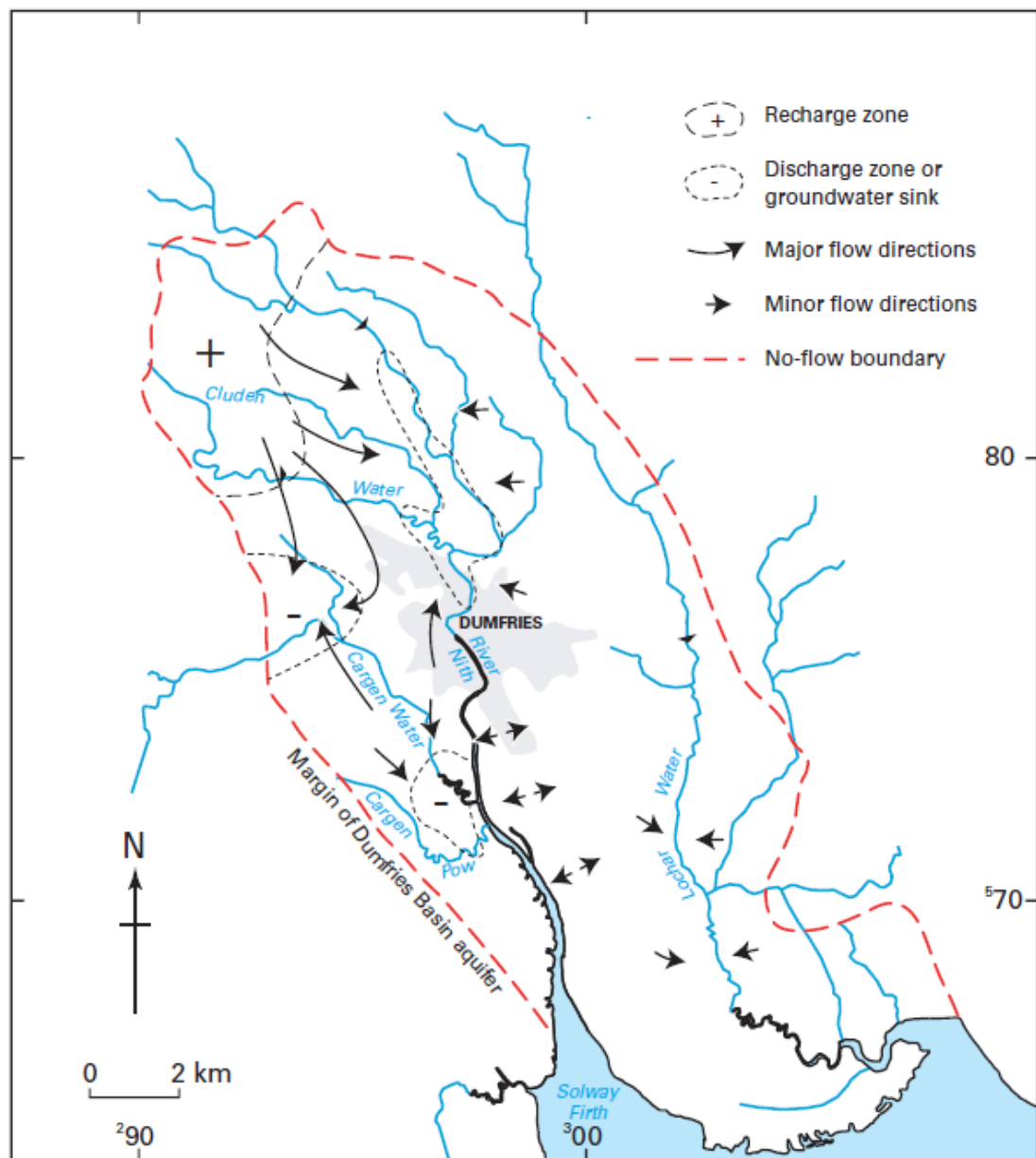
A schematic summary of the DB conceptual model after Robins and Ball (2006) is presented in Figure 6.4. Generally, the conceptual model can be summarized as follows (Robins and Ball, 2006);

- The basin boundary is constrained as a no-flow boundary owing to the presence of low hydraulic conductivity Palaeozoic rocks surrounding the basin.
- Most of the recharge to the bedrock aquifer is believed to occur in the north-western and central part of the basin via the superficial deposits. In areas of the basin underlain by clay or silt grade deposits, direct rainfall recharge may be significantly inhibited. Furthermore, some indirect recharge to the aquifer is expected in the northernmost part of the basin.
- Groundwater lateral flow is indicated to be towards the River Nith and also towards the western-central part of the basin where a heavily pumped groundwater sink is located.
- Hydraulic contact between the superficial deposits and the bedrock aquifer does not occur throughout the basin.
- Discharge from the basin directly to the sea is inhibited by marine and alluvial silts.

## 6.3.2 Model Development

### 6.3.2.1 Spatial Discretization

The DB model domain has an areal extent of about 187 km<sup>2</sup> with a grid coverage comprising a total of 93 columns and 106 rows, each at a 200 m horizontal



**Figure 6.4** Schematic conceptual flow model of the Dumfries Basin aquifer (Fig. 5.5, Robins and Ball, 2006)

resolution. The model is vertically discretized into 2 layers namely, superficial deposits (~ 20m thickness) and a lower layer representing the bedrock aquifers (~ 200m thickness). The lower layer was divided into two zones representing the Doweel Breccia and Locharbriggs Sandstone formations (see Figure 6.1). The

superficial deposits vary in depth across the basin but for purposes of numerical representation, the upper layer was set to 20m depth but can be as thin as 10m in some sections (Jackson et al., 2004).

### 6.3.2.2 Temporal Discretization

Groundwater flow for the DB was simulated from January 1981 to December 2005 (same time discretization as the RNC SWAT model). Initially, because this model was intended to be subsequently coupled with the corresponding SWAT model, the model was run in ‘steady-state’ mode for a period of two years (i.e. 1981 and 1982) after which transient flow was simulated from 2007 to 2005. The steady-state simulation was used to generate starting heads which were subsequently used in solving the groundwater flow equation at the beginning of the transient simulation. The transient period was discretized into monthly time-steps initially for calibration purposes but when coupled with the SWAT model, the model was forced to run on daily time-steps.

### 6.3.2.3 Hydrologic Boundaries

The DB is surrounded by low hydraulic conductivity Palaeozoic rocks hence the active area of the DB groundwater flow model is characterized as a ‘no flow’ (i.e., specified flow or Neumann conditions) boundary, except for a small portion towards the south-east of the basin where the prevalence of Carboniferous limestones and calcareous sandstones allow for some leakage across the boundary (Akhurst et al., 2006; Jackson et al., 2004). Here the model is specified as a specified head (i.e., Dirichlet conditions). Internal boundaries specified as *sources* and *sinks* include rivers, recharge zones (calculated using SWAT and passed to MODFLOW cells)

and pumping wells defined using MODFLOW packages RIV, RCH and MNW2 respectively.

#### 6.3.2.4 Hydraulic Properties

The horizontal hydraulic conductivities (HK) of the Superficial and Quaternary deposits were calculated via a ‘pilot-point’ method using geostatistical methods implemented in PEST. This is an automated parameterization method where hydraulic conductivity values of model cells are assigned by interpolation based on pilot points. The advantage of using PEST for this exercise versus other methods where geostatistical algorithms such as *inverse-distance weighting* or *kriging* are applied to assign HK cell values via interpolation, lies in the unique feature of PEST referred to as *regularization*. This feature ensures that the inversion process is stable by minimizing an objective function subject to constraints provided by the user (i.e. *prior information*) that define the expected ranges of the values. This is a slight departure from the zonation method employed by Jackson et al. (2004) to define the hydraulic conductivity zones used for their DB groundwater flow model. The vertical hydraulic conductivities (VK) for layers 1 and 2 were initially set at values of 10 and 20 respectively. Thereafter, PEST determined the values to be 6 and 27 for layers 1 and 2 respectively.

#### 6.3.2.5 Calibration

Calibration of the groundwater model was done separately using the automated parameter estimation tool PEST. As mentioned in Section 6.3.2.4, PEST calibration was run with the assistance of regularization. We used field measurement data (groundwater wells) collected by Jackson et al. (2004) to calibrate the groundwater

flow model. Although the groundwater levels were recorded on different dates with possible interference from pumping in others, the collated data represents the most complete collection of groundwater heads in the DB (Jackson et al., 2004). For the transient period, one borehole with a long record of groundwater levels was used to calibrate the model. Despite the UK being a data-rich region when compared to other developing regions such as Malawi, the Dumfries Aquifer is considered to be among data-scarce aquifers in Scotland (Gaus and Dochartaigh, 2000), despite being studied for over 30 years (MacDonald et al., 2000). Thus, little groundwater data was available for a more comprehensive calibration campaign. Where data is available, there is limited access to the data which is held by institutions such as SEPA and the BGS. Notwithstanding this limitation, access to a long record of groundwater level observations coupled with variable recharge values from the SWAT model (which benefited from the rich and freely available hydrological data), the transient model was considered to be adequately calibrated for this thesis' objectives. The accuracy of the calibration was checked by comparing the observed and simulated heads.

Calibration of the SWAT model is detailed in Section 5.4.2. The SWAT parameters that produced the best simulation for the baseline period calibration were used to set-up the initial baseline coupled model. The coupled SWAT-MODFLOW model was calibrated using the classical trial-and-error method and then optimised using PEST. In order to check the effectiveness of the coupled model in simulating hydrologic processes within the basin and watershed, a comparison was made between observed streamflow hydrographs and those obtained using SWAT and SWAT-MODFLOW respectively. Goodness-of-fit statistics are presented in Table 6.1.

**Table 6.1** Goodness-of-fit statistics used to compare the performance of SWAT and SWAT-MODFLOW (SWAT-MF) in simulating monthly streamflow in the RNC

Metric	Station							
	Scar Water at Capenoch		Cluden Water at Fiddlers Ford		Nith at Friars Carse		Lochar Water at Kirkblain Bridge	
	SWAT	SWAT-MF	SWAT	SWAT-MF	SWAT	SWAT-MF	SWAT	SWAT-MF
ME	0.53	0.37	0.85	0.60	7.00	5.00	-0.19	-0.13
MAE	1.81	1.52	2.58	2.25	10.10	8.33	0.44	0.37
MSE	5.53	3.54	12.11	7.70	159.58	96.49	0.34	0.25
RMSE	2.35	1.88	3.48	2.77	12.63	9.82	0.58	0.50
NRMSE %	55.10	44.00	55.40	44.20	60.20	46.80	35.30	30.50
PBIAS %	8.90	6.30	10.00	7.10	23.80	17.00	-8.60	-6.00
RSR	0.55	0.44	0.55	0.44	0.60	0.47	0.35	0.30
rSD	0.79	0.72	0.85	0.73	0.83	0.72	0.93	0.79
NSE	0.70	0.81	0.69	0.80	0.64	0.78	0.87	0.91
mNSE	0.49	0.57	0.51	0.57	0.42	0.52	0.68	0.73
rNSE	-3.13	-2.59	-2.48	-2.24	-2.59	-1.76	0.69	0.72
d	0.90	0.93	0.90	0.93	0.89	0.93	0.97	0.97
md	0.70	0.74	0.72	0.74	0.68	0.72	0.84	0.85
rd	-0.36	-0.26	-0.08	-0.11	-0.07	0.07	0.91	0.91
cp	0.73	0.83	0.72	0.82	0.65	0.79	0.87	0.90
r	0.84	0.93	0.84	0.92	0.87	0.94	0.94	0.97
R <sup>2</sup>	0.71	0.86	0.71	0.85	0.75	0.89	0.89	0.94
bR <sup>2</sup>	0.67	0.79	0.68	0.79	0.71	0.88	0.80	0.83
KGE	0.73	0.70	0.76	0.71	0.68	0.67	0.87	0.78
VE	0.69	0.74	0.70	0.73	0.66	0.72	0.80	0.83



SWAT-MODFLOW improved the simulation of monthly streamflow at all the stations. It should be noted here that the statistics for the SWAT model presented in Table 6.1 are a composite of the calibrated and validation periods for a fair comparison with SWAT-MODFLOW since groundwater model calibration in modern times omits the validation process. Thus, goodness-of-fit statistics provided as insets in Figure 5.4 may slightly differ from those presented here.

#### **6.3.2.6 Sensitivity Analysis**

Sensitivity analysis of the groundwater model was also done using PEST. Unlike SWAT-CUP, sensitivity values are calculated during the last iteration of the optimization campaign (Fisher et al., 2016). As expected, the parameter that was found to be most sensitive to input parameters is hydraulic conductivity.

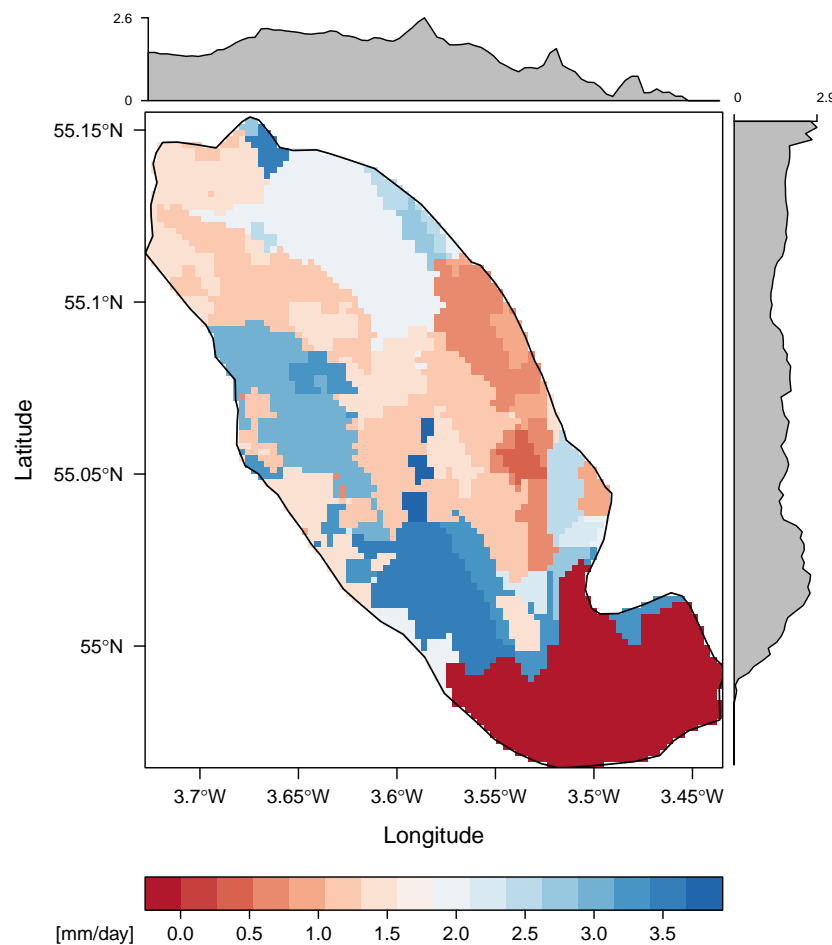
### **6.3.3 Description of the Coupling Process**

At the core of the SWAT-MODFLOW coupling process is the concept of hydrologic response units (HRUs) and disaggregated HRUs (DHRUs). DHRUs divide each original HRU into contiguous areas within a sub-basin in order to allow HRU calculations to be geo-located (Bailey et al., 2016). “Mapping” subroutines are used within SWAT-MODFLOW to relate HRUs to MODFLOW grid cells and MODFLOW river cells to SWAT stream channels. SWAT calculates daily deep percolation or recharge for each HRU. The HRUs are subsequently mapped to each individual DHRU and then mapped to each MODFLOW grid cell in accordance to the percent area of the DHRU contained in the respective grid cell for use by the Recharge package. Groundwater hydraulic heads and groundwater-surface water interactions are thereafter calculated by MODFLOW. To accurately simulate

groundwater-surface water interactions, MODFLOW computes groundwater discharge volumes computed on a cell-by-cell basis, sums and adds them to in-stream flow for each SWAT sub-basin. Finally, SWAT completes the stream routing calculations for the day on a continuous loop to the end of the simulation (Bailey et al., 2016).

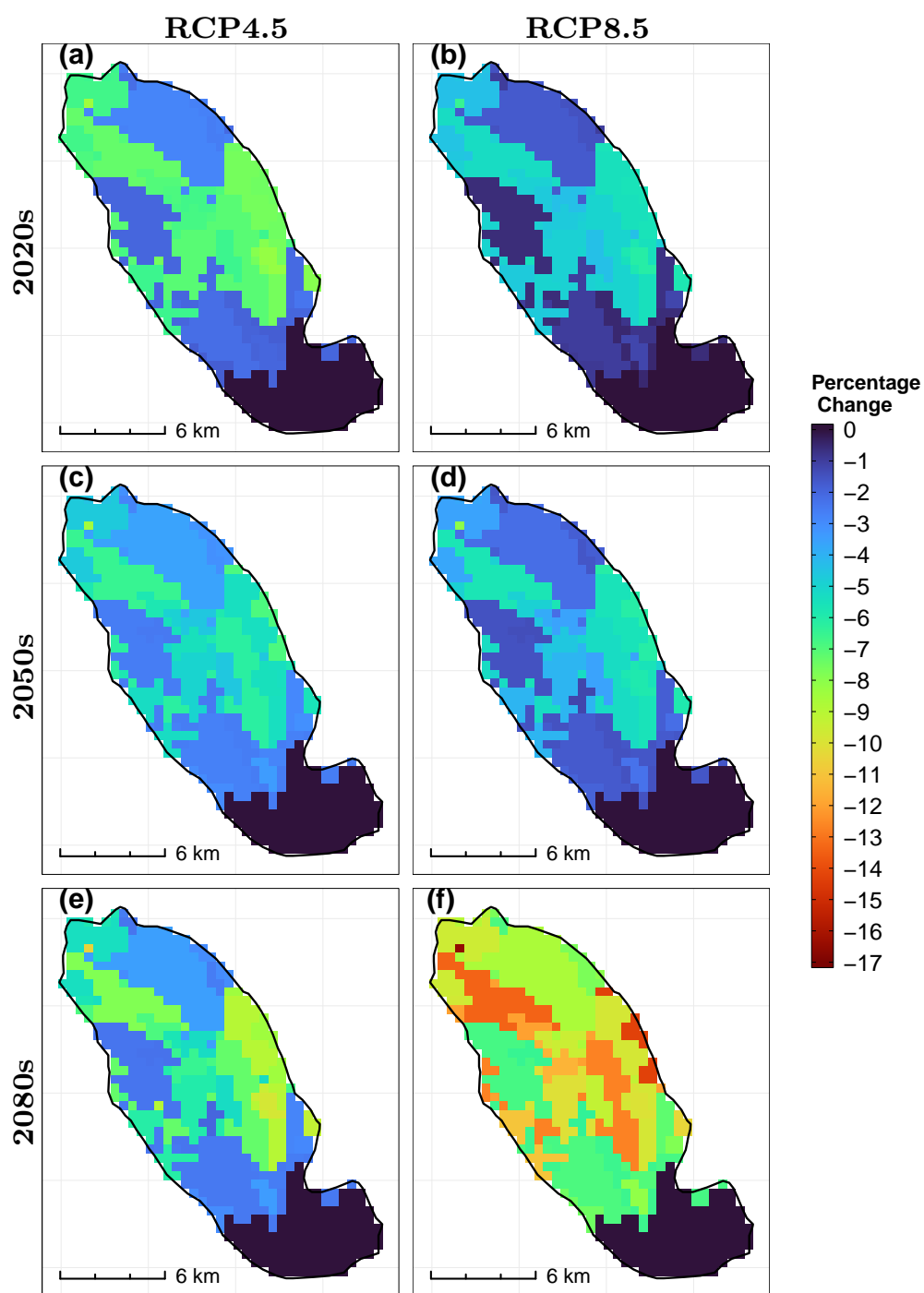
#### 6.3.4 Baseline and Future Recharge Estimation

Average recharge over the baseline period was calculated in mm/day (see Figure 6.5) using the SWAT-MODFLOW model. Daily recharge values are passed onto the groundwater model from the SWAT model during the simulation. From Figure 6.5, the average recharge in the DB is about  $1.5 \text{ mm day}^{-1}$  with the most recharge, contrary to the results published by Jackson et al. (2004), occurring in the Doweel Breccia as can be inferred from the latitudinal and longitudinal density plots of mean Groundwater Recharge (GWRch) on the top and right axes of the figure. The initial conceptualization of the Dumfries Aquifer hydrologic processes based on Jackson et al. (2004) may thus need to be revised and/or investigated further following this integrated modelling campaign. However, it should be noted that there could be structural differences in the formulations of this model versus their model which could lead to a discrepancy in results. The recharge appears to be mostly dominated by the hydraulic properties of the aquifers as opposed to the land-use since approximately 74.6% of the landuse is cropland and pasture (denoted as CRDY in SWAT). The higher recharge zones in the central portion of the basin may not be apparent in the hydrograph analyses due to possible interference from abstraction wells for domestic, agricultural and industrial water needs.

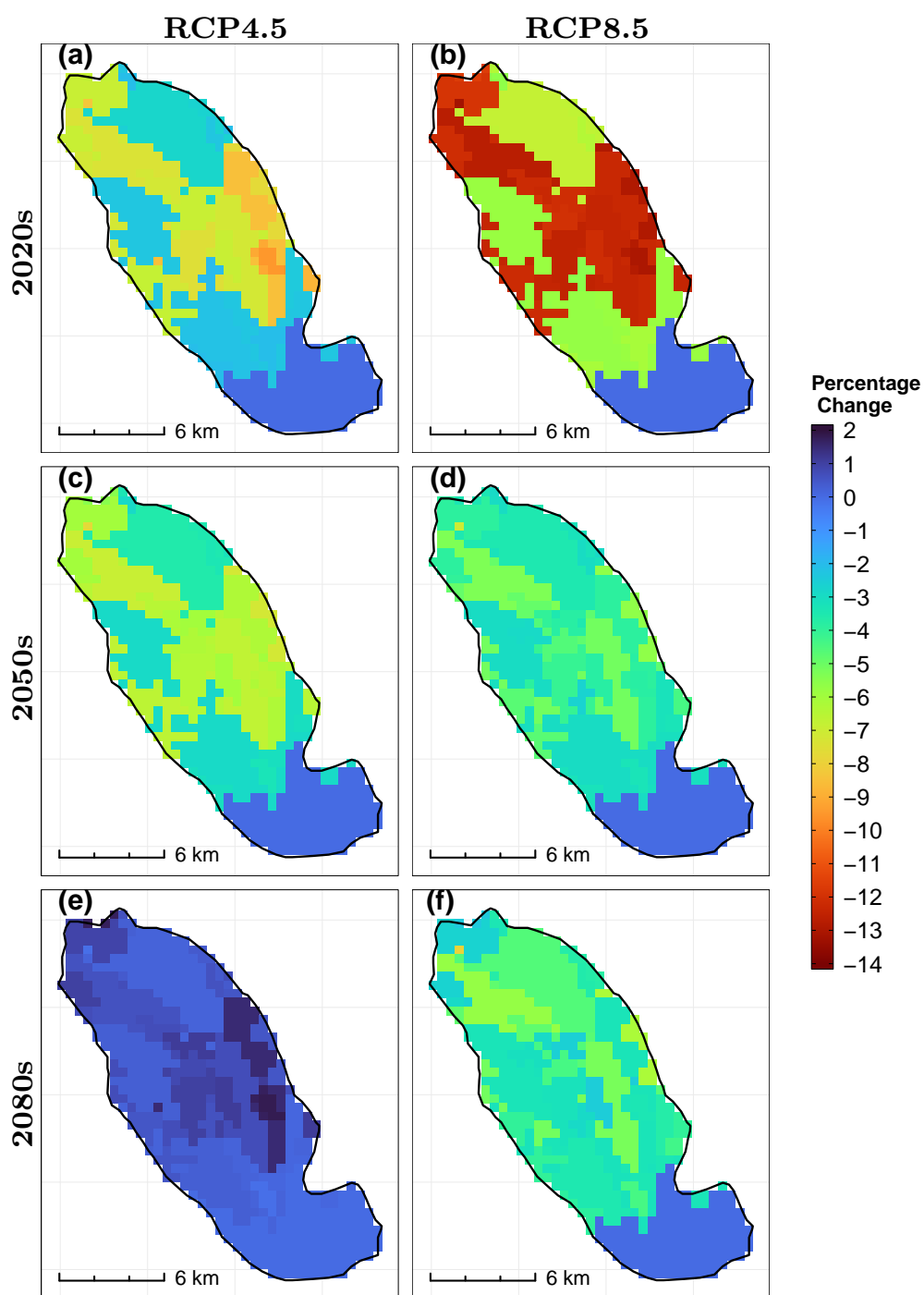


**Figure 6.5** Average baseline daily recharge (mm/day) provided by SWAT to each MODFLOW Grid Cell. Gray margins along the top and right axes are density plots of latitudinal and longitudinal averages of GWRch

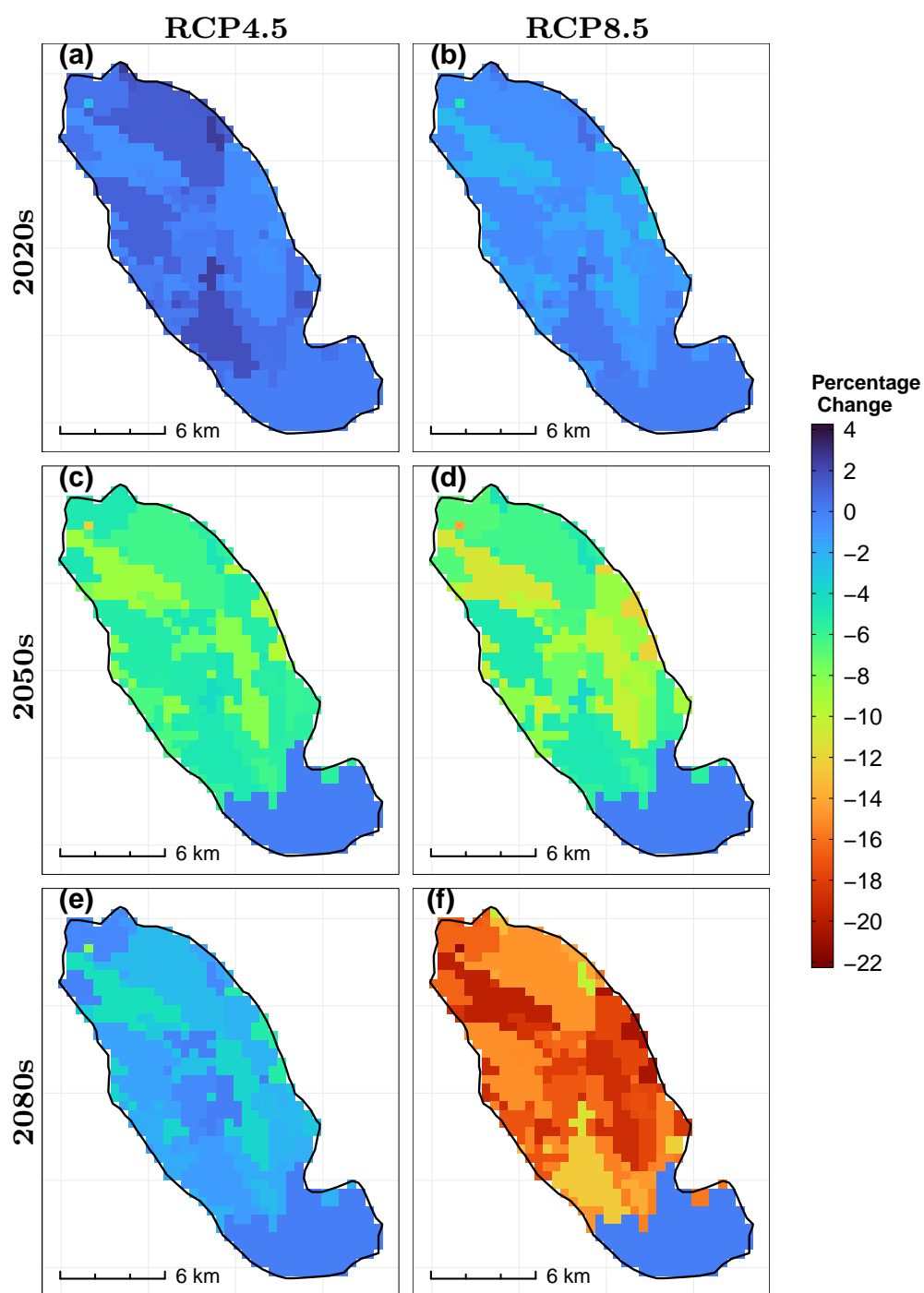
Once the long term baseline recharge was established, comparisons between baseline recharge conditions versus future projections was made as shown in Figures 6.6 to 6.10. Thereafter, a simple average of five separate IHMs (hereinafter River Nith Catchment SWAT-MODFLOW Ensemble Model Mean [RNC-SWATMFEMM]) was used to compare differences in recharge values between future projections and baseline values (Figure 6.11) whereas one IHM whose SWAT model is driven by the RNC-EGCMM was used to compare differences in recharge values between baseline and future periods (Figure 6.12).



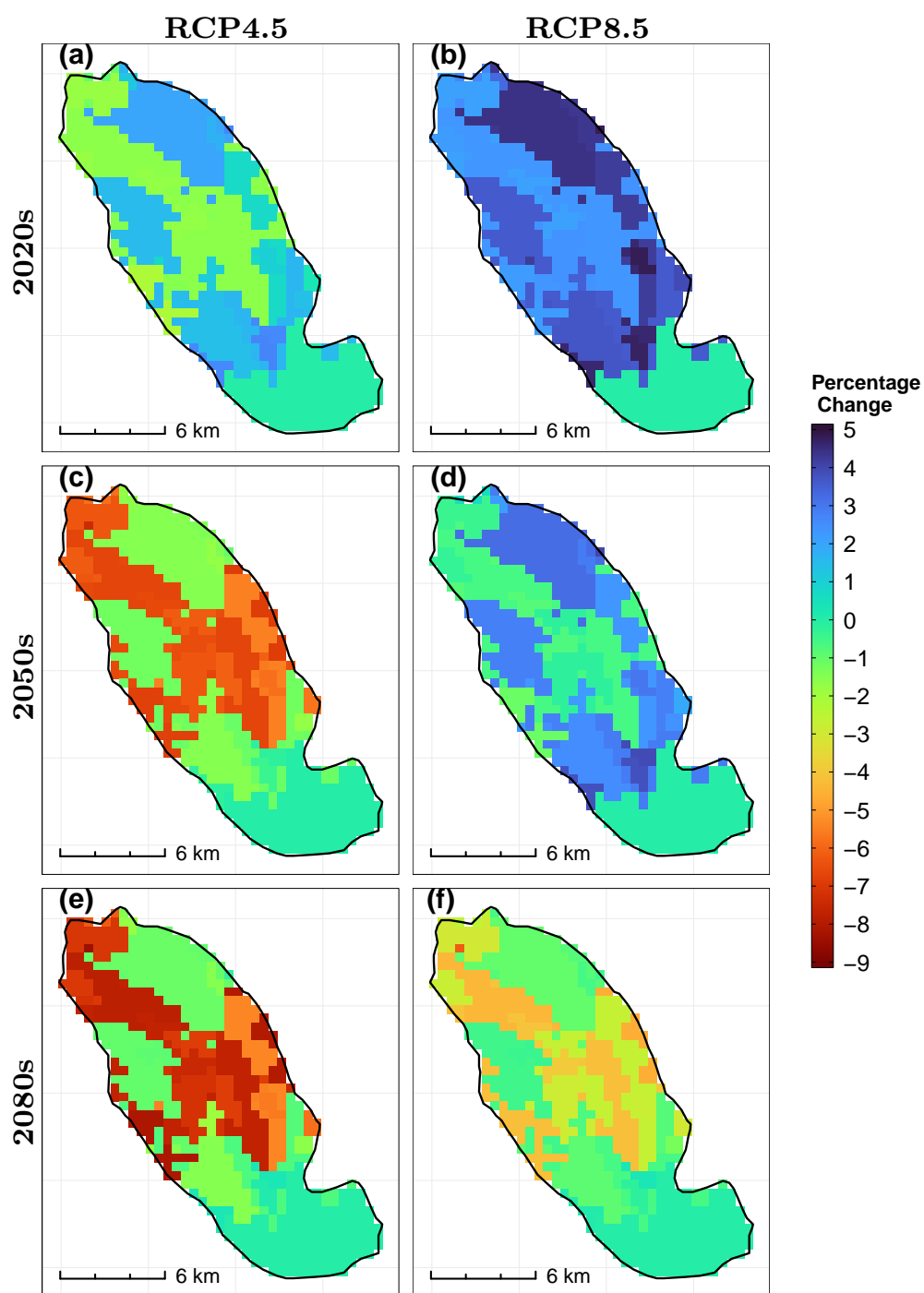
**Figure 6.6** Percentage differences in groundwater recharge (GWRch) between the baseline period and future periods for the Dumfries Basin as simulated by CCSM4



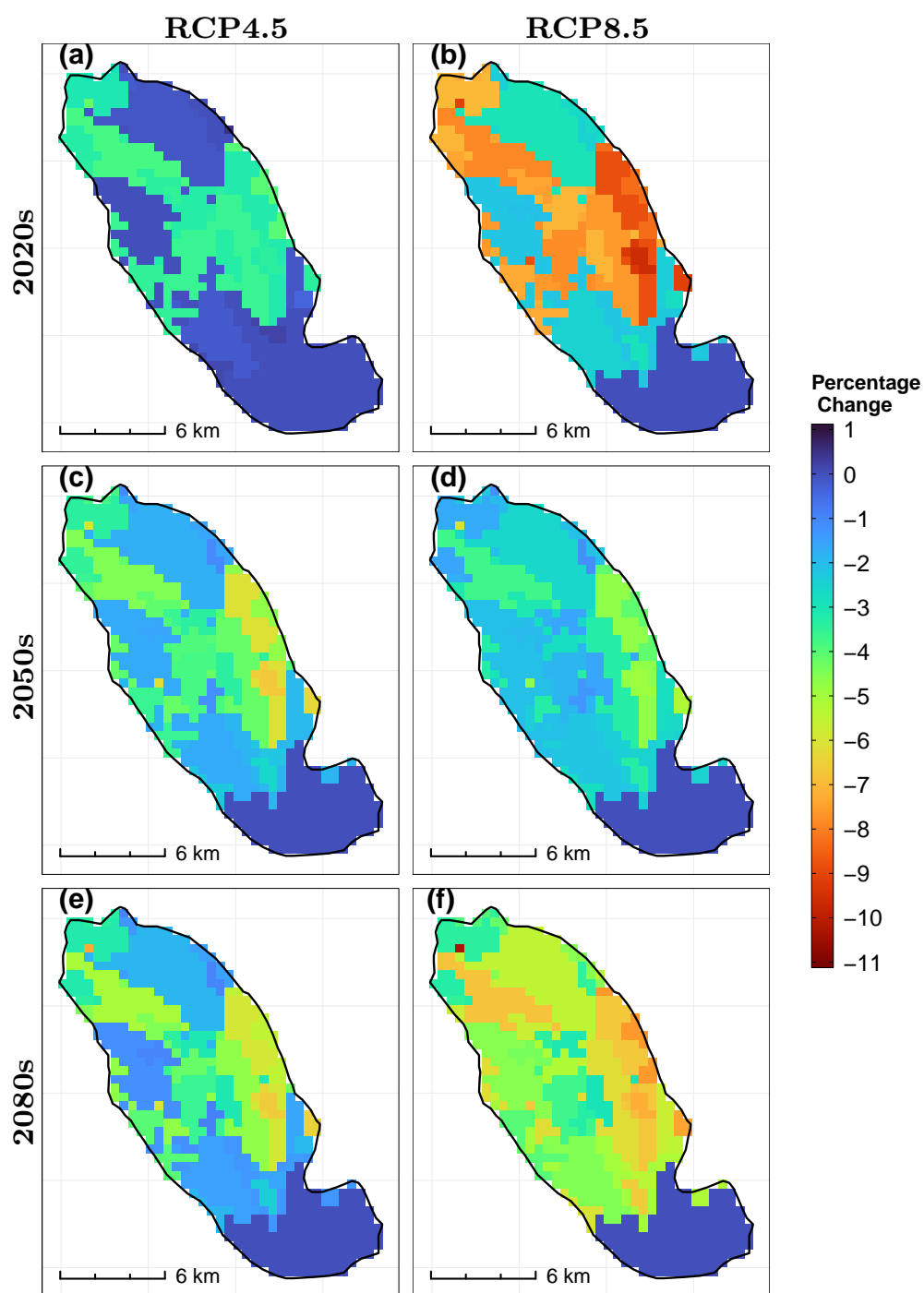
**Figure 6.7** Percentage differences in groundwater recharge (GWRch) between the baseline period and future periods for the Dumfries Basin as simulated by GFDL-ESM2G



**Figure 6.8** Percentage differences in groundwater recharge (GWRch) between the baseline period and future periods for the Dumfries Basin as simulated by HadGEM2-ES



**Figure 6.9** Percentage differences in groundwater recharge (GWRch) between the baseline period and future periods for the Dumfries Basin as simulated by INMCM4



**Figure 6.10** Percentage differences in groundwater recharge (GWRch) between the baseline period and future periods for the Dumfries Basin as simulated by MPI-ESM-LR

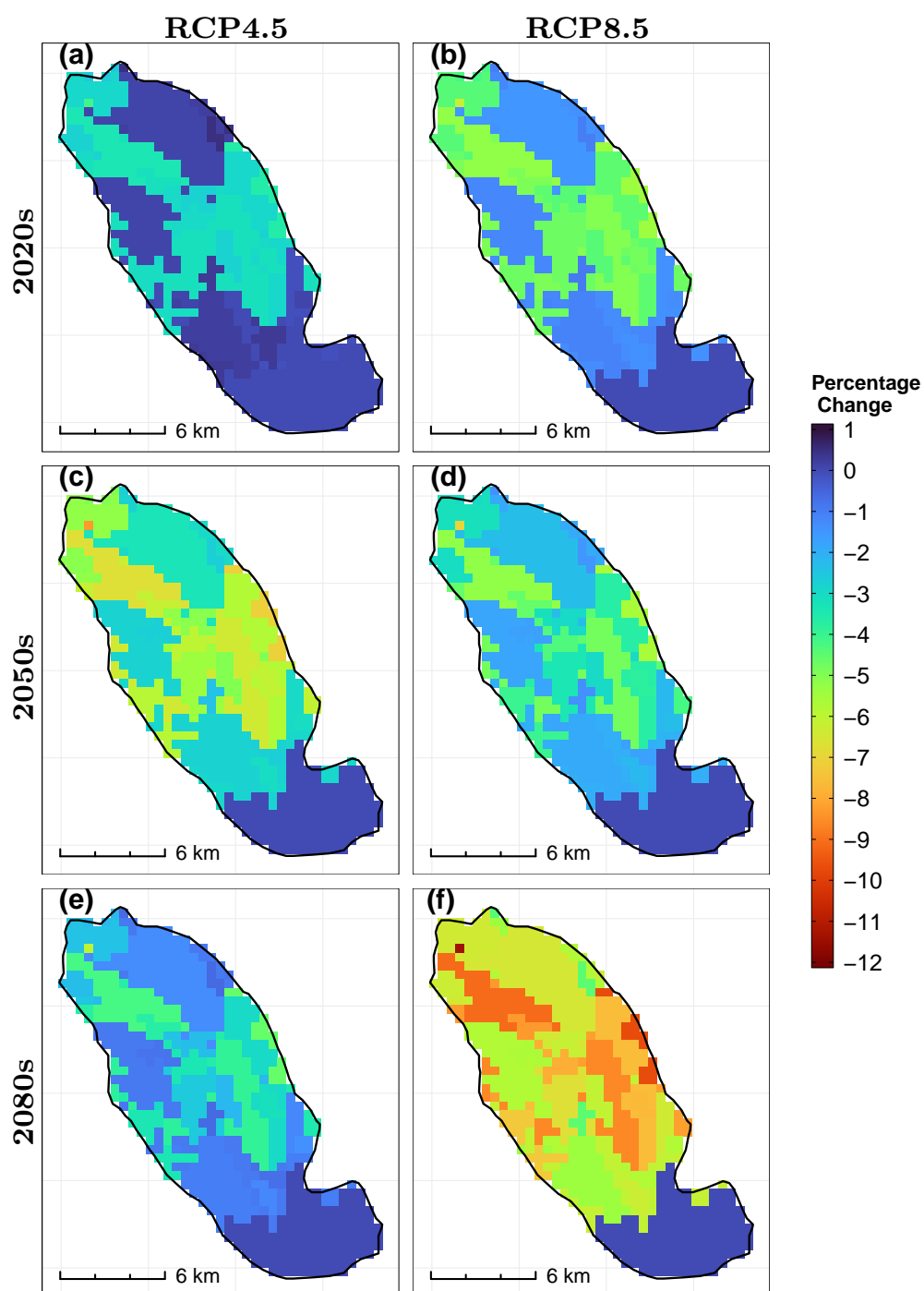


As expected, there were slight differences in GWRch values from one model to another both in the sign and magnitude of change. Ensemble models, also, seem to disagree along the same lines. In almost all cases, the RNC-EGCMM driven IHM suggests increased GWRch in some parts of the Locharbriggs Sandstone of about +30% to +40%. For the rest of the basin, the model predicts up to +10% increase in GWRch in the 2020s, up to +12% in the 2050s and up to +18% in selected regions of the DB in the 2080s under RCP4.5. Slightly higher ranges are expected under RCP8.5 with GWRch increasing by up to +12% in the 2020s, +5% to +15% in the mid-century and only up to +6% in the late century. The RNC-EGCMM forced IHM did not predict any decrease in GWRch when compared with the baseline period. It is unclear whether this is an artefact of the model construction and parametrisation or that of the climate. In any case and for most of the basin, the changes in GWRch are considered negligible save for a few regions.

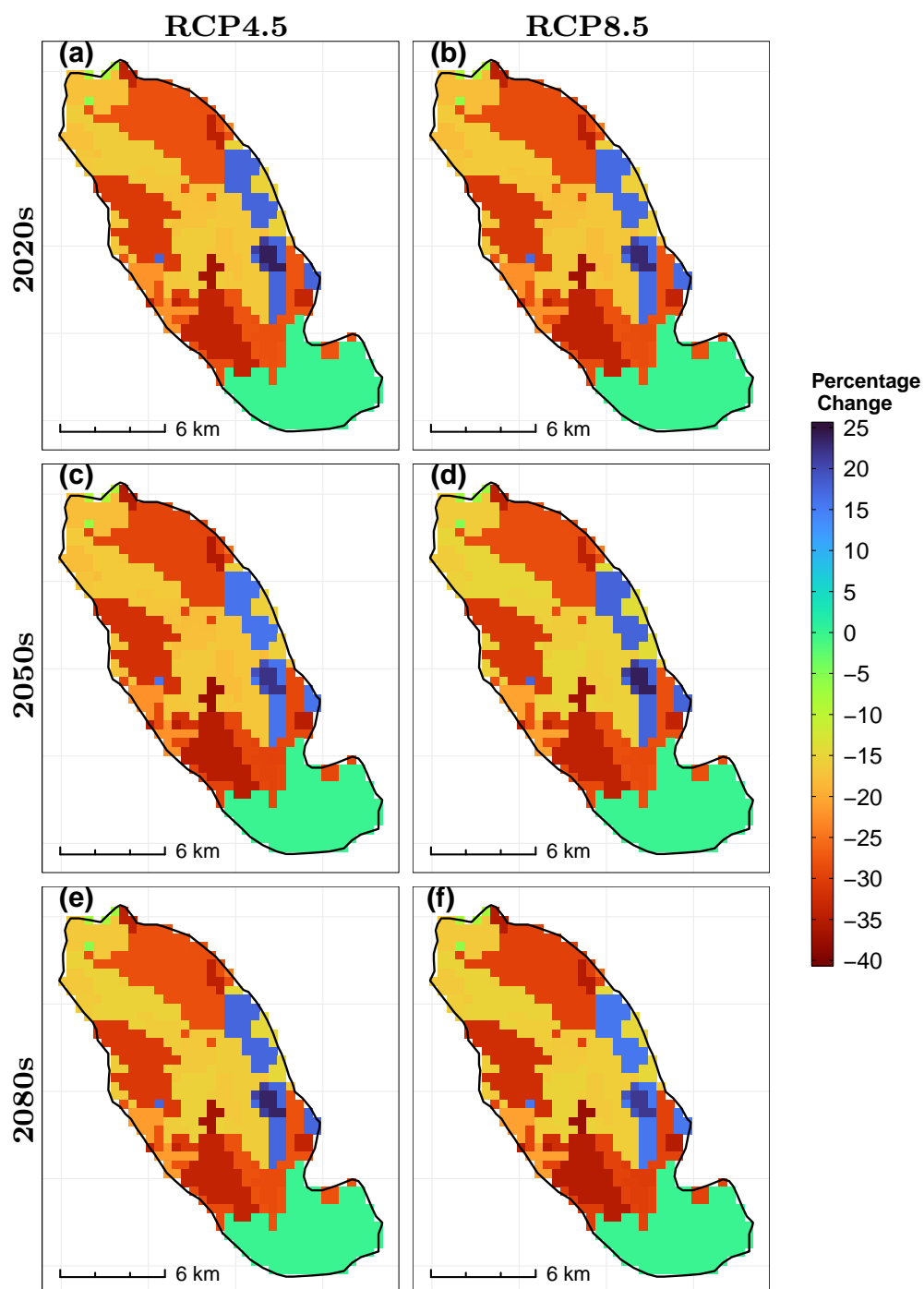
The RNC-SWATMFEMM predicts an increase of up to +2% in the 2020s, a decrease of GWRch of between -2% to -4% in the mid-century and an increase of up to +6% in the late-century under RCP4.5. An increase of up to +22% is observed in the 2020s and 2050s under RCP8.5 while the 2080s are expected to see an increase of up to +3% under the same emission scenario.

Both models are in agreement that under RCP8.5, higher GWRch is expected, perhaps due to increased precipitation especially in the winter season. In the 2050s, spring precipitation is expected to fall by about -3% so it could possibly explain the drop in GWRch under RCP4.5 in the same time period as predicted by DG-Ens-IHM. Both models predict decreased GWRch in the 2080s under the two emission scenarios. This can be confirmed by the climate projection results of Chapter 4 which show no significant changes in winter precipitation,

decreased summer precipitation and increased temperatures in the 2080s. Again, it cannot be conclusively decided whether the RNC-EGCMM driven IHM or RNC-SWATMFEMM can be considered to be a better representation of the future. Both models take into consideration the inherent variability of the single GCMs and how the associated uncertainty can be reduced via ensemble averaging. Improved GCM skill, sufficient watershed and groundwater observations can certainly help to improve the quality of IHMs especially in the case where they are used as predictive models.



**Figure 6.11** Percentage differences in groundwater recharge (GWRch) as simulated by SWAT-MODFLOW between the baseline period and future periods for the Dumfries Basin. Results are a simple average of the separate SWAT-MODFLOW models (RNC-SWATMFEMM)



**Figure 6.12** Percentage differences in groundwater recharge (GWRch) as simulated by SWAT-MODFLOW between the baseline period and future periods in the SRB. MODFLOW was coupled with a SWAT model forced with the RNC-EGCMM.

### 6.3.5 RNC Groundwater Recharge Modelling Summary

Table 6.2 provides a summary of areal mean percentage change in GWRch in the RNC. With the exception of the model forced with the RNC-EGCMM, all models projected insignificant change in GWRch when compared with baseline values. The sign of change, even though the magnitudes are classified as insignificant, is not always in harmony across the models. However, as already established in the preceding chapters, this is expected due to many factors but including inherent variability in the GCM models.

The model forced with the RNC-EGCMM projects a significant decrease in groundwater recharge across all time horizons under RCP4.5 and 8.5. However, results from this model and particularly for the RNC, as discussed in Chapter 5, should be treated with caution. Again, the cause for this behaviour is unknown but suspected to be an artefact of the random forest algorithm when averaging the models.


Historically, Robins and Ball (2006) report of a sharp increase in groundwater abstraction in the DB during the late 1980s and early 1990s followed by a steady increase up to around 2015. In the future, uncontrolled and indiscriminate abstraction of groundwater can be a potential issue in vulnerable regions of the DB that are projected to be in a recharge deficit. Further studies are recommended aimed at understanding recharge mechanisms in the DB that are not diffuse-based but largely controlled by flow through fracture networks.

In general there is little to no threat to groundwater resources in the DB based on anticipated anthropogenic climate change as simulated under RCP4.5 and 8.5 scenarios.


**Table 6.2** Summary areal mean percentage change in projected groundwater recharge (GWRch) in the RNC with respect to the baseline period. Changes within  $\pm 10\%$  of baseline values are considered to be insignificant (green boxes) whereas changes above  $+10\%$  (red boxes) and below  $-10\%$  (blue boxes) are considered to be significant.

GCM	Scenario					
	RCP4.5			RCP8.5		
	2020s	2050s	2080s	2020s	2050s	2080s
CCSM4	-4.0	-3.6	-4.2	-2.6	-2.8	-7.8
GFDL-ESM2G	-4.2	-4.0	0.5	-7.7	-3.2	-3.3
HadGEM2-ES	0.4	-5.0	-1.8	-0.8	-6.0	-13.4
INMCM4	0.2	-3.2	-3.5	2.7	1.2	-1.8
MPI-ESM-LR	-1.5	-2.6	-2.6	-4.4	-2.3	-4.3
Ensemble (RNC-EGCMM)	-16.2	-17.0	-16.1	-16.6	-16.0	-16.8
Ensemble (RNC-SWATMFEMM)	-1.3	-3.7	-1.8	-2.6	-2.6	-5.7


**Increase**



**Insignificant Change**



**Decrease**



## 6.4 SRB Groundwater Modelling

### 6.4.1 Conceptual Model

#### 6.4.1.1 Aquifer definition

The major aquifers in the valley, in increasing importance, as noted by Bradford (1973) are, weathered and fractured basement rocks, Karro and Cretaceous sedimentary rocks, weathered and fractured basalt, and finally the unconsolidated deposits on the valley floor (Bradford, 1973). Generally, there exists three types of aquifers in Malawi that can be summarised (CGS, 2018; JICA, 2014) as follows;

- The Weathered Basement (WB) aquifers of the plateau that are extensive and low yielding,
- Higher yielding Quaternary Alluvial (QA) aquifers of the lakeshore plains and the Shire Valley.

- Fractured Basement (FB) aquifer whose groundwater resource potential is considered negligible.

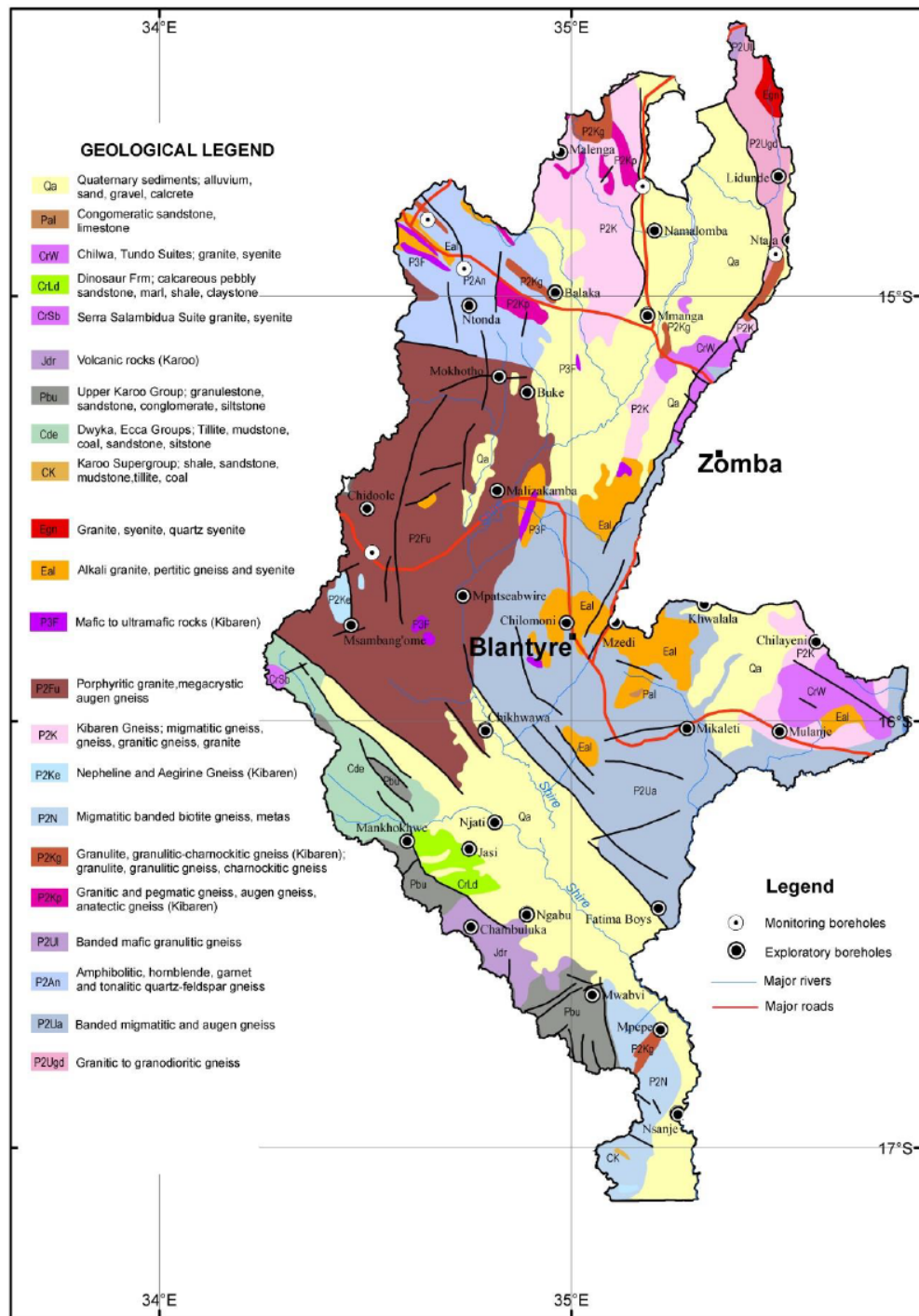
#### **6.4.1.2 Geologic Setting**

The Lower Shire Valley has a complex geological structure because it is located within the East African Rift System. Consequently, there are a number of faults in the region with considerable throw (Bradford, 1973). The most notable faults are the Mwanza, Thyolo and Namalambo faults. The valley floor is occupied mostly by Quaternary sediments such as gravels, sands and poorly-sorted silts. The Malawi Basement Complex underlies the valley and is composed mostly of biotite gneisses. Alluvial formations are in abundance in the SRB covering the northern-most parts of the basin from Mangochi to Matope and also in the low-lying regions of Chikwawa and Ngabu (see Figure 6.13).

Precambrian to lower Palaeozoic age crystalline metamorphic and igneous rocks form what is mainly referred to as the basement complex which supplies approximately 60% of potable water to the population (Chilton and Smith-Carington, 1984; Chilton and Foster, 1995; Mapoma and Xie, 2014).

#### **6.4.1.3 Surface Water**

The SRB is mainly drained by the Shire River (largest river in Malawi) which flows south towards Mozambique where it flows into the Zambezi River. Acting as the only outlet of Lake Malawi, flows in the Shire River are highly regulated via the Kamuzu Barrage at Liwonde. The Shire River has many benefits to Malawi such as hydroelectric power generation at Nkula, Tedzani and Kapichira falls, supply of water to the city of Blantyre and its peri-urban areas by the Blantyre



**Figure 6.13** Geology of the SRB with names of the sites that were surveyed during exploratory drilling for the SRB Hydrogeological and Water Quality Mapping under the SRB Management Program (Phase 1) Project. (Fig. 2, CGS, 2018)



Water Board, irrigation of sugar plantations at Nchalo and also supporting the fisheries industry in the Elephant Marsh of the Lower Shire River flood plains.

#### **6.4.1.4 Groundwater**

The weathered basement aquifers mainly occur on the highland areas and are an important source of rural water supply (JICA, 2014). The weathered basement aquifers are generally divided into three layers: the laterite layer mainly composed of red clay or completely weathered silt; saprolite layer and the medium weathered layer, considered to be the best water yielding zone within the weathered basement aquifer, occurring between 15 and 30m (JICA, 2014).

### **6.4.2 Model Development**

#### **6.4.2.1 Spatial Discretization**

In order to develop a fully integrated model, it was necessary that the surface-water model developed in Chapter 5 fully overlaps the groundwater model. It should be noted, however, that SWAT-MODFLOW is capable of linking separate SWAT and MODFLOW models that only partially overlap. The regional groundwater model developed for the SRB overlapped with about 70% of the SWAT model. This is because the groundwater model was spatially restricted to areas for which data was available i.e. part of the Shire Basin within the Malawi boundary. The SRB groundwater model domain spans an area of about 21,751 km<sup>2</sup>.

#### **6.4.2.2 Temporal Discretization**

The SRB groundwater model is simulated from January, 1975 to December, 2005. A ‘warm-up’ period of 6 years was included at the beginning of the simulation to

account for uncertainties in model initialization; thus a period of 25 years should be considered as the simulated period. Moreover, when the MODFLOW model was coupled with SWAT, the same warm-up period was used and thus results of the first six years are discarded and not recorded in the simulation results files. As, alluded to earlier, this is because of the uncertainty related to model initialization that renders the first few years' results less reliable.

For the future scenarios, the calibrated groundwater model was coupled with SWAT to simulate future recharge and groundwater/surface-water interactions in the basin. Each future-scenario 30 year time slice was simulated independently since the associated future SWAT models were developed separately too.

#### **6.4.2.3 Hydraulic Properties**

Similar to the approach used for the DB, PEST was used in regularization mode to parameterize the model HK. Layers 1 and 2 of the model were defined as 'convertible' so that where the layers are partially saturated, the storage coefficient (SC) would be, for all intents and purposes, equal to the specific yield (SY). Layer 3 was defined as confined. Initial values of HK were assigned based on tests done by CGS (2018). A single vertical anisotropy value of 10 was initially assigned to the model before calibration. This means that the VK is assumed to be 10 times smaller than the HK. After calibration, the vertical anisotropy was determined to be 18. For the alluvium deposits, this value seems to be a little higher than expected. This is expected for a regional model with sparse ground truth data. Thus aquifer property values at a finer scale are required to verify and/or improve parameterization of the model.

#### 6.4.2.4 Hydrologic Boundaries

Due to the vast expanse of the SRB groundwater model, three types of hydraulic boundaries were defined. The East and West boundaries were defined under Neumann conditions as no-flow boundaries. This is easily done in ModelMuse by setting the cells outside the perimeter of the model as ‘inactive’ because the model does not support the use of IBOUND arrays to define which cells belong to the modelled area. The northern portion of the model which borders with the lake is specified as a constant head boundary and defined by the GHB package in ModelMuse. The southern boundary of the basin is defined as a general head boundary by the GHB package. Internal boundaries were defined by the RIV and RCH packages.

#### 6.4.2.5 Model Calibration

Groundwater monitoring data for the SRB during the baseline period are non-existent and as such calibration efforts for the SRB groundwater model were riddled with a lot of uncertainty. Between 2009 and 2015, a number of hydrometric stations in the SRB commenced groundwater level monitoring activities. Even so, where such records exist, data are sparse and range from a few months to 3 or 4 years on a monthly time-scale. Thus it was difficult to calibrate the MODFLOW model using reliable long-term spatio-temporal hydrometric data. Aquifer and baseline heads characterization was dependent on data collected on behalf of the Malawi Government by the Council for Geoscience and PBM Consultants in 2017.

Initially, the coupled model was run using parameters obtained from individual SWAT and MODFLOW (steady-state) calibrations. This resulted in an initial set of results such as hydraulic heads, recharge and groundwater/surface-water

fluxes for the baseline period. The simulated hydraulic heads, in particular, were compared to the observed spatial hydraulic head distribution to check for departures from the stand-alone MODFLOW model. As expected, there was significant departure from the observed heads simulated by the stand-alone MODFLOW model especially at higher elevations. To correct this, simulated recharge supplied to the MODFLOW cells during the coupled simulations were obtained and used to constrain the MODFLOW model in a fresh calibration campaign. Furthermore, other parameters that control GW/SW interactions (i.e River Package parameters) such as the stage, elevation of the bottom of the river bed and hydraulic conductance of the riverbed, were calibrated using the trial-and-error method. Using volume fluxes and observed heads as calibration targets, PEST was used to calibrate the transient MODFLOW model. Table 6.3 provides a summary of the goodness-of-fit statistics that were used to compare hydrographs obtained from SWAT and SWAT-MODFLOW. The coupling of the groundwater model to the SWAT model marginally improved streamflow simulation at some stations and significantly at others – consolidating the claims made by the developers and users of SWAT-MODFLOW about the enhanced simulation capabilities of such a combination.

Again, goodness-of-fit statistics provided as insets in Figure 5.29 may slightly differ from those presented here since the statistics for the SWAT model presented in Table 6.3 are a composite of the calibrated and validation periods for a fair comparison with SWAT-MODFLOW.

**Table 6.3** Goodness-of-fit statistics used to compare the performance of SWAT and SWAT-MODFLOW (SWAT-MF) in simulating monthly streamflow in the SRB.

Metric	Station					
	Rivi-Rivi River at Balaka		Ruo River at M1 Roadbridge		Lichenya River at Mini Mini Estate	
	SWAT	SWAT-MF	SWAT	SWAT-MF	SWAT	SWAT-MF
ME	0.52	0.50	-0.41	-0.42	0.29	0.14
MAE	4.04	3.69	3.84	3.18	3.20	2.61
MSE	37.51	34.10	30.44	21.61	22.88	16.12
RMSE	6.12	5.84	5.52	4.65	4.78	4.01
NRMSE %	62.50	59.60	48.10	40.50	56.20	47.20
PBIAS %	8.10	7.70	-3.20	-3.20	2.80	1.40
RSR	0.63	0.60	0.48	0.41	0.56	0.47
rSD	0.73	0.75	0.89	0.86	1.02	0.96
NSE	0.60	0.64	0.77	0.83	0.68	0.78
mNSE	0.41	0.46	0.56	0.64	0.52	0.60
rNSE	-2.44	-1.71	0.73	0.77	0.71	0.75
d	0.85	0.87	0.93	0.95	0.92	0.94
md	0.66	0.69	0.77	0.81	0.76	0.80
rd	-0.26	0.03	0.92	0.93	0.92	0.93
cp	0.67	0.69	0.74	0.81	0.63	0.74
r	0.78	0.80	0.88	0.92	0.85	0.88
R <sup>2</sup>	0.61	0.65	0.77	0.84	0.71	0.78
bR <sup>2</sup>	0.44	0.48	0.68	0.74	0.69	0.74
KGE	0.65	0.67	0.83	0.83	0.84	0.88
VE	0.37	0.43	0.70	0.76	0.69	0.75

#### 6.4.2.6 Summary of the Conceptual Model

There is limited data in the SRB to form a conclusive picture of the hydrogeological processes therein. From the sparse data that has been collated within the SRB by various consultants, researchers and agencies, conceptualization of the SRB groundwater processes is as follows;

1. Groundwater flow is inferred to flow in a north-south direction. In reality, preferential pathways such as faults and local topography plays an important role in the direction of flow.

2. It is assumed that the Shire River and its tributaries are in hydraulic contact with the alluvial aquifer units in the SRB.
3. Most of the groundwater recharge is assumed to take place in the highlands (north-west of the basin) and consequently discharge in the lower Shire basin valleys.
4. Unconsolidated sedimentary aquifers are assumed to be highly responsive to precipitation events
5. Although groundwater is abstracted for industrial, agricultural and domestic use in the SRB, these abstractions have not been incorporated into the model. Instead, the focus is on more regional phenomena such as recharge and GW/SW interactions and how these processes respond to future climate conditions.

### 6.4.3 Description of the Coupling Process

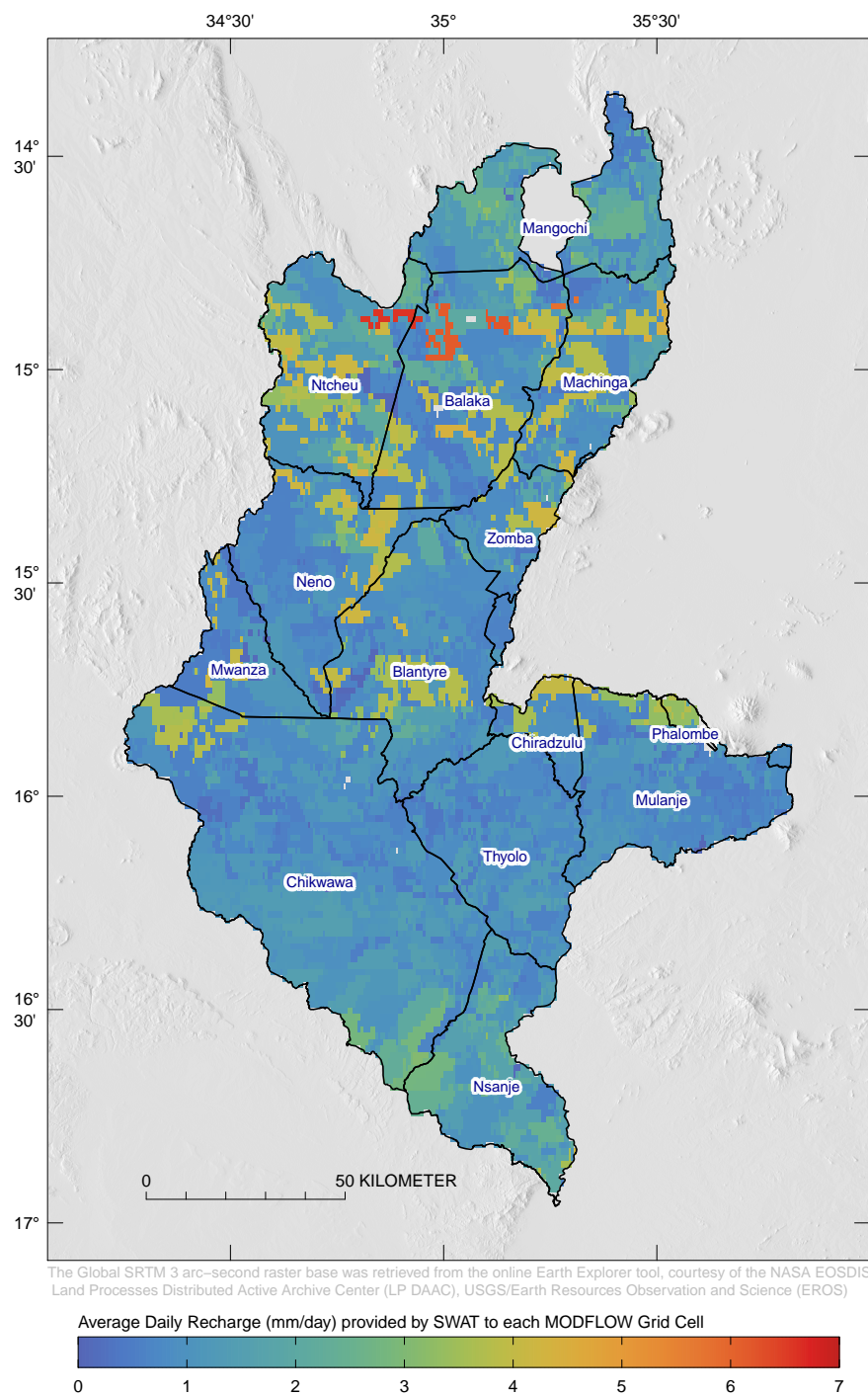
Unlike the DB, the SRB SWAT model extent fully overlaps the groundwater model. SWAT model HRUs were mapped onto MODFLOW grid cells and MODFLOW river cells defined by the RIV package mapped to SWAT stream channels using subroutines within SWAT-MODFLOW. Details of the mapping schemes can be found in Bailey et al. (2016) although a brief description has been provided in Section 6.3.3.

### 6.4.4 Baseline Recharge Estimation

The long term average daily recharge and head for the baseline (1981 – 2005) period in the SRB is presented in Figures 6.14 and 6.15. The calculated recharge is related to the spatial distribution of rainfall in the basin. Groundwater level

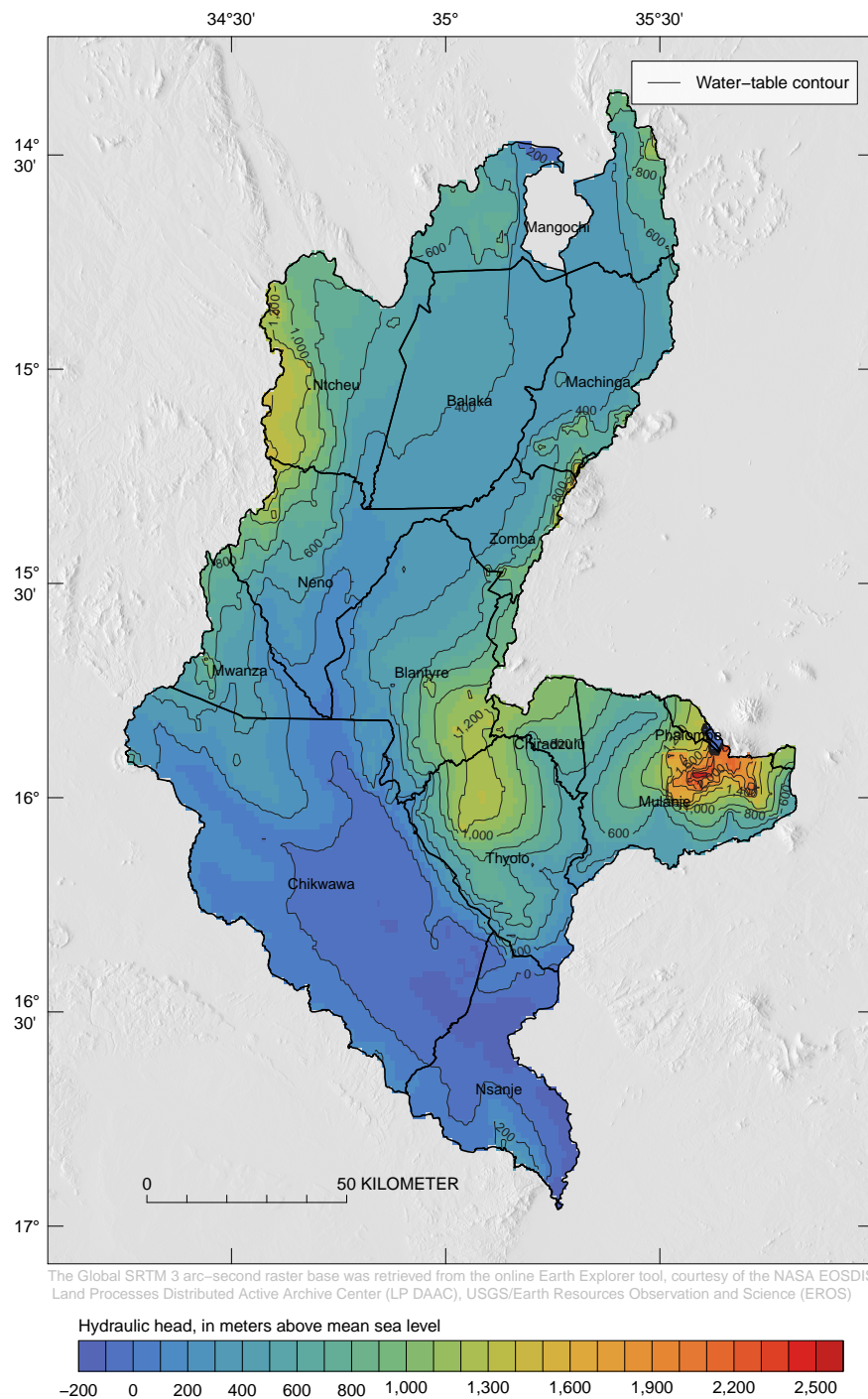
response to precipitation variability is affected by a lot of factors among which are; spatial variability in hydraulic properties and distance from recharge areas (Green et al., 2011a). Thus it is important to study current and future groundwater recharge mechanisms and trends in order to predict availability and impact of climate change on groundwater resources.

According to Sherif and Singh (1999), groundwater resources can be divided into four categories namely; confined aquifers with impermeable upper layers, phreatic aquifers in wet regions, unconfined aquifers in dry and arid regions and finally, coastal aquifers subject to sea water intrusions. Most of the SRB can be classified as semi-arid (Joshua et al., 2016) with groundwater aquifers that respond almost immediately to precipitation events and thus fall into the third category of the aforementioned classifications.



**Figure 6.14** Long term daily average recharge for the rainy season in the SRB for the baseline period (1981 – 2005).





**Figure 6.15** Average Cell-by-Cell Groundwater Hydraulic Head in the SRB for the baseline period (1981 – 2005).

### 6.4.5 Future Groundwater Recharge Estimation

As was discussed in Section 2.6, numerical models were employed to calculate climate change impacts on groundwater recharge. Aquifers are mainly recharged via direct precipitation and interaction with surface-water bodies such as rivers and lakes. The coupled SWAT-MODFLOW model was used to calculate potential climate change impacts on future recharge (i.e. diffuse and focussed recharge) in the SRB. The SWAT-MODFLOW model produces, as one of its outputs, spatial groundwater recharge results for the simulation period that are useful in visualizing temporal changes due to climate (Molina-Navarro et al., 2019b). Groundwater recharge is one of the most important inputs to groundwater models simulated with MODFLOW. However, in most cases, groundwater modellers use simplistic assumptions and the zonal approach to estimate recharge for groundwater models. As noted by Semiromi and Koch (2019), while such groundwater models calibrated for recharge are capable of satisfactorily reproducing groundwater heads, they can simply be considered to be “mathematical marionettes, dancing to match the calibration data even if their underlying premises are unrealistic” (Kirchner, 2006). This is because such methods fail to account for spatial variability of recharge rates due to many factors such as varying geology, irrigation practices, landuse and landcover (Semiromi and Koch, 2019). Because SWAT-MODFLOW is a tightly coupled hydrologic model, most of the weaknesses of stand-alone SWAT (e.g. simplified groundwater module in SWAT) and MODFLOW (e.g. inability to capture most of the hydro-climatic processes owing to surface and atmospheric processes) are eliminated and thus greatly improving the simulation of surface- and groundwater processes and interactions for better water resources management and adaptation planning.

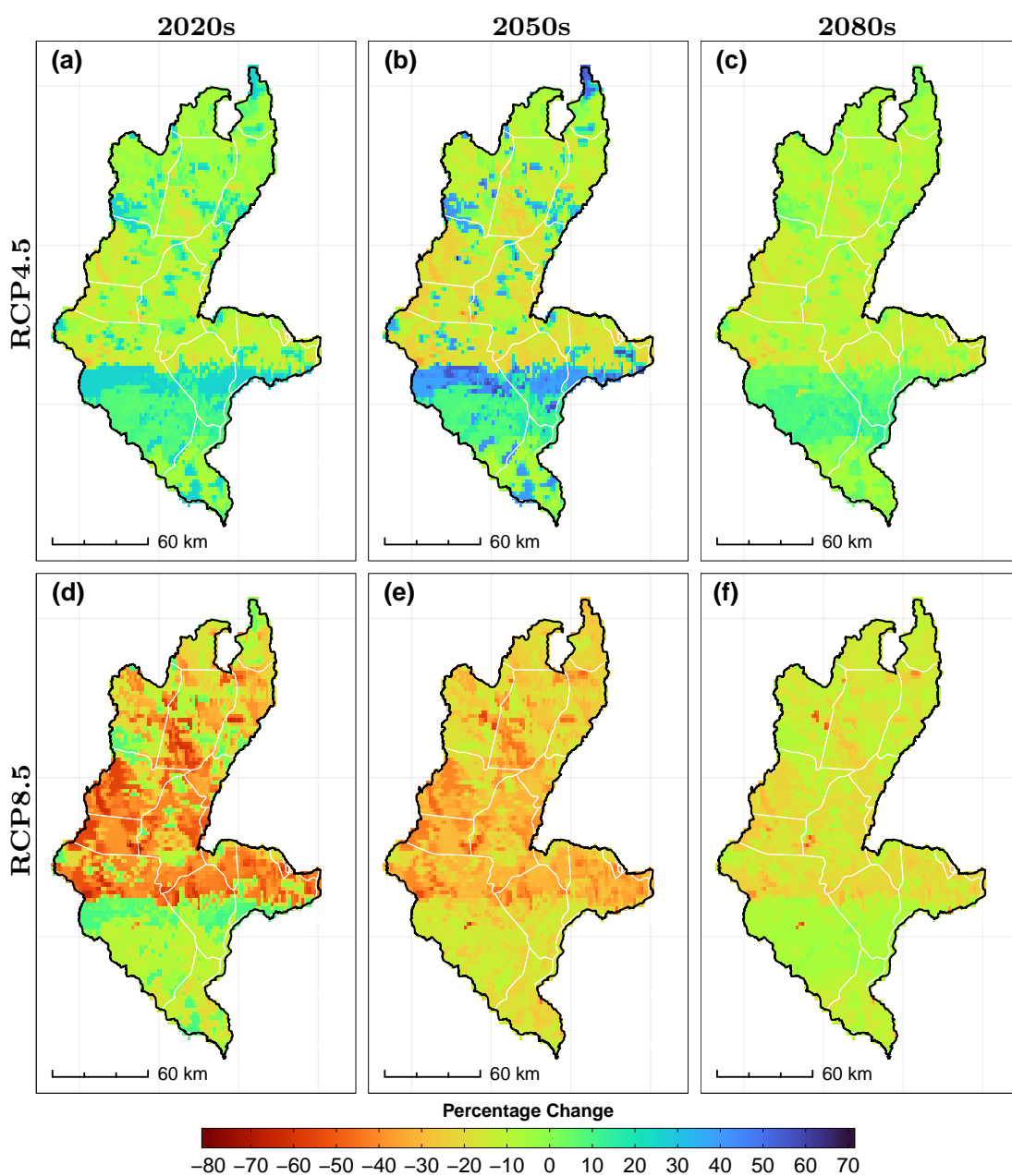
Groundwater recharge for the SRB was calculated differently than for the RNC because the SRB SWAT model overlaps the groundwater model. The wet period in the SRB usually stretches from November to April where approximately 95% of precipitation takes place. This means that there is little to no precipitation for half of the year in the SRB, as is typical of semi-arid regions in sub-Saharan Africa. However, because of agricultural and irrigation activities and GW/SW interactions in some parts of the SRB, groundwater recharge is calculated and presented as an annual average. Again, the SWAT-MODFLOW models were forced with 6 GCMs and percentage differences in recharge between the future period and baseline periods calculated (i.e. positive values indicate increase in recharge while negative values indicate a decrease in wet season recharge).

Figures 6.16 to 6.21 show the percentage differences in groundwater recharge (GWRch) from the baseline period. SWAT-MODFLOW calculates the groundwater recharge for each HRU (HRUs were mapped onto MODFLOW grid cells). This approach is advantageous over other simplistic methods mentioned earlier in that the estimated daily deep percolation or groundwater recharge is a function of the LU/LC and other land surface-atmosphere interactions.

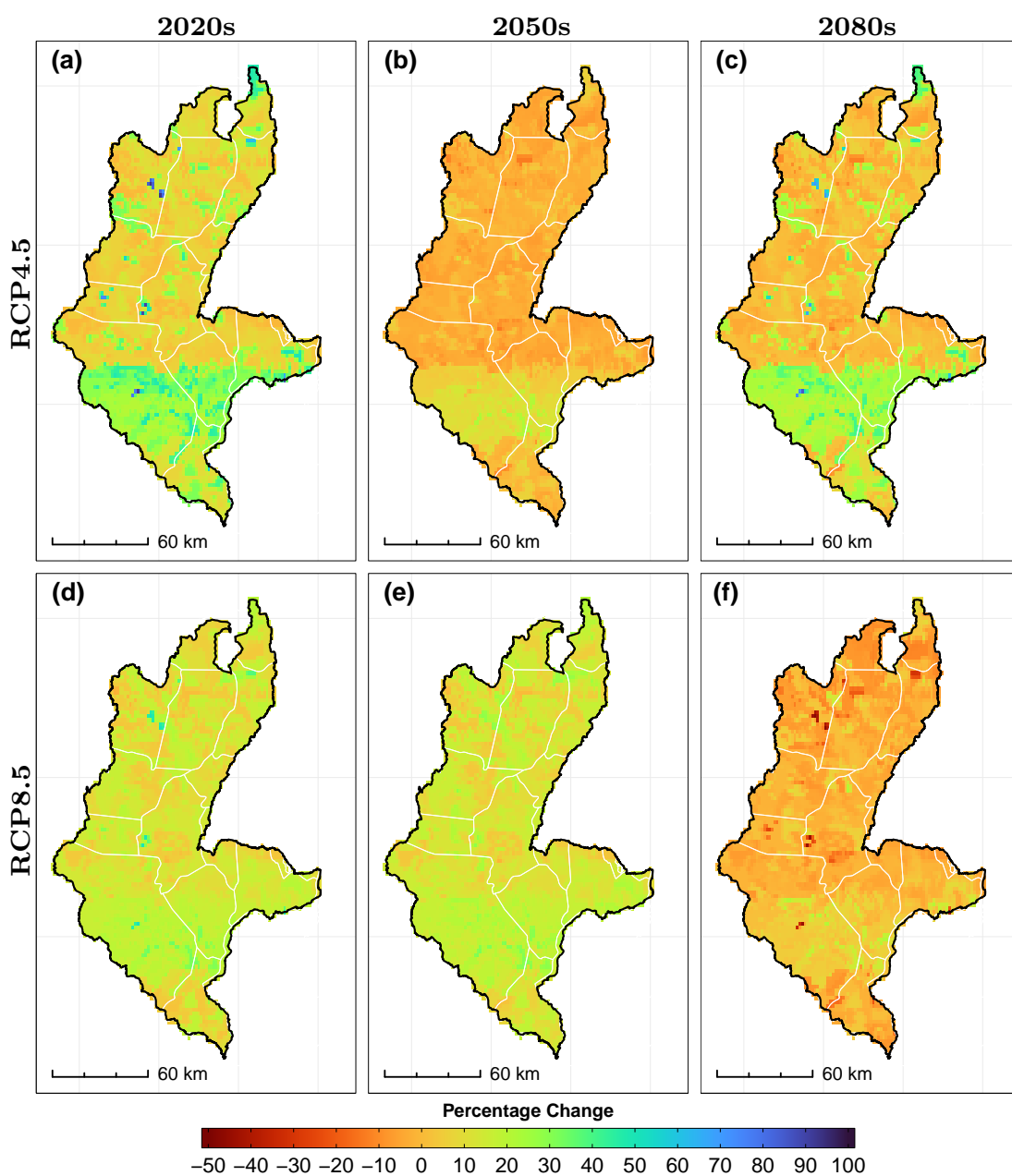
As was observed in Chapter 4, GCMs vary widely in terms of their representation of climate, particularly precipitation. The same trend was observed in Chapter 5 when assessing the impacts of climate on future streamflow. Similarly, there is relatively wide disagreement and uncertainty between models about future groundwater recharge. Under the RCP4.5 scenario, BCC-CSM1-1-M generally predicts a decrease in groundwater recharge in the short term of up to 20% for most of the basin except parts of Chikwawa and Thyolo where an increase of around 10% is predicted. In the mid- to late-century, areas surrounding the

southern parts of Chikwawa and Thyolo experience a surplus in groundwater recharge whereas the rest of the basin experiences mostly a slight decrease of up to -25% especially in the 2050s. Under the same conditions CCSM4 predicts even higher (+30% to +50% change in the short term and up to +40% change in the late century) ranges for the surplus in GWRch in Southern Chikwawa and Thyolo with little to negligible change in the rest of the basin. CNRM-CM5 predicts little to insignificant increase in GWRch in most areas of the basin except for the southern part of the basin increases of up to +30% can be observed throughout the century. GFDL-ESM2G predicts slightly increased (up to 15%) levels of GWRch in the early century for most parts of the basin whereas the high recharge zones in the highlands and down the basin in the valleys of Chikwawa and Thyolo, recharge values are expected to go up by up to +60%. In the late century, the values drop to baseline levels with a few areas showing elevated levels of GWRch of up to +15%. HadGEM2-ES shows the same trend as GFDL-ESM2G except where a surplus in GWRch is predicted, it is approximately 2 times higher than GFDL-ESM2G. MPI-ESM-LR predicts on average about +20% increase in GWRch, in the 2020s and minimal changes (0 to +5%) in GWRch in the mid- to late-century.

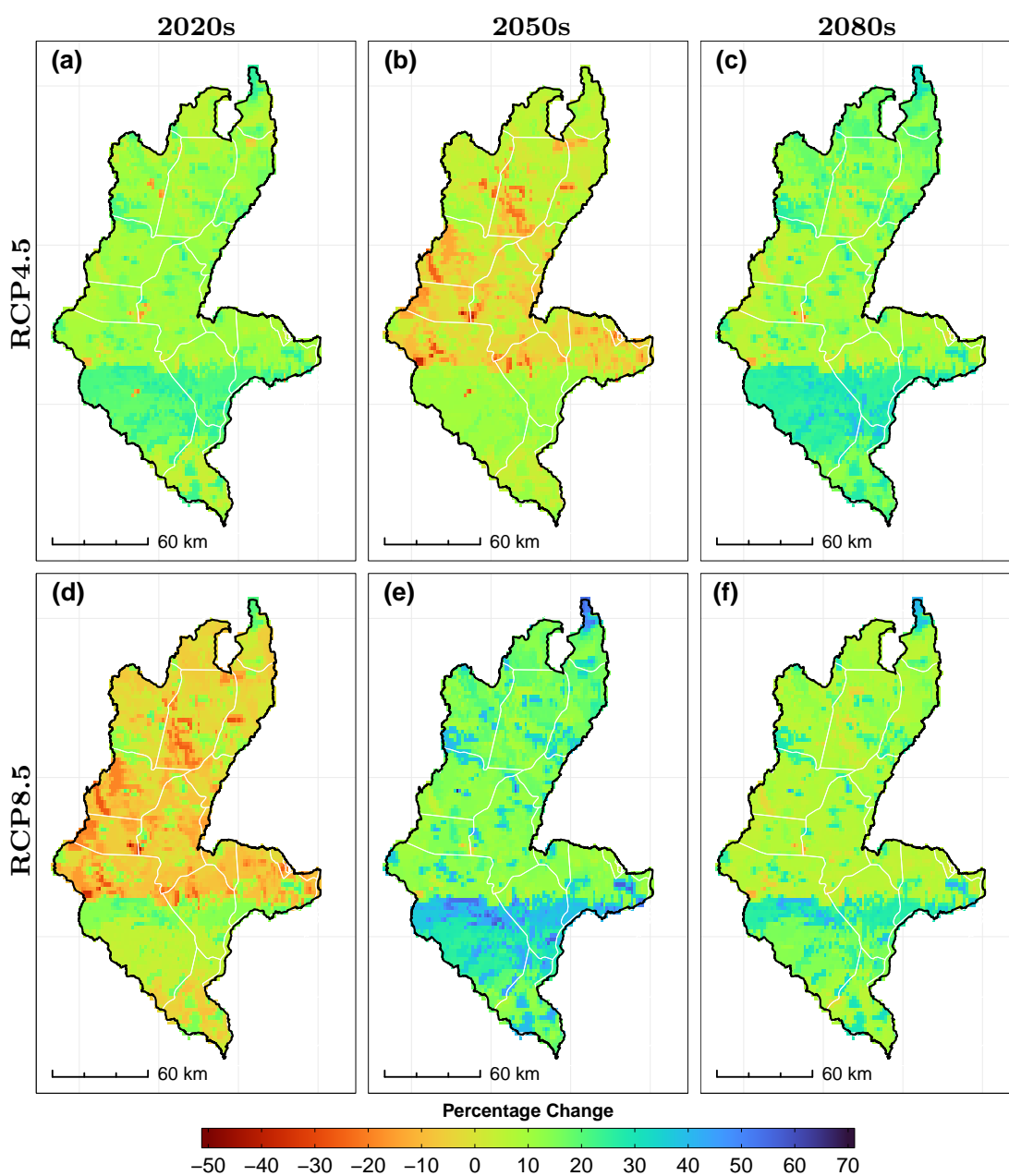
Similarly, under RCP8.5, results vary from one GCM to another. Also, the direction of change for each time slice is not in agreement among the GCMs. The percentage differences in GWRch between the future periods and the baseline varies between -20% to +30% for most of the basin.



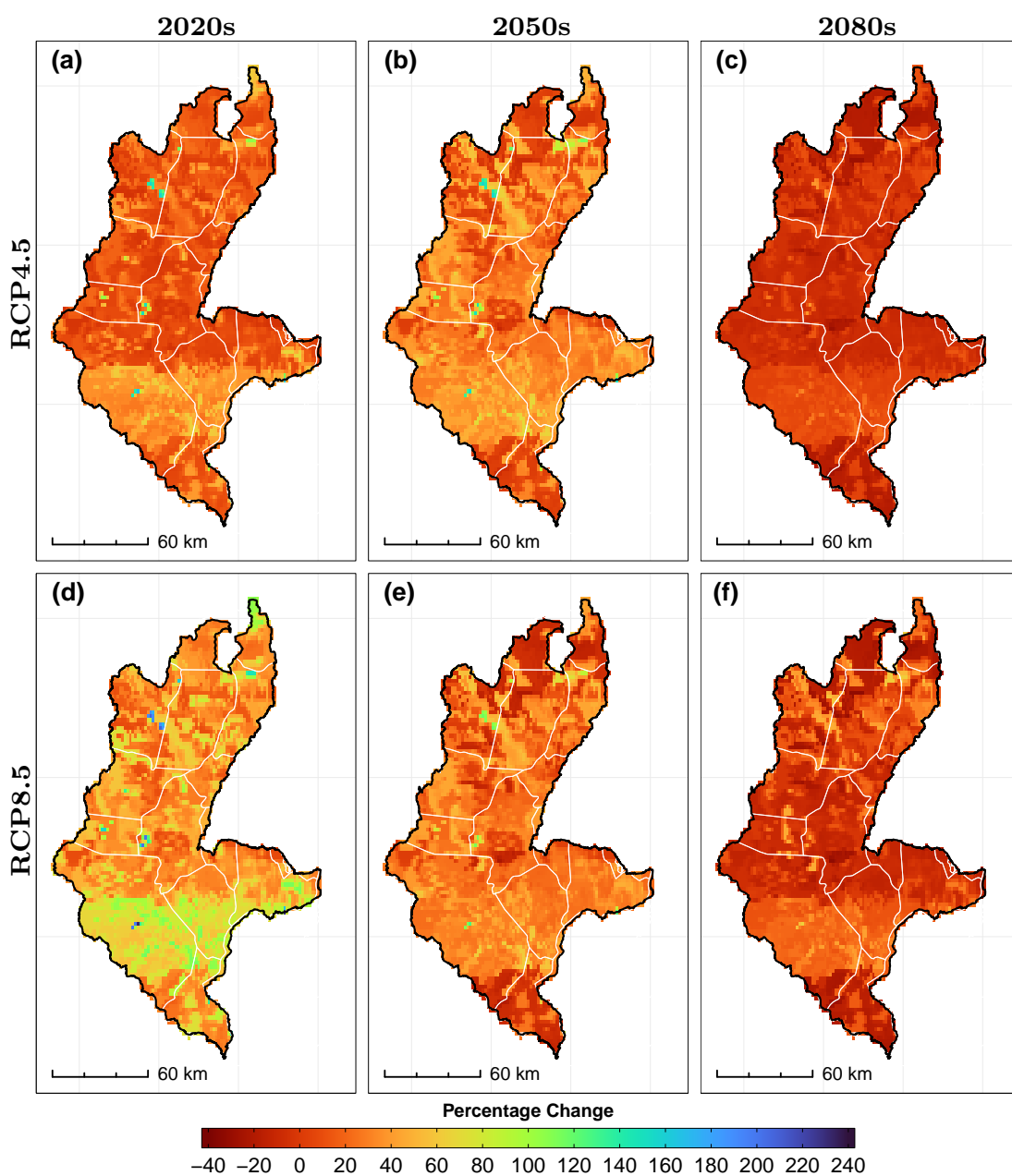
**Figure 6.16** Percentage differences in groundwater recharge (GWRch) as simulated by SWAT-MODFLOW between the baseline period and future periods in the SRB. MODFLOW was coupled with a SWAT model forced with the BCC-CSM1-1-M GCM



**Figure 6.17** Percentage differences in groundwater recharge (GWRch) as simulated by SWAT-MODFLOW between the baseline period and future periods in the SRB. MODFLOW was coupled with a SWAT model forced with the CCSM4 GCM

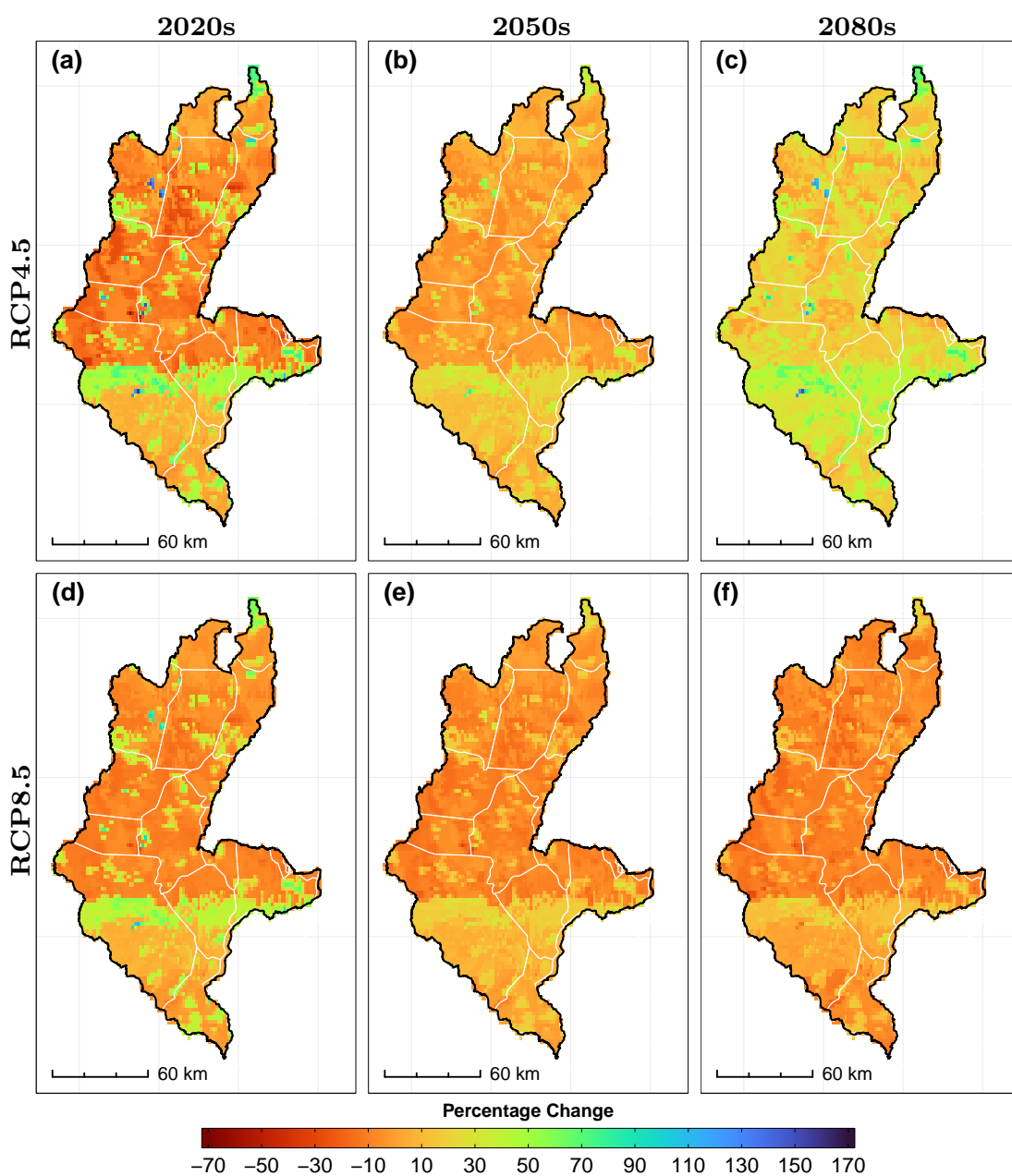


**Figure 6.18** Percentage differences in groundwater recharge (GWRch) as simulated by SWAT-MODFLOW between the baseline period and future periods in the SRB. MODFLOW was coupled with a SWAT model forced with the CNRM-CM5 GCM

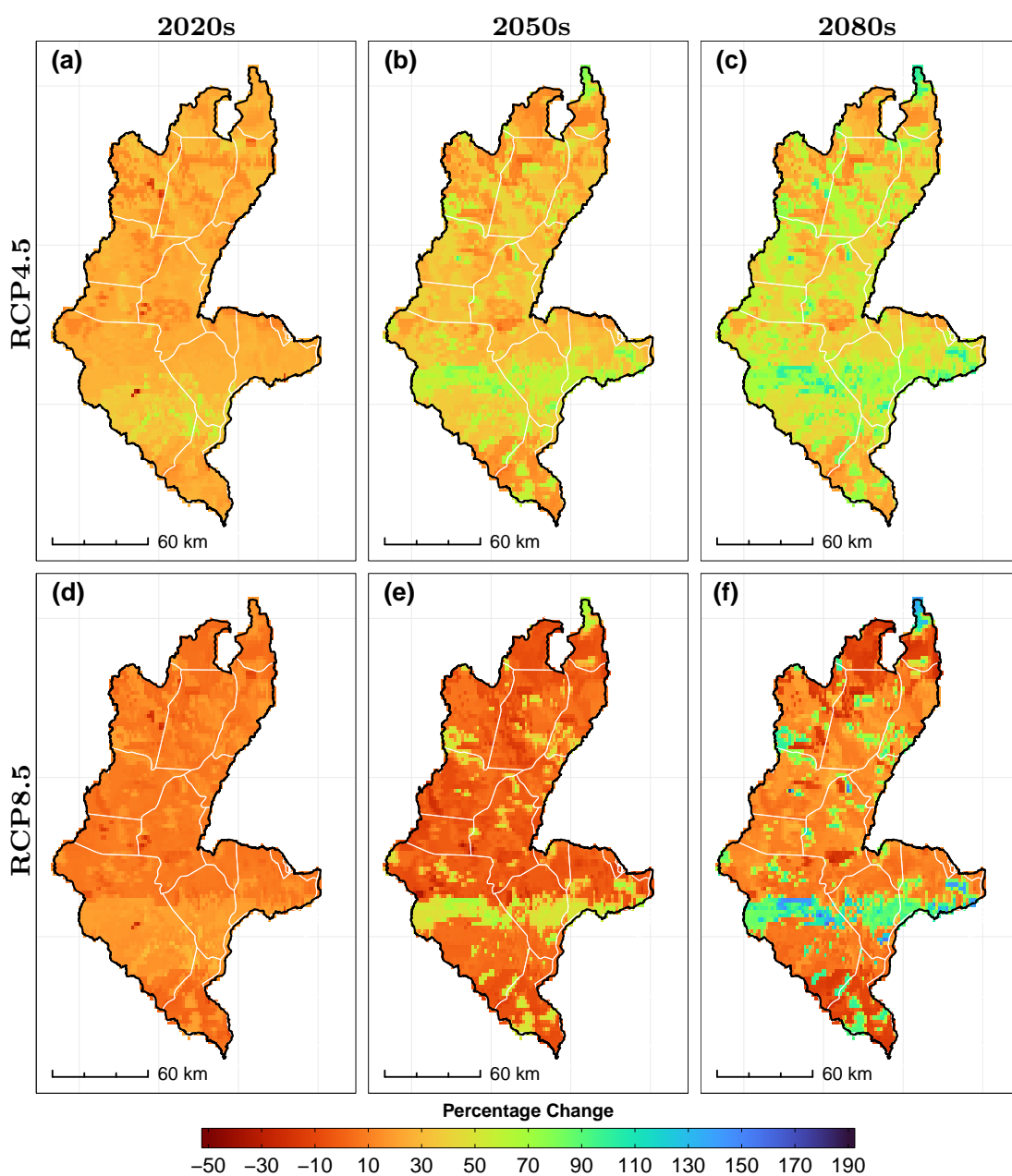


**Figure 6.19** Percentage differences in groundwater recharge (GWRch) as simulated by SWAT-MODFLOW between the baseline period and future periods in the SRB. MODFLOW was coupled with a SWAT model forced with the GFDL-ESM2G GCM





**Figure 6.20** Percentage differences in groundwater recharge (GWRch) as simulated by SWAT-MODFLOW between the baseline period and future periods in the SRB. MODFLOW was coupled with a SWAT model forced with the HadGEM2-ES GCM



**Figure 6.21** Percentage differences in groundwater recharge (GWRch) as simulated by SWAT-MODFLOW between the baseline period and future periods in the SRB. MODFLOW was coupled with a SWAT model forced with the MPI-ESM-LR GCM

In Chapter 4, it has already been demonstrated that, due to the structural differences in the GCMs and the inherent variability and uncertainty associated with rainfall simulation in hydrometric studies, results may differ from one study to another depending on a number of factors – some of which are GCM selection and the baseline period selected for model training and future comparisons. In keeping up with one of the sub-aims of this thesis – that of testing the most suitable way of combining GCMs and hydrologic models for impact assessments – results of the ensemble models that were considered in this study are presented here. Particularly, a comparison is made between two sets of results, namely a) a simple average of the separate hydrologic (SWAT-MODFLOW) models (hereinafter SRB-SWATMFEMM) and b) results of an integrated hydrologic model whose SWAT model is forced with the SRB-EGCMM.

Under RCP4.5, SRB-SWATMFEMM (Figure 6.22) predicts no change in GWRch up to an upper limit of +15% change in the 2020s for most of the basin. The percentage changes in the high recharge zones referred to earlier are expected to be as high as +40% but mostly within +15% to +25%. The SRB-EGCMM forced model (Figure 6.23) gives a similar prediction of +15% increase in recharge for most of the basin with a few isolated areas showing a minor decrease of about -15%. Similarly, some areas in the southern part of the basin are predicted to receive up to +25% more recharge than baseline. In the 2050s, up to +10% more GWRch is expected for most parts of the basin as predicted by both models whereas in the 2080s, this model predicts at least +5% higher GWRch than SRB-SWATMFEMM which generally predicts up to +15% increase in GWRch for most of the basin.

Under RCP8.5, SRB-SWATMFEMM generally predicts a fluctuation in GWRch

of between -5% to +5% in the 2020s, up to +10% in the 2050s and no change for most of the basin in the 2080s compared to baseline conditions. The SRB-EGCMM forced IHM predicts a range of +10% to +25% increase in GWRch in the 2020s, a slight drop of +5% to +10% in the 2050s and a similar range of +5% to +12% in the 2080s.

Comparing the two models, it can be concluded that averaging the separate IHMs resulted in a reduction of the biases inherent in each model. Moreover, as established in Chapter 5, the SWAT models are sensitive to the climate data input and hence uncertainty propagates from the GCMs all the way to the hydrologic processes within the SWAT models. Thus, the importance of using multi-model ensembles in IWRM models as demonstrated previously by many other studies in the literature cannot be overemphasized.

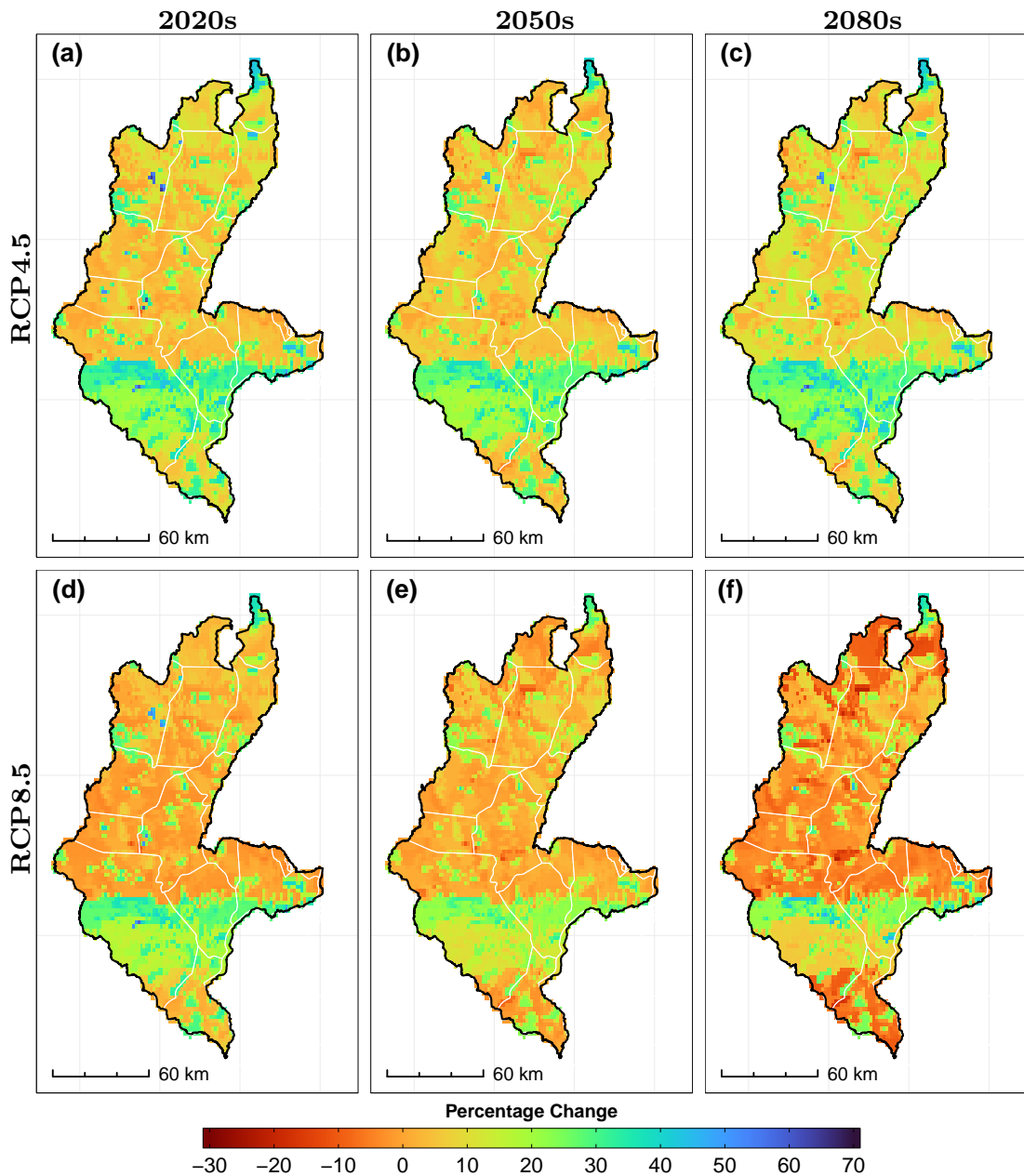
Groundwater recharge changes in the basin are not significant in most parts of the SRB. While there were some slight variations in predictions among the IHMs, results from the SRB-SWATMFEMM and SRB-EGCMM forced IHM are in agreement with each other at basin-scale. Furthermore, these results are in agreement with those of Cuthbert et al. (2019b) who show that groundwater in sub-Saharan Africa, contrary to previous studies (e.g. Jimenez Cisneros et al., 2014), is more resilient than previously thought, especially in arid to semi-arid areas. In areas that are humid to sub-humid and where the water-table is shallow, their study suggests pumping of groundwater could potentially create “room for recharge to occur” (Cuthbert et al., 2019b) as these areas show the least potential for GWRch. In contrast, in arid and semi-arid climates, recharge potential and groundwater response time (GRT) is higher than in more humid climates. The results here indicate that higher recharge is expected in areas that receive less

than 800mm of rainfall annually (parts of Chikwawa and Thyolo) than in areas where annual rainfall is in excess of 1200mm. Thus groundwater resources in these areas could very well be less vulnerable to climate change impacts on precipitation and could potentially take up to a century before equilibrating or reacting to current anthropogenic effects on climate (Cuthbert et al., 2019a).

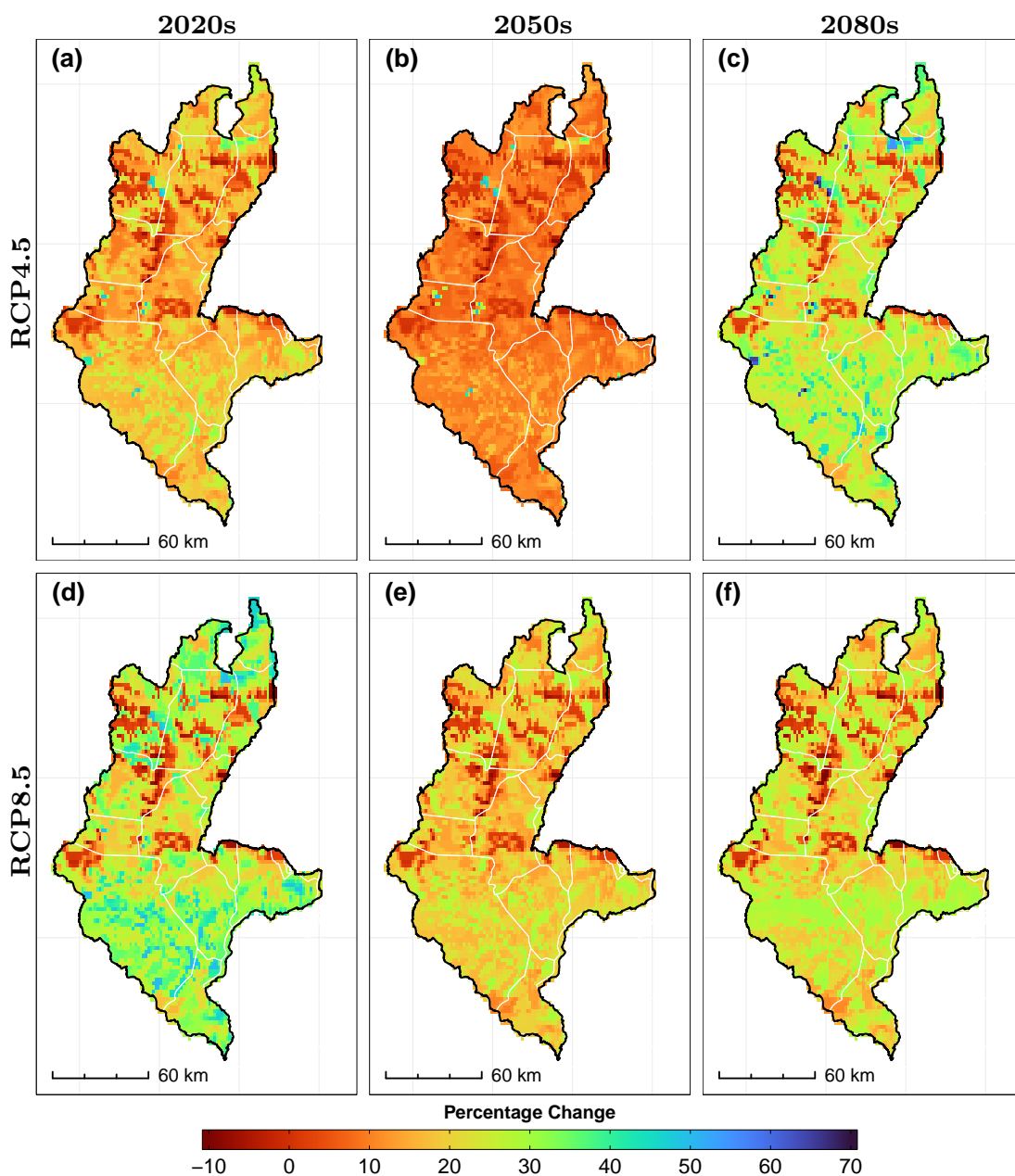
Another often overlooked insight from the study of Cuthbert et al. (2019a,b) is the importance of losing rivers and streams in recharging aquifers. A possible explanation of why the regions in Chikwawa could be expected to receive higher amounts of recharge when compared to the rest of the basin is related to the higher probability and prevalence of floods in these areas as opposed to higher areas and thus receive a lot of water from the highlands via several pathways such as “flash-like” streamflow culminating into floods in this region and also via groundwater flow from the north. These areas are prone to flooding during intense episodic rainfall events which could lead to increased recharge during the flood periods. Thus, the importance of the intensity of rainfall and/or the occurrence of floods are important pathways for aquifer recharge in arid and semi-arid regions (Cuthbert et al., 2019b). In Chapter 4, results indicate rainfall in the SRB is expected to increase slightly at an annual scale but more importantly, on average a 20% increase in rainfall is expected in the wet months of December–January. While climate change is expected to bring along extreme precipitation events (e.g. intense rainfall and floods), groundwater in the shallow and deep aquifers is expected to be replenished during these extreme episodic rainfall events.

From a climate preparedness and adaptability point of view, it is recommended, that during intense rainfall events, measures should be put in place to capture and store flood flows so as to enhance “focussed” (see Section 2.6) groundwater

recharge in the SRB (Cuthbert et al., 2019b) via a known strategy referred to as ‘managed aquifer recharge’ (MAR).

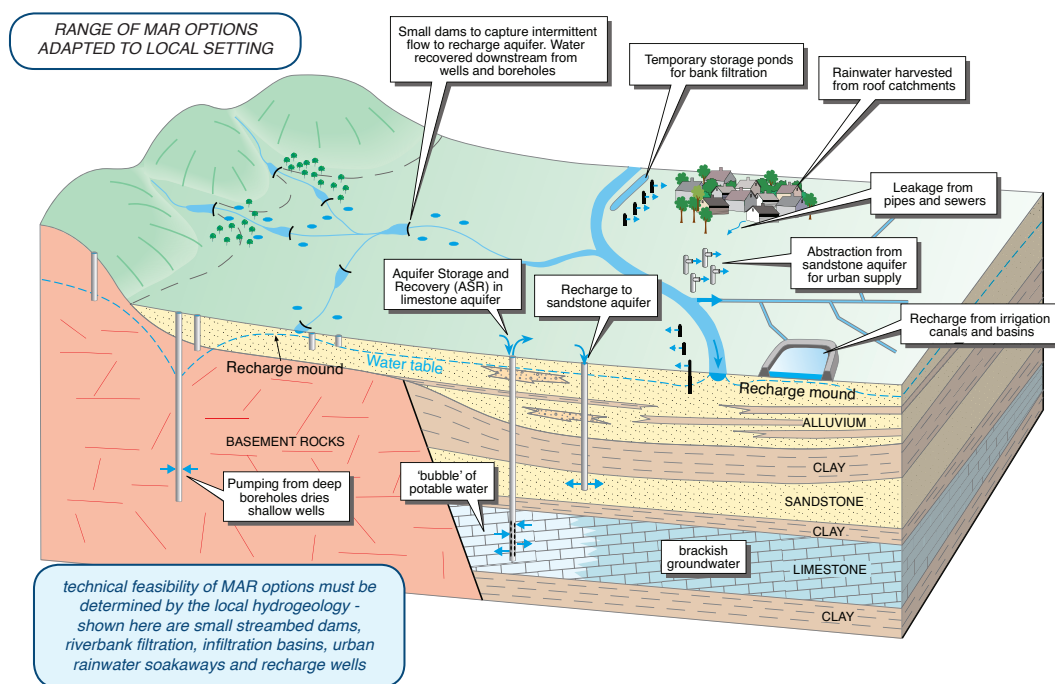


**Figure 6.22** Percentage differences in groundwater recharge (GWRch) as simulated by SWAT-MODFLOW between the baseline period and future periods in the SRB. Results are a simple average of the models (SRB-SWATMFEMM) presented in Figures 6.16 to 6.21



**Figure 6.23** Percentage differences in groundwater recharge (GWRch) as simulated by SWAT-MODFLOW between the baseline period and future periods in the SRB. MODFLOW was coupled with a SWAT model forced with the SRB-EGCMM model

MAR is widely documented in the literature (e.g. Assaf, 2009; MacDonald and Calow, 2009; Scanlon et al., 2012; Shah, 2009; Usher et al., 2006; Wu et al., 2012) as an efficient method of recycling storm-water or treated sewerage effluent (Dillon et al., 2010) in developed countries and regions such as the USA, Canada, Australia and Europe. MAR is suitable for both rural and urban water supply needs and has great potential for contributing to water security especially under the threats posed by climate change and variability.



**Figure 6.24** Managed Aquifer Recharge options that can be adopted by water management agencies (Fig. 3 IAH, 2019).

Figure 6.24 depicts the range of MAR options that can be adopted by national agencies and adapted to their local settings. A *suitability for MAR* mapping exercise is recommended for the SRB to identify regions where efficient focussed recharge is feasible via MAR schemes. In the Lower Shire Valley (LSV), the prevalence of alluvial deposits leaves limited space for storage of storm-water



since groundwater levels tend to be shallow in these deposits. However, where groundwater levels are indicated to be at depth, MAR is recommended as these aquifers have good storage and transmissive capacities (Gale, 2005).

#### **6.4.6 Impacts of Land-use/Land-cover**

While there is particular emphasis on reforestation in Malawi, there seems to be no proper guidance from professionals in the hydrology/hydrogeological and ecological sectors on how this is to be implemented. In the first instance, an understanding of the soil type and its memory (i.e. how well soils preserve the properties of the forest with respect to hydrology after clearing), needs to be established. Secondly, the rooting characteristics, which are important for groundwater recharge, need to be understood before a species of plants is adopted in the rehabilitation process. For example, it has been documented that eucalypts are capable of mining groundwater up to a depth of 18 m in the subsurface and thus lead to dramatic changes in soil moisture content and groundwater storages (Bloeschl et al., 2007).

Even though the results of this research were premised on a stationary LU/LC, the importance of changes in LU/LC on catchment processes such as evapotranspiration that has been demonstrated (i.e. higher ET) to be a cause of decreased groundwater recharge in warmer climates (Aslam et al., 2018) cannot be ignored. Thus an important recommendation is for relevant authorities to ensure that LU/LC is controlled and preserved for optimised groundwater recharge. In reality, this is much easier said than done as a balance should be struck between ecological conservation and agricultural/livelihood needs. For example, the main cause of deforestation in Malawi is due to the search for arable land by peasant farmers

and also due to the indiscriminate cutting of trees for charcoal which is a major source of energy in most communities. An emphasis again is made of the need for increased capacity in tackling complex and wicked problems associated with the water-energy-food (WEF) nexus.


### 6.4.7 SRB Groundwater Recharge Modelling Summary

A summary of the areal percentage change in groundwater recharge with respect to the baseline period in the SRB is provided in Table 6.4.

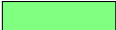
**Table 6.4** Summary areal mean percentage change in projected groundwater recharge (GWRch) in the SRB with respect to the baseline period. Changes within  $\pm 10\%$  of baseline values are considered to be insignificant (green boxes) whereas changes above  $+10\%$  (red boxes) and below  $-10\%$  (blue boxes) are considered to be significant.

GCM	Scenario					
	RCP4.5			RCP8.5		
	2020s	2050s	2080s	2020s	2050s	2080s
BCC-CSM1-1-M	-0.5	-1.5	-6.0	-24.2	-25.7	-15.1
CCSM4	14.3	-0.1	8.1	13.4	13.7	-1.1
CNRM-CM5	12.6	2.0	15.6	-1.8	20.7	12.0
GFDL-ESM2G	20.0	28.7	-3.6	47.5	23.4	2.7
HadGEM2-ES	4.1	6.3	24.4	3.3	-0.7	-4.0
MPI-ESM-LR	25.6	35.1	47.3	10.5	7.4	22.8
Ensemble (SRB-EGCMM)	16.1	9.2	24.0	25.3	17.6	20.4
Ensemble (SRB-SWATMFEMM)	12.7	11.7	14.3	8.1	6.5	2.9


**Increase**



**Insignificant Change**



**Decrease**



Here, it can be seen that the models indicate significant increase in groundwater recharge in at least 50% of the time horizons while the rest indicate no significant change from baseline values. BCC-CSM1-1-M is an outlier as it is the only model that projected significant decrease in GWRch under RCP8.5. Under RCP8.5, the ensemble models are not entirely in agreement with the magnitude of change

especially under RCP8.5. Again, the areal mean values do not reflect the entire picture as they are influenced to a great degree by outliers and extreme values.

## 6.5 Limitations

As is prevalent with any modelling exercise, the following limitations were identified with modelling efforts in the SRB and DB;

- For the SRB models, the construction of the regional groundwater model did not take into consideration the occurrence of geological faults that may have a bearing on localised flows, GW/SW interactions and groundwater recharge.
- To reduce the time and computational burden due to the vast extent of the modelled area, cell sizes were deliberately exaggerated. This could lead to a loss in information and accuracy especially with respect to GW/SW interactions. However, other studies that involved the use of isotope data and sub-regional models support the conclusions made in this chapter and thus the results can be used as an initial estimate and understanding of the complex groundwater processes in the SRB.
- For the DB and SRB, only one conceptualization was used but studies have shown that this can lead to ‘underdispersive and prone-to-bias predictions’ (Rojas et al., 2008). Thus future modelling efforts beyond the scope of this thesis will endeavour to reduce conceptual model uncertainty by considering multiple representations of the subsurface hydrology.

## 6.6 Chapter Summary

This chapter is a culmination of the attempts in this thesis to model the atmospheric and terrestrial phases of the hydrologic cycle. SWAT models described in Chapter 5 were coupled with MODFLOW-NWT in order to achieve this task. Here, again, a similar methodology was applied in both the DB and SRB in line with objective number 5 presented in Section 1.3. According to the results presented in this chapter, the SWAT-MODFLOW model can be used successfully by water resources managers to understand and quantify risk and vulnerability to surface- and groundwater resources.

In the case of the DB, a large portion of the Locharbriggs Sandstone Formation and the northernmost portion of the Doweel Breccia Formation are projected to experience a slight decrease in groundwater recharge under RCP4.5 (up to -6%) and significant decrease under RCP8.5 (up to -22%). The rest of the basin is projected to experience little to no change in groundwater recharge under both RCP4.5 and 8.5. However, recharge pathways in the DB have been documented to be heavily controlled by flow through near vertical fractures particularly in the north-west and other areas with the basin. Thus, the results presented in this chapter may not fully capture all the mechanisms that control recharge through the Quaternary and Permian deposits. From a general perspective, there is no significant change in groundwater recharge from baseline values except towards the late-century under RCP8.5. Thus, the threat to future groundwater availability in the DB due to anthropogenic climate change is minimal based solely on the ability of the aquifer to recharge itself. Other external stresses on the aquifer such as uncontrolled and indiscriminate water abstractions may lead to unsustainable

water levels.

Results indicate that groundwater resources, especially in the low-lying alluvial formations of the SRB, are more resilient to climate change than previously hypothesized. Shallow basement and alluvial aquifers in the SRB generally depict temporal fluctuations in response to seasonal precipitation trends. Groundwater recharge to the deeper aquifers may exhibit a different recharge mechanism altogether. While BWF in the central and southern parts of the SRB is indicated to be in a slight deficit according to results presented in Chapter 5, there is potential for increased groundwater recharge to the shallow but especially deeper aquifers in these regions. Under RCP4.5 groundwater recharge is expected to increase by up to +30% by mid- to late-century in the southern region of the SRB while recharge in the rest of the SRB is expected to be similar to baseline values. Under RCP8.5, groundwater recharge south of the SRB is expected to increase by up to +20%. Groundwater recharge in the rest of the basin is expected to remain unchanged from baseline values except in the mid- to late-century when recharge is expected to decrease by up to -10%. Thus, groundwater may act as a buffer against droughts in rural communities of the SRB if it is managed and exploited in a sustainable manner. It should be mentioned, however, that these results reflect future changes with the condition that LU/LC is held constant. Changes in LU/LC and abstraction scenarios which are unsustainable could result in potentially different outcomes than presented here.

It terms of the modelling aspect, it has been shown that integrated modelling is an approach that can be applied both in data-rich and data-sparse regions as an initial step in understanding GW/SW interactions and as a decision-making tool in the allocation of surface- and groundwater resources. Additionally, it

has been shown that integrated modelling can improve the representation of the hydrologic system and consequently confidence in the projections. This is a crucial requirement for water managers and policy makers alike since insights gained from such scientific endeavours impact entire communities and nations from a policy perspective. Moreover, the IWRM community can benefit greatly from knowledge generation and sharing of how hydrological processes in different settings and environments evolve in the presence of climate change.

Uncertainty in the results and non-agreement between models for the same GCM scenarios remains a challenge. Uncertainty in the results are probably due to what many other researchers have unanimously observed, namely choice of GCM, choice of downscaling method and choice of representative concentration pathway (or emission scenario in some cases) (Smerdon, 2017).

In view of the foregoing, the following recommendations have been proposed;

1. There is need to introduce deliberate and aggressive hydrometric data collection in the SRB in order to increase current understanding of the complex system dynamics in the region. In addition to gaining insights about the quantity of groundwater in any region, high integrity groundwater level monitoring data is also required for adequate calibration of groundwater models. Currently, the MoAIWD has assessed that the few groundwater monitoring boreholes in the SRB are either vandalised, inaccessible, clogged or simply not maintained. In order to enhance IWRM efforts in the SRB, heavy investment in the installation of monitoring points and training of site caretakers and loggers should be prioritised.
2. The feasibility of Managed Aquifer Recharge (MAR) should be given consideration as an adaptation measure to mitigate against the impacts of climate

---

change and variability especially in the most vulnerable zones of the SRB.

*—I never guess. It is a capital mistake to theorize before one has data. Insensibly one begins to twist facts to suit theories, instead of theories to suit facts.*

Sir Arthur Conan Doyle

# 7

## **IWRM in Developing and Transition Countries - A Case of Malawi**

*The application of scientific techniques aimed at understanding and quantifying water resources availability in the Shire River Basin and the threats thereof, have yielded insights that could support the implementation of robust decision-making in the context of the IWRM framework. Challenges and opportunities for IWRM implementation and/or improvement in Malawi are discussed here.*



## 7.1 Introduction

In light of the many threats to the sustainability of water resources, there is need to revisit the issue of IWRM and its application, especially in developing and transition countries. While it is true that there are challenges of IWRM application are more pronounced in developing and transition countries, there also exists many opportunities for applying some of the solutions discussed and proposed in this chapter to IWRM challenges in such regions.

Thus far, in trying to meet the objectives set out for this thesis, the focus has been limited to the quantification of surface and groundwater resources at the exclusion of other equally pressing and important aspects of SDG 6. Hopefully, through the pages of this chapter, IWRM needs and challenges in the face of climate change in southern Malawi can be highlighted. From the results presented in Chapters 4 to 6, it has been shown that climate change is a potential threat to water security in the SRB. Interventions are needed to ensure that the SRB and the entire Malawi attains SDG 6 by 2030. A recent report by UN-Water (2018) has indicated that “at current progress SDG 6 is not on track to be achieved by 2030”. Most of the challenges cited in their report resonate with IWRM challenges that have been identified in Malawi and other developing nations. In this chapter, IWRM challenges in Malawi that can hamper the implementation of interventions suggested in the preceding chapters are discussed and possible solutions offered.

## 7.2 Overview of IWRM Challenges in Developing Countries

At the very core of the IWRM paradigm is the desire and aim to develop coherent policies that will guide the distribution of freshwater resources in an equitable and sustainable way (GWP, 2011). This means adopting an approach that recognizes the integration between water and parallel policy sectors ((Benson et al., 2015)) such as energy, food and climate change (hence the *nexus* approach discussed in Chapter 2). Inevitably, it is not difficult to immediately see the need for trans-disciplinary assessment of competing needs within the IWRM and/or WEF nexus paradigms. For example, among the competing water needs in the SRB is hydropower generation, irrigated agriculture and domestic water supply. These different sectors need to work together to ensure sustainable distribution and usage of water resources in the face of imminent water scarcity.

From a general perspective in developing countries such as Malawi, for IWRM to be successfully implemented, there is need to consider the strengthening of human resources development (Al Radif, 1999), development of infrastructure for the monitoring and control of water resources and establishment of institutions that will superintend the implementation of IWRM objectives and describe normative procedures for integrating the many aspects of IWRM at policy, economic and scientific levels. Many studies (e.g. Allan and Rieu-Clarke, 2010; Braune and Xu, 2008; Swatuk, 2005) have highlighted the important role of government and governance structures in the successful implementation of IWRM. Thus, here, we reiterate the need for sectoral and cultural reforms within the GoM governance structures with respect to IWRM needs. While a lot of progress has been made

by both governmental and non-governmental players in the IWRM space and ultimately towards the attainment of SDG 6 in Malawi, a lot of ground is yet to be covered before this is a reality. In the following sections, these challenges are discussed with consideration of the potential threats to water resources in the SRB that have been uncovered in the preceding chapters.

## **7.3 Technical and Institutional IWRM challenges in Malawi**

### **7.3.1 Capacity Building Needs**

A study by Mkandawire and Mulwafu (2006) revealed a scarcity of well trained water resources personnel and professionals in both public and private sector organizations. The study highlighted that most training institutions in Malawi do not offer courses in IWRM proper and that most respondents in the survey from the government and private sectors received some aspects of IWRM training from meetings and workshops (Mkandawire and Mulwafu, 2006). Of note is the authors' recommendation for Malawi to deliberately engage in capacity building by way of equipping technicians and other water personnel with formal IWRM training, as opposed to the sole reliance of donor agencies or other professional networks to provide the required training and equipment (Mkandawire and Mulwafu, 2006).

The Water Resources Act of 2013 and the National Water Policy (GoM, 2005) are key pieces of legislation and policy/procedure respectively for management of water resources in Malawi. The former supersedes the 1969 act and provides updated guidelines on the management of water resources in Malawi including

the establishment of the National Water Resources Authority (NWRA), whose main duty is to superintend the development and management of water resources in Malawi. The latter acknowledges “IWRM as the basis for sustainable water development” (Chidammodzi and Muhandiki, 2017), the application of which is specified in the 2013 Act. This is an important step in the successful implementation of IWRM in Malawi. However, as noted by Chidammodzi and Muhandiki (2017) in a recent study, the main IWRM challenges in Malawi are related to (i) “inadequate awareness of IWRM and lack of motivation among water professionals”, (ii) “lack of specialized training in water institutions”, (iii) “lack of human resources”, (iv) “irresponsibility of officials” and (v) “lack of IWRM models”. Addressing these challenges should be one of Malawi’s most urgent needs but should not be treated as a panacea for IWRM challenges and shortcomings. Rather, the process itself should be seen as a learning expedition which should be refined iteratively until the attainment of SDG 6 by 2030. In this thesis, lack of quality climate and streamflow records has been acknowledged and cosmetic treatment of the data applied before hydroclimatic models were developed. One of the reasons for poor ground truth data, *inter alia* (see also Section 3.6), is the lack of personnel to record readings and maintain malfunctioning instruments. Thus, addressing operational and capacity needs in this area can positively impact environmental data collection and hydroclimatic modelling campaigns in the SRB and Malawi at large.

### **7.3.2 Limited Availability of Ground Truth Data**

The lack of reliable streamflow gauging station records in Malawi and the SRB in particular presents a lot of challenges when it comes to water resources management

and modelling and implementation of adaption strategies. A quick browse through the GRDC catalogue reveals a reasonable number of gauging stations across the Malawi hydrologic network. However, one quickly gets frustrated at the numerous gaps in the streamflow records and thus rendering them unsuitable for identification and interpretation of long-term hydrological variability and change. While attempts were made in this thesis and other works (e.g. Mwale et al., 2012) to obtain complete streamflow records by use of infilling techniques, care has to be applied to avoid the potential introduction of biases and unwanted signals into the data. Furthermore, data cleaning and preparation, while unavoidable and certainly a prerequisite to most modelling tasks, requires an enormous amount of effort on the modeller or data analyst to ensure ground truth data is validated and that the signal in the actual observations is conserved following the application of infilling and/or other time-series analysis techniques. This, often, is an unwelcome distraction to the modeller or scientist from focussing on the objectives for which ground truth data was collected in the first place. Thus, as already mentioned, establishment of more weather and water monitoring stations equipped with state-of-the-art instruments and skilled operators is of supreme importance to alleviate this challenge.

### 7.3.3 Policy Coherence Issues

IWRM in the context of climate change introduces extra complexity with regard to policy formulation and coherence across multiple sectors. For example, climate adaptation strategies and related policies between the agricultural and water sectors need to be interlinked as climate change introduces interacting challenges across the WEF nexus as discussed in Section 2.4 (England et al., 2018). A multi-

sectoral adaptation planning paradigm is essential when dealing with the cross-cutting issues associated with climate change. According to a study by Stringer et al. (2014), the importance of cross-sectoral partnerships and collaborations in the management of climate change impacts have been recognised by the establishment of inter-ministerial climate change committees and task forces in Southern African countries including Malawi. However, in the particular case of Malawi, England et al. (2018) note that there are challenges with “institutional and governance arrangements” aimed at tackling climate change adaptation strategies. According to the study, the main issues identified were related to 1) limited use of climate information (also highlighted by Vincent et al. (2017)) 2) policies with different time-frames and ages across sectors and 3) “the lack of integrated planning between national policies and international environmental agreement communications” (England et al., 2018; Stringer et al., 2014, 2010). With regard to the first issue, Vincent et al. (2017) observes that only 5–10 day and seasonal forecasts are being used in government decision making and that there is no evidence of any department using “*short-, medium- or long-term climate projections in their current decision making, despite the availability of regionally downscaled information from various sources*”. The authors further argue that more relevant and useful information include a) the distribution of rainfall within a season b) 2–3 week lead-time climate forecasts c) extreme event projections in the short term (1–5 years) and d) climate projections in the medium term (typically 6–20 years). Use of climate projections enable water professionals to predict and quantify the availability and occurrence of water resources. Thus, at the very least, agricultural, water and energy sectors need to collaborate to ensure that they are in agreement with respect to water availability, allocation,

management and adaptation planning.

## 7.4 Way Forward

Based on results from this research, recommendations have been made that will highlight areas for improvement in terms of implementation of IWRM in the SRB under the threat of climate change. It has long been recognised that IWRM is not meant to be a prescriptive tool but rather an approach that should guide water resources managers and other relevant stakeholders in their pursuit for better water resources management (Chidammodzi and Muhandiki, 2017). Similarly, the recommendations made here are based on experience and international best practice; they are in no way prescriptive but can be used as a guide to enhance the use and assimilation of climate and hydrologic data into water policy formulation and adaptation planning as guided by the IWRM framework.

### 7.4.1 Data Collection and Sharing

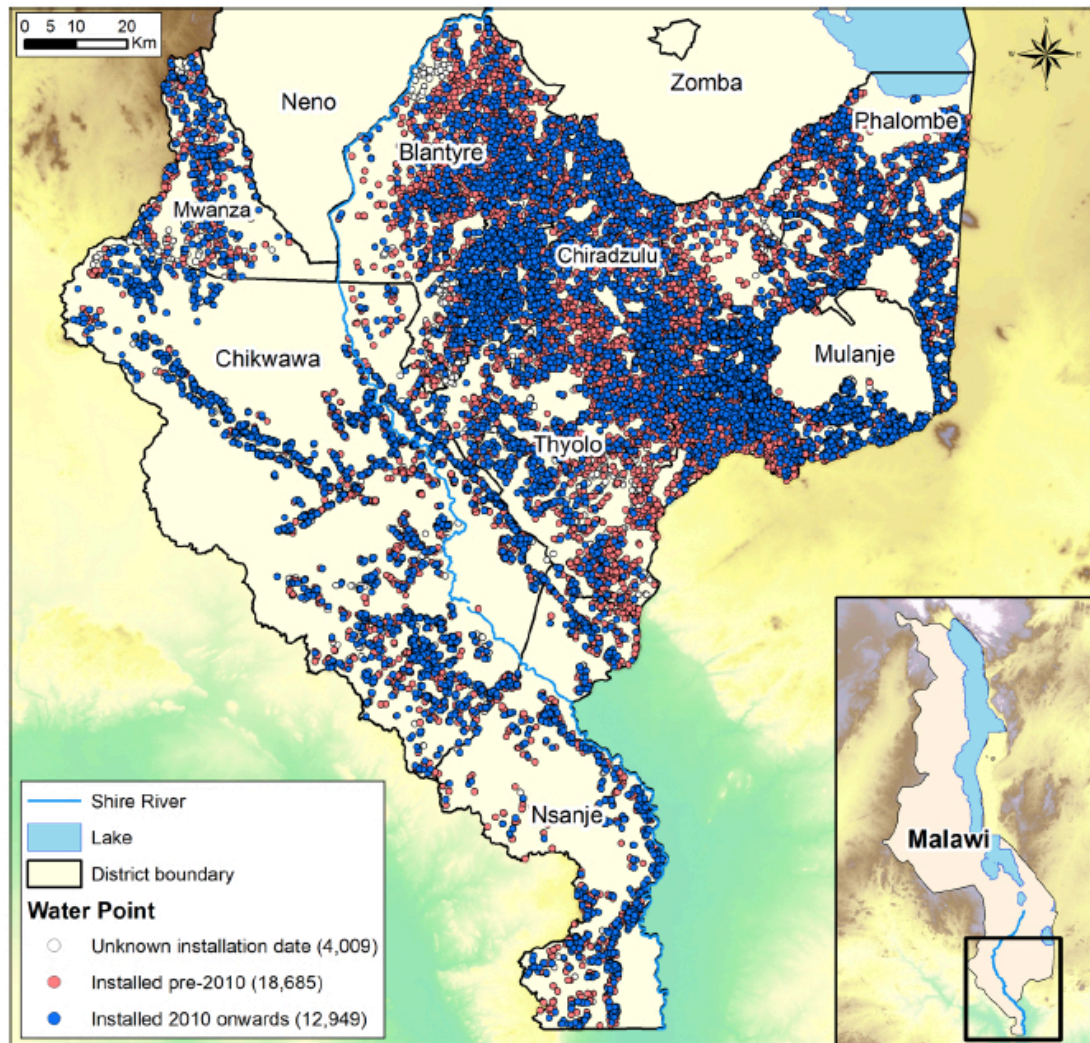
Understanding climate change and other societal problems related to the WEF nexus requires concerted efforts by various scientists and institutes to both generate and share hydro-meteorological and related data. Discovery science, especially in poor and developing regions, should be given the utmost attention as it is the very foundation of scientific inquiry in the hydrological sciences and forms the evidence base for sustainable water resources management (Tetzlaff et al., 2017). The evidence from this research work in Malawi shows that there is urgent need of data generation that may be useful in understanding environmental systems and their evolution in the face of climate change. The main challenge that was

encountered in the SRB with respect to hydrological modelling is the limited and in some cases non-existent groundwater level monitoring data. This presents challenges when it comes to groundwater model calibration. Continuous daily or monthly groundwater level data of sufficient length (typically 20 years or more) is required for adequate calibration of groundwater models. Another issue that is equally important when it comes to groundwater modelling is the density of groundwater monitoring points hence the need to install multiple groundwater monitoring points across the basin.

While a lot of effort from various stakeholders has been directed towards ensuring that the SRB is able to cope with the adverse effects of climate change by 2030 in line with SDG 6, more effort is required to build capacity on the technical and planning aspects of IWRM. There is evidence of attempts to collect hydrometric data in the past, particularly streamflow data across the stream network in Malawi. However, this data is encumbered with a lot of gaps and inconsistencies so that a lot of treatment is required before working with it. For example, in Chapter 5, only three stations free of the influence of controlled flows from Lake Malawi via the Kamuzu Barrage were used to calibrate the SRB SWAT model. A lot more streamflow gauge records of high integrity would have enhanced the quality of the model, as opposed to the current available records that are plagued with a lot of gaps. Consequently, uncertainty in the SRB simulations is more pronounced than in the RNC. Thus investments in water quantity and quality monitoring in the basin should be of paramount priority in addition to the efforts that are concentrated on providing potable water to rural communities. Capacity building in terms of training personnel to install, record and maintain a network of streamflow gauges across developing countries such as Malawi should



be given urgent attention. Similarly, installation of groundwater monitoring wells and the subsequent recording of high quality groundwater quantity and quality data should be prioritised in the interest of quality and timely science.



**Figure 7.1** Water points in Southern Malawi mapped by the CJF between 2011 – 2018 (Fig. 1, Miller et al., 2018)

In the past decades, there has been a lot of aid to the WASH sector in Malawi from the donor community to lessen the burden of access to clean water especially in rural areas. Consequently, a lot of boreholes have been sunk over the years by various donors to alleviate this pressure. However, there has been little to no

follow-up by the donor community in terms of finding out what the impact of these interventions have been on the communities. There are a few organisations have invested resources to monitor borehole functionality in these areas post-installation. WaterAid (2003 – 2005) and Engineers Without Borders – Canada (2009 – 13) are among the few organisations that have endeavoured to establish water point database systems (Miller et al., 2018). What should be encouraged is the establishment of a platform from which such data could be shared and accessed by various stakeholders.

In the last eight years, the Scottish Government Climate Justice Fund (CJF) under the Water Futures Programme has worked with the Malawi Ministry of Irrigation, Agriculture and Water Development (MoAIWD) to not only help Malawi achieve SDG 6 by providing infrastructure and access to fresh water supplies in rural Malawi, but to also collect valuable data (e.g., Figure 7.1) from new and existing water points across southern Malawi (Miller et al., 2018). To this end, the CJF Programme in 2011 embarked on a thorough scoping exercise of all Management Information System (MIS) platforms which culminated into the adoption of *mWater*, an online MIS tool (Miller et al., 2018). Using this tool, various data such as functionality of boreholes, water point surveys, sanitation surveys, irrigation, drilling and water quality data shall be collated and made accessible to stakeholders in real time. Thus, management of water resources by relevant stakeholders can be enhanced by targeting development and/or attention to regions of greatest need. Adoption and further development of the *mWater* tool by the wider WASH sectors is recommended by Miller et al. (2018).

Discovery science, data collection and generation in developing countries is an urgent and immediate need. The emergence of tools and technologies (e.g. machine

and deep learning algorithms) that can help organisations derive insight from complex and multi-faceted environmental data provides a unique opportunity to help develop solutions that, hitherto, seemed unattainable. The use of such technologies and innovations will spur the integration of “socio-economic and stakeholder factors” with GCMs and hydrologic models that are better suited for decision making in developing countries and other semi- to arid regions (Burt and McDonnell, 2015). The availability of ground truth and other forms of data of high integrity will help researchers improve existing and future hydrologic models and also ease the development and adoption of robust decision support systems (DSS).

## **7.4.2 Capacity Building in IWRM Sectors**

### **7.4.2.1 Skilled Workers Shortage**

As noted in Section 7.3.1, there is a shortage of skilled personnel in the Malawi WASH sectors (includes government ministries and NGOs). Consequently, efforts to collect and generate high integrity data on which most of the decisions and policies should be predicated, are frustrated. Outside other logistical challenges such as access to monitoring stations (e.g., blocked access roads, limited transportation etc.), shortages of skilled water resources personnel can be alleviated by implementing recommendations such as those of Mkandawire and Mulwafu (2006). The same challenges apply when it comes to implementation of IWRM measures especially in rural and remote areas of the SRB. This research has established that effects of climate change are more severe in Malawi, and by extension other areas of similar climate, than in temperate regions. Climate change adaptation and preparedness demands that all stakeholders such as the

GoM, NGOs and communities are all aware of the different but coordinated roles they are supposed to play. Rural communities are constantly to be engaged on the practice of sustainable water use (e.g. borehole-garden permaculture advocated for by Rivett et al. (2018)). However, most of these efforts are spearheaded by NGOs as observed by Mkandawire and Mulwafu (2006). Adequate training of personnel working in IRWM and related departments will ensure that enough manpower is on the ground to implement and share IWRM principles within rural communities in the SRB. Here, universities and other tertiary institutions will play a major role to supplement efforts being made by NGOs and the donor community.

#### **7.4.2.2 Role of the Donor Community**

Chapters 4 to 6 have highlighted possible challenges associated with rainfall and freshwater shortages in rivers, streams and lakes. Furthermore, Chapter 6 has highlighted the potential robustness of groundwater aquifers in the central portion of the SRB even under climatic stress. The donor community such as the CJF, JICA and the World Bank have funded and supported the installation of groundwater abstraction points fitted with hand pumps in rural communities of the SRB. While such efforts are welcome, they should be preceded by proper feasibility studies and robust well design and installation programmes. Multiple wells in the SRB are non-functional due to poor borehole drilling and pump installation.

In terms of training, recently the CJF programme has provided short courses to water resources personnel from the government and private sectors. Participants have been taught at a minimum, the basics of IWRM and international best practice in this sector. Shared experiences from various fora such as workshops

organised by the CJF have also helped in ensuring various IWRM stakeholders learn from the successes and mistakes of their colleagues in different regions of Malawi. There is need for other donor agencies to come on board and offer basic IWRM training in addition to installation of boreholes and other reticulation systems in rural communities. More importantly, such investments either by the donor community or GoM, should be done with full consideration of the concept of “Stranded Assets” as proposed by Kalin et al. (2019) to ensure sustainable and judicious SDG 6 investment strategies.

#### **7.4.2.3 Role of Tertiary Institutions**

Tertiary institutions such as universities and colleges should encourage the training of highly skilled IWRM personnel such as hydrologists, hydrogeologists and many other related fields and sub-fields. Where more specialized training beyond the current ability of local universities are required, training could be outsourced elsewhere or capacity built over time in both government and private tertiary institutions. The emergence of tools and paradigms to identify solutions to water problems such as IWRM and the *nexus* approach require transdisciplinary efforts in order to satisfy the water needs of interacting social and natural systems (Grigg, 2019). Thus, critical skills training for IWRM personnel should be of paramount importance especially for Malawian Government MoAIWD officials. In addition, similar to what the CJF WFP have done in recent years, exchange programmes where officials travel to learn and share experiences from first world countries should be encouraged. Short courses such as MOOCs offering water resources management and related training should be subscribed to as these can be accessed remotely.

#### 7.4.2.4 Software and Computing Infrastructure

The ubiquity of open-source hydrologic modelling software tools is a positive step in ensuring collaboration and sharing of research findings among key WASH sectors such as NGOs, Government institutions and private agencies. Commercial and proprietary software can be inhibitive expensive for many individuals and organisations in developing countries. Furthermore, collaborations between different organizations or groups would require all parties to have the same software and thus limiting or hindering participation from groups that do not have the requisite software.

Free and open-source software (FOSS) <sup>1</sup> tools commonly used and required in hydrologic modelling include but not limited to the following; QGIS (QGIS Development Team and others, 2015), SWAT, MODFLOW, HEC-RAS (Brunner, 2002), HEC-HMS (Feldman, 2000), MT3D-USGS (Bedekar et al., 2016), MT3DMS (Zheng and Wang, 1999), PRMS (Markstrom et al., 2015) and GSFLOW (Markstrom et al., 2008). In this thesis, a deliberate choice was made to use freely available software to promote reproducibility and sharing of research findings, a stance which, in recent years, has been supported by many other scientists (Baker, 2016; Mair, 2016). Scientific programming tools such as R and Python have been used extensively in hydrological and climate studies. Researchers often publish the code and associated data in repositories such as GitHub <sup>2</sup> or as supplementary material to their published papers. Often-times such scripts are finally collated and bundled into a library or package that can be installed from public code repositories along with vignettes that describe how functions in the library can be

---

<sup>1</sup>In this thesis, free software tools that are free but not necessarily open-source are included in this definition.

<sup>2</sup><https://github.com/>

applied to solve a particular problem. This is an important advantage for scientists and researchers in developing countries who have limited access to proprietary software such as MATLAB® and ArcGIS among many others. Additionally, using open-source scientific languages such as R and Python, one can easily automate the entire workflow from data collection via web-scraping to data analysis and visualization. In the R programming environment, tools such as R Markdown (Xie, 2017; Xie et al., 2018) can integrate analysis, visualization and publication so that the end result is a document or vignette complete with results and associated code.

However, adopting FOSS for IWRM scientific needs requires a lot of investment in training scientists and other practitioners in the efficient use of these tools. From experience, hydrologic modelling using FOSS requires considerable effort and knowledge of related pieces of software to achieve the same result using a commercial GUI. For example, commercial groundwater modelling software such as Groundwater Modelling System (GMS) and Visual MODFLOW incorporate GIS and groundwater modelling tools in the same package so that most of the data preparation using external GIS tools is diminished or eliminated. Although free tools such as ModelMuse are now catching up to these commercial software, it is still considerably easy to pre-process, model, calibrate and post-process results in commercial tools than in FOSS. Thus, a balance needs to be made between productivity (including reliability of results) and cost-saving. If available personnel are not yet well versed in the use of FOSS tools, a slow transition is recommended.

With specific reference to surface- and groundwater model calibration, commercial software has a lot to offer than FOSS which often has isolated tools that make it almost impossible to streamline the modelling workflow. Furthermore,

there is a lot of time investment required to learn these tools and be able to use them efficiently. This is in contrast to the commercial software tools alluded to earlier that incorporate the whole process from conceptual design to model calibration. Model calibration, an often underrated and neglected step in the modelling workflow, is one of the most computation intensive tasks requiring not only a deep understanding of the watershed/aquifer being simulated, but of the underlying physics of the calibration tools themselves. For example, the two most popular groundwater model calibration software tools employed by many hydrogeologists, UCODE and PEST, have not been integrated into free groundwater modelling tools such as ModelMuse. Although, some progress has been made to integrate PEST++ (Welter et al., 2015) and PEST into free groundwater modelling tools such as FloPy, not many people have adopted these tools due to the huge overhead required to successfully use and adopt these tools. Consider, too, the works of Fisher et al. (2016) who are proponents of reproducibility in groundwater modelling. Although most of their model is reproducible, it is not possible to reproduce the calibrated model as the calibration was done outside of the R Programming environment which handled the reproducible components. Similarly, free surface hydrologic modelling platforms such as SWAT and PRMS do not offer inbuilt calibration, perhaps due to the fact that initial developers' interests and experience were not in mathematical optimization. Thus, development in calibration tools for these popular software remains in the domain of mathematical optimization specialists and programmers who are interested in building stand-alone applications. Again, the importance of having well trained personnel working with these tools versus commercial packages such as FEFLOW, GMS, SMS, MIKE-SHE and Visual MODFLOW cannot be stressed enough.



On the hardware front, experience shows that integrated modelling is a compute intensive exercise often requiring high-end graphics and processing hardware. As a minimum, the recommendation is to use machines with at least 16 GB RAM and i5 processors. In this research, for example, processing the SRB DEM using QGIS took prohibitively long processing times. To mitigate this, powerful and faster computer hardware is recommended. Ideally, laptops and desktops specifically designated as ‘workstations’ would be a cost effective option where high-performance computing (HPC) is inaccessible. With respect to operating systems, it is generally observed that most hydrologic software are developed for Microsoft Windows based operating systems. Hence the recommendation here is biased towards computers running Windows based operating systems. It is possible to install two or more operating systems on one computer so that a switch to another can be made when required. For example, experience shows that it is faster to run some optimization modules on a Linux OS (also free and open-source) or its variants than on Windows based OS. Hence the ability to dual-boot Linux and Windows on one machine is desired as it eliminates the need of having two computers host the operating systems. Ultimately, access to HPC services would be recommended to shorten simulation times. For example, calibration of SRB SWAT model took close to 2 months to achieve acceptable results on a machine with 16 GB RAM and a 2.7 GHz intel core i7 processor. On an HPC cluster, this can be processed in under an hour leading to faster delivery of research results to relevant stakeholders.

Another important aspect is that of data storage. With the advent of cloud storage services, many organizations and institutions are migrating their data from local data centres to cloud storage facilities. The advantage of cloud storage

is that end-users do not need to worry about maintaining their local storage databases. Moreover, cloud storage and related services allow on-demand and high-quality access to applications and services without implementing the same locally (Wang et al., 2013).

#### **7.4.2.5 Modelling and Research Centres**

Finally, there is need to strengthen research centres in Malawi and related regions so that they are capable of generating high quality hydrometric data and models that are more representative of local conditions. It was highlighted, for example, in Section 4.9.5.2 that climate modelling is still a challenge in Africa as has been observed in many GCMs (James et al., 2018). GCMs that are more representative of African climate and conditions coupled with high integrity ground truth data will enable climate scientists and hydrologists build robust models that can be used to underpin IWRM decisions and policies in their respective countries.

### **7.4.3 Robust Adaptation Strategies**

#### **7.4.3.1 Dealing with uncertainty**

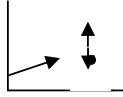
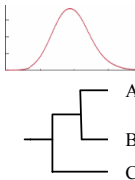

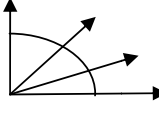
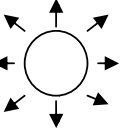
In Section 2.2, various sources of uncertainty associated with climate change and impact studies were presented. Furthermore, it was demonstrated how that climate change and variability is expected to affect the quantity of both surface- and groundwater resources. Many plausible scenarios and outcomes, all necessitating the need for adaptation measures, were also presented and discussed. The question, which naturally arises, is *how to deal with the uncertainty and formulate the best adaptation plan given the plausibility of multiple future scenarios?* Given the many challenges related to future scenario modelling and inter-sectoral policy coherence

issues in developing countries, conditions arise where the uncertainty can be classified as “deep” according to Walker et al. (2013). From their definition, deep uncertainty arises when “one is able to enumerate multiple plausible alternatives without being able to rank the alternatives in terms of perceived likelihood” (Roach et al., 2018; Walker et al., 2013).

From Fig. 7.2, it can be seen that under Walker et al.’s (2013) classification of deep uncertainty (i.e., Level 4 uncertainty), multiple unranked plausible futures with known outcomes exist, typical of climate change and related impact studies. Maier et al. (2016) present a multi-disciplinary perspective on the interaction of 1) uncertainties, 2) scenarios, 3) robustness and 4) adaptive strategies. In the case of Malawi and other developing countries, the interplay between the third and fourth components is of the utmost importance since deep uncertainty is a feature of all climate change and adaptation studies. From a quantitative perspective, a special emphasis is made for the need to have all key stakeholder institutions across the WEF nexus to first of all agree on the level of involvement in the mathematical modelling of the future. In other words, a consensus needs to be reached on which software to use, which scenarios to consider, purpose of the model, which metrics to use to quantify model errors and uncertainty and so on. In most cases, a multi-model and integrated approach may be required so that all systems in the WEF nexus are catered for.

#### **7.4.4 Multi-objective Optimization**

Following on from the previous section, the goal of efficient and effective water resources management in the face of uncertainty and multiple competing interests is not an easy one. In the face of climate change, managers and decision makers

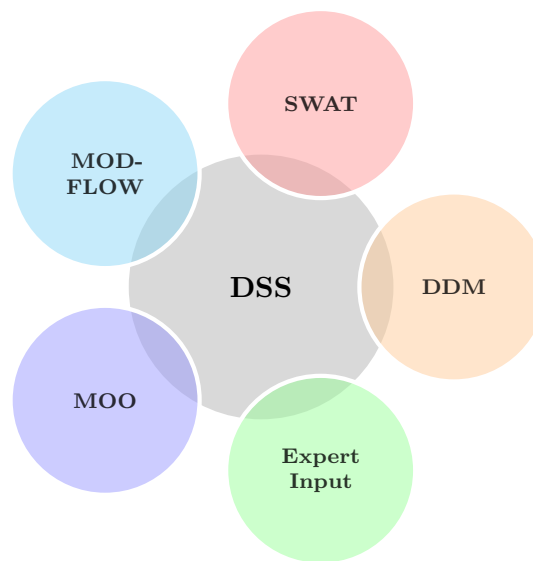
Complete Certainty		Level 1	Level 2	Level 3	Level 4	Level 5	Total Ignorance
	Context	A clear enough future (with sensitivity) 	Alternate futures (with probabilities) 	Alternate futures (with ranking) 	A multiplicity of plausible futures (unranked) 	Unknown future 	
	Systemmodel	A single system model	A single system model with a probabilistic parameterization	Several system models, one of which is most likely	Several system models, with different structures	Unknown system model; know we don't know	
	Systemoutcomes	Point estimates with sensitivity	Several sets of point estimates with confidence intervals, with a probability attached to each set	Several sets of point estimates, ranked according to their perceived likelihood	A known range of outcomes	Unknown outcomes; know we don't know	
	Weightsonoutcomes	A single estimate of the weights	Several sets of weights, with a probability attached to each set	Several sets of weights, ranked according to their perceived likelihood	A known range of weights	Unknown weights; know we don't know	

**Figure 7.2** Figure depicting uncertainty levels and how they evolve (Fig. 1, Walker et al., 2013)

are faced with a complex task of choosing the optimal solution that satisfies water demands from multiple sectors at the lowest cost possible (Nouiri, 2014).

In this thesis, an integrated GWSW modelling methodology that provides a quantitative measure of available future water resources under a changing climate has been developed. The methodology relied upon FOSS tools such as

MODFLOW and SWAT. These can easily be adopted by IWRM personnel to build a powerful and robust decision support system (DSS). A robust decision according to Rosenhead and Mingers's (2001) definition is "one that opens many paths towards favourable outcomes while closing off many paths towards unfavourable ones" (Lempert and Groves, 2010). However, due to the challenges of multi-decision making highlighted earlier, there is need to enhance the DSS process by adopting multi-objective optimization (MOO) techniques as shown in Figure 7.3.



**Figure 7.3** Components of a proposed Decision Support System for IWRM in Malawi

Multi-objective optimization techniques have been used in many parts of the world to determine the best management decisions and policies. A list of some recent applications of MOO to the solution of water management problems is given in Table 7.1.

Due to competing water demands, it is becoming increasingly necessary to employ MOO as a tool that can help decision-makers to arrive at optimal solutions that will satisfy the demands economically. The tools (i.e. algorithms) for MOO with respect to their application in IWRM are becoming better, efficient and

**Table 7.1** Applications of multi-objective optimization techniques in water resources management

Objective	Algorithm/Software	Reference
River basin management	Borg MOEA, $\varepsilon$ -DSEA	Al-Jawad et al. (2019)
Wastewater system management	Triangle Splitting Method, CPLEX 12.7	Rezaei et al. (2019)
Optimization of water consumption structure based on water shortage risk	LFP, MOP, BP, BMLFP	Wang et al. (2019)
Allocation of agricultural land and water resources	CCP	Li et al. (2019b)
Quantifying predictive uncertainty associated with groundwater flow and reactive transport models	MOPSO	Siade et al. (2019)
Optimize the allocation of surface and groundwater resources	NSGA-II	Banihabib et al. (2019)
Optimal allocation of water resources	NSGA-II	Gao et al. (2019b)
Equality and benefit for water allocation	GBSO, CCP, NSGA-II	Dai et al. (2018)
Sustainable irrigation water allocation	IFMONLP	Li et al. (2017)
Inclusion of deeply uncertain factors directly into a multi-objective search procedure	Borg MOEA, MORDM	Watson and Kasprzyk (2017)

more parsimonious due to the active research in this area as indicated by the publications listed in Table 7.1. Thus these tools can be adopted and applied

using minimal computing resources even though HPC would be favoured. This is an advantage for the IWRM community in developing countries where informed policy formulation is of the utmost importance to avert the negative impacts of climate change. To the best of the author's knowledge at the time of writing this thesis, there is no published records indicating the application of a methodology such as the one depicted in Figure 7.3 for optimum water resources allocation using open-source tools specifically in Malawi. It is hoped that this work will open channels of dialogue and further inquiry into the adoption of these methods for robust decision-making in the IWRM sector – especially in developing countries such as Malawi.

#### **7.4.5 Policy formulation and Implementation**

Policy formulation and planning of adaptation strategies should be done in a way that ensures that all parallel and competing interests within the WEF nexus paradigm are addressed. More importantly, there is need for coherent trans-sectoral policy and adaptation planning for a highly uncertain future (i.e., multiple plausible futures) due to climate and socio-economic changes. Chapter 4 highlighted the possible shortening of the rainy season and how this could affect the timing of the planting season for most cash crops in the SRB like maize, a staple food in Malawi. Also, Chapter 5 highlighted possible future blue and green water scarcity and how this could also affect irrigated agriculture and freshwater supply. Robust policies and initiatives aimed at ensuring optimized and sustainable utilization of blue water resources is highly recommended to mitigate against future BWF shortages especially in the central and southernmost regions of the SRB. Significant strides in this area at local village level have already

been made as pointed out by Rivett et al. (2018) in their study on the use of borehole-garden permaculture to realise the full potential of rural water supplies in Malawi. However, similar and advanced basin scale efforts in the face of possible climate change and competing water requirements must be implemented to ensure that the SRB is both economically and technologically capable to adapt to climate change.

Synchronization of policies between agricultural, energy and water supply sectors is important and recommended to ensure adequate preparedness during times of water scarcity. Additionally, policy synchronization may help to eliminate duplication of similar efforts across sectors. The role of local government is also important in coordinating implantation of water management policies and planning of settlements to ensure that water resources, both surface- and groundwater, are not stressed due to increasing populations.

## 7.5 Summary

Due to increasing water risks identified in Chapters 4 to 6, systematic and coordinated efforts towards climate change preparedness are required to ensure the attainment of SDG 6 in the SRB. In this chapter, challenges that can hinder implementation of IWRM policies and climate adaptation agendas in the SRB have been discussed and recommendations provided. IWRM challenges in the developing world and particularly Malawi – but directly related to the work presented in this thesis – were identified at the exclusion of many other equally important challenges.

Capacity building in the water sector is the most important challenge that was identified and one that needs urgent attention. Recommendations made in



Chapters 4 to 6 can only be realised if there are coordinated efforts from the GoM, NGOs and other stake holders at the policy formulation and implementation stages. Lack of adequate well trained water resources personnel, lack of adequate and well maintained water monitoring equipment, lack of facilities and other logistical issues are among the challenges identified with respect to capacity building. Additionally, lack of adequate investment and financing in rural water supply and sanitation was identified as a major challenge in the SRB. Investment in the training of personnel and establishment of adequate infrastructure that will improve the management of water resources in the SRB should not be seen as a cost but an investment that will result in positive contributions to the Gross Domestic Product (GDP) in the long term.

Finally, inter-sectoral policy coherence was recommended to ensure that climate adaptability planning is done in a holistic manner especially in the face of competing water needs.

*Life can only be understood backwards; but it must be lived forwards.*

Soren Kierkegaard

# 8

## Conclusions and Recommendations

*In this chapter, a summary discussion of the findings from each chapter of this thesis with respect to the objectives defined in Chapter 1 is provided. Thereafter, recommendations arising from the findings of this research along with considerations for future works are discussed.*

## 8.1 Summary of Findings

- ✍ In Chapter 2, a detailed literature review discussing aspects of anthropogenic climate change and the resulting impact on surface- and groundwater resources was presented. The state-of-the-art in surface- and groundwater modelling was reviewed and discussed. The core finding from the literature review is that climate change impact assessment is a trans-disciplinary exercise requiring a holistic assessment all the components of the hydrologic cycle. Secondly, most of the literature is in agreement that there are many sources of uncertainty and error in this process hence any assessment should quantify and report the uncertainty so that policy and decision makers are able to make informed and unbiased decisions.
- ✍ Chapter 3 provides a discussion of the methodologies developed and/or adapted for this research. The main hydrological tools that were used in this research (i.e. SWAT and MODFLOW) were introduced. The main focus in this chapter was to propose a methodology that relied mostly on free and open-source software for ease of collaboration and reproducibility. With respect to climate analyses and projections, a novel GCM subset selection methodology that employs the SU, PDF and a machine learning method was presented. For purposes of data preparation and cleaning, a parsimonious univariate method for infilling of missing data in streamflow records was tested and applied. The ubiquity of gaps in streamflow and climate data in developing regions makes this method appealing since it is not as compute-intensive as most of the methods used in literature such as neural networks. The methodology proposed in this chapter was intended to

be applied in the RNC (temperate climate) and SRB (mild tropical climate).

✍ In Chapter 4, the bias correction and spatial downscaling (BCSD) method proposed in Chapter 3 was tested and applied in downscaling a total of twenty-nine GCMs, of which seven were finally selected for the two study sites in line with objectives 1 and 2 of this research. The method was found to be useful for downscaling global scale climate forecasts to local watershed scales for hydrological analyses in both the RNC and SRB. The BCSD method was applied to GCM future projections to obtain local-scale forecasts for 3 time horizons referred to as the 2020s (early-century), 2050s (mid-century) and 2080s (late-century). In the case of the RNC, significant changes in precipitation under RCP4.5 and 8.5 are observed in winter of up to +24% and +28% respectively by the late century. These results are consistent with previous research which shows that future winter rainfall is likely to increase. Summer precipitation in the RNC decreases (up to -16%) across all forecast horizons and for all scenarios considered. Maximum and minimum temperatures are expected to increase by 1.9°C and up to 3.8°C by the end of the century. In the SRB, there could be increased rainfall by the late-century of up to +15% in the middle stages of the rainy season while the early and late stages of the rainy season could experience decreased rainfall by up to -40% and -18% respectively. This could result in late onset and early cessation of rainfall and thus affect timing of the planting of cash crops such as maize for subsistence farmers in the SRB. Adequate climate adaptation planning and the migration to climate resilient sustainable agriculture is recommended especially in the rural parts of the SRB. Maximum and minimum temperatures in the SRB increases by up to

2.5 °C and in the worst case by up to 5.0 °C under RCP8.5. The ensembles of GCM projections created by combining the GCM subset (6 for the SRB and 5 for the RNC) via the *Random Forest* algorithm was used in subsequent hydrological analyses.

📖 Chapter 5 presents results of hydrological modelling in the RNC and SRB as a fulfilment of objective number 3. The main idea in this chapter was to force SWAT models with a subset of GCMs identified in Chapter 4. Most importantly, a comparison was made between the performance of SWAT models developed for a data-rich region (RNC) versus a data-sparse region (SRB). Future streamflow and blue/green water availability in the RNC and SRB was assessed successfully using open-source software tools. Modelling results indicate that there is little impact on future streamflow and water balance components in the RNC. The southern part of the RNC is expected to be in slight deficit with respect to BWF (approximately 7 to 9% lower than baseline values) in the short- to medium term (i.e. 2020s and 2050s). Similarly, future streamflow in the RNC varies by about  $\pm 9\%$  from baseline values indicating no significant change. RNC modelling results indicate that, generally, temperate regions are more robust to climate change and variability. In the SRB, it was found that some regions (especially northern portions of the SRB) will experience an increase in streamflow while others are expected to experience a decrease in streamflow. Regions with increased streamflow may basically be more vulnerable to floods while regions with decreased streamflow may experience challenges in the agricultural, energy and domestic water supply sectors. Central and southern portions of the SRB are expected to receive reduced BWF or “liquid” water which can also

affect agricultural, energy and water supply sectors. It becomes imperative, therefore, to substitute inefficient and unsustainable irrigation practices with more efficient systems such as drip irrigation. Robust climate change adaptation and preparedness plans in the SRB to mitigate against potential future water risks should be a priority. Thus, results and recommendations arising from this chapter should be taken into consideration by relevant policy makers and water management authorities.

✍ In Chapter 6, development of integrated hydrologic models (IHMs) for the RNC and SRB was presented. In line with objectives 4 and 5, groundwater flow models developed using MODFLOW-NWT and coupled with SWAT models were tested and applied first in the Dumfries Basin (DB) and subsequently the SRB. Groundwater recharge for future time horizons was computed and presented. In DB, a large portion of the Locharbriggs Sandstone Formation and the northernmost portion of the Doweel Breccia Formation are projected to experience a slight decrease in groundwater recharge under RCP4.5 (up to -6%) and significant decrease under RCP8.5 (up to -22%). The rest of the basin is projected to experience little to no change in groundwater recharge under both RCP4.5 and 8.5. Again, the threat to future groundwater availability in the DB due to anthropogenic climate change is minimal based solely on the ability of the aquifer to recharge itself although other external stresses on the aquifer such as uncontrolled and indiscriminate water abstractions may lead to unsustainable water levels. In the SRB, it was discovered that the low-lying alluvial formations of the SRB are more resilient to climate change than previously hypothesized. Under RCP4.5 groundwater recharge is expected to increase by up to +30% by

mid- to late-century in the southern region of the SRB while recharge in the rest of the SRB is expected to be similar to baseline values. Under RCP8.5, groundwater recharge south of the SRB is expected to increase by up to +20%. For the rest of the basin, groundwater recharge is expected to remain unchanged from baseline values except in the mid- to late-century when recharge is expected to decrease by up to -10%. Thus, groundwater may act as a buffer against potential droughts and water scarcity in rural communities of the SRB if it is managed and exploited in a sustainable manner.

✍ Chapter 7 discusses important aspects of IWRM and climate change adaptation implementation in developing countries like Malawi in light of insights gained from this research. Persistent and endemic IWRM challenges such as lack of capacity in terms of well trained water resources personnel and infrastructure are discussed and recommendations for the GoM proposed. The significance of this chapter is that it highlights IWRM challenges that can hinder consideration and implementation of the findings and recommendations of Chapters 4 to 6. Finally, possible solutions that may help mitigate against adverse effects of climate change in the SRB in the context of IWRM were presented.

## 8.2 Recommendations

Recommendations arising from this research have been presented in previous chapters including and especially Chapter 7. Here, a brief summary of the recommendations is provided as follows;

- ✓ In the SRB, there is potential for shortening of the rainy season. Even though

our models indicate that DJF rainfall is expected to slightly increase, the mechanisms under which this may happen is not known. For example, it is possible to have half a month's rainfall in one day while the rest of the month is relatively dry (case of intra-seasonal and intra-monthly drought). Monthly mean values, in this case, do not mean anything more than just an indication of the possible rainfall quantity expected. Thus, the recommendation is that in the future, subsistence and commercial farmers in the SRB should be encouraged to plant drought-resistant crops such as cassava in place of crops such as maize which require a lot of water.

- ✓ Because of the potential for decreased BWF and GWF in the southern part of the SRB, farmers using ineffective and unsustainable irrigation methods should be encouraged to substitute them with more efficient and sustainable methods such as drip irrigation and other permaculture farming practices.
- ✓ The resilience of groundwater aquifers to climate change is a positive result for SRB communities. Investment in borehole drilling within rural SRB is thereby recommended to ensure that communities have access to potable water. However, the CJF-WFP has identified that the most important cause of non-functional boreholes is poor drilling and installation of the boreholes. Thus, hydrogeological feasibility studies should judiciously performed prior to siting of borehole locations including proper well design and drilling considerations.
- ✓ Hydro-meteorological data collection, summarized in three themes below, is one of the major issues in the SRB. The following specific recommendations were made:
  1. Climate impact studies rely on historical climate observations as well



as GCM outputs to project and prepare for possible future climate scenarios. While the role of satellite remote sensing in climate impact studies cannot be overemphasized, climate data recorded from meteorological stations are important in understanding local ground conditions. The ubiquity of remotely sensed climate products should be complemented with ground observations for completeness. Thus the GoM through the Ministry of Natural Resources, Energy and Environment and other stakeholders in the SRB should aim at ensuring that climate variables are recorded on a daily or sub-daily basis at the current weather stations. Setting up of new climate stations to increase the density of meteorological stations in the SRB should also be considered as a priority. Most importantly, quality assurance and control should be emphasized by screening the data and storing it in a format that lends itself easily to analyses without much pre-processing. Some climate stations in the SRB had unrealistic values which, unless detected early during the pre-processing stage, could adversely affect downscaled GCM results.

2. There should be deliberate efforts aimed at improving the quality and integrity of data collected from the streamflow gauge network in the SRB and the rest of Malawi. Historical streamflow records in the SRB are fraught with gaps and inconsistencies that, for the most part, reduces the efficacy of the said data in hydrological modelling. Lessons can be learned from the United Kingdom Benchmark Network 2 (UKBN2) campaign in the UK (result of which were used in this thesis) that aims at ensuring that streamflow records are screened and assessed

for suitability in climate-driven hydrological trends interpretation. Lack of capacity in terms of adequate training of water monitoring assistants (WMAs), including modern streamflow monitoring equipment, should be given urgent attention by the Ministry of Agriculture, Irrigation and Water Development (MoAIWD).

3. There is need for continuous monitoring of groundwater levels in the SRB and the rest of the country. The sparseness of historical groundwater level data makes it difficult to calibrate and constrain groundwater models for more robust predictive modelling. Some of the major problems associated with sparse or non-existent groundwater data is the issue of vandalism and lack of personnel (WMAs) to record the readings. Introduction of automatic groundwater level loggers in monitoring wells protected with locking steel lids can mitigate against these limitations.
- ✓ There should be deliberate plans and policies to meet training requirements for WASH sector personnel in the SRB. The role of local and international tertiary learning institutions in ensuring ease of access to IWRM training in whatever form cannot be overemphasized. The donor community, NGOs and GoM should work in tandem to identify and provide training opportunities for water resources personnel to ensure effective application of IWRM across all sectors.
- ✓ The tools and methods developed in this thesis may be incorporated as part of a decision support system (DSS) to assist the GoM and aligned stakeholders in their short-, medium- and long-term climate-change adaptation and water security planning. More specifically, an understanding of the spatial distribution of future water resources (both surface- and groundwater) in the

SRB is invaluable in the identification of vulnerable regions – consequently leading to timely climate preparedness and adaptation strategies. Another advantage is the open-source nature of the tools employed in this thesis; leading to a zero- or low-cost yet robust DSS that easily be adopted by IWRM professionals across all sectors.

- ✓ A multi-sectoral adaptation planning paradigm should be adopted by all IWRM stakeholders especially and including the GoM to ensure policy coherence with respect to water, energy, climate and food.
- ✓ Managed aquifer recharge (MAR) is recommended as a viable method for capturing and storing flood flows to enhance groundwater recharge.

## 8.3 Limitations

Limitations associated with this research are summarized below:

**Stationary LU/LC:** LU/LC for the HRUs in the SRB and RNC was considered to be stationary throughout the 21<sup>st</sup> century; that is, LU/LC conditions that prevailed during the baseline period were assumed to remain constant throughout the future simulated period. This is a significant limitation as conditions in the future may neither be reflective of past nor present conditions. While this approach is conservative, there is need for an independent LU/LC projected changes study that will feed into the models developed in this research for refined understanding of future hydrological impacts.

**Downscaling Method:** Another important source of uncertainty as discussed in Section 2.2.1 is the choice of GCM downscaling method. In this thesis, only one downscaling method was employed and hence limitations associated with the method selected in this research can be propagated to the hydrologic

models. Moreover, because the experiments were conducted using only one downscaling method, it was difficult to quantify the uncertainty associated with the methodology adopted here versus other downscaling methods. One known limitation with the methodology adopted in this thesis is that of the *stationarity assumption*; that is, an assumption is made that the performance of an empirical statistical downscaling (ESD) method for baseline conditions is indicative of the skill it exhibits when applied to future climate projections (Dixon et al., 2016). It has been shown that, depending on the region, there exists some downscaling errors, especially in coastal areas and also during warmer months arising from the use of ESDs (Dixon et al., 2016).

**Conceptual Modelling:** Another source of uncertainty that needs to be considered is the surface and groundwater conceptual modelling. The issue of multiple conceptual models has been given enough attention in the literature (e.g. Hojberg and Refsgaard, 2005; Troldborg et al., 2007) to the extent that different conceptualizations may lead to different results.

## 8.4 Research Contribution

A summary of the contributions to research that this thesis has yielded is presented in the box frame below.

### Summary of Research Novelty

1. In this thesis, a novel method for GCM selection that can potentially reduce inherent bias and uncertainty in future projections has been proposed. The application of the SU and PDF methods, combined with machine learning based methods for selection of a subset of GCMs for hydrological simulations is a parsimonious methodology that can be applied by researchers in both and temperate and semi-arid climates.
2. To the best of the author's knowledge, this is the first time a regional integrated (i.e., both surface- and groundwater) modelling approach has been applied to the RNC and SRB to quantify availability of future water resources up to the end of the 21<sup>st</sup> century. The results from this work can be used for climate adaptation planning and as a baseline for future research especially in the SRB.
3. This work has demonstrated that, for hydrological modelling, available remotely-sensed and reanalysis climate data can be used in lieu of missing point meteorological data. Furthermore, it has been shown that it is imperative to test different reanalysis products for a particular region to determine which product is the most suitable. For example, applying the same methodology to the SRB and RNC, it was discovered that CRU reanalysis data was more suitable for the RNC while CFSR products were suitable for the RNC.
4. This work provides a basis for a unified framework and methodology

for integrated hydrologic modelling that can be applied in different climatic settings using freely available hydro-climatic data products.

## 8.5 Considerations for Future Works

In this section, a summary of proposed future works is presented. It is the author's hope that the following suggestions shall be implemented in the shortest possible time so as to advance and/or enhance the methodology and results presented in this thesis.

1. While only two RCP scenarios (i.e. RCP4.5 and 8.5) were considered, it is intended to extend the models to include RCP6 which is consistent with a future where the application of a range of technologies and strategies for reducing greenhouse gas emissions are applied.
2. Due to the multiple future scenarios generated by this study and following the discussion presented in Section 7.4.4, it is the view of the author that multi-objective optimization be employed to address the trade-offs between model calibration and an uncertain or contested predictive model outcome(s); the result of which would allow decision-makers to consider the likelihood of a model prediction or outcome to occur in spite of the parameters chosen to calibrate the model (see Section 2.5.3.2 on non-uniqueness) (Siade et al., 2019).
3. Since LU/LC was considered to be stationary in the future (see Section 8.3), it is possible that results presented in this thesis could be conservative especially for Malawi where issues of deforestation and significant land-cover change/removal are prevalent. Thus it is planned to take into consideration

the effects of a changing climate and land-use on hydrologic components in the SRB and RNC. Recently a tool developed by Moriasi et al. (2019) is capable of updating land-use in the SWAT model while running multi-year simulations.

4. The issue of model structure uncertainty is one that needs to be considered in future works to assess the significance of this uncertainty on the results of this research. This objective will also include current and projected LU/LC scenarios as has been stated above.
5. It is intended to test the feasibility of incorporating data-based models as predictive tools for surface- and groundwater resources availability. The machine- and deep-learning models will be trained and validated against results obtained in this thesis. The idea is to improve the methodology used in this thesis so that similar results can be obtained with great confidence parsimoniously.
6. SWAT and MODFLOW models created in this thesis are not reproducible programmatically. This means that one has to rely completely on GUIs such as ModelMuse and QSWAT to create similar models. In the future, the model creation process will be automatized using the Python programming language to facilitate ease of reproducibility.
7. Currently, the authors of QSWATMOD have decided to port it to Python 3.x since FloPY, the groundwater modelling engine, will cease Python 2.7x support. Thus, all SWAT-MODFLOW models developed in this thesis will be converted into a future Python 3.x QSWATMOD compatible version programmatically as suggested above.

# References

- Abbaspour, K., Johnson, C., and van Genuchten, M. (2004). Estimating uncertain flow and transport parameters using a sequential uncertainty fitting procedure. *VADOSE ZONE JOURNAL*, 3(4):1340–1352.
- Abbaspour, K. C., Faramarzi, M., Ghasemi, S. S., and Yang, H. (2009). Assessing the impact of climate change on water resources in Iran. *WATER RESOURCES RESEARCH*, 45.
- Abbaspour, K. C., Rouholahnejad, E., Vaghefi, S., Srinivasan, R., Yang, H., and Klove, B. (2015). A continental-scale hydrology and water quality model for Europe: Calibration and uncertainty of a high-resolution large-scale SWAT model. *JOURNAL OF HYDROLOGY*, 524:733–752.
- Abbaspour, K. C., Vaghefi, S. A., and Srinivasan, R. (2018). A Guideline for Successful Calibration and Uncertainty Analysis for Soil and Water Assessment: A Review of Papers from the 2016 International SWAT Conference. *WATER*, 10(1).
- Abbaspour, K. C., Yang, J., Maximov, I., Siber, R., Bogner, K., Mieleitner, J., Zobrist, J., and Srinivasan, R. (2007). Modelling hydrology and water quality in the pre-alpine/alpine Thur watershed using SWAT. *JOURNAL OF HYDROLOGY*, 333(2-4):413–430.
- Adeloye, A. J. and Rustum, R. (2012). Self-organising map rainfall-runoff multivariate modelling for runoff reconstruction in inadequately gauged basins. *HYDROLOGY RESEARCH*, 43(5):603–617.
- Adhikari, U. and Nejadhashemi, A. P. (2016). Impacts of Climate Change on Water Resources in Malawi. *JOURNAL OF HYDROLOGIC ENGINEERING*, 21(11).
- Afshar, A. A., Hassanzadeh, Y., Pourreza-Bilondi, M., and Ahmadi, A. (2018). Analyzing long-term spatial variability of blue and green water footprints in a semi-arid mountainous basin with MIROC-ESM model (case study: Kashafrud River Basin, Iran). *THEORETICAL AND APPLIED CLIMATOLOGY*, 134(3-4):885–899.
- Ahani, A., Shourian, M., and Rad, P. R. (2018). Performance Assessment of the Linear, Nonlinear and Nonparametric Data Driven Models in River Flow Forecasting. *WATER RESOURCES MANAGEMENT*, 32(2):383–399.



- Ahmad, I., Tang, D., Wang, T., Wang, M., and Wagan, B. (2015). Precipitation Trends over Time Using Mann-Kendall and Spearman's rho Tests in Swat River Basin, Pakistan. *ADVANCES IN METEOROLOGY*.
- Ahmed, K. F., Wang, G., Silander, J., Wilson, A. M., Allen, J. M., Horton, R., and Anyah, R. (2013). Statistical downscaling and bias correction of climate model outputs for climate change impact assessment in the US northeast. *GLOBAL AND PLANETARY CHANGE*, 100:320–332.
- Akhurst, M. C., Ball, D. R., Brady, L., Buckley, D. K., Burns, J., Darling, W. G., MacDonald, A. M., McMillan, A. A., Dochartaigh, B. E. O., Peach, D. W., Robins, N. S., and Wealthall, G. P. (2006). Towards understanding the Dumfries Basin aquifer, SW Scotland. In Barker, RD and Tellam, JH, editor, *FLUID FLOW AND SOLUTE MOVEMENT IN SANDSTONES: THE ONSHORE UK PERMO-TRIASSIC RED BED SEQUENCE*, volume 263 of *Geological Society Special Publication*, pages 187+. Environm & Ind Geophys Grp; Hydrogeol Grp Geol Soc London. Meeting of the Environmental-and-Industrial-Geophysics-Group/Hydrogeological-Group of the Geological-Society-of-London, London, ENGLAND, 2003.
- Al-Abed, N. and Whiteley, H. (2002). Calibration of the Hydrological Simulation Program Fortran (HSPF) model using automatic calibration and geographical information systems. *HYDROLOGICAL PROCESSES*, 16(16):3169–3188.
- Al-Jawad, J. Y., Alsaffar, H. M., Bertram, D., and Kalin, R. M. (2019). Optimum socio-environmental flows approach for reservoir operation strategy using many-objectives evolutionary optimization algorithm. *SCIENCE OF THE TOTAL ENVIRONMENT*, 651(2):1877–1891.
- Al Radif, A. (1999). Integrated water resources management (IWRM): an approach to face the challenges of the next century and to avert future crises. *DESALINATION*, 124(1-3):145–153. European Conference on Desalination and the Environment, LAS PALMAS, SPAIN, NOV 09-12, 1999.
- Aliyari, F., Bailey, R. T., Tasdighi, A., Dozier, A., Arabi, M., and Zeiler, K. (2019). Coupled SWAT-MODFLOW model for large-scale mixed agro-urban river basins. *ENVIRONMENTAL MODELLING & SOFTWARE*, 115:200–210.
- Alizamir, M., Moghadam, M. A., Monfared, A. H., and Shamsipour, A. (2018). Statistical downscaling of global climate model outputs to monthly precipitation via extreme learning machine: A case study. *ENVIRONMENTAL PROGRESS & SUSTAINABLE ENERGY*, 37(5):1853–1862.
- Allan, A. and Rieu-Clarke, A. (2010). Good governance and iwrn—a legal perspective. *Irrigation and Drainage Systems*, 24(3):239–248.
- Allen, M. and Ingram, W. (2002). Constraints on future changes in climate and the hydrologic cycle. *NATURE*, 419(6903):224+.

- Allison, G. B. (1988). A Review of Some of the Physical, Chemical and Isotopic Techniques Available for Estimating Groundwater Recharge. In Simmers, I., editor, *Estimation of Natural Groundwater Recharge*, pages 49–72. Springer Netherlands, Dordrecht.
- Anderson, J. R. (1976). *A land use and land cover classification system for use with remote sensor data*, volume 964. US Government Printing Office.
- Anderson, M., Woessner, W., and Hunt, R. (2015). Applied Groundwater Modeling: Simulation of Flow and Advective Transport, 2nd Edition. In *APPLIED GROUNDWATER MODELING: SIMULATION OF FLOW AND ADVECTIVE TRANSPORT, 2ND EDITION*, pages 1–564.
- ARNOLD, J., ALLEN, P., and BERNHARDT, G. (1993). A COMPREHENSIVE SURFACE-GROUNDWATER FLOW MODEL. *JOURNAL OF HYDROLOGY*, 142(1-4):47–69.
- Arnold, J., Muttiah, R., Srinivasan, R., and Allen, P. (2000). Regional estimation of base flow and groundwater recharge in the Upper Mississippi river basin. *JOURNAL OF HYDROLOGY*, 227(1-4):21–40.
- Arnold, J. G., Moriasi, D. N., Gassman, P. W., Abbaspour, K. C., White, M. J., Srinivasan, R., Santhi, C., Harmel, R. D., van Griensven, A., Van Liew, M. W., Kannan, N., and Jha, M. K. (2012). SWAT: MODEL USE, CALIBRATION, AND VALIDATION. *TRANSACTIONS OF THE ASABE*, 55(4):1491–1508.
- Arnold, J. G., Srinivasan, R., Muttiah, R. S., and Williams, J. R. (1998). Large area hydrologic modeling and assessment part i: model development. *JAWRA Journal of the American Water Resources Association*, 34(1):73–89.
- Aslam, R. A., Shrestha, S., and Pandey, V. P. (2018). Groundwater vulnerability to climate change: A review of the assessment methodology. *SCIENCE OF THE TOTAL ENVIRONMENT*, 612:853–875.
- Assaf, H. (2009). A hydro-economic model for managing groundwater resources in semi-arid regions. In Brebbia, CA and Popov, V, editor, *WATER RESOURCES MANAGEMENT V*, volume 125 of *WIT Transactions on Ecology and the Environment*, pages 85–96. Wessex Inst Technol; WIT Transact Ecol & Environm. 5th International Conference on Sustainable Water Resources Management, MALTA, SEP 09-11, 2009.
- Ayele, G. T., Teshale, E. Z., Yu, B., Rutherford, I. D., and Jeong, J. (2017). Streamflow and Sediment Yield Prediction for Watershed Prioritization in the Upper Blue Nile River Basin, Ethiopia. *WATER*, 9(10).
- Ayers, J., Ficklin, D. L., Stewart, I. T., and Strunk, M. (2016). Comparison of CMIP3 and CMIP5 projected hydrologic conditions over the Upper Colorado River Basin. *INTERNATIONAL JOURNAL OF CLIMATOLOGY*, 36(11):3807–3818.

- Baginska, B., Milne-Home, W., and Cornish, P. (2003). Modelling nutrient transport in Currency Creek, NSW with AnnAGNPS and PEST. *ENVIRONMENTAL MODELLING & SOFTWARE*, 18(8-9, SI):801–808. Conference on Modelling of Hydrologic Systems (MODSIM 2001), CANNBERRA, AUSTRALIA, DEC 10-13, 2001.
- Bailey, R., Rathjens, H., Bieger, K., Chaubey, I., and Arnold, J. (2017). SWATMOD-PREP: GRAPHICAL USER INTERFACE FOR PREPARING COUPLED SWAT-MODFLOW SIMULATIONS. *JOURNAL OF THE AMERICAN WATER RESOURCES ASSOCIATION*, 53(2):400–410.
- Bailey, R. T., Wible, T. C., Arabi, M., Records, R. M., and Ditty, J. (2016). Assessing regional-scale spatio-temporal patterns of groundwater-surface water interactions using a coupled SWAT-MODFLOW model. *HYDROLOGICAL PROCESSES*, 30(23):4420–4433.
- Baker, M. (2016). 1,500 scientists lift the lid on reproducibility. *Nature News*, 533(7604):452.
- Banihabib, M. E., Tabari, M. M. R., and Tabari, M. M. R. (2019). Development of a Fuzzy Multi-Objective Heuristic Model for Optimum Water Allocation. *WATER RESOURCES MANAGEMENT*, 33(11):3673–3689.
- Bardossy, A. and Pegram, G. (2014). Infilling missing precipitation records - A comparison of a new copula-based method with other techniques. *JOURNAL OF HYDROLOGY*, 519(A):1162–1170.
- Bates, B., Kundzewicz, Z., and Wu, S. (2008). Climate Change and Water. <https://www.ipcc.ch/pdf/technical-papers/climate-change-water-en.pdf>. (Accessed on 02/11/2016).
- Bazilian, M., Rogner, H., Howells, M., Hermann, S., Arent, D., Gielen, D., Steduto, P., Mueller, A., Komor, P., Tol, R. S. J., and Yumkella, K. K. (2011). Considering the energy, water and food nexus: Towards an integrated modelling approach. *ENERGY POLICY*, 39(12):7896–7906.
- Bedekar, V., Morway, E. D., Langevin, C. D., and Tonkin, M. J. (2016). MT3D-USGS version 1: A U.S. Geological Survey release of MT3DMS updated with new and expanded transport capabilities for use with MODFLOW. Technical report, Reston, VA. Report.
- Bedekar, V., Niswonger, R. G., Kipp, K., Panday, S., and Tonkin, M. (2012). Approaches to the Simulation of Unconfined Flow and Perched Groundwater Flow in MODFLOW. *GROUND WATER*, 50(2):187–198.
- Behnke, R., Vavrus, S., Allstadt, A., Albright, T., Thogmartin, W. E., and Radeloff, V. C. (2016). Evaluation of downscaled, gridded climate data for the - conterminous United States. *ECOLOGICAL APPLICATIONS*, 26(5):1338–1351.

- Bekele, E. G. and Nicklow, J. W. (2007). Multi-objective automatic calibration of SWAT using NSGA-II. *JOURNAL OF HYDROLOGY*, 341(3-4):165–176.
- Bennis, S., Berrada, F., and Kang, N. (1997). Improving single-variable and multivariable techniques for estimating missing hydrological data. *JOURNAL OF HYDROLOGY*, 191(1-4):87–105.
- Benson, D., Gain, A. K., and Rouillard, J. J. (2015). Water Governance in a Comparative Perspective: From IWRM to a ‘Nexus’ Approach? *WATER ALTERNATIVES-AN INTERDISCIPLINARY JOURNAL ON WATER POLITICS AND DEVELOPMENT*, 8(1, SI):756–773.
- Betrie, G. D., Mohamed, Y. A., van Griensven, A., and Srinivasan, R. (2011a). Sediment management modelling in the Blue Nile Basin using SWAT model. *HYDROLOGY AND EARTH SYSTEM SCIENCES*, 15(3):807–818.
- Betrie, G. D., van Griensven, A., Mohamed, Y. A., Popescu, I., Mynett, A. E., and Hummel, S. (2011b). LINKING SWAT AND SOBEK USING OPEN MODELING INTERFACE (OPENMI) FOR SEDIMENT TRANSPORT SIMULATION IN THE BLUE NILE RIVER BASIN. *TRANSACTIONS OF THE ASABE*, 54(5):1749–1757.
- Beven, K. (2006a). A manifesto for the equifinality thesis. *JOURNAL OF HYDROLOGY*, 320(1-2, SI):18–36. 3rd MOPEX Workshop, Sapporo, JAPAN, JUL, 2003.
- Beven, K. (2006b). A manifesto for the equifinality thesis. *JOURNAL OF HYDROLOGY*, 320(1-2, SI):18–36. 3rd MOPEX Workshop, Sapporo, JAPAN, JUL, 2003.
- BEVEN, K. and BINLEY, A. (1992). THE FUTURE OF DISTRIBUTED MODELS - MODEL CALIBRATION AND UNCERTAINTY PREDICTION. *HYDROLOGICAL PROCESSES*, 6(3):279–298.
- Beven, K. and Young, P. (2013). A guide to good practice in modeling semantics for authors and referees. *WATER RESOURCES RESEARCH*, 49(8):5092–5098.
- Biemans, H., Speelman, L. H., Ludwig, F., Moors, E. J., Wiltshire, A. J., Kumar, P., Gerten, D., and Kabat, P. (2013). Future water resources for food production in five South Asian river basins and potential for adaptation - A modeling study. *SCIENCE OF THE TOTAL ENVIRONMENT*, 468(SI):S117–S131.
- Bjørnæs, C. (2013). A guide to representative concentration pathways. *Center for International Climate and Environmental Research*. Available at: <https://www.sei-international.org/mediamanager/documents/A-guide-to-RCPs.pdf> (Accessed on 1 June 2017).
- Bloeschl, G., Ardoin-Bardin, S., Bonell, M., Dorninger, M., Goodrich, D., Gutknecht, D., Matamoros, D., Merz, B., Shand, P., and Szolgay, J. (2007). At

- what scales do climate variability and land cover change impact on flooding and low flows? *HYDROLOGICAL PROCESSES*, 21(9):1241–1247.
- Bonell, M. (1999). Tropical forest hydrology and the role of the UNESCO International Hydrological Programme. *HYDROLOGY AND EARTH SYSTEM SCIENCES*, 3(4):451–461.
- Bradford, R. (1973). Groundwater reconnaissance study: lower shire valley. *Report RB/5 File T601 Geol Surv Malawi*.
- Braganza, K., Karoly, D., and Arblaster, J. (2004). Diurnal temperature range as an index of global climate change during the twentieth century. *GEOPHYSICAL RESEARCH LETTERS*, 31(13).
- Braune, E. and Xu, Y. (2008). Groundwater management issues in Southern Africa - An IWRM perspective. *WATER SA*, 34(6):699–706. International Conference on Integrated Water Resources Management, Cape Town, SOUTH AFRICA, MAR 10-12, 2008.
- Breiman, L. (2001). Random forests. *MACHINE LEARNING*, 45(1):5–32.
- Brisson, E., Demuzere, M., Willems, P., and van Lipzig, N. P. M. (2015). Assessment of natural climate variability using a weather generator. *CLIMATE DYNAMICS*, 44(1-2):495–508.
- Bronstert, A. (2004). Rainfall-runoff modelling for assessing impacts of climate and land-use change. *HYDROLOGICAL PROCESSES*, 18(3):567–570.
- Brookfield, M. (1978). Revision of the stratigraphy of permian and supposed permian rocks of southern scotland. *Geologische Rundschau*, 67(1):110–149.
- Bruijnzeel, L. A. (2006). *Land Use and Landcover Effects on Runoff Processes: Forest Harvesting and Road Construction*, chapter 119, page 1815. American Cancer Society.
- Brunner, G. W. (2002). Hec-ras (river analysis system). In *North American Water and Environment Congress & Destructive Water*, pages 3782–3787. ASCE.
- Brunner, G. W. (2010). *HEC-RAS river analysis system: hydraulic reference manual*. US Army Corps of Engineers, Institute for Water Resources, Hydrologic Engineering Center.
- Bunn, C., Laederach, P., Ovalle Rivera, O., and Kirschke, D. (2015). A bitter cup: climate change profile of global production of Arabica and Robusta coffee. *CLIMATIC CHANGE*, 129(1-2):89–101.
- Burt, T. P. and McDonnell, J. J. (2015). Whither field hydrology? The need for discovery science and outrageous hydrological hypotheses. *WATER RESOURCES RESEARCH*, 51(8):5919–5928.

- Byun, K. and Hamlet, A. F. (2018). Projected changes in future climate over the Midwest and Great Lakes region using downscaled CMIP5 ensembles. *INTERNATIONAL JOURNAL OF CLIMATOLOGY*, 38(1):E531–E553.
- Cannon, A. J., Sobie, S. R., and Murdock, T. Q. (2015). Bias Correction of GCM Precipitation by Quantile Mapping: How Well Do Methods Preserve Changes in Quantiles and Extremes? *JOURNAL OF CLIMATE*, 28(17):6938–6959.
- Carrera, J., Alcolea, A., Medina, A., Hidalgo, J., and Slooten, L. (2005). Inverse problem in hydrogeology. *HYDROGEOLOGY JOURNAL*, 13(1):206–222.
- Castro, J. E. (2007). Water governance in the twentieth-first century. *Ambiente & sociedade*, 10(2):97–118.
- CBEC, Mott MacDonald, Walking-the-Talk (2013). Physical restoration options to address morphology and flood pressures on the river nith - a pilot study. <https://www.sepa.org.uk/media/105436/nith-final-report.pdf>. (Accessed on 11/07/2017).
- CGS (2018). EXPLORATORY DRILLING REPORT - SHIRE RIVER BASIN MANAGEMENT PROGRAM (PHASE 1) PROJECT.
- Chang, Y., Li, G., Yao, Y., Zhang, L., and Yu, C. (2016). Quantifying the Water-Energy-Food Nexus: Current Status and Trends. *ENERGIES*, 9(2).
- Chen, H., Xu, C.-Y., and Guo, S. (2012). Comparison and evaluation of multiple GCMs, statistical downscaling and hydrological models in the study of climate change impacts on runoff. *JOURNAL OF HYDROLOGY*, 434:36–45.
- Chen, J., Brissette, F. P., Chaumont, D., and Braun, M. (2013). Performance and uncertainty evaluation of empirical downscaling methods in quantifying the climate change impacts on hydrology over two North American river basins. *JOURNAL OF HYDROLOGY*, 479:200–214.
- Chen, J., Brissette, F. P., and Leconte, R. (2011). Uncertainty of downscaling method in quantifying the impact of climate change on hydrology. *JOURNAL OF HYDROLOGY*, 401(3-4):190–202.
- Chen, J., St-Denis, B. G., Brissette, F. P., and Lucas-Picher, P. (2016). Using Natural Variability as a Baseline to Evaluate the Performance of Bias Correction Methods in Hydrological Climate Change Impact Studies. *JOURNAL OF HYDROMETEOROLOGY*, 17(8):2155–2174.
- Cherkassky, V., Krasnopolsky, V., Solomatine, D. P., and Valdes, J. (2006). Computational intelligence in earth sciences and environmental applications: Issues and challenges. *NEURAL NETWORKS*, 19(2):113–121. IEEE International Joint Conference on Neural Networks (IJCNN 2005), Montreal, CANADA, JUL 31-AUG 04, 2005.

- Chidammodzi, C. L. and Muhandiki, V. S. (2017). Water resources management and integrated water resources management implementation in malawi: Status and implications for lake basin management. *Lakes & Reservoirs: Science, Policy and Management for Sustainable Use*, 22(2):101–114.
- Chiew, F. and McMahon, T. (2002). Modelling the impacts of climate change on Australian streamflow. *HYDROLOGICAL PROCESSES*, 16(6, SI):1235–1245.
- Chilton, P. and Smith-Carington, A. (1984). *Characteristics of the weathered basement aquifer in Malawi in relation to rural water supplies*. IAHS Press.
- Chilton, P. J. and Foster, S. (1995). Hydrogeological characterisation and water-supply potential of basement aquifers in tropical africa. *Hydrogeology journal*, 3(1):36–49.
- Cho, J., Oh, C., Choi, J., and Cho, Y. (2016). Climate change impacts on agricultural non-point source pollution with consideration of uncertainty in CMIP5. *IRRIGATION AND DRAINAGE*, 65(2, SI):209–220. 22nd International Congress of the International-Commission-on-Irrigation-and-Drainage (ICID) on Securing Water for Food and Rural Community under Climate Change, Gwangju, SOUTH KOREA, SEP, 2014.
- Christensen, N. and Lettenmaier, D. P. (2006). A multimodel ensemble approach to assessment of climate change impacts on the hydrology and water resources of the Colorado River basin. *Hydrology and Earth System Sciences Discussions*, 3(6):3727–3770.
- Christensen, N. S. and Lettenmaier, D. P. (2007). A multimodel ensemble approach to assessment of climate change impacts on the hydrology and water resources of the Colorado River Basin. *HYDROLOGY AND EARTH SYSTEM SCIENCES*, 11(4):1417–1434.
- Chung, I.-M., Kim, N.-W., Lee, J., and Sophocleous, M. (2010). Assessing distributed groundwater recharge rate using integrated surface water-groundwater modelling: application to Mihocheon watershed, South Korea. *HYDROGEOLOGY JOURNAL*, 18(5):1253–1264.
- Chung, I.-M., Lee, J., Kim, N. W., Na, H., Chang, S. W., Kim, Y., and Kim, G.-B. (2015). Estimating exploitable amount of groundwater abstraction using an integrated surface water-groundwater model: Mihocheon watershed, South Korea. *HYDROLOGICAL SCIENCES JOURNAL-JOURNAL DES SCIENCES HYDROLOGIQUES*, 60(5, SI):863–872.
- Chunn, D., Faramarzi, M., Smerdon, B., and Alessi, D. S. (2019). Application of an Integrated SWAT-MODFLOW Model to Evaluate Potential Impacts of Climate Change and Water Withdrawals on Groundwater-Surface Water Interactions in West-Central Alberta. *WATER*, 11(1).

- Clarke, L., Edmonds, J., Jacoby, H., Pitcher, H., Reilly, J., and Richels, R. (2007). Scenarios of greenhouse gas emissions and atmospheric concentrations. *US Department of Energy Publications*.
- Costa, M., Botta, A., and Cardille, J. (2003). Effects of large-scale changes in land cover on the discharge of the Tocantins River, Southeastern Amazonia. *JOURNAL OF HYDROLOGY*, 283(1-4):206–217.
- Costa, M. and Foley, J. (1997). Water balance of the Amazon Basin: Dependence on vegetation cover and canopy conductance. *JOURNAL OF GEOPHYSICAL RESEARCH-ATMOSPHERES*, 102(D20):23973–23989.
- Coulibaly, P. and Evora, N. D. (2007). Comparison of neural network methods for infilling missing daily weather records. *JOURNAL OF HYDROLOGY*, 341(1-2):27–41.
- Creswell, J. W. and Creswell, J. D. (2017). *Research design: Qualitative, Quantitative, and Mixed Methods Approaches*. Sage Publications.
- Cuceloglu, G., Abbaspour, K. C., and Ozturk, I. (2017). Assessing the Water-Resources Potential of Istanbul by Using a Soil and Water Assessment Tool (SWAT) Hydrological Model. *WATER*, 9(10).
- Cuthbert, M. O., Gleeson, T., Moosdorf, N., Befus, K. M., Schneider, A., Hartmann, J., and Lehner, B. (2019a). Global patterns and dynamics of climate-groundwater interactions. *NATURE CLIMATE CHANGE*, 9(2):137+.
- Cuthbert, M. O., Taylor, R. G., Favreau, G., Todd, M. C., Shamsudduha, M., Villholth, K. G., MacDonald, A. M., Scanlon, B. R., Kotchoni, D. O. V., Vouillamoz, J.-M., Lawson, F. M. A., Adjomayi, P. A., Kashaigili, J., Seddon, D., Sorensen, J. P. R., Ebrahim, G. Y., Owor, M., Nyenje, P. M., Nazoumou, Y., Goni, I., Ousmane, B. I., Sibanda, T., Ascott, M. J., Macdonald, D. M. J., Agyekum, W., Koussoube, Y., Wanke, H., Kim, H., Wada, Y., Lo, M.-H., Oki, T., and Kukuric, N. (2019b). Observed controls on resilience of groundwater to climate variability in sub-Saharan Africa. *NATURE*, 572(7768):230+.
- da Silva, R. M., Santos, C. A. G., Moreira, M., Corte-Real, J., Silva, V. C. L., and Medeiros, I. C. (2015). Rainfall and river flow trends using Mann-Kendall and Sen's slope estimator statistical tests in the Cobres River basin. *NATURAL HAZARDS*, 77(2):1205–1221.
- Dai, C., Qin, X. S., Chen, Y., and Guo, H. C. (2018). Dealing with equality and benefit for water allocation in a lake watershed: A Gini-coefficient based stochastic optimization approach. *JOURNAL OF HYDROLOGY*, 561:322–334.
- de Moraes Takafuji, E. H., da Rocha, M. M., and Manzione, R. L. (2019). Groundwater Level Prediction/Forecasting and Assessment of Uncertainty Using SGS and ARIMA Models: A Case Study in the Bauru Aquifer System (Brazil). *NATURAL RESOURCES RESEARCH*, 28(2):487–503.



- Dehghanipour, A. H., Zahabiyoun, B., Schoups, G., and Babazadeh, H. (2019). A weap-modflow surface water-groundwater model for the irrigated miyandoab plain, urmia lake basin, iran: Multi-objective calibration and quantification of historical drought impacts. *Agricultural Water Management*, 223:105704.
- Deng, W. and Wang, G. (2017). A novel water quality data analysis framework based on time-series data mining. *JOURNAL OF ENVIRONMENTAL MANAGEMENT*, 196:365–375.
- Deng, Z., Liu, J., Qiu, X., Zhou, X., and Zhu, H. (2017). Downscaling RCP8.5 daily temperatures and precipitation in Ontario using localized ensemble optimal interpolation (EnOI) and bias correction. *Climate Dynamics*, pages 1–21.
- Dessai, S., Hulme, M., Lempert, R., and Pielke Jr., R. (2009). Do we need better predictions to adapt to a changing climate? *Eos, Transactions American Geophysical Union*, 90(13):111–112.
- DeWalle, D., Swistock, B., Johnson, T., and McGuire, K. (2000). Potential effects of climate change and urbanization on mean annual streamflow in the United States. *WATER RESOURCES RESEARCH*, 36(9):2655–2664.
- Diallo, I., Giorgi, F., and Stordal, F. (2018). Influence of Lake Malawi on regional climate from a double-nested regional climate model experiment. *CLIMATE DYNAMICS*, 50(9-10):3397–3411.
- Dibike, Y., Velickov, S., Solomatine, D., and Abbott, M. (2001). Model induction with support vector machines: Introduction and applications. *JOURNAL OF COMPUTING IN CIVIL ENGINEERING*, 15(3):208–216.
- Dibike, Y. B. and Coulibaly, P. (2005). Hydrologic impact of climate change in the saguenay watershed: comparison of downscaling methods and hydrologic models. *Journal of hydrology*, 307(1):145–163.
- Dierauer, J. R., Whitfield, P. H., and Allen, D. M. (2017). Assessing the suitability of hydrometric data for trend analysis: The ‘FlowScreen’ package for R. *CANADIAN WATER RESOURCES JOURNAL*, 42(3):269–275.
- Dile, Y. T. and Srinivasan, R. (2014). EVALUATION OF CFSR CLIMATE DATA FOR HYDROLOGIC PREDICTION IN DATA-SCARCE WATERSHEDS: AN APPLICATION IN THE BLUE NILE RIVER BASIN. *JOURNAL OF THE AMERICAN WATER RESOURCES ASSOCIATION*, 50(5):1226–1241.
- Dillon, P., Toze, S., Page, D., Vanderzalm, J., Bekele, E., Sidhu, J., and Rinck-Pfeiffer, S. (2010). Managed aquifer recharge: rediscovering nature as a leading edge technology. *WATER SCIENCE AND TECHNOLOGY*, 62(10):2338–2345.
- Dixon, K. W., Lanzante, J. R., Nath, M. J., Hayhoe, K., Stoner, A., Radhakrishnan, A., Balaji, V., and Gaitan, C. F. (2016). Evaluating the stationarity

- assumption in statistically downscaled climate projections: is past performance an indicator of future results? *CLIMATIC CHANGE*, 135(3-4):395–408.
- Doherty, J. (2001). Improved calculations for dewatered cells in MODFLOW. *GROUND WATER*, 39(6):863–869.
- Doherty, J. (2003). Ground water model calibration using pilot points and regularization. *GROUND WATER*, 41(2):170–177. MODFLOW 2001 and Other Modeling Odysseys Conference, COLORADO SCH MINES, GOLDEN, COLORADO, SEP 12-14, 2001.
- Doherty, J. (2015). *Calibration and uncertainty analysis for complex environmental models*. Watermark Numerical Computing.
- Doherty, J. et al. (1994). PEST: a unique computer program for model-independent parameter optimisation. *Water Down Under 94: Groundwater/Surface Hydrology Common Interest Papers; Preprints of Papers*, page 551.
- Doherty, J. E. and Hunt, R. J. (2010). *Approaches to highly parameterized inversion: a guide to using PEST for groundwater-model calibration*. US Department of the Interior, US Geological Survey Reston, VA, USA.
- Donevska, K. and Panov, A. (2019). Climate change impact on water supply demands: case study of the city of Skopje. *WATER SCIENCE AND TECHNOLOGY-WATER SUPPLY*, 19(7):2172–2178.
- Douglas-Mankin, K., Srinivasan, R., and Arnold, J. (2010). Soil and water assessment tool (swat) model: Current developments and applications. *Transactions of the ASABE*, 53(5):1423–1431.
- Eberhart, R. and Kennedy, J. (1995). A new optimizer using particle swarm theory. In *Micro Machine and Human Science, 1995. MHS'95., Proceedings of the Sixth International Symposium on*, pages 39–43. IEEE.
- Eckhardt, K., Breuer, L., and Frede, H. (2003). Parameter uncertainty and the significance of simulated land use change effects. *JOURNAL OF HYDROLOGY*, 273(1-4):164–176.
- Eckhardt, K. and Ulbrich, U. (2003). Potential impacts of climate change on groundwater recharge and streamflow in a central European low mountain range. *JOURNAL OF HYDROLOGY*, 284(1-4):244–252.
- Eden, J. M., Widmann, M., Grawe, D., and Rast, S. (2012). Skill, Correction, and Downscaling of GCM-Simulated Precipitation. *JOURNAL OF CLIMATE*, 25(11):3970–3984.
- Emori, S., Taylor, K., Hewitson, B., Zermoglio, F., Juckes, M., Lautenschlager, M., Stockhause, M., Emori, S., Taylor, K., Hewitson, B., et al. (2016). CMIP5 data provided at the IPCC Data Distribution Centre.

- Engelbrecht, F. A., McGregor, J. L., and Engelbrecht, C. J. (2009). Dynamics of the Conformal-Cubic Atmospheric Model projected climate-change signal over southern Africa. *INTERNATIONAL JOURNAL OF CLIMATOLOGY*, 29(7, SI):1013–1033. 28th Joint Scientific-Committee-of-the-World-Climate-Research-Programme Meeting on African Climate and Applications, Tanzania Meteorol Agcy, Zanzibar, TANZANIA, MAR 26-30, 2007.
- England, M. I., Dougill, A. J., Stringer, L. C., Vincent, K. E., Pardoe, J., Kalaba, F. K., Mkwambisi, D. D., Namaganda, E., and Afonis, S. (2018). Climate change adaptation and cross-sectoral policy coherence in southern Africa. *REGIONAL ENVIRONMENTAL CHANGE*, 18(7, SI):2059–2071.
- Erler, A. R., Frey, S. K., Khader, O., d’Orgeville, M., Park, Y.-J., Hwang, H.-T., Lapen, D. R., Peltier, W. R., and Sudicky, E. A. (2019). Simulating Climate Change Impacts on Surface Water Resources Within a Lake-Affected Region Using Regional Climate Projections. *WATER RESOURCES RESEARCH*, 55(1):130–155.
- Falkenmark, M. and Rockstrom, J. (2006). The new blue and green water paradigm: Breaking new ground for water resources planning and management. *JOURNAL OF WATER RESOURCES PLANNING AND MANAGEMENT-ASCE*, 132(3):129–132.
- Fang, G., Yang, J., Chen, Y., Zhang, S., Deng, H., Liu, H., and De Maeyer, P. (2015). Climate Change Impact on the Hydrology of a Typical Watershed in the Tianshan Mountains. *ADVANCES IN METEOROLOGY*.
- FAO (2016). [www.fao.org/aquastat/en/overview/methodology/water-use](http://www.fao.org/aquastat/en/overview/methodology/water-use). <http://www.fao.org/aquastat/en/overview/methodology/water-use>. (Accessed on 10/02/2017).
- Feldman, A. D. (2000). *Hydrologic modeling system HEC-HMS: technical reference manual*. US Army Corps of Engineers, Hydrologic Engineering Center.
- Fetter, C. W. (2000). *Applied hydrogeology*. Prentice hall.
- Ficklin, D. L., Letsinger, S. L., Stewart, I. T., and Maurer, E. P. (2016). Assessing differences in snowmelt-dependent hydrologic projections using CMIP3 and CMIP5 climate forcing data for the western United States. *HYDROLOGY RESEARCH*, 47(2):483–500.
- Ficklin, D. L., Luo, Y., Luedeling, E., and Zhang, M. (2009). Climate change sensitivity assessment of a highly agricultural watershed using SWAT. *JOURNAL OF HYDROLOGY*, 374(1-2):16–29.
- Fischer, A. M., Weigel, A. P., Buser, C. M., Knutti, R., Kuensch, H. R., Liniger, M. A., Schaer, C., and Appenzeller, C. (2012). Climate change projections for Switzerland based on a Bayesian multi-model approach. *INTERNATIONAL JOURNAL OF CLIMATOLOGY*, 32(15):2348–2371.

- Fisher, J. C., Bartolino, J. R., Wylie, A. H., Sukow, J., and McVay, M. (2016). Groundwater-flow model for the wood river valley aquifer system, south-central idaho. Technical report, Reston, VA. Report.
- Flannery, B. P., Press, W. H., Teukolsky, S. A., and Vetterling, W. (1992). Numerical recipes in C. *Press Syndicate of the University of Cambridge, New York*, 24:78.
- Fowler, H. J., Blenkinsop, S., and Tebaldi, C. (2007). Linking climate change modelling to impacts studies: recent advances in downscaling techniques for hydrological modelling. *INTERNATIONAL JOURNAL OF CLIMATOLOGY*, 27(12):1547–1578. General Assembly of the European-Geosciences-Union, Vienna, AUSTRIA, APR 02-07, 2006.
- Freyberg, D. (1988). AN EXERCISE IN GROUNDWATER MODEL CALIBRATION AND PREDICTION. *GROUND WATER*, 26(3):350–360.
- Fujino, J., Nair, R., Kainuma, M., Masui, T., and Matsuoka, Y. (2006). Multi-gas mitigation analysis on stabilization scenarios using aim global model. *ENERGY JOURNAL*, pages 343–353.
- Fuka, D. R., Walter, M. T., MacAlister, C., Degaetano, A. T., Steenhuis, T. S., and Easton, Z. M. (2014a). Using the Climate Forecast System Reanalysis as weather input data for watershed models. *Hydrological Processes*, 28(22):5613–5623. HYP-13-0038.R2.
- Fuka, D. R., Walter, M. T., MacAlister, C., Degaetano, A. T., Steenhuis, T. S., and Easton, Z. M. (2014b). Using the Climate Forecast System Reanalysis as weather input data for watershed models. *HYDROLOGICAL PROCESSES*, 28(22):5613–5623.
- Galbiati, L., Bouraoui, E., Elorza, F., and Bidoglio, G. (2006). Modeling diffuse pollution loading into a Mediterranean lagoon: Development and application of an integrated surface-sub surface model tool. *ECOLOGICAL MODELLING*, 193(1-2):4–18. 1st International Conference on Southern European Coastal Lagoons, Ferrara, ITALY, NOV 10-12, 2003.
- Gale, I. (2005). *Strategies for Managed Aquifer Recharge (MAR) in semi-arid areas*. UNESCO.
- Gao, F., Feng, G., Han, M., Dash, P., Jenkins, J., and Liu, C. (2019a). Assessment of Surface Water Resources in the Big Sunflower River Watershed Using Coupled SWAT-MODFLOW Model. *WATER*, 11(3).
- Gao, Y., Zhang, X., Zhang, X., Li, D., Yang, M., and Tian, J. (2019b). Application of NSGA-II and Improved Risk Decision Method for Integrated Water Resources Management of Malian River Basin. *WATER*, 11(8).

- Gardner, M. A., Morton, C. G., Huntington, J. L., Niswonger, R. G., and Henson, W. R. (2018). Input data processing tools for the integrated hydrologic model GSFLOW. *ENVIRONMENTAL MODELLING & SOFTWARE*, 109:41–53.
- Gassman, P. W., Reyes, M. R., Green, C. H., and Arnold, J. G. (2007). The soil and water assessment tool: Historical development, applications, and future research directions. *TRANSACTIONS OF THE ASABE*, 50(4):1211–1250.
- Gaus, I. and Dochartaigh, B. Ó. (2000). Conceptual modelling of data-scarce aquifers in scotland: the sandstone aquifers of fife and dumfries. *Geological Society, London, Special Publications*, 182(1):157–168.
- Gaye, C. and Edmunds, W. (1996). Groundwater recharge estimation using chloride, stable isotopes and tritium profiles in the sands of northwestern Senegal. *ENVIRONMENTAL GEOLOGY*, 27(3):246–251.
- Gilbert, R. O. (1987). *Statistical methods for environmental pollution monitoring*. John Wiley & Sons.
- Githui, F., Gitau, W., Mutua, F., and Bauwens, W. (2009). Climate change impact on SWAT simulated streamflow in western Kenya. *INTERNATIONAL JOURNAL OF CLIMATOLOGY*, 29(12):1823–1834.
- Gocic, M. and Trajkovic, S. (2013). Analysis of changes in meteorological variables using Mann-Kendall and Sen’s slope estimator statistical tests in Serbia. *GLOBAL AND PLANETARY CHANGE*, 100:172–182.
- GoM (2005). *National Water Policy*. Ministry of Irrigation and Water Development.
- Gong, W., Gupta, H. V., Yang, D., Sricharan, K., and Hero, III, A. O. (2013). Estimating epistemic and aleatory uncertainties during hydrologic modeling: An information theoretic approach. *WATER RESOURCES RESEARCH*, 49(4):2253–2273.
- Govender, M. and Everson, C. (2005). Modelling streamflow from two small South African experimental catchments using the SWAT model. *HYDROLOGICAL PROCESSES*, 19(3, SI):683–692. 1st International SWAT Conference, Rauischholzhausen, GERMANY, AUG, 2001.
- Government of Malawi (2017). The Malawi Growth and Development Strategy (MGDS III)(2017–2022).
- Green, T. R., Taniguchi, M., Kooi, H., Gurdak, J. J., Allen, D. M., Hiscock, K. M., Treidel, H., and Aureli, A. (2011a). Beneath the surface of global change: Impacts of climate change on groundwater. *Journal of Hydrology*, 405(3-4):532–560.

- Green, T. R., Taniguchi, M., Kooi, H., Gurdak, J. J., Allen, D. M., Hiscock, K. M., Treidel, H., and Aureli, A. (2011b). Beneath the surface of global change: Impacts of climate change on groundwater. *Journal of Hydrology*, 405(3):532–560.
- Greve, P., Kahil, T., Mochizuki, J., Schinko, T., Satoh, Y., Burek, P., Fischer, G., Tramberend, S., Burtscher, R., Langan, S., and Wada, Y. (2018). Global assessment of water challenges under uncertainty in water scarcity projections. *NATURE SUSTAINABILITY*, 1(9):486–494.
- Grigg, N. S. (2019). IWRM and the Nexus Approach: Versatile Concepts for Water Resources Education. *JOURNAL OF CONTEMPORARY WATER RESEARCH & EDUCATION*, 166(1):24–34.
- Gudmundsson, L., Bremnes, J. B., Haugen, J. E., and Engen-Skaugen, T. (2012). Technical Note: Downscaling RCM precipitation to the station scale using statistical transformations - a comparison of methods. *HYDROLOGY AND EARTH SYSTEM SCIENCES*, 16(9):3383–3390.
- Gupta, H. V., Sorooshian, S., and Yapo, P. O. (1999). STATUS OF AUTOMATIC CALIBRATION FOR HYDROLOGIC MODELS: COMPARISON WITH MULTILEVEL EXPERT CALIBRATION. *JOURNAL OF HYDROLOGIC ENGINEERING*, 4(2):135–143.
- GWP (2011). What is IWRM? - GWP. <https://www.gwp.org/en/GWP-CEE/about/why/what-is-iwrn/>. (Accessed on 03/11/2017).
- GYAUBOAKYE, P. and SCHULTZ, G. (1994). FILLING GAPS IN RUNOFF TIME-SERIES IN WEST-AFRICA. *HYDROLOGICAL SCIENCES JOURNAL-JOURNAL DES SCIENCES HYDROLOGIQUES*, 39(6):621–636.
- Hamed, K. and Rao, A. (1998). A modified Mann-Kendall trend test for autocorrelated data. *JOURNAL OF HYDROLOGY*, 204(1-4):182–196.
- Hanson, R. T., Boyce, S. E., Schmid, W., Hughes, J. D., Mehl, S. W., Leake, S. A., Maddock III, T., and Niswonger, R. G. (2014). One-water hydrologic flow model (MODFLOW-OWHM). Technical report, US Geological Survey.
- Harbaugh, A. W., Banta, E. R., Hill, M. C., and McDonald, M. G. (2000). Modflow-2000, the u. s. geological survey modular ground-water model-user guide to modularization concepts and the ground-water flow process. *Open-file Report. U. S. Geological Survey*, (92):134.
- Harrigan, S., Hannaford, J., Muchan, K., and Marsh, T. J. (2018). Designation and trend analysis of the updated UK Benchmark Network of river flow stations: the UKBN2 dataset. *HYDROLOGY RESEARCH*, 49(2):552–567. 29th Nordic Water Conference, Vytautas Magnus Univ, Kaunas, LITHUANIA, AUG 08-10, 2016.

- Harris, G. (2002). Energy, water and food scenarios on the future of sustainable development. *Best Partners*.
- Hashmi, M. Z., Shamseldin, A. Y., and Melville, B. W. (2011). Comparison of SDSM and LARS-WG for simulation and downscaling of extreme precipitation events in a watershed. *Stochastic Environmental Research and Risk Assessment*, 25(4):475–484.
- Hassan, Z., Shamsudin, S., and Harun, S. (2014). Application of SDSM and LARS-WG for simulating and downscaling of rainfall and temperature. *Theoretical and applied climatology*, 116(1-2):243–257.
- Havril, T., Toth, A., Molson, J. W., Galsa, A., and Madl-Szonyi, J. (2018). Impacts of predicted climate change on groundwater flow systems: Can wetlands disappear due to recharge reduction? *JOURNAL OF HYDROLOGY*, 563:1169–1180.
- Healy, R. W. (2010). *Estimating groundwater recharge*. Cambridge University Press.
- Hewitson, B. C., Daron, J., Crane, R. G., Zermoglio, M. F., and Jack, C. (2014). Interrogating empirical-statistical downscaling. *CLIMATIC CHANGE*, 122(4):539–554.
- HIJIOKA, Y., MATSUOKA, Y., NISHIMOTO, H., MASUI, T., and KAINUMA, M. (2008). Global ghg emission scenarios under ghg concentration stabilization targets. *Journal of Global Environment Engineering*, 13:97–108.
- Hill, M. C. and Tiedeman, C. R. (2006). *Effective groundwater model calibration: with analysis of data, sensitivities, predictions, and uncertainty*. John Wiley & Sons.
- Hoff, H. (2011). Understanding the nexus: Background paper for the Bonn2011 Nexus Conference.
- Hojberg, A. and Refsgaard, J. (2005). Model uncertainty - parameter uncertainty versus conceptual models. *WATER SCIENCE AND TECHNOLOGY*, 52(6):177–186. International Symposium on Uncertainty and Precaution in Environment Management, Copenhagen, DENMARK, JUN 07-09, 2004.
- Hughes, J. D., Langevin, C. D., and Banta, E. R. (2017). Documentation for the MODFLOW 6 Framework. Technical report, US Geological Survey.
- Hunt, R. J. and Feinstein, D. T. (2012). MODFLOW-NWT: Robust Handling of Dry Cells Using a Newton Formulation of MODFLOW-2005. *GROUND WATER*, 50(5):659–663.
- Hunt, R. J., Fienen, M. N., and White, J. T. (2019). Revisiting "an exercise in groundwater model calibration and prediction" after 30 years: Insights and new directions. *Groundwater*.

- Hunt, R. J., Walker, J. F., Selbig, W. R., Westenbroek, S. M., and Regan, R. S. (2013). Simulation of climate-change effects on streamflow, lake water budgets, and stream temperature using GSFLOW and SNTEMP, Trout Lake Watershed, Wisconsin. Technical report, US Geological Survey.
- Hunter, J. D. (2007). Matplotlib: A 2d graphics environment. *Computing In Science & Engineering*, 9(3):90–95.
- IAH (2019). Climate-change adaptation & groundwater. [https://iah.org/wp-content/uploads/2019/07/IAH\\_Climate-ChangeAdaptationGdwtr.pdf](https://iah.org/wp-content/uploads/2019/07/IAH_Climate-ChangeAdaptationGdwtr.pdf). (Accessed on 09/09/2019).
- Immerzeel, W. W., Pellicciotti, F., and Bierkens, M. F. P. (2013). Rising river flows throughout the twenty-first century in two Himalayan glacierized watersheds. *NATURE GEOSCIENCE*, 6(9):742–745.
- IPCC (2001). Contribution of Working Group I to the Third Assessment Report of the Intergovernmental Panel on Climate Change. Technical Report November.
- Jackson, C., Hughes, A., and Dochartaigh, B. O. (2004). Preliminary numerical modelling of groundwater flow in the dumfries basin. This item has been internally reviewed but not externally peer-reviewed.
- James, G., Witten, D., Hastie, T., and Tibshirani, R. (2013). An Introduction to Statistical Learning with Applications in R Introduction. In *INTRODUCTION TO STATISTICAL LEARNING: WITH APPLICATIONS IN R*, volume 103 of *Springer Texts in Statistics*, pages 1–14.
- James, R., Washington, R., Abiodun, B., Kay, G., Mutemi, J., Pokam, W., Hart, N., Artan, G., and Senior, C. (2018). EVALUATING CLIMATE MODELS WITH AN AFRICAN LENS. *BULLETIN OF THE AMERICAN METEOROLOGICAL SOCIETY*, 99(2):313–336.
- Javier Miro, J., Caselles, V., and Jose Estrela, M. (2017). Multiple imputation of rainfall missing data in the Iberian Mediterranean context. *ATMOSPHERIC RESEARCH*, 197:313–330.
- Jha, M., Gassman, P., Secchi, S., Gu, R., and Arnold, J. (2004a). Effect of watershed subdivision on swat flow, sediment, and nutrient predictions. *JOURNAL OF THE AMERICAN WATER RESOURCES ASSOCIATION*, 40(3):811–825.
- Jha, M., Pan, Z., Takle, E., and Gu, R. (2004b). Impacts of climate change on streamflow in the Upper Mississippi River Basin: A regional climate model perspective. *JOURNAL OF GEOPHYSICAL RESEARCH-ATMOSPHERES*, 109(D9).
- JICA (2014). Final Report: Part I Existing Condition - Project for National Water Resources Master Plan in the Republic of Malawi. [http://open\\_jicareport.jica.go.jp/pdf/12184537\\_01.pdf](http://open_jicareport.jica.go.jp/pdf/12184537_01.pdf). (Accessed on 08/07/2018).



- Jimenez Cisneros, B. E., Oki, T., Arnell, N. W., Benito, G., Cogley, J. G., Doell, P., Jiang, T., Mwakalila, S. S., Fischer, T., Gerten, D., Hock, R., Kanae, S., Lu, X., Jose Mata, L., Pahl-Wostl, C., Strzepek, K. M., Su, B., and van den Hurk, B. (2014). Freshwater Resources. In Field, CB and Barros, VR and Dokken, DJ and Mach, KJ and Mastrandrea, MD and Bilir, TB and Chatterjee, M and Ebi, KL and Estrada, YO and Genova, RC and Girma, B and Kissel, ES and Levy, AN and MacCracken, S and Mastrandrea, PR and White, LL, editor, *CLIMATE CHANGE 2014: IMPACTS, ADAPTATION, AND VULNERABILITY, PT A: GLOBAL AND SECTORAL ASPECTS: WORKING GROUP II CONTRIBUTION TO THE FIFTH ASSESSMENT REPORT OF THE INTERGOVERNMENTAL PANEL ON CLIMATE CHANGE*, pages 229–269.
- Jones, R. N., Chiew, F. H. S., Boughton, W. C., and Zhang, L. (2006). Estimating the sensitivity of mean annual runoff to climate change using selected hydrological models. *ADVANCES IN WATER RESOURCES*, 29(10):1419–1429.
- Joshi, D., St-Hilaire, A., Ouarda, T., and Daigle, A. (2015). Statistical downscaling of precipitation and temperature using sparse Bayesian learning, multiple linear regression and genetic programming frameworks. *CANADIAN WATER RESOURCES JOURNAL*, 40(4):392–408.
- Joshua, M. K., Ngongondo, C., Chipungu, F., Monjerezi, M., Liwenga, E., Majule, A. E., Stathers, T., and Lamboll, R. (2016). Climate change in semi-arid Malawi: Perceptions, adaptation strategies and water governance. *JAMBA-JOURNAL OF DISASTER RISK STUDIES*, 8(3).
- Jung, I.-W., Moradkhani, H., and Chang, H. (2012). Uncertainty assessment of climate change impacts for hydrologically distinct river basins. *JOURNAL OF HYDROLOGY*, 466:73–87.
- Jury, M. and Gwazantini, M. (2002). Climate variability in Malawi, part 2: sensitivity and prediction of lake levels. *International Journal of Climatology*, 22(11):1303–1312.
- Jury, M. and Mwafulirwa, N. (2002). Climate variability in Malawi, part 1: Dry summers, statistical associations and predictability. *INTERNATIONAL JOURNAL OF CLIMATOLOGY*, 22(11):1289–1302.
- Kadioglu, M. (1997). Trends in surface air temperature data over Turkey. *INTERNATIONAL JOURNAL OF CLIMATOLOGY*, 17(5):511–520.
- Kalin, R. M. (2000). Radiocarbon Dating of Groundwater Systems. In Cook, P. G. and Herczeg, A. L., editors, *Environmental Tracers in Subsurface Hydrology*, pages 111–144. Springer US, Boston, MA.
- Kalin, R. M., Mwanamveka, J., Coulson, A. B., Robertson, D. J. C., Clark, H., Rathjen, J., and Rivett, M. O. (2019). Stranded Assets as a Key Concept to Guide Investment Strategies for Sustainable Development Goal 6. *WATER*, 11(4).

- Kalteh, A. M. and Berndtsson, R. (2007). Interpolating monthly precipitation by self-organizing map (SOM) and multilayer perceptron (MLP). *HYDROLOGICAL SCIENCES JOURNAL-JOURNAL DES SCIENCES HYDROLOGIQUES*, 52(2):305–317.
- Kalteh, A. M. and Hjorth, P. (2009). Imputation of missing values in a precipitation-runoff process database. *HYDROLOGY RESEARCH*, 40(4):420–432.
- Kannan, S. S. and Ramaraj, N. (2010). A novel hybrid feature selection via Symmetrical Uncertainty ranking based local memetic search algorithm. *KNOWLEDGE-BASED SYSTEMS*, 23(6):580–585.
- Keeling, C. D., Bacastow, R. B., Bainbridge, A. E., Ekdahl, C. A., Guenther, P. R., Waterman, L. S., and Chin, J. F. S. (1976). ATMOSPHERIC CARBON-DIOXIDE VARIATIONS AT MAUNA-LOA OBSERVATORY, HAWAII. *Tellus*, 28(6):538–551.
- Keenan, T., Maria Serra, J., Lloret, F., Ninyerola, M., and Sabate, S. (2011). Predicting the future of forests in the Mediterranean under climate change, with niche- and process-based models: CO2 matters! *GLOBAL CHANGE BIOLOGY*, 17(1):565–579.
- Kelly, L., Bertram, D., Kalin, R., and Ngongondo, C. (2019). Characterization of groundwater discharge to rivers in the shire river basin, malawi. *American Journal of Water Science and Engineering*, 5(4):127–138.
- Kendall, M. G. (1975). Rank correlation methods.
- Kennedy, J. and Eberhart, R. (1995). Particle swarm optimization. In *Neural Networks, 1995. Proceedings., IEEE International Conference on*, volume 4, pages 1942–1948 vol.4.
- Khalil, M., Panu, U., and Lennox, W. (2001). Groups and neural networks based streamflow data infilling procedures. *JOURNAL OF HYDROLOGY*, 241(3-4):153–176.
- Khan, M. S., Coulibaly, P., and Dibike, Y. (2006). Uncertainty analysis of statistical downscaling methods using Canadian Global Climate Model predictors. *HYDROLOGICAL PROCESSES*, 20(14):3085–3104.
- Kiersch, B., Tognetti, S., et al. (2002). Land-water linkages in rural watersheds: results from the FAO electronic workshop. *Land Use Water Resour. Res.*, 2:1–1.
- Kim, J.-T., Choo, C.-O., Kim, M.-I., and Jeong, G.-C. (2017). Validity evaluation of a groundwater dam in Oshipcheon River, eastern Korea using a SWAT-MODFLOW model. *ENVIRONMENTAL EARTH SCIENCES*, 76(22).

- Kim, J.-W. and Pachepsky, Y. A. (2010). Reconstructing missing daily precipitation data using regression trees and artificial neural networks for SWAT streamflow simulation. *JOURNAL OF HYDROLOGY*, 394(3-4):305–314.
- Kim, N. W., Chung, I. M., Won, Y. S., and Arnold, J. G. (2008). Development and application of the integrated SWAT-MODFLOW model. *JOURNAL OF HYDROLOGY*, 356(1-2):1–16.
- Kingra, P. K., Setia, R., Kaur, S., Singh, S., Singh, S. P., Kukal, S. S., and Pateriya, B. (2018). Spatio-temporal analysis of the climate impact on rice yield in north-west India. *SPATIAL INFORMATION RESEARCH*, 26(4):381–395.
- Kirchner, J. (2006). Getting the right answers for the right reasons: Linking measurements, analyses, and models to advance the science of hydrology. *WATER RESOURCES RESEARCH*, 42(3).
- Kishiwa, P., Nobert, J., Kongo, V., and Ndomba, P. (2018). Assessment of impacts of climate change on surface water availability using coupled SWAT and WEAP models: case of upper Pangani River Basin, Tanzania. In Makurira, H and Mazvimavi, D and KileshyeOnema, JM and Kapangaziwiri, E and Gumindoga, W, editor, *UNDERSTANDING SPATIO-TEMPORAL VARIABILITY OF WATER RESOURCES AND THE IMPLICATIONS FOR IWRM IN SEMI-ARID EASTERN AND SOUTHERN AFRICA*, VOL 378, volume 378 of *Proceedings of the International Association of Hydrological Sciences (IAHS)*, pages 23–27. Int Assoc Hydrol Sci. International-Association-of-Hydrological-Sciences Scientific Assembly, Port Elizabeth, SOUTH AFRICA, JUL 10-14, 2017.
- Knighton, J., Pleiss, G., Carter, E., Lyon, S., Walter, M. T., and Steinschneider, S. (2019). Potential Predictability of Regional Precipitation and Discharge Extremes Using Synoptic-Scale Climate Information via Machine Learning: An Evaluation for the Eastern Continental United States. *JOURNAL OF HYDROMETEOROLOGY*, 20(5):883–900.
- Knutti, R. (2010). The end of model democracy? *CLIMATIC CHANGE*, 102(3-4):395–404.
- Knutti, R. and Sedlacek, J. (2013). Robustness and uncertainties in the new CMIP5 climate model projections. *NATURE CLIMATE CHANGE*, 3(4):369–373.
- Kohonen, T. (1998). The self-organizing map. *Neurocomputing*, 21(1-3):1–6.
- Kothari, C. R. (2004). *Research methodology: Methods and techniques*. New Age International.
- Krause, P., Boyle, D., and Bäse, F. (2005). Comparison of different efficiency criteria for hydrological model assessment. *Advances in geosciences*, 5:89–97.
- Kresic, N. (2006). *Hydrogeology and groundwater modeling*. CRC press.

- Kresic, N. and Mikszewski, A. (2012). *Hydrogeological conceptual site models: data analysis and visualization*. CRC press.
- Kriegler, E., O'Neill, B. C., Hallegatte, S., Kram, T., Lempert, R. J., Moss, R. H., and Wilbanks, T. (2012). The need for and use of socio-economic scenarios for climate change analysis: A new approach based on shared socio-economic pathways. *GLOBAL ENVIRONMENTAL CHANGE-HUMAN AND POLICY DIMENSIONS*, 22(4):807–822.
- Kuczera, G. and Parent, E. (1998). Monte Carlo assessment of parameter uncertainty in conceptual catchment models: the Metropolis algorithm. *JOURNAL OF HYDROLOGY*, 211(1-4):69–85.
- Kumambala, P. G. (2010). *Sustainability of water resources development for Malawi with particular emphasis on North and Central Malawi*. PhD thesis, University of Glasgow.
- Langevin, C. D., Hughes, J. D., Banta, E. R., Niswonger, R. G., Panday, S., and Provost, A. M. (2017). Documentation for the MODFLOW 6 Groundwater Flow Model. Technical report, US Geological Survey.
- Lanzante, J. (1996). Resistant, robust and non-parametric techniques for the analysis of climate data: Theory and examples, including applications to historical radiosonde station data. *INTERNATIONAL JOURNAL OF CLIMATOLOGY*, 16(11):1197–1226.
- Le Brocque, A. F., Kath, J., and Reardon-Smith, K. (2018). Chronic groundwater decline: A multi-decadal analysis of groundwater trends under extreme climate cycles. *JOURNAL OF HYDROLOGY*, 561:976–986.
- Leavesley, G. H., Lichty, R., Thoutman, B., and Saindon, L. (1983). *Precipitation-runoff modeling system: User's manual*. USGS Washington, DC.
- Leck, H., Conway, D., Bradshaw, M., and Rees, J. (2015). Tracing the Water-Energy-Food Nexus: Description, Theory and Practice. *GEOGRAPHY COMPASS*, 9(8):445–460.
- Leemhuis, C., Thonfeld, F., Naeschen, K., Steinbach, S., Muro, J., Strauch, A., Lopez, A., Daconto, G., Games, I., and Diekkruieger, B. (2017). Sustainability in the Food-Water-Ecosystem Nexus: The Role of Land Use and Land Cover Change for Water Resources and Ecosystems in the Kilombero Wetland, Tanzania. *SUSTAINABILITY*, 9(9).
- Legates, D. R. and McCabe, G. J. (1999). Evaluating the use of “goodness-of-fit” measures in hydrologic and hydroclimatic model validation. *Water resources research*, 35(1):233–241.
- Lemann, T., Zeleke, G., Amsler, C., Giovanoli, L., Suter, H., and Roth, V. (2016). Modelling the effect of soil and water conservation on discharge and sediment

- yield in the upper Blue Nile basin, Ethiopia. *APPLIED GEOGRAPHY*, 73:89–101.
- Lempert, R. and Schlesinger, M. (2000). Robust strategies for abating climate change - An editorial essay. *CLIMATIC CHANGE*, 45(3-4):387–401.
- Lempert, R. J. and Groves, D. G. (2010). Identifying and evaluating robust adaptive policy responses to climate change for water management agencies in the American west. *TECHNOLOGICAL FORECASTING AND SOCIAL CHANGE*, 77(6):960–974.
- Li, F.-F., Wang, Z.-Y., and Qiu, J. (2019a). Long-term streamflow forecasting using artificial neural network based on preprocessing technique. *JOURNAL OF FORECASTING*, 38(3):192–206.
- Li, M., Fu, Q., Singh, V. P., Ma, M., and Liu, X. (2017). An intuitionistic fuzzy multi-objective non-linear programming model for sustainable irrigation water allocation under the combination of dry and wet conditions. *JOURNAL OF HYDROLOGY*, 555:80–94.
- Li, M., Li, J., Singh, V. P., Fu, Q., Li, D., and Yang, G. (2019b). Efficient allocation of agricultural land and water resources for soil environment protection using a mixed optimization-simulation approach under uncertainty. *GEODERMA*, 353:55–69.
- Liu, T., Chen, Y., Li, B., Hu, Y., Qiu, H., and Liang, Z. (2019). Long-term streamflow forecasting for the Cascade Reservoir System of Han River using SWAT with CFS output. *HYDROLOGY RESEARCH*, 50(2):655–671.
- Lo Presti, R., Barca, E., and Passarella, G. (2010). A methodology for treating missing data applied to daily rainfall data in the Candelaro River Basin (Italy). *ENVIRONMENTAL MONITORING AND ASSESSMENT*, 160(1-4):1–22.
- Luo, Y., Ficklin, D. L., Liu, X., and Zhang, M. (2013). Assessment of climate change impacts on hydrology and water quality with a watershed modeling approach. *SCIENCE OF THE TOTAL ENVIRONMENT*, 450:72–82.
- Luo, Y. and Sophocleous, M. (2011). Two-way coupling of unsaturated-saturated flow by integrating the SWAT and MODFLOW models with application in an irrigation district in arid region of West China. *JOURNAL OF ARID LAND*, 3(3):164–173.
- Luo, Y., Su, B., Yuan, J., Li, H., and Zhang, Q. (2011). GIS Techniques for Watershed Delineation of SWAT Model in Plain Polders. In Wu, Y, editor, *2011 3RD INTERNATIONAL CONFERENCE ON ENVIRONMENTAL SCIENCE AND INFORMATION APPLICATION TECHNOLOGY ESIAT 2011, VOL 10, PT C*, volume 10 of *Procedia Environmental Sciences*, pages 2050–2057. Hong Kong Educ; Engn Technol Press; Asia Pacific Environm Sci Res Ctr; Wuhan Univ; Huazhong Normal Univ; China Univ Geosci; Wuhan Inst Technol. 3rd

- International Conference on Environmental Science and Information Application Technology (ESIAT), Xian, PEOPLES R CHINA, AUG 20-21, 2011.
- Lutz, A. F., ter Maat, H. W., Biemans, H., Shrestha, A. B., Wester, P., and Immerzeel, W. W. (2016). Selecting representative climate models for climate change impact studies: an advanced envelope-based selection approach. *INTERNATIONAL JOURNAL OF CLIMATOLOGY*, 36(12):3988–4005.
- MacDonald, A., Ball, D., and Darling, W. (2000). The permian aquifer of dumfries : groundwater chemistry and age. This item has been internally reviewed but not externally peer-reviewed.
- MacDonald, A., Robins, N., Ball, D., and Dochartaigh, B. (2005). An overview of groundwater in Scotland. *SCOTTISH JOURNAL OF GEOLOGY*, 41(1):3–11.
- MacDonald, A. M. and Calow, R. C. (2009). Developing groundwater for secure rural water supplies in Africa. *DESALINATION*, 248(1-3):546–556. International Workshop on Water and Sanitation in International Development and Disaster Relief, Edinburgh, SCOTLAND, MAY 28-30, 2008.
- Mahlman, J. (1997). Uncertainties in projections of human-caused climate warming. *SCIENCE*, 278(5342):1416–1417.
- Maier, H. R., Guillaume, J. H. A., van Delden, H., Riddell, G. A., Haasnoot, M., and Kwakkel, J. H. (2016). An uncertain future, deep uncertainty, scenarios, robustness and adaptation: How do they fit together? *ENVIRONMENTAL MODELLING & SOFTWARE*, 81:154–164.
- Mair, P. (2016). Thou Shalt Be Reproducible! A Technology Perspective. *FRONTIERS IN PSYCHOLOGY*, 7.
- Mann, H. B. (1945). NONPARAMETRIC TESTS AGAINST TREND. *ECONOMETRICA*, 13(3):245–259.
- Mansour, M. M., Wang, L., Whiteman, M., and Hughes, A. G. (2018). Estimation of spatially distributed groundwater potential recharge for the United Kingdom. *QUARTERLY JOURNAL OF ENGINEERING GEOLOGY AND HYDROGEOLOGY*, 51(2):247–263.
- Mapoma, H. W. and Xie, X. (2014). Basement and alluvial aquifers of malawi: an overview of groundwater quality and policies. *African Journal of Environmental Science and Technology*, 8(3):190–202.
- Marchenko, Y. V. and Genton, M. G. (2010). Multivariate log-skew-elliptical distributions with applications to precipitation data. *ENVIRONMETRICS*, 21(3-4, SI):318–340. 4th International Workshop on Spatio-Temporal Modelling, Alghero, ITALY, SEP 24-26, 2008.

- Margat, J. and VanDerGun, J. (2013). Groundwater around the World: A Geographic Synopsis. In *GROUNDWATER AROUND THE WORLD: A GEOGRAPHIC SYNOPSIS*, pages 1–341.
- Markstrom, S. L., Niswonger, R. G., Regan, R. S., Prudic, D. E., and Barlow, P. M. (2008). GSFLOW-Coupled Ground-water and Surface-water FLOW model based on the integration of the Precipitation-Runoff Modeling System (PRMS) and the Modular Ground-Water Flow Model (MODFLOW-2005). *US Geological Survey techniques and methods*, 6:240.
- Markstrom, S. L., Regan, R. S., Hay, L. E., Viger, R. J., Webb, R. M., Payn, R. A., and LaFontaine, J. H. (2015). Prms-iv, the precipitation-runoff modeling system, version 4. *US Geological Survey Techniques and Methods*, (6-B7).
- Maurer, E. P. (2007). Uncertainty in hydrologic impacts of climate change in the Sierra Nevada, California, under two emissions scenarios. *CLIMATIC CHANGE*, 82(3-4):309–325.
- Maurer, E. P. and Hidalgo, H. G. (2008). Utility of daily vs. monthly large-scale climate data: an intercomparison of two statistical downscaling methods. *HYDROLOGY AND EARTH SYSTEM SCIENCES*, 12(2):551–563.
- McCallum, J. L., Crosbie, R. S., Walker, G. R., and Dawes, W. R. (2010). Impacts of climate change on groundwater in Australia: a sensitivity analysis of recharge. *HYDROGEOLOGY JOURNAL*, 18(7):1625–1638.
- McDonald, J. and Harbaugh, A. (1988). Modflow, a modular 3d finite difference ground-water flow model, open-file report 83-875. *US Geological Survey*.
- McDonald, M. G., Harbaugh, A. W., Orr, B. R., and Ackerman, D. J. (1991). A method of converting no-flow cells to variable-head cells for the US Geological Survey modular finite-difference ground-water flow model. Technical report, US Dept. of the Interior, US Geological Survey; Books and Open-File Reports Section [distributor],.
- McMillan, A., Merritt, J., Auton, C., and Golledge, N. (2011). The quaternary geology of the solway. Technical report, Nottingham, UK.
- McSweeney, C., New, M., and Lizcano, G. (2014). UNDP climate change country profiles Malawi. <http://www.ndr.mw:8080/xmlui/bitstream/handle/123456789/1117/UNDP%20Climate%20Change%20Country%20Profiles.pdf?sequence=1>. (Accessed on 07/15/2017).
- McSweeney, C. F., Jones, R. G., Lee, R. W., and Rowell, D. P. (2015). Selecting CMIP5 GCMs for downscaling over multiple regions. *CLIMATE DYNAMICS*, 44(11-12):3237–3260.
- Mechoso, C., ROBERTSON, A., BARTH, N., DAVEY, M., DELECLUSE, P., GENT, P., INESON, S., KIRTMAN, B., LATIF, M., LETREUT, H., NAGAI,

- T., NEELIN, J., PHILANDER, S., POLCHER, J., SCHOPF, P., STOCKDALE, T., SUAREZ, M., TERRAY, L., THUAL, O., and TRIBBIA, J. (1995). THE SEASONAL CYCLE OVER THE TROPICAL PACIFIC IN COUPLED OCEAN-ATMOSPHERE GENERAL-CIRCULATION MODELS. *MONTHLY WEATHER REVIEW*, 123(9):2825–2838.
- Mekonnen, M. M. and Hoekstra, A. Y. (2016). Four billion people facing severe water scarcity. *SCIENCE ADVANCES*, 2(2).
- Miller, A., Nhlema, M., Kumwenda, S., Mbalame, E., Uka, Z., Feighery, J., and Kalin, R. M. (2018). Evolving water point mapping to strategic decision making in rural malawi.
- Miller, N., Bashford, K., and Strem, E. (2003). Potential impacts of climate change on California hydrology. *JOURNAL OF THE AMERICAN WATER RESOURCES ASSOCIATION*, 39(4):771–784.
- Minville, M., Brissette, F., and Leconte, R. (2008). Uncertainty of the impact of climate change on the hydrology of a nordic watershed. *JOURNAL OF HYDROLOGY*, 358(1-2):70–83.
- Mirmasoudi, S., Byrne, J., MacDonald, R., Johnson, D., and Kroebel, R. (2019). Modelling historical and potential future climate impacts on Keremeos Creek, an Okanagan-Similkameen watershed, British Columbia, Canada: Part I. Forecasting change in spring and summer water supply and demand. *CANADIAN WATER RESOURCES JOURNAL*, 44(4):350–366.
- Mitchell, T. and Jones, P. (2005). An improved method of constructing a database of monthly climate observations and associated high-resolution grids. *INTERNATIONAL JOURNAL OF CLIMATOLOGY*, 25(6):693–712.
- Mkandawire, T. W. and Mulwafu, W. O. (2006). An analysis of IWRM capacity needs in Malawi. *Physics and Chemistry of the Earth, Parts A/B/C*, 31(15-16):738–744.
- MMSD (2017). Malawi Meteorological Services. <http://www.metmalawi.com/about.php>. (Accessed on 01/07/2017).
- MMSD (2018). Malawi Meteorological Services. <http://www.metmalawi.com/about.php>. (Accessed on 02/09/2018).
- MoAIWD (2017). Shire river basin plan: Executive summary. <http://shirebasinplanning.wris.info/>. (Accessed on 12/23/2017).
- Molina-Navarro, E., Bailey, R. T., Andersen, H. E., Thodsen, H., Nielsen, A., Park, S., Jensen, J. S., Jensen, J. B., and Trolle, D. (2019a). Comparison of abstraction scenarios simulated by SWAT and SWAT-MODFLOW. *HYDROLOGICAL SCIENCES JOURNAL-JOURNAL DES SCIENCES HYDROLOGIQUES*, 64(4):434–454.



- Molina-Navarro, E., Bailey, R. T., Andersen, H. E., Thodsen, H., Nielsen, A., Park, S., Jensen, J. S., Jensen, J. B., and Trolle, D. (2019b). Comparison of abstraction scenarios simulated by SWAT and SWAT-MODFLOW. *Hydrological Sciences Journal*, 0(ja):null.
- Monhart, S., Spirig, C., Bhend, J., Bogner, K., Schar, C., and Liniger, M. A. (2018). Skill of Subseasonal Forecasts in Europe: Effect of Bias Correction and Downscaling Using Surface Observations. *JOURNAL OF GEOPHYSICAL RESEARCH-ATMOSPHERES*, 123(15):7999–8016.
- Moriasi, D. N., Arnold, J. G., Van Liew, M. W., Bingner, R. L., Harmel, R. D., and Veith, T. L. (2007). Model evaluation guidelines for systematic quantification of accuracy in watershed simulations. *TRANSACTIONS OF THE ASABE*, 50(3):885–900.
- Moriasi, D. N., Pai, N., Steiner, J. L., Gowda, P. H., Winchell, M., Rathjens, H., Starks, P. J., and Verser, J. A. (2019). SWAT-LUT: A Desktop Graphical User Interface for Updating Land Use in SWAT. *JOURNAL OF THE AMERICAN WATER RESOURCES ASSOCIATION*, 55(5):1102–1115.
- Moritz, S. and Bartz-Beielstein, T. (2017). imputeTS: time series missing value imputation in R. *The R Journal*, 9(1):207–218.
- Moss, R., Babiker, W., Brinkman, S., Calvo, E., Carter, T., Edmonds, J., Elgizouli, I., Emori, S., Erda, L., Hibbard, K., et al. (2008). Towards new scenarios for the analysis of emissions: Climate change, impacts and response strategies.
- Moss, R. H., Edmonds, J. A., Hibbard, K. A., Manning, M. R., Rose, S. K., van Vuuren, D. P., Carter, T. R., Emori, S., Kainuma, M., Kram, T., Meehl, G. A., Mitchell, J. F. B., Nakicenovic, N., Riahi, K., Smith, S. J., Stouffer, R. J., Thomson, A. M., Weyant, J. P., and Wilbanks, T. J. (2010). The next generation of scenarios for climate change research and assessment. *NATURE*, 463(7282):747–756.
- Mucher, C., Stomph, T., and Fresco, L. (1993). Proposal for a global land use classification. Technical report, FAO/ITC/WAU.
- Murphy, J., Harris, G., Sexton, D., Kendon, E., Bett, P., Clark, R., Eagle, K., Fosser, G., Fung, F., Lowe, J., et al. (2018). Ukcpl8 land projections: Science report. *Met Office*.
- Mwale, F. D., Adeloye, A. J., and Rustum, R. (2012). Infilling of missing rainfall and streamflow data in the Shire River basin, Malawi - A self organizing map approach. *PHYSICS AND CHEMISTRY OF THE EARTH*, 50-52(SI):34–43.
- Mwale, F. D., Adeloye, A. J., and Rustum, R. (2014). Application of self-organising maps and multi-layer perceptron-artificial neural networks for streamflow and water level forecasting in data-poor catchments: the case of the Lower Shire floodplain, Malawi. *HYDROLOGY RESEARCH*, 45(6):838–854.

- Nanda, T., Sahoo, B., and Chatterjee, C. (2017). Enhancing the applicability of Kohonen Self-Organizing Map (KSOM) estimator for gap-filling in hydrometeorological timeseries data. *JOURNAL OF HYDROLOGY*, 549:133–147.
- Nash, J. E. and Sutcliffe, J. V. (1970a). River flow forecasting through conceptual models part i – a discussion of principles. *Journal of Hydrology*, 10(3):282–290.
- Nash, J. E. and Sutcliffe, J. V. (1970b). River flow forecasting through conceptual models part i—a discussion of principles. *Journal of hydrology*, 10(3):282–290.
- Neitsch, S. L., Arnold, J. G., Kiniry, J. R., and Williams, J. R. (2011). Soil and water assessment tool theoretical documentation version 2009. Technical report, Texas Water Resources Institute.
- Neuman, S. (2003a). Accounting for conceptual model uncertainty via maximum likelihood Bayesian model averaging. In Kovar, K and Hrkal, Z, editor, *CALIBRATION AND RELIABILITY IN GROUNDWATER MODELLING: A FEW STEPS CLOSER TO REALITY*, number 277 in IAHS PUBLICATION, pages 303–313. Conference on Calibration and Reliability in Groundwater Modelling (ModelCARE 2002), PRAGUE, CZECH REPUBLIC, JUN 17-20, 2002.
- Neuman, S. (2003b). Maximum likelihood Bayesian averaging of uncertain model predictions. *STOCHASTIC ENVIRONMENTAL RESEARCH AND RISK ASSESSMENT*, 17(5):291–305. ModelCARE 2002 Conference, PRAGUE, CZECH REPUBLIC, JUN 17-20, 2002.
- Ngai, S. T., Tangang, F., and Juneng, L. (2017). Bias correction of global and regional simulated daily precipitation and surface mean temperature over Southeast Asia using quantile mapping method. *GLOBAL AND PLANETARY CHANGE*, 149:79–90.
- Ngongondo, C. (2006). An analysis of long-term rainfall variability, trends and groundwater availability in the Mulunguzi river catchment area, Zomba mountain, Southern Malawi. *QUATERNARY INTERNATIONAL*, 148:45–50. Pan-Africa PAGES Workshop on African Palaeoperspectives, Nairobi, KENYA, JUL 19-20, 2004.
- Ngongondo, C. S., Xu, C.-Y., Tallaksen, L. M., Alemaw, B., and Chirwa, T. (2011). Regional frequency analysis of rainfall extremes in Southern Malawi using the index rainfall and L-moments approaches. *STOCHASTIC ENVIRONMENTAL RESEARCH AND RISK ASSESSMENT*, 25(7):939–955.
- Nicholson, S. E., Klotter, D., and Chavula, G. (2014). A detailed rainfall climatology for Malawi, Southern Africa. *INTERNATIONAL JOURNAL OF CLIMATOLOGY*, 34(2):315–325.
- Niswonger, R. G., Panday, S., and Ibaraki, M. (2011). MODFLOW-NWT, a Newton formulation for MODFLOW-2005. *US Geological Survey Techniques and Methods*, 6(A37):44.

- Niswonger, R. G. and Prudic, D. E. (2005). Documentation of the streamflow-routing (sfr2) package to include unsaturated flow beneath streams-a modification to sfr1. Technical report, US Geological Survey.
- Niswonger, R. G., Prudic, D. E., and Regan, R. S. (2006). Documentation of the unsaturated-zone flow (uzf1) package for modeling unsaturated flow between the land surface and the water table with modflow-2005. Technical report.
- Niu, W.-J., Feng, Z.-K., Feng, B.-F., Min, Y.-W., Cheng, C.-T., and Zhou, J.-Z. (2019). Comparison of Multiple Linear Regression, Artificial Neural Network, Extreme Learning Machine, and Support Vector Machine in Deriving Operation Rule of Hydropower Reservoir. *WATER*, 11(1).
- Nouiri, I. (2014). Multi-Objective tool to optimize the Water Resources Management using Genetic Algorithm and the Pareto Optimality Concept. *WATER RESOURCES MANAGEMENT*, 28(10):2885–2901.
- Olivera, F., Valenzuela, M., Srinivasan, R., Choi, J., Cho, H., Koha, S., and Agrawal, A. (2006a). ArcGIS-SWAT: A geodata model and GIS interface for SWAT (vol 2, pg 295, 2006). *JOURNAL OF THE AMERICAN WATER RESOURCES ASSOCIATION*, 42(3):807.
- Olivera, F., Valenzuela, M., Srinivasan, R., Choi, J., Cho, H., Koka, S., and Agrawal, A. (2006b). ArcGIS-SWAT: A geodata model and GIS interface for SWAT. *JOURNAL OF THE AMERICAN WATER RESOURCES ASSOCIATION*, 42(2):295–309.
- Oriani, F., Ohana-Levi, N., Marra, F., Straubhaar, J., Mariethoz, G., Renard, P., Karnieli, A., and Morin, E. (2017). Simulating Small-Scale Rainfall Fields Conditioned by Weather State and Elevation: A Data-Driven Approach Based on Rainfall Radar Images. *WATER RESOURCES RESEARCH*, 53(10):8512–8532.
- Pahl-Wostl, C., Gupta, J., and Petry, D. (2008). Governance and the Global Water System: A Theoretical Exploration. *GLOBAL GOVERNANCE*, 14(4):419–435.
- Painter, S., Basagaoglu, H., and Liu, A. (2008). Robust Representation of Dry Cells in Single-Layer MODFLOW Models. *GROUND WATER*, 46(6):873–881.
- Palamuleni, L. G., Ndomba, P. M., and Annegarn, H. J. (2011). Evaluating land cover change and its impact on hydrological regime in Upper Shire river catchment, Malawi. *REGIONAL ENVIRONMENTAL CHANGE*, 11(4):845–855.
- Panday, S. and Huyakorn, P. S. (2008). MODFLOW SURFACT: A state-of-the-art use of vadose zone flow and transport equations and numerical techniques for environmental evaluations. *VADOSE ZONE JOURNAL*, 7(2):610–631.

- Panday, S., Langevin, C. D., Niswonger, R. G., Ibaraki, M., and Hughes, J. D. (2013). MODFLOW–USG version 1: an unstructured grid version of MODFLOW for simulating groundwater flow and tightly coupled processes using a control volume finite-difference formulation. Technical report, US Geological Survey.
- Pandey, B. K., Gosain, A. K., Paul, G., and Khare, D. (2017). Climate change impact assessment on hydrology of a small watershed using semi-distributed model. *APPLIED WATER SCIENCE*, 7(4):2029–2041.
- Park, S., Nielsen, A., Bailey, R. T., Trolle, D., and Bieger, K. (2019). A QGIS-based graphical user interface for application and evaluation of SWAT-MODFLOW models. *ENVIRONMENTAL MODELLING & SOFTWARE*, 111:493–497.
- Park, Y.-Y., Buizza, R., and Leutbecher, M. (2008). TIGGE: Preliminary results on comparing and combining ensembles. *QUARTERLY JOURNAL OF THE ROYAL METEOROLOGICAL SOCIETY*, 134(637, B):2029–2050.
- Patil, A. and Ramsankaran, R. A. A. J. (2017). Improving streamflow simulations and forecasting performance of SWAT model by assimilating remotely sensed soil moisture observations. *JOURNAL OF HYDROLOGY*, 555:683–696.
- Perkins, S. E. and Pitman, A. J. (2009). Do weak AR4 models bias projections of future climate changes over Australia? *CLIMATIC CHANGE*, 93(3-4):527–558.
- Perkins, S. E., Pitman, A. J., Holbrook, N. J., and McAneney, J. (2007). Evaluation of the AR4 climate models’ simulated daily maximum temperature, minimum temperature, and precipitation over Australia using probability density functions. *JOURNAL OF CLIMATE*, 20(17):4356–4376.
- Perkins, S. E., Pitman, A. J., and Sisson, S. A. (2013). Systematic differences in future 20 year temperature extremes in AR4 model projections over Australia as a function of model skill. *INTERNATIONAL JOURNAL OF CLIMATOLOGY*, 33(5):1153–1167.
- Petit, J. R., Jouzel, J., Raynaud, D., Barkov, N. I., Barnola, J. M., Basile, I., Bender, M., Chappellaz, J., Davis, M., Delaygue, G., Delmotte, M., Kotlyakov, V. M., Legrand, M., Lipenkov, V. Y., Lorius, C., Pepin, L., Ritz, C., Saltzman, E., and Stievenard, M. (1999). Climate and atmospheric history of the past 420,000 years from the Vostok ice core, Antarctica. *Nature*, 399(6735):429–436.
- Pilskaln, C. (2004). Seasonal and interannual particle export in an African Rift Valley Lake: A 5-yr record from Lake Malawi, southern East Africa. *LIMNOLOGY AND OCEANOGRAPHY*, 49(4):964–977.
- Poeter, E. and Anderson, D. (2005). Multimodel ranking and inference in ground water modeling. *GROUND WATER*, 43(4):597–605.

- Pour, S. H., Shahid, S., Chung, E.-S., and Wang, X.-J. (2018). Model output statistics downscaling using support vector machine for the projection of spatial and temporal changes in rainfall of Bangladesh. *ATMOSPHERIC RESEARCH*, 213:149–162.
- QGIS Development Team and others (2015). QGIS geographic information system. *Open Source Geospatial Foundation Project, Versão*, 2(7).
- Qian, J., Zhao, J., Liu, Y., Feng, X., and Gui, D. (2018). Simulation and prediction of monthly accumulated runoff, based on several neural network models under poor data availability. *SCIENCES IN COLD AND ARID REGIONS*, 10(6):468–481.
- R Core Team (2017). *R: A Language and Environment for Statistical Computing*. R Foundation for Statistical Computing, Vienna, Austria.
- Racsko, P., Szeidl, L., and Semenov, M. (1991). A serial approach to local stochastic weather models. *Ecological Modelling*, 57(1-2):27–41.
- Rahman, K., Maringanti, C., Beniston, M., Widmer, F., Abbaspour, K., and Lehmann, A. (2013). Streamflow Modeling in a Highly Managed Mountainous Glacier Watershed Using SWAT: The Upper Rhone River Watershed Case in Switzerland. *WATER RESOURCES MANAGEMENT*, 27(2):323–339.
- Raju, K. S. and Kumar, D. N. (2014). Ranking of global climate models for India using multicriterion analysis. *CLIMATE RESEARCH*, 60(2):103–117.
- Randall, D. A. and Wood, R. A. (2007). Climate Models and Their Evaluation. In Solomon, S and Qin, D and Manning, M and Marquis, M and Averyt, K and Tignor, MMB and Miller, HL and Chen, ZL, editor, *CLIMATE CHANGE 2007: THE PHYSICAL SCIENCE BASIS*, pages 589–662.
- Ratan, R. and Venugopal, V. (2013). Wet and dry spell characteristics of global tropical rainfall. *WATER RESOURCES RESEARCH*, 49(6):3830–3841.
- Rees, J. (2013). Geography and the nexus: Presidential Address and record of the Royal Geographical Society (with IBG) AGM 2013. *GEOGRAPHICAL JOURNAL*, 179(3):279–282.
- Refsgaard, J. C., Christensen, S., Sonnenborg, T. O., Seifert, D., Hojberg, A. L., and Trolborg, L. (2012). Review of strategies for handling geological uncertainty in groundwater flow and transport modeling. *ADVANCES IN WATER RESOURCES*, 36(SI):36–50.
- Refsgaard, J. C., van der Sluijs, J. P., Brown, J., and van der Keur, P. (2006). A framework for dealing with uncertainty due to model structure error. *ADVANCES IN WATER RESOURCES*, 29(11):1586–1597.

- Ren, M., Pang, B., Xu, Z., Yue, J., and Zhang, R. (2019). Downscaling of daily extreme temperatures in the Yarlung Zangbo River Basin using machine learning techniques. *THEORETICAL AND APPLIED CLIMATOLOGY*, 136(3-4):1275–1288.
- Ren, W. W., Yang, T., Huang, C. S., Xu, C. Y., and Shao, Q. X. (2018). Improving monthly streamflow prediction in alpine regions: integrating HBV model with Bayesian neural network. *STOCHASTIC ENVIRONMENTAL RESEARCH AND RISK ASSESSMENT*, 32(12):3381–3396.
- Rezaei, N., Sierra-Altamiranda, A., Diaz-Elsayed, N., Charkhgard, H., and Zhang, Q. (2019). A multi-objective optimization model for decision support in water reclamation system planning. *JOURNAL OF CLEANER PRODUCTION*, 240.
- Rhee, J. and Im, J. (2017). Meteorological drought forecasting for ungauged areas based on machine learning: Using long-range climate forecast and remote sensing data. *AGRICULTURAL AND FOREST METEOROLOGY*, 237:105–122.
- Riahi, K., Gruebler, A., and Nakicenovic, N. (2007). Scenarios of long-term socio-economic and environmental development under climate stabilization. *TECHNOLOGICAL FORECASTING AND SOCIAL CHANGE*, 74(7):887–935.
- Rivett, M. O., Haicrow, A. W., Schmalfuss, J., Stark, J. A., Truslove, J. P., Kumwenda, S., Harawa, K. A., Nhlema, M., Songola, C., Wanangwa, G. J., Miller, A. V. M., and Kalin, R. M. (2018). Local scale water-food nexus: Use of borehole-garden permaculture to realise the full potential of rural water supplies in Malawi. *JOURNAL OF ENVIRONMENTAL MANAGEMENT*, 209:354–370.
- Roach, T., Kapelan, Z., and Ledbetter, R. (2018). A Resilience-Based Methodology for Improved Water Resources Adaptation Planning under Deep Uncertainty with Real World Application. *WATER RESOURCES MANAGEMENT*, 32(6):2013–2031.
- Robins, N. and Ball, D. (2006). *The Dumfries Basin aquifer*. British Geological Survey.
- Rodrigues da Silva, V. d. P., Silva, M. T., Singh, V. P., de Souza, E. P., Braga, C. C., de Holanda, R. M., Almeida, R. S. R., Salviano de Sousa, F. d. A., and Rodrigues Braga, A. C. (2018). Simulation of stream flow and hydrological response to land-cover changes in a tropical river basin. *CATENA*, 162:166–176.
- Rogers, P. and Hall, A. W. (2003). *Effective Water Governance*, volume 7. Global Water Partnership Stockholm.
- Rojas, R., Feyen, L., Batelaan, O., and Dassargues, A. (2010a). On the value of conditioning data to reduce conceptual model uncertainty in groundwater modeling. *WATER RESOURCES RESEARCH*, 46.

- Rojas, R., Feyen, L., and Dassargues, A. (2008). Conceptual model uncertainty in groundwater modeling: Combining generalized likelihood uncertainty estimation and Bayesian model averaging. *WATER RESOURCES RESEARCH*, 44(12).
- Rojas, R., Kahunde, S., Peeters, L., Batelaan, O., Feyen, L., and Dassargues, A. (2010b). Application of a multimodel approach to account for conceptual model and scenario uncertainties in groundwater modelling. *JOURNAL OF HYDROLOGY*, 394(3-4):416–435.
- Rosenhead, J. and Mingers, J. (2001). *Rational analysis for a problematic world revisited: Problem structuring methods for complexity, uncertainty and conflict*. Wiley Chichester.
- Rushton, K. (2017). Recharge from permanent water bodies. *Recharge of Phreatic Aquifers in (Semi-) Arid Areas: IAH International Contributions to Hydrogeology 19*, page 215.
- Rushton, K. R. (2003). *Groundwater Hydrology - Conceptual and computational models*. Wiley Online Library.
- Sachindra, D. A., Ahmed, K., Rashid, M. M., Shahid, S., and Perera, B. J. C. (2018). Statistical downscaling of precipitation using machine learning techniques. *ATMOSPHERIC RESEARCH*, 212:240–258.
- Saha, S., Moorthi, S., Pan, H.-L., Wu, X., Wang, J., Nadiga, S., Tripp, P., Kistler, R., Woollen, J., Behringer, D., Liu, H., Stokes, D., Grumbine, R., Gayno, G., Wang, J., Hou, Y.-T., Chuang, H.-y., Juang, H.-M. H., Sela, J., Iredell, M., Treadon, R., Kleist, D., Van Delst, P., Keyser, D., Derber, J., Ek, M., Meng, J., Wei, H., Yang, R., Lord, S., van den Dool, H., Kumar, A., Wang, W., Long, C., Chelliah, M., Xue, Y., Huang, B., Schemm, J.-K., Ebisuzaki, W., Lin, R., Xie, P., Chen, M., Zhou, S., Higgins, W., Zou, C.-Z., Liu, Q., Chen, Y., Han, Y., Cucurull, L., Reynolds, R. W., Rutledge, G., and Goldberg, M. (2010). The ncep climate forecast system reanalysis. *Bulletin of the American Meteorological Society*, 91(8):1015–1058.
- Salman, S. A., Shahid, S., Ismail, T., Ahmed, K., and Wang, X.-J. (2018). Selection of climate models for projection of spatiotemporal changes in temperature of Iraq with uncertainties. *ATMOSPHERIC RESEARCH*, 213:509–522.
- Sangelantoni, L., Russo, A., and Gennaretti, F. (2018). Impact of bias correction and downscaling through quantile mapping on simulated climate change signal: a case study over Central Italy. *Theoretical and Applied Climatology*.
- Sanikhani, H., Kisi, O., Mirabbasi, R., and Meshram, S. G. (2018). Trend analysis of rainfall pattern over the Central India during 1901-2010. *ARABIAN JOURNAL OF GEOSCIENCES*, 11(15).
- Scanlon, B. R., Faunt, C. C., Longuevergne, L., Reedy, R. C., Alley, W. M., McGuire, V. L., and McMahon, P. B. (2012). Groundwater depletion and

- sustainability of irrigation in the US High Plains and Central Valley. *PROCEEDINGS OF THE NATIONAL ACADEMY OF SCIENCES OF THE UNITED STATES OF AMERICA*, 109(24):9320–9325.
- Schoof, J. and Pryor, S. (2001). Downscaling temperature and precipitation: A comparison of regression-based methods and artificial neural networks. *INTERNATIONAL JOURNAL OF CLIMATOLOGY*, 21(7):773–790.
- Schulzweida, U., Kornblueh, L., and Quast, R. (2006). Cdo user’s guide. *Climate data operators, Version*, 1(6).
- Schuol, J., Abbaspour, K. C., Srinivasan, R., and Yang, H. (2008a). Estimation of freshwater availability in the West African sub-continent using the SWAT hydrologic model. *JOURNAL OF HYDROLOGY*, 352(1-2):30–49.
- Schuol, J., Abbaspour, K. C., Yang, H., Srinivasan, R., and Zehnder, A. J. B. (2008b). Modeling blue and green water availability in Africa. *WATER RESOURCES RESEARCH*, 44(7).
- See, L., Solomatine, D., Abrahart, R., and Toth, E. (2007). Hydroinformatics: computational intelligence and technological developments in water science applications - Editorial. *HYDROLOGICAL SCIENCES JOURNAL-JOURNAL DES SCIENCES HYDROLOGIQUES*, 52(3):391–396.
- Semenov, M. A. (2007). Development of high-resolution UKCIP02-based climate change scenarios in the UK. *AGRICULTURAL AND FOREST METEOROLOGY*, 144(1-2):127–138.
- Semenov, M. A. and Barrow, E. M. (1997). Use of a stochastic weather generator in the development of climate change scenarios. *Climatic Change*, 35(4):397–414.
- Semenov, M. A., Barrow, E. M., and Lars-Wg, A. (2002). A stochastic weather generator for use in climate impact studies. *User’s manual, Version*, 3.
- Semenov, M. A., Brooks, R. J., Barrow, E. M., and Richardson, C. W. (1998). Comparison of the WGEN and LARS-WG stochastic weather generators for diverse climates. *Climate Research*, 10(2):95–107.
- Semenov, M. A. and Stratonovitch, P. (2010). Use of multi-model ensembles from global climate models for assessment of climate change impacts. *CLIMATE RESEARCH*, 41(1):1–14.
- Semiromi, M. T. and Koch, M. (2019). Analysis of spatio-temporal variability of surface-groundwater interactions in the Gharehsoo river basin, Iran, using a coupled SWAT-MODFLOW model. *ENVIRONMENTAL EARTH SCIENCES*, 78(6).
- Sen, P. K. (1968). Estimates of the regression coefficient based on Kendall’s tau. *Journal of the American statistical association*, 63(324):1379–1389.



- Setegn, S. G., Srinivasan, R., Melesse, A. M., and Dargahi, B. (2010). SWAT model application and prediction uncertainty analysis in the Lake Tana Basin, Ethiopia. *HYDROLOGICAL PROCESSES*, 24(3):357–367.
- Setyorini, A., Khare, D., and Pingale, S. M. (2017). Simulating the impact of land use/land cover change and climate variability on watershed hydrology in the Upper Brantas basin, Indonesia. *APPLIED GEOMATICS*, 9(3):191–204.
- Shah, T. (2009). Climate change and groundwater: India's opportunities for mitigation and adaptation. *ENVIRONMENTAL RESEARCH LETTERS*, 4(3).
- Sharannya, T. M., Mudbhatkal, A., and Mahesha, A. (2018). Assessing climate change impacts on river hydrology - A case study in the Western Ghats of India. *JOURNAL OF EARTH SYSTEM SCIENCE*, 127(6).
- Sharma, M. and Hughes, M. (1985). GROUNDWATER RECHARGE ESTIMATION USING CHLORIDE, DEUTERIUM AND O-18 PROFILES IN THE DEEP COASTAL SANDS OF WESTERN AUSTRALIA. *JOURNAL OF HYDROLOGY*, 81(1-2):93–109.
- Sharpley, A. and Williams, J. (1990). EPIC erosion productivity impact calculator: 2. User manual. *US Department of Agriculture Technical Bulletin*, (1768):127.
- Shen, M., Chen, J., Zhuan, M., Chen, H., Xu, C.-Y., and Xiong, L. (2018). Estimating uncertainty and its temporal variation related to global climate models in quantifying climate change impacts on hydrology. *JOURNAL OF HYDROLOGY*, 556:10–24.
- Sherif, M. M. and Singh, V. P. (1999). Effect of climate change on sea water intrusion in coastal aquifers. *Hydrological Processes*, 13(8):1277–1287.
- Shreem, S. S., Abdullah, S., and Nazri, M. Z. A. (2016). Hybrid feature selection algorithm using symmetrical uncertainty and a harmony search algorithm. *INTERNATIONAL JOURNAL OF SYSTEMS SCIENCE*, 47(6):1312–1329.
- Siade, A. J., Rath, B., Prommer, H., Welter, D., and Doherty, J. (2019). Using heuristic multi-objective optimization for quantifying predictive uncertainty associated with groundwater flow and reactive transport models. *JOURNAL OF HYDROLOGY*, 577.
- Simmers, I. (2017). *Recharge of Phreatic Aquifers in (Semi-) Arid Areas: IAH International Contributions to Hydrogeology 19*. Routledge.
- Singh, R. M. and Datta, B. (2007). Artificial neural network modeling for identification of unknown pollution sources in groundwater with partially missing concentration observation data. *WATER RESOURCES MANAGEMENT*, 21(3):557–572.
- Smerdon, B. D. (2017). A synopsis of climate change effects on groundwater recharge. *JOURNAL OF HYDROLOGY*, 555:125–128.

- Smith, I. G. (1978). Climate variation and its effects on our land and water : Part a, earth science in climate research. Technical report. Report.
- Smith, S. J. and Wigley, T. M. L. (2006). Multi-gas forcing stabilization with Minicam. *ENERGY JOURNAL*, pages 373–391.
- Somers, L. D., McKenzie, J. M., Mark, B. G., Lagos, P., Ng, G.-H. C., Wickert, A. D., Yarleque, C., Baraër, M., and Silva, Y. (2019). Groundwater buffers decreasing glacier melt in an andean watershed - but not forever. *Geophysical Research Letters*.
- Sophocleous, M. and Perkins, S. (2000). Methodology and application of combined watershed and ground-water models in Kansas. *JOURNAL OF HYDROLOGY*, 236(3-4):185–201.
- Stocker, T., Dahe, Q., Plattner, G.-k., Tignor, M., and Midgley, P. (2010). IPCC Expert Meeting on Assessing and Combining Multi Model Climate Projections Good Practice Guidance Paper on Assessing and Combining Multi Model Climate Projections. *IPCC Expert Meeting on Assessing and Combining Multi Model Climate Projections*, page 15.
- Stonefelt, M., Fontaine, T., and Hotchkiss, R. (2000). Impacts of climate change on water yield in the Upper Wind River Basin. *JOURNAL OF THE AMERICAN WATER RESOURCES ASSOCIATION*, 36(2):321–336.
- Strauch, M., Bernhofer, C., Koide, S., Volk, M., Lorz, C., and Makeschin, F. (2012). Using precipitation data ensemble for uncertainty analysis in SWAT streamflow simulation. *JOURNAL OF HYDROLOGY*, 414:413–424.
- Stringer, L. C., Dougill, A. J., Dyer, J. C., Vincent, K., Fritzsche, F., Leventon, J., Falcao, M. P., Manyakaidze, P., Syampungani, S., Powell, P., and Kalaba, G. (2014). Advancing climate compatible development: lessons from southern Africa. *REGIONAL ENVIRONMENTAL CHANGE*, 14(2, SI):713–725.
- Stringer, L. C., Mkwambisi, D. D., Dougill, A. J., and Dyer, J. C. (2010). Adaptation to climate change and desertification: Perspectives from national policy and autonomous practice in Malawi. *CLIMATE AND DEVELOPMENT*, 2(2, SI):145–160.
- Swatuk, L. (2005). Political challenges to implementing IWRM in Southern Africa. *PHYSICS AND CHEMISTRY OF THE EARTH*, 30(11-16):872–880. 5th WaterNet/Warfsa/GWP-SA Symposium, Windhoek, NAMIBIA, NOV 02-04, 2004.
- Tabari, H. and Talaei, P. H. (2011). Temporal variability of precipitation over Iran: 1966-2005. *JOURNAL OF HYDROLOGY*, 396(3-4):313–320.
- Taormina, R. and Chau, K.-W. (2015). Data-driven input variable selection for rainfall-runoff modeling using binary-coded particle swarm optimization and Extreme Learning Machines. *JOURNAL OF HYDROLOGY*, 529(3):1617–1632.

- Taylor, R. G., Scanlon, B., Doell, P., Rodell, M., van Beek, R., Wada, Y., Longuevergne, L., Leblanc, M., Famiglietti, J. S., Edmunds, M., Konikow, L., Green, T. R., Chen, J., Taniguchi, M., Bierkens, M. F. P., MacDonald, A., Fan, Y., Maxwell, R. M., Yechieli, Y., Gurdak, J. J., Allen, D. M., Shamsudduha, M., Hiscock, K., Yeh, P. J. F., Holman, I., and Treidel, H. (2013). Ground water and climate change. *NATURE CLIMATE CHANGE*, 3(4):322–329.
- Tebaldi, C. and Knutti, R. (2007). The use of the multi-model ensemble in probabilistic climate projections. *Philosophical Transactions of the Royal Society of London A: Mathematical, Physical and Engineering Sciences*, 365(1857):2053–2075.
- Tebaldi, C., Mearns, L., Nychka, D., and Smith, R. (2004). Regional probabilities of precipitation change: A Bayesian analysis of multimodel simulations. *GEOPHYSICAL RESEARCH LETTERS*, 31(24).
- Tebaldi, C. and Sanso, B. (2009). Joint projections of temperature and precipitation change from multiple climate models: a hierarchical Bayesian approach. *JOURNAL OF THE ROYAL STATISTICAL SOCIETY SERIES A-STATISTICS IN SOCIETY*, 172(1):83–106.
- Tebaldi, C., Smith, R., Nychka, D., and Mearns, L. (2005). Quantifying uncertainty in projections of regional climate change: A Bayesian approach to the analysis of multimodel ensembles. *JOURNAL OF CLIMATE*, 18(10):1524–1540.
- Teegavarapu, R. and Chandramouli, V. (2005). Improved weighting methods, deterministic and stochastic data-driven models for estimation of missing precipitation records. *JOURNAL OF HYDROLOGY*, 312(1-4):191–206.
- Tetzlaff, D., Carey, S. K., McNamara, J. P., Laudon, H., and Soulsby, C. (2017). The essential value of long-term experimental data for hydrology and water management. *WATER RESOURCES RESEARCH*, 53(4):2598–2604.
- Thampi, S. G., Raneesh, K. Y., and Surya, T. V. (2010). Influence of Scale on SWAT Model Calibration for Streamflow in a River Basin in the Humid Tropics. *WATER RESOURCES MANAGEMENT*, 24(15):4567–4578.
- Themessl, M. J., Gobiet, A., and Leuprecht, A. (2011). Empirical-statistical downscaling and error correction of daily precipitation from regional climate models. *INTERNATIONAL JOURNAL OF CLIMATOLOGY*, 31(10):1530–1544.
- Thiel, H. (1950a). A rank-invariant method of linear and polynomial regression analysis, Part 1. In *Proceedings of Koninklijke Nederlandse Akademie van Wetenschappen A*, volume 53, pages 386–392.
- Thiel, H. (1950b). A rank-invariant method of linear and polynomial regression analysis, Part 2. In *Proceedings of Koninklijke Nederlandse Akademie van Wetenschappen A*, volume 53, pages 521–525.

- Thiel, H. (1950c). A rank-invariant method of linear and polynomial regression analysis, Part 3. In *Proceedings of Koninklijke Nederlandse Akademie van Wetenschappen A*, volume 53, pages 1397–1412.
- Thoning, K. W., Tans, P. P., and Komhyr, W. D. (1989). ATMOSPHERIC CARBON-DIOXIDE AT MAUNA LOA OBSERVATORY .2. ANALYSIS OF THE NOAA GMCC DATA, 1974-1985. *Journal of Geophysical Research-Atmospheres*, 94(D6):8549–8565.
- Tian, Y., Zheng, Y., Han, F., Zheng, C., and Li, X. (2018). A comprehensive graphical modeling platform designed for integrated hydrological simulation. *Environmental Modelling & Software*, 108:154–173.
- Tikhonov, A. N. and Arsenin, V. I. (1977). *Solutions of ill-posed problems*, volume 14. Winston, Washington, DC.
- Torrance, J. (1972). Malawi, Rhodesia and Zambia. *World survey of climatology*, 10:409–460.
- Tortajada, C. (2010). Water Governance: Some Critical Issues. *INTERNATIONAL JOURNAL OF WATER RESOURCES DEVELOPMENT*, 26(2, SI):297–307.
- Troldborg, L., Refsgaard, J. C., Jensen, K. H., and Engesgaard, P. (2007). The importance of alternative conceptual models for simulation of concentrations in a multi-aquifer system. *HYDROGEOLOGY JOURNAL*, 15(5):843–860.
- UN-Water (2018). Sustainable Development Goal 6 Synthesis Report on Water and Sanitation. *United Nations New York, New York*, 10017.
- UNFCCC (1992). *United Nations Framework Convention on Climate Change*. 1992. Available on the Internet: <http://www.unfccc.de>.
- USGS (2018). What is the difference between global warming and climate change? [https://www.usgs.gov/faqs/what-difference-between-global-warming-and-climate-change-1?qt-news\\_science\\_products=0#qt-news\\_science\\_products](https://www.usgs.gov/faqs/what-difference-between-global-warming-and-climate-change-1?qt-news_science_products=0#qt-news_science_products). (Accessed on 10/23/2018).
- Usher, B., Pretorius, J., and van Tonder, G. (2006). Management of a karoo fractured-rock aquifer system - Kalkveld water user association (WUA). *WATER SA*, 32(1):9–19.
- van Griensven, A. and Bauwens, W. (2003). Multiobjective autocalibration for semidistributed water quality models. *WATER RESOURCES RESEARCH*, 39(12).
- Van Vuuren, D. and O'Neill, B. (2006). The consistency of IPCC's SRES scenarios to recent literature and recent projections. *CLIMATIC CHANGE*, 75(1-2):9–46.

- van Vuuren, D. P., Den Elzen, M. G. J., Lucas, P. L., Eickhout, B., Strengers, B. J., van Ruijven, B., Wonink, S., and van Houdt, R. (2007). Stabilizing greenhouse gas concentrations at low levels: an assessment of reduction strategies and costs. *CLIMATIC CHANGE*, 81(2):119–159.
- van Vuuren, D. P., Edmonds, J., Kainuma, M., Riahi, K., Thomson, A., Hibbard, K., Hurtt, G. C., Kram, T., Krey, V., Lamarque, J.-F., Masui, T., Meinshausen, M., Nakicenovic, N., Smith, S. J., and Rose, S. K. (2011). The representative concentration pathways: an overview. *CLIMATIC CHANGE*, 109(1-2, SI):5–31.
- van Vuuren, D. P., Eickhout, B., Lucas, P. L., and den Elzen, M. G. J. (2006). Long-term multi-gas scenarios to stabilise radiative forcing - Exploring costs and benefits within an integrated assessment framework. *ENERGY JOURNAL*, pages 201–233.
- van Zyl, J. (2001). The Shuttle Radar Topography Mission (SRTM): A breakthrough in remote sensing of topography. *ACTA ASTRONAUTICA*, 48(5-12, SI):559–565. 51st International Astronautical Federation Congress, RIO JANEIRO, BRAZIL, OCT 02-06, 2000.
- Vazquez-Amabile, G. and Engel, B. (2005). Use of SWAT to compute groundwater table depth and streamflow in the Muscatatuck River watershed. *TRANSACTIONS OF THE ASAE*, 48(3):991–1003.
- Veldkamp, T. I. E., Wada, Y., Aerts, J. C. J. H., and Ward, P. J. (2016). Towards a global water scarcity risk assessment framework: incorporation of probability distributions and hydro-climatic variability. *ENVIRONMENTAL RESEARCH LETTERS*, 11(2).
- Viglione, A., Borga, M., Balabanis, P., and Blöschl, G. (2010). Barriers to the exchange of hydrometeorological data in Europe Results from a survey and implications for data policy. *JOURNAL OF HYDROLOGY*, 394(1-2, SI):63–77.
- Vincent, K., Dougill, A. J., Dixon, J. L., Stringer, L. C., and Cull, T. (2017). Identifying climate services needs for national planning: insights from Malawi. *CLIMATE POLICY*, 17(2):189–202.
- vonStorch, H. (1995). Misuses of statistical analysis in climate research. In vonStorch, H and Navarra, A, editor, *ANALYSIS OF CLIMATE VARIABILITY: APPLICATIONS OF STATISTICAL TECHNIQUES*, pages 11–26. Commiss European Community. Autumn School on Analysis of Climate Variability - Applications of Statistical Techniques, ISL ELBA, ITALY, OCT 30-NOV 06, 1993.
- Walker, W., Lempert, R., and Kwakkel, J. (2013). Deep uncertainty.
- Wang, B., Zheng, L., Liu, D. L., Ji, F., Clark, A., and Yu, Q. (2018). Using multi-model ensembles of CMIP5 global climate models to reproduce observed monthly rainfall and temperature with machine learning methods in Australia. *INTERNATIONAL JOURNAL OF CLIMATOLOGY*, 38(13):4891–4902.

- Wang, C., Chow, S. S. M., Wang, Q., Ren, K., and Lou, W. (2013). Privacy-Preserving Public Auditing for Secure Cloud Storage. *IEEE TRANSACTIONS ON COMPUTERS*, 62(2):362–375.
- Wang, X., Yang, W., and Melesse, A. M. (2008). Using hydrologic equivalent wetland concept within swat to estimate streamflow in watersheds with numerous wetlands. *TRANSACTIONS OF THE ASABE*, 51(1):55–72.
- Wang, Y., Liu, L., Guo, S., Yue, Q., and Guo, P. (2019). A bi-level multi-objective linear fractional programming for water consumption structure optimization based on water shortage risk. *JOURNAL OF CLEANER PRODUCTION*, 237.
- Warszawski, L., Frieler, K., Huber, V., Piontek, F., Serdeczny, O., and Schewe, J. (2014). The Inter-Sectoral Impact Model Intercomparison Project (ISI-MIP): Project framework. *PROCEEDINGS OF THE NATIONAL ACADEMY OF SCIENCES OF THE UNITED STATES OF AMERICA*, 111(9):3228–3232.
- Watson, A. A. and Kasprzyk, J. R. (2017). Incorporating deeply uncertain factors into the many objective search process. *ENVIRONMENTAL MODELLING & SOFTWARE*, 89:159–171.
- Watts, G., Battarbee, R. W., Bloomfield, J. P., Crossman, J., Daccache, A., Durance, I., Elliott, J. A., Garner, G., Hannaford, J., Hannah, D. M., Hess, T., Jackson, C. R., Kay, A. L., Kernan, M., Knox, J., Mackay, J., Monteith, D. T., Ormerod, S. J., Rance, J., Stuart, M. E., Wade, A. J., Wade, S. D., Weatherhead, K., Whitehead, P. G., and Wilby, R. L. (2015). Climate change and water in the UK - past changes and future prospects. *PROGRESS IN PHYSICAL GEOGRAPHY*, 39(1, SI):6–28.
- WEF (2017). World Economic Forum. In *Global Risks Report: World Economic Forum*.
- Wei, X. and Bailey, R. T. (2019). Assessment of System Responses in Intensively Irrigated Stream-Aquifer Systems Using SWAT-MODFLOW. *WATER*, 11(8).
- Welter, D. E., White, J. T., Hunt, R. J., and Doherty, J. E. (2015). Approaches in highly parameterized inversion—pest++ version 3, a parameter estimation and uncertainty analysis software suite optimized for large environmental models. Technical report, US Geological Survey.
- WHO (2017). Factsheet on drinking-water. <https://www.who.int/news-room/fact-sheets/detail/drinking-water>. (Accessed on 08/19/2017).
- Wilby, R., Charles, S., Zorita, E., Timbal, B., Whetton, P., and Mearns, L. (2004). Guidelines for use of climate scenarios developed from statistical downscaling methods. *Supporting material of the Intergovernmental Panel on Climate Change, available from the DDC of IPCC TG CIA*, 27.

- Wilby, R., Dawson, C., and Barrow, E. (2002a). SDSM - a decision support tool for the assessment of regional climate change impacts. *ENVIRONMENTAL MODELLING & SOFTWARE*, 17(2):147–159.
- Wilby, R. and Harris, I. (2006). A framework for assessing uncertainties in climate change impacts: Low-flow scenarios for the River Thames, UK. *WATER RESOURCES RESEARCH*, 42(2).
- Wilby, R., Tomlinson, O., and Dawson, C. (2003). Multi-site simulation of precipitation by conditional resampling. *CLIMATE RESEARCH*, 23(3):183–194.
- Wilby, R. L., Dawson, C. W., and Barrow, E. M. (2002b). SDSM—a decision support tool for the assessment of regional climate change impacts. *Environmental Modelling & Software*, 17(2):145–157.
- Wilby, R. L. and Wigley, T. M. L. (1997). Downscaling general circulation model output: a review of methods and limitations. *Progress in Physical Geography*, 21(4):530–548.
- Willmott, C. J. (1981). On the validation of models. *Physical geography*, 2(2):184–194.
- Wilson, P. and Toumi, R. (2005). A fundamental probability distribution for heavy rainfall. *GEOPHYSICAL RESEARCH LETTERS*, 32(14).
- Winston, R. (2009). Modelmuse-a graphical user interface for modflow-2005 and phast: Us geological survey techniques and methods 6-a29. *US Geological Survey*. Available online at <http://pubs.usgs.gov/tm/tm6A29>.
- Wise, M., Calvin, K., Thomson, A., Clarke, L., Bond-Lamberty, B., Sands, R., Smith, S. J., Janetos, A., and Edmonds, J. (2009). Implications of Limiting CO<sub>2</sub> Concentrations for Land Use and Energy. *SCIENCE*, 324(5931):1183–1186.
- Worland, S. C., Farmer, W. H., and Kiang, J. E. (2018). Improving predictions of hydrological low-flow indices in ungaged basins using machine learning. *ENVIRONMENTAL MODELLING & SOFTWARE*, 101:169–182.
- World Economic Forum Water Initiative and others (2012). *Water security: the water-food-energy-climate nexus*. Island Press.
- Wu, H. and Chen, B. (2015). Evaluating uncertainty estimates in distributed hydrological modeling for the Wenjing River watershed in China by GLUE, SUFI-2, and Para Sol methods. *ECOLOGICAL ENGINEERING*, 76:110–121.
- Wu, Z., McKay, J., and Keremane, G. (2012). Issues Affecting Community Attitudes and Intended Behaviours in Stormwater Reuse: A Case Study of Salisbury, South Australia. *WATER*, 4(4):835–847.
- Xie, Y. (2017). *Dynamic Documents with R and knitr*. Chapman and Hall/CRC.

- Xie, Y., Allaire, J. J., and Grolemond, G. (2018). *R markdown: The definitive guide*. Chapman and Hall/CRC.
- Yan, J., Jia, S., Lv, A., and Zhu, W. (2019). Water Resources Assessment of China's Transboundary River Basins Using a Machine Learning Approach. *WATER RESOURCES RESEARCH*, 55(1):632–655.
- Yang, J., Reichert, P., Abbaspour, K. C., Xia, J., and Yang, H. (2008). Comparing uncertainty analysis techniques for a SWAT application to the Chaohe Basin in China. *JOURNAL OF HYDROLOGY*, 358(1-2):1–23.
- Yaseen, Z. M., Allawi, M. F., Yousif, A. A., Jaafar, O., Hamzah, F. M., and El-Shafie, A. (2018). Non-tuned machine learning approach for hydrological time series forecasting. *NEURAL COMPUTING & APPLICATIONS*, 30(5):1479–1491.
- Yilmaz, A. G. and Imteaz, M. A. (2011). Impact of climate change on runoff in the upper part of the Euphrates basin. *HYDROLOGICAL SCIENCES JOURNAL-JOURNAL DES SCIENCES HYDROLOGIQUES*, 56(7):1265–1279.
- Yin, Z., Feng, Q., Yang, L., Deo, R. C., Wen, X., Si, J., and Xiao, S. (2017a). Future Projection with an Extreme-Learning Machine and Support Vector Regression of Reference Evapotranspiration in a Mountainous Inland Watershed in North-West China. *WATER*, 9(11).
- Yin, Z., Feng, Q., Yang, L., Wen, X., Si, J., and Zou, S. (2017b). Long Term Quantification of Climate and Land Cover Change Impacts on Streamflow in an Alpine River Catchment, Northwestern China. *SUSTAINABILITY*, 9(7).
- Yue, S., Pilon, P., and Cavadias, G. (2002a). Power of the Mann-Kendall and Spearman's rho tests for detecting monotonic trends in hydrological series. *JOURNAL OF HYDROLOGY*, 259(1-4):254–271.
- Yue, S., Pilon, P., Phinney, B., and Cavadias, G. (2002b). The influence of autocorrelation on the ability to detect trend in hydrological series. *Hydrological Processes*, 16(9):1807–1829.
- Yue, S. and Wang, C. (2002). Applicability of prewhitening to eliminate the influence of serial correlation on the Mann-Kendall test. *WATER RESOURCES RESEARCH*, 38(6).
- Zelenakova, M., Purcz, P., Blist'an, P., Vranayova, Z., Hlavata, H., Diaconu, D. C., and Portela, M. M. (2018). Trends in Precipitation and Temperatures in Eastern Slovakia (1962-2014). *WATER*, 10(6).
- Zhang, X., Srinivasan, R., and Van Liew, M. (2010). On the use of multi-algorithm, genetically adaptive multi-objective method for multi-site calibration of the SWAT model. *HYDROLOGICAL PROCESSES*, 24(8):955–969.



- Zhao, A., Zhu, X., Liu, X., Pan, Y., and Zuo, D. (2016). Impacts of land use change and climate variability on green and blue water resources in the Weihe River Basin of northwest China. *CATENA*, 137:318–327.
- Zhao, G., Gao, H., Kao, S.-C., Voisin, N., and Naz, B. S. (2018). A modeling framework for evaluating the drought resilience of a surface water supply system under non-stationarity. *JOURNAL OF HYDROLOGY*, 563:22–32.
- Zheng, C. and Wang, P. P. (1999). Mt3dms: a modular three-dimensional multi-species transport model for simulation of advection, dispersion, and chemical reactions of contaminants in groundwater systems; documentation and user's guide. Technical report, Alabama Univ University.
- Zhou, Y. and Li, W. (2011). A review of regional groundwater flow modeling. *Geoscience Frontiers*, 2(2):205 – 214.
- Zhu, S., Luo, X., Xu, Z., and Ye, L. (2019). Seasonal streamflow forecasts using mixture-kernel GPR and advanced methods of input variable selection. *HYDROLOGY RESEARCH*, 50(1):200–214.
- Zuzani, P., Ngongondo, C., Mwale, F., and Willems, P. (2019a). Examining trends of hydro-meteorological extremes in the shire river basin in malawi. *Physics and Chemistry of the Earth, Parts A/B/C*.
- Zuzani, P. N., Ngongondo, C. S., Mwale, F. D., and Willems, P. (2019b). Examining trends of hydro-meteorological extremes in the Shire River Basin in Malawi. *PHYSICS AND CHEMISTRY OF THE EARTH*, 112(SI):91–102. 18th WaterNet/WARFSA/GWPSA Symposium on Integrated Water Resources Development and Management - Innovative Technological Advances for Water Security in Eastern and Southern Africa, Swakopmund, NAMIBIA, OCT 25-27, 2017.



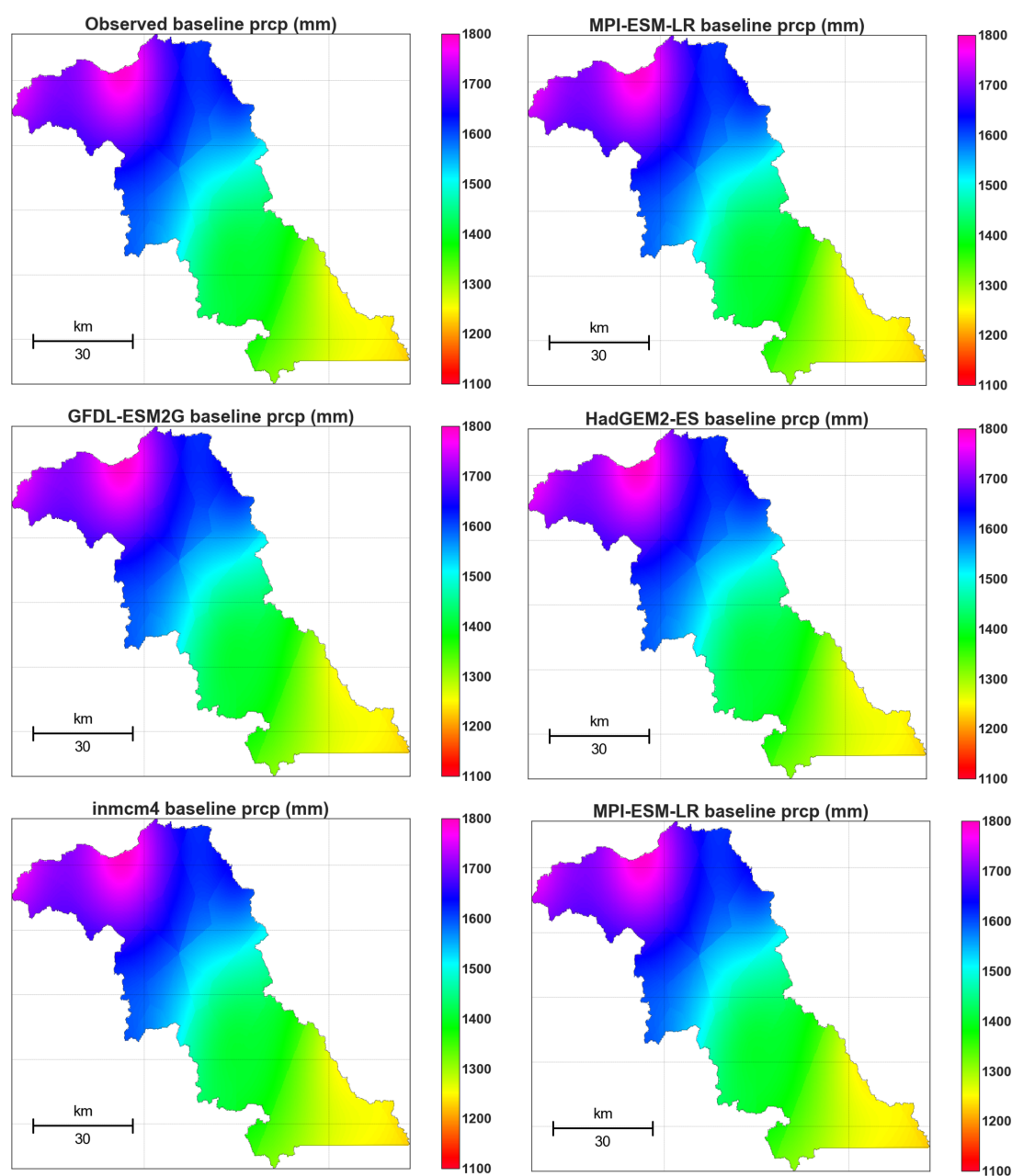
## **Supplementary data**

**Table A.1** Main characteristics of each RCP after van Vuuren et al. (2011)

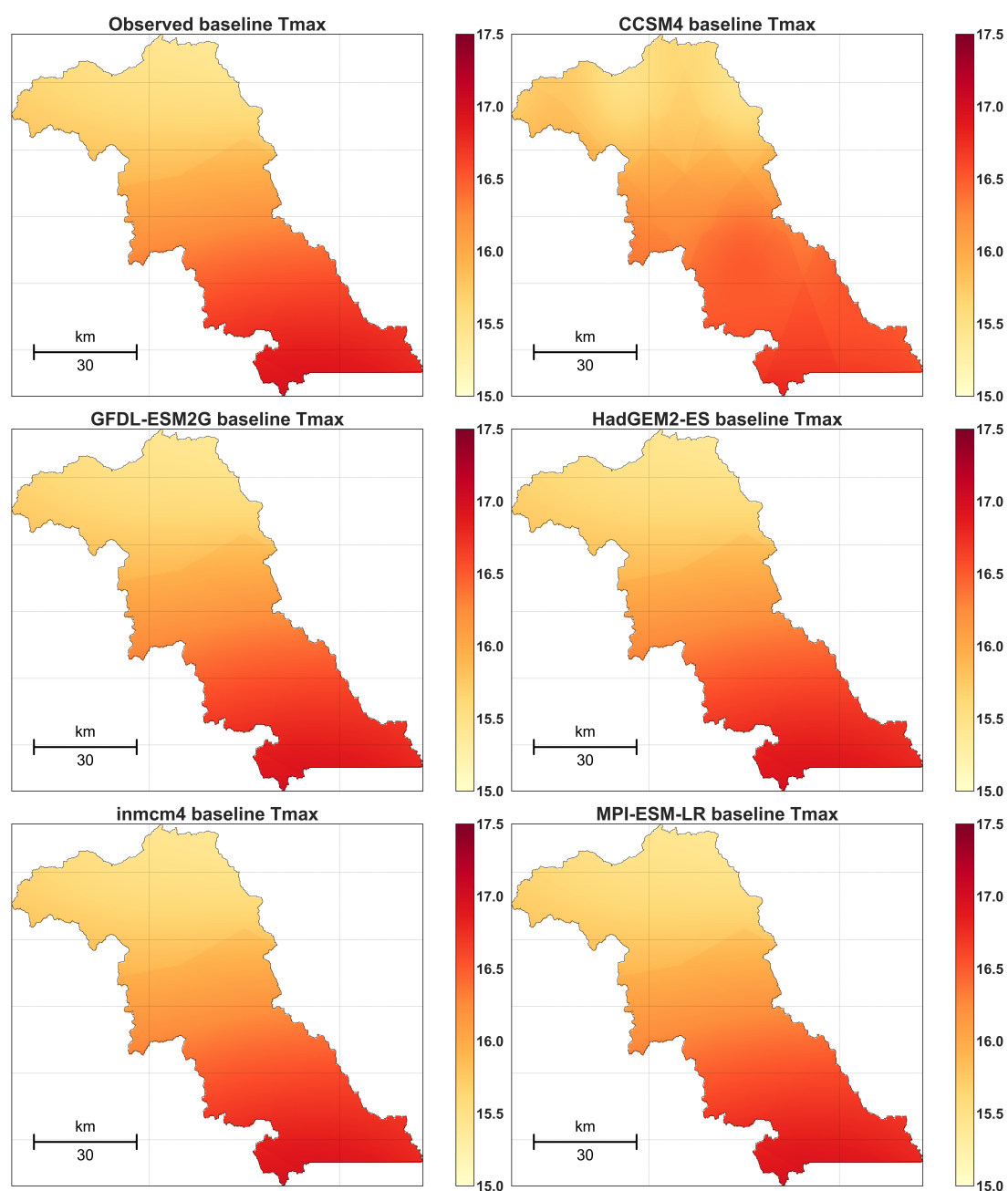
Scenario Component	RCP2.6	RCP4.5	RCP6	RCP8.5
Greenhouse gas emissions	Very low	Medium-low mitigation Very low baseline	high mitigation Medium baseline	High baseline
Agricultural Area	Medium for cropland and pasture	Very low for both cropland and pasture	Medium for cropland but very low for pasture (total low)	Medium for both cropland and pasture
Air pollution	Medium-Low	Medium	Medium	Medium-high

B

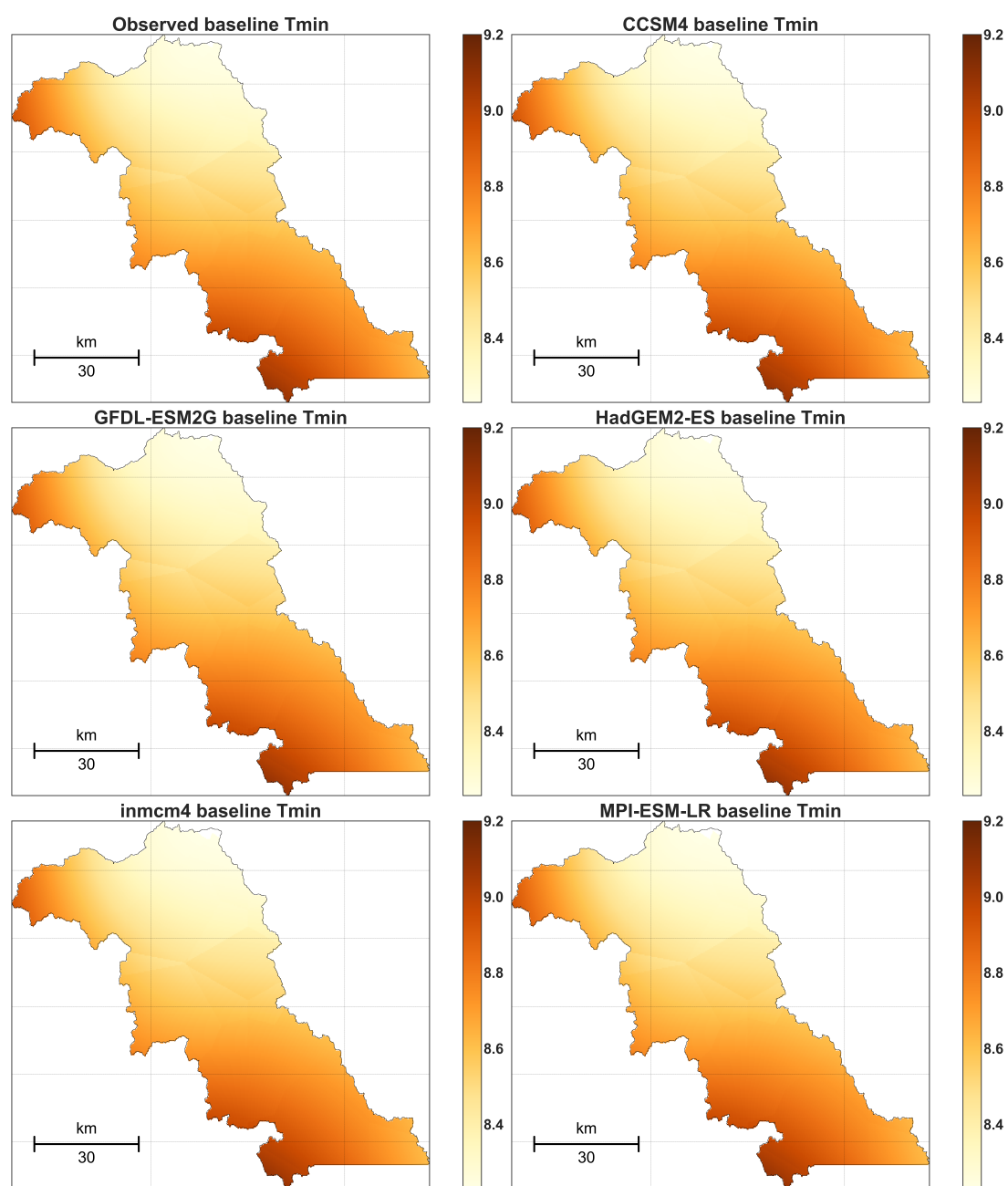
## **Supplementary climate data**



**Figure B.1** GCMs' ability to simulate precipitation for the baseline period (1981–2005) in the River Nith Catchment after bias correction.

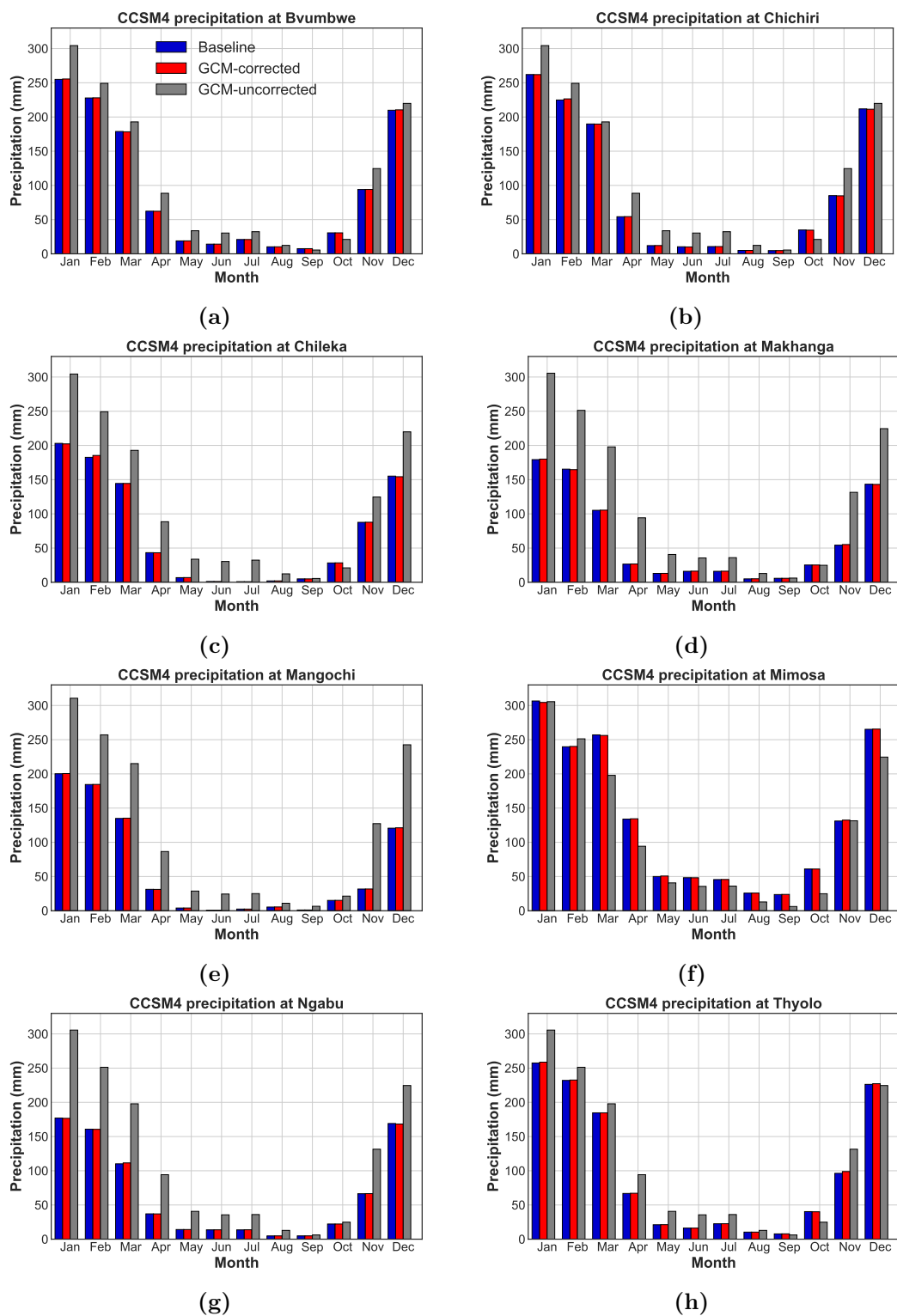


**Figure B.2** GCMs' ability to simulate summer maximum temperature for the baseline period (1981–2005) in the River Nith Catchment after bias correction.



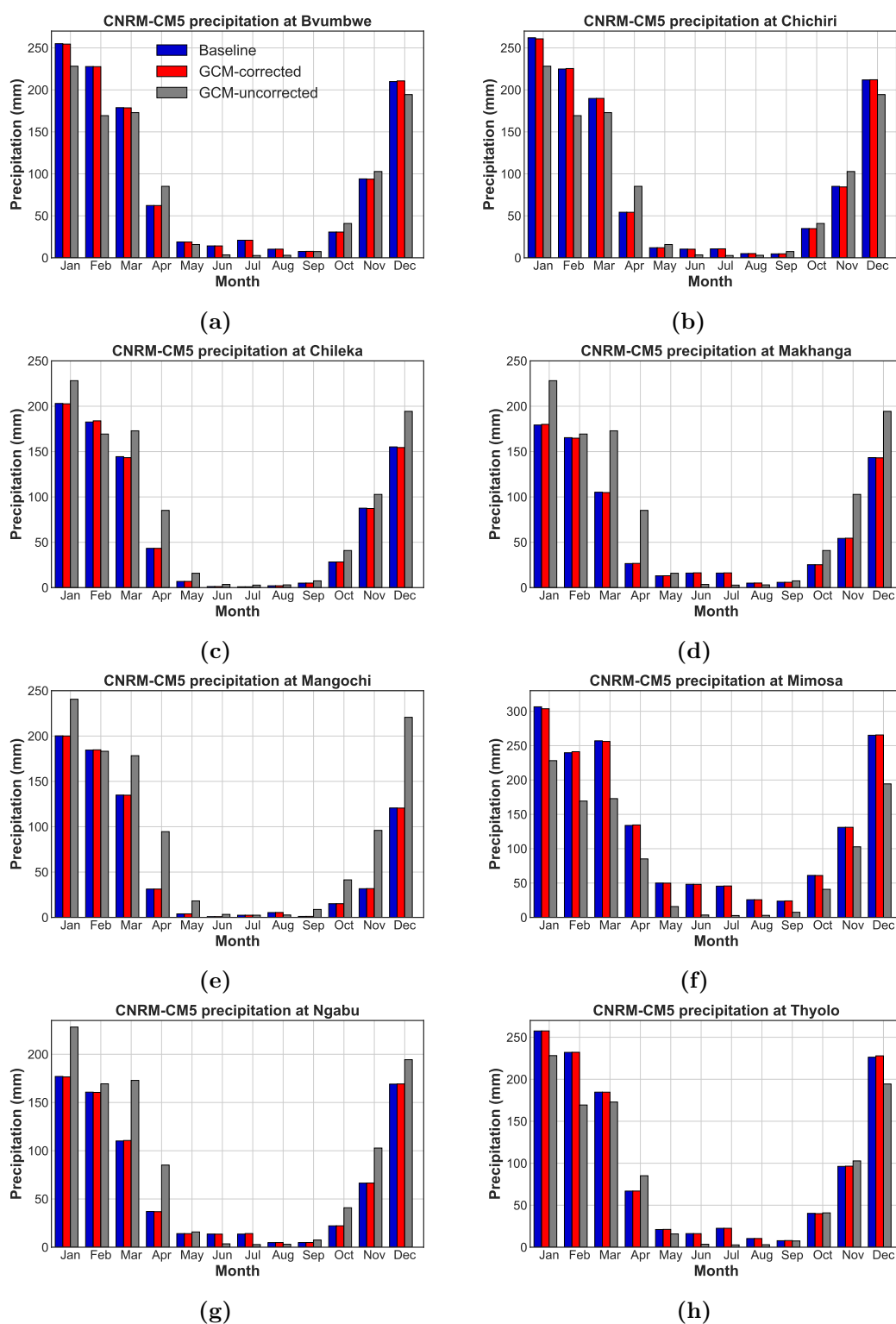
**Figure B.3** GCMs' ability to simulate summer minimum temperature for the baseline period (1981–2005) in the River Nith Catchment after bias correction.

## B.1 Shire Basin climate modelling

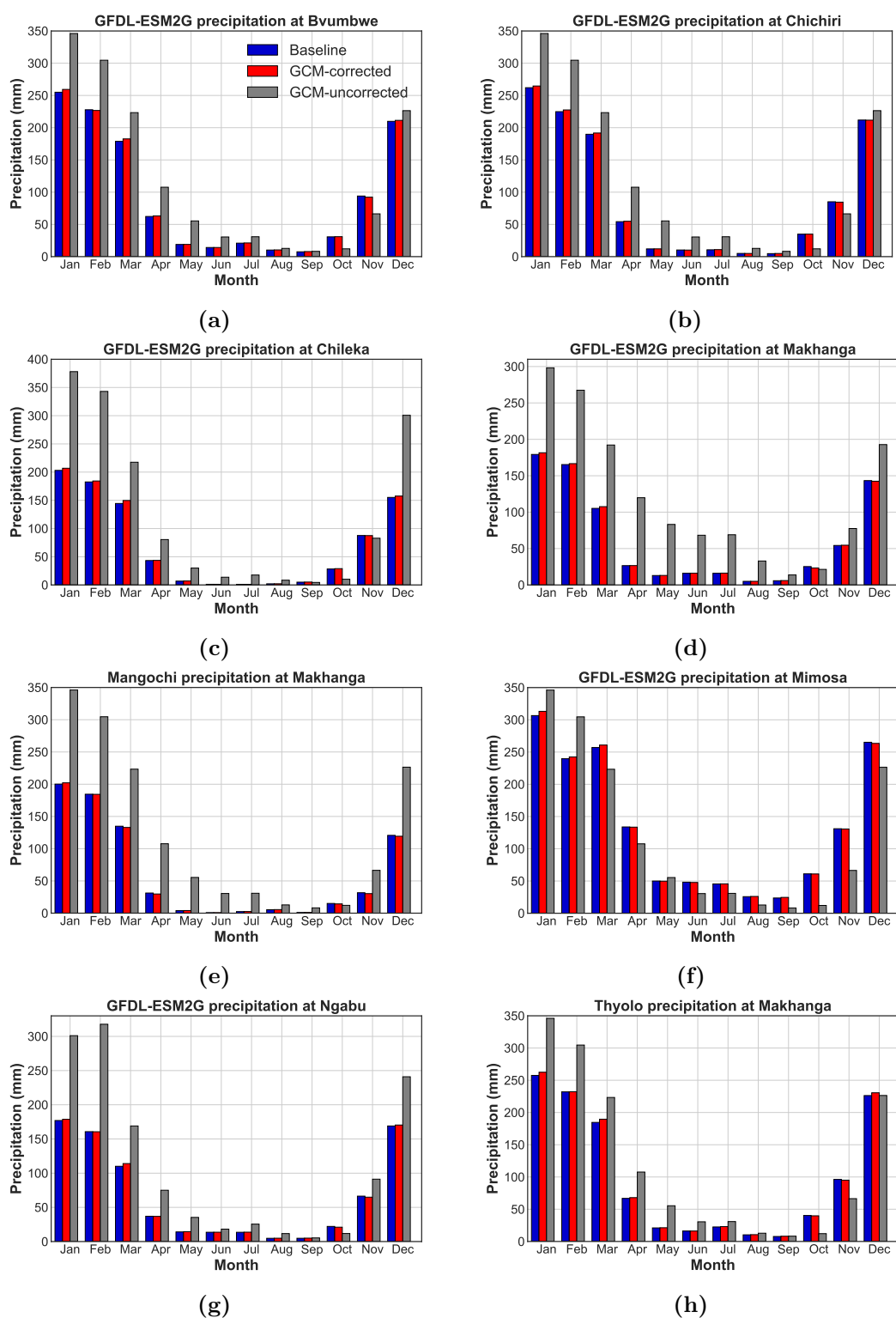


**Figure B.4** Performance of CCSM4 downscaled precipitation in the SRB

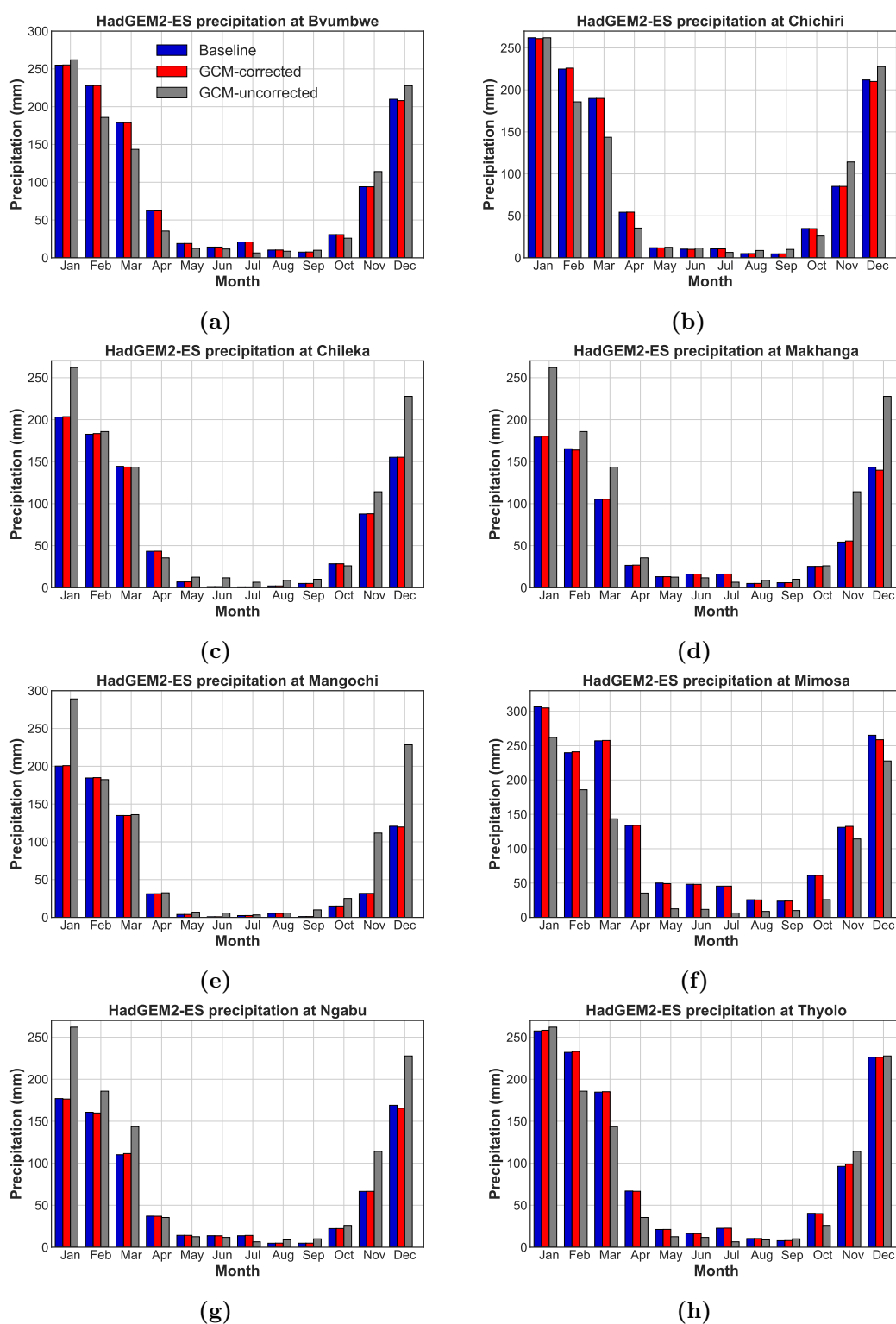




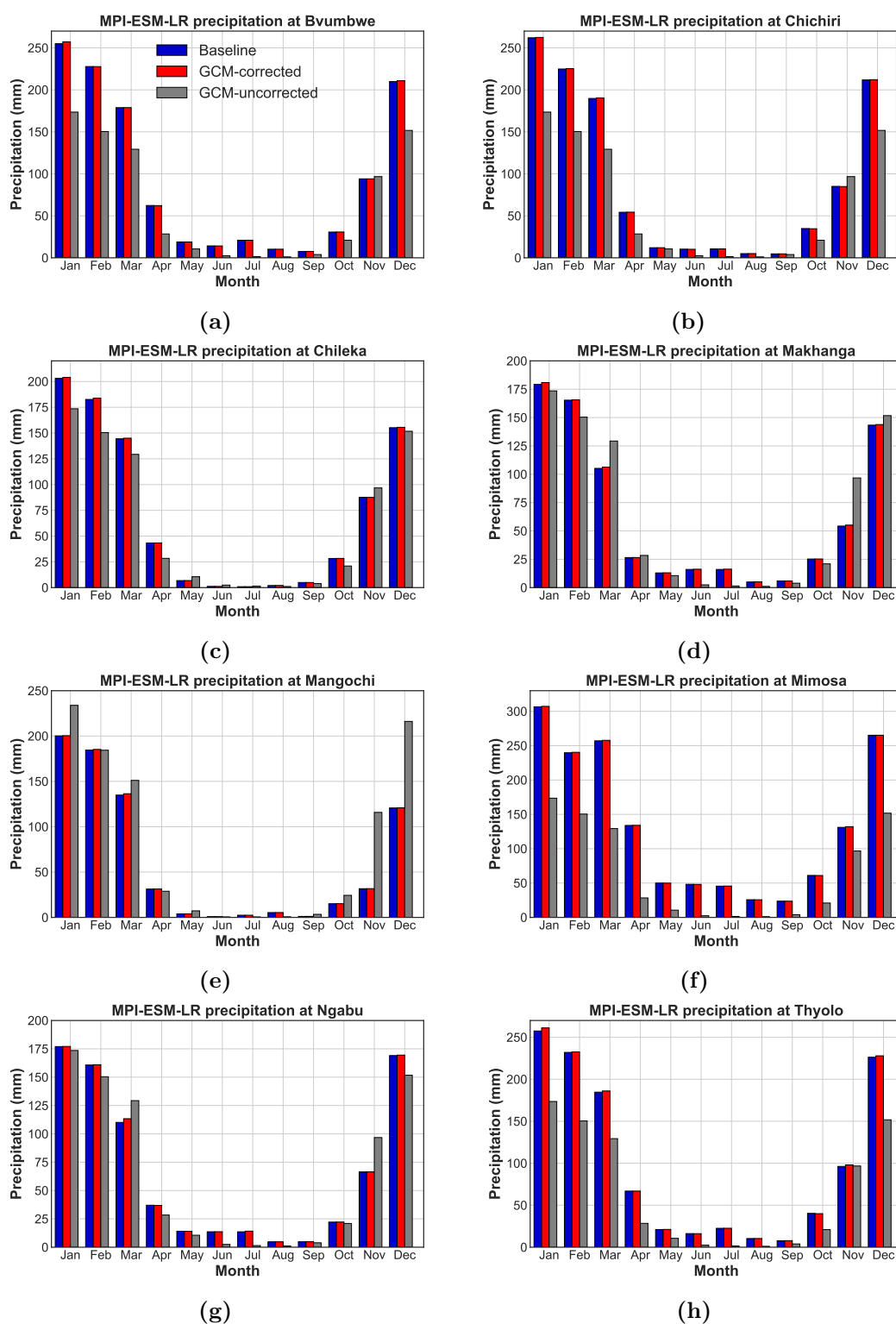
**Figure B.5** Performance of CNRM-CM5 downscaled precipitation in the SRB



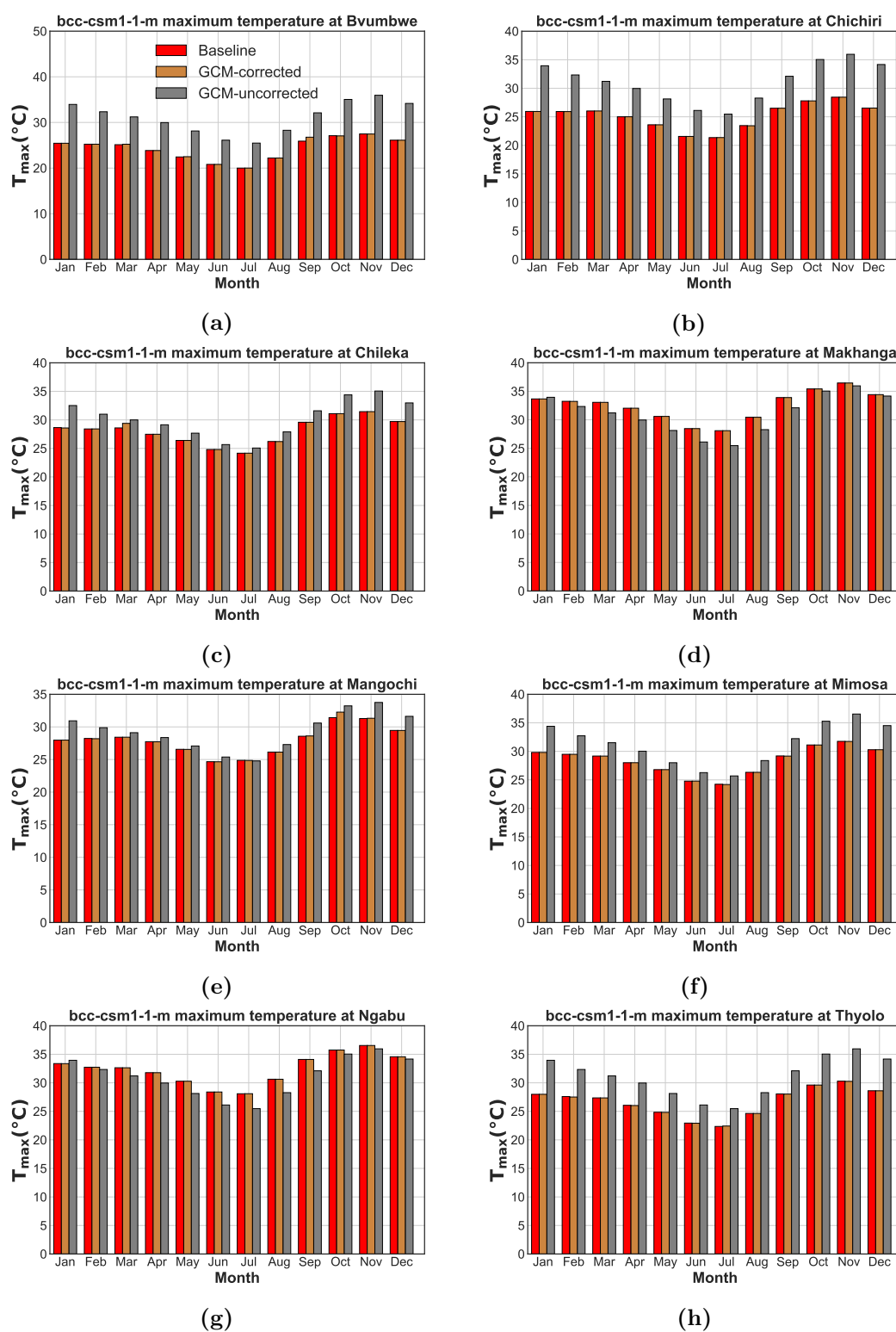
**Figure B.6** Performance of GFDL-ESM2G downscaled precipitation in the SRB



**Figure B.7** Performance of HadGEM2-ES downscaled precipitation in the SRB



**Figure B.8** Performance of MPI-ESM-LR downscaled precipitation in the SRB



**Figure B.9** Performance of bcc-csm1-1m downscaled maximum temperature in the SRB

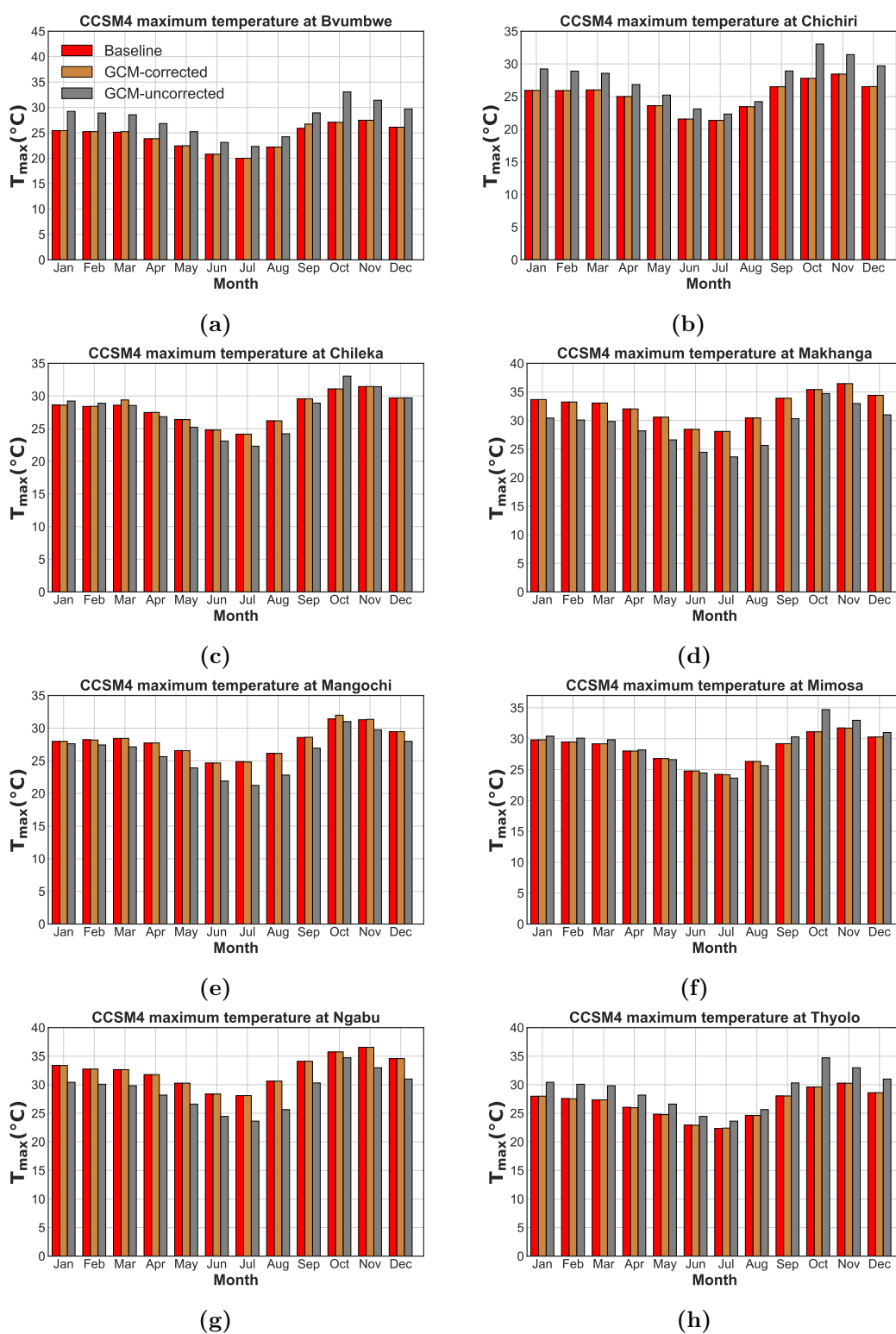
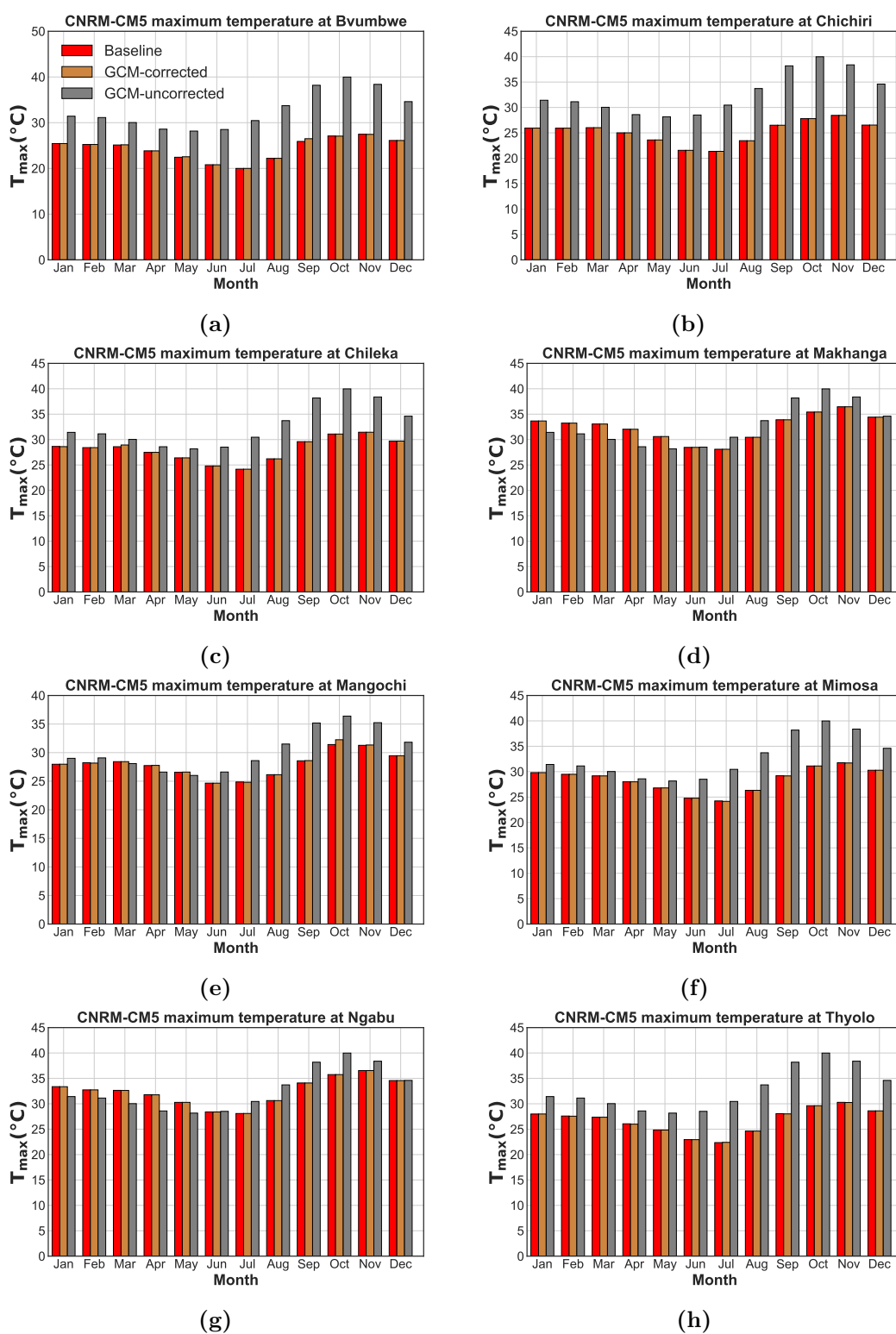
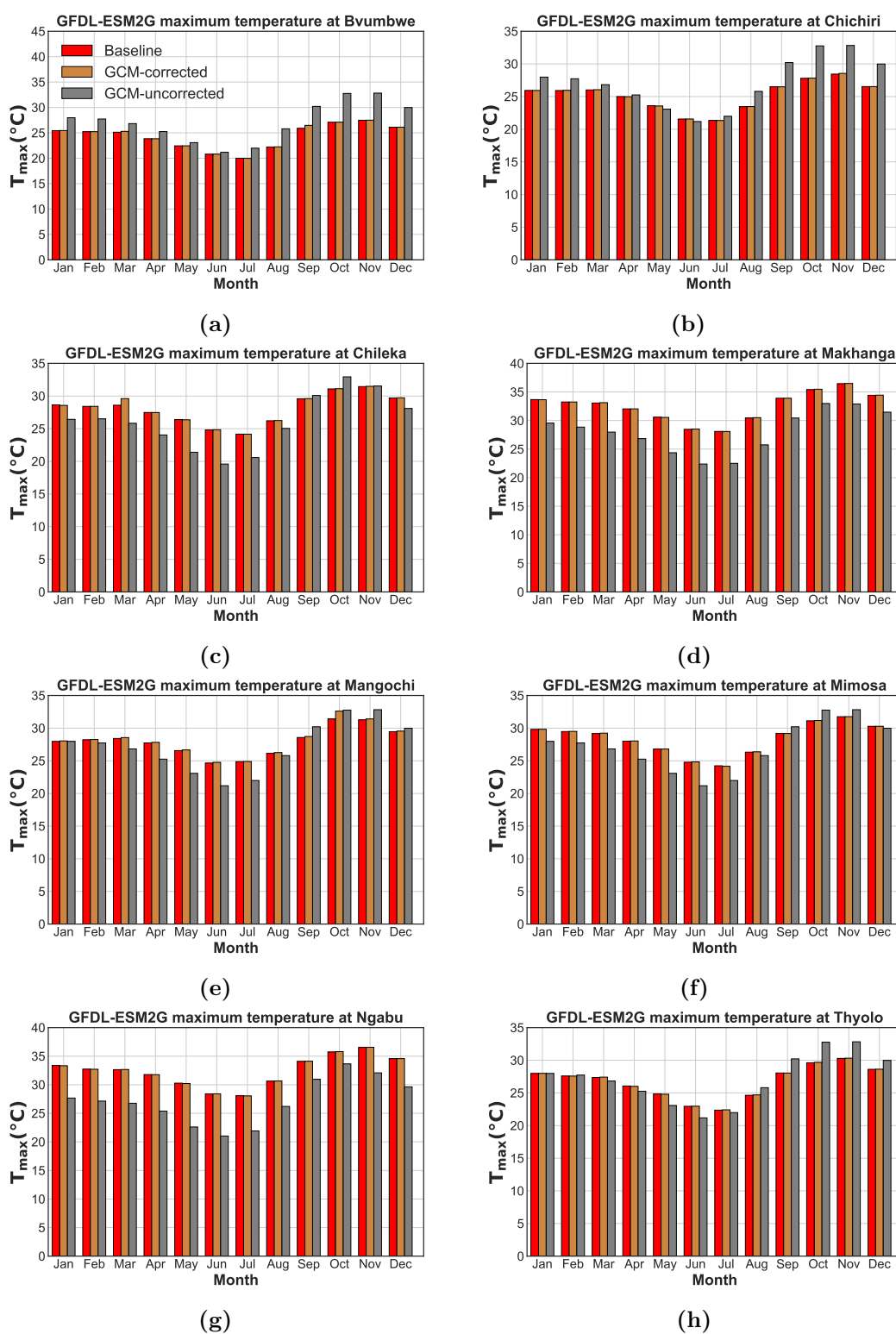


Figure B.10 Performance of CCSM4 downscaled precipitation in the SRB

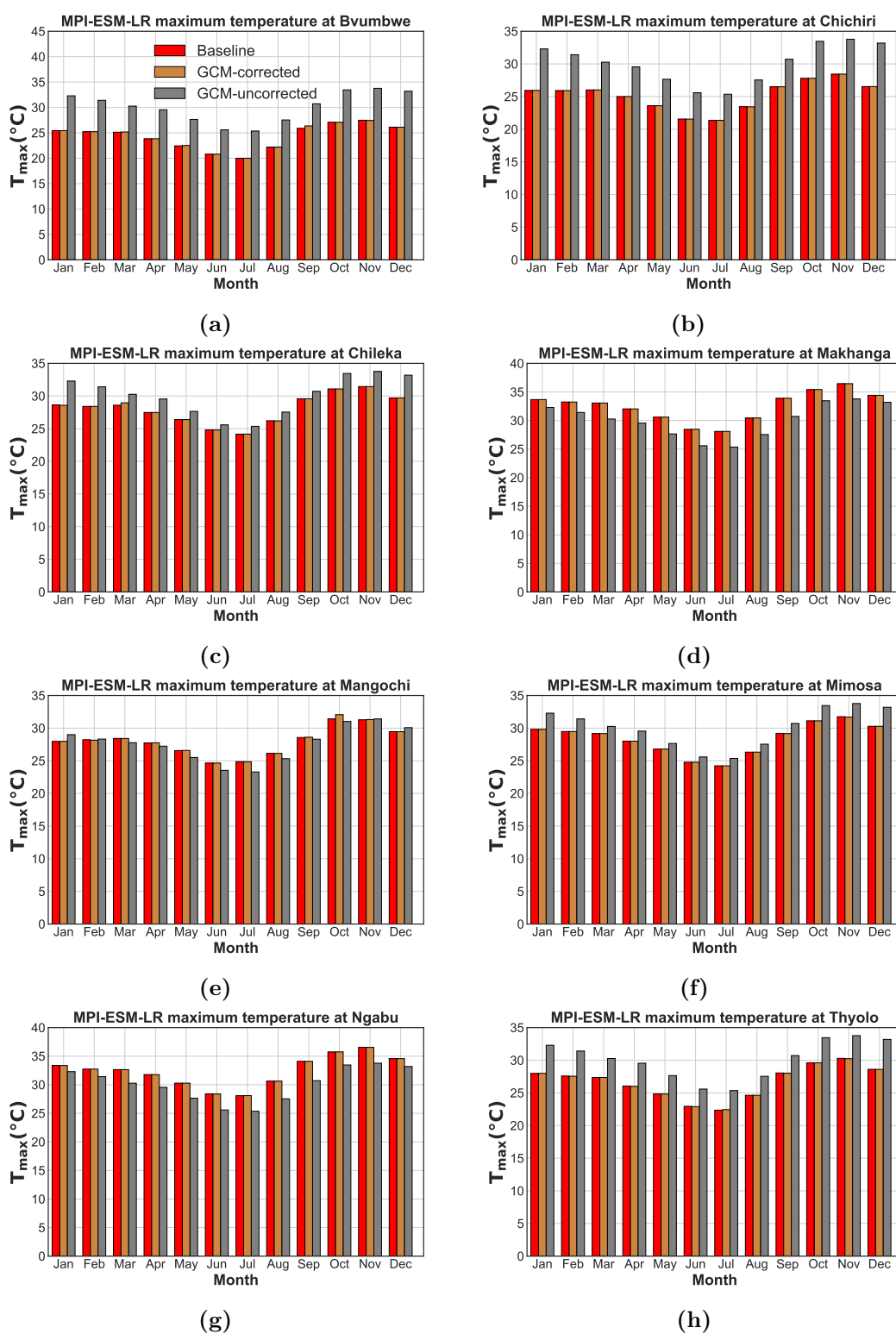


**Figure B.11** Performance of CNRM-CM5 downscaled maximum temperature in the SRB

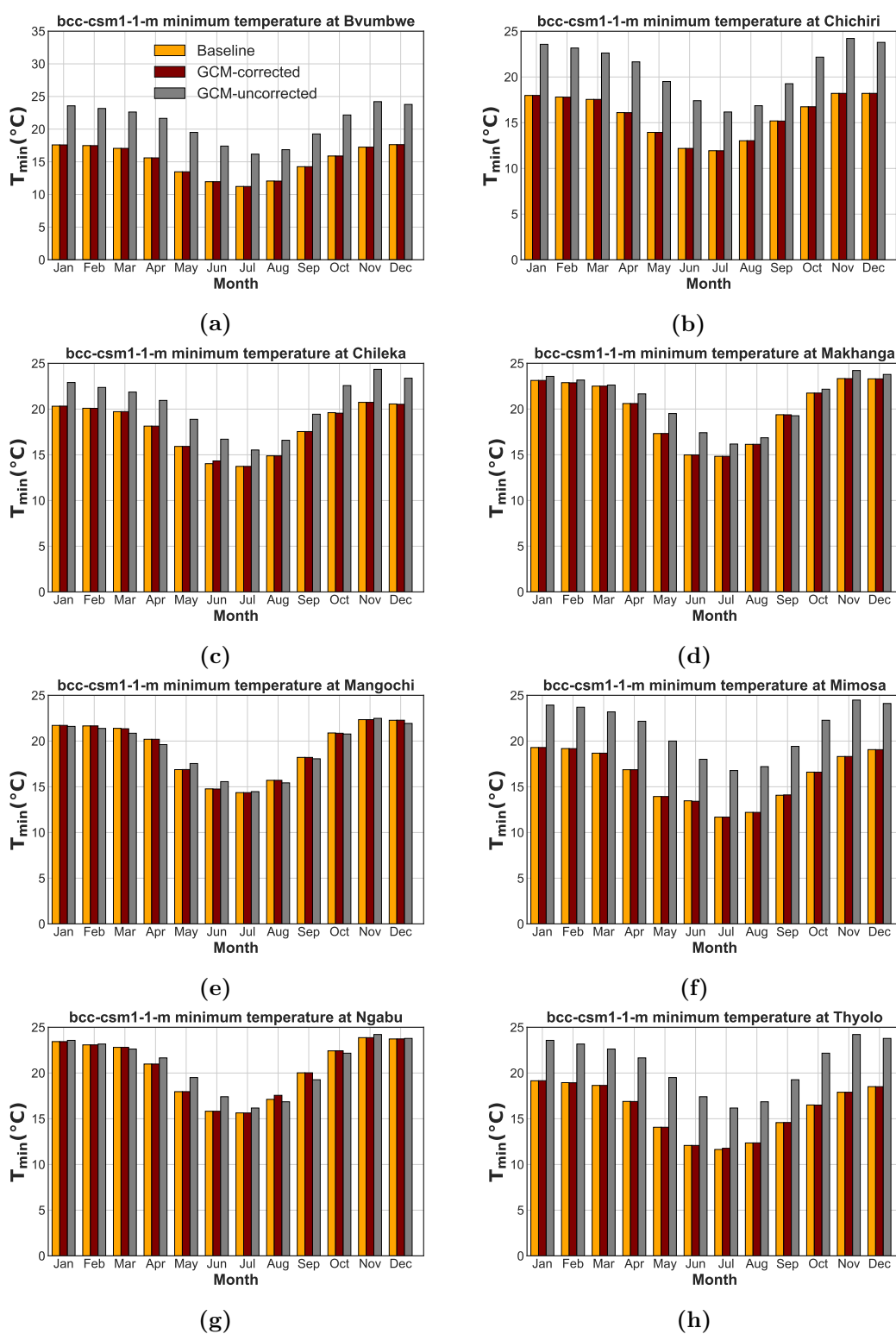


**Figure B.12** Performance of GFDL-ESM2G downscaled maximum temperature in the SRB





**Figure B.13** Performance of MPI-ESM-LR downscaled maximum temperature in the SRB



**Figure B.14** Performance of bcc-csm1-1m downscaled minimum temperature in the SRB

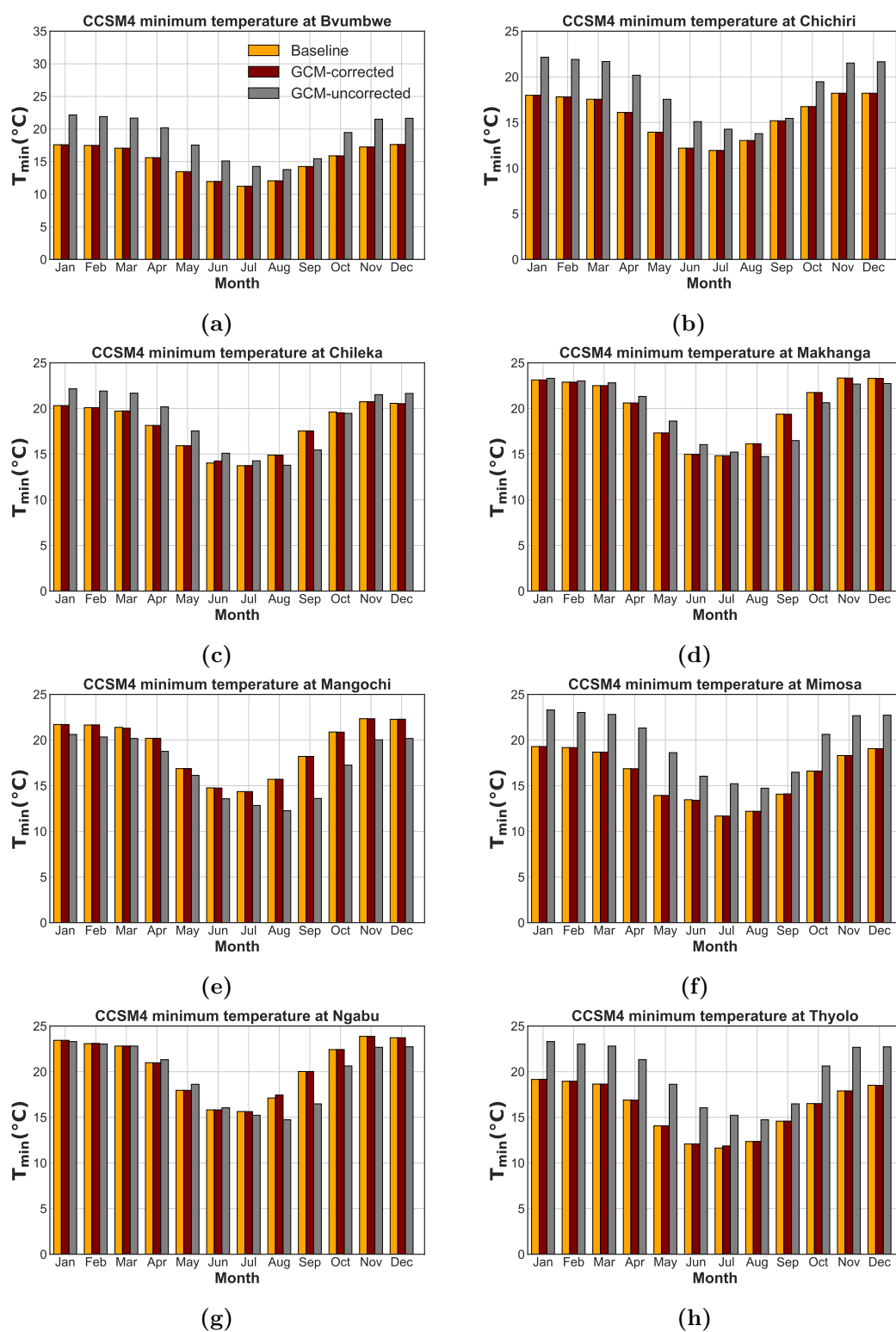
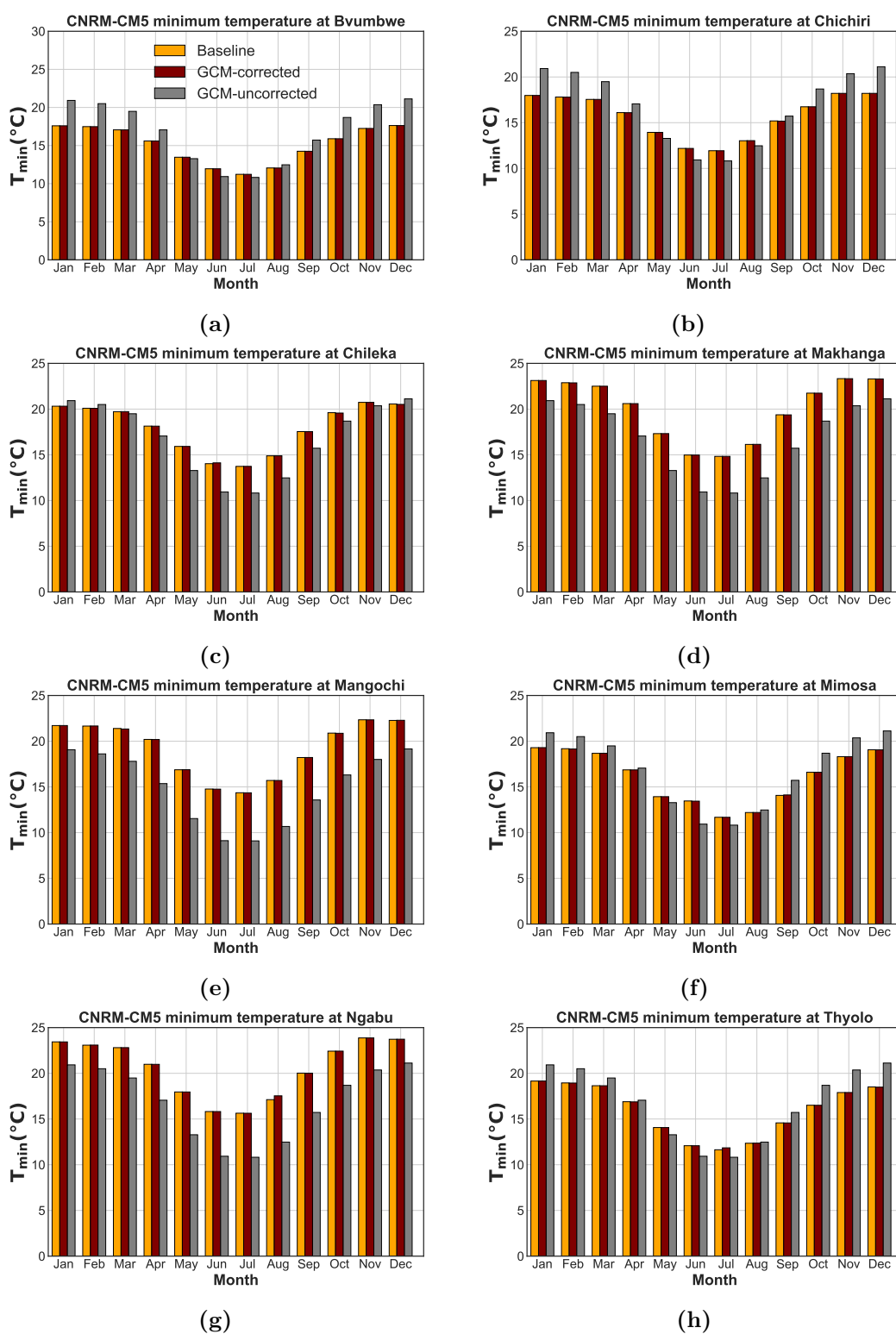
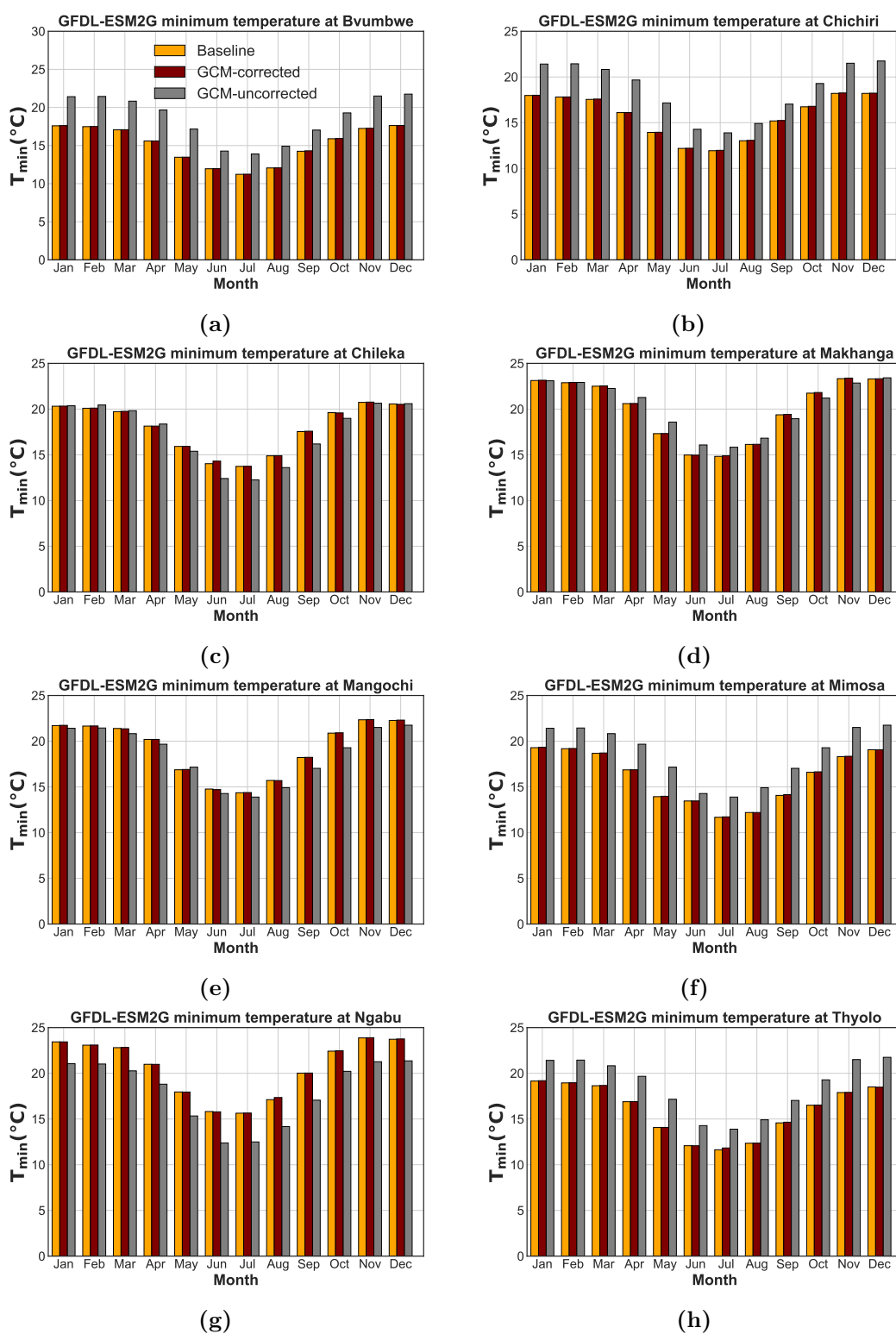


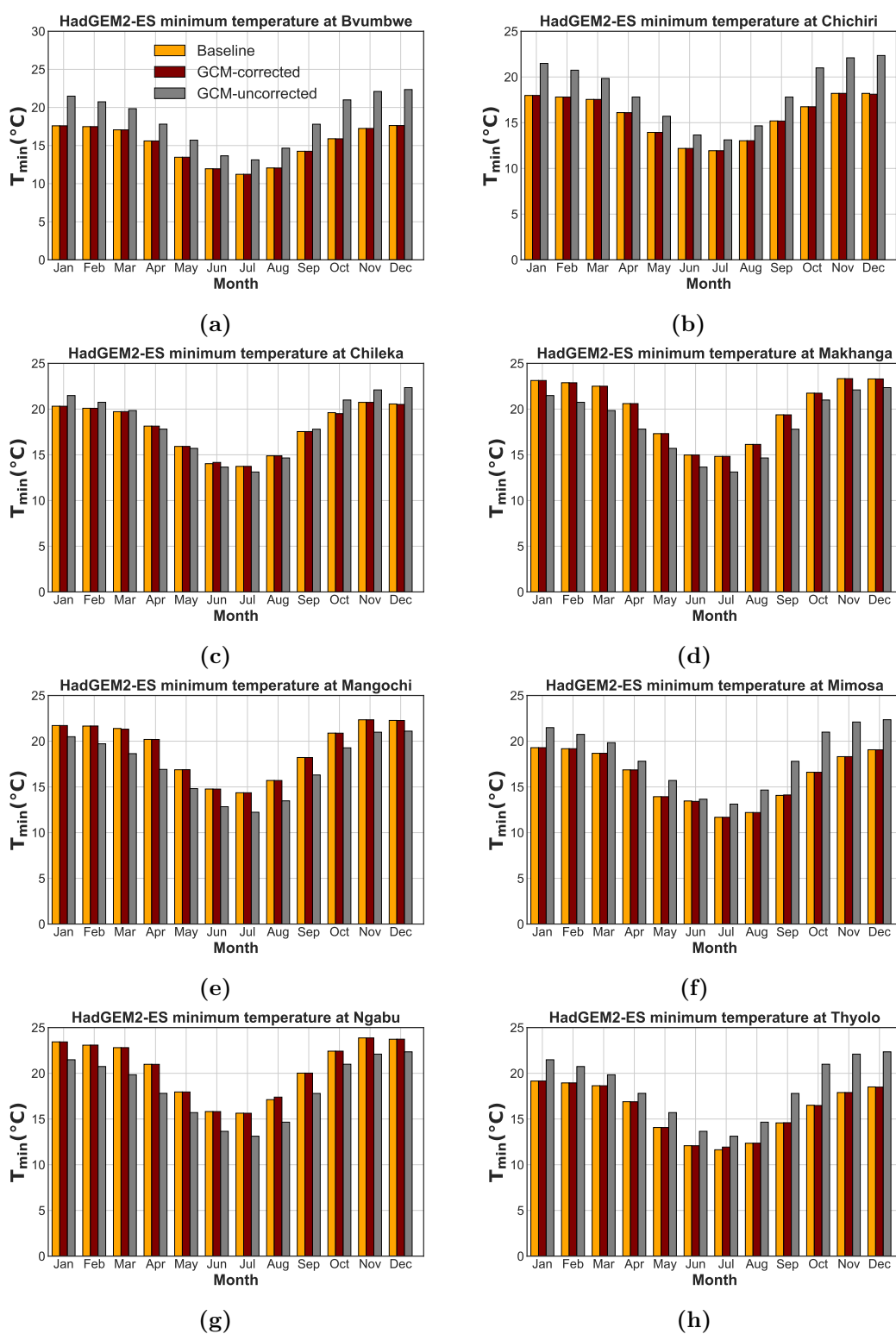
Figure B.15 Performance of CCSM4 downscaled minimum temperature in the SRB



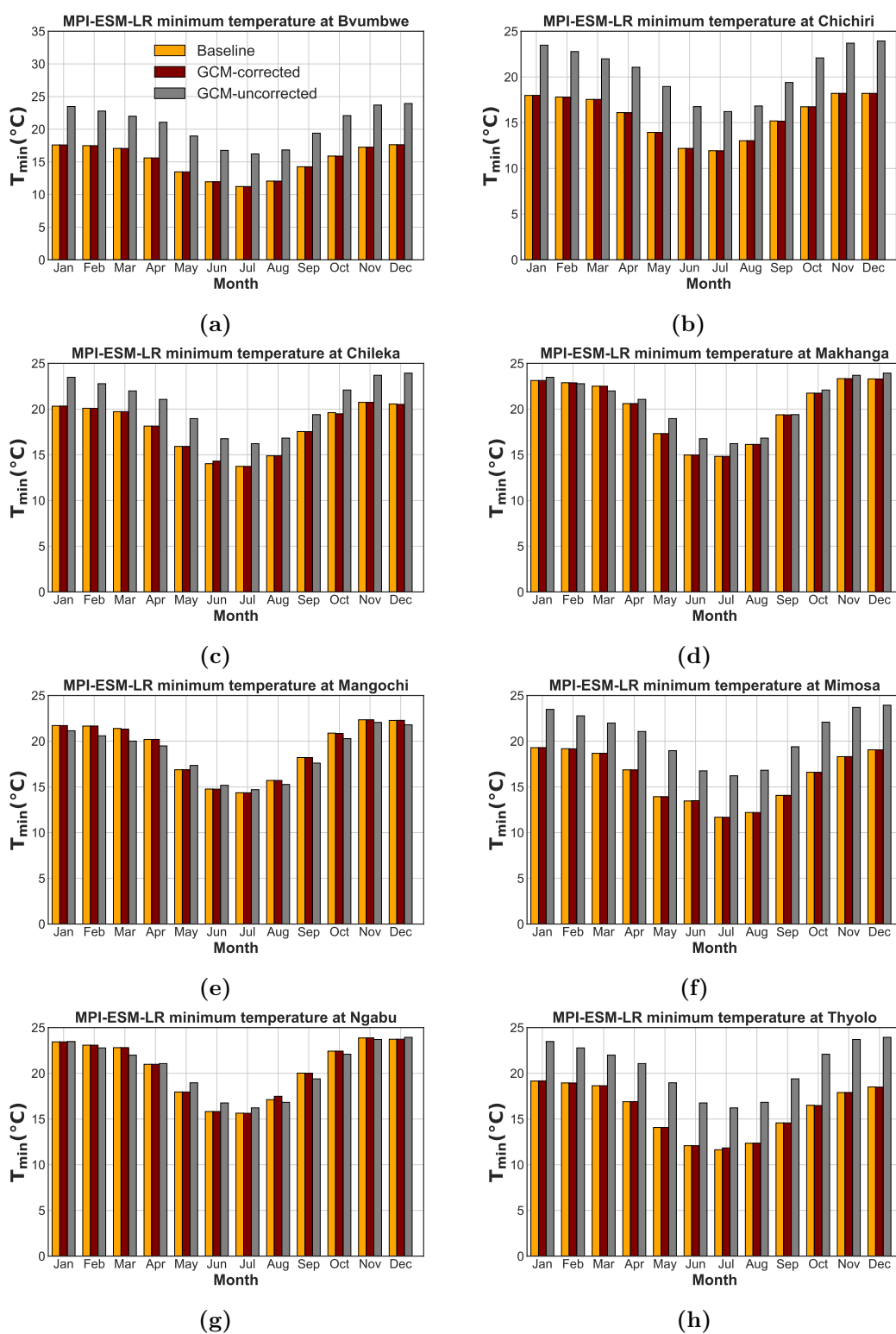
**Figure B.16** Performance of CNRM-CM5 downscaled minimum temperature in the SRB



**Figure B.17** Performance of GFDL-ESM2G downscaled minimum temperature in the SRB



**Figure B.18** Performance of HadGEM2-ES downscaled minimum temperature in the SRB



**Figure B.19** Performance of MPI-ESM-LR downscaled minimum temperature in the SRB

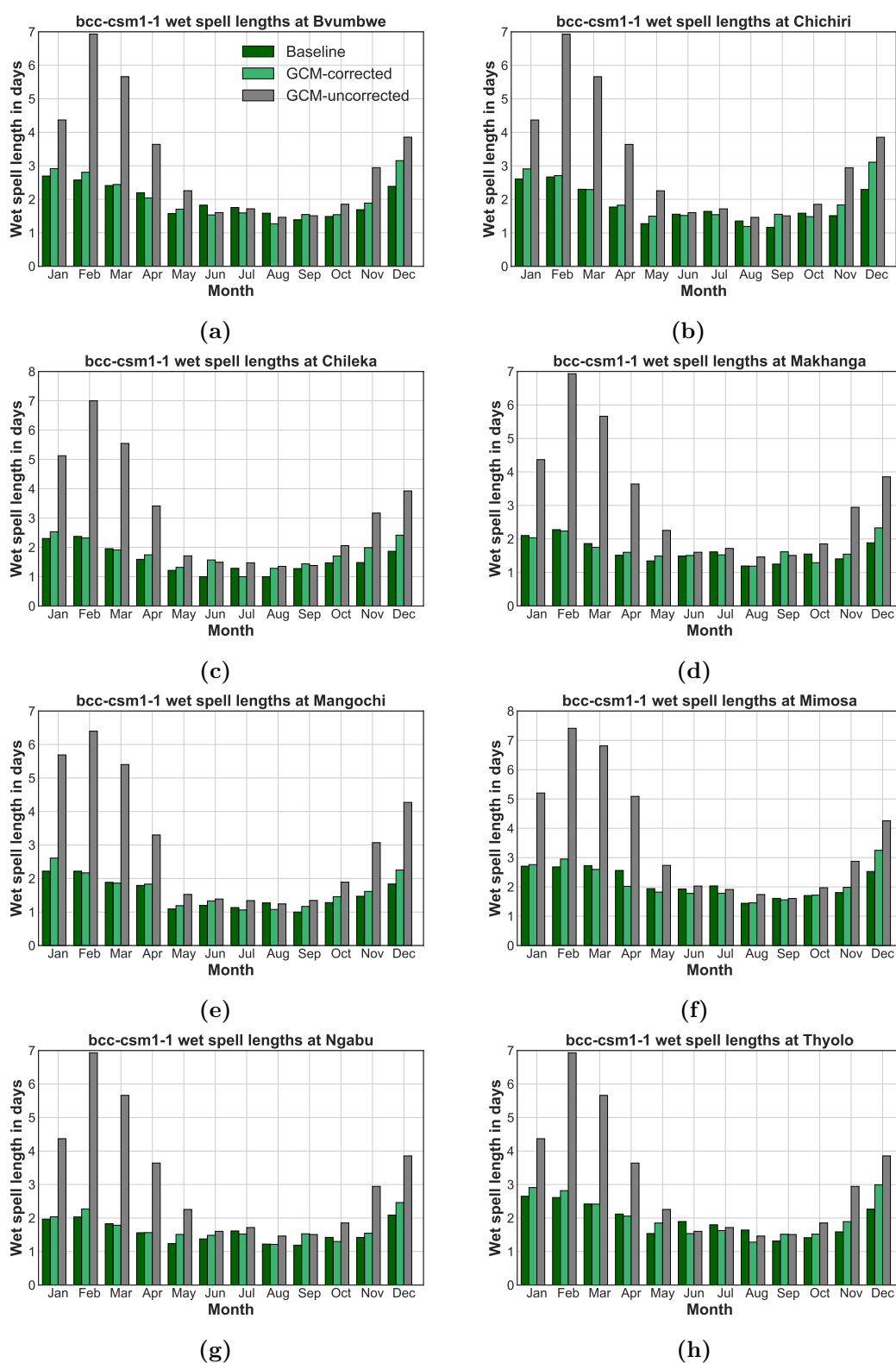


Figure B.20 Performance of bcc-csm1-1-1m in predicting wet spell lengths in the SRB



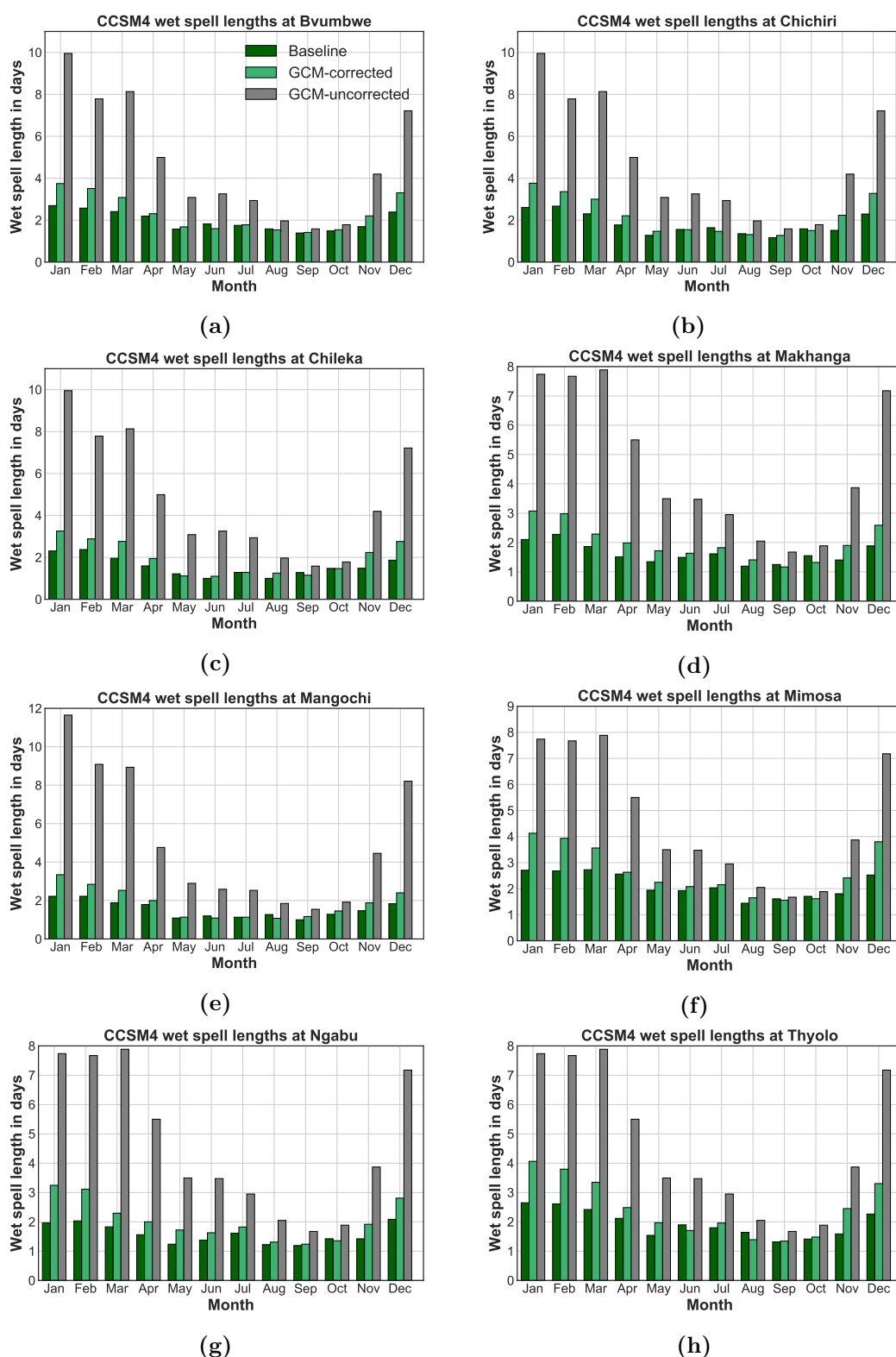
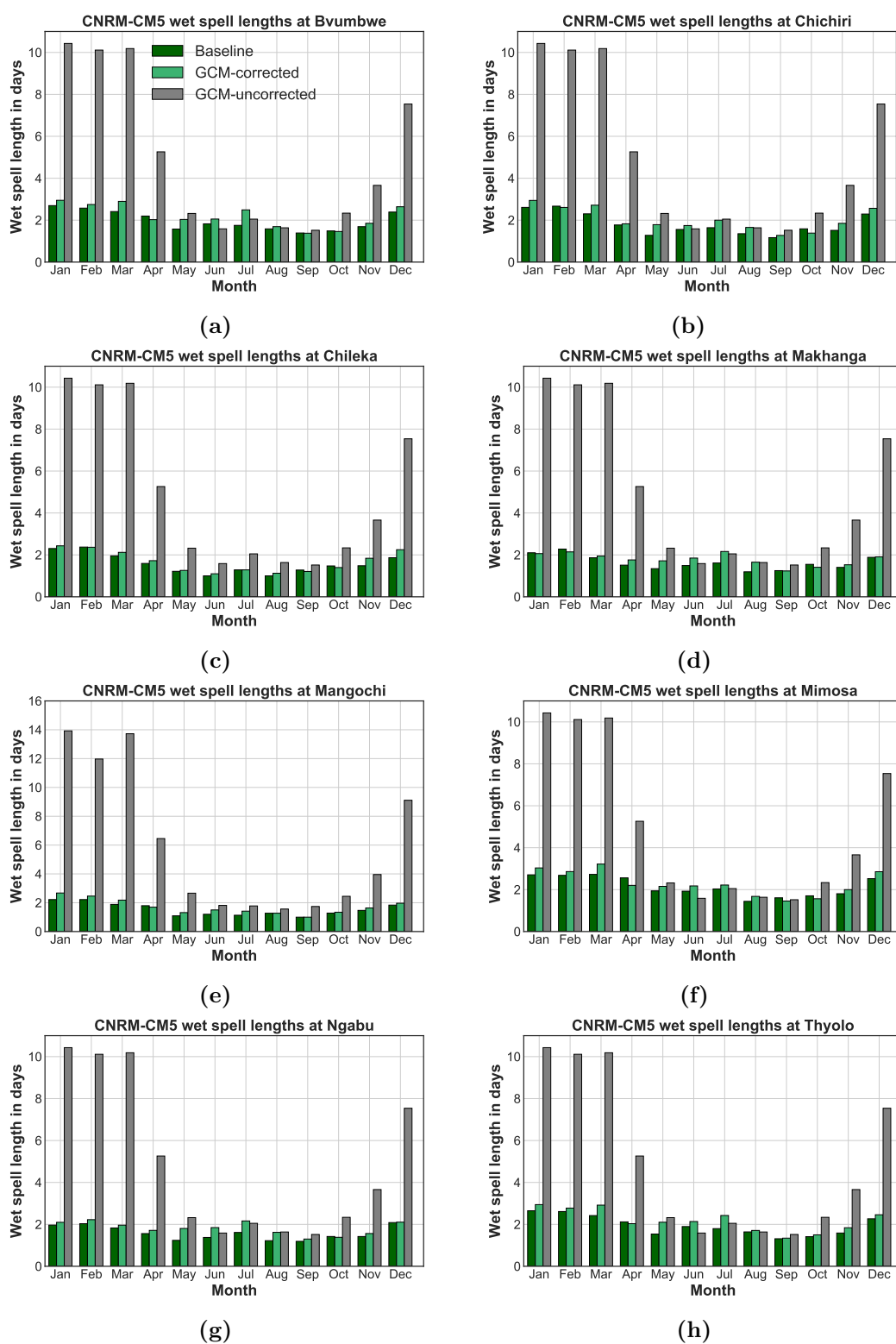
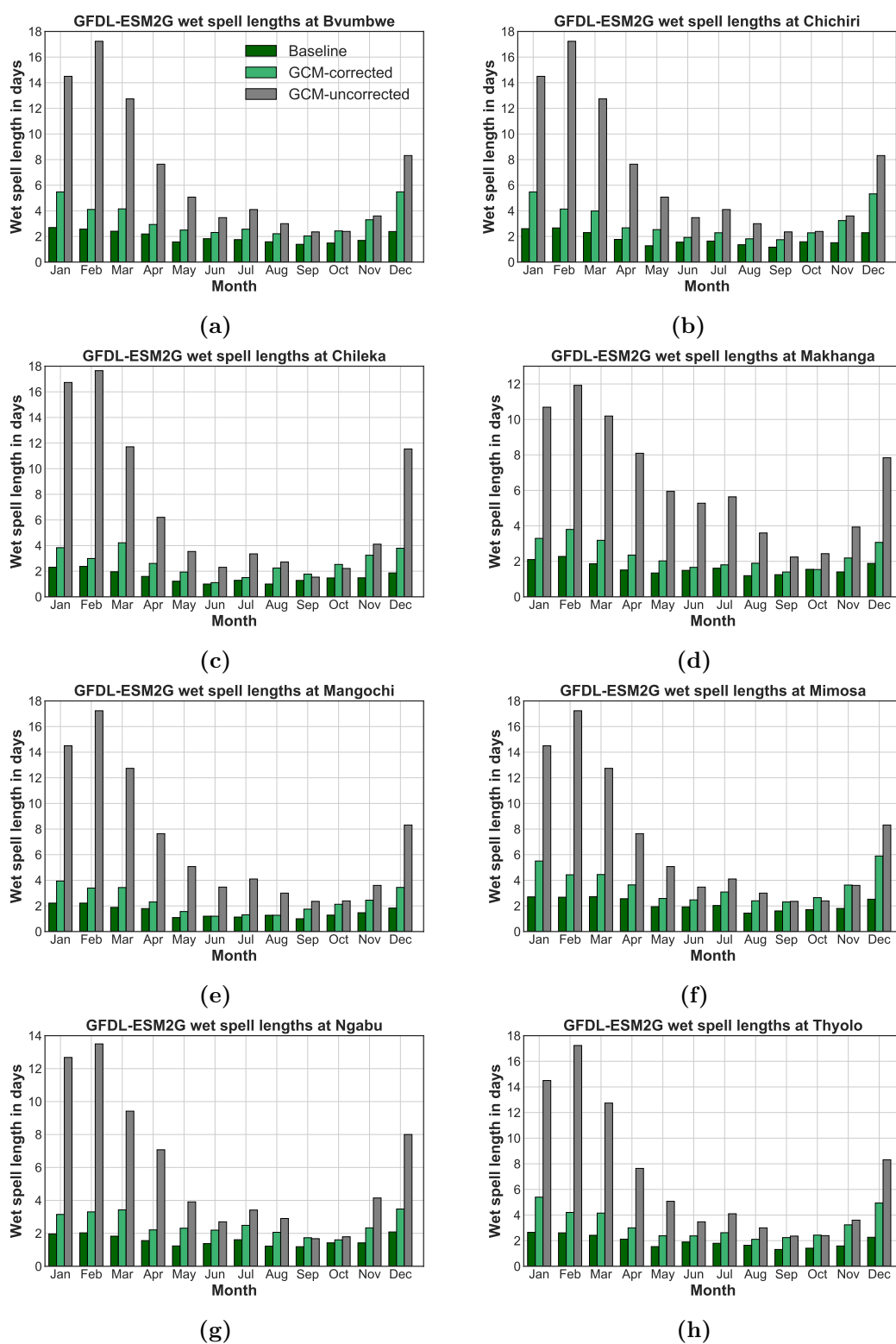


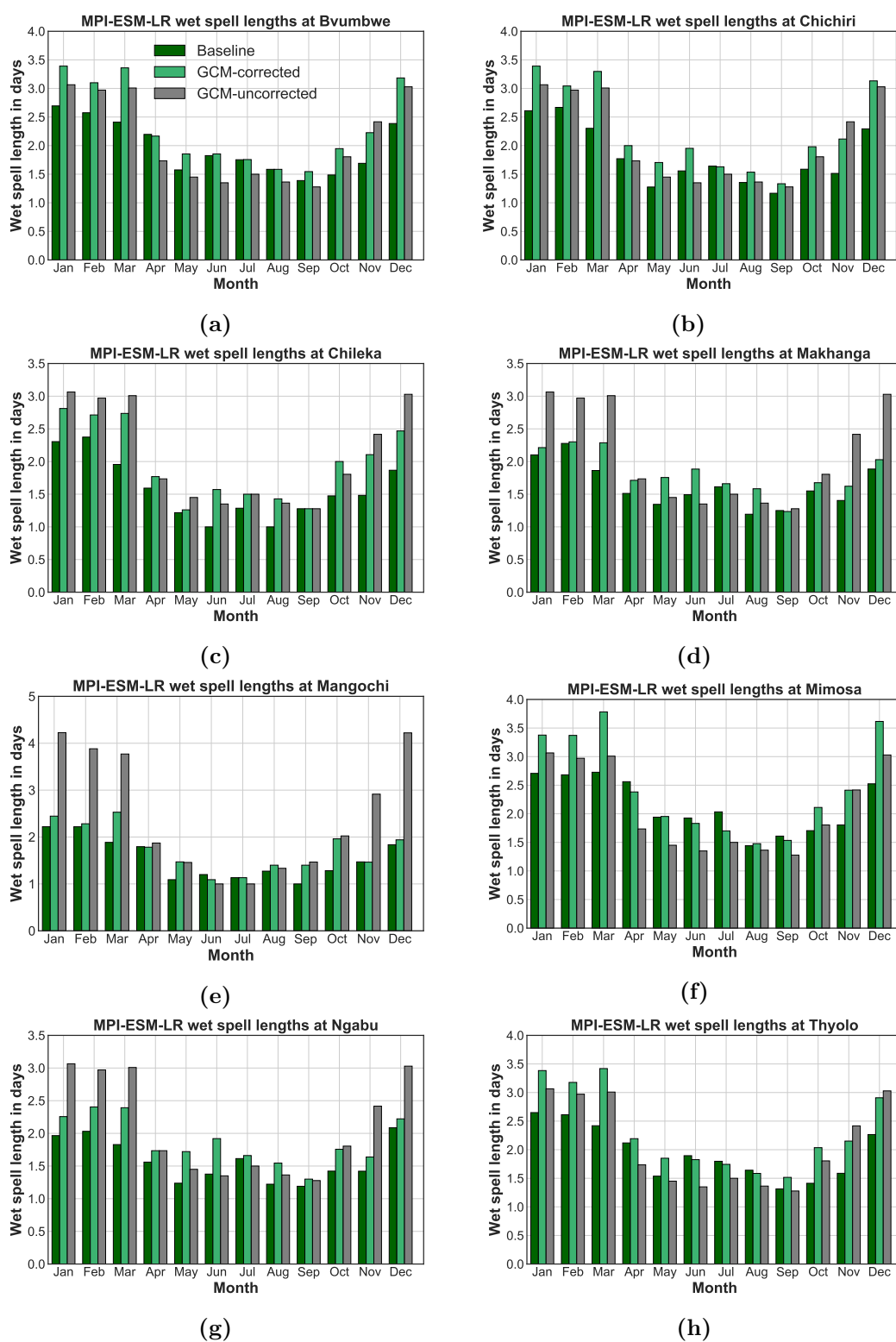
Figure B.21 Performance of CCSM4 in predicting wet spell lengths in the SRB



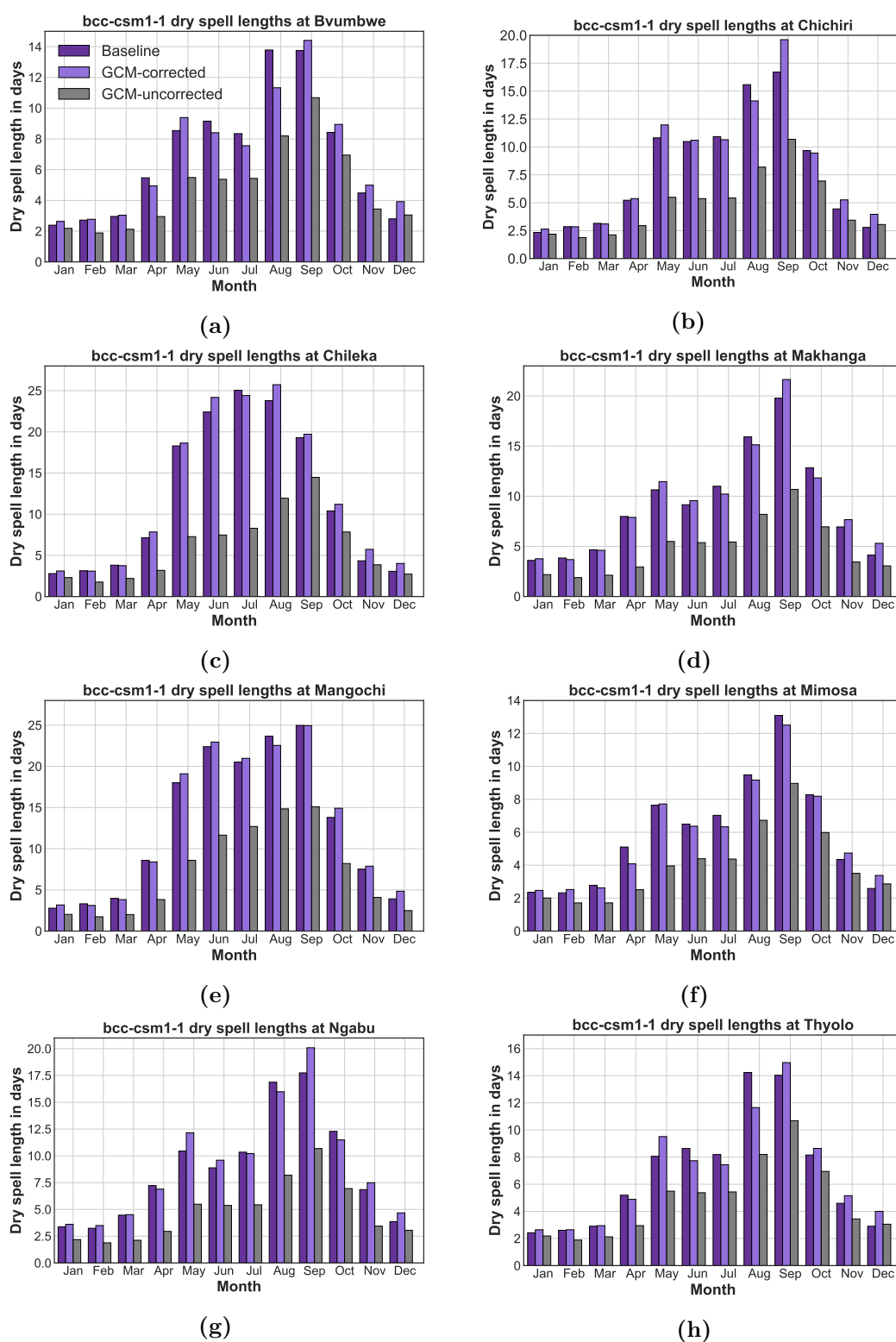
**Figure B.22** Performance of CNRM-CM5 in predicting wet spell lengths in the SRB



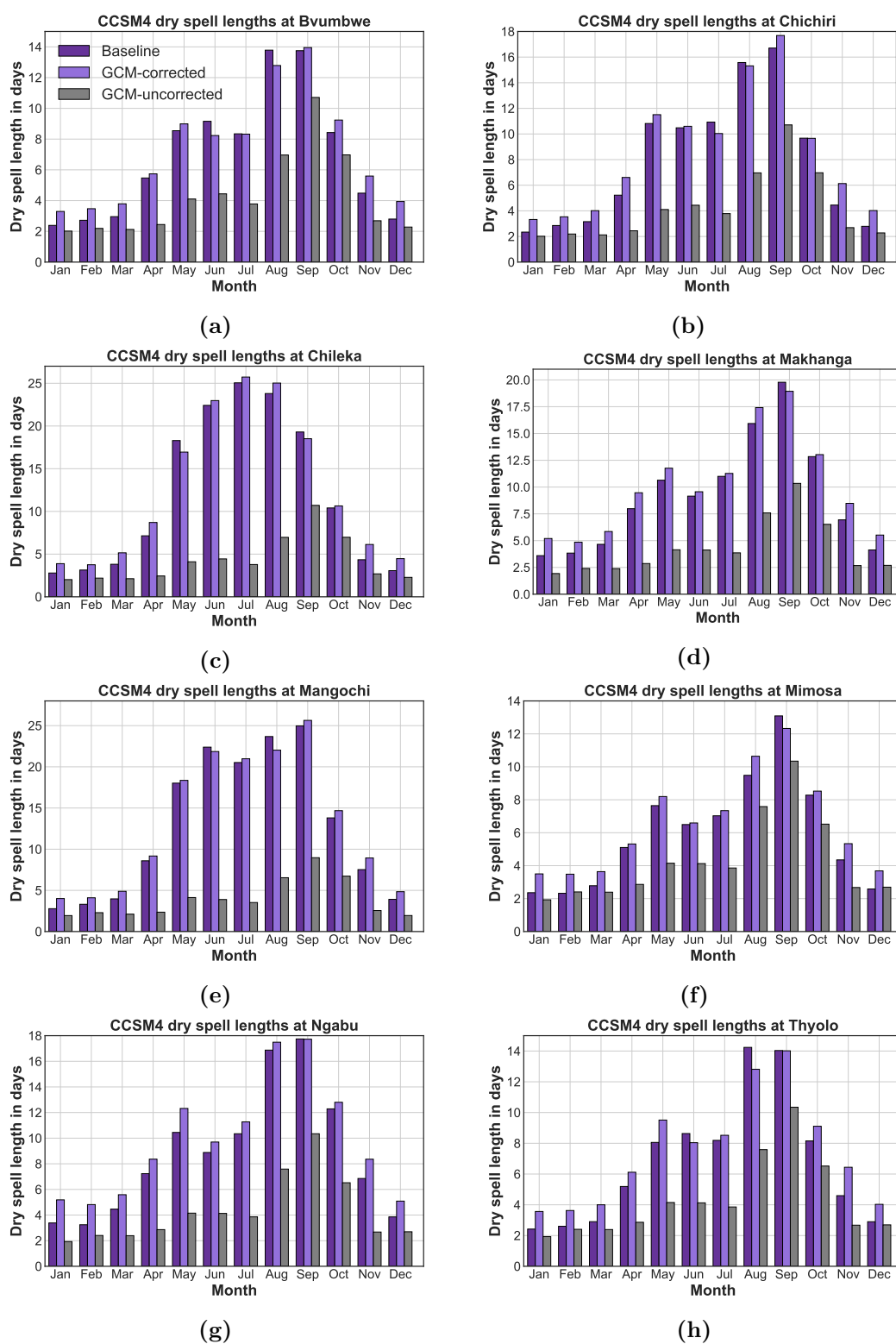
**Figure B.23** Performance of GFDL-ESM2G in predicting wet spell lengths in the SRB



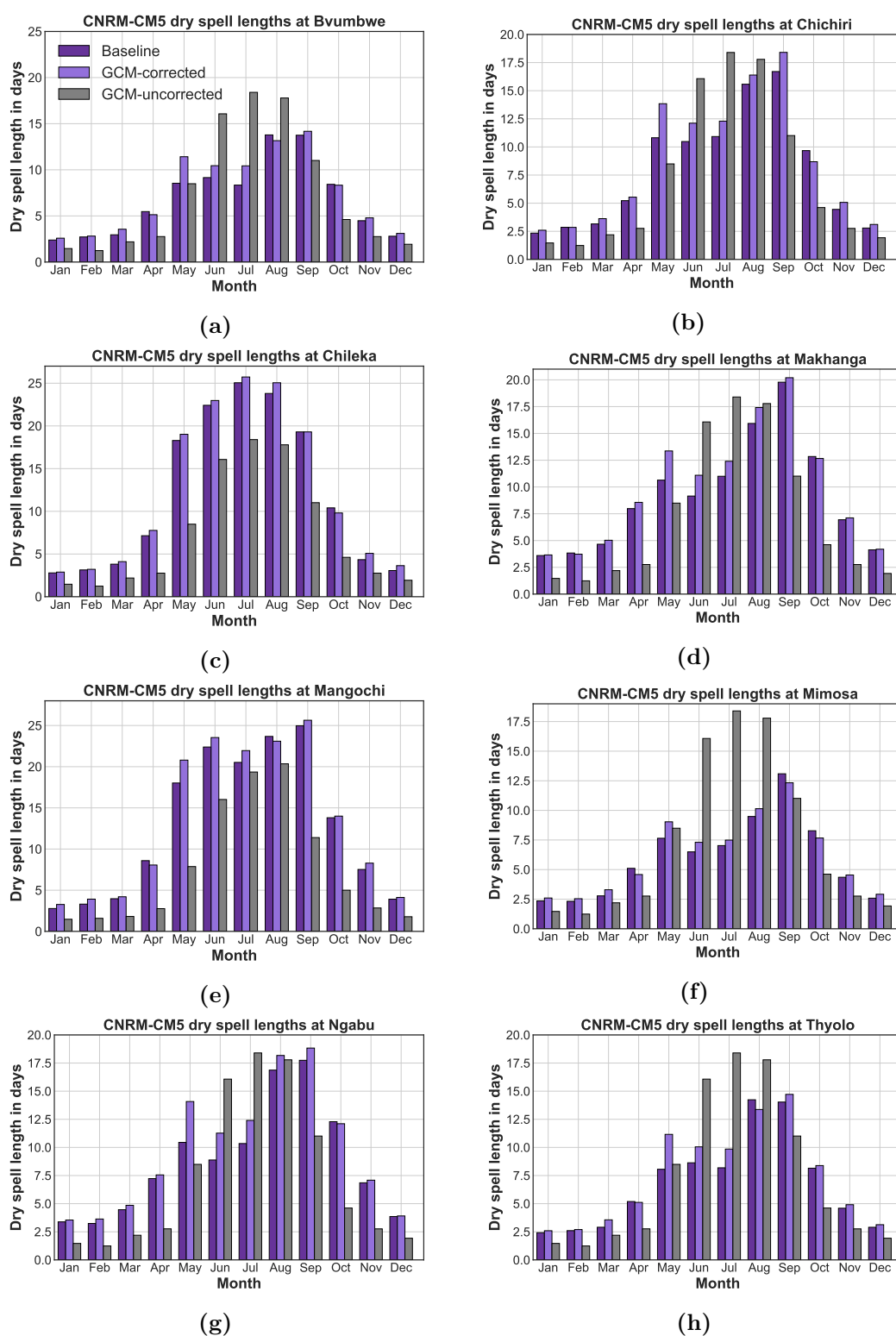
**Figure B.24** Performance of MPI-ESM-LR in predicting wet spell lengths in the SRB



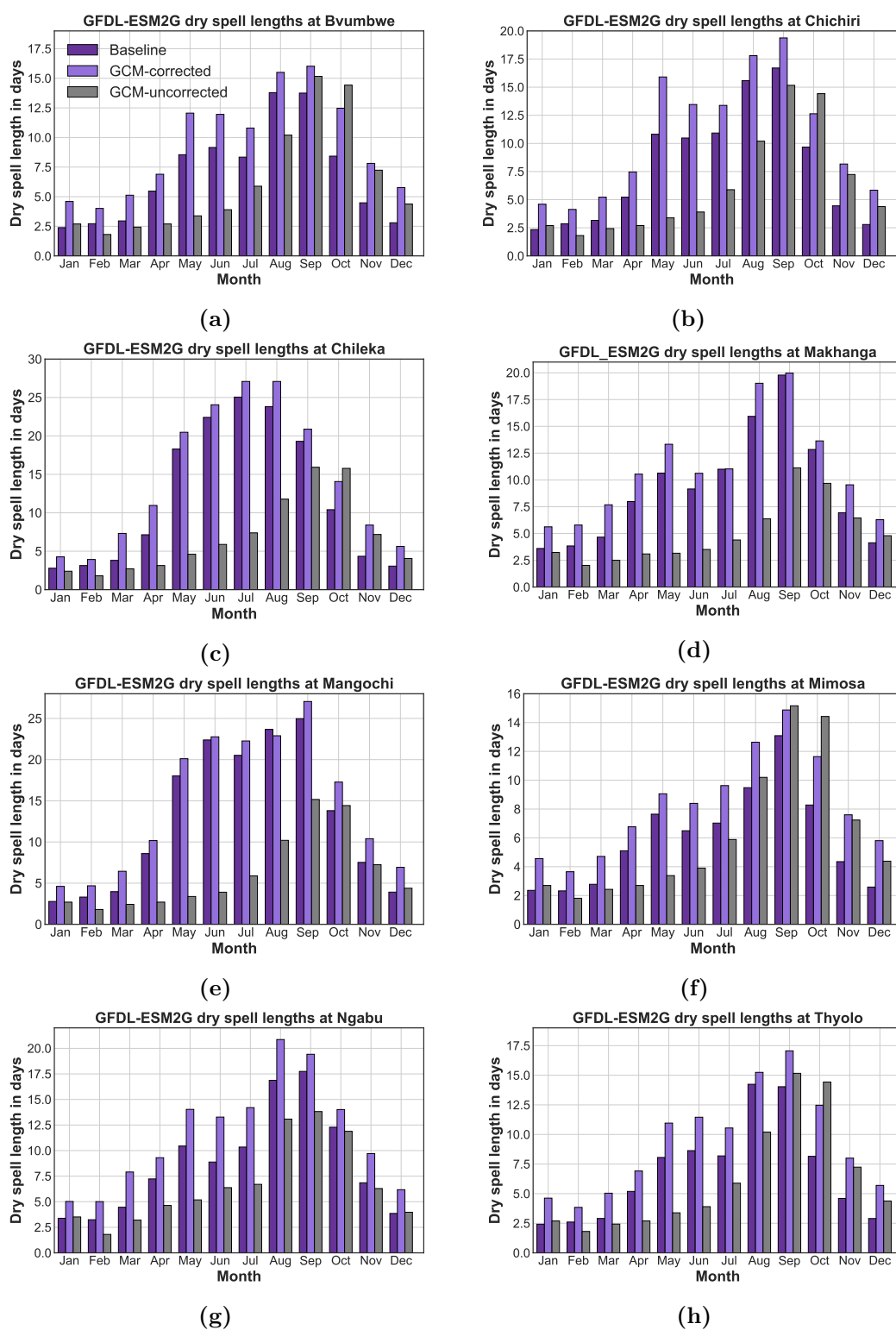
**Figure B.25** Performance of bcc-csm1-1-m in predicting dry spell lengths in the SRB



**Figure B.26** Performance of CCSM4 in predicting dry spell lengths in the SRB

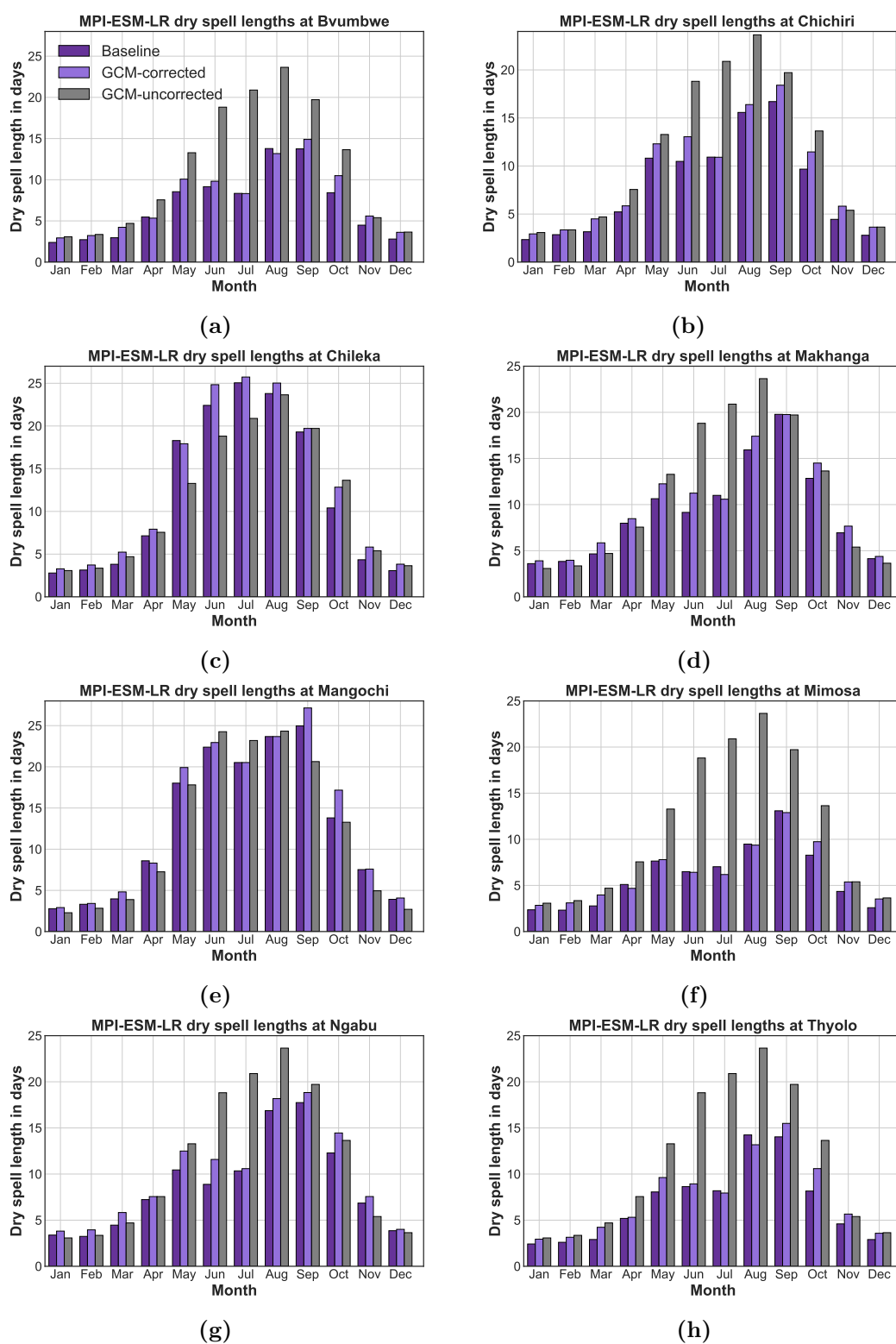


**Figure B.27** Performance of CNRM-CM5 in predicting dry spell lengths in the SRB

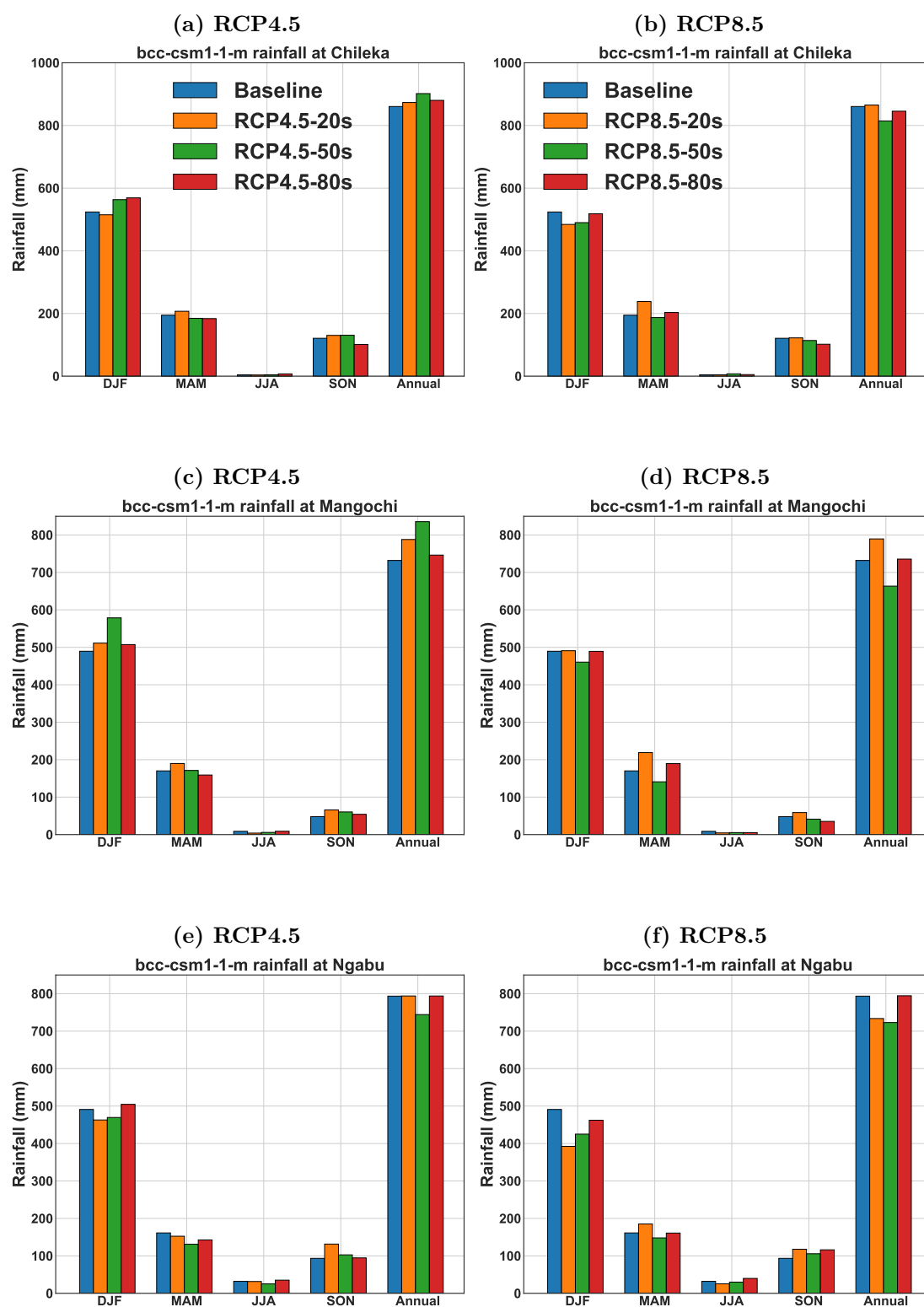


**Figure B.28** Performance of GFDL-ESM2G in predicting dry spell lengths in the SRB





**Figure B.29** Performance of MPI-ESM-LR in predicting dry spell lengths in the SRB



**Figure B.30** bcc-csm1-1-1-m seasonal and annual future projections for rainfall in the SRB.

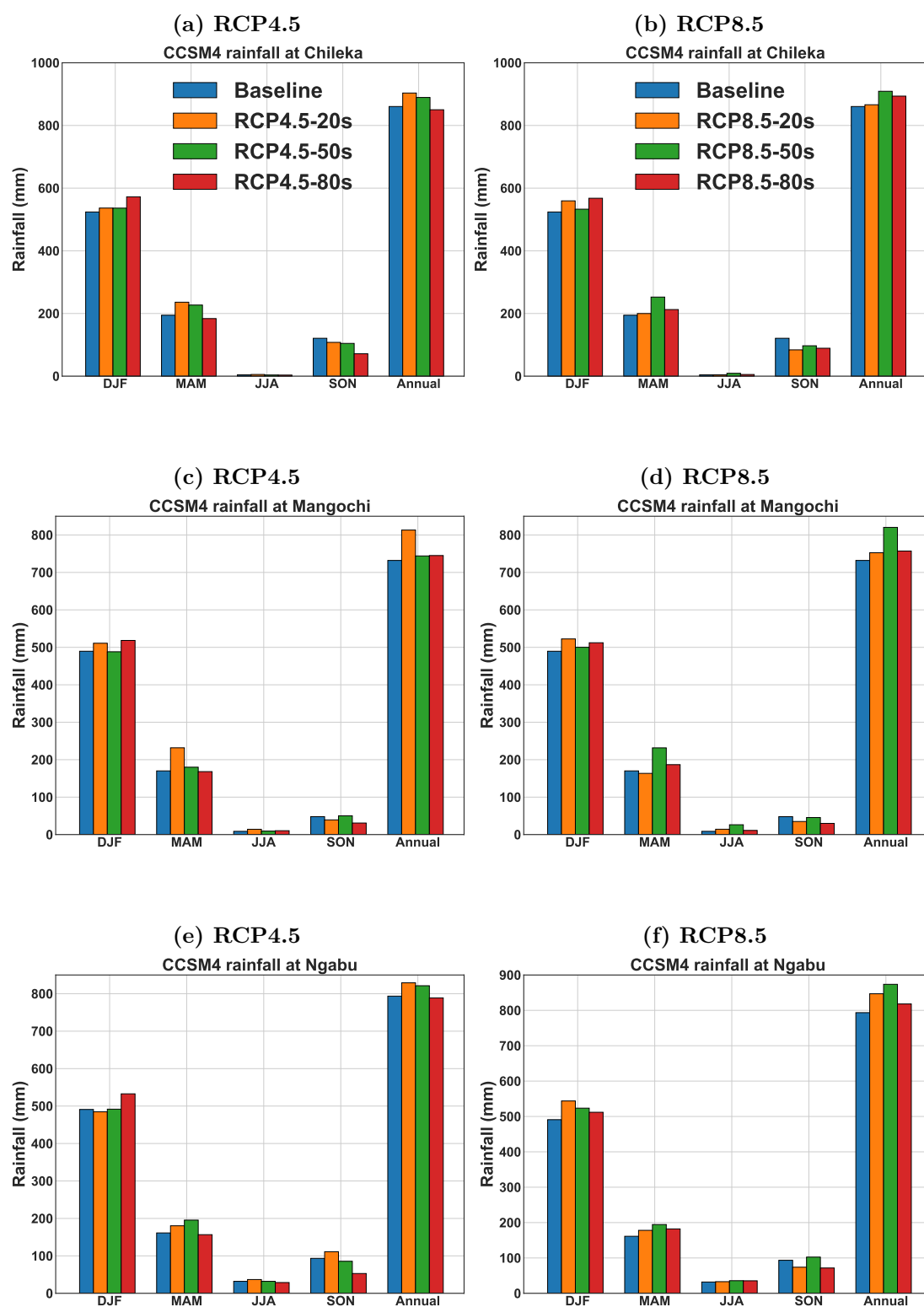
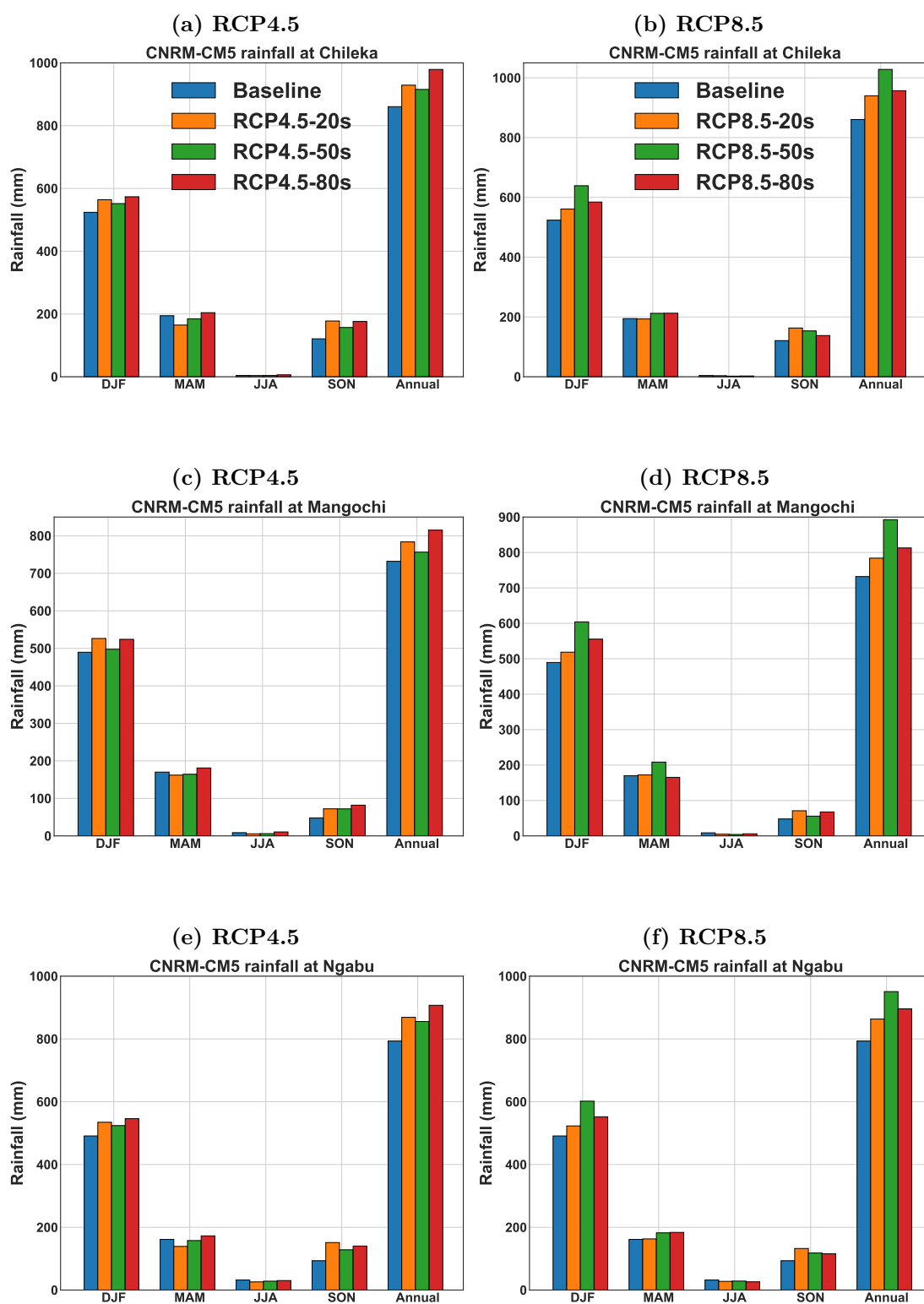
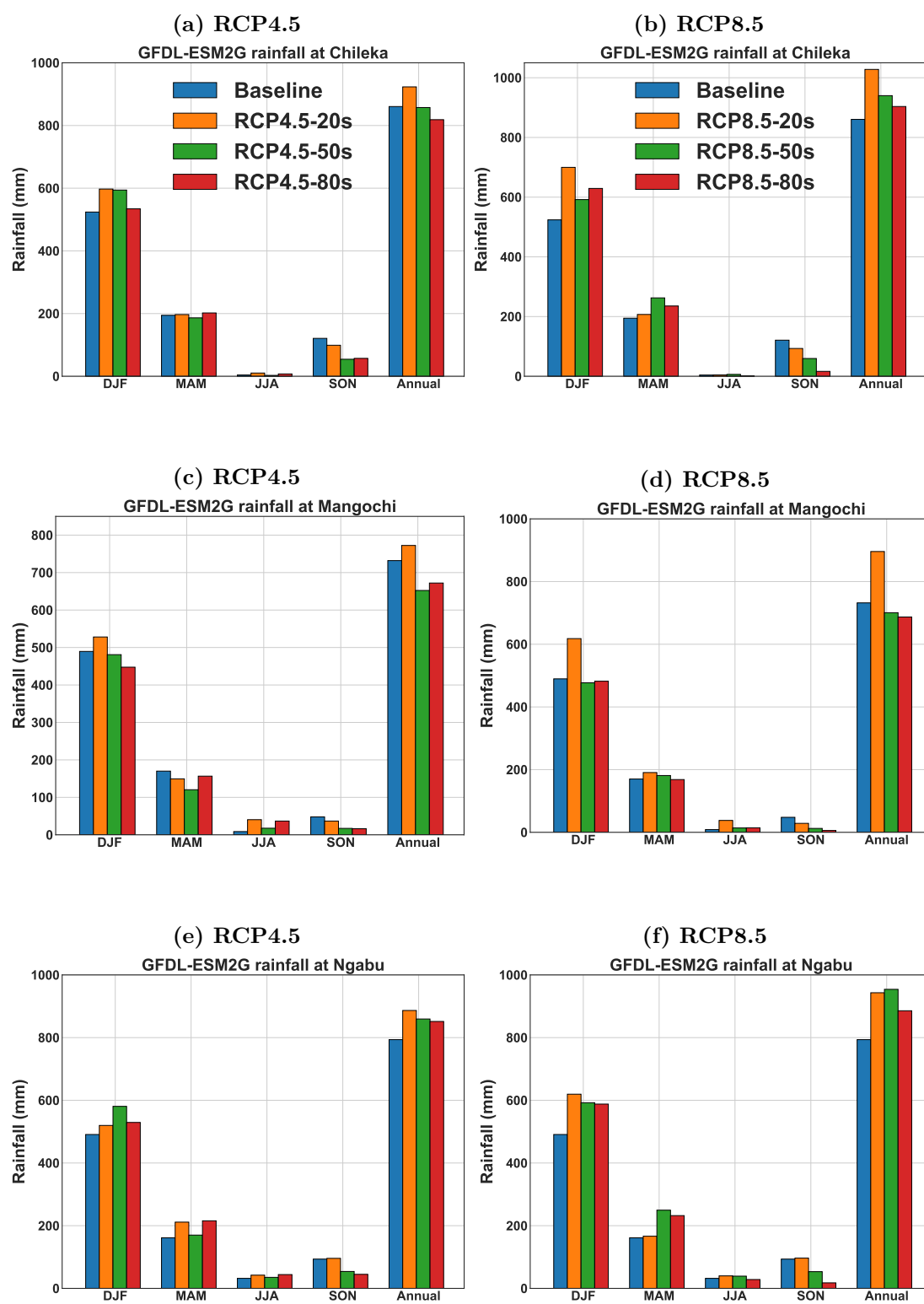


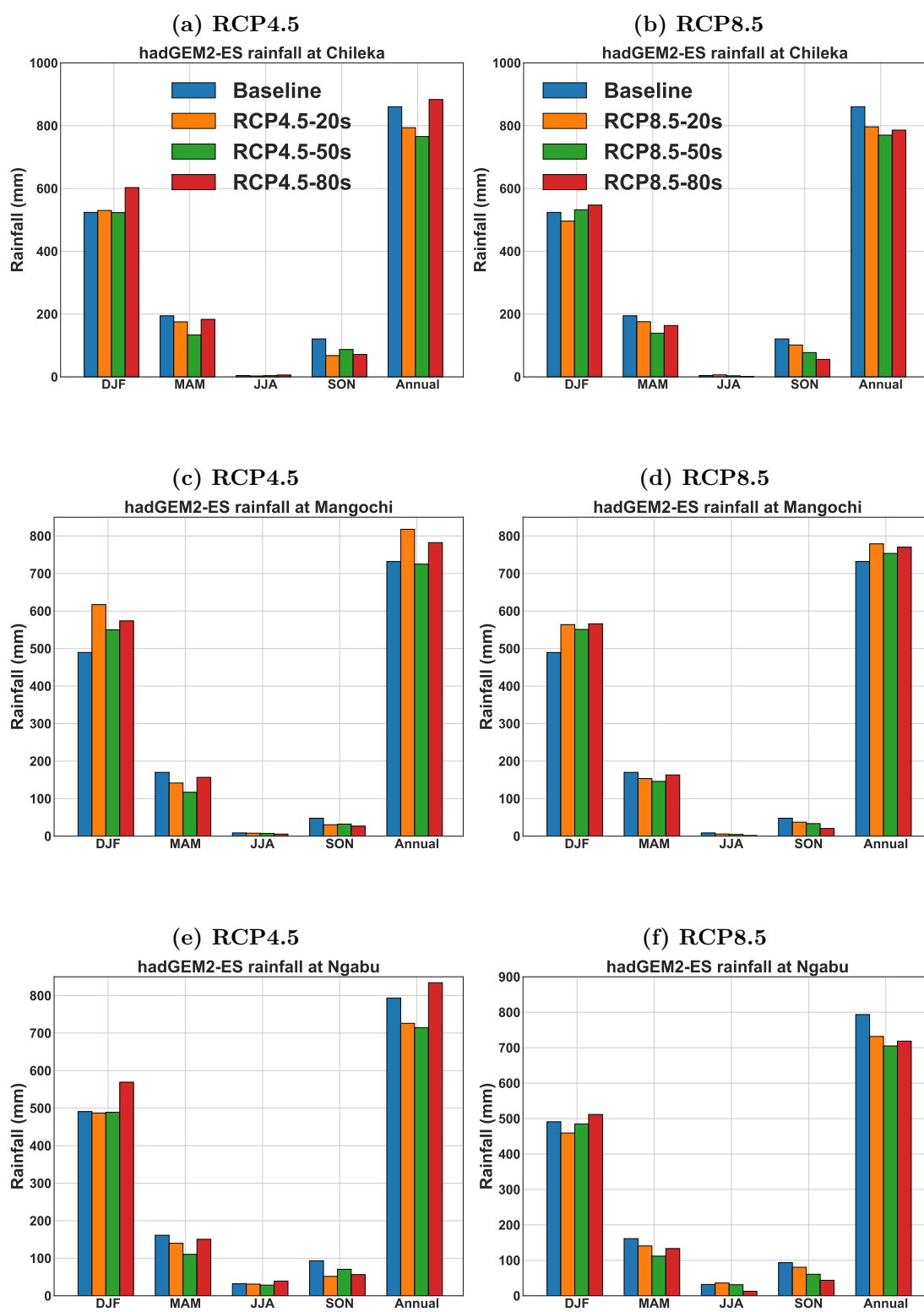
Figure B.31 CCSM4 seasonal and annual future projections for rainfall in the SRB.



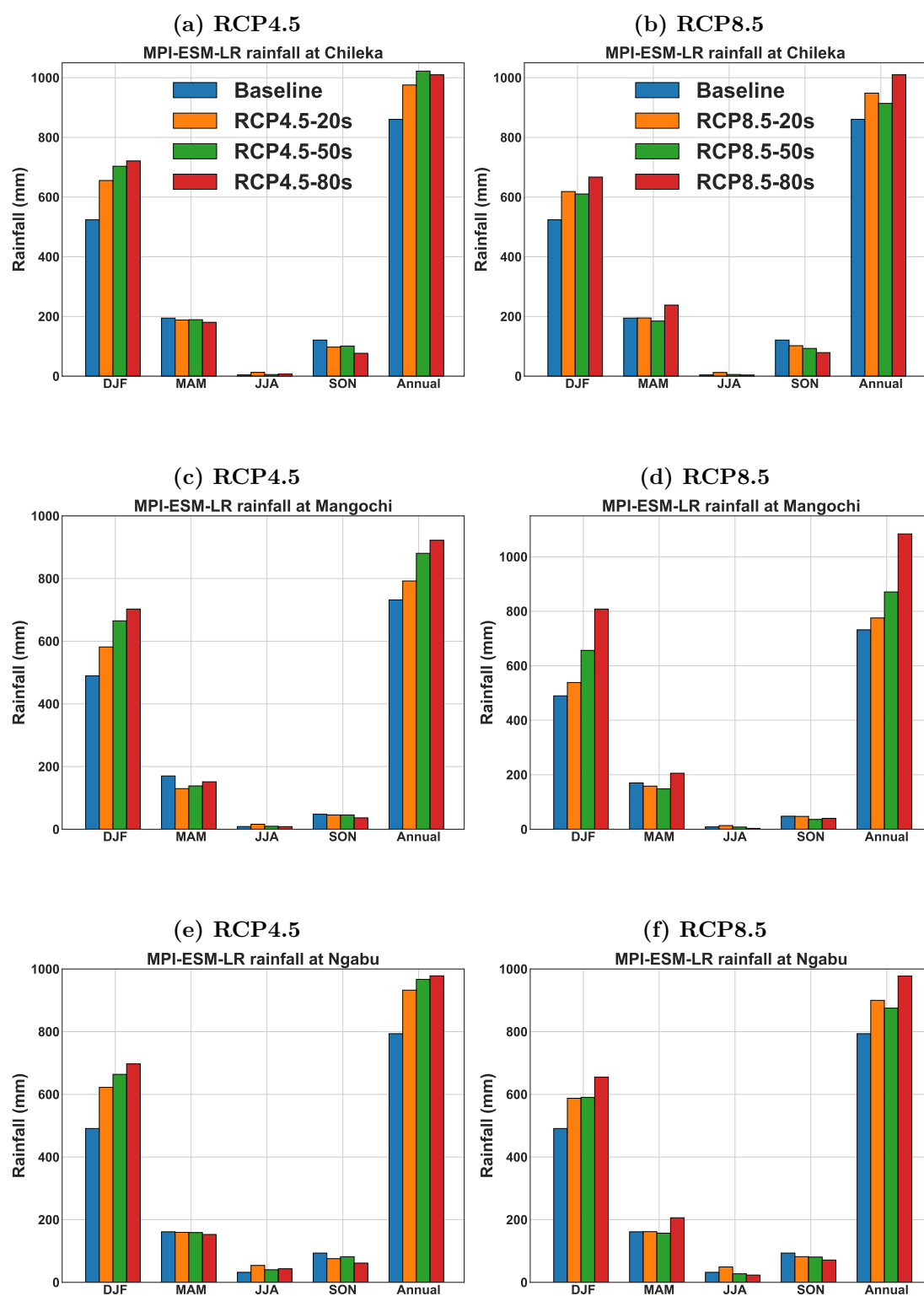
**Figure B.32** CNRM-CM5 seasonal and annual future projections for rainfall in the SRB.



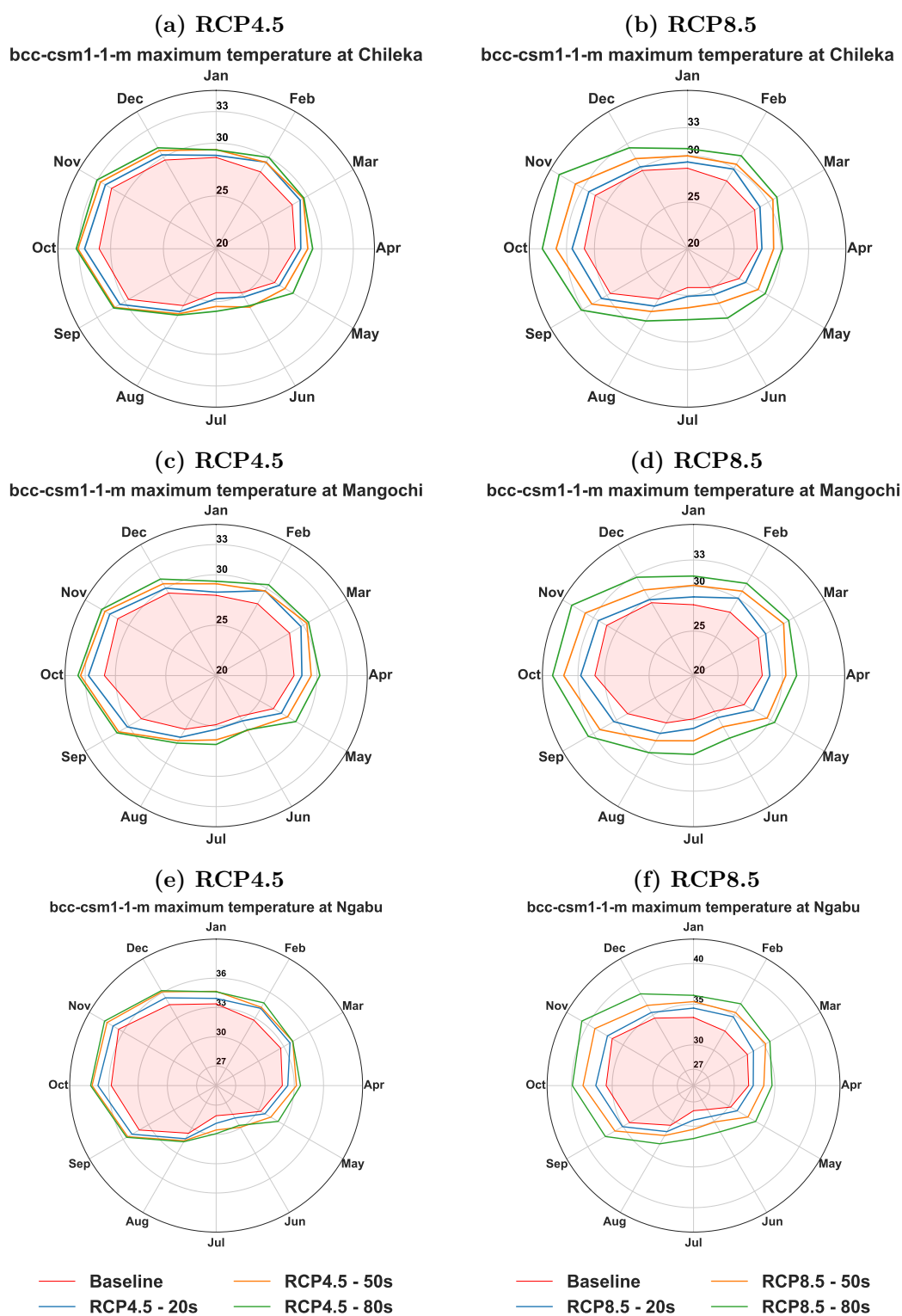
**Figure B.33** GFDL-ESM2G seasonal and annual future projections for rainfall in the SRB.



**Figure B.34** HadGEM2-ES seasonal and annual future projections for rainfall in the SRB.

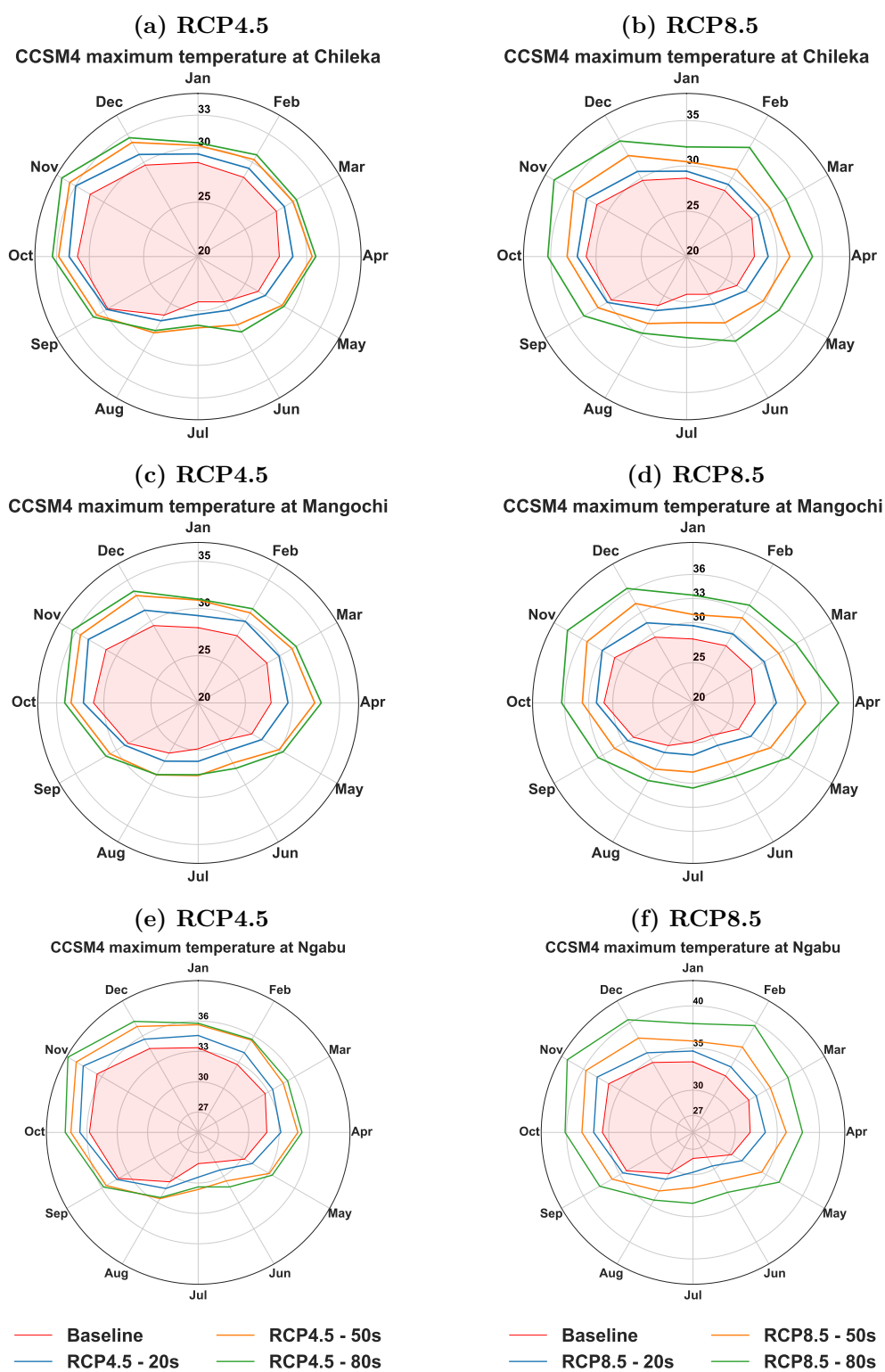


**Figure B.35** MPI-ESM-LR seasonal and annual future projections for rainfall in the SRB.

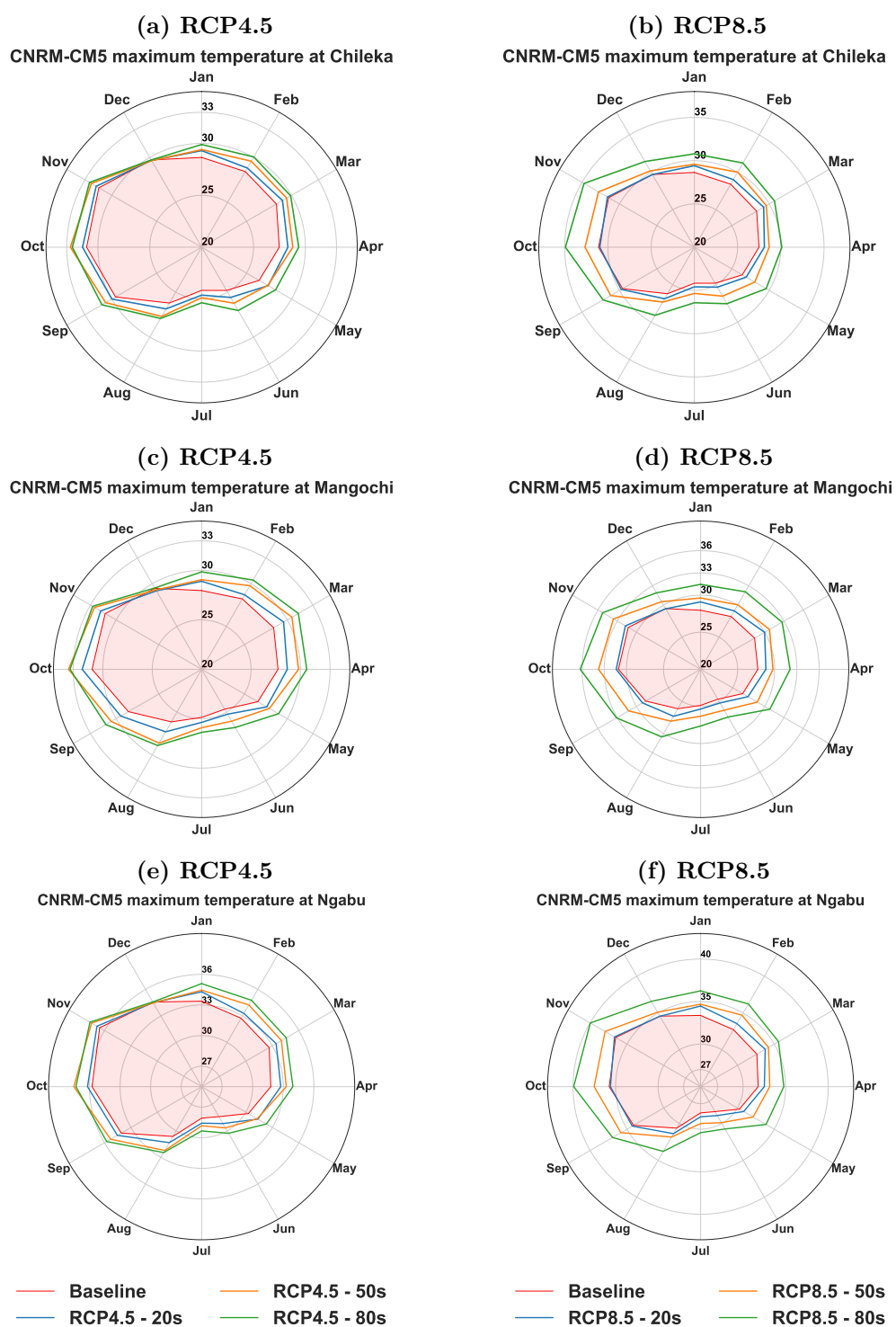


**Figure B.36** bcc-csm1-1-1-m future projections for maximum temperature in degree Celsius. Shaded region represents baseline period (1975–2005)

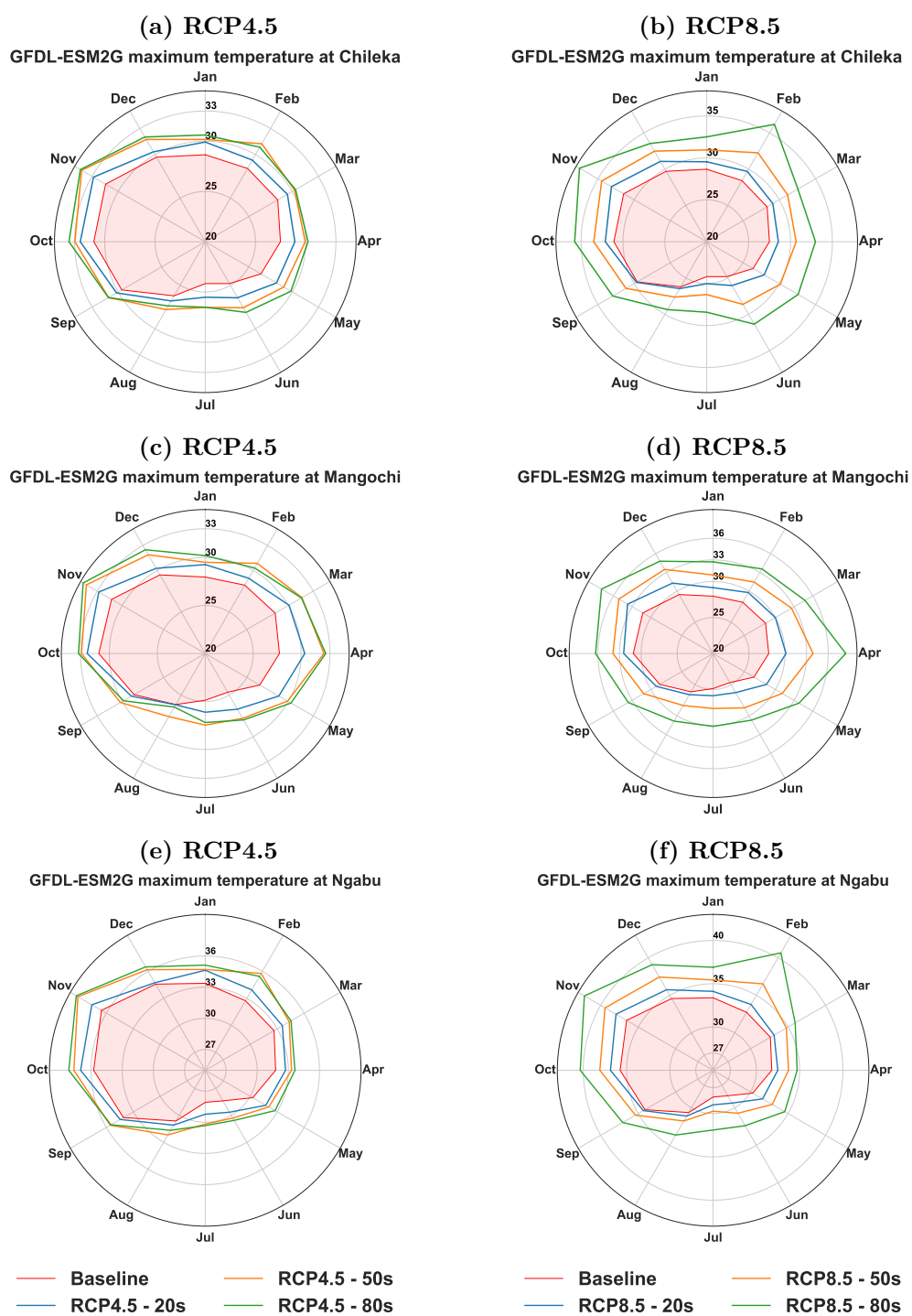




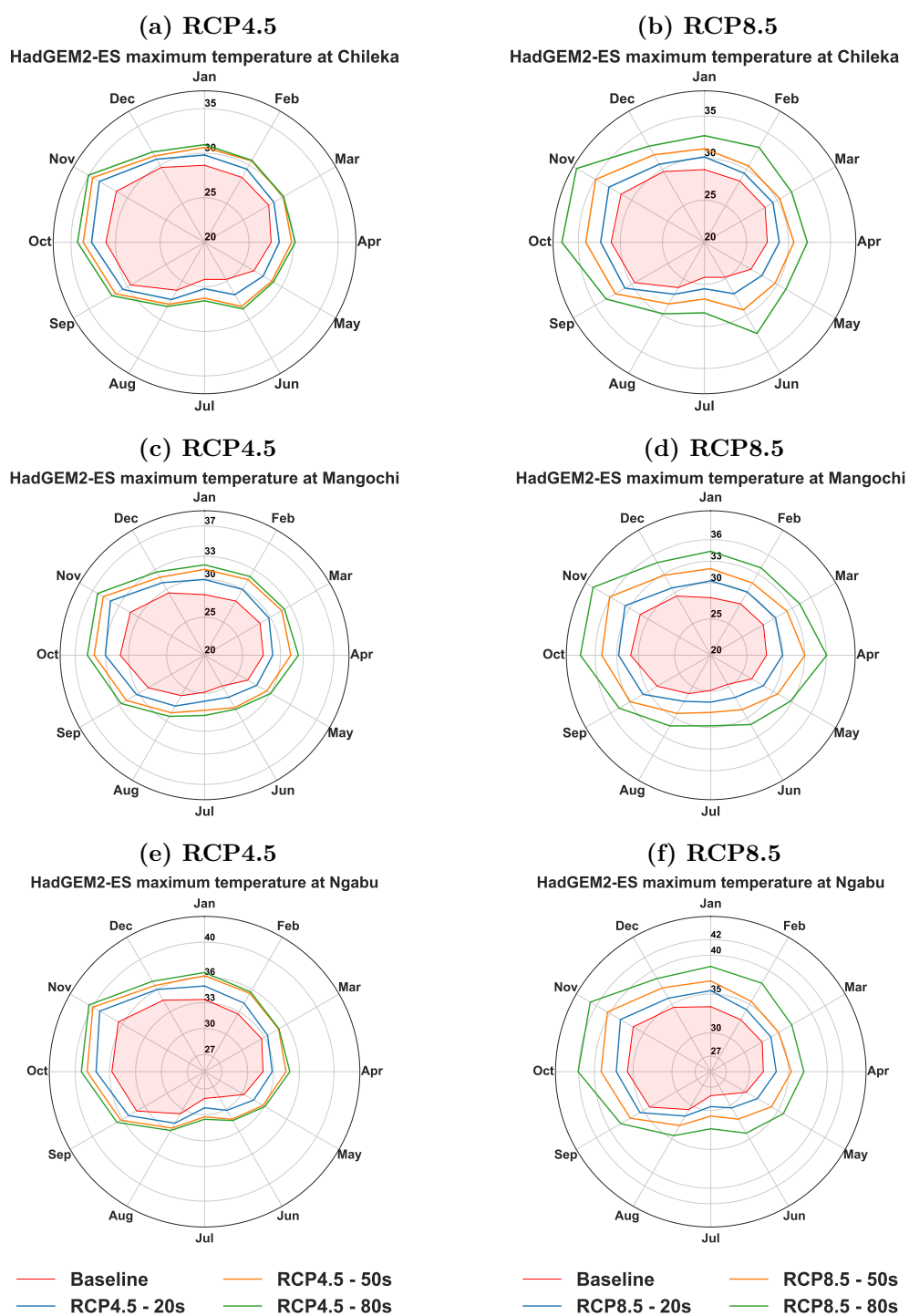
**Figure B.37** CCSM4 future projections for maximum temperature in degree Celsius. Shaded region represents baseline period (1975–2005)



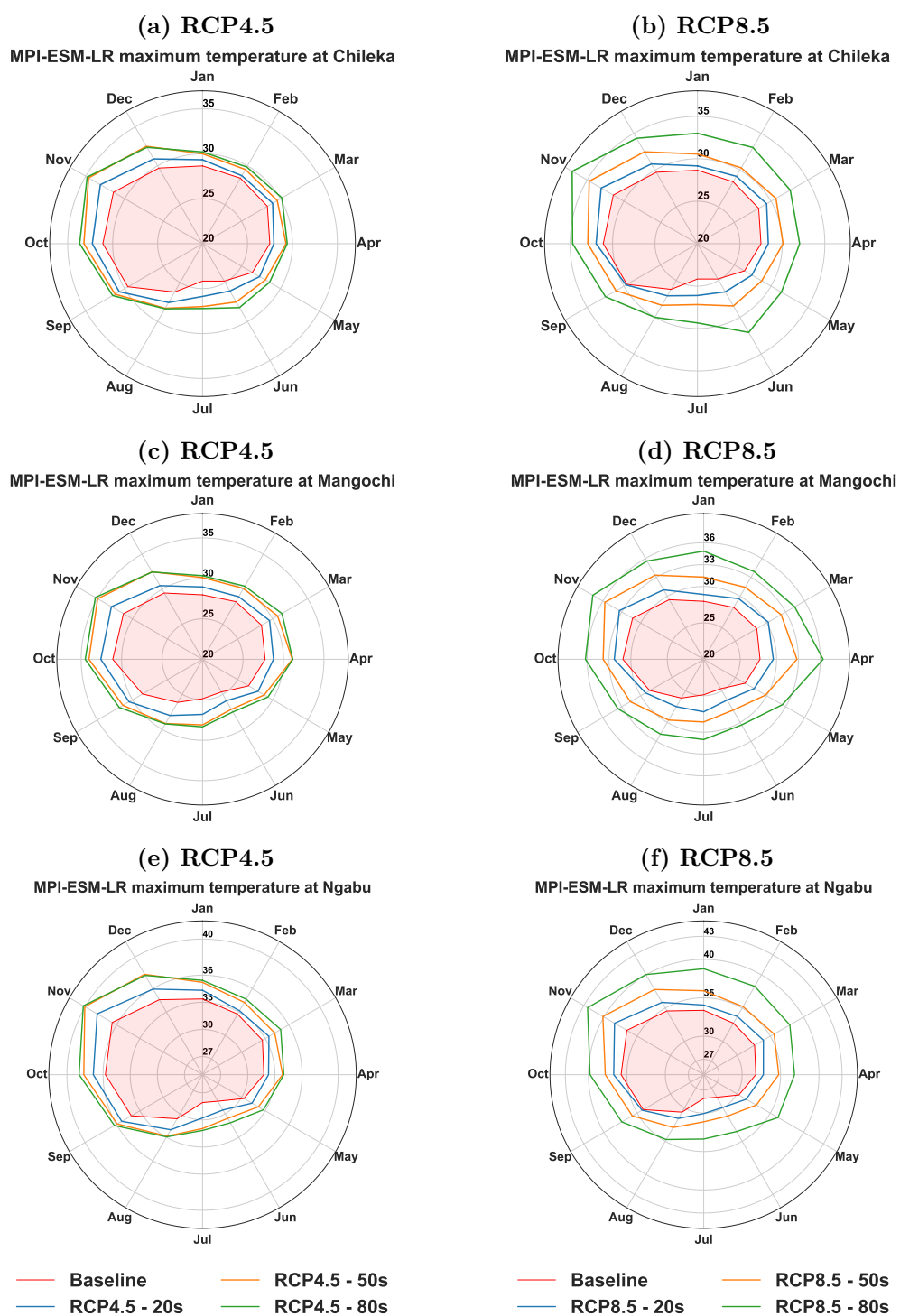
**Figure B.38** CNRM-CM5 future projections for maximum temperature in degree Celsius. Shaded region represents baseline period (1975–2005)



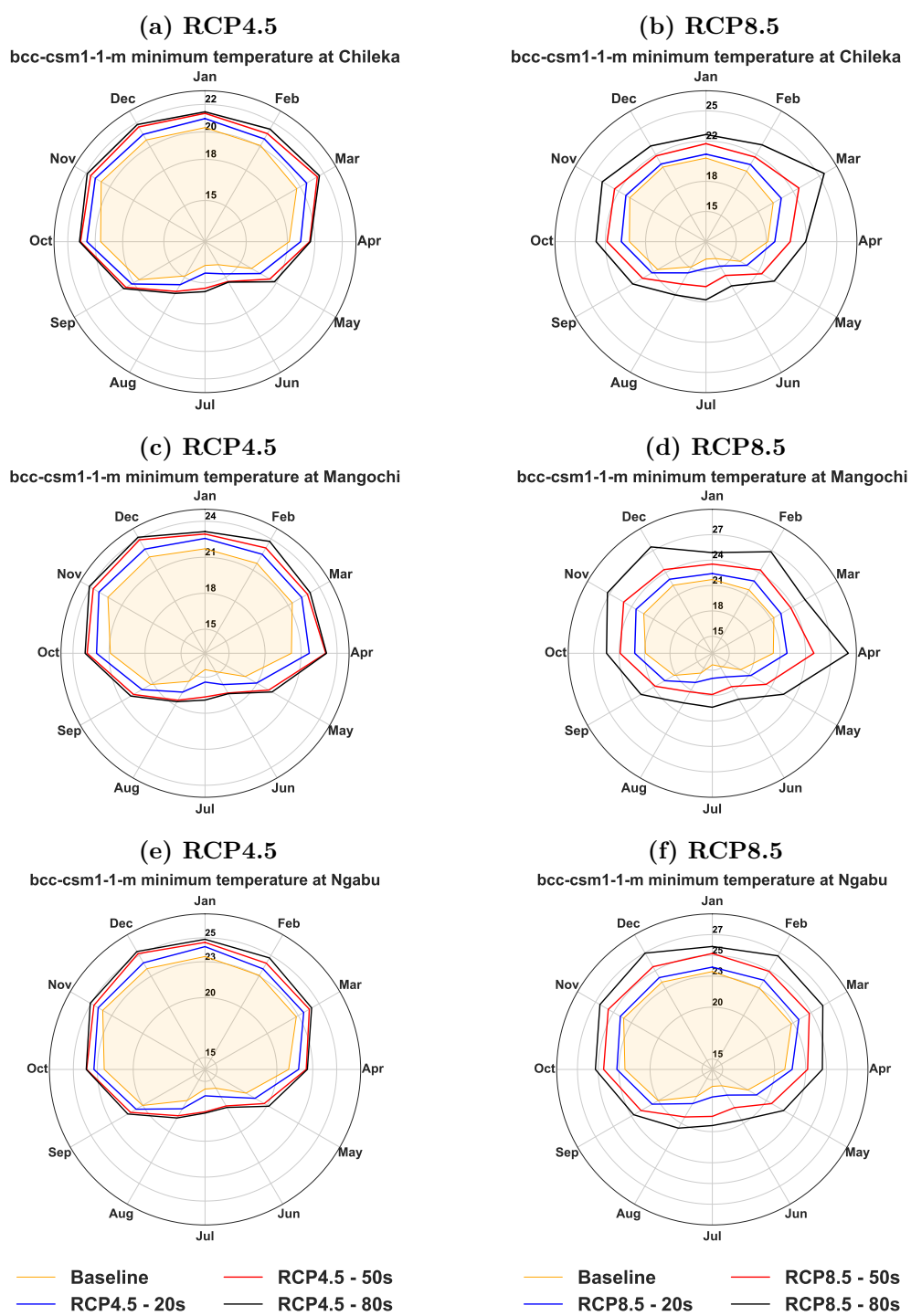
**Figure B.39** GFDL-ESM2G future projections for maximum temperature in degree Celsius. Shaded region represents baseline period (1975–2005)



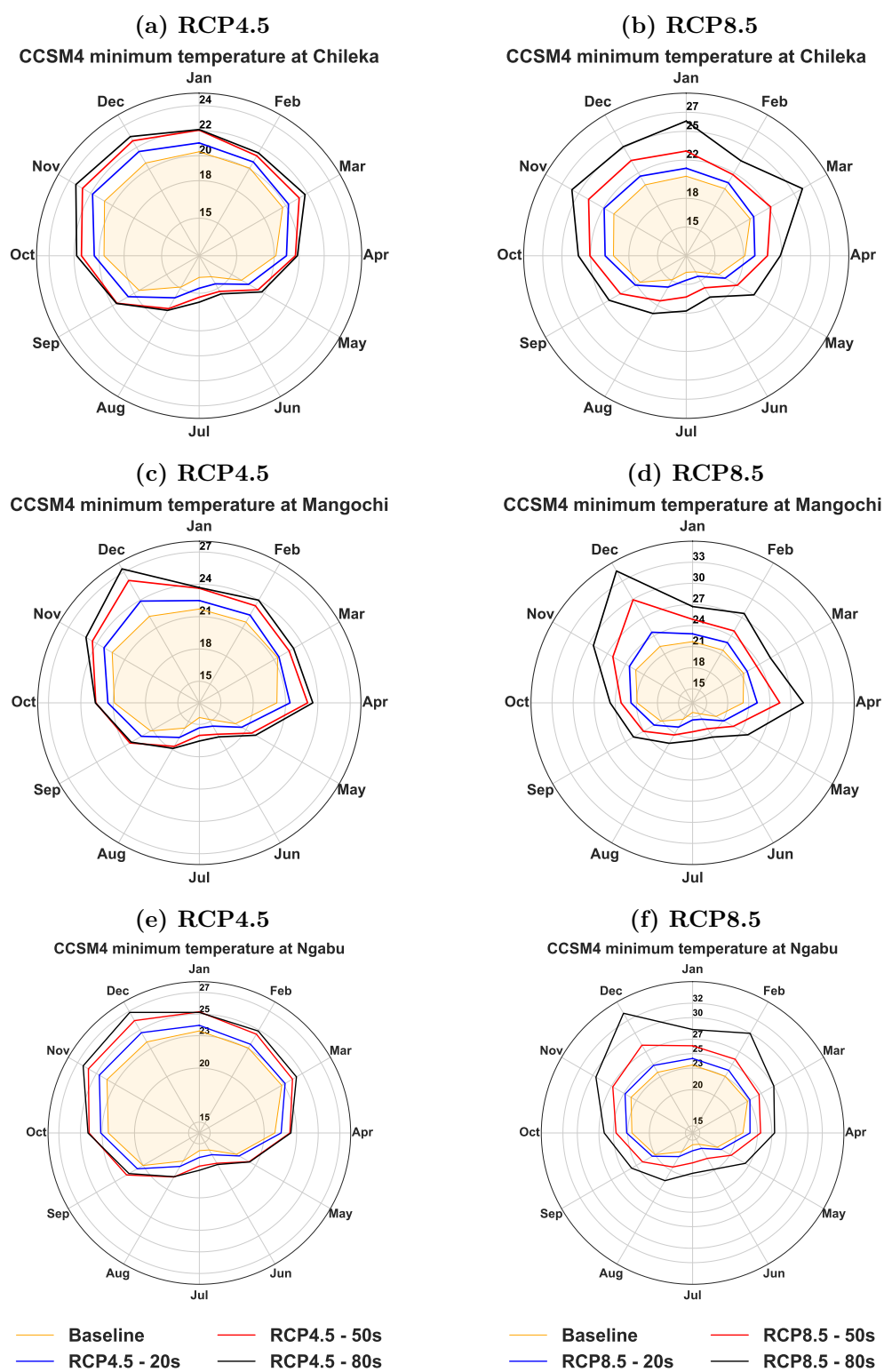
**Figure B.40** hadGEM2-ES future projections for maximum temperature in degree Celsius. Shaded region represents baseline period (1975–2005)



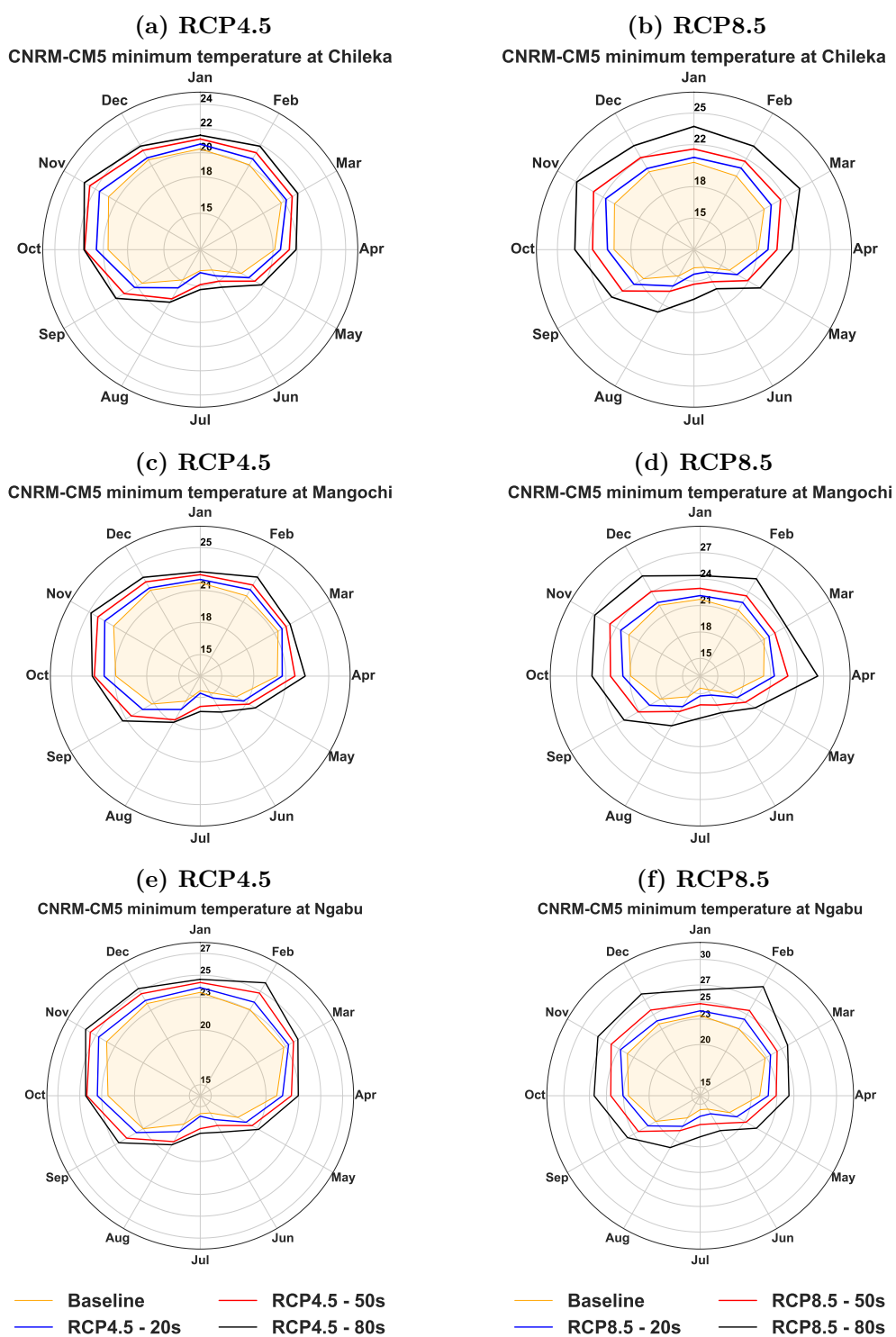
**Figure B.41** MPI-ESM-LR future projections for maximum temperature in degree Celsius. Shaded region represents baseline period (1975–2005)



**Figure B.42** bcc-csm1-1-m future projections for minimum temperature in degree Celsius. Shaded region represents baseline period (1975–2005)

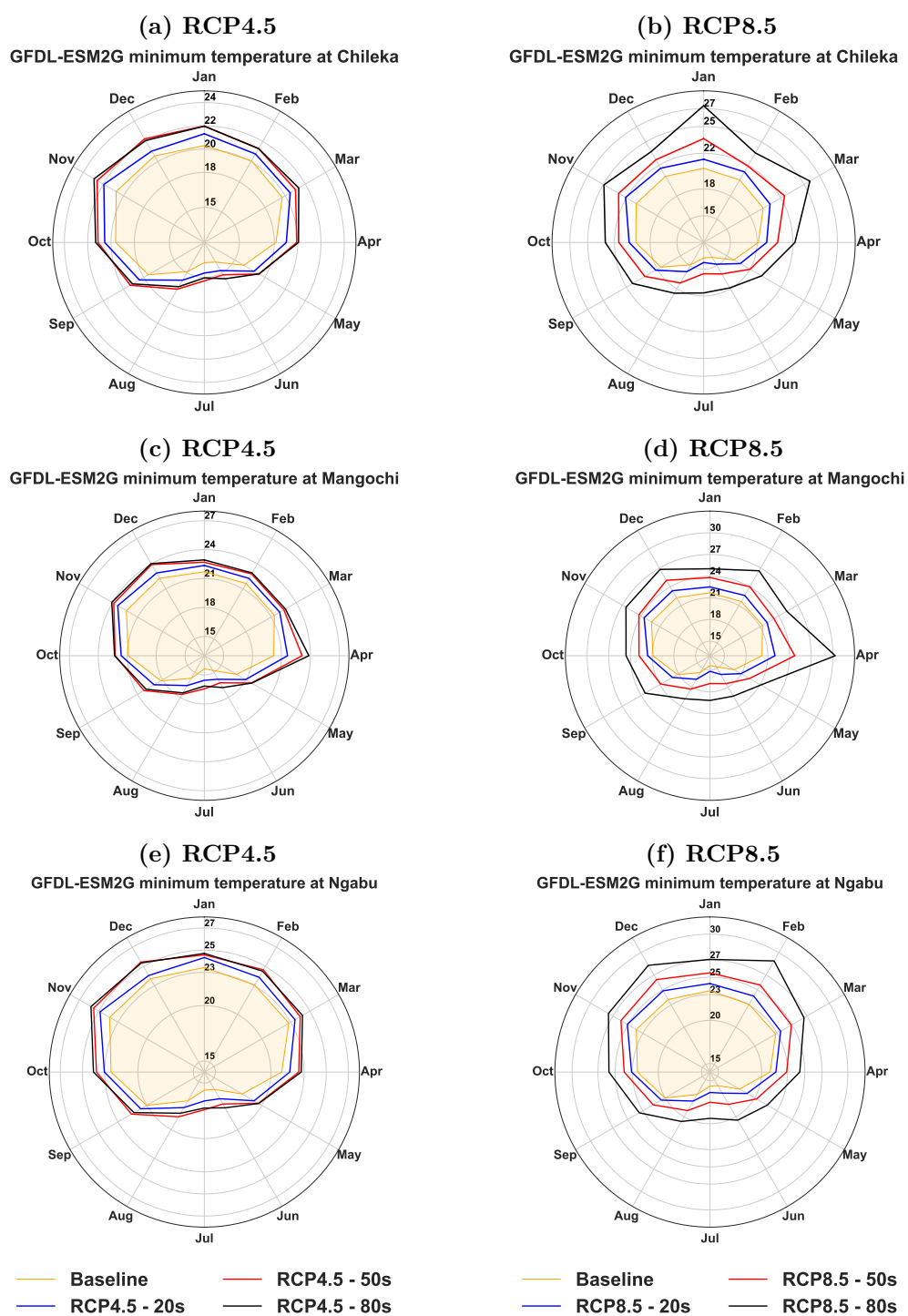


**Figure B.43** CCSM4 future projections for minimum temperature in degree Celsius. Shaded region represents baseline period (1975–2005)

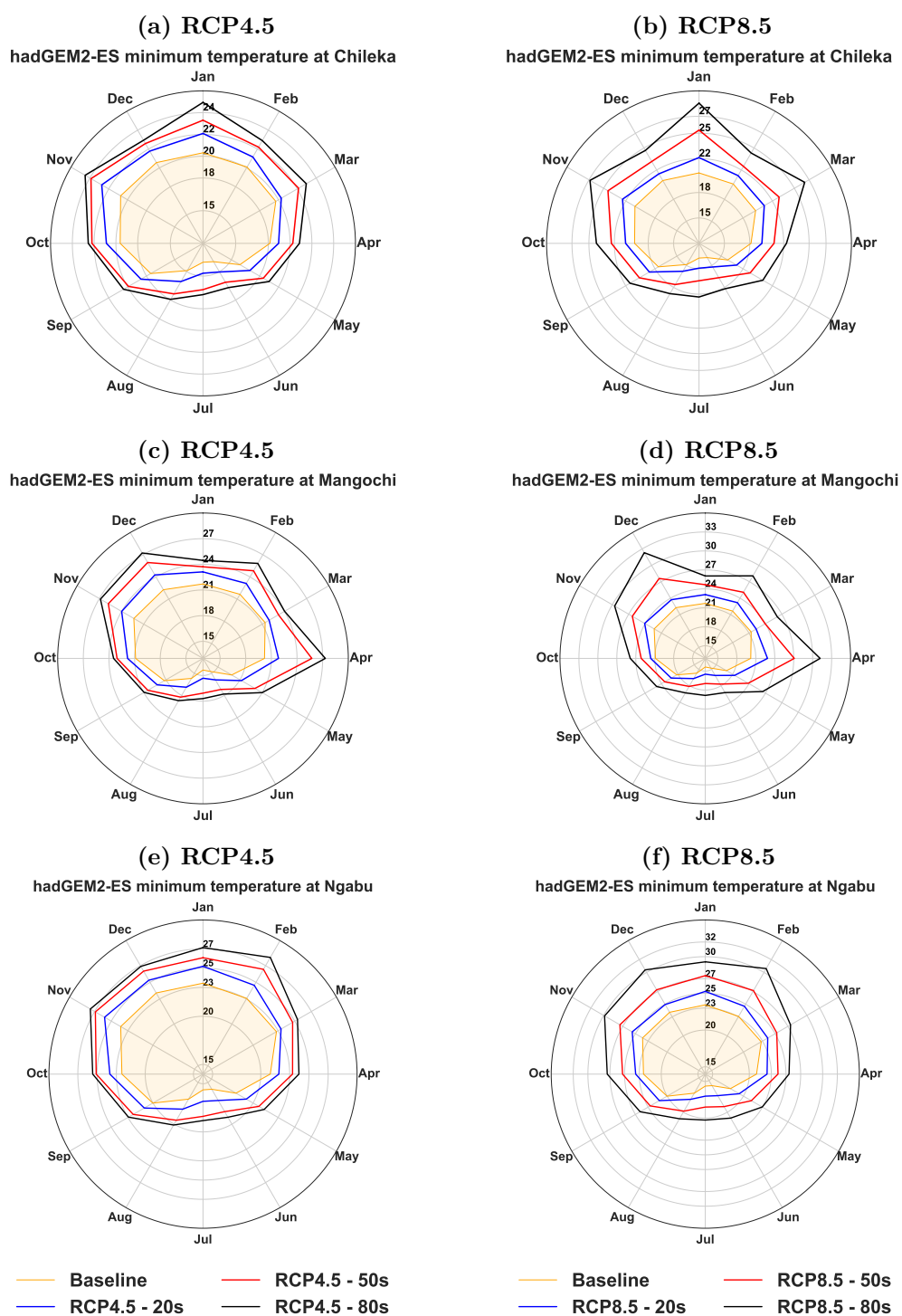


**Figure B.44** CNRM-CM5 future projections for minimum temperature in degree Celsius. Shaded region represents baseline period (1975–2005)

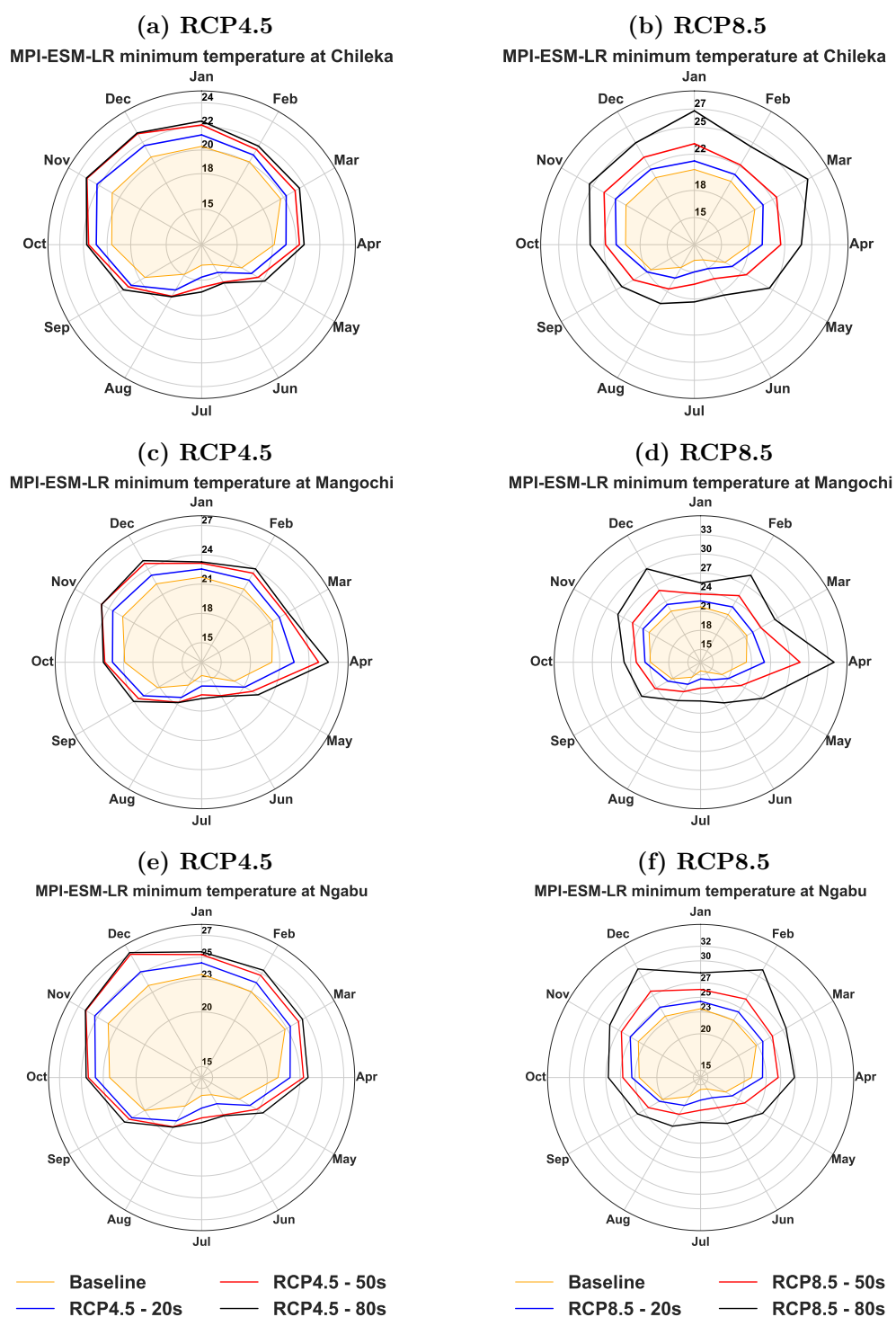




**Figure B.45** GFDL-ESM2G future projections for minimum temperature in degree Celsius. Shaded region represents baseline period (1975–2005)



**Figure B.46** hadGEM2-ES future projections for minimum temperature in degree Celsius. Shaded region represents baseline period (1975–2005)



**Figure B.47** MPI-ESM-LR future projections for minimum temperature in degree Celsius. Shaded region represents baseline period (1975–2005)